Evidence-Based Complementary and Alternative Medicine

Traditional Medicine in Diabetes

Lead Guest Editor: Youhua Xu
Guest Editors: Dingkun Gui and Xu-Jie Zhou

Traditional Medicine in Diabetes

Evidence-Based Complementary and Alternative Medicine

Traditional Medicine in Diabetes

Lead Guest Editor: Youhua Xu
Guest Editors: Dingkun Gui and Xu-Jie Zhou

Contents

A Meta-Analysis of the Effects of Tai Chi on Glucose and Lipid Metabolism in Middle-Aged and Elderly Diabetic Patients: Evidence from Randomized Controlled Trials
Ya-nv Liu, Lin Wang, Xin Fan, Shijie Liu, Qi Wu, and You-Ling Qian
Review Article (13 pages), Article ID 6699935, Volume 2021 (2021)

Effect of Bushen Huoxue Prescription on Cognitive Dysfunction of KK-Ay Type 2 Diabetic Mice
Shao-Yang Zhao, Huan-Huan Zhao, Ting-Ting Hao, Wei-Wei Li, and Hao- Guo
Research Article (14 pages), Article ID 6656362, Volume 2021 (2021)

Ethnopharmacological Use and Biological Activities of *Tragia involucrata* L.
Mumtaz S. Pallie, Pathirage K. Perera, Nishantha Kumarasinghe, Menuka Arawwawala, and Charitha L. Goonasekara
Review Article (17 pages), Article ID 8848676, Volume 2020 (2020)

The Role of Oxymatrine in Amelioration of Acute Lung Injury Subjected to Myocardial I/R by Inhibiting Endoplasmic Reticulum Stress in Diabetic Rats
Yongpan Huang, Xian Long, Xinliang Li, Saihua Li, and Jianbin He
Research Article (13 pages), Article ID 8836904, Volume 2020 (2020)

Hindawi
Evidence-Based Complementary and Alternative Medicine
Volume 2021, Article ID 9972386, 22 pages
https://doi.org/10.1155/2021/9972386

Research Article

Cost-Effectiveness of Oral Antidiabetic Drugs: A Prospective Multicenter Study of Real-World Patients

Gordon Liu,[1] Zhiyong Huang,[2] and Qian Xin[3]

[1]*Institute for Global Health and Development, Peking University, Beijing 100871, China*
[2]*Center of Health Policy and Governance, Southwestern University of Finance and Economics, Chengdu 611130, China*
[3]*Visible Analytics, Oxford OX20DP, UK*

Correspondence should be addressed to Qian Xin; qian.xin@visibleanalytics.co.uk

Received 2 April 2021; Accepted 17 September 2021; Published 28 October 2021

Academic Editor: Youhua Xu

This real-world, multicenter, prospective study aims to analyze the cost-effectiveness of prevalent oral antidiabetic drugs, including traditional Chinese medicine and its compounds, used in China. Type 2 diabetes patients initiated on one or several of the most prevalent antidiabetic drugs were recruited on the baseline and followed up over one year with no restriction on drug discontinuation, switching, and add-on. Different drugs were evaluated on their efficacy, adverse effect (AE), health-related quality of life (HRQoL), and cost. Treatments were defined as the intent-to-treat in the primary analysis and on-treatment in the sensitivity analyses. A rich set of patients' baseline characteristics was collected and controlled using the multivariate linear model in the primary analysis and inverse probability weighting and double selection—a machine learning algorithm—in the sensitivity analyses. Estimates of "raw" outcomes, which are not adjusted by covariates and calculated as subgroup means, show that the use of Xiaoke Pill alone and in combination is among the most effective therapies with 50% and 54% of patients reaching the control target of HbA1c < 6.5%. In terms of cost, Xiaoke Pill and gliclazide, which cost participants 4,350 and 5,150 RMB per year on average, are among the least costly therapies. After adjusting patient characteristics, monotherapy and combination therapy using the Xiaoke Pill again display the best control rates, of 45% and 43% against 33% of metformin. Regarding cost, the Xiaoke Pill costs a patient 5,340 RMB per year, in sharp contrast with 8,550 RMB for metformin and 10,330 RMB for acarbose. Our study suggests that the use of Xiaoke Pill—alone or in combination—is associated with better glycemic control and lower cost than some allopathic medications such as metformin or acarbose and shows a similar incidence of hypoglycemia.

1. Introduction

In 2019, 463 million adults (one in 11 adults) aged between 20 and 79 years had diabetes mellitus worldwide, and the number is projected to reach 578 million by 2030 and 700 million by 2045 [1]. The high prevalence of diabetes represents huge health and economic burdens. In 2016, diabetes caused 1.599 million deaths, which ranked it the seventh leading cause of death [2]. In 2019, an estimated $ 760 billion was spent on diabetes treatment, making up 10% of the global health expenditure spent on adults [1]. With the rising prevalence of diabetes globally, low- and middle-income countries have experienced the greatest increase in recent years [1]. In China, an estimated 129.8 million adults have diabetes, which accounts for 11.2% of its adult population [3], and the health expenditure attributed to diabetes was estimated to be $ 63 billion [1].

In China, diabetes is treated with both allopathic medicines and traditional Chinese medicine (TCM). The history of using TCMs as a treatment for diabetes is over 2000 years [4]. Nowadays, many of the TCMs have been included in the national reimbursement plan and TCM alone or in combination with allopathic drugs has been widely prescribed in clinical settings [5]. A survey conducted at 75 hospitals in nine cities found that the proportions of patients treated with biguanides, sulfonylurea, meglitinides, glitazones, α-glucosidase inhibitors, and others (including TCMs) were 78.4%, 65.1%, 14.0%, 12.6%, 31.1%, and 18.1%,

respectively. Oral antidiabetic drugs on 2018 China's National Essential Medicines, which is the most recently issued guidance for purchase and reimbursement of essential drugs by healthcare providers in China, include both allopathic drugs, such as metformin, glibenclamide, glipizide, glimepiride, gliquidone, gliclazide, acarbose, dapagliflozin, liraglutide, repaglinide, pioglitazone, sitagliptin, and linagliptin, and TCMs, such as the Xiaoke Pill (*Xiao Ke Wan* in Chinese).

Among TCMs used in treating diabetes, the Xiaoke Pill, a compound of glibenclamide and several Chinese herbs, was widely used to treat diabetes in China [6]. The Xiaoke Pill contains 0.25 micrograms of glibenclamide (per pill) and Chinese herbs such as Radix Puerariae, Radix Rehmanniae, Radix Astragali, Radix Trichosanthis, Stylus Zeae Maydis, Fructus Schisandrae Sphenantherae, and Rhizoma Dioscoreae, selected according to two ancient TCM formulas, namely, "Yuquan San" and "Xiaoke Fang." An experiment using rats showed that Radix Astragali, one of the TCM substances of the Xiaoke Pill, could amplify the glucose counterregulatory response to insulin-induced hypoglycemia [7]. A randomized, double-blind, and multicenter clinical trial found that the Xiaoke Pill, compared with glibenclamide, had similar glucose control efficacy but a reduced risk of hypoglycemia, which indicated that TCM herbs in the Xiaoke Pill were protective against hypoglycemia caused by glibenclamide [8].

Given the high prevalence and economic burden of diabetes, studies on the cost-effectiveness of antidiabetic drugs are needed to plan treatment programs. One previous study, which compared five oral antidiabetic drugs in the Chinese market, found that metformin was cost-effective [9]. Another study found metformin to be cost-effective against acarbose [10]. However, a systematic review of 16 cost-effectiveness studies conducted in China found that metformin was the least cost-effective therapy when compared to rosiglitazone, glipizide, and α-glucosidase inhibitors [11]. There are some other studies regarding the cost-effectiveness of antidiabetic drugs other than metformin in China [12]. However, most of the existing studies on the cost-effectiveness of antidiabetic drugs used in the Chinese market are limited by their relatively small sample sizes, retrospective or model-based designs, and lack of information on the actual cost undertaken by patients.

In this study, we aim to analyze the cost-effectiveness of currently existing oral antidiabetic drugs in the management of type 2 diabetes in China, including TCMs and TCM compounds. In particular, we compare the efficacy, adverse effect, HRQoL, and cost among the most commonly used oral antidiabetic drugs in China with real-world evidence. We contribute to the existing literature in several ways. First, the cost-effectiveness studies of oral antidiabetic drugs in the Chinese market are lacking, especially for TCMs, although TCMs are routinely used for diabetes treatment. In this study, we analyze the cost-effectiveness of TCMs and their compounds, among other commonly used antidiabetic drugs. Second, the real-world design of this study can help us better assess the cost-effectiveness of different types of diabetes therapies in medical practice where discontinuation, switching, and add-on behaviors are common but difficult to incorporate into the model-based analysis. Third, our study is of multicenter and prospective design and of a relatively large size, providing us with enough statistical power to capture significant differences in key outcomes of interest.

As a complementary source to conventional randomized controlled trials (RCTs), real-world evidence has become increasingly important in healthcare decision-making [13]. Cost-effectiveness analysis based on real-world evidence has advantages, such as focusing on effectiveness rather than efficacy, simultaneous comparison of multiple treatment options, and rich data on resource use, but confounding bias associated with real-world data should be addressed with great caution [14]. To date, there have been very few real-world studies on the cost-effectiveness of antidiabetic drugs. A retrospective study compared liraglutide with exenatide, in which the multivariate regression was used to control confounding bias [15]. Another retrospective study compared canagliflozin with dapagliflozin, in which the propensity score-based method was used to adjust the confounding bias [16]. In this study, we adopted a prospective, observational cohort design [14] and collected a wide range of potential confounding factors of health outcomes and costs associated with diabetes, following a systematic review of the existing evidence. During the analysis stage, several statistical methods, including multivariate regression, inverse probability weighting, and double selection, were used to mitigate confounding bias.

2. Materials and Methods

2.1. Study Design and Sample. This study was a prospective multicenter study of real-world patients. The Ethics Review Committee of The Third Affiliated Hospital of Peking University of Traditional Chinese and Western Medicine approved the study. All the participants provided their written informed consent to participate in this study. Participants were recruited from 66 community health centers located in five Chinese cities (i.e., Beijing, Chengdu, Guangzhou, Nanjing, and Shenyang) between December 2010 and December 2011. Recruitment was facilitated by an endocrinologist (or a general practitioner if the health center did not have an endocrine department) and was assisted by trained interviewers. All clinically diagnosed patients with type 2 diabetes who visited the healthcare centers in 2010 and provided phone numbers were contacted and screened for eligibility for inclusion. (1) Patients aged 16 years or older who were clinically diagnosed with type 2 diabetes; (2) those who were taking oral antidiabetic drugs, without any cognitive impairment, severe vision problems, or hearing problems; (3) those who were able to read and communicate in Mandarin; and (4) those who were willing to participate in the study were considered eligible. Among all eligible patients, 3,000 subjects (with a target of 600 in each city) were randomly sampled with a quota of 600 subjects for users of the Xiaoke Pill.

Upon completing the baseline interview, the patients were invited to participate in follow-up surveys every three months, four times per year. In addition, two medical tests were administrated, one at the time of the baseline interview and the other at the last follow-up, to collect physiological indicators associated with patients' diabetic conditions.

A number of quality control measures were taken throughout the survey. First, a pilot test was conducted before the baseline survey to test the survey design. Second, both investigators and supervisors were screened and trained. Investigators were recruited from our cooperators, including Beijing University of Chinese Medicine in Beijing, Shenyang Pharmaceutical University in Shenyang, China Pharmaceutical University in Nanjing, Southwestern University of Finance and Economics in Chengdu, and Guangzhou Academy of Social Sciences in Guangzhou, while supervisors were recruited from the China Center of Health Economics Research. A survey guide was provided to both investigators and supervisors. Third, every filled questionnaire was checked by two reviewers independently. Fourth, 20% of filled questionnaires were randomly selected and called back by phone. Last, a double-entry method was adopted to ensure the accuracy of data entry.

In the statistical analysis stage, we kept those who had participated in the baseline, all follow-up surveys, and the two medical tests. We excluded those taking insulin at the baseline but imposed no restriction on initial oral drug use, following discontinuation, switching, and add-on of drugs (Figure 1). There were 1903 subjects remaining in our working sample, with 440 from Shenyang, 314 from Beijing, 403 from Chengdu, 366 from Nanjing, and 380 from Guangzhou. The power of results from each city might not be even due to differences in sample sizes. However, there were enough observations for each city so that meaningful inference can be reached.

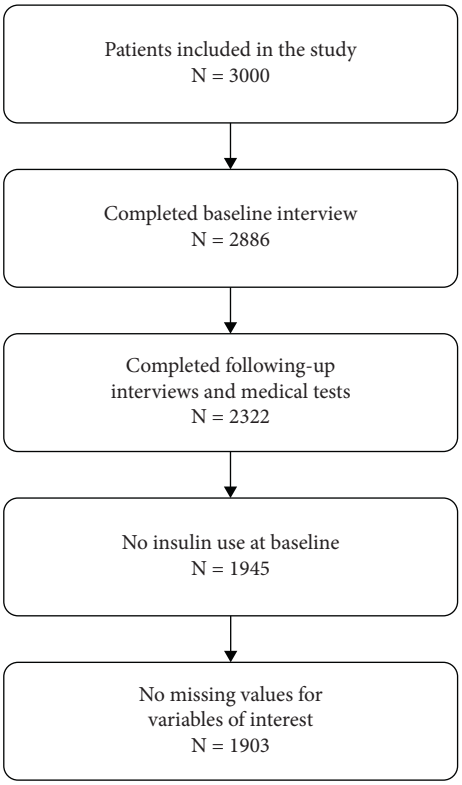

Figure 1: Study sample.

2.2. Measures. Table 1 describes the variables of outcomes, treatments, and controls used in this study.

2.2.1. Outcomes. We evaluated the outcome of each drug in terms of its efficacy, AE, HRQoL, and associated costs, including hospitalizations, outpatient encounters, and OTC pharmacy prescriptions. Note that hospitalizations include the expense for drugs used in the episode of inpatient care and outpatient encounters include the expense for drugs in the episode of outpatient care.

(1) Efficacy. Efficacy was measured as the level of glycemic control with the glycated hemoglobin (HbA1c) target of <6.5% recommended by the American Diabetes Association, the European Association for the Study of Diabetes, the International Diabetes Federation, and the WHO [17]. The indicator variable takes the value of one under control target or zero out of control target.

(2) AE. As a side effect associated with antidiabetic drugs, hypoglycemia (also known as low blood sugar) is considered a major AE concern in diabetes treatment. This study asked patients whether they had experienced hypoglycemia since the last survey. If they had, the AE indicator was coded as one and if not, zero during that period. The AE measure was then calculated as the sum of the AE indicators over the four follow-up surveys and ranged from zero to four.

(3) HRQoL. Patients were asked to complete an EQ-5D-3L questionnaire at baseline and follow-up surveys [18]. Answers to these questions were transformed into HRQoL scores using the value set for the Chinese population [19]. The HRQoL score is defined as a continuous measure ranging between zero and one.

(4) Costs. Given our real-world setup, we measured the all-cause medical costs incurred to diabetic patients without making a distinction between costs directly attributable to diabetes and other indirect medical costs [20]. We measured the costs of the inpatient and outpatient services (including the cost of drugs prescribed and purchased within hospitals and clinics), as well as OTC drug costs. The total cost was defined as the sum of inpatient cost, outpatient cost, and OTC drug costs.

2.2.2. Treatment. In this real-world study, we monitored the use of up to 15 different types of oral antidiabetic medications, including biguanides (metformin and phenformin), sulfonylureas (glibenclamide, glipizide, gliquidone, gliclazide, and glimepiride), α-glucosidase inhibitors (acarbose and voglibose), secretagogue (repaglinide and nateglinide), thiazolidinediones (rosiglitazone and pioglitazone), TCMs, and the Xiaoke Pill. No restriction on drug use behaviors such as discontinuation, switching, and add-on of drugs was imposed. Using this design, we could observe a pyramid of therapies for diabetes adopted in medical practice. To maintain sufficient statistical power, we restrict our analysis on several drugs most widely used.

Table 1: Description of variables.

Variables	Description
Outcomes	
HbA1c < 6.5%	1 if HbA1c < 6.5% at the last follow-up; 0 otherwise
Inci. of hypoglycemia	Incidence of reported hypoglycemia in one year (spanning the period of all four follow-up surveys)
EQ-5D HRQoL	HRQoL measured through EQ-5D
Inpatient cost	Inpatient cost in one year, including all costs related to tests, medication, and treatment in hospitals (unit: 1000 yuan)
Outpatient cost	Outpatient cost in one year, including all costs related to tests, medication, and treatment in clinics (unit: 1000 yuan)
OTC drug cost	OTC drug cost in one year (unit: 1000 yuan)
Total cost	Inpatient cost + outpatient cost + OTC drug cost (unit: 1000 yuan)
Treatments	
Metformin	Use of metformin alone
Xiaoke Pill	Use of Xiaoke Pill alone
TCMs	Use of other TCMs (with no chemical substance, other than Xiaoke Pill) alone
Gliclazide	Use of gliclazide alone
Acarbose	Use of acarbose alone
Xiaoke Pill+	Use of Xiaoke Pill in combination with other agents
Glibenclamide	Use of glibenclamide alone
Others	All other medication therapies
Control variables	
Age	Age categories: 1, younger than 50 (reference group); 2, aged between 50 and 60; 3, aged between 60 and 70; 4, older than 70
Gender	0, female; 1, male
Education	Education levels: 1, primary or below (reference group); 2, lower secondary; 3, upper secondary; 4, tertiary or above
City of residence	1, Beijing (reference group); 2, Shenyang; 3, Chengdu; 4, Nanjing; 5, Guangzhou
Income	Monthly income: 1, less than 1000 yuan (reference group); 2, between 1000 and 2000 yuan; 3, more than 2000 yuan
Medical insurance	1, urban resident basic medical insurance (URBMI) (reference group); 2, urban employee basic medical insurance (UEBMI); 3, new rural cooperative medical insurance (NRCM); 4, government insurance
Currently smoking	1 if smoking at the time of baseline survey, 0 otherwise
Currently during	1 if consuming alcohol at the time of baseline survey, 0 otherwise
Any physical exercise	1 if doing any physical exercise at the time of baseline survey, 0 otherwise
Diet control	1 if doing diet control at the time of baseline survey, 0 otherwise
Duration	Duration of diabetes. 1, less than five years (reference group); 2, between 5 and 10 years; 3, more than ten years
Heart disease	1 if heart disease, 0 otherwise
Hypertension	1 if hypertension, 0 otherwise
Dyslipidemia	1 if dyslipidemia, 0 otherwise
Stroke	1 if stroke, 0 otherwise
BMI	1 if BMI ≥ 24 at the time of baseline survey, 0 otherwise
HbA1c	1 if hemoglobin A1c < 6.5% at the time of baseline survey, 0 otherwise
FBS	1 if fasting blood sugar level <7 mmol/L at the time of baseline survey, 0 otherwise
Hypoglycemia	1 if reporting hypoglycemia at the time of baseline survey, 0 otherwise
SBP	1 if systolic blood pressure ≥ 140 at the time of baseline survey, 0 otherwise
DBP	1 if diastolic blood pressure ≥ 90 at the time of baseline survey, 0 otherwise
TC	1 if total cholesterol ≥ 5.2 mmol/L at the time of baseline survey, 0 otherwise
TG	1 if triglycerides ≥ 1.7 mmol/L at the time of baseline survey, 0 otherwise
HRQoL	1 if EQ-5D HRQoL ≥ 0.9 at the time of baseline survey, 0 otherwise

In this study, we focus on intent-to-treat (ITT), defined as therapies chosen by patients at the time of the baseline survey [21]. At baseline, we observed 132 different plans, including monotherapies and combination therapies among patients. We kept the top five monotherapies with the largest proportions of users but also glibenclamide, which constituted one important substance of the Xiaoke Pill. In addition, we included a combination therapy of the Xiaoke Pill. All other therapies were merged into the category of "others" for comparison. Therefore, our ITT treatment variable was defined as a categorical variable representing the eight therapies. The number of patients in each therapy group is summarized in Table 2. Metformin and the Xiaoke Pill accounted for 10.67% and 12.24%, respectively, while another 9.3% of patients used the Xiaoke Pill in combination with other drugs. Complete descriptions of the composition of all therapies in our sample are listed in Table 3.

In addition to the estimates of ITT, we estimated the on-treatment effect by only including patients who adhered to the same therapy without discontinuation, switching, or add-on of drugs throughout the study. Although the on-treatment effect could avoid the "dilution effect" caused by dropping out and switching, it is criticized for reduced sample size and bias due to using only compliers [22].

Table 2: Treatment therapies at baseline.

	Number of subjects	Proportion (%)	Cumulative proportion (%)
Metformin	203	10.67	10.67
Xiaoke Pill	233	12.24	22.91
Other TCMs	137	7.20	30.11
Gliclazide	128	6.73	36.84
Acarbose	110	5.78	42.62
Xiaoke Pill+	177	9.30	51.92
Glibenclamide	12	0.63	52.55
Others	903	47.45	100.00
Total	1903	100.00	

Note: we only kept those who have completed the baseline and all four follow-up surveys as well as two medical checks. Therapies in the category "others" are detailed in Appendix. TCMs refer to TCMs other than the Xiaoke Pill.

Table 3: Other observed plans on drug use.

Therapy	No. of cases	Prop.	Cum. prop.
Gliclazide + metformin	119	13.18	13.18
Metformin + acarbose	67	7.42	20.60
Other than these 15 drugs	57	6.31	26.91
Glipizide + metformin	50	5.54	32.45
Glimepiride + metformin	42	4.65	37.10
Glipizide	42	4.65	41.75
Gliquidone	36	3.99	45.74
Repaglinide	36	3.99	49.72
Gliclazide + acarbose	35	3.88	53.60
Gliclazide + metformin + acarbose	35	3.88	57.48
Repaglinide + metformin	29	3.21	60.69
Gliquidone + acarbose	26	2.88	63.57
Glimepiride	25	2.77	66.33
Glimepiride + acarbose	23	2.55	68.88
Glipizide + acarbose	20	2.21	71.10
Glimepiride + metformin + acarbose	18	1.99	73.09
Repaglinide + acarbose	17	1.88	74.97
Gliquidone + metformin	16	1.77	76.74
Metformin + TCMs	12	1.33	78.07
Acarbose + TCMs	9	1.00	79.07
Gliclazide + metformin + rosiglitazone	9	1.00	80.07
Rosiglitazone	9	1.00	81.06
Glibenclamide + metformin	8	0.89	81.95
Glipizide + metformin + acarbose	8	0.89	82.83
Nateglinide	8	0.89	83.72
Gliquidone + metformin + acarbose	7	0.78	84.50
Repaglinide + metformin + acarbose	7	0.78	85.27
Gliclazide + TCMs	6	0.66	85.94
Glimepiride + rosiglitazone	6	0.66	86.60
Glipizide + metformin + TCMs	6	0.66	87.26
Metformin + rosiglitazone	6	0.66	87.93
Pioglitazone	5	0.55	88.48
Gliclazide + metformin + TCMs	4	0.44	88.93
Metformin + pioglitazone	4	0.44	89.37
Phenformin	4	0.44	89.81
Gliclazide + rosiglitazone	3	0.33	90.14
Glimepiride + metformin + pioglitazone	3	0.33	90.48
Glipizide + gliclazide	3	0.33	90.81
Glipizide + gliclazide + metformin	3	0.33	91.14
Glipizide + TCMs	3	0.33	91.47
Metformin + rosiglitazone + acarbose	3	0.33	91.81
Repaglinide + rosiglitazone	3	0.33	92.14
Rosiglitazone + acarbose	3	0.33	92.47

Table 3: Continued.

Therapy	No. of cases	Prop.	Cum. prop.
Gliclazide + metformin + pioglitazone	2	0.22	92.69
Gliclazide + repaglinide	2	0.22	92.91
Glimepiride + metformin + pioglitazone + acarbose	2	0.22	93.13
Glimepiride + metformin + rosiglitazone	2	0.22	93.36
Glimepiride + pioglitazone	2	0.22	93.58
Glipizide + rosiglitazone	2	0.22	93.80
Gliquidone + acarbose + TCMs	2	0.22	94.02
Gliquidone + gliclazide	2	0.22	94.24
Gliquidone + rosiglitazone	2	0.22	94.46
Nateglinide + metformin	2	0.22	94.68
Pioglitazone + acarbose	2	0.22	94.91
Repaglinide + metformin + TCMs	2	0.22	95.13
Glibenclamide + acarbose	1	0.11	95.24
Glibenclamide + voglibose	1	0.11	95.35
Gliclazide + acarbose + TCMs	1	0.11	95.46
Gliclazide + glimepiride	1	0.11	95.57
Gliclazide + glimepiride + metformin	1	0.11	95.68
Gliclazide + metformin + rosiglitazone + acarbose	1	0.11	95.79
Gliclazide + metformin + rosiglitazone + acarbose + TCMs	1	0.11	95.90
Gliclazide + pioglitazone	1	0.11	96.01
Gliclazide + pioglitazone + acarbose	1	0.11	96.12
Gliclazide + rosiglitazone + acarbose	1	0.11	96.23
Gliclazide + rosiglitazone + voglibose	1	0.11	96.35
Glimepiride + metformin + TCMs	1	0.11	96.46
Glimepiride + nateglinide	1	0.11	96.57
Glimepiride + repaglinide	1	0.11	96.68
Glimepiride + rosiglitazone + acarbose	1	0.11	96.79
Glipizide + acarbose + TCMs	1	0.11	96.90
Glipizide + gliclazide + acarbose	1	0.11	97.01
Glipizide + glimepiride + acarbose	1	0.11	97.12
Glipizide + glimepiride + metformin + acarbose	1	0.11	97.23
Glipizide + gliquidone + metformin	1	0.11	97.34
Glipizide + gliquidone + metformin + rosiglitazone	1	0.11	97.45
Glipizide + metformin + pioglitazone	1	0.11	97.56
Glipizide + metformin + pioglitazone + acarbose	1	0.11	97.67
Glipizide + metformin + rosiglitazone	1	0.11	97.79
Glipizide + metformin + rosiglitazone + acarbose	1	0.11	97.90
Glipizide + pioglitazone	1	0.11	98.01
Glipizide + rosiglitazone + acarbose	1	0.11	98.12
Gliquidone + gliclazide + metformin	1	0.11	98.23
Gliquidone + metformin + acarbose + TCMs	1	0.11	98.34
Gliquidone + metformin + rosiglitazone	1	0.11	98.45
Gliquidone + metformin + TCMs	1	0.11	98.56
Gliquidone + nateglinide	1	0.11	98.67
Gliquidone + TCMs	1	0.11	98.78
Metformin + acarbose + TCMs	1	0.11	98.89
Metformin + phenformin + rosiglitazone	1	0.11	99.00
Metformin + pioglitazone + acarbose	1	0.11	99.11
Nateglinide + acarbose	1	0.11	99.22
Phenformin + acarbose	1	0.11	99.34
Repaglinide + acarbose + TCMs	1	0.11	99.45
Repaglinide + metformin + pioglitazone	1	0.11	99.56
Repaglinide + metformin + rosiglitazone	1	0.11	99.67
Repaglinide + pioglitazone	1	0.11	99.78
Repaglinide + TCMs	1	0.11	99.89
Rosiglitazone + TCMs	1	0.11	100.00
Total	903	100.00	

Table 4: Baseline characteristics (%).

	Metformin	Xiaoke Pill	Other TCMs	Glimepiride	Acarbose	Xiaoke Pill + others	Glibenclamide	Others	Total	ANOVA: p value
60 > age ≥ 50	25	31	26	20	15	25	17	25	25	0.06
70 >age ≥ 60	31	27	35	40	37	26	33	35	33	0.05
Age ≥ 70	22	20	31	30	34	24	8	28	27	0.03
Male	46	41	45	45	46	41	50	45	44	0.88
Lower secondary education	40	41	39	34	38	34	42	34	36	0.44
Upper secondary education	24	21	28	15	26	20	33	25	24	0.12
Tertiary education	14	16	7	9	17	16	0	13	13	0.07
Shenyang	33	42	74	17	18	10	33	12	23	0.00
Chengdu	24	27	6	16	26	33	25	19	21	0.00
Nanjing	16	8	4	53	12	5	42	24	19	0.00
Guangzhou	11	14	7	10	15	39	0	24	20	0.00
2000 > income ≥ 1000	49	37	53	31	31	28	58	38	38	0.00
Income ≥ 2000	31	33	20	23	51	46	0	39	36	0.00
UEBMI	65	64	69	41	72	63	58	65	64	0.00
NRCM	5	5	3	30	2	9	8	11	10	0.00
Govern. insur.	4	3	2	5	9	6	0	6	5	0.24
Currently smoking	25	21	27	16	19	18	33	19	20	0.18
Currently drinking	29	27	18	27	28	20	25	25	25	0.25
Any physical exercise	81	84	79	68	80	81	58	79	79	0.02
Diet control	89	85	84	88	93	92	92	91	90	0.03
10 > duration ≥ 5	19	20	24	35	19	29	42	28	26	0.00
Duration ≥ 10	17	17	34	16	15	24	17	29	24	0.00
Heart disease	18	21	40	20	25	16	17	19	21	0.00
Hypertension	53	35	55	48	64	46	8	51	49	0.00
Dyslipidemia	27	16	26	20	26	11	8	20	20	0.00
Stroke	11	5	16	13	10	5	0	7	8	0.00
Baseline BMI	67	54	59	70	55	47	42	58	58	0.00
Baseline HbA1c	42	53	29	37	51	46	33	33	39	0.00
Baseline FBS	47	61	31	42	59	54	33	39	45	0.00
Baseline hypoglycemia	12	9	9	10	8	9	8	13	11	0.35
Baseline SBP	44	33	44	54	39	38	50	39	40	0.01
Baseline DBP	33	27	28	37	18	27	42	23	26	0.00
Baseline TC	42	41	52	22	28	40	33	40	39	0.00
Baseline TG	51	39	46	39	33	38	50	41	41	0.04
Baseline HRQoL	47	52	46	45	55	53	50	46	48	0.46
Observations	203	233	137	128	110	177	12	903	1903	1903

Note: the last column includes significant levels derived from ANOVA tests regarding variable difference between different therapies.

Analysis of the on-treatment effect was included in the sensitivity analyses.

2.2.3. Covariates. To reduce confounding bias, we collected and controlled a rich set of individual baseline characteristics of survey patients, which was crucial to real-world analysis to recover the treatment effect. We controlled factors such as demographics including age and sex; socioeconomic factors including education, household income, type of medical insurance, and city of residence; diabetes-related morbidities including heart disease, hypertension, dyslipidemia, and stroke; duration of diabetes; behavior factors including alcoholic use, smoking, physical exercise, and diet control; hypoglycemia as the primary adverse effect; anthropometric and physiological indicators including body mass index (BMI), fasting blood sugar level (FBS), HbA1c, systolic blood pressure (SBP), diastolic blood pressure (DBP), total cholesterol (TC), triglycerides (TG), and HRQoL measured as EQ-5D scores. All covariates were measured at the time of the baseline survey. BMI, FBS, HbA1c, TC, and TG were coded as dichotomous variables with clinically relevant cutoffs [17, 23, 24]. The descriptive statistics of covariates by therapies are shown in Table 4 with the last column including significant levels derived from ANOVA tests regarding variance among different therapies. Most characteristics were imbalanced among different therapies at conventionally significant levels.

2.3. Statistical Methods. Similar to other observational studies, we imposed conditional independence (CI) to identify treatment effects among different therapies [25]. The CI assumption says that, after conditioning on covariates, the treatment variable is independent of the outcome variable. The CI assumption is justified by the rich set of covariates we have controlled for. In addition to this crucial assumption, we have some other model-specific assumptions, which we illustrate in the following.

2.3.1. Multivariate Linear Regression. In our primary analysis, we used multivariate linear regression to estimate the treatment effects of drugs. The multivariate linear regression has the advantage of establishing meaningful inference when some treatment arms have very few observations. It is helpful for our study since one treatment arm in our study, glibenclamide, has few observations, precluding us from implementing data-driven statistical models. The disadvantage of multivariate linear regression is that it relies on the correct specification of functional forms. We addressed this potential problem in the sensitivity analysis, in which the propensity score-based method and machine learning methods were used for comparison.

2.3.2. Inverse Probability Weighting. As an alternative to multivariate regression, the inverse treatment assignment as weights is widely used to estimate treatment effects with multiple treatment arms [26–28]. Note that there are some other popular propensity score-based methods such as matching, stratification, and imputation, which, however, are hard to be implemented on studies with many treatment arms like ours. Inverse probability weighting (IPW) reduces confounding bias by reweighting treatment arms to mimic a random assignment, in which the weights are typically calculated as the functions of propensity score defined as the probability of receiving treatment conditional on covariates [29]. The IPW is less susceptible to functional misspecification; however, it requires more data than regression models. In this study, we used multinomial logistic regression to obtain the propensity score of each treatment arm.

2.3.3. A Machine Learning Algorithm: Double Selection Lasso on High-Dimensional Control Variables. Including a large set of covariates can help minimize confounding bias, but it has the cost of the reduced efficiency of estimation, as it inflates both the signal and noise. The least absolute shrinkage and selection operator (lasso) [30] and its variations such as adaptive lasso [31] have been widely used to select covariates in high-dimensional models in the context of prediction. However, designed for prediction, not for causal inference, lasso and adaptive lasso are likely to produce an unreliable estimate for the treatment effect [32], which is the central goal of our study. Recently, some lasso-like estimators were proposed to make causal inference in a high-dimensional model [33–35]. In this study, we used a double selection lasso estimator to estimate treatment effects [33, 34]. First, we created a pool of potential covariates, including the variables listed in Table 1 and their interaction terms. Note that, technically, we also included squared terms of these variables but they were identical to the original variables which were defined as dummies. After dropping the variables with collinearity, we were left with 69 covariates. We then used the adaptive lasso method to select covariates for the outcome and treatments. Finally, we operated multivariate regressions using the union of selected covariates for the outcome and treatments as control variables. The detailed algorithm is displayed in Appendix.

3. Results

3.1. Unadjusted Outcomes on Effects and Costs. Estimates of "raw" outcomes that are not adjusted by covariates are calculated as subgroup means (Figures 2 and 3). Results of pairwise tests among different therapies are included in Table 5, where the estimates sharing a letter in the group label are not significantly different at the 5% level.

In terms of glycemic control, the use of the Xiaoke Pill alone and in combination was among the most effective therapies, with 50% and 54% of patients reaching the control target of HbA1c level <6.5%, respectively. At the conventional statistical level, the effects were significantly different for metformin (with a control rate of 33%). On the other hand, TCMs other than Xiaoke Pill had the lowest control rate, with only 20% of the patients having attained the control target.

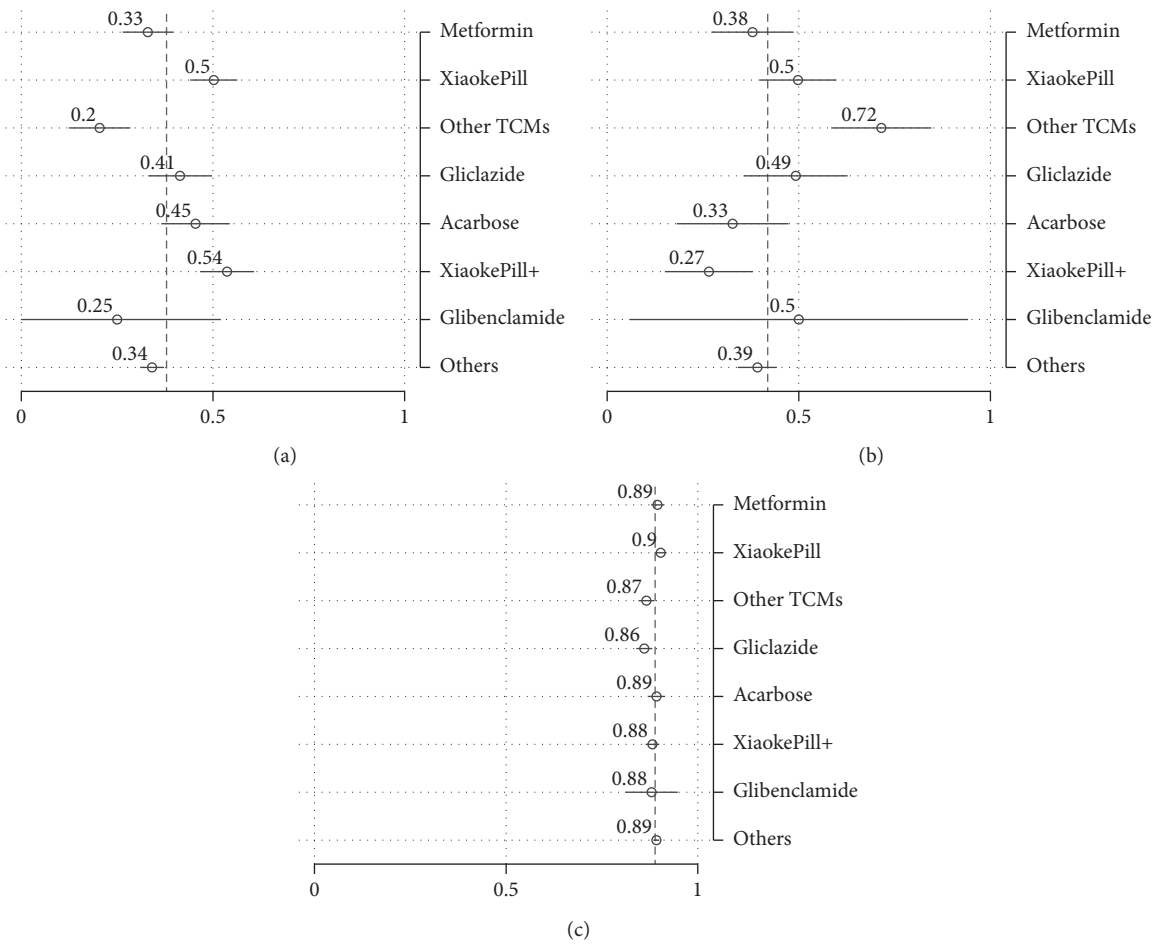

Figure 2: Unadjusted outcomes: efficacy, AE, and HRQoL. Note: point estimates of subgroup means and their 95% confidence intervals are drawn as circles and spikes. Dashed lines represent estimates of population means. Xiaoke Pill + refers to the use of Xiaoke Pill in combination with other antidiabetic drugs. (a) HbA1c < 6.5%. (b) Hypoglycemia. (c) EQ-5D.

In terms of AE measured as the incidence of hypoglycemia, patients using the Xiaoke Pill in combination with other drugs experienced the least number of adverse events, with the incidence of 0.27 times in one year on average, while TCMs other than Xiaoke Pill had the highest reported occurrence of low-blood-sugar events, 0.72 times per year. No significant difference was found among other therapies, including the use of the Xiaoke Pill alone or metformin alone. The HRQoL difference among different therapies was relatively marginal although the Xiaoke Pill and metformin show statistically significant higher uses.

Regarding the total cost, defined as the sum of costs of inpatient and outpatient care, and OTC drugs, the Xiaoke Pill and gliclazide, which cost participants 4,350 (around $670) and 5,150 RMB per year on average, are among the least costly therapies (significantly lower than other therapies at the 5% significance level). Note that even with the lowest point estimate of the cost, the cost of glibenclamide is not statistically lower than other plans in our analysis. The most expensive therapy is acarbose which users, on average, need to spend 11,370 RMB in one year.

3.2. Adjusted Outcomes on Effects and Costs: Intent-to-Treat Treatment Effect. Table 6 provides a point estimate of treatment effects of different therapies with covariates adjusted using multivariate linear regressions. The use of the Xiaoke Pill alone and its combination with other drugs revealed superior effects, with control rates of 12% and 10% higher than those of the reference group of metformin, respectively, and the differences are significant at conventional levels. No statistically significant differences are found among drugs in terms of incidence of hypoglycemia, and the Xiaoke Pill in combination with other drugs shows slightly lower HRQoL than metformin. Regarding costs, compared with metformin, the Xiaoke Pill has significantly lower inpatient costs, acarbose displays higher outpatient costs, and TCMs and acarbose also show higher OTC drug costs. When considering the total cost, the cost reduction of the Xiaoke Pill against metformin is large and statistically significant.

To better understand the size of estimated treatment effects and make comparisons among all therapies rather than just contrasting one therapy with the reference drug, which is, in our case, metformin, we have calculated, in

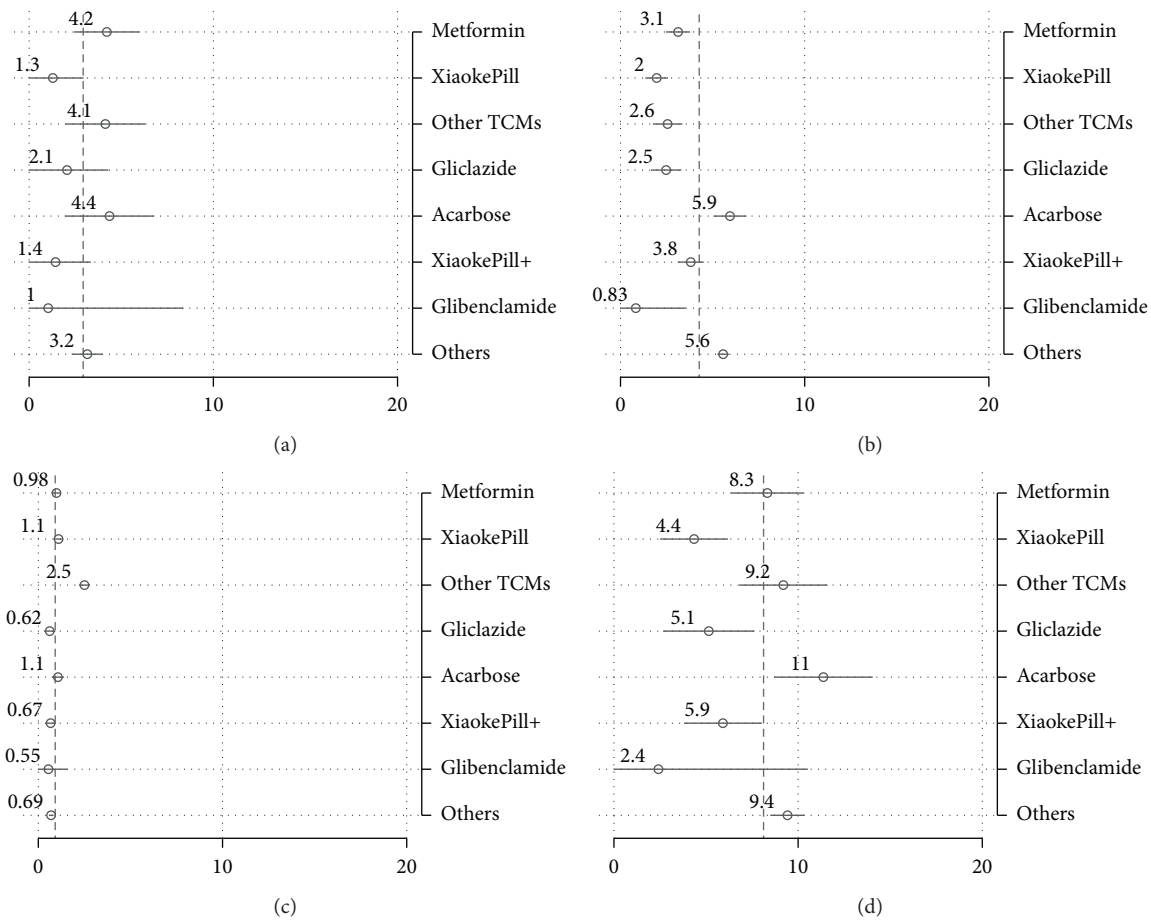

Figure 3: Unadjusted outcomes: costs. Note: point estimates of subgroup means and their 95% confidence intervals are drawn as circles and spikes. Dashed lines represent estimates of population means. Xiaoke Pill + refers to the use of Xiaoke Pill in combination with other antidiabetic drugs. (a) Inpatient cost. (b) Outpatient cost. (c) OTC drug cost. (d) Total cost.

Table 5: Unadjusted outcomes.

	HbA1c < 6.5%	Hypoglycemia	Endpoint HRQoL	Inpatient cost	Outpatient cost	OTC drug cost	Total cost
Metformin	0.33^{b}	0.38^{ab}	0.89^{c}	4.22^{c}	3.13^{bc}	0.98^{ab}	8.33^{bcd}
	(0.03)	(0.05)	(0.01)	(0.91)	(0.34)	(0.13)	(1.01)
Xiaoke Pill	0.50^{cd}	0.50^{b}	0.90^{c}	1.29^{a}	1.96^{a}	1.10^{b}	4.35^{a}
	(0.03)	(0.05)	(0.01)	(0.85)	(0.31)	(0.12)	(0.94)
Other TCMs	0.20^{a}	0.72^{c}	0.87^{ab}	4.14^{bc}	2.56^{ab}	2.50	9.20^{cd}
	(0.04)	(0.07)	(0.01)	(1.11)	(0.41)	(0.15)	(1.22)
Gliclazide	0.41^{bc}	0.49^{b}	0.86^{a}	2.06^{abc}	2.48^{ab}	0.62^{a}	5.15^{a}
	(0.04)	(0.07)	(0.01)	(1.15)	(0.42)	(0.16)	(1.27)
Acarbose	0.45^{cd}	0.33^{ab}	0.89^{bc}	4.36^{bc}	5.94^{d}	1.07^{ab}	11.37^{d}
	(0.05)	(0.07)	(0.01)	(1.24)	(0.46)	(0.17)	(1.37)
Xiaoke Pill+	0.54^{d}	0.27^{a}	0.88^{abc}	1.43^{ab}	3.82^{c}	0.67^{a}	5.92^{ab}
	(0.04)	(0.06)	(0.01)	(0.98)	(0.36)	(0.14)	(1.08)
Glibenclamide	0.25^{abc}	0.50^{abc}	0.88^{abc}	1.04^{abc}	0.83^{ab}	0.55^{ab}	2.42^{abc}
	(0.14)	(0.23)	(0.03)	(3.74)	(1.38)	(0.52)	(4.14)
Others	0.34^{b}	0.39^{b}	0.89^{c}	3.16^{abc}	5.57^{d}	0.69^{a}	9.42^{cd}
	(0.02)	(0.03)	(0.00)	(0.43)	(0.16)	(0.06)	(0.48)
Observations	1903	1903	1903	1903	1903	1903	1903

Note: inpatient cost, outpatient cost, medication cost, and total cost are measured with the unit of 1000 RMB. Estimates sharing a letter in the group label are not significantly different at the 5% level.

Table 6: Adjusted outcomes: point estimates.

	HbA1c < 6.5%	Inci. of hypoglycemia	EQ-5D HRQoL	Inpatient cost	Outpatient cost	OTC drug cost	Total cost
Xiaoke Pill	0.12***	0.07	0.00	−2.66**	−0.52	−0.02	−3.20**
	(0.04)	(0.07)	(0.01)	(1.27)	(0.39)	(0.16)	(1.37)
Other TCMs	0.03	0.13	−0.00	−1.26	0.45	0.70***	−0.12
	(0.05)	(0.09)	(0.01)	(1.49)	(0.46)	(0.19)	(1.62)
Gliclazide	0.08	0.08	−0.02	−2.34	0.40	−0.10	−2.03
	(0.05)	(0.09)	(0.01)	(1.52)	(0.47)	(0.19)	(1.65)
Acarbose	0.07	0.05	−0.01	0.16	1.28***	0.34*	1.78
	(0.05)	(0.09)	(0.01)	(1.56)	(0.48)	(0.20)	(1.69)
Xiaoke Pill+	0.10**	0.01	−0.02*	−2.29*	−0.03	0.05	−2.27
	(0.05)	(0.08)	(0.01)	(1.38)	(0.43)	(0.18)	(1.50)
Glibenclamide	−0.05	0.08	0.00	−3.75	−0.17	−0.50	−4.42
	(0.13)	(0.22)	(0.03)	(3.88)	(1.20)	(0.49)	(4.20)
Others	0.02	0.09	−0.00	−1.15	1.65***	0.03	0.53
	(0.03)	(0.06)	(0.01)	(1.04)	(0.32)	(0.13)	(1.13)
60 > age ≥ 50	−0.05	0.01	0.00	0.41	1.28***	−0.02	1.67
	(0.03)	(0.06)	(0.01)	(1.02)	(0.31)	(0.13)	(1.10)
70 > age ≥ 60	−0.11***	−0.00	−0.01	2.18**	1.03***	0.14	3.36***
	(0.03)	(0.06)	(0.01)	(1.03)	(0.32)	(0.13)	(1.12)
Age ≥ 70	−0.10***	−0.03	−0.04***	2.71**	1.19***	0.19	4.10***
	(0.04)	(0.07)	(0.01)	(1.14)	(0.35)	(0.14)	(1.23)
Male	−0.00	−0.03	−0.00	0.64	−0.03	0.11	0.72
	(0.02)	(0.04)	(0.01)	(0.75)	(0.23)	(0.10)	(0.81)
Lower secondary education	0.01	−0.09*	0.00	0.04	0.26	0.16	0.45
	(0.03)	(0.05)	(0.01)	(0.83)	(0.25)	(0.11)	(0.90)
Upper secondary education	−0.02	−0.03	0.00	0.53	0.80***	0.56***	1.89*
	(0.03)	(0.05)	(0.01)	(0.94)	(0.29)	(0.12)	(1.01)
Tertiary education	0.01	−0.01	0.01	−0.11	0.46	0.34**	0.69
	(0.04)	(0.07)	(0.01)	(1.16)	(0.36)	(0.15)	(1.26)
Shenyang	−0.04	0.56***	−0.02*	0.58	−6.94***	1.93***	−4.43***
	(0.04)	(0.06)	(0.01)	(1.07)	(0.33)	(0.14)	(1.16)
Chengdu	0.24***	0.01	0.01	0.08	−3.14***	0.78***	−2.28*
	(0.04)	(0.06)	(0.01)	(1.09)	(0.34)	(0.14)	(1.18)
Nanjing	0.11***	0.21***	−0.00	0.11	−5.72***	0.39***	−5.22***
	(0.04)	(0.07)	(0.01)	(1.15)	(0.35)	(0.15)	(1.25)
Guangzhou	0.19***	0.05	−0.00	0.07	−4.19***	0.42***	−3.71***
	(0.03)	(0.06)	(0.01)	(1.05)	(0.32)	(0.13)	(1.14)
2000 > income ≥ 1000	−0.03	−0.04	0.01	−0.11	0.62**	0.01	0.52
	(0.03)	(0.05)	(0.01)	(0.89)	(0.27)	(0.11)	(0.97)
Income ≥ 2000	0.01	−0.04	0.02***	−0.26	1.09***	−0.09	0.75
	(0.03)	(0.06)	(0.01)	(1.01)	(0.31)	(0.13)	(1.09)
UEBMI	0.00	−0.03	0.00	0.58	0.13	−0.10	0.62
	(0.03)	(0.05)	(0.01)	(0.80)	(0.25)	(0.10)	(0.87)
NRCM	0.04	0.13*	0.00	−1.37	−0.73*	−0.13	−2.22
	(0.04)	(0.08)	(0.01)	(1.31)	(0.40)	(0.17)	(1.42)
Govern. insur.	0.00	−0.03	0.02	−2.12	−0.00	−0.15	−2.27
	(0.05)	(0.09)	(0.01)	(1.50)	(0.46)	(0.19)	(1.62)
Currently smoking	−0.03	0.02	−0.00	0.53	−0.33	−0.14	0.07
	(0.03)	(0.05)	(0.01)	(0.88)	(0.27)	(0.11)	(0.95)
Currently drinking	−0.03	−0.02	0.02**	−0.28	−0.21	−0.17*	−0.66
	(0.03)	(0.05)	(0.01)	(0.79)	(0.24)	(0.10)	(0.86)
Any physical exercise	−0.03	−0.08*	0.03***	−1.54**	−0.10	0.05	−1.58*
	(0.03)	(0.04)	(0.01)	(0.77)	(0.24)	(0.10)	(0.83)
Diet control	−0.03	0.03	−0.01	−0.64	0.64**	−0.05	−0.05
	(0.03)	(0.06)	(0.01)	(1.00)	(0.31)	(0.13)	(1.09)
Duration ≥ 5	−0.01	0.03	−0.01**	0.06	0.40*	0.09	0.54
	(0.02)	(0.04)	(0.01)	(0.75)	(0.23)	(0.10)	(0.81)
Duration ≥ 10	−0.07***	0.07	−0.01	1.34*	0.44*	0.42***	2.20**
	(0.03)	(0.05)	(0.01)	(0.79)	(0.24)	(0.10)	(0.86)

Table 6: Continued.

	HbA1c < 6.5%	Inci. of hypoglycemia	EQ-5D HRQoL	Inpatient cost	Outpatient cost	OTC drug cost	Total cost
Heart disease	0.07***	0.04	−0.01	0.53	0.87***	0.40***	1.80**
	(0.03)	(0.05)	(0.01)	(0.79)	(0.24)	(0.10)	(0.86)
Hypertension	0.05**	0.04	0.01*	−0.51	0.93***	−0.10	0.31
	(0.02)	(0.04)	(0.01)	(0.68)	(0.21)	(0.09)	(0.74)
Dyslipidemia	−0.02	0.01	0.00	0.07	0.57**	0.28***	0.92
	(0.03)	(0.05)	(0.01)	(0.80)	(0.25)	(0.10)	(0.87)
Stroke	−0.05	−0.04	−0.05***	1.30	0.77**	0.17	2.25*
	(0.04)	(0.07)	(0.01)	(1.13)	(0.35)	(0.14)	(1.22)
Baseline BMI	−0.02	0.01	0.00	−0.47	0.08	0.01	−0.38
	(0.02)	(0.04)	(0.01)	(0.64)	(0.20)	(0.08)	(0.69)
Baseline HbA1c	0.26***	0.03	0.00	−0.16	0.32	−0.01	0.15
	(0.02)	(0.04)	(0.01)	(0.73)	(0.22)	(0.09)	(0.79)
Baseline FBS	0.12***	0.09**	0.00	−0.23	−0.19	0.02	−0.40
	(0.02)	(0.04)	(0.01)	(0.70)	(0.22)	(0.09)	(0.76)
Baseline hypoglycemia	0.03	0.21***	0.00	−0.88	0.09	0.08	−0.72
	(0.03)	(0.05)	(0.01)	(0.95)	(0.29)	(0.12)	(1.02)
Baseline SBP	−0.06***	−0.06	0.01	0.03	−0.24	0.14	−0.07
	(0.02)	(0.04)	(0.01)	(0.74)	(0.23)	(0.09)	(0.81)
Baseline DBP	0.04	0.02	−0.02***	0.53	−0.04	0.06	0.55
	(0.03)	(0.05)	(0.01)	(0.81)	(0.25)	(0.10)	(0.87)
Baseline TC	−0.03	0.02	−0.00	−0.68	−0.10	0.17**	−0.61
	(0.02)	(0.04)	(0.01)	(0.65)	(0.20)	(0.08)	(0.70)
Baseline TG	0.03	−0.01	−0.00	1.06	−0.24	−0.09	0.74
	(0.02)	(0.04)	(0.01)	(0.65)	(0.20)	(0.08)	(0.70)
Baseline HRQoL	−0.02	−0.11***	0.05***	−1.35**	−0.30	−0.05	−1.70**
	(0.02)	(0.04)	(0.01)	(0.62)	(0.19)	(0.08)	(0.67)
Constant	0.24***	0.24*	0.86***	4.45**	4.56***	−0.45	8.57***
	(0.07)	(0.13)	(0.02)	(2.21)	(0.68)	(0.28)	(2.39)
Observations	1903	1903	1903	1903	1903	1903	1903

Note: metformin is the reference group. Significance level: *0.10, **0.05, and ***0.01. Inpatient cost, outpatient cost, medication cost, and total cost are measured with the unit of 1000 RMB.

Table 7: Adjusted outcomes: predictive margins.

	HbA1c < 6.5%	Hypoglycemia	Endpoint HRQoL	Inpatient cost	Outpatient cost	OTC drug cost	Total cost
Metformin	0.33^{a}	0.35^{a}	0.89^{ab}	4.28^{b}	3.42^{ab}	0.84^{ab}	8.55^{bcd}
	(0.03)	(0.05)	(0.01)	(0.93)	(0.29)	(0.12)	(1.00)
Xiaoke Pill	0.45^{b}	0.42^{a}	0.90^{b}	1.63^{a}	2.90^{a}	0.81^{ab}	5.34^{a}
	(0.03)	(0.05)	(0.01)	(0.89)	(0.27)	(0.11)	(0.96)
Other TCMs	0.36^{ab}	0.48^{a}	0.89^{ab}	3.02^{ab}	3.87^{bc}	1.54^{c}	8.43^{bcd}
	(0.04)	(0.07)	(0.01)	(1.19)	(0.37)	(0.15)	(1.29)
Gliclazide	0.41^{ab}	0.43^{a}	0.88^{ab}	1.94^{ab}	3.83^{bc}	0.74^{a}	6.52^{abc}
	(0.04)	(0.07)	(0.01)	(1.20)	(0.37)	(0.15)	(1.30)
Acarbose	0.40^{ab}	0.40^{a}	0.88^{ab}	4.44^{ab}	4.70^{cd}	1.18^{bc}	10.33^{d}
	(0.04)	(0.07)	(0.01)	(1.26)	(0.39)	(0.16)	(1.37)
Xiaoke Pill+	0.43^{b}	0.36^{a}	0.87^{a}	1.99^{ab}	3.40^{ab}	0.89^{ab}	6.28^{ab}
	(0.03)	(0.06)	(0.01)	(1.01)	(0.31)	(0.13)	(1.09)
Glibenclamide	0.28^{ab}	0.42^{a}	0.89^{ab}	0.53^{ab}	3.26^{abcd}	0.34^{ab}	4.13^{abcd}
	(0.12)	(0.22)	(0.03)	(3.77)	(1.16)	(0.48)	(4.09)
Others	0.36^{a}	0.44^{a}	0.89^{b}	3.13^{ab}	5.07^{d}	0.87^{ab}	9.07^{cd}
	(0.01)	(0.03)	(0.00)	(0.45)	(0.14)	(0.06)	(0.48)
Observations	1903	1903	1903	1903	1903	1903	1903

Note: inpatient cost, outpatient cost, medication cost, and total cost are measured with the unit of 1000 RMB. When calculating the predictive margins, covariates including age, sex, education, household income, type of medical insurance, city of residence, diabetes-related morbidities including AMI, hypertension, dyslipidemia, and stroke, duration of diabetes, alcoholic use, smoking, physical exercise, diet control, BMI, blood glucose level, HbA1c, blood pressure, TCH, TG, and EQ-5D score are controlled. Estimates sharing a letter in the group label are not significantly different at the 5% level.

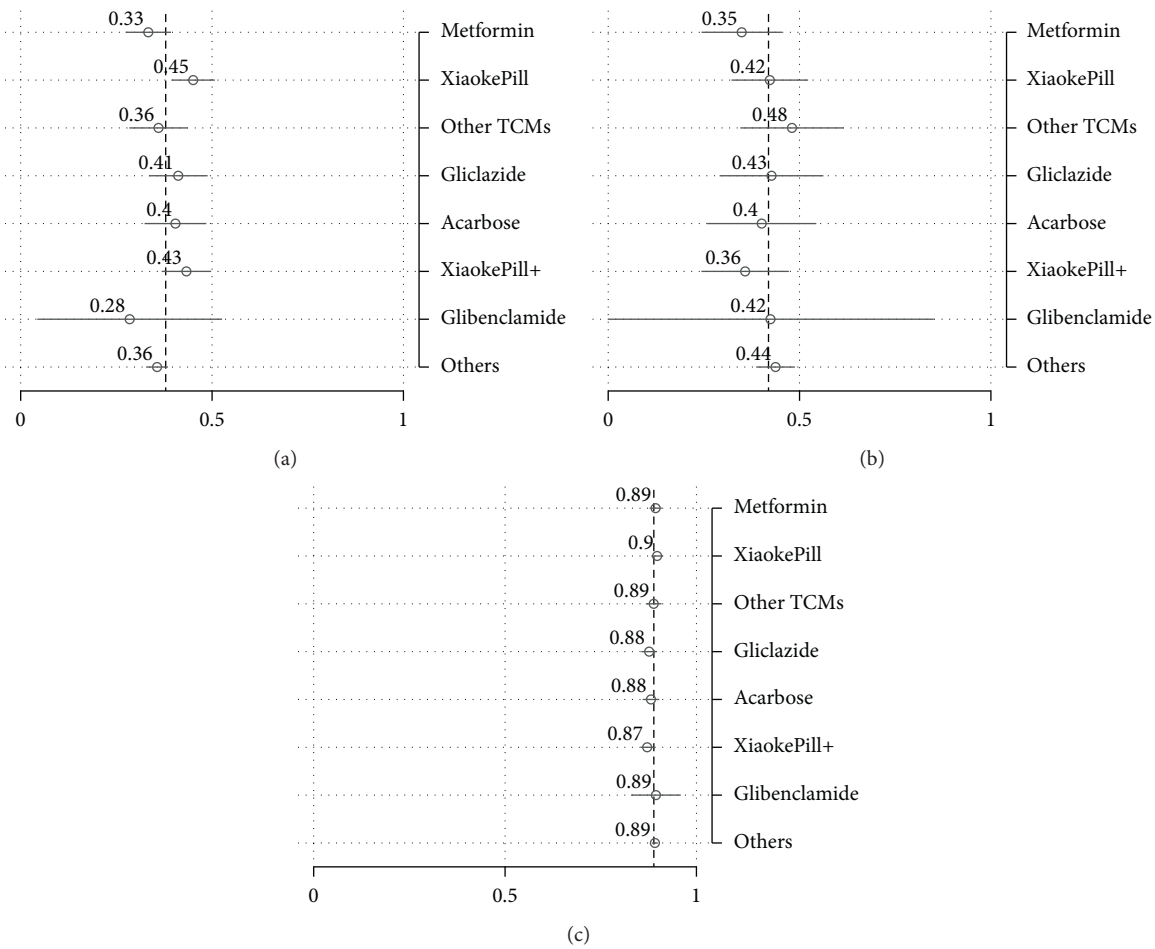

Figure 4: Risk factor-adjusted outcomes: efficacy, AE, and HRQoL. (a) HbA1c < 6.5%. (b) Hypoglycemia. (c) EQ-5D.

addition to the point estimates, the predictive margins. These are defined as predictive outcomes by fixing the treatment variable and averaging over covariates after regression. Note that the predictive margins for each treatment without covariates are just subgroup means. Therefore, predictive margins are comparable with subgroup means in the above analysis. The results of predictive margins are shown in Table 7 and Figures 4 and 5, respectively. In terms of glycemic control, monotherapy and combination therapy using the Xiaoke Pill again display the best control rates, of 45% and 43%, respectively, against 33% of metformin. However, the difference became smaller in comparison with the unadjusted outcomes, as shown in Table 5. The Xiaoke Pill costs a patient 5,340 RMB per year, in sharp contrast with 8,550 RMB for metformin and 10,330 RMB for acarbose. Although being lower than the unadjusted results, the cost difference among different therapies is still remarkable and statistically significant.

3.3. Sensitivity Analysis. Sensitivity analyses using a more conservative definition for treatment samples and more data-driven statistical methods such as inverse probability weighting and machine learning have provided consistent results on the effectiveness and cost of antidiabetic therapies. The detailed estimates are included in Appendix.

4. Discussion

Our study is one of the few studies that explore the cost-effectiveness of oral antidiabetic therapies, including TCM and its compounds, based on real-world evidence.

Our results show that metformin underperforms some other widely used antidiabetic drugs, including gliclazide and Xiaoke Pill, in terms of efficacy and cost. However, it has a lower incidence of adverse effects. This finding is consistent with some other studies. One meta-study found that thiazolidinediones, metformin, sulfonylureas, dipeptidyl peptidase-4 (DPP-4) inhibitors, and sodium-glucose cotransporter 2 inhibitors have similar efficacy [36]. Another study found that rosiglitazone, as compared with metformin, is associated with more extended glycemic durability from a clinical trial [37].

Our study provides some suggestive evidence that the Xiaoke Pill, as a compound formula of glibenclamide and Xiaoke herbal substance, may achieve better glycemic control than glibenclamide. However, the difference is not statistically significant given the small sample size of

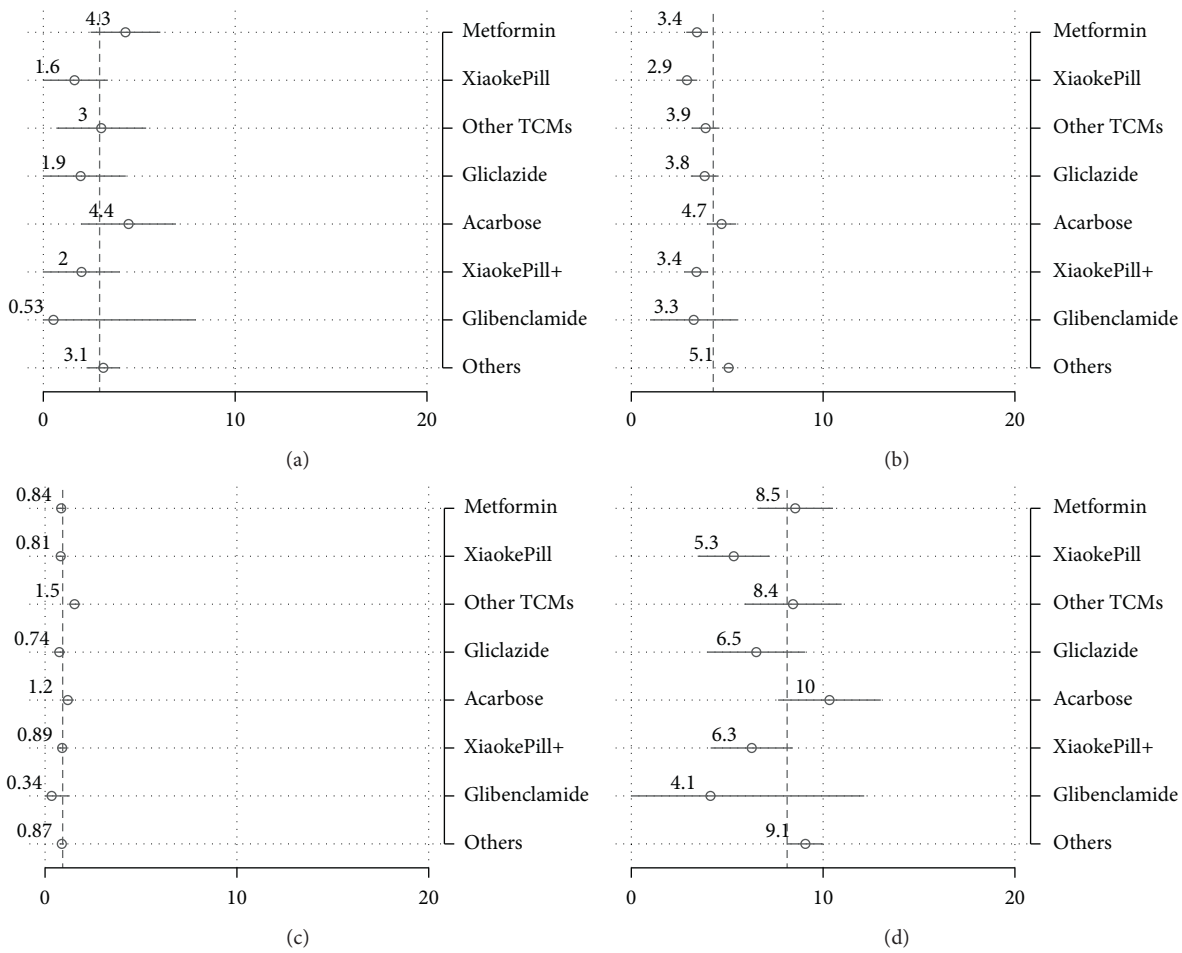

Figure 5: Risk factor-adjusted outcomes: costs. (a) Inpatient cost. (b) Outpatient cost. (c) Drug cost. (d) Total cost.

Table 8: Adjusted outcomes: predictive margins.

	HbA1c < 6.5%	Hypoglycemia	Endpoint HRQoL	Inpatient cost	Outpatient cost	OTC drug cost	Total cost
Metformin	0.25 A (0.07)	0.25 A (0.12)	0.90 B (0.02)	2.73 A (2.09)	3.36 A (0.73)	0.60 BC (0.21)	6.69 A (2.29)
Xiaoke Pill	0.42 B (0.06)	0.37 A (0.10)	0.89 B (0.01)	2.59 A (1.76)	3.80 A (0.62)	0.24 AB (0.18)	6.63 A (1.92)
Other TCMs	0.22 A (0.08)	0.47 A (0.14)	0.88 B (0.02)	1.96 A (2.47)	6.01 B (0.86)	2.05 (0.25)	10.01 A (2.69)
Gliclazide	0.39 AB (0.07)	0.26 A (0.12)	0.90 B (0.02)	0.21 A (2.04)	4.06 AB (0.72)	0.54 ABC (0.21)	4.82 A (2.23)
Acarbose	0.46 B (0.08)	0.24 A (0.14)	0.87 AB (0.02)	11.25 B (2.39)	5.42 AB (0.84)	1.08 C (0.24)	17.75 B (2.61)
Xiaoke Pill+	0.33 AB (0.07)	0.45 A (0.12)	0.82 A (0.02)	1.58 A (2.02)	3.26 A (0.71)	0.66 BC (0.21)	5.49 A (2.21)
Glibenclamide	0.37 AB (0.25)	0.44 A (0.45)	0.90 AB (0.06)	−0.25 AB (7.59)	3.39 AB (2.66)	−0.96 A (0.77)	2.18 AB (8.29)
Others	0.36 AB (0.02)	0.44 A (0.03)	0.89 B (0.00)	2.88 A (0.56)	5.42 B (0.19)	0.64 C (0.06)	8.95 A (0.61)
Observations	878	878	878	878	878	878	878

Note: inpatient cost, outpatient cost, medication cost, and total cost are measured with the unit of 1000 RMB. When calculating the predictive margins, covariates including age, sex, education, household income, type of medical insurance, city of residence, diabetes-related morbidities including AMI, hypertension, dyslipidemia, and stroke, duration of diabetes, alcoholic use, smoking, physical exercise, diet control, BMI, blood glucose level, HbA1c, blood pressure, TCH, TG, and EQ-5D score are controlled. Estimates sharing a letter in the group label are not significantly different at the 5% level.

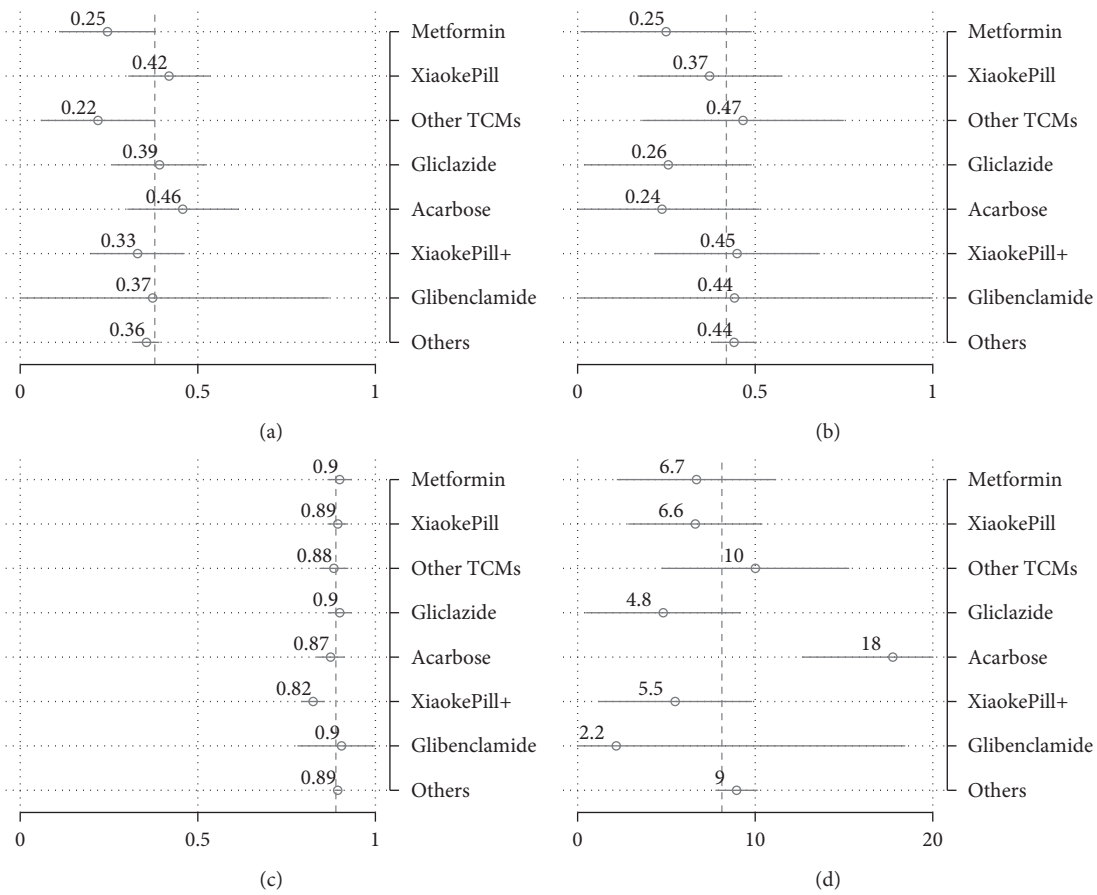

Figure 6: Risk factor-adjusted outcomes: efficacy, AE, HRQoL, and cost.

Table 9: Inverse-probability-weighted outcomes.

	HbA1c < 6.5%	Hypoglycemia	Endpoint HRQoL	Inpatient cost	Outpatient cost	OTC drug cost	Total cost
Metformin	0.36	0.38	0.90	4.09	3.21	0.85	8.15
	(0.04)	(0.05)	(0.01)	(1.02)	(0.25)	(0.09)	(1.16)
Xiaoke Pill	0.39	0.36	0.90	2.45	2.68	0.99	6.12
	(0.04)	(0.05)	(0.01)	(1.31)	(0.25)	(0.15)	(1.34)
Other TCMs	0.38	0.34	0.91	1.31	6.39	1.60	9.30
	(0.08)	(0.09)	(0.01)	(0.42)	(2.23)	(0.55)	(2.25)
Gliclazide	0.42	0.52	0.85	1.87	5.67	0.79	8.32
	(0.08)	(0.13)	(0.02)	(0.54)	(1.38)	(0.24)	(1.18)
Acarbose	0.39	0.43	0.88	4.58	4.73	1.35	10.66
	(0.05)	(0.08)	(0.01)	(1.57)	(0.48)	(0.42)	(1.75)
Xiaoke Pill+	0.39	0.41	0.87	1.26	3.94	1.01	6.21
	(0.05)	(0.10)	(0.02)	(0.40)	(0.42)	(0.27)	(0.70)
Others	0.35	0.43	0.89	3.01	5.04	0.88	8.93
	(0.02)	(0.03)	(0.00)	(0.41)	(0.15)	(0.09)	(0.45)
Observations	1903	1903	1903	1903	1903	1903	1903

Note: inpatient cost, outpatient cost, medication cost, and total cost are measured with the unit of 1000 RMB. Inverse probability weighting needs enough observations in each treatment arm during estimation, and we therefore merge glibenclamide into the category "others." The predictive margins are calculated after multivariate regressions. When calculating the predictive margins, covariates including age, sex, education, household income, type of medical insurance, city of residence, diabetes-related morbidities including AMI, hypertension, dyslipidemia, and stroke, duration of diabetes, alcoholic use, smoking, physical exercise, diet control, BMI, blood glucose level, HbA1c, blood pressure, TCH, TG, and EQ-5D score are controlled.

glibenclamide in our study. Our finding is consistent with a clinical trial [8], which evidenced that the Xiaoke Pill had either a similar or better effect in treating hyperglycemia in diabetic patients than glibenclamide. The benefit of the Xiaoke Pill may be linked to its Xiaoke herbs. It has been reported that the Xiaoke Pill not only exerts its antidiabetic

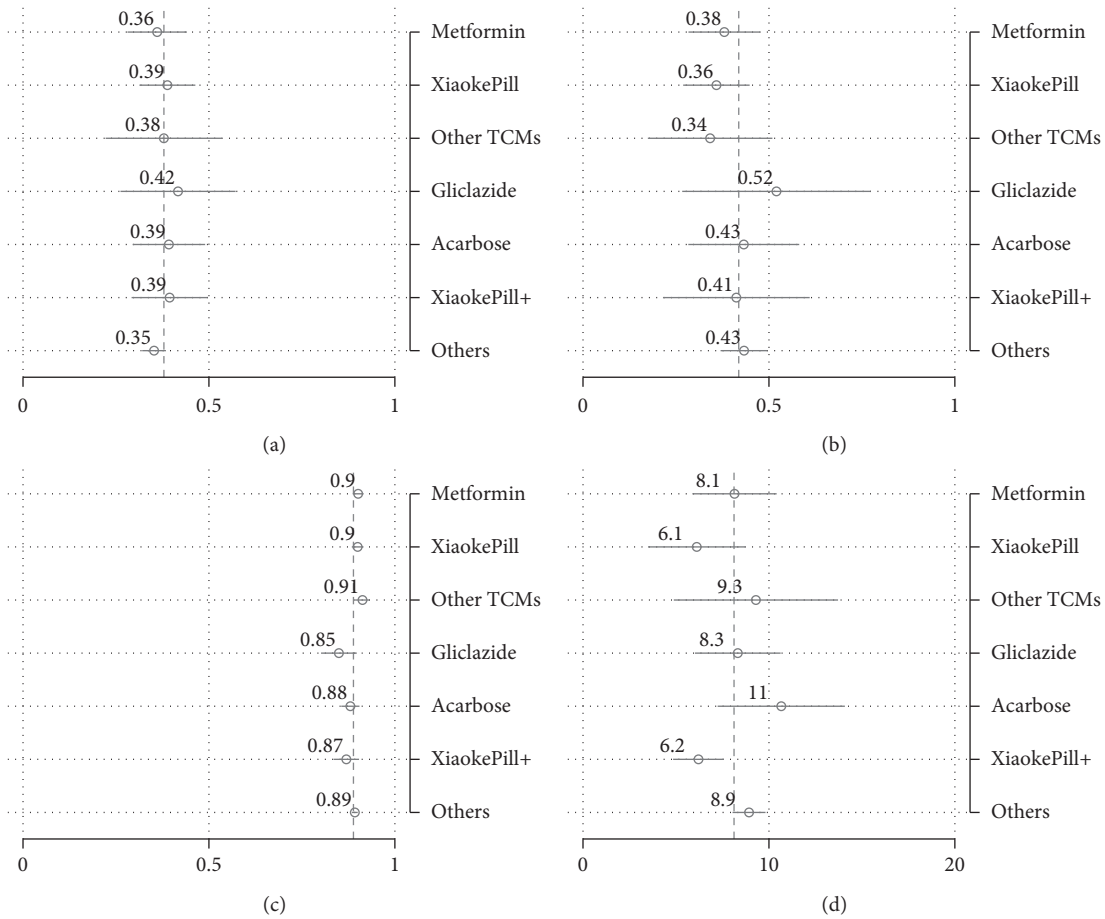

Figure 7: Inverse-probability-weighted outcomes.

Table 10: Baseline characteristics weighted by the inverse propensity score.

	Metformin	Xiaoke Pill	Other TCMs	Glimepiride	Acarbose	Xiaoke Pill + others	Others	ANOVA: + p value
60 > age ≥ 50	0.22	0.23	0.18	0.29	0.20	0.30	0.23	0.83
70 > age ≥ 60	0.33	0.29	0.27	0.19	0.35	0.29	0.34	0.17
Age ≥ 70	0.32	0.35	0.45	0.38	0.29	0.29	0.28	0.44
Male	0.42	0.45	0.50	0.44	0.51	0.44	0.43	0.92
Lower secondary education	0.34	0.30	0.34	0.29	0.41	0.37	0.35	0.75
Upper secondary education	0.24	0.27	0.26	0.40	0.27	0.23	0.23	0.80
Tertiary education	0.11	0.14	0.20	0.08	0.11	0.12	0.14	0.50
Shenyang	0.24	0.24	0.20	0.22	0.24	0.24	0.24	0.98
Chengdu	0.24	0.18	0.13	0.20	0.19	0.19	0.21	0.59
Nanjing	0.19	0.23	0.30	0.14	0.23	0.23	0.19	0.61
Guangzhou	0.18	0.21	0.22	0.13	0.14	0.16	0.20	0.55
2000 > income ≥ 1000	0.43	0.44	0.42	0.47	0.40	0.34	0.39	0.81
Income ≥ 2000	0.31	0.33	0.35	0.32	0.38	0.36	0.36	0.96
UEBMI	0.62	0.65	0.67	0.63	0.70	0.56	0.65	0.78
NRCM	0.11	0.08	0.12	0.09	0.05	0.14	0.10	0.80
Govern. insur.	0.06	0.04	0.03	0.03	0.04	0.04	0.05	0.88
Currently smoking	0.19	0.21	0.18	0.13	0.22	0.24	0.19	0.72
Currently drinking	0.20	0.30	0.29	0.37	0.24	0.31	0.25	0.43
Any physical exercise	0.76	0.81	0.91	0.79	0.82	0.79	0.79	0.01
Diet control	0.89	0.87	0.95	0.81	0.87	0.93	0.90	0.17
10 > duration ≥ 5	0.29	0.31	0.29	0.17	0.22	0.24	0.26	0.35

Table 10: Continued.

	Metformin	Xiaoke Pill	Other TCMs	Glimepiride	Acarbose	Xiaoke Pill + others	Others	ANOVA: + p value
Duration ≥ 10	0.27	0.26	0.13	0.32	0.21	0.35	0.25	0.04
Heart disease	0.23	0.19	0.21	0.34	0.19	0.24	0.20	0.85
Hypertension	0.47	0.54	0.49	0.33	0.60	0.47	0.49	0.14
Dyslipidemia	0.20	0.22	0.17	0.12	0.24	0.21	0.20	0.54
Stroke	0.06	0.08	0.05	0.04	0.06	0.05	0.08	0.58
Baseline BMI	0.57	0.59	0.56	0.43	0.65	0.61	0.57	0.50
Baseline HbA1c	0.37	0.35	0.26	0.39	0.38	0.36	0.40	0.61
Baseline FBS	0.43	0.44	0.53	0.52	0.50	0.41	0.45	0.84
Baseline hypoglycemia	0.13	0.09	0.12	0.08	0.13	0.17	0.11	0.74
Baseline SBP	0.41	0.43	0.48	0.52	0.47	0.41	0.42	0.88
Baseline DBP	0.24	0.33	0.22	0.37	0.28	0.20	0.28	0.36
Baseline TC	0.38	0.44	0.40	0.49	0.32	0.44	0.39	0.63
Baseline TG	0.39	0.47	0.38	0.47	0.43	0.42	0.42	0.90
Baseline HRQoL	0.45	0.49	0.42	0.41	0.47	0.51	0.49	0.92

Note: observations are weighted by inverse propensity scores calculated from multinomial logistic regressions with regressors including demographic factors such as age and sex, socioeconomic factors such as education, household income, type of medical insurance, and city of residence, diabetes-related morbidities such as AMI, hypertension, dyslipidemia, and stroke, duration of diabetes, behavior factors such as alcohol use, smoking, physical exercise, and diet control, anthropometric and physiological indicators such as BMI, blood glucose level, HbA1c, blood pressure, TCH, TG, and HRQoL measured as EQ-5D score. The last column includes significant levels derived from ANOVA tests regarding the variable difference between treatment plans.

Table 11: Algorithm of double selection for variable selection.

(1) Select predictors of the outcome variable using adaptive lasso
(2) For each treatment arm {
Select predictors for treatment variable using adaptive lasso
}
(3) Take the covariates as the union of all predictors selected in steps 1 and 2
(4) Apply multivariate regression to the covariates selected

Table 12: Variable selected for post-LASSO OLS.

	HbA1c < 6.5%	Hypoglycemia	EQ-5D HRQoL	Inpatient cost	Outpatient cost	OTC drug cost	Total cost
60>age ≥ 50					Y		
70>age ≥ 60					Y		
Age ≥ 70			Y		Y		Y
Male							
Lower secondary education							
Upper secondary education					Y	Y	
Tertiary education							
Shenyang	Y	Y	Y	Y	Y	Y	Y
Chengdu	Y	Y	Y	Y	Y	Y	Y
Nanjing	Y	Y	Y	Y	Y	Y	Y
Guangzhou	Y	Y	Y	Y	Y	Y	Y
2000 > income ≥ 1000					Y		
Income ≥ 2000			Y		Y		
UEBMI							
NRCM	Y	Y	Y	Y	Y	Y	Y
Govern. insur.							
Currently smoking							
Currently drinking			Y				
Any physical exercise			Y				
Diet control							
10 > duration ≥ 5							
Duration ≥ 10	Y	Y	Y	Y	Y	Y	Y
Heart disease					Y	Y	
Hypertension	Y	Y	Y	Y	Y	Y	Y
Dyslipidemia							

Table 12: Continued.

	HbA1c < 6.5%	Hypoglycemia	EQ-5D HRQoL	Inpatient cost	Outpatient cost	OTC drug cost	Total cost
Stroke			Y				
Baseline BMI							
Baseline HbA1c	Y	Y	Y	Y	Y	Y	Y
Baseline FBS	Y						
Baseline hypoglycemia							
Baseline SBP	Y						
Baseline DBP			Y				
Baseline TC	Y	Y	Y	Y	Y	Y	Y
Baseline TG							
Baseline HRQoL		Y	Y				
(60 > age ≥ 50) × (B/L HbA1c ctrl)							
(70 > age ≥ 60) × (B/L HbA1c ctrl)	Y						
(Age ≥ 70) × (B/L HbA1c ctrl)	Y	Y	Y	Y	Y	Y	Y
(Male) × (B/L HbA1c ctrl)							
(Lower secondary education) × (B/L HbA1c ctrl)							
(Upper secondary education) × (B/L HbA1c ctrl)	Y	Y	Y	Y	Y	Y	Y
(Tertiary education) × (B/L HbA1c ctrl)							
(Shenyang) × (B/L HbA1c ctrl)	Y						
(Chengdu) × (B/L HbA1c ctrl)					Y		
(Nanjing) × (B/L HbA1c ctrl)							
(Guangzhou) × (B/L HbA1c ctrl)							
(2000 > income ≥ 1000) × (B/L HbA1c ctrl)	Y	Y	Y	Y	Y	Y	Y
(Income ≥ 2000) × (B/L HbA1c ctrl)	Y	Y	Y	Y	Y	Y	Y
(UEBMI) × (B/L HbA1c ctrl)							
(NRCM) × (B/L HbA1c ctrl)							
(Govern. insur.) × (B/L HbA1c ctrl)							
(Currently smoking) × (B/L HbA1c ctrl)							
(Currently drinking) × (B/L HbA1c ctrl)							
(Any physical exercise) × (B/L HbA1c ctrl)							
(Diet control) × (B/L HbA1c ctrl)							
(10 > duration ≥ 5) × (B/L HbA1c ctrl)	Y	Y	Y	Y	Y	Y	Y
(Duration ≥ 10) × (B/L HbA1c ctrl)	Y						
(Heart disease) × (B/L HbA1c ctrl)							
(Hypertension) × (B/L HbA1c ctrl)							
(Dyslipidemia) × (B/L HbA1c ctrl)					Y		
(Stroke) × (B/L HbA1c ctrl)							
(Baseline BMI) × (B/L HbA1c ctrl)							
(Baseline FBS) × (B/L HbA1c ctrl)	Y	Y	Y	Y	Y	Y	Y
(Baseline hypoglycemia) × (B/L HbA1c ctrl)		Y					
(Baseline SBP) × (B/L HbA1c ctrl)							
(Baseline DBP) × (B/L HbA1c ctrl)							
(Baseline TC) × (B/L HbA1c ctrl)							
(Baseline TG) × (B/L HbA1c ctrl)							
(Baseline HRQoL) × (B/L HbA1c ctrl)					Y		

Note: B/L HbA1c ctrl is the abbreviation for baseline HbA1c control rate. The post-lasso linear regression is a two-step procedure where firstly confounding variables are selected using lasso and then they are used as controls in multivariate linear regression. To minimize the risk of overpenalization, variables selected for post-lasso regression are taken as the union of variables selected using both outcome and treatment arms as dependent variables of lasso. The choice of the tuning parameter of lasso is based on empirical BIC.

Table 13: Double selection.

	HbA1c < 6.5%	Hypoglycemia	Endpoint HRQoL	Inpatient cost	Outpatient cost	OTC drug cost	Total cost
Metformin	0.33[a]	0.35[a]	0.89[ab]	4.13[b]	3.46[ab]	0.86[a]	8.34[bc]
	(0.03)	(0.05)	(0.01)	(0.92)	(0.28)	(0.12)	(1.00)
Xiaoke Pill	0.44[b]	0.42[a]	0.90[b]	1.38[a]	2.86[a]	0.81[a]	5.04[a]
	(0.03)	(0.05)	(0.01)	(0.89)	(0.27)	(0.11)	(0.97)
Other TCMs	0.35[ab]	0.48[a]	0.89[ab]	3.34[ab]	3.80[bc]	1.53[b]	8.84[bc]
	(0.04)	(0.07)	(0.01)	(1.19)	(0.36)	(0.15)	(1.29)
Gliclazide	0.41[ab]	0.42[a]	0.87[ab]	2.16[ab]	3.82[bc]	0.80[a]	6.82[abc]
	(0.04)	(0.07)	(0.01)	(1.19)	(0.37)	(0.15)	(1.30)
Acarbose	0.40[ab]	0.39[a]	0.88[ab]	4.37[ab]	4.74[cd]	1.18[ab]	10.24[c]
	(0.04)	(0.07)	(0.01)	(1.26)	(0.39)	(0.16)	(1.37)
Xiaoke Pill+	0.44[b]	0.37[a]	0.87[a]	1.95[ab]	3.38[ab]	0.85[a]	5.95[ab]
	(0.03)	(0.06)	(0.01)	(1.01)	(0.31)	(0.13)	(1.09)
Glibenclamide	0.32[ab]	0.42[a]	0.89[ab]	0.95[ab]	3.26[abcd]	0.34[a]	4.07[abc]
	(0.12)	(0.22)	(0.03)	(3.77)	(1.16)	(0.48)	(4.10)
Others	0.36[ab]	0.44[a]	0.89[ab]	3.16[ab]	5.09[d]	0.87[a]	9.17[c]
	(0.01)	(0.03)	(0.00)	(0.45)	(0.14)	(0.06)	(0.48)
Observations	1903	1903	1903	1903	1903	1903	1903

Note: inpatient cost, outpatient cost, medication cost, and total cost are measured with the unit of 1000 RMB. The predictive margins are calculated after multivariate regressions. When calculating the predictive margins, covariates including age, sex, education, household income, type of medical insurance, city of residence, diabetes-related morbidities including AMI, hypertension, dyslipidemia, and stroke, duration of diabetes, alcoholic use, smoking, physical exercise, diet control, BMI, blood glucose level, HbA1c, blood pressure, TCH, TG, and EQ-5D score are controlled. Estimates sharing a letter in the group label are not significantly different at the 5% level.

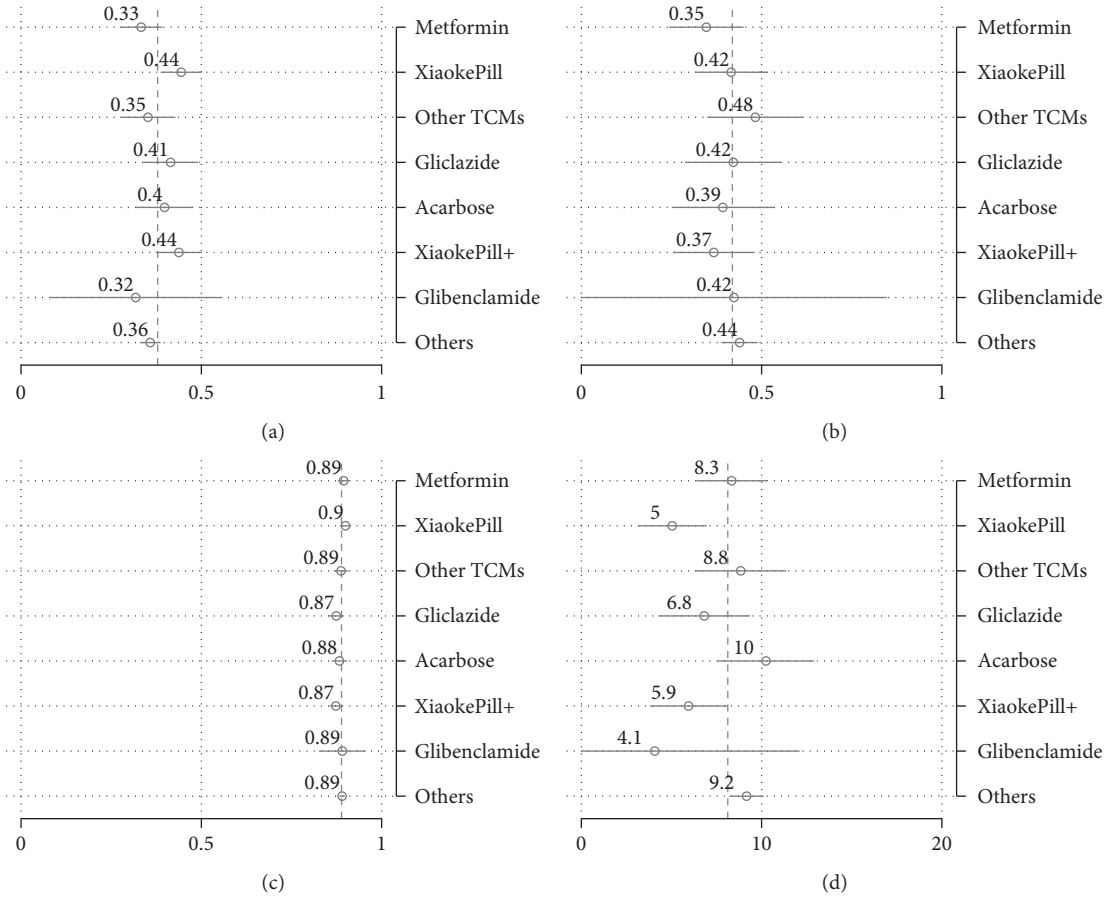

Figure 8: Double selection.

activity by stimulation of insulin secretion mainly mediated by glibenclamide but also enhances the sensitivity of receptors towards insulin mediated by promoting adiponectin secretion in patients with diabetes [38]. Another study shows that several DPP-4 inhibitors are screened in the Xiaoke herbal substance [39].

Regarding add-on effects, our study suggests that the Xiaoke Pill added to metformin results in higher efficacy and lower incidence of AE. Another study also showed that DPP-4 on top of prior metformin monotherapy results in similar HbA1c reductions within 12 months but a significant reduction in hypoglycemia compared with sulfonylurea added to metformin [40].

Our study had several limitations of our study. First, we did not impose any restrictions on initiation, discontinuation, switching, and add-on of drug use, and we, therefore, had many different therapies used as treatments in our sample. Although with a relatively large sample, some treatment arms may not have enough observations to make meaningful statistical inference owing to the lack of power. Second, while we have included many baseline characteristics of patients as control variables, we may still have the omission of variables—a commonly criticized problem for all real-world studies. To address this concern, in sensitivity analyses, we utilize lasso to preselect a set of control variables from an extensive list of variables, including all baseline characteristics and their squared and interaction terms, and our conclusion is essentially the same. Third, our indicators on adverse effects are not complete in the sense that we did not include outcomes of risk of CVD and mortality [41]. However, including these outcomes require a much longer follow-up than is designed in this study.

Finally, it is worth noticing that it has been ten years since the data were collected and this lag may render some change on the cost of drugs and may undermine the validity of our results. Nevertheless, hopefully, readers may still find our study useful and relevant given the scant real-world evidence on the cost-effectiveness of antidiabetic drugs so far. Besides, we are assured by some aspects of our study, making our results less sensitive to this time lag. First, our analysis on efficacy and adverse events is unlikely to be biased by this time lag. Second, inpatient and outpatient costs are mainly driven by the efficacy, side effects, and quality of life change and thus less likely to be affected. In contrast, OTC medication cost, which is more subject to time change, accounts for relatively a small part of the total cost (23%). The last thing we want to emphasize is that even though ten years have passed, there are still minimal cost-effectiveness studies on antidiabetic drugs based on real-world evidence. We hope our study can generate some interest of researchers in this topic as it is very important for policy-making given the large and growing diabetes population in China.

5. Conclusions

Our study suggests that the use of Xiaoke Pill—alone or in combination—is associated with better glycemic control and lower cost than some allopathic medications such as metformin and shows a similar incidence of hypoglycemia.

Appendix

A. Other Observed Therapies

B. On-Treatment Approach Treatment Effect

Table 8 and Figure 6 illustrate treatment effects based on the on-treatment approach, which admits a much smaller sample. No statistically significant difference among therapies in terms of control rate and adverse events was found, except that TCMs showed a lower control rate than the Xiaoke Pill and acarbose. Regarding costs, acarbose shows a higher total cost, which is statistically different from other plans. However, these differences should be read with caution as on-treatment analyses are based on a sample with a smaller size.

C. Inverse Probability Weighting

Table 9 and Figure 7 show inverse-probability-weighted treatment effects, respectively, which are largely comparable with estimates from our multivariate linear regression. Both the control rate and the number of adverse events show no statistically significant difference among therapies. When cost is concerned, monotherapy or combination therapy using the Xiaoke Pill has the lowest costs, 6,200 and 6,200 RMB, respectively, per year. However, these values are not statistically different from the cost of metformin.

As indicated in Table 10, after propensity score weighting, almost all covariates became balanced among different therapies. For example, the baseline glycemic control rate (HbA1c < 6.5%) is similar among therapies and the difference is insignificant after weighting.

D. Double Selection

To address causal treatment effect when making a variable selection, we use double selection [33] in the context of multiple treatment arms. The algorithm is described in Table 11.

In particular, we used lasso to select covariates from a large pool generated by including all control variables and their interactions, as shown in Table 12.

Table 13 and Figure 8 display estimates of multiple regressions after lasso selection. The results are very similar to the estimates from our multivariate regressions. The use of the Xiaoke Pill alone and its combination with other drugs has achieved better control rates, 44% against 33% of metformin. No significant difference is found in terms of hypoglycemia among different therapies, and the HRQoL difference is marginal. On average, the Xiaoke Pill costs each patient 5,040 RMB and metformin costs 8,340 RMB, respectively, per year, and the difference between the two is statistically different.

Data Availability

The data that support the findings of this study are available from the corresponding author upon reasonable request.

Disclosure

The funder had no role in study design, data collection, and analysis, decision to publish, or manuscript preparation.

Conflicts of Interest

The authors declare that have no conflicts of interest.

Authors' Contributions

Study concept and design and acquisition of data were contributed by GL; analysis and interpretation of data and manuscript drafting were carried out by QX and ZH. All authors critically reviewed and revised the manuscript and have read and approved the final version.

Acknowledgments

This work was supported by a grant from Guangzhou Zhongyi Pharmaceutical (funding number: 8203703643).

References

[1] M. Duke, A. Fereira de Moura, S. Gorban de Lapertosa et al., *IDF Diabetes Atlas*, International Diabetes Federation, Brussels, Belgium, 9th edition, 2019.

[2] World Health Organization, *Global Health Estimates 2018: Disease Burden by Cause, Sex, by Country and Region, 2000–2016*, World Health Organization, Geneva, Switzerland, 2018.

[3] Y. Li, D. I. Teng, and X. Shi, "Prevalence of diabetes recorded in mainland China using 2018 diagnostic criteria from the American Diabetes Association: national cross sectional study," *BMJ*, vol. 369, 2020.

[4] J. Tian, D. Jin, Q. Bao et al., "Evidence and potential mechanisms of traditional Chinese medicine for the treatment of type 2 diabetes: a systematic review and meta-analysis," *Diabetes, Obesity and Metabolism*, vol. 21, no. 8, pp. 1801–1816, 2019.

[5] F. Zhang, L.-L. Kong, Y.-Y. Zhang, and S.-C. Li, "Evaluation of impact on health-related quality of life and cost effectiveness of Traditional Chinese Medicine: a systematic review of randomized clinical trials," *Journal of Alternative & Complementary Medicine*, vol. 18, no. 12, pp. 1108–1120, 2012.

[6] G. Y. Yeh, D. M. Eisenberg, T. J. Kaptchuk, and R. S. Phillips, "Systematic review of herbs and dietary supplements for glycemic control in diabetes," *Diabetes Care*, vol. 26, no. 4, pp. 1277–1294, 2003.

[7] Z. Sang, L. Zhou, X. Fan, and R. J. McCrimmon, "Radixz astragali (huangqi) as a treatment for defective hypoglycemia counterregulation in diabetes," *American Journal of Chinese Medicine*, vol. 38, no. 6, pp. 1027–1038, 2010.

[8] L. Ji, X. Tong, H. Wang et al., "Efficacy and safety of traditional Chinese medicine for diabetes: a double-blind, randomised, controlled trial," *PLoS One*, vol. 8, no. 2, Article ID e56703, 2013.

[9] X. Cai, H. Lu, R. Zhao, and L. Shang, "Analysis on pharmaceutical economics of different oral antidiabetic drugs for treating type-2 diabetes mellitus," *China Pharmaceuticals*, vol. 13, 2009.

[10] S. Gu, Z. Tang, L. Shi, M. Sawhney, H. Hu, and H. Dong, "Cost-minimization analysis of metformin and acarbose in treatment of type 2 diabetes," *Value in Health Regional Issues*, vol. 6, pp. 84–88, 2015.

[11] M. Ding and J. Wu, "Economic evaluation of oral antidiabetic drugs in the national essential medicine list," *Evaluation of Drugs*, vol. 11, pp. 10–14, 2013, in Chinese.

[12] L. Gao, F.-L. Zhao, and S.-C. Li, "Cost-utility analysis of liraglutide versus glimepiride as add-on to metformin in type 2 diabetes patients in China," *International Journal of Technology Assessment in Health Care*, vol. 28, no. 4, pp. 436–444, 2012.

[13] R. E. Sherman, S. A. Anderson, G. J. D. Pan et al., "Real-world evidence—what is it and what can it tell us?" *New England Journal of Medicine*, vol. 375, no. 23, pp. 2293–2297, 2016.

[14] L. P. Garrison, P. Erickson, D. Marshall, and C. Daniel Mullins, "Using real-world data for coverage and payment decisions: the ISPOR real-world data Task Force report," *Value in Health*, vol. 10, no. 5, pp. 326–335, 2007.

[15] M. DeKoven, W. C. Lee, J. Bouchard, M. Massoudi, and J. Langer, "Real-world cost-effectiveness: lower cost of treating patients to glycemic goal with liraglutide versus exenatide," *Advances in Therapy*, vol. 31, no. 2, pp. 202–216, 2014.

[16] B. Lawrence, C. Patel, B. Bookhart, M. Pfeifer, Y.-W. Chen, and B. Wu, "A real-world analysis of glycemic control among patients with type 2 diabetes treated with canagliflozin versus dapagliflozin," *Current Medical Research and Opinion*, vol. 34, no. 6, pp. 1143–1152, 2018.

[17] D. M. Nathan, B. Balkau, and E. Bonora, "International expert committee report on the role of the A1C assay in the diagnosis of diabetes," *Diabetes Care*, vol. 32, no. 7, pp. 1327–1334, 2009.

[18] M. van Reenen and M. Oppe, "EQ-5D-3L user guide: basic information on how to use the EQ-5D-3L instrument," *EuroQol Research Foundation*, 2015.

[19] G. G. Liu, H. Wu, M. Li, C. Gao, and N. Luo, "Chinese time trade-off values for EQ-5D health states," *Value in Health*, vol. 17, no. 5, pp. 597–604, 2014.

[20] V. J. Willey, S. Kong, B. Wu et al., "Estimating the real-world cost of diabetes mellitus in the United States during an 8-year period using 2 cost methodologies," *American Health and Drug Benefits*, vol. 11, no. 6, pp. 310–318, 2018.

[21] S. K. Gupta, "Intention-to-treat concept: a review," *Perspectives in Clinical Research*, vol. 2, no. 3, pp. 109–112, 2011.

[22] Y. J. Lee, J. H. Ellenberg, D. G. Hirtz, and K. B. Nelson, "Analysis of clinical trials by treatment actually received: is it really an option?" *Statistics in Medicine*, vol. 10, no. 10, pp. 1595–1605, 1991.

[23] National Cholesterol Education Program (NCEP) Expert Panel on Detection, Evaluation, and Treatment of High Blood Cholesterol in Adults (Adult Treatment Panel III), "Third report of the national cholesterol education program (NCEP) expert panel on detection, evaluation, and treatment of high blood cholesterol in adults (adult treatment panel III) final report," *Circulation*, vol. 106, no. 25, pp. 3143–3421, 2002.

[24] T. Unger, C. Borghi, and F. Charchar, "2020 international society of hypertension global hypertension practice guidelines," *Hypertension*, vol. 75, no. 6, 2020.

[25] D. B. Rubin, "Estimating causal effects of treatments in randomized and nonrandomized studies," *Journal of Educational Psychology*, vol. 66, no. 5, pp. 688–701, 1974.

[26] G. W. Imbens, "The role of the propensity score in estimating dose-response functions," *Biometrika*, vol. 87, no. 3, pp. 706–710, 2000.

[27] P. Feng, X. H. Zhou, Q. M. Zou, M. Y. Fan, and X. S. Li, "Generalized propensity score for estimating the average treatment effect of multiple treatments," *Statistics in Medicine*, vol. 31, 2012.

[28] D. F. Mccaffrey, B. A. Griffin, D. Almirall, M. E. Slaughter, R. Ramchand, and L. F. Burgette, "A tutorial on propensity score estimation for multiple treatments using generalized boosted models," *Statistics in Medicine*, vol. 32, no. 19, pp. 3388–3414, 2013.

[29] P. C. Austin, "An introduction to propensity score methods for reducing the effects of confounding in observational studies," *Multivariate Behavioral Research*, vol. 46, no. 3, pp. 399–424, 2011.

[30] R. Tibshirani, "Regression shrinkage and selection via the lasso," *Journal of the Royal Statistical Society: Series B*, vol. 58, 1996.

[31] H. Zou, "The adaptive lasso and its oracle properties," *Journal of the American Statistical Association*, vol. 101, 2006.

[32] H. Leeb and B. M. Pötscher, "Sparse estimators and the oracle property, or the return of Hodges' estimator," *Journal of Econometrics*, vol. 142, no. 1, pp. 201–211, 2008.

[33] B. Alexandre, V. V. Chernozhukov, and C. Hansen, "High-dimensional methods and inference on structural and treatment effects," *Journal of Economic Perspectives*, vol. 28, 2014.

[34] B. Alexandre, V. Chernozhukov, and W. Ying, "Post-selection inference for generalized linear models with many controls," *Journal of Business & Economic Statistics*, vol. 34, 2016.

[35] V. Chernozhukov, D. Chetverikov, and M. Demirer, "Double/debiased machine learning for treatment and structural parameters," *The Econometrics Journal*, vol. 21, no. 1, 2018.

[36] N. M. Maruthur, E. Tseng, S. Hutfless et al., "Diabetes medications as monotherapy or metformin-based combination therapy for type 2 diabetes: a systematic review and meta-analysis," *Annals of Internal Medicine*, vol. 164, no. 11, pp. 740–751, 2016.

[37] S. E. Kahn, S. M. Haffner, M. A. Heise et al., "Glycemic durability of rosiglitazone, metformin, or glyburide monotherapy," *New England Journal of Medicine*, vol. 355, no. 23, pp. 2427–2443, 2006.

[38] J. Weng, L. Ji, and W. Jia, "Standards of care for type 2 diabetes in China," *Diabetes*, vol. 32, no. 5, 2016.

[39] S. Jiang, X. Wu, Yi Wang, J. Zou, and X. Zhao, "The potential DPP-4 inhibitors from Xiao-Ke-An improve the glucolipid metabolism via the activation of AKT/GSK-3β pathway," *European Journal of Pharmacology*, vol. 882, 2020.

[40] A. K. Gitt, P. Bramlage, and C. Binz, "Prognostic implications of DPP-4 inhibitor vs. sulfonylurea use on top of metformin in a real world setting - results of the 1 year follow-up of the prospective DiaRegis registry," *International Journal of Clinical Practice*, vol. 67, no. 10, pp. 1005–1014, 2013.

[41] C. C. Chan, H. W. Zhang, K. Chan, and Z. X. Lin, "Xiaoke pill and anti-diabetic drugs: a review on clinical evidence of possible herb-drug interactions," *Chinese Journal of Integrative Medicine*, 2016.

Hindawi
Evidence-Based Complementary and Alternative Medicine
Volume 2021, Article ID 9011168, 20 pages
https://doi.org/10.1155/2021/9011168

Research Article

Mineral Composition, Phenolic Content, and *In Vitro* Antidiabetic and Antioxidant Properties of Aqueous and Organic Extracts of *Haloxylon scoparium* Aerial Parts

Nacima Lachkar, Fatima Lamchouri, Khadija Bouabid, Mohamed Boulfia, Souad Senhaji, Mourad Stitou, and Hamid Toufik

Laboratory of Natural Substances, Pharmacology, Environment, Modeling, Health & Quality of Life (SNAMOPEQ), Polydisciplinary Faculty of Taza, Sidi Mohamed Ben Abdellah University of Fez, B.P.: 1223 Taza-Gare, Taza, Morocco

Correspondence should be addressed to Fatima Lamchouri; fatima.lamchouri@usmba.ac.ma

Received 20 May 2021; Accepted 29 September 2021; Published 14 October 2021

Academic Editor: Youhua Xu

Haloxylon scoparium is a plant widely used in traditional medicine for the treatment of diabetes. Hence, this study focuses on the mineralogical and chemical composition and evaluation of the antidiabetic and antioxidant activities of the aerial part of this species. The mineralogical analysis was done by inductively coupled plasma atomic emission spectrometry (ICP-AES). The phytochemical study consisted in the preparation of different extracts from the aerial part by aqueous and organic extraction using Soxhlet and cold maceration. Then, phytochemical screening was performed on the plant powder and on the extracts, which is completed by spectrophotometric quantification of total polyphenols, flavonoids, and catechic tannins. The evaluation of antidiabetic activity was done by three enzymes: *a*-amylase, *a*-glucosidase, and *ß*-galactosidase, and that of antioxidant activity was done by five methods: H_2O_2, DPPH, ABTS, FRAP, and reducing power (RP). Mineralogical analysis revealed the presence of iron, potassium, magnesium, phosphorus, sodium, copper, calcium, strontium, selenium, and zinc. The studied part is rich in alkaloids, flavonoids, catechic tannins, and saponins. The methanolic extract is rich in total polyphenols (161.65 ± 1.52 Ug EAG/mg E), and the ethyl acetate extract has high levels of catechic tannins (23.69 ± 0.6 Ug EC/mg E). In addition, the decoctate expresses a high flavonoid content of 306.59 ± 4.35 Ug EQ/mg E. The *in vitro* evaluation of the antidiabetic activity showed that the decoctate has a higher inhibitory capacity on *a*-glucosidase (IC50 = 181.7 ± 21.15 ug/mL) than acarbose (IC50 = 195 ± 6.12 ug/mL). The results of the antioxidant activity showed that the methanolic extract and the decoctate present a percentage of hydrogen peroxide (H_2O_2) scavenging (20.91 ± 0.27 and 16.21 ± 0.39%) higher than that of ascorbic acid (14.35 ± 0.002%). Positive correlations obtained between the total polyphenol content and the antioxidant activity of the extracts were studied. A positive correlation of *a*-amylase inhibitory activity was also recorded with the antioxidant activity tests.

1. Introduction

Oxidative stress causes adverse effects on human health and can be the cause of several diseases such as cancer, diabetes, and cardiovascular diseases [1]. It is also responsible for respiratory distress syndrome [2].

Antioxidants are able to combat this oxidative stress and prevent free radical damage, and antioxidant-rich micronutrients can help prevent cancer and diabetes [3]. Some minerals are involved in the regulation of insulin secretion and the insulin signalling pathway influencing insulin sensitivity [4]. Antioxidant molecules in plants protect against complications of type 2 diabetes [5] and protect against cardiovascular disease, atherosclerosis, and hypertension [6].

Among the sources of antidiabetic and antioxidant molecules available in nature, there are medicinal plants that are frequently used in traditional herbal medicine, which are

reputed to be effective in treating several diseases. Hence, it is important to expand research on natural antioxidants of plant origin.

Haloxylon scoparium is a medicinal plant that belongs to the Chenopodiaceae family, which has 120 genera and more than 1300 species [7], and is a small, highly branched shrub distributed in North Africa, southeastern Spain, and parts of Iran, Turkey, Iraq, and Syria [8]. Several ethnobotanical and ethnopharmacological surveys have shown that *Haloxylon scoparium* is used in Moroccan traditional medicine against several diseases such as hypertension and diabetes [9,10]. Previous work in our laboratory has shown that *H. scoparium* does not have antifungal activity, and of different organic extracts tested (methanol, chloroform, ethyl acetate, and petroleum ether), only the ethyl acetate extract has moderate antibacterial activity (7–12 mm) against the *Staphylococcus aureus* strain [7].

In the present study, we were interested in the mineralogical investigation by determining the mineral content of the aerial part of *Haloxylon scoparium*, phytochemical investigation by preparing different aqueous (decocted, infused, and macerated) and organic extracts using solvents of decreasing polarity (methanol, chloroform, ethyl acetate, and petroleum ether), the characterisation of the composition of secondary metabolites by carrying out a phytochemical screening on both the powder and the different aqueous and organic extracts prepared, and finally the quantification of phenolic compounds contained in the aerial part of *Haloxylon scoparium*. The biological and pharmacological study consisted of an *in vitro* evaluation of the antidiabetic activity of the prepared aqueous and organic extracts by the three enzyme inhibition tests of *a*-amylase, *a*-glucosidase, and *ß*-galactosidase, and that of the antioxidant capacity using five tests: hydrogen peroxide (H_2O_2) scavenging test; DPPH (2,2-diphenyl-1-picrylhydrazyl) free radical scavenging test; ABTS (2,2-azinobis (3-ethyl-benzothiazoline-6-sulphonate) or TEAC (Trolox equivalent antioxidant capacity) test; iron reduction antioxidant power (FRAP) test, and the reducing power (RP) test. To investigate the correlations between the chemical composition of the different extracts and the antioxidant and antidiabetic activities, we used principal component analysis (PCA).

2. Materials and Methods

2.1. Plant Material. The plant material consists of the aerial part of *Haloxylon scoparium* collected in July 2019 near the region of Taddart located 42.1 km from the city of Taza (geographical coordinates: N 34°12.530′, W 003°32.917') (Figure 1).

The botanical identification of the plant *Haloxylon scoparium* was carried out by Dr. Abdelmajid Khabbach at the Laboratory of Natural Substances, Pharmacology, Environment, Modeling, Health and Quality of Life (SNAMOPEQ), Polydisciplinary Faculty of Taza (FPT), Sidi Mohamed Ben Abdellah University of Fez (USMBA), B.P.: 1223, Taza-Gare, Taza, Morocco. A reference sample (ST2019/07) of the plant was deposited in the herbarium of the SNAMOPEQ laboratory of the FPT.

2.2. Mineralogical Study. Quantitative mineralogical analysis was carried out by inductively coupled plasma atomic emission spectroscopy (ICP-AES), which is a multielement analytical method that allows the measurement of several elements while using the quantitative measurement of the optical emission from the stimulated atoms, to determine the concentration of the analyte. It was carried out according to the protocol of Arora et al. [11], where 0.5 g of the powder of the aerial part of *Haloxylon scoparium* was placed in test tubes, a solution of perchloric acid and nitric acid (1 : 4) was added to digest the mixture, and then the samples were placed in the oven at 80°C. The samples were then allowed to cool, and the contents were filtered through Whatman filter paper. The sample solution was made up to a final volume of 25 ml with distilled water and analysed by HORIBA Jobin Yvon inductively coupled plasma atomic emission spectrometry (ICP-AES) [11].

2.3. Phytochemical Study

2.3.1. Preparation of Aqueous and Organic Extracts. The bioactive content of the aerial part of *Haloxylon scoparium* was extracted by two processes: an aqueous extraction using distilled water according to 3 modalities: decoction, infusion, and maceration, and another organic one in hot Soxhlet using organic solvents of different polarities: methanol, chloroform, ethyl acetate, and petroleum ether and in cold by maceration with methanol. The extraction methodology used is described in our previous work [12–16]. After removal of the solvents using a rotary evaporator (Buchi R-210), extraction yields were calculated and all extracts obtained were weighed and stored at 4°C.

2.3.2. Phytochemical Screening. The families of secondary metabolites such as catechic tannins, gall tannins, flavonoids, saponins, alkaloids, anthracenosides, free quinones, and anthraquinones were searched in the powder of the plant material and in the aqueous and organic extracts prepared from the aerial part of *Haloxylon scoparium* by staining and precipitation reactions as described in previous works of our laboratory [12–16].

2.3.3. Determination of Phenolic Compounds. The quantitative analysis was based on the results obtained by phytochemical screening; the determination of total polyphenols, flavonoids, and catechic tannins was carried out on the aqueous and organic extracts of the aerial part of *Haloxylon scoparium* as defined in previous publications of our laboratory [12,14–16].

2.3.4. Determination of Total Polyphenols. The determination of total polyphenols in extracts from the aerial part of *Haloxylon scoparium* was carried out according to the Folin–Ciocalteu reagent method [17] as presented in our previous articles [13–16].

Figure 1: *Haloxylon scoparium* (pictures taken on 17 July 2019 in Taddart located 42.1 km from the city of Taza; geographical coordinates: N 34°12.530′, W 003°32.917′).

2.3.5. Determination of Flavonoids. Total flavonoids were quantified using the method adapted by Mihai et al. [18] using aluminium trichloride and sodium hydroxide; the protocol is referred to in previous works [13–16].

2.3.6. Determination of Catechic Tannins. Catechic tannins are determined by the vanillin method based on the ability of vanillin to react with condensed tannins in the presence of acid to form a coloured complex measurable at 500 nm. The procedure has been described previously in [13–16,19].

2.4. In Vitro Study of Antidiabetic Activity

2.4.1. Inhibitory Activity of the Enzyme a-Amylase. The *a*-amylase inhibitory power of our aqueous and organic extracts was found *in vitro* by colorimetric assay based on the quantification of glucose released into the reaction medium. Because of the reducing properties of sugar, 3,5-dinitrosalicylic acid which acts as an oxidant is reduced to 3-amino-5-nitrosalicylic acid [20]. A mixture of 200 μL of sample and 200 μL of 0.02 M sodium phosphate buffer (pH = 6.9) containing the enzyme *a*-amylase (10 U/mL) was incubated at 30°C for 10 min. Then, 200 μL of 1% starch solution was added to the reaction mixture. The mixture was incubated at 30°C for 3 min. Then, 1 mL of the solution (DNS) was added and the reaction mixture was incubated at 90°C for 10 min. The reaction mixture was then diluted by adding 5 mL of distilled water, and the absorbance was measured at 540 nm in the type spectrophotometer (UviLine 9100–94000 UV/Vis). Acarbose was used as a positive control.

2.4.2. Inhibitory Activity of the Enzyme a-Glucosidase. The effect of our aqueous and organic extracts on the catalytic activity of *a*-glucosidase was identified according to the method in [21]. A mixture of 150 μL of the sample and 100 μL of 0.1 M sodium phosphate buffer (pH = 6.7) containing the *a*-glucosidase enzyme solution (0.1 U/mL) was incubated at 37°C for 10 min. After preincubation, 200 μL of 1 mM pNPG solution in 0.1 M sodium phosphate buffer was added. The reaction mixtures were incubated at 37°C for 30 min. After incubation, 1 mL Na_2CO_3 (0.1 M) was added and we measured the absorbance at 405 nm using the spectrophotometer (UviLine 9100–94000 UV/Vis). The inhibitory activity of *a*-glucosidase was expressed as percentage inhibition, and IC50 values were determined. Acarbose was used as a positive control.

2.4.3. Inhibitory Activity of the Enzyme ß-Galactosidase. The *in vitro ß*-galactosidase inhibition assay was done by colorimetric assay [22]; for this, a volume of 150 μL of different extracts and 100 μL of sodium phosphate buffer (0.1 M) at pH = 7.6 containing *ß*-galactosidase enzyme solution (1 U/mL) was incubated at 37°C for 10 min. Afterwards, we added 200 μL of the substrate 2-nitrophenyl beta-D-galactopyranoside (1 mM) prepared in sodium phosphate buffer (0.1 M) at pH = 7.6. The mixtures were incubated at 37°C for 30 min. After incubation, we added 1 mL Na_2CO_3 to stop the reaction and recorded the absorbance at 410 nm using a spectrophotometer. Quercetin is used as a positive control.

The results of the three tests for antidiabetic activity were expressed as %inhibition and calculated using the following equation:

$$\%\,\text{inhibition} = \left(\frac{((\text{Ac}(+) - \text{Acb}(-)) - (\text{As} - \text{Ab}))}{(\text{Ac}(+) - \text{Acb}(-))}\right) * 100, \quad (1)$$

where Ac+ is the absorbance of control with enzyme, Ac- is the absorbance of control without enzyme, As is the

absorbance of sample with enzyme, and Ab is the absorbance of sample without enzyme

2.5. In Vitro Study of Antioxidant Activity. Five methods were chosen to evaluate the antioxidant activity of the aqueous and organic extracts of the aerial part of *Haloxylon scoparium*, namely, hydrogen peroxide (H_2O_2) scavenging test, DPPH (2,2-diphenyl-1-picrylhydrazyl) free radical scavenging test, ABTS (2,2-azinobis (3-ethyl-benzothiazoline-6-sulphonate) or TEAC (Trolox equivalent antioxidant capacity) test, iron reduction antioxidant power (FRAP) test, and the reducing power (RP) test.

2.5.1. Hydrogen Peroxide (H_2O_2) Scavenging Activity. The evaluation of H_2O_2 scavenging capacity was carried out by the method described by Ruch and coworkers [23]: The experimental protocol has been detailed by previous works [13–16]. The percentage of hydrogen peroxide scavenging was determined by the following formula:

$$\% = \left[\frac{(\mathrm{AC} - \mathrm{AE})}{\mathrm{AC}}\right] \times 100, \quad (2)$$

where AC is the absorbance of the control and AE is the absorbance of the sample.

2.5.2. DPPH Free Radical Scavenging Test. The test for the scavenging of the DPPH radical (2,2-diphenyl-1-picrylhydrazyl (C18H12N5O6)) radical from the aerial part of *Haloxylon scoparium* was performed according to the protocol described by previous works [13–16,24]. The results obtained are compared with Trolox, BHT, and ascorbic acid which are employed as standard antioxidants. For each extract, the test is repeated three times.

The results are expressed as percentage inhibition using the following formula:

$$I\,(\%) = \left[\frac{(\mathrm{Abs} - \mathrm{Abss})}{\mathrm{Abs}}\right] \times 100, \quad (3)$$

where $I(\%)$ denotes the percentage inhibition, Abs is the absorbance of the negative control, and Abss is the absorbance of the sample.

The percentage of inhibition allowed us to establish a linear regression curve linking the different concentrations and the percentages of inhibition, and from this curve, we determined the IC50, the concentration that results in 50% inhibition of the DPPH• radical.

2.5.3. Equivalent Antioxidant Capacity of Trolox (TEAC or ABTS). The inhibitory power of the $ABTS^{\bullet+}$ radical is evaluated by the method described by Re et al. in 1999 [25]. For detailed protocol, refer to our previous works [13–16]. The reading is taken at 734 nm by using a spectrophotometer (UviLine 9100–94000 UV/Vis). Trolox is used as a standard, and the results obtained are expressed as mg Trolox equivalent per gram of extract (mg TE.g-1E).

2.5.4. Ferric Reducing Antioxidant Power (FRAP) Assay. The antioxidant capacity of the tested extracts was determined based on the method of Benzie and Strain [26]. The experimental protocol was detailed in our previous work [13–16]. The antioxidant capacity of the different extracts is represented as mg Trolox equivalent/g extract (mg TE.g-1E).

2.5.5. Reducing Power Assay. The reducing power of our extracts was determined according to the method described by [13–16,27], based on the reduction of ferric iron Fe^{3+} to ferrous iron Fe^{2+}. The absorbance reading was taken at 700 nm. Ascorbic acid was used as a positive control. The final result is represented as milligrams of ascorbic acid equivalent per gram of extract.

2.6. Statistical Analysis and Principal Component Analysis (PCA). The statistical study was carried out using the statistical software GraphPad Prism 5. All experiments were performed in triplicate. The results are expressed as mean ± SEM. The results are analysed by the one-way ANOVA test followed by the Tukey test for multiple comparisons and determination of significance levels. Values of $p \leq 0.05$ are considered statistically significant.

Principal component analysis (PCA) was used to analyse the relationships between the chemical composition of the aqueous and organic extracts tested and the biological activities and also to better visualise the correlations between the chemical composition of the eight prepared *Haloxylon scoparium* extracts and their antidiabetic and antioxidant activity *in vitro*.

3. Results

3.1. Mineralogical Study of the Aerial Part of Haloxylon scoparium. The analysis of the mineral composition by inductively coupled plasma atomic emission spectrometry (ICP-AES) carried out for the first time allowed the quantification of the mineral elements iron, potassium, phosphorus, magnesium, sodium, copper, calcium, strontium, selenium, and zinc in the aerial part of *Haloxylon scoparium*. The results obtained are presented in Table 1.

Table 1 shows the results of the study of the mineral content of the aerial part of *Haloxylon scoparium*. The analysis of minerals showed that this part of the plant contains high levels of iron, potassium, magnesium, phosphorus, and sodium with values of 60909.00, 27452.10, 10059.90, 1125.39, and 1054.65 mg/kg dry matter, respectively. Copper, calcium, and strontium are present in average amounts, respectively, of the order of 438.93, 313.29, and 280.23 mg/kg of dry matter. Selenium and zinc are present in low levels of 3.00 mg/kg for each.

3.2. Phytochemical Study of the Aerial Part of Haloxylon scoparium

3.2.1. Yield of Aqueous and Organic Extractions. The aqueous extractions with distilled water carried out hot by decoction and infusion and cold by maceration and the

Table 1: Mineral composition of the aerial part of *Haloxylon scoparium*.

Mineral elements	Fe	K	Mg	P	Na	Cu	Ca	Sr	Se	Zn
Content in mg/kg of dry matter	**60909.00**	**27452.10**	**10059.90**	**1125.39**	**1054.65**	438.93	313.29	280.23	3.00	3.00

Fe: iron; K: potassium; Mg: magnesium; P: phosphorus; Na: sodium; Cu: copper; Ca: calcium; Sr: strontium; Se: selenium; Zn: zinc.

organic extractions hot with Soxhlet with four solvents of different polarities (methanol, ethyl acetate, chloroform, and petroleum ether) and cold by methanol maceration of the aerial part of *Haloxylon scoparium* allowed us to calculate the yield of each aqueous and organic extract. The results obtained are presented in Table 2.

The yields obtained for the aqueous and organic extractions of the aerial part of *Haloxylon scoparium* are presented in Table 2. For the aqueous extracts, the decocted recorded the highest yield followed by the infused and lastly the macerated with percentages of 16, 8, and 5%, respectively. As for the organic extraction, the yields vary according to the solvent used and the extraction method; the methanolic extract prepared with the Soxhlet presents the highest yield of 14.35%, which is higher than the methanolic macerate (10.68%), followed by the chloroform and ethyl acetate extracts which present close values of 2.34 and 2.17%, respectively, the petroleum ether extract comes last with a low yield of 0.89%. In addition, the yield of the decocted aqueous extract (16%) is higher than that of all organic extracts.

3.2.2. Phytochemical Screening. The qualitative evaluation of the chemical composition of the powder of the aerial part of *Haloxylon scoparium* and of the different aqueous and organic extracts prepared from it revealed the presence of the chemical families represented in Table 3.

Phytochemical screening on the powder of the aerial part of the plant showed a strong positive reaction with catechic tannins and alkaloids, a medium positive reaction for flavonoids and saponins, and a weak reaction towards anthracenosides and free quinones.

The aqueous extracts also showed a strong positive reaction for catechic tannins, saponins, and alkaloids except for the aqueous macerate which showed a medium content of saponins. Free quinones are low in the decoctate. For the five organic extracts, catechic tannins were moderately present and alkaloids were strongly present. In addition, the methanolic extract prepared with Soxhlet and the methanolic macerate show a medium reaction with flavonoids, saponins, anthracenosides, and free quinones, and the latter are low in the ethyl acetate and chloroform extracts.

3.2.3. Determination of Polyphenols, Flavonoids, and Catechic Tannins. The results of the phytochemical screening of the aerial part of *Haloxylon scoparium* guided us in the selection of the secondary metabolites to be determined: total phenols, flavonoids, and catechic tannins. The results of the assay are presented in Table 4.

The phytochemical study on the determination of secondary metabolites revealed that the tested extracts contain polyphenols, flavonoids, and catechic tannins (Table 4).

Table 2: Yields of aqueous and organic extractions of the aerial part of *Haloxylon scoparium*.

	Extracts	Yield in %
Aqueous extracts	**Decocted**	**16**
	Infused	8
	Macerated	5
Organic extracts	**Methanol extract**	**14.35**
	Macerated methanol	**10.68**
	Ethyl acetate extract	2.17
	Chloroform extract	2.34
	Petroleum ether extract	0.89

Concerning polyphenols, the aqueous, decocted, infused, and macerated extracts present values of 6.83 ± 0.04, 3.81 ± 0.21, and 3.96 ± 0.07 Ug EAG/mg E, respectively, with a statistically insignificant difference between all aqueous extracts. Polyphenols are more abundant in the methanolic extract prepared in Soxhlet (161.65 ± 1.52 Ug EAG/mg E) and in the methanolic macerate (147.11 ± 6.11 Ug EAG/mg E) with a significant difference, followed, respectively, by ethyl acetate extracts (54.24 ± 2, 70 Ug EAG/mg E) and chloroformic extract (49.42 ± 1.02 Ug EAG/mg E) with a nonsignificant difference. Petroleum ether extract comes in the last position with a polyphenol content of 11.30 ± 1.58 Ug EAG/mg E.

For flavonoids measured in aqueous extracts, the decocted had the highest content (306.59 ± 4.35 Ug EQ/mg E) followed, respectively, by the infused (228.67 ± 10.87 Ug EQ/mg E) and then the macerated (135.78 ± 3.57 Ug EQ/mg E), with a significant difference between them. For the organic extracts, the highest flavonoid content was obtained in the methanolic extract prepared in Soxhlet (612.47 ± 10.10 Ug EQ/mg E) and the methanolic macerate (641.03 ± 7.8 Ug EQ/mg E) with a statistically nonsignificant difference, followed, respectively, by the ethyl acetate extract (416.73 ± 10.18 Ug EQ/mg E) and chloroformic extract (263.25 ± 2.59 Ug EQ/mg E) with a statistically significant difference between the two and lastly the petroleum ether extract (168.3 ± 7.91 Ug EQ/mg E). A significant difference was observed between the decocted and the two organic extracts: the chloroform and petroleum ether extracts expressed by a higher flavonoid content in the decocted compared to the chloroform and petroleum ether extracts.

Concerning the determination of catechic tannins, we found that the aqueous extracts have similar contents; the decoctate has a content of 3.78 ± 0.35 Ug EC/mg E, followed by the infused (1.1 ± 0.13 Ug EC/mg E) and the aqueous macerate (2.25 ± 0.12 Ug EC/mg E), with a nonsignificant difference between the three extracts. As for the organic extracts, the ethyl acetate extract has the highest tannin content (23.69 ± 0.6 Ug EC/mg E) followed by the chloroform extract (21.25 ± 2.25 Ug EC/mg E), petroleum ether

Table 3: Phytochemical screening of the powder and the aqueous and organic extracts of the aerial part of *Haloxylon scoparium*.

Plant powder and aqueous and organic extracts		Catechic tannins	Gallic tannins	Flavonoids	Saponins	Alkaloids	Sterols	Anthracenosides	Anthraquinones	Free quinones
Powder of the aerial part of the plant		+++	−	++	++	+++	−	+	−	+
Aqueous extracts	Decocted	+++	−	++	+++	+++	−	−	−	−
	Infused	+++	−	++	+++	+++	−	−	−	−
	Macerated	+++	−	++	++	+++	−	−	−	−
Organic extracts	Methanol	++	−	++	++	+++	−	++	−	++
	Macerated methanol	++	−	++	++	+++	−	++	−	++
	Ethyl acetate	++	−	−	−	+++	−	−	−	+
	Chloroform	++	−	−	−	+++	−	−	−	+
	Petroleum ether	++	−	−	−	+++	−	−	−	−

+++: very abundant; ++: moderately abundant; +: present; −: absent.

Table 4: Contents of total polyphenols, flavonoids, and catechic tannins in aqueous and organic extracts of the aerial part of *Haloxylon scoparium*.

Extracts		Total phenolic content (μg GAE mg^{-1}E)	Total flavonoid content (μg QE mg^{-1}E)	Total catechic tannin content (μg CE mg^{-1}E)
Aqueous	Decocted	**6.83 ± 0.04^{a}**	**306.59 ± 4.35^{a}**	**$3.78 \pm 0.35^{a,b,c,e}$**
	Infused	$3.81 \pm 0.21^{a,b}$	228.67 ± 10.87^{b}	$1.1 \pm 0.13^{a,c}$
	Macerated	$3.96 \pm 0.07^{a,b}$	135.78 ± 3.57^{c}	$2.25 \pm 0.12^{a,b,c}$
Organic	Methanol	**161.65 ± 1.52^{c}**	**612.47 ± 10.10^{d}**	6.02 ± 0.11^{b}
	Macerated methanol	147.11 ± 6.11^{d}	**641.03 ± 7.8^{d}**	0.26 ± 0.2^{c}
	Ethyl acetate	54.24 ± 2.70^{e}	416.73 ± 10.18^{e}	**23.69 ± 0.6^{d}**
	Chloroform	49.42 ± 1.02^{e}	263.25 ± 2.59^{b}	21.25 ± 2.25^{d}
	Petroleum ether	$11.30 \pm 1.58^{b,f}$	168.3 ± 7.91^{c}	$7.55 \pm 1.18^{b,e}$

All results expressed are mean of three individual replicates ($n = 3 \pm$ SEM). Values with the same letter superscript in the same row are not significantly different ($p < 0.05$).

extract (7.55 ± 1.18 Ug EC/mg E), and methanolic Soxhlet extract (6.02 ± 0.11 Ug EC/mg E) with a nonsignificant difference, and methanolic macerate comes the last (0.26 ± 0.2 Ug EC/mg E).

3.3. In Vitro Study of Antidiabetic Activity. The study of the *in vitro* antihyperglycaemic effect of the aqueous and organic extracts of *Haloxylon scoparium* was carried out by the three tests of enzymatic inhibition of *a*-amylase, *a*-glucosidase, and *ß*-galactosidase. The results were expressed as IC50 and are shown in Table 5.

For the *a*-amylase enzyme inhibition test, the results obtained in Table 5 show that the aqueous and organic extracts evaluated present an inhibitory activity with an IC50 which varies between 39096.66 ± 4174.94 ug/mL and 80277.33 ± 7609.97 ug/mL. Concerning the aqueous extracts, the decoctate presents the best inhibitory activity (IC50 = 66855.66 ± 10519.25 ug/mL), followed, respectively, by the infused (IC50 = 78892.33 ± 14448.37 ug/mL) and the macerated (IC50 = 80277.33 ± 7609.97 ug/mL) with a statistically nonsignificant difference between the three extracts. For the organic extracts, ethyl acetate shows inhibitory activity with IC50 = 39096.66 ± 4174.94 ug/mL, followed, respectively, by methanolic macerate (IC50 = 46351 ± 4882.68 ug/mL), chloroformic extract (IC50 = 51261 ± 4786, 07 ug/mL), methanolic extract (IC50 = 56156.33 ± 2580.20 ug/mL), and lastly petroleum ether extract (IC50 = 66601 ± 12217.29 ug/mL) with a statistically insignificant difference between all organic extracts. The aqueous and organic extracts have a lower inhibitory activity for *a*-amylase than the acarbose standard (IC50 = 616.33 ± 5.00 ug/mL).

The study of the inhibition of the enzyme *a*-glucosidase *in vitro* shows that all extracts had high inhibitory activity. For aqueous extracts, decoctate shows an inhibitory activity with IC50 = 181.7 ± 21.15 ug/mL, followed by aqueous macerate (IC50 = 202.1 ± 75.44 ug/mL) and infused (IC50 = 225.44 ± 58.43 ug/mL), respectively; aqueous extracts recorded statistically insignificant difference between them. In addition, the decoctate has a better inhibitory activity compared to acarbose (IC50 = 195 ± 6.12 ug/mL) with a statistically nonsignificant difference. For the organic extracts, the methanolic extract shows an inhibitory activity with IC50 = 193.4 ± 8.57 ug/mL, followed, respectively, by the methanolic macerate (IC50 = 200.86 ± 1.99 ug/mL), ethyl

Table 5: IC50 (μg/mL) of *a*-amylase, *a*-glucosidase, and *ß*-galactosidase inhibitory activity of aqueous and organic extracts of the aerial part of *Haloxylon scoparium*.

Extracts	α-Amylase	α-Glucosidase	β-Galactosidase
Decocted	**66855.66** ± 10.51^{a,b,c}	**181.7 ± 21.15**^{a}	1361.66 ± 188.40^{a,b,c}
Infused	78892.33 ± 14.44^{a,b,c}	225.44 ± 58.43^{a,b}	**915.23 ± 68.86**^{a}
Macerated	80277.33 ± 7.61^{a,b}	202.10 ± 75.44^{a,b}	1072.73 ± 369.28^{a,c}
Methanol	56156.33 ± 2.58^{b,c}	**193.4 ± 8.57**^{a,b}	**1735.66 ± 269.50**^{a,b}
Macerated methanol	**46351** ± 4.88^{b,c}	200.86 ± 1.99^{a,b}	1984.66 ± 61.65^{a,b}
Ethyl acetate	39096.66 ± 4.17^{b,c}	235.9 ± 35.56^{a,b}	1601.66 ± 107.21^{a,b}
Chloroform	51261 ± 4.78^{b,c}	341.73 ± 13.92^{a,b}	**1707.66 ± 12.99**^{a,b}
Petroleum ether	66601 ± 12.21^{b,c}	357.16 ± 2.50^{a,b}	1819.66 ± 172.29^{a,b,c}
Acarbose	616.33 ± 5.00^{d}	195 ± 6.12^{a,b}	—
Quercetin	—	—	171.16 ± 5.00^{d}

All results expressed are mean of three individual replicates ($n = 3 \pm$ SEM). Values with the same letter superscript in the same row are not significantly different ($p < 0.05$).

acetate extract (IC50 = 235.9 ± 35.56 ug/mL), chloroform extract (IC50 = 341, 73 ± 13.92 ug/mL), and lastly the petroleum ether extract with an IC50 value of 357.16 ± 2.50 ug/mL; a statistically nonsignificant difference was found between the organic extracts studied and between the latter and acarbose (IC50 = 195 ± 6.12 ug/mL).

The results of the *ß*-galactosidase inhibition test carried out reveal that all the aqueous and organic extracts had inhibitory activity with IC50s ranging between 915.23 ± 68.86 ug/mL and 1984.66 ± 61.65 ug/mL. For the aqueous extracts, infused comes first with an IC50 of 915.23 ± 68.86 ug/mL, followed, respectively, by aqueous macerated (IC50 = 1072.73 ± 369.28 ug/mL) and decocted (IC50 = 1361.66 ± 188.40 ug/mL), with a statistically significant difference between the three extracts. Concerning the organic extracts, the ethyl acetate extract shows the highest inhibitory activity with an IC50 of 1735.66 ± 269.50 ug/mL, followed, respectively, by the chloroform extract (IC50 = 1601.66 ± 107.21 ug/mL), methanolic extract (IC50 = 1735.66 ± 269.50 ug/mL), petroleum ether (IC50 = 1819.66 ± 172.29 ug/mL), and lastly the methanolic macerate (IC50 = 1984.66 ± 61.65 ug/mL). The organic extracts in this test showed a nonsignificant difference between them and a statistically significant difference with quercetin (IC50 = 171.16 ± 5.00 ug/mL).

3.4. Antioxidant Activity. The evaluation of the *in vitro* antioxidant activity of the aqueous and organic extracts of the aerial part of *Haloxylon scoparium* was carried out by five tests: H_2O_2 scavenging activity test, DPPH radical scavenging test, ABTS radical scavenging test, FRAP test, and PR test. The results obtained are presented in Table 6.

All the extracts studied showed strong antioxidant and free radical scavenging properties, which varied according to the nature of the extract tested and the test used. Moreover, aqueous and organic extracts take the same ranking for all tests; decoctate comes first followed, respectively, by infused and aqueous macerated for aqueous extracts. For the organic extracts, we found the following order for the five tests: methanolic extract > methanolic macerate > ethyl acetate extract > chloroformic extract > petroleum ether extract.

The results of the hydrogen peroxide (H_2O_2) scavenging activity reveal that the aqueous extract decoctate has the highest hydrogen peroxide (H_2O_2) scavenging capacity (16.21 ± 0.39%), followed by the infused (8.78 ± 0.41%) and the aqueous macerate (4.15 ± 0.43%), respectively, with a significant difference between the three aqueous extracts. For the organic extracts, the methanolic extract shows the highest percentage of hydrogen peroxide (H_2O_2) scavenging (20.91 ± 0.27%) with a significant difference with the chloroform, ethyl acetate, and petroleum ether extracts, followed, respectively, by methanolic macerate (7.36 ± 0.09%), ethyl acetate (7.26 ± 0.11%), chloroformic (5.84 ± 0.39%), and lastly petroleum ether extract (5.76 ± 0.4%), with a statistically nonsignificant difference between the four organic extracts. In addition, the hydrogen peroxide scavenging capacity of the decoctate surpassed the methanolic macerated, ethyl acetate, chloroformic, and petroleum ether extracts, as presented in Table 6.

The study of the anti-free radical activity by the DPPH test reveals that all the tested extracts present a considerable anti-free radical activity. Concerning the aqueous extracts, the decoctate showed the highest DPPH scavenging activity with an IC50 of 439.3 ± 7.74 μg/mL, followed, respectively, by the infused (IC50 = 518.96 ± 5.66 μg/mL) and the aqueous macerate (IC50 = 582.8 ± 14.72 μg/mL), with a nonsignificant difference between the three aqueous extracts. For the organic extracts, we found that the methanolic extract shows a very high DPPH radical scavenging power with an IC50 of 39.63 ± 2.03 μg/mL, followed, respectively, by the methanolic macerate (IC50 = 57.87 ± 1.50 μg/mL) with a nonsignificant difference, then by the ethyl acetate extract (IC50 = 62.27 ± 1.82 μg/mL) and chloroform extract (IC50 = 72.00 ± 1.88 μg/mL), with a nonsignificant difference between the two, and lastly petroleum ether (IC50 = 297.8 ± 1.15 μg/mL) which shows a significant difference with all other organic extracts. The free radical scavenging activity of the organic extracts is higher than that of the aqueous extracts, with the exception of the petroleum ether extract, which shows a lower free radical scavenging activity than the decoctate. In spite of the antiradical power of these extracts, it remains significantly lower than the reference standards (ascorbic acid = 0.17 ± 0.02 μg/ml, BHA = 1.59 ± 0.13 μg/ml, and Trolox = 1.75 ± 0.09 μg/ml).

Table 6: Results of *in vitro* antioxidant activity of aqueous and organic extracts of the aerial part of *Haloxylon scoparium* via five tests: H_2O_2, DPPH, ABTS, FRAP, and PR.

Extracts		H_2O_2 (%)	DPPH (IC50)	ABTS (ug E AA/mg E)	FRAP (ug E T/mg E)	PR (ug E AA/mg E)
Aqueous extracts	Decocted	**16.21 ± 0.39**^{a}	**439.3 ± 7.74** ^{a}	**8.20 ± 0.01**^{a}	**37.66 ± 1.29**^{a,g}	**21.89 ± 1.04**^{a}
	Infused	8.78 ± 0.41^{b}.^{e}	518.96 ± 5.66^{b}	5.14 ± 0.37^{a,d}	27.94 ± 1.08^{a,b,g}	14.09 ± 0.74^{a}
	Macerated	4.15 ± 0.43^{c}	582.8 ± 14.72^{c}	3.99 ± 0.26^{a,d}	17.81 ± 3.50^{b,g}	6.63 ± 0.40^{a}
Organic extracts	Methanol	**20.91 ± 0.27**^{d}	**39.63 ± 2.03**^{d}	**50.75 ± 0.72**^{b}	**163.37 ± 1.52**^{c}	**116.18 ± 8.19**^{b}
	Macerated methanol	7.36 ± 0.09^{e}	57.87 ± 1.50^{d,e}	47.71 ± 1.21^{b}	124.08 ± 6.97^{d}	110.11 ± 7.47^{b}
	Ethyl acetate	7.26 ± 0.11^{e}	62.27 ± 1.82^{d,e}	39.74 ± 1.41^{c}	106.14 ± 5.26^{e}	79.27 ± 4.78^{c}
	Chloroform	5.84 ± 0.39^{e,f}	72.00 ± 1.88^{e}	36.99 ± 1.34^{c}	85.02 ± 2.96^{f}	59.35 ± 0.65^{c}
	Petroleum ether	5.76 ± 0.4^{e,f,c}	297.8 ± 1.15^{f}	1.72 ± 0.53^{d}	24.51 ± 0.53^{g}	0.96 ± 0.3^{a}
Reference standards	Ascorbic acid	**14.35 ± 0.002**^{g}	**0.17 ± 0.02**^{g}			
	BHT		**1.59 ± 0.13**^{g}	—	—	—
	Trolox		**1.75 ± 0.09**^{g}			

All results expressed are mean of three individual replicates ($n = 3 \pm$ SEM). Values with the same letter superscript in the same row are not significantly different ($p < 0.05$).

Concerning the ABTS test, we found that the decoctate has the highest antiradical capacity (8.20 ± 0.01 Ug E AA/mg E), higher than the infused (5.14 ± 0.37 Ug E AA/mg E) and the aqueous macerate (3.99 ± 0.26 Ug E AA/mg E); however, they present a statistically nonsignificant difference between them. For the organic extracts, we noticed that the methanolic extract has the highest antiradical capacity (50.75 ± 0.72 Ug E AA/mg E), followed by the methanolic macerate (47.71 ± 1.21 Ug E AA/mg E) with a nonsignificant difference, then by the ethyl acetate extract (39.74 ± 1.41 Ug E AA/mg E) and chloroformic extract (36.99 ± 1.34 Ug E AA/mg E) with a nonsignificant difference, and lastly petroleum ether extract (1.72 ± 0.53 Ug E AA/mg E) with a statistically significant difference with all the organic extracts (Soxhlet methanolic, methanolic macerated, chloroformic, and ethyl acetate). The organic extracts in this test have a higher free radical scavenging activity than the aqueous extracts with a significant difference, except for the petroleum ether extract, which has a lower free radical scavenging capacity than the aqueous extracts with a significant difference with the decoctate and a nonsignificant difference with the infused and aqueous macerate.

The results of the antioxidant activity by the FRAP test reveal that the decoctate comes first with a reducing capacity of 37.66 ± 1.29 Ug E T/mg E, followed, respectively, by the infused (27.94 ± 1.08 Ug *E* T/mgE) with a nonsignificant difference and the aqueous macerate (17.81 ± 3.50 Ug E T/mg E) with a significant difference with the decoctate and a nonsignificant difference with the infused.

Concerning the organic extracts, the methanolic extract presents the highest reducing capacity of ferric iron (Fe3+) to ferrous iron (Fe2+) with a value of 163.37 ± 1.52 Ug E T/mg E, followed, respectively, by the methanolic macerate, ethyl acetate, chloroformic, and petroleum ether extracts with values of 124.08 ± 6.97, 106.14 ± 5.2, 85.02 ± 2.96, and 24.51 ± 0.53 Ug *E* T/mg E, respectively. Statistical analysis showed a significant difference between all organic extracts.

According to the results obtained, the aqueous extracts also show a higher reducing power in this test than the petroleum ether extract with a statistically nonsignificant difference between the 3 aqueous extracts: decocted (37.66 ± 1.29 Ug E T/mg E), infused (27.94 ± 1.08 Ug E T/mg E), and macerated (17.81 ± 3.50 Ug E T/mg E).

The results of the reducing power test show that the decoctate has a higher reducing capacity than the infused and aqueous macerated extracts, which are, respectively, in the order of 21.89 ± 1.04, 14.09 ± 0.74, and 6.63 ± 0.40 Ug E AA/mg E with a nonsignificant difference.

For organic extracts, methanolic extract and methanolic macerate show the highest reducing power of 116.18 ± 8.19 and 110.11 ± 7.47 Ug E AA/mg E, respectively, with a nonsignificant difference between the two extracts, followed by ethyl acetate extract (79, 27 ± 4.78 Ug E AA/mg E) and chloroformic extract (59.35 ± 0.65 Ug *E* AA/mg E) with a nonsignificant difference between them and finally petroleum ether extract (0.96 ± 0.3 Ug E AA/mg E) which shows a significant difference with all organic extracts. The aqueous extracts have a higher iron reduction capacity than the petroleum ether extract with a statistically nonsignificant difference.

3.5. Principal Component Analysis (PCA). The principal component analysis (PCA) allowed us to highlight the correlation between the aqueous and organic extracts and their antioxidant capacity evaluated by the different tests and the correlation between these extracts and their chemical compound content.

The objective of the PCA carried out on eight individuals divided into three aqueous extracts and five organic extracts of the aerial part of *Haloxylon scoparium* was to highlight the possible correlations existing between the individuals and the variables tested, in relation to eight variables represented the content of chemical compounds (total polyphenols, flavonoids, and catechic tannins) and, on the other hand, in relation to the *in vitro* inhibitory activity of *a*-amylase, *a*-glucosidase, and *ß*-galactosidase and with the five tests used for the evaluation of antioxidant activity: H_2O_2, DPPH, ABTS, FRAP, and PR.

3.5.1. Correlation Matrix. Principal component analysis (PCA) showed that the DPPH test is highly positively correlated with the ABTS ($r^2 = 0.9716$), PR ($r^2 = 0.9333$), and FRAP ($r^2 = 0.9495$) tests. The ABTS test is highly positively correlated with the FRAP ($r^2 = 0.9713$) and PR ($r^2 = 0.9809$) tests. The FRAP and PR tests have a high positive correlation with each other of $r^2 = 0.9845$.

Polyphenol content is highly positively correlated with all antioxidant activity tests except the H_2O_2 test (DPPH, $r^2 = 0.8549$; ABTS, $r^2 = 0.8944$; FRAP, $r^2 = 0.9372$; and PR, $r^2 = 0.9429$). Flavonoid content was also strongly positively correlated with the tests (DPPH, $r^2 = 0.7909$; ABTS, $r^2 = 0.8567$; FRAP, $r^2 = 0.8730$; and PR, $r^2 = 0.8983$). In addition, total polyphenols showed a high positive correlation with flavonoid content ($r^2 = 0.9416$) (Table 7).

The inhibitory activity of *a*-amylase was highly positively correlated with antioxidant activity assays: DPPH ($r^2 = 0.8094$), ABTS ($r^2 = 0.8237$), FRAP ($r^2 = 0.8115$), and PR ($r^2 = 0.8508$); *a*-amylase was highly positively correlated with total polyphenol ($r^2 = 0.7721$) and flavonoid ($r^2 = 0.7162$) content. The *in vitro* inhibitory activity by *a*-glucosidase and *ß*-galactosidase is moderately positively correlated with the H_2O_2 antioxidant activity test with values of $r^2 = 0.4885$ and $r^2 = 0.0412$, respectively.

3.5.2. Graphical Representation of the Principal Component Analysis (PCA). According to the principal component analysis (PCA) (Figure 2), the two main axes (F1 and F2) describe 83.39% of the total variance of the observations. Therefore, the interpretations made from this analysis will be highly significant. This analysis allowed us to discriminate three groups:

Group 1: it contains the methanolic extract and the methanolic macerate, presents the highest contents of total polyphenols and flavonoids, and also expresses a better antiradical activity via the DPPH, ABTS, and H_2O_2 tests and a high reducing power via the FRAP and PR tests. In addition, both extracts show inhibitory activity of *a*-amylase and *a*-glucosidase enzymes.

Group 2: it includes the chloroformic extract which has high tannin content and intermediate *in vitro* antioxidant and antidiabetic activity.

Group 3: it consists of the organic ethyl acetate extract which expresses a high content of catechic tannins and presents a strong inhibitory activity of the enzymes *ß*-galactosidase and *a*-amylase. This group also includes the petroleum ether extract and the aqueous extracts, decocted, infused, and macerated, which have low levels of phenolic compounds, but are rich in flavonoids and have moderate antioxidant and antidiabetic activity *in vitro*.

4. Discussion

4.1. Study of the Mineral Composition of the Aerial Part of Haloxylon scoparium. The results of the mineralogical analysis reveal the richness of the aerial part of *Haloxylon scoparium* in minerals, with a high content of iron, potassium, and magnesium and a significant content of phosphorus, sodium, and copper. Calcium and strontium are present at medium levels. The aerial part of *Haloxylon scoparium* is characterised by its richness in minerals that could be responsible for its biological activities. From the mineralogical study, we have highlighted the presence of a high content of Fe, K, P, Na, Cu, Mg, Ca, and Sr compared to those obtained in a recent work carried out by Boulfia and his collaborators (Fe (33552), K (1843.14), P (756.36), Na (439.65), Cu (303.9), Mg (272.37), and Ca (20.55) mg/kg of plant material), and the antioxidant capacity that we recorded is higher than that obtained by Boulfia his collaborators for the ethanolic extract with Soxhlet [28], which could confirm that some minerals may be responsible for the antioxidant capacity of the aerial part of *Haloxylon scoparium*. In this sense, a study conducted on *Phoenix dactylifera* fruits showed a high correlation between antioxidant activity and mineral composition; K content is highly correlated with the FRAP test ($r^2 = 0.800$) and with the H_2O_2 test ($r^2 = 0.889$) [29]. This is in agreement with our results on antioxidant activity for both tests. Minerals play a crucial role in antioxidant activity; according to Grela et al., the antioxidant activity is attributed to mineral components such as copper, manganese, and iron [30]. Furthermore, an imbalance of mineral elements would change the content of flavonoids considered as a proven antioxidant compound [31]. Some antioxidant enzymes require metal ions for their activity; other metals have been directly classified as antioxidants [32]. Many antioxidant defence pathways are dependent on micronutrients. Some minerals are components of antioxidant enzymes: superoxide dismutase depends on Mn, Cu, and Zn; catalase depends on Fe, and glutathione peroxidase on Se [33]. Minerals may also be responsible for antidiabetic activity; several minerals are involved in glucose metabolism such as Ca, K, Mg, and Na [34]; in addition, several studies have shown the relationship between oxidative stress and the development of diabetes. An increase in oxidative stress can cause an alteration of the insulin signalling pathway, either by a decrease in glucose capture by insulin-sensitive tissues or by an increase in hepatic glucose production, which leads to the development of insulin resistance and subsequently noninsulin-dependent diabetes [35].

4.2. Phytochemical Study

4.2.1. Yield of Aqueous and Organic Extracts. The results of the phytochemical study show that among the aqueous extracts, the decoctate presented a better yield in comparison with the infused and macerated with percentages of 16%, 8%, and 5%, respectively. These extracts were prepared with distilled water but at different temperatures, which means that the amount of extractable material from the aerial part of *Haloxylon scoparium* increases with the increase of temperature during the aqueous extraction.

For the organic extracts, the yields vary according to the polarity of the solvent used and the method and modality of

Table 7: Correlation coefficient between the antioxidant variables, *a*-amylase, *a*-glucosidase, and *β*-galactosidase enzyme inhibitory activities, and the chemical contents of aqueous and organic extracts of the aerial part of *Haloxylon scoparium*.

Variables	H_2O_2	DPPH	ABTS	FRAP	RP	Total phenolics	Flavonoids	Catechic tannins	α-Amylase	α-Glucosidase	β-Galactosidase
H_2O_2	**1**										
DPPH	0.2581	**1**									
ABTS	0.3023	**0.9693**	**1**								
FRAP	0.4676	**0.9424**	**0.9713**	**1**							
RP	0.3906	**0.9255**	**0.9809**	**0.9845**	**1**						
Total phenolics	0.4477	**0.8563**	**0.8944**	**0.9372**	**0.9429**	**1**					
Flavonoids	0.5243	**0.8055**	**0.8567**	**0.8730**	**0.8983**	**0.9416**	**1**				
Catechic tannins	−0.2149	0.4813	0.3640	0.2451	0.1921	−0.0338	−0.0433	**1**			
α-Amylase	0.1604	**0.8094**	**0.8237**	**0.8115**	**0.8508**	**0.7721**	**0.7162**	0.1979	**1**		
α-Glucosidase	0.4885	−0.0822	0.1413	0.2234	0.2832	0.2696	0.2851	−0.5792	0.1484	**1**	
β-Galactosidase	0.0412	−0.6996	−0.5983	−0.5705	−0.5658	−0.6320	−0.5357	−0.2659	−0.7078	0.2847	**1**

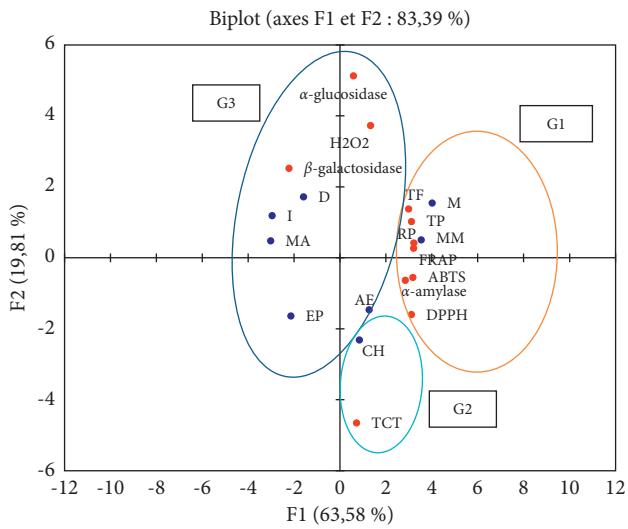

Figure 2: Correlation circle of the variables and the positioning of the individuals on the first main plane (83.39% information) (D: decocted; I: infused; MA: aqueous macerated; MM: methanolic macerated; M: methanolic extract; AE: ethyl acetate extract; CH: chloroformic extract; EP: petroleum ether extract; G1: Group 1; G2: Group 2; G3: Group 3; DPPH: 2,2-diphenyl-1-picrylhydrazyl; H_2O_2: hydrogen peroxide; ABTS: 2,2′-azino-bis(3-ethylbenzothiazoline-6-sulphonic acid); FRAP: iron reducing antioxidant power; PR: iron reducing power; TP: total polyphenols; TF: total flavonoids; TCT: total catechic tannins).

extractions; the yield of the methanolic extract prepared with Soxhlet is higher than that of the methanolic macerate with 14.35 and 10.68%, respectively. This variation is probably due to the temperature used, the extraction time, and the technique used. The Soxhlet methanolic extract has the highest amount of extracted material, which suggests that the use of methanol as an organic solvent may be suitable for the extraction of natural chemical compounds from the studied part of the plant.

The extraction yield varies depending on the plant species, the part used in the extraction, the harvesting period, the type of soil, the climate, the geographical position, the drying conditions including the duration, the form of the plant material (powder or fragments), the nature of the solvent used in the extraction and its polarity and the extraction conditions: temperature, extraction duration, solvent/plant material ratio.

According to Jurinjak Tušek et al., the extraction yield of the Asteraceae family increases by increasing the extraction temperature [36]. According to Kwon and Chung, the maximum extraction yield of *Curcuma longa* was obtained at 135°C/5 min with a ratio of water: ethanol (50 : 50, v/v) as extraction solvent [37]. Wu et al. also found that temperature, extraction time, and solvent/plant material ratio affect the yield of *Ziziphus jujuba* [38].

In 2012, Lamchouri and his collaborators conducted a phytochemical study on the aerial part of *Haloxylon scoparium* and obtained yields of 10.50% for the decoctate, 10.47% for the Soxhlet methanolic extract, and 10.00% for the methanolic macerate. These yields are lower than those obtained in our study [7]. This variation could be explained by the difference in the harvesting period which was between March and April in 2012 and by the plant material/solvent ratio which was 20 g of plant material/250 ml of each solvent for the 2012 study. In contrast, the 2019 harvest was done in July, and the plant material to solvent ratio was 20 g plant material/200 ml of each solvent.

According to work conducted on other plants from the region of Taza, Morocco, in our laboratory under the same operating conditions, Bouabid and collaborators found that the best yields are obtained with polar solvents and that hot extraction gives the higher yields when compared to cold extraction for aqueous and organic extracts of the underground part of *Atractylis gummifera* [12]. Senhaji and her collaborators found that the aqueous macerate and hot methanolic extract of *Ajuga iva* had the high yield of 13.31% and 9%, respectively. Similarly, aqueous macerate and methanolic extract prepared hot in Soxhlet from the aerial part of *Anabasis aretioides* of the family Chenopodiaceae show the highest yield of 3.41% and 3.39%, respectively [15,16]. Boulfia and his collaborators found that the hot-prepared ethanolic extract and the decoctate of *Juglans regia* had the highest yields of 22.04% and 14% [14].

4.2.2. Phytochemical Screening. The phytochemical screening carried out on the powder of the aerial part of *Haloxylon scoparium* and on the aqueous and organic extracts prepared from it allowed us to highlight the presence of different secondary metabolites; the plant is highly rich in catechic tannins and alkaloids that are contained in the powder of the plant material and in all the aqueous and organic extracts. Our results are in agreement with other works that indicated the richness of *Haloxylon scoparium* in alkaloids; Zerriouh and collaborators reported that the aerial part of *Hammada scoparia* collected in Algeria contains the alkaloids [39]. In addition, Jarraya and collaborators described the isolation and structural elucidation of N-methylisososaloline extracted from *Haloxylon scoparium* leaves collected in Tunisia [40].

The plant material and the aqueous and organic extracts contain catechic tannins, which are known to possess multiple pharmacological properties, antiinflammatory [41], antidiabetic [42], antimicrobial, and antiviral activity [43]. In this sense, a study conducted in our laboratory by Lamchouri and collaborators showed that the *Staphylococcus aureus* strain presented a good sensitivity of 7–12 mm to ethyl acetate extract of *H. scoparium* [7].

Saponins are strongly present in aqueous extracts, mainly decocted and infused, and moderately present in methanolic extract and its macerate; saponins are best extracted at high temperature. According to Nafiunisa and collaborators, the amount of extracted saponin increases with increasing extraction temperature [44]. Concerning flavonoids, the reaction of their detection was moderately positive at the level of the three aqueous extracts, the methanolic extract prepared with Soxhlet, and the methanolic macerate. Quinones and anthracenosides were present in the decoctate and the methanolic, methanolic macerated, ethyl acetate, and chloroform extracts.

A study done by Zerriouh and collaborators in Algeria showed that the aqueous extract of the aerial part of *Hammada scoparia* is devoid of flavonoids but contains the alkaloids and saponins, while the methanolic extract prepared in Soxhlet contains flavonoids, alkaloids, and tannins [39]. Furthermore, a study done by Bourogaa and collaborators in Algeria revealed the presence of flavonoids and alkaloids, while sterols and quinones are absent from the aqueous extract of *H. scoparia* leaves [45].

In the same operating conditions, works carried out on plants collected in the same region as *Haloxylon scoparium* in our laboratory by Senhaji and collaborators, Bouabid and collaborators, and Boulfia and collaborators revealed that phytochemical screening showed the presence of catechic tannins, saponins, and sterols in the aerial part of *Anabasis aretioïdes* which belongs to the same Chenopodiaceae family as our *H. scoparium* plant [16]. The underground part of *Atractylis gummifera* is characterised by the presence of tannins and flavonoids [12], and the bark of *Juglans regia* is rich in catechic tannins, flavonoids, anthraquinones, and free quinones [14]. Catechic tannins, flavonoids, saponins, and sterols are present in the aerial part of *Ajuga iva* [15].

4.2.3. Determination of Total Polyphenols, Flavonoids, and Catechic Tannins. The quantitative analysis of phenolic compounds in the aerial part of *Haloxylon scoparium* showed that all extracts are richer in total polyphenols, flavonoids, and tannins.

The aqueous extracts show low amounts of total polyphenols, and the decoctate comes first with a value of 6.83 ± 0.04 Ug EAG/mg E, followed by the aqueous macerate (3.96 ± 0.07 Ug EAG/mg E) and the infused (3.81 ± 0.21 Ug EAG/mg E) with a statistically nonsignificant difference. For the organic extracts, the total polyphenols are better extracted by methanol; moreover, the polyphenol content in the Soxhlet methanolic extract exceeds that of the methanolic macerate with a significant difference. This variation may be due to the factor of the technique used; in fact, the Soxhlet extraction allows the total exhaustion of the plant material through the successive repetition of the extraction cycles at a temperature of 64.7°C for 7 hours, which allows the maximum extraction of total polyphenols. The organic extracts have the highest content of total polyphenols compared to the aqueous extracts. The richness of organic extracts compared to aqueous extracts could be explained by the capacity of organic solvents to extract bioactive molecules. According to Toledo-Guillén and collaborators, extraction by organic solvents is more efficient to obtain bioactive compounds [46].

In the same operating conditions, the work carried out in our laboratory by Senhaji and her collaborators on a plant of the same family showed that the decoctate and the aqueous macerate have high contents of total polyphenols (1.78 ± 0.003 and 0.92 ± 0.03 mg EAG/g E); moreover, ethyl acetate is the recommended solvent for the extraction of polyphenols from the aerial part of *Anabasis aretioïdes* [16]. Another study conducted by Bouabid and her collaborators revealed that polyphenols are very abundant in the methanolic macerate of *Atractylis gummifera* (102.88 ± 1.38 mg EAG/g E) [13]. According to Senhaji and her collaborators, decoction is the mode that allows a high extraction of polyphenols (3.75 ± 0.02 EAG/g E) from the aerial part of *Ajuga iva* subsp. pseudoiva [15]. Boulfia and his collaborators found that the acetone macerate of *Juglans regia* bark is the richest in phenolic compounds (327.972 ± 0.06 μg EAG/mg E) [14].

As for the flavonoids, they are clearly abundant in all the aqueous extracts of the aerial part of *Haloxylon scoparium*; the decoctate comes first with a content of 306.59 ± 4.35 Ug EAG/mg E, followed, respectively, by the infused (228.67 ± 10.87 Ug EAG/mg E) and the macerated (135.78 ± 3.57 Ug EAG/mg E), with a significant difference between the three aqueous extracts.

The flavonoid content of the organic extracts increased with the degree of polarity of the organic solvents used for extraction; this could be explained by the variation in the solubility of phenolic compounds depending on the polarity of the extraction solvent used. Furthermore, in the present study, the highest content was obtained in the methanolic extract prepared hot in Soxhlet and methanolic macerate with a statistically insignificant difference; methanol could be recommended for the extraction of flavonoids.

However, the content recorded by the decoctate exceeds that of the chloroform and petroleum ether extracts, which could be explained, on the one hand, by the high polarity of water compared to chloroform and petroleum ether and, on the other hand, by the high polarity and water solubility of the flavonoids present in the aerial part of *Haloxylon scoparium*. In addition, the high temperature could favour the solubility of the flavonoids contained in the plant. Tan and Kassim conducted a phytochemical study on the plant *R. apiculata* and found that the flavonoid content increases with increasing temperature and that the amount of flavonoids extracted by water at 90°C exceeds that of ethanolic and acetone extracts [47].

According to a study conducted in Algeria, Ziani and collaborators found that the infused aerial part of *Haloxylon scoparium* has a polyphenol content of 230 ± 8 mg GAE/g E and a flavonoid content of 56 ± 1 mg CE/g E [48]. Another study conducted in Algeria by Chaouche and collaborators revealed that the hydromethanolic extract of the aerial part of *H. articulatum* has low contents of total polyphenols and flavonoids compared to the content of our methanolic extract [49]. Another Tunisian study was conducted by Bouaziz and collaborators [50] and revealed that the total polyphenol content of the methanolic extract of *H. scoparium* leaves is 59.75 ± 1.80 mg GAE/g, which is low compared to that of our methanolic extract. The difference in these results can be explained by factors related to the harvesting of the plant such as geographical location, harvesting season, maturity stage of the harvested plant, part of the plant harvested, and factors related to the experiment such as plant/solvent ratio, temperature, and extraction time. These same deductions and conclusions were found from several works carried out on several plants from the same region of Taza, Morocco, in our laboratory [13–16]. Indeed, Bouabid and collaborators found that the methanolic macerate of the aerial part of *Atractylis*

gummifera has a flavonoid content of the order of 17.25 ± 0.06 mg ER/g E [13]. Boulfia and collaborators found that the acetone macerate of *Juglans regia* bark contains the highest flavonoid content (1267.981 ± 2.911 μg EQ/mg E) [14]. According to Senhaji and collaborators, the ethyl acetate extract of *Ajuga iva* is the mode that allows high flavonoid extraction (22.40 ± 0.36 mg ER/g E) [15]. In contrast, a phytochemical study conducted by Senhaji and collaborators on the aerial part of *Anabasis aretioides*, which belongs to the Chenopodiaceae family, showed a complete absence of flavonoids [16].

Concerning the tannin content, it varies according to the extracts analysed. For the aqueous extracts, tannins are poorly present, which could be explained by the low solubility of condensed tannins in water. According to Gun'ko et al., tannins are less soluble in water due to the low surface area accessible to water molecules [51]. In addition, the large value recorded for aqueous extracts was for the decoctate (3.78 ± 0.35 Ug EC/mg E), which could be due to the ability of hot water to extract condensed tannins. These results agree with those obtained by Tan and Kassim on *R. apiculata*, who found that condensed tannins are more soluble in water at high temperatures [47]. A study done in Algeria by Chaouche and collaborators revealed that the hydromethanolic extract of the aerial part of *H. articulatum* presents a content of 9.98 ± 1.6 mg EC/g dry matter [49].

For the organic extracts, the highest tannin value was recorded by ethyl acetate (23.69 ± 0.6 mg EC/g E) and chloroform (21.25 ± 2.25 mg EC/g E) with a statistically nonsignificant difference, followed by petroleum ether and Soxhlet methanolic extracts, respectively. However, the methanolic macerate showed low tannin content. The difference obtained between the two extracts (methanolic extract and methanolic macerate) prepared with the same methanolic solvent allows us to confirm that hot extraction allows better extraction of tannins.

These differences could be due to the properties of the tannins in the test portion to solubilise in the solvents used. According to Bele et al., tannins are generally divided into hydrolysable and condensed tannins; the former can be hydrolysed by weak acids and bases to produce carbohydrates and phenolic acids. However, condensed tannins are not susceptible to hydrolytic cleavage [52].

As a comparison, work carried out under the same operating conditions in our laboratory by Bouabid and collaborators revealed that the methanolic macerate of *Atractylis gummifera* is richer in catechic tannins (144.09 ± 3.96 mg EC/g E) [13]; acetone macerate of *Juglans regia* bark is rich in tannins (38.056 ± 1.886 μg EC/g E) [14]; aqueous macerated of *Ajuga iva* allows a high extraction of catechic tannins (15.49 ± 0.17 mg EC/g E) [15]; and ethyl acetate extract of the aerial part of *Anabasis aretioides* of the Chenopodiaceae family has the highest tannin content (46.46 ± 0.67 mg EC/g E) [16].

4.3. In Vitro Study of Antidiabetic Activity. The *in vitro* antihyperglycaemic effect of aqueous and organic extracts of *Haloxylon scoparium* carried out by the enzymatic inhibition tests of *a*-amylase, *a*-glucosidase, and *ß*-galactosidase showed that all the extracts possess inhibitory activity with different degrees. The decoctate had an inhibitory effect against *a*-amylase with IC50 = 66855.66 ± 10519.25 ug/mL, which is higher than those of the infused and aqueous macerate, which could be explained by the ability of the high temperature to extract molecules that have the capacity to inhibit *a*-amylase. Ethyl acetate shows the best *a*-amylase inhibitory activity compared to other organic extracts; this *a*-amylase inhibitory activity is probably related to the presence of phenolic compounds in this plant. Hanhineva and collaborators reported that flavonoids, phenolic acids, and tannins inhibit the activity of enzymes such as *a*-amylase and *a*-glucosidase [53]. This is proved by the phytochemical study we performed, which revealed that ethyl acetate extract has the high content of catechic tannins (23.69 ± 0.6 Ug EC/mg E) among other organic extracts.

For the *a*-glucosidase assay, all products showed a very high activity compared to the reference standard. For the aqueous extracts, the decoctate showed an inhibitory activity with IC50 = 181.7 ± 21.15 ug/mL, which is higher than those obtained by the infused (IC50 = 225.44 ± 58.43 ug/mL) and the aqueous macerate (IC50 = 202.1 ± 75.44 ug/mL). The decoctate shows a significantly higher activity than acarbose (IC50 = 195 ± 6.12 ug/mL) with a statistically nonsignificant difference. This effect may be due to the presence of secondary metabolites extracted at high temperature. For organic extracts, the inhibitory activity of *a*-glucosidase was recorded according to this order: methanolic extract > methanolic macerate > ethyl acetate extract > chloroformic extract > petroleum ether extract, which shows that the inhibitory activity varies according to the polarity of the solvents used for extraction; a recent study carried out in Japan by Dirar and collaborators showed that polar extracts of *G. senegalensis* exhibited better inhibitory activity on *a*-glucosidase [54].

The results of enzymatic inhibition of *ß*-galactosidase of the aqueous extracts show that the infused comes first, followed, respectively, by the aqueous macerated and lastly the decocted which could be explained by the nature of the molecules responsible for the activity which are degradable at high temperature at a longer duration. For the organic extracts, ethyl acetate extract presents the best inhibitory activity with an IC50 of 1601.66 ± 107.21 ug/mL followed, respectively, by chloroformic extract (IC50 = 1707.66 ± 12.99 ug/mL), methanolic extract (IC50 = 1735.66 ± 269.50 ug/mL), petroleum ether extract (IC50 = 1819.66 ± 172.29 ug/mL), and finally methanolic macerate (IC50 = 1984.66 ± 61.65 ug/mL). These results are in agreement with those obtained by El Omari and collaborators on *A. longa* who found that the ethyl acetate fraction had the highest inhibitory activity against *ß*-galactosidase (12.70 ± 1.27%) and the methanolic fraction showed moderate inhibition of *ß*-galactosidase (2.05 ± 1.22%) [55]. The degree of inhibitory activity of aqueous and organic extracts of *Haloxylon scoparium* varies from test to test; according to Chiba and collaborators the differences between the enzymes *a*-amylase and *ß*-galactosidase is due to structural differences related to the origin of the enzymes [56].

The antidiabetic activity could be not only due to the phenolic compounds, flavonoids, and catechic tannins but also due to the mineral compounds contained in the studied part: calcium, potassium, magnesium, and sodium are involved in the glucose metabolism [34]. Calcium improves glucose tolerance. In case of deficiency, its metabolism may be directly involved in the occurrence of noninsulin-dependent diabetes [57]. Potassium is involved in the production of glycogen and the secretion of hormones, particularly insulin. Its deficiency is responsible for glucose intolerance [58]. Magnesium is an enzyme activator; it increases insulin secretion and facilitates the use of glucose [59]. The aerial part of *Haloxylon scoparium* is rich in mineral elements (Fe, K, Mg, P, Na, Cu, Ca, and Sr) that can contribute to glucose metabolism. A recent study conducted by Boulfia and his collaborators found that *Juglans regia* L. bark has several minerals (Fe (19849.8), K (3487.8), Mg (2631.03), and P (691.02) mg/kg); these values remain lower than those found by our study. Similarly the antidiabetic activity that we obtained is higher compared to the ethanolic extract of *Juglans regia* L. bark for the *a*-amylase (IC50 = 7806.33 ± 85.08 μg/mL) and *a*-glucosidase (IC50 = 488.83 ± 36.34 μg/mL) inhibition tests [60]. Therefore, a richness of the aerial part of *Haloxylon scoparium* in mineral compounds could explain the hypoglycemic effect of its extracts.

An *in vitro* antihyperglycaemic study conducted by Bouabid and her collaborators in our laboratory under the same experimental conditions on extracts prepared at different polarity from *Atractylis gummifera* harvested in the region of Taza, Morocco, showed that the methanolic macerate presents the highest inhibitory activity for the three enzymes *a*-amylase (IC50 = 557 ± 0.013 ug/mL), *a*-glucosidase (IC50 = 743 ± 0.017 ug/mL), and *ß*-galactosidase(IC50 = 2443 ± 0.071 ug/mL) [12].

4.4. In Vitro Antioxidant Activity. The study showed that the aqueous and organic extracts studied have an interesting antioxidant power, mainly those prepared by the solvents methanol, ethyl acetate, and chloroform for the organic extracts and the decoctate for the aqueous extracts.

4.4.1. Hydrogen Peroxide Scavenging Activity. The results of the activity of the aqueous extracts obtained reveal that the decoctate has the best hydrogen peroxide scavenging activity compared to the infused and the aqueous macerate which can be attributed to its high flavonoid content. According to Ghedira, the best described property of flavonoids is their antioxidant activity and their ability to neutralise free radicals through their highly reactive hydroxyl group (C3-OH) [61].

For the organic extracts, the hydrogen peroxide (H_2O_2) blocking activity revealed that the methanolic extract has the highest free radical scavenging capacity with a value of 20.91 ± 0.27%, which is in agreement with the high polyphenol and flavonoid contents of this extract. However, the methanolic macerated extract shows a lower free radical scavenging activity against hydrogen peroxide, but very close to those of ethyl acetate, chloroformic, and petroleum ether extracts with a statistically nonsignificant difference.

With the hydrogen peroxide (H_2O_2) blocking test, we noted a strong capacity to neutralise hydrogen peroxide of the methanolic extract and the aqueous decoctate superior to that of the reference standard ascorbic acid. Thus, we can deduce that the molecules responsible for hydrogen peroxide scavenging are best extracted by high polarity and high temperature solvents. Furthermore, the hydrogen peroxide scavenging capacity may be due to the richness of the studied part in mineral compounds (Fe, K, Mg, P, Na, Cu, Ca, and Sr); this is in agreement with a study conducted on *Phoenix dactylifera* fruits which showed a high correlation between the H_2O_2 test and K content ($r^2 = 0.889$) [29].

In the same operating conditions, the phytochemical study conducted on *Atractylis gummifera* revealed that the best antioxidant activity via the H_2O_2 test (19.24 ± 1.102%) was obtained by the methanolic macerate [13]. Furthermore, the acetone-macerated extract of *Juglans regia* showed a high antioxidant activity by the H_2O_2 test (24.13 ± 1.81%) [14]. In addition, a phytochemical study conducted on *Ajuga iva* showed that the methanolic macerate had an antioxidant activity of 22.17 ± 0.30% for the H_2O_2 test [15]. Another phytochemical study conducted on *Anabasis aretioides* which belongs to the same family of *Haloxylon scoparium* showed that the aqueous macerate exhibits the highest antioxidant activity for the H_2O_2 test (7.84 ± 0.44%) [16].

4.4.2. DPPH Radical Scavenging Activity. According to the results obtained with the DPPH test, the aqueous extracts present relatively high IC50 values which indicates a low antiradical power in contrast to the organic extracts which present a high antiradical power; we noticed that the IC50 values of the organic extracts range from 39.63 ± 2.03 for the methanolic extract to 297.8 ± 1.15 μg/mL for the petroleum ether extract. A strong free radical scavenging capacity is noted for the methanolic extract prepared under hot Soxhlet conditions, the aqueous macerate, and the ethyl acetate extract with a statistically nonsignificant difference. This is probably due to the richness of these extracts in phenolic compounds including total polyphenols, tannins, and flavonoids, which gives a better antiradical activity. These results are in agreement with the contents of quantified phenolic compounds. Similarly, Turkmen and collaborators found a significant correlation between total polyphenols extracted from black tea and free radical scavenging activity via the DPPH test [62]. Additionally, the antiradical activity of the different extracts studied could be due to the mineralogical richness of *Haloxylon scoparium*. According to Tamuly and his collaborators, there is a positive correlation between the K content and the capacity to trap the free radical DPPH [63].

For the comparative purposes, the antiradical power of our methanolic and methanolic macerated extract are stronger than that of the hydromethanolic extract of the aerial part of *Haloxylon scoparium* tested by Chaouche and collaborators in Algeria (IC50 = 6.32±0.25 mg/mL) [49]. Furthermore, our extracts are more potent compared to a

study done by Miguel and collaborators in Portugal on the hydroalcoholic extract of the aerial part of *H. articulatum* (IC50 = 1.867 ± 0.061 mg/ml) [64]. The results obtained by Bouaziz and collaborators with the aqueous extract of *H. scoparia* leaves from Tunisia showed a high antiradical activity with an IC50 value in the range of 28 ± 0.70 μg/mL [50].

In the same conditions of operation, phytochemical studies recently conducted in our laboratory with the DPPH test showed that the best antioxidant activity of *Atractylis gummifera* was obtained with the aqueous macerate which was found to be the most active (IC50 = 2.78 ± 1.03 μg/mL) [13]. Moreover, the acetone macerate of *Juglans regia* has the highest antioxidant activity (IC50 = 5.573 µg/ml) [14]. In addition, the methanolic extract of *Ajuga iva* is the most active (IC50 = 78.40 ± 5.24 µg/mL) [15]. Another phytochemical study conducted on the aerial part of a plant of the Chenopodiaceae family, *Anabasis aretioides*, indicated that the methanolic macerate has the high level of antioxidant activity (IC50 = 52.91 ± 0.24 μg/ml) [16].

4.4.3. Equivalent Antioxidant Capacity of Trolox (TEAC or ABTS). According to the ABTS test, we noticed that the aqueous extracts present an antiradical activity with a nonsignificant difference; this could be explained by the composition of these extracts in polyphenols and catechic tannins with statistically nonsignificant values.

The results also show that the organic extracts present a remarkable antioxidant effect towards the ABTS radical. The best antioxidant activity to trap the ABTS free radical was obtained by the methanolic extract (50.75 ± 0.72 Ug E AA/mg E) and the methanolic macerate (47.71 ± 1.21 Ug E AA/mg E) with a statistically nonsignificant difference. This activity is correlated with their high content of total polyphenol and flavonoids compared to the other extracts.

In addition, the decoctate presents a significant antiradical activity among the aqueous extracts, which is also higher than that of the organic petroleum ether extract; this could be explained, on the one hand, by the variability of the solubilisation capacity of the $ABTS^{\bullet+}$ radical in the organic and aqueous media and, on the other hand, by the richness of the decoctate in flavonoids. Bhouri and collaborators reported that flavonoids have a potential activity towards the $ABTS^{\bullet+}$ radical due to the fact that they are rich in hydroxyl groups and therefore stabilise the reactive oxygen species by reaction with the reactive compound of the radical. Because of the high reactivity of the hydroxyl group of flavonoids, the radicals are inactivated [65]. Moreover, the free radical scavenging activity of the ABTS test could be due to the neutralisation of the $ABTS^{\bullet+}$ radical by some minerals contained in the plant; according to Gordon, K plays a role in the activation of enzymes that promote the biosynthesis of flavonoids and phenolic compounds, the latter being endowed with an important antioxidant power [66]. Furthermore, in a study conducted by Chaouche and collaborators in Algeria on the hydromethanolic extract of the aerial part of *Haloxylon articulatum* with the ABTS assay, they obtained an IC50 value in the order of 40.94 ± 3.30 mg/mL [49].

With the same operating conditions, Bouabid and collaborators found that the methanolic macerate of *Atractylis gummifera L* has given the strongest antioxidant activity in the ABTS test (122.6 ± 0.63 mg TE/g E) [13]. Boulfia and collaborators found that the acetone macerate showed the most strong antioxidant activity in the ABTS test (602.29 ± 0.34 μg ET/mg E) [14]. In addition, Senhaji et al. conducted a study on *Ajuga iva* under the same operating conditions as our work and found that the chloroform extract was the most active in the ABTS test (27.33 ± 1.08 μg TE mg-1E) [15]. Another study conducted on a plant of the Chenopodiaceae family, *Anabasis aretioides*, showed that the methanolic macerate exhibited the most high level of antioxidant activity in the ABTS test (48.99 ± 1.316 μg TE/mg E) [16].

4.4.4. Ferric Reducing Antioxidant Power (FRAP) Assay. For the FRAP test, all extracts showed reducing power. The aqueous, decocted and infused extracts show high iron reducing capacity with a statistically insignificant difference, while the aqueous macerate exerts a less remarkable reducing activity with a significant difference to the decocted and a nonsignificant difference to the infused. The compounds responsible for iron reduction are present in the aqueous extracts prepared at high temperature. This activity of the aqueous extract is probably due to the presence of a high level of flavonoids demonstrated in the secondary metabolite assay. Our results are in agreement with a recent work by Hmidani and collaborators on *Thymus atlanticus*; they found that the decoctate has a significant reducing power (19.06 ± 0.54 μmol Trolox E/1 g DM) than the aqueous macerate (4.37 ± 0.24 μmol Trolox E/1 g DM) [67].

Concerning the organic extracts, the reducing power increases with the increase of the polarity of the solvent used; the methanolic extract, the methanolic macerated extract, and the ethyl acetate extract present the highest powers to convert ferric (Fe^{3+}) into ferrous (Fe^{2+}) with a significant difference. This could be related to the high amount of total polyphenols and flavonoids in these extracts. In addition, the chloroformic extract shows an average but higher reducing capacity than the petroleum ether extract with a significant difference; the latter contains lower contents of total polyphenols (11.30 ± 1.58 Ug EAG/mg E) than the other organic extracts. This result is in agreement with a study done by Saffarzadeh-Matin and Khosrowshahi in which they found a correlation between the FRAP test and the content of phenolic compounds and flavonoids contained in the ethanolic extract of *Punica granatum* harvested in Iran [68]. In addition, according to Mohamed and his collaborators, the FRAP test of date fruits showed a highly significant positive correlation with K ($r^2 = 0.800$) and Ca ($r^2 = 0.664$) [29].

In the same operating conditions with the FRAP test, Bouabid and collaborators found that the aqueous macerate of *Atractylis gummifera L* showed the strongest antioxidant activity (102.5 ± 1.66 mg TE/g E) [13]. The macerated

acetone extract of *Juglans regia* bark showed the best antioxidant activity (759.11 ± 0.27 μg TE/mg E) [14]. In addition, a phytochemical study on the aerial part of *Ajuga iva* subsp. revealed that the methanolic extract had a reducing power of 22.70 ± 0.19 mg TE/g E [15]. Another phytochemical study conducted on *Anabasis aretioides* of the Chenopodiaceae family showed that the methanolic macerate had the highest antioxidant activity (99.73 ± 3.570 μg TE/mg E) [16].

4.4.5. Reducing Power Assay. Concerning the reducing power (RP) test, we found that the iron reduction profile of the aqueous extracts increases with the increase of temperature; this increase is more marked for the decoctate with a value of 21.89 ± 1.04 Ug E AA/mg E, and this same extract showed a high content of phenolic compounds that are probably responsible for its reducing power. According to El Moussaoui and collaborators, the presence of hydroxylated compounds in the phytochemicals of plant extracts gives them a reducing power and they can be used as electron donors [69].

For the organic extracts, we found that the reducing capacity is proportional to the increase of the polarity of the extracts. The highest reducing power was recorded by the methanolic extract and the methanolic macerate with a statistically nonsignificant difference. In the secondary metabolite assay performed, these two extracts showed higher contents of total polyphenols and flavonoids. The ethyl acetate and chloroform extracts also expressed a high reducing power with a nonsignificant difference; although they had lower quantities of polyphenols, but they had the highest contents of catechic tannins compared to the other organic extracts, which are probably responsible for the reducing power for these two extracts.

A comparison with studies conducted in our laboratory under the same operating conditions on the RP test showed that the aqueous macerated of *Atractylis gummifera L* had the highest antioxidant activity with the PR test (96.15 ± 1.12 mg EAA/g E) [13]. For *Juglans regia*, acetone macerate has the best antioxidant activity (685.68 ± 0.82 μg EAA/g E) [14]. In addition, the methanolic extract of *Ajuga iva* had the highest reducing power (21.55 ± 0.18 μg AAE/mg E) [15]. Another study conducted on a plant of the same family of *Haloxylon scoparium*, *Anabasis aretioides*, showed that the methanolic macerate had the best antioxidant activity (72.176 ± 0.540 μg AAE/mg E) [16].

4.5. Principal Component Analysis (PCA). According to the results obtained from the correlation matrix, the ABTS test is highly positively correlated with the DPPH test ($r^2 = 0.9693$), which can be explained by the fact that both tests involve the same mechanisms of action, which consist in giving up electrons or hydrogens to eliminate free radicals. The FRAP test is highly positively correlated with the reducing power (RP) test ($r^2 = 0.9845$) and with the DPPH ($r^2 = 0.9424$) and ABTS ($r^2 = 0.9713$) test. The high positive correlation between all the tests probably testifies to the presence in our extracts of antioxidant molecules which can intervene by two types of reaction mechanisms. In the FRAP and RP tests, there is a reduction of Fe(III), based only on electron transfer, whereas in the DPPH and ABTS tests, the radicals can be neutralised either by direct reduction via electron transfer or by radical scavenging via hydrogen atom transfer [70]. Similar results were obtained in our laboratory with other plants from the region of Taza, Morocco, and reported by Senhaji and collaborators showing the presence of a strong correlation among DPPH, ABTS, FRAP, and PR tests realised on *Ajuga iva* and on *Anabasis aretioïdes* which belong to the same family of *Haloxylon scoparium*, Chenopodiaceae [15,16].

The four antioxidant activity tests, DPPH, ABTS, FRAP, and PR, had shown a strong positive correlation with the total polyphenol content of the aqueous and organic extracts; this correlation suggests that these phenolic compounds thus contribute to antioxidant power by two mechanisms. They have redox properties allowing them to act as both hydrogen and electron donating agents [71]. A study by Kourouma and collaborators on twenty-five sweet potato varieties showed a high positive correlation between total phenols and DPPH, ABTS, and FRAP tests [72]. Prior and collaborators also report that the antioxidant capacity assessed by the FRAP test appears to be related to the degree of hydroxylation and conjugation capacity of polyphenols [70]. According to Lv and collaborators, the high antioxidant activities exhibited by plant extracts are due to the presence of polyphenolic compound [73]. Other studies have not established this correlation and have reported that antioxidant activity is positively correlated with the structure of polyphenols [74].

In the same operative conditions, works carried out in our laboratory on other plants of the region of Taza and reported by Boulfia and his collaborators have revealed that phenolic compounds, flavonoids, and tannins are strongly correlated with the antioxidant activity of *Juglans regia* [13]. In addition, Senhaji and collaborators showed a strong correlation among DPPH, ABTS, FRAP, and PR assays carried out on the aerial part of *Ajuga iva* subsp. pseudoiva and on the aerial part of *Anabasis aretioides*, a plant of the Chenopodiaceae family [15,16].

Our results from PCA analysis also show a strong positive correlation between total polyphenol content and flavonoid content, which probably indicates that total polyphenols in the aerial part are predominantly in the form of flavonoids. In concordance with our results, a recent study by Senhaji and her collaborators reported a strong positive correlation between total polyphenol and flavonoid content in the aerial part of *Ajuga iva* [15].

The study of the antihyperglycaemic activity *in vitro* showed a high correlation between the *a*-amylase inhibitory activity and the DPPH ($r^2 = 0.8094$), ABTS ($r^2 = 0.8237$), FRAP ($r^2 = 0.8115$), and PR ($r^2 = 0.8508$) tests. The correlation between antioxidant activity and antidiabetic activity could be explained, on the one hand, by the particularity of the molecules contained in the aerial part of *Haloxylon scoparium* to have both antioxidant and antidiabetic power and, on the other hand, by the existence of a

link between oxidative stress and diabetes. Reactive oxygen species (ROS) can participate in the development of diabetes by altering the action of insulin and destroying the beta cells of the pancreas [75]. A study conducted in Iran on *R. turkestanicum* reported a high correlation between DPPH assay and inhibitory activity by *a*-amylase ($r^2 = 0.897$) [75].

The *a*-amylase is strongly positively correlated with total polyphenol ($r^2 = 0.7721$) and flavonoid ($r^2 = 0.7162$) content. According to Sales et al., polyphenols and flavonoids inhibit the enzyme *a*-amylase through the formation of hydrogen bonds between its hydroxyl groups and the residues of the binding site of this enzyme [76].

The *in vitro* inhibitory activity by the enzymes *a*-glucosidase and *ß*-galactosidase is moderately positively correlated with the H_2O_2 antioxidant activity test with values of $r^2 = 0.4885$ and $r^2 = 0.0412$, respectively. A study conducted in Malaysia reported the existence of a strong correlation between antioxidant activity and *a*-glucosidase assay of *Ficus deltoidea* water fraction ($R = 0.998$) [77].

According to the results presented in this study, among the organic extracts tested, we found that the methanolic extract with Soxhlet showed high antioxidant and antidiabetic activity compared to the other organic extracts prepared. Similarly, for the aqueous extracts, it was the decoctate that showed high antioxidant and antidiabetic capacity among the other aqueous extracts. It seems from these results that polarity and temperature would play a crucial role in extracting molecules that are responsible for the antioxidant and antidiabetic activity of the aerial part of *Haloxylon scoparium*.

5. Conclusion

The results obtained in this study show that the aerial part of *Haloxylon scoparium* is rich in mineral elements (Fe, k, Mg, P, Na, Cu, Ca, and Sr), which may be responsible for the biological effects found in this part of the plant. Furthermore, the phytochemical screening carried out by means of characterisation reactions revealed the richness of the studied aerial part of the *Haloxylon scoparium* plant in secondary metabolites: alkaloids, tannins, saponins, flavonoids, quinones, and anthracenosides.

The quantification by spectrophotometric methods of the contents of secondary metabolites showed that the extracts tested have high contents of total polyphenols, flavonoids, and catechic tannins which may confer biological and pharmacological activities to the plant. This contributes to confirm its use in traditional medicine for the treatment of several anomalies.

The *in vitro* evaluation of the antidiabetic activity showed that the decoctate has a higher inhibitory capacity on *a*-glucosidase than acarbose, ethyl acetate extract has the best inhibitory capacity on *ß*-galactosidase and *a*-amylase, and methanolic extract and macerated methanol had an inhibitory effect on *a*-glucosidase.

The study of antioxidant properties of aqueous and organic extracts showed that the aerial part of *Haloxylon scoparium* has free radical scavenging potential. The decoctate showed the best antioxidant activity among the aqueous extracts and for the organic extracts, the methanolic extract and the macerated methanol showed the highest antioxidant activity, respectively.

The principal component analysis (PCA) showed a positive correlation of the antidiabetic activity with the polyphenol and catechic tannin content and with the antioxidant activity tests. PCA also showed a high positive correlation between the four antioxidant activity tests, DPPH, ABTS, FRAP, and PR, performed on the aerial part of *Haloxylon scoparium* and between the antioxidant power and the content of total polyphenols and flavonoids.

These results represent a first step in the research on the mineral composition and active principles of the secondary metabolites and their antioxidant activity of *Haloxylon scoparium* and constitute a support to carry out, on the one hand, *in vivo* tests to confirm the results obtained *in vitro* and, on the other hand, to continue the chemical study in order to identify precisely the compounds responsible for the biological and pharmacological activities of the plant.

Abbreviations

H. scoparium:	*Haloxylon scoparium*
ROS:	Reactive oxygen species
H_2O_2:	Hydrogen peroxide scavenging assay
TEAC or ABTS:	Trolox equivalent antioxidant capacity method/ABTS radical cation decolorization assay
FRAP:	Ferric reducing antioxidant power assay
RP:	Reducing power method
DPPH:	1,1-diphenyl-2-picrylhydrazyl scavenging activity
PCA:	Principal component analysis
ANOVA:	Analysis of variance
IC50:	Concentration that causes 50% inhibition.

Data Availability

The experimental data used to support the findings of this study are incorporated into the article.

Conflicts of Interest

The authors declare that they have no conflicts of interest.

Authors' Contributions

NL performed experimental studies, statistical analysis, and manuscript preparation. FL designed the experiments, provided consistent guidance, analysed the data, prepared manuscript, reviewed and edited the final version, and submitted it for publication. KB, MB, and SS participated in the experimental studies. MS participated in the statistical analysis. HT designed the experiments, provided consistent guidance, and performed manuscript preparation and review.

Acknowledgments

The authors thank the CURI Center (Regional University Interface Center), Sidi Mohamed Ben Abdellah University of Fez (USMBA), Morocco, for the determination of the mineral composition of the plant and Dr. Abdelmajid Khabbach for the botanical identification of the plant. This study was conducted with the support of Sidi Mohamed Ben Abdellah University (USMBA).

References

[1] M. A. Martín and S. Ramos, "Cocoa polyphenols in oxidative stress: potential health implications," *Journal of Functional Foods*, vol. 27, pp. 570–588, 2016.

[2] L. Marseglia, G. D'Angelo, R. Granese et al., "Role of oxidative stress in neonatal respiratory distress syndrome," *Free Radical Biology and Medicine*, vol. 142, pp. 132–137, 2019.

[3] M. Goodman, R. M. Bostick, O. Kucuk, and D. P. Jones, "Clinical trials of antioxidants as cancer prevention agents: past, present, and future," *Free Radical Biology and Medicine*, vol. 51, no. 5, pp. 1068–1084, 2011.

[4] A. Sallé, "Le diabète, facteur de dénutrition et de carences en micronutriments?" *Nutrition Clinique et Metabolisme*, vol. 32, no. 1, pp. 8–21, 2018.

[5] M. Rahimi-Madiseh, A. Malekpour-Tehrani, M. Bahmani, and M. Rafieian-Kopaei, "The research and development on the antioxidants in prevention of diabetic complications," *Asian Pacific Journal of Tropical Medicine*, vol. 9, no. 9, pp. 825–831, 2016.

[6] A. Taleb, K. A. Ahmad, A. U. Ihsan et al., "Antioxidant effects and mechanism of silymarin in oxidative stress induced cardiovascular diseases," *Biomedicine & Pharmacotherapy*, vol. 102, pp. 689–698, 2018.

[7] F. Lamchouri, T. Benali, B. Bennani, H. Toufik, L. I. M. Hassani, and B. Lyoussi, "Preliminary phytochemical and antimicrobial investigations of extracts of Haloxylon scoparium," *Journal of Materials and Environmental Science*, vol. 3, no. 4, pp. 754–759, 2012.

[8] H. Najjaa, A. B. Arfa, Á. Máthé, and M. Neffati, "Aromatic and medicinal plants of Tunisian arid and desert zone used in traditional medicine, for drug discovery and biotechnological applications," *Medicinal and Aromatic Plants of the World*, vol. 3, pp. 157–230, 2017.

[9] M. Eddouks, M. Maghrani, A. Lemhadri, M.-L. Ouahidi, and H. Jouad, "Ethnopharmacological survey of medicinal plants used for the treatment of diabetes mellitus, hypertension and cardiac diseases in the south-east region of Morocco (Tafilalet)," *Journal of Ethnopharmacology*, vol. 82, no. 2-3, pp. 97–103, 2002.

[10] M. Bnouham, H. Mekhfi, A. Legssyer, and A. Ziyyat, "Medicinal plants used in the treatment of diabetes in Morocco," *International Journal of Diabetes and Metabolism*, vol. 10, pp. 33–50, 2002.

[11] M. Arora, B. Kiran, S. Rani, A. Rani, B. Kaur, and N. Mittal, "Heavy metal accumulation in vegetables irrigated with water from different sources," *Food Chemistry*, vol. 111, no. 5, pp. 811–815, 2008.

[12] K. Bouabid, F. Lamchouri, H. Toufik, K. Sayah, Y. Cherrah, and M. E. A. Faouzi, "Phytochemical screening and in vitro evaluation of alpha amylase, alpha glucosidase and beta galactosidase inhibition by aqueous and organic Atractylis gummifera L. extracts," *Plant Science Today*, vol. 5, no. 3, pp. 103–112, 2018.

[13] K. Bouabid, F. Lamchouri, H. Toufik, and M. E. A. Faouzi, "Phytochemical investigation, in vitro and in vivo antioxidant properties of aqueous and organic extracts of toxic plant: Atractylis gummifera L," *Journal of Ethnopharmacology*, vol. 253, Article ID 112640, 2020.

[14] M. Boulfia, F. Lamchouri, and H. Toufik, "Chemical analysis, phenolic content, and antioxidant activities of aqueous and organic Moroccan *Juglans regia* L. Bark extracts," *Current Bioactive Compounds*, vol. 16, no. 9, pp. 1328–1339, 2020.

[15] S. Senhaji, F. Lamchouri, K. Bouabid et al., "Phenolic contents and antioxidant properties of aqueous and organic extracts of a Moroccan Ajuga iva subsp. pseudoiva," *Journal of Herbs, Spices, & Medicinal Plants*, vol. 26, no. 3, pp. 248–266, 2020.

[16] S. Senhaji, F. Lamchouri, and H. Toufik, "Phytochemical content, antibacterial and antioxidant potential of endemic plant anabasis aretioïdes Coss. & Moq. (Chenopodiaceae)," *BioMed Research International*, vol. 2020, Article ID 6152932, 16 pages, 2020.

[17] V. L. Singleton, R. Orthofer, and R. M. Lamuela-Raventós, "Analysis of total phenols and other oxidation substrates and antioxidants by means of folin-ciocalteu reagent," *Oxidants and Antioxidants Part A*, vol. 299, pp. 152–178, 1999.

[18] C. M. Mihai, L. A. Mărghitaş, O. Bobiş, D. Dezmirean, and M. Tămaş, "Estimation of flavonoid content in propolis by two different colorimetric methods," *Scientific Papers Animal Science and Biotechnologies*, vol. 43, no. 1, pp. 407–410, 2010.

[19] R. Julkunen-Tiitto, "Phenolic constituents in the leaves of northern willows: methods for the analysis of certain phenolics," *Journal of Agricultural and Food Chemistry*, vol. 33, no. 2, pp. 213–217, 1985.

[20] M. N. Wickramaratne, J. C. Punchihewa, D. B. M. Wickramaratne, and D. B. M. Wickramaratne, "*In-vitro* alpha amylase inhibitory activity of the leaf extracts of *Adenanthera pavonina*," *BMC Complementary and Alternative Medicine*, vol. 16, no. 1, p. 466, 2016.

[21] S. Lordan, T. J. Smyth, A. Soler-Vila, C. Stanton, and R. P. Ross, "The &-amylase and & glucosidase inhibitory effects of Irish seaweed extracts," *Food Chemistry*, vol. 141, pp. 2170–2176, 2003.

[22] M. Pastore, F. Morisi, and A. Viglia, "Reduction of lactose of Milk by entrapped β-galactosidase. II. Conditions for an industrial continuous process," *Journal of Dairy Science*, vol. 57, no. 3, pp. 269–272, 1974.

[23] R. J. Ruch, S.-j. Cheng, and J. E. Klaunig, "Prevention of cytotoxicity and inhibition of intercellular communication by antioxidant catechins isolated from Chinese green tea," *Carcinogenesis*, vol. 10, no. 6, pp. 1003–1008, 1989.

[24] O. P. Sharma and T. K. Bhat, "DPPH antioxidant assay revisited," *Food Chemistry*, vol. 113, no. 4, pp. 1202–1205, 2009.

[25] R. Re, N. Pellegrini, A. Proteggente, A. Pannala, M. Yang, and C. Rice-Evans, "Antioxidant activity applying an improved ABTS radical cation decolorization assay," *Free Radical Biology and Medicine*, vol. 26, no. 9-10, pp. 1231–1237, 1999.

[26] I. F. F. Benzie and J. J. Strain, "The ferric reducing ability of plasma (FRAP) as a measure of "antioxidant power": the FRAP assay," *Analytical Biochemistry*, vol. 239, no. 1, pp. 70–76, 1996.

[27] M. Oyaizu, "Studies on products of browning reaction. Antioxidative activities of products of browning reaction prepared from glucosamine," *The Japanese journal of nutrition and dietetics*, vol. 44, no. 6, pp. 307–315, 1986.

[28] M. Boulfia, F. Lamchouri, S. Senhaji, N. Lachkar, K. Bouabid, and H. Toufik, "Mineral content, chemical analysis, *in vitro* antidiabetic and antioxidant activities, and antibacterial power of aqueous and organic extracts of Moroccan *Leopoldia comosa* (L.) parl. Bulbs," *Evidence-based Complementary and Alternative Medicine*, vol. 2021, pp. 1–17, 2021.

[29] R. M. A. Mohamed, A. S. M. Fageer, M. M. Eltayeb, and I. A. Mohamed Ahmed, "Chemical composition, antioxidant capacity, and mineral extractability of S udanese date palm (P hoenix dactylifera L.) fruits," *Food Sciences and Nutrition*, vol. 2, no. 5, pp. 478–489, 2014.

[30] E. R. Grela, W. Samolińska, B. Kiczorowska, R. Klebaniuk, and P. Kiczorowski, "Content of minerals and fatty acids and their correlation with phytochemical compounds and antioxidant activity of leguminous seeds," *Biological Trace Element Research*, vol. 180, no. 2, pp. 338–348, 2017.

[31] S. F. Sulaiman, N. A. M. Yusoff, I. M. Eldeen et al., "Correlation between total phenolic and mineral contents with antioxidant activity of eight Malaysian bananas (*Musa* sp.)," *Journal of Food Composition and Analysis*, vol. 24, no. 1, pp. 1–10, 2011.

[32] A. C. Akinmoladun, E. O. Ibukun, E. Afor et al., "Chemical constituents and antioxidant activity of *Alstonia boonei*," *African Journal of Biotechnology*, vol. 6, no. 10, pp. 1197–1201, 2007.

[33] P. Evans and B. Halliwell, "Micronutrients: oxidant/antioxidant status," *British Journal of Nutrition*, vol. 85, no. S2, p. S67, 2001.

[34] P. J. Lefebvre and A. J. Scheen, "Improving the action of insulin. Clinical and investigative medicine," *Medecine clinique et experimentale18*, no. 4, pp. 340–347, 1995.

[35] M. Hokayem, C. Bisbal, K. Lambert, and A. Avignon, "Quelle place pour les antioxydants dans la prévention du diabète de type 2 ?" *Médecine des Maladies Métaboliques*, vol. 6, no. 4, pp. 327–331, 2012.

[36] A. Jurinjak Tušek, M. Benković, A. Belščak Cvitanović, D. Valinger, T. Jurina, and J. Gajdoš Kljusurić, "Kinetics and thermodynamics of the solid-liquid extraction process of total polyphenols, antioxidants and extraction yield from Asteraceae plants," *Industrial Crops and Products*, vol. 91, pp. 205–214, 2016.

[37] H.-L. Kwon and M.-S. Chung, "Pilot-scale subcritical solvent extraction of curcuminoids from Curcuma long L," *Food Chemistry*, vol. 185, pp. 58–64, 2015.

[38] Z. Wu, H. Li, Y. Wang et al., "Optimization extraction, structural features and antitumor activity of polysaccharides from Z. jujuba cv. Ruoqiangzao seeds," *International Journal of Biological Macromolecules*, vol. 135, pp. 1151–1161, 2019.

[39] M. Zerriouh, S. Merghache, R. Djaziri, C. Selles, and F. Z. Sekkal, "Investigation of Hammada scoparia antidiabetic activity and toxicity in rat," *International Journal of Phytomedicine*, vol. 8, pp. 327–334, 2014.

[40] R. M. Jarraya, A. Bouaziz, B. Hamdi, A. Ben Salah, and M. Damak, "N-Methylisosalsoline from Hammada scoparia," *Acta Crystallographica Section E Structure Reports Online*, vol. 64, no. 9, p. o1714, 2008.

[41] M. L. R. M. G. Thomas and J. M. B. Filho, "Anti-inflammatory actions of tannins isolated from the bark of Anacardwm occidentale L," *Journal of Ethnopharmacology*, vol. 13, no. 3, pp. 289–300, 1985.

[42] C. N. Kunyanga, J. K. Imungi, M. Okoth, C. Momanyi, H. K. Biesalski, and V. Vadivel, "Antioxidant and antidiabetic properties of condensed tannins in acetonic extract of selected raw and processed indigenous food ingredients from Kenya," *Journal of Food Science*, vol. 76, no. 4, pp. C560–C567, 2011.

[43] P. Buzzini, P. Arapitsas, M. Goretti et al., "Antimicrobial and antiviral activity of hydrolysable tannins," *Mini Reviews in Medicinal Chemistry*, vol. 8, no. 12, pp. 1179–1187, 2008.

[44] A. Nafiunisa, N. Aryanti, and D. H. Wardhani, "Kinetic study of saponin extraction from sapindus rarak DC by ultrasound-assisted extraction methods," *Bulletin of Chemical Reaction Engineering and Catalysis*, vol. 14, no. 2, p. 468, 2019.

[45] E. Bourogaa, R. M. Jarraya, R. Nciri, M. Damak, and A. Elfeki, "Protective effects of aqueous extract of *Hammada scoparia* against hepatotoxicity induced by ethanol in the rat," *Toxicology and Industrial Health*, vol. 30, no. 2, pp. 113–122, 2014.

[46] A. R. Toledo-Guillén, I. Higuera-Ciapara, G. García-Navarrete, and J. C. De la Fuente, "Extraction of bioactive flavonoid compounds from orange (Cit-rus sinensis) peel using supercritical CO2," *Atherosclerosis*, vol. 178, pp. 25–32, 2010.

[47] K. W. Tan and M. J. Kassim, "A correlation study on the phenolic profiles and corrosion inhibition properties of mangrove tannins (*Rhizophora apiculata*) as affected by extraction solvents," *Corrosion Science*, vol. 53, no. 2, pp. 569–574, 2011.

[48] B. E. C. Ziani, R. C. Calhelha, J. C. M. Barreira, L. Barros, M. Hazzit, and I. C. F. R. Ferreira, "Bioactive properties of medicinal plants from the Algerian flora: selecting the species with the highest potential in view of application purposes," *Industrial Crops and Products*, vol. 77, pp. 582–589, 2015.

[49] T. M. Chaouche, F. Haddouchi, R. Ksouri, and F. Atik-Bekkara, "Evaluation of antioxidant activity of hydromethanolic extracts of some medicinal species from South Algeria," *Journal of the Chinese Medical Association*, vol. 77, no. 6, pp. 302–307, 2014.

[50] A. Bouaziz, D. Mhalla, I. Zouari et al., "Antibacterial and antioxidant activities of *Hammada scoparia* extracts and its major purified alkaloids," *South African Journal of Botany*, vol. 105, pp. 89–96, 2016.

[51] V. M. Gun'ko, T. Lupascu, T. V. Krupska, A. P. Golovan, E. M. Pakhlov, and V. V. Turov, "Influence of tannin on aqueous layers at a surface of hydrophilic and hydrophobic nanosilicas," *Colloids and Surfaces A: Physicochemical and Engineering Aspects*, vol. 531, pp. 9–17, 2017.

[52] A. A. Bele, V. M. Jadhav, and V. J. Kadam, "Potential of tannnins: a review," *Asian Journal of Plant Sciences*, vol. 9, no. 4, pp. 209–214, 2010.

[53] K. Hanhineva, R. Törrönen, I. Bondia-Pons et al., "Impact of dietary polyphenols on carbohydrate metabolism," *International Journal of Molecular Sciences*, vol. 11, no. 4, pp. 1365–1402, 2010.

[54] A. I. Dirar, D. H. M. Alsaadi, M. Wada, M. A. Mohamed, T. Watanabe, and H. P. Devkota, "Effects of extraction solvents on total phenolic and flavonoid contents and biological activities of extracts from Sudanese medicinal plants," *South African Journal of Botany*, vol. 120, pp. 261–267, 2019.

[55] N. El Omari, K. Sayah, S. Fettach et al., "Evaluation of in vitro antioxidant and antidiabetic activities of aristolochia longa extracts," *Evidence-based Complementary and Alternative Medicine*, vol. 2019, Article ID 7384735, 9 pages, 2019.

[56] S. Chiba, "Molecular mechanism inα-glucosidase and glucoamylase," *Bioscience Biotechnology and Biochemistry*, vol. 61, no. 8, pp. 1233–1239, 1997.

[57] P. Vexiau, G. Cathelineau, A. Luyckx, and P. Lefebvre, "Amelioration of glucose tolerance and correction of reactive hypoglycemias induced by intravenous calcium infusion cannot be explained by modifications in blood glucagon

levels," *Diabete & Metabolisme*, vol. 12, no. 4, pp. 177–185, 1986.

[58] P. F. Jacques, A. Cassidy, G. Rogers, J. J. Peterson, J. B. Meigs, and J. T. Dwyer, "Higher dietary flavonol intake is associated with lower incidence of type 2 diabetes," *Journal of Nutrition*, vol. 143, no. 9, pp. 1474–1480, 2013.

[59] C. Voma and A. M. P. Romani, "Role of magnesium in the regulation of hepatic glucose homeostasis," in *Glucose Homeostasis*, L. Szablewski, Ed., InTech, London, UK, 2014.

[60] M. Boulfia, F. Lamchouri, and H. Toufik, "Mineral analysis, in vitro evaluation of alpha-amylase, alpha-glucosidase, and beta-galactosidase inhibition, and antibacterial activities of *Juglans regia* L. Bark extracts," *BioMed Research International*, vol. 2021, Article ID 1585692, 14 pages, 2021.

[61] K. Ghedira, "Les flavonoïdes: structure, propriétés biologiques, rôle prophylactique et emplois en thérapeutique," *Phytothérapie*, vol. 3, no. 4, pp. 162–169, 2005.

[62] N. Turkmen, Y. Velioglu, F. Sari, and G. Polat, "Effect of extraction conditions on measured total polyphenol contents and antioxidant and antibacterial activities of black tea," *Molecules*, vol. 12, no. 3, pp. 484–496, 2007.

[63] C. Tamuly, B. Saikia, M. Hazarika, J. Bora, M. J. Bordoloi, and O. P. Sahu, "Correlation between phenolic, flavonoid, and mineral contents with antioxidant activity of underutilized vegetables," *International Journal of Vegetable Science*, vol. 19, no. 1, pp. 34–44, 2013.

[64] M. Miguel, N. Bouchmaaa, S. Aazza, F. Gaamoussi, and B. Lyoussi, "Antioxidant, anti-inflammatory and anti-acetylcholinesterase activities of eleven extracts of moroccan plants," *Fresenius Environmental Bulletin*, vol. 23, no. 6, pp. 1–14, 2014.

[65] W. Bhouri, S. Derbel, I. Skandrani et al., "Study of genotoxic, antigenotoxic and antioxidant activities of the digallic acid isolated from Pistacia lentiscus fruits," *Toxicology in Vitro*, vol. 24, no. 2, pp. 509–515, 2010.

[66] B. Gordon, "Manganese nutrition of glyphosate-resistant and conventional soybeans," *Better Crops*, vol. 91, no. 4, pp. 12-13, 2007.

[67] A. Hmidani, E. d. T. Bouhlali, T. Khouya et al., "Effect of extraction methods on antioxidant and anticoagulant activities of Thymus atlanticus aerial part," *Scientific African*, vol. 5, Article ID e00143, 2019.

[68] S. Saffarzadeh-Matin and F. M. Khosrowshahi, "Phenolic compounds extraction from Iranian pomegranate (Punica granatum) industrial waste applicable to pilot plant scale," *Industrial Crops and Products*, vol. 108, pp. 583–597, 2017.

[69] A. El Moussaoui, F. Z. Jawhari, A. M. Almehdi et al., "Antibacterial, antifungal and antioxidant activity of total polyphenols of Withania frutescens.L," *Bioorganic Chemistry*, vol. 93, Article ID 103337, 2019.

[70] R. L. Prior, X. Wu, and K. Schaich, "Standardized methods for the determination of antioxidant capacity and phenolics in foods and dietary supplements," *Journal of Agricultural and Food Chemistry*, vol. 53, no. 10, pp. 4290–4302, 2005.

[71] C. Manach, G. Williamson, C. Morand, A. Scalbert, and C. Rémésy, "Bioavailability and bioefficacy of polyphenols in humans. I. Review of 97 bioavailability studies," *American Journal of Clinical Nutrition*, vol. 81, no. 1, pp. 230S–242S, 2005.

[72] V. Kourouma, T. H. Mu, M. Zhang, and H. N. Sun, "Comparative study on chemical composition, polyphenols, flavonoids, carotenoids and antioxidant activities of various cultivars of sweet potato," *International Journal of Food Science and Technology*, vol. 55, no. 1, pp. 369–378, 2020.

[73] H. Lv, X. Zhang, X. Chen et al., "Phytochemical compositions and antioxidant and anti-inflammatory activities of Crude extracts from Ficus pandurata H. (Moraceae)," *Evidence-based Complementary and Alternative Medicine*, vol. 8, Article ID 215036, 2013.

[74] A. A. Mariod, R. M. Ibrahim, M. Ismail, and N. Ismail, "Antioxidant activities of phenolic rich fractions (PRFs) obtained from black mahlab (Monechma ciliatum) and white mahlab (Prunus mahaleb) seedcakes," *Food Chemistry*, vol. 118, no. 1, pp. 120–127, 2010.

[75] H. Dehghan, P. Salehi, and M. S. Amiri, "Bioassay-guided purification of α-amylase, α-glucosidase inhibitors and DPPH radical scavengers from roots of Rheum turkestanicum," *Industrial Crops and Products*, vol. 117, pp. 303–309, 2018.

[76] P. M. Sales, P. M. Souza, L. A. Simeoni, P. O. Magalhães, and D. Silveira, "α-Amylase inhibitors: a review of raw material and isolated compounds from plant source," *Journal of Pharmacy & Pharmaceutical Sciences*, vol. 15, no. 1, p. 141, 2012.

[77] M. Farsi, A. Shafaei, S. Yee Hor et al., "Correlation between enzymes inhibitory effects and antioxidant activities of standardized fractions of methanolic extract obtained from Ficus deltoidea leaves," *African Journal of Biotechnology*, vol. 10, no. 67, pp. 15184–15194, 2011.

Hindawi
Evidence-Based Complementary and Alternative Medicine
Volume 2021, Article ID 9991454, 13 pages
https://doi.org/10.1155/2021/9991454

Research Article

Antibacterial and Anti-Inflammatory Potential of Polyherbal Formulation Used in Chronic Wound Healing

Ilona Mandrika,[1,2] Somit Kumar,[1,3] Baiba Zandersone,[1] Sujith Subash Eranezhath,[3] Ramona Petrovska,[2] Iveta Liduma,[1] Arnolds Jezupovs,[1] Valdis Pirags,[1] and Tatjana Tracevska[1]

[1]*Faculty of Medicine, University of Latvia, Riga 1004, Latvia*
[2]*Latvian Biomedical Research and Study Centre, Riga 1067, Latvia*
[3]*AVP Research Foundation, Coimbatore 641045, India*

Correspondence should be addressed to Ilona Mandrika; ilona@biomed.lu.lv

Received 4 April 2021; Revised 16 June 2021; Accepted 25 June 2021; Published 7 July 2021

Academic Editor: Youhua Xu

Objective. Polyherbal formulations *Jathyadi Thailam* and *Jatyadi Ghritam* (*JT*) are used in Indian traditional medicine for diabetic chronic wounds, fistula, fissure, eczema, and burn management. We aimed to investigate the antibacterial and anti-inflammatory properties of crude hexane and ethanol extracts of *JT* formulations. *Methods*. Antibacterial activity of *JT* extracts was tested to estimate minimum inhibitory concentrations (MICs) against nine reference bacterial strains, including one methicillin-resistant *Staphylococcus aureus* (MRSA) and multidrug-resistant (MDR) *Pseudomonas aeruginosa*, and clinical strains of methicillin-susceptible *S.aureus* (MSSA), all involved in diabetic foot infection. The anti-inflammatory activity of plant extracts was evaluated in LPS-treated macrophage cells by measuring the mRNA levels and secretion of inflammatory mediators. *Results*. The antibacterial activity of *JT* extracts was higher against Gram (+) bacteria, with the MICs varying from 1.95 to 62.5 mg/mL. Gram (−) bacteria were only susceptible to ethanol extracts of *JT*. Plant extracts were found to be the most active against the reference and clinical strains of MSSA, MRSA, and biofilm-forming *S. epidermidis*. *JT* extracts efficiently inhibited in a dose-dependent manner the mRNA expression and protein secretion of proinflammatory cytokines IL-6 and IL-1β, and chemokines MCP-1 and CXCL10 in LPS-challenged macrophages. *Conclusion*. In the present study, we have shown that extracts of *JT* formulations possess potent antibacterial and anti-inflammatory properties that could be involved in chronic wound healing activity and has the potential to be used as external add-on therapy in the management of multidrug-resistant bacterial infections at the wound.

1. Introduction

Diabetes is a chronic metabolic disease characterized by prolonged hyperglycemia, which can lead to eyes, kidneys, nerves, blood vessel damage, and nonhealing wounds [1, 2]. The normal wound healing process involves overlapping phases of hemostasis, inflammation, proliferation, and remodelling and requires a coordinated interplay between macrophages, fibroblasts, keratinocytes, epithelial cells, and signalling molecules. Macrophages play a critical role in the inflammatory phase of wound repair by killing pathogens, clearing damaged tissues, and producing growth factors that induce angiogenesis, collagen deposition, and wound closure [3]. During impaired healing of wounds associated with diabetes, it exhibits prolonged accumulation of M1-polarized macrophages associated with elevated levels of proinflammatory cytokines and reduced levels of various growth factors. It has been demonstrated that IL-1β, TNF-α, IL-6, and MCP-1 levels are sustained at high levels in chronic wounds of diabetic mice and humans [4].

Further, the diabetic wound environment with the resident cells and their secreted signalling molecules could be significantly influenced by the bacterial colonisation in the wound. It has been shown that diabetic mouse wounds

inoculated with *Pseudomonas aeruginosa* biofilm displayed higher levels of IL-1β and IL-6 than control wounds even at 4 weeks postwounding [5]. Diabetic foot ulcer infections (DFI) are mostly polymicrobial, involving both aerobic and anaerobic bacteria that grow in synergy [6, 7]. Recent studies have revealed that Gram (+) cocci, mostly *Staphylococcus aureus*, are the main microorganisms responsible for DFI in occidental countries, but in Asia and Africa, Gram (-) bacilli are predominant. Among the *S. aureus* pathogen, methicillin-resistant *S. aureus* (MRSA) was found in 11% of the DFI isolates [8]. Multidrug-resistant bacterial infections are growing worldwide as a serious problem and this urges the immediate need for the search for alternatives.

The use of medicinal plants and herbs with oils or clarified butter as oleaginous products is a common practice in Indian traditional medicine. These practices have got enshrined in the traditional books as medicated oil (Thailam) and medicated clarified butter or ghee (Ghritam) [9, 10]. This study looks into the prospects of an Ayurveda-based polyherbal formulation, *Jatyadi* widely used in traditional medicine for chronic wounds (including diabetic wounds), ulcers, eczema, scalds, and burns healing as a topical application [11, 12]. The pharmacopoeia version of *Jatyadi (Jatyadi Ghritam)*, as in Ayurveda Formulary of India (AFI), consists of 11 herbs along with honey bee wax (*Sikta*) and copper sulfate (*Tuttha*) [10]. *Jatyadi Thailam* (JT_{AFI}) is also prepared in a sesame oil base instead of clarified butter as mentioned in the pharmacopoeia version of *Jatyadi Ghritam,* without changing the herbal ingredients. JT_{AFI} has shown significant clinical efficacy in healing diabetic wounds after application for 10 days, with a follow-up of 45 days showing no recurrence [13]. Another clinical case of acute erythroderma showed complete remission in lesions after three months of external application of JT_{AFI} along with other parenteral drugs [14]. A very preliminary attempt has been made to understand the mechanism of action of *JT Thailam* through healing in excision wound model in rats [15] and *JT Ghritam* in diabetes-induced rats [16]. Interestingly, there is another traditional version of this formulation, namely, *Jatyadi Thailam* (JT_{YG}) itself, which is used for similar indications in South India. The composition of this formulation (JT_{YG}) is different from JT_{AFI} and is referenced in the Yogagrantha text [17]. JT_{YG} is composed of 13 herbs fortified in coconut oil. The JT_{YG} formulation has not been evaluated using contemporary methods, even though it is used in clinical practice for healing chronic wounds [18].

The aim of this study was to evaluate the biological activities of hexane (JT_{AFI}-Hex, JT_{YG}-Hex) and 90% ethanol (JT_{AFI}-EE, JT_{YG}-EE) extracts of herbal fractions of JT_{AFI} and JT_{YG} formulations *in vitro.* Antibacterial study on *JT* extracts was done through broth microdilution method to estimate its MICs against nine reference Gram (+) and Gram (−) bacterial strains and on clinical strains of MSSA, all involved in diabetic foot infection. The effects of plant extracts on proinflammatory cytokine and chemokine gene expression and protein secretion were examined using lipopolysaccharide-(LPS-) stimulated human THP-1 macrophage cells as a model to understand the network of reactions at the molecular plane during the inflammatory phase of diabetic wounds.

2. Materials and Methods

2.1. Collection and Authentication of Plant Material. Fresh plant materials were collected in and around Palghat District, Kerala, India, and the dried herbs were collected from respective herb dealers across India. The samples were then authenticated at Fischer Herbarium (FRC) at the Institute of Forest Genetics and Tree Breeding, Coimbatore, recognised by the Royal Botanical Gardens of UK and certified by Dr. Kunjikanan. The specimens were deposited in the FRC with voucher numbers for all individual herbs, except *Berberis aristata*, covered from 24222 to 24242. The details of the herbs and voucher numbers are summarized in Table 1 and Table 2. *Berberis aristata* root was identified based on the phytopharmacognostic method as stated in API [19].

2.2. Preparation of Plant Material and Extraction. All the plant materials were air-dried under shade and pulverized. 1000 g of both variants of *JT* herb mixtures was sequentially extracted in 4 L of nonpolar solvent hexane (Hex) and polar solvent 90% ethanol (EE) for 6 h at room temperature by hot percolation method using Soxhlet apparatus. Hexane and 90% ethanol extracts were concentrated up to 200 mL and 250 mL, respectively, and subjected to qualitative and quantitative analysis for the phytochemical profile. The concentrated extracts were further evaporated, and EE extract was lyophilized to remove the last traces of the water. The obtained yields were 2.14% (w/w) for JT_{YG}-Hex, 3.58% (w/w) for JT_{YG}-EE (semisolid), 0.72% (w/w) for JT_{AFI}-Hex, and 3.33% (w/w) for JT_{AFI}-EE (semisolid).

Stock solutions of 0.1 g/mL of extracts with 90% of final DMSO concentration have been made for cell culture analysis and stock solutions of 0.5 g/mL with 50% of final DMSO and 0.25% Tween 20 concentrations have been made for antibacterial studies.

2.3. Phytochemical Analysis of the JT Extracts. Extracts were tested initially for the presence of phytochemicals qualitatively according to standard methods such as precipitation or colouration tests as described by Evance [20] and further quantitative estimation was done only for the detected phytochemicals. Quantification of the total phenolic and tannin content of extracts was done by the Folin-Ciocalteu method according to [21, 22]. The concentrations of the phenols and tannins were estimated from gallic and tannic acids calibration curves, respectively. The aluminium chloride colorimetric method with a quercetin as a standard was used for the determination of the total flavonoid content of extracts as previously described [23]. The total anthocyanin content of extracts was determined by the pH differential method according to [24]. The Liebermann–Burchard test was used for determination of sterols, with cholesterol used as the standard as previously described [25]. The quantification of terpenoids, cardiac glycosides, and saponins was performed by gravimetric methods according to [26–28]. Quantitative determination of alkaloids and proteins was according to the methodology by Harborne [26] and Lowry [29].

Table 1: Herbal ingredients used for JT_{YG} preparation.

Specimens No.	Botanical name	Family	Vernacular name	Specimen Acc No.	Part used	Amount used of herbs
1	*Aerva lanata* (L.) Juss.	Amaranthaceae	Cherula	24229	Whole plant	1 part
2	*Calycopteris floribunda* (Roxb.) Lam. ex. Poir.	Combretaceae	Pullani	24227	leaf	1 part
3	*Curcuma longa* L.	Zingiberaceae	Manjal	24235	Rhizome	1 part
4	*Cynodon dactylon* (L.) Pers.	Poaceae (Graminae)	Arugampul	24222	Whole plant	1 part
5	*Erythrina variegate* L. (= *Erythrina indica* Lam.)	Fabaceae	Muruku	24224	Leaf	1 part
6	*Glycyrrhiza glabra* L.	Fabaceae	Erati mathuram	24236	Root	1 part
7	Jasminum flexile Vahl	Oleaceae	Jasmine	24241	Leaf	1 part
8	*Murraya koenigii* (L.) Spreng.	Rutaceae	Karuvepu	24231	Leaf	1 part
9	*Nigella sativa* L.	Ranunculaceae	Karujeeragam	24242	Seed	1 part
10	*Oldenlandia corymbosa* L.	Rubiaceae	Parpadagam	24230	Whole plant	1 part
11	*Physalis minima* L.	Solanaceae	Njotta	24237	Whole plant	1 part
12	*Pupalia atropurpurea*	Amaranthaceae	Cherukadaladi	24238	Whole plant	1 part
13	*Vitex negundo* L.	Lamiaceae	Karunochi	24228	Leaf	1 part

Table 2: Herbal ingredients used for JT_{AFI} preparation.

Specimens No.	Botanical name	Family	Vernacular name	Specimen Acc No.	Part used	Amount used of herbs
1	*Azadirachta indica* A. Juss.	Meliaceae	Nimba	24223	Leaf	1 part
2	*Chrysopogon zizanioides* (L.) Roberty (*Vetiveria zizanioides* (L.) Nash)	Poaceae (Graminae)	Usira	24233	Root	1 part
3	*Berberis aristata*	Menispermaceae	Darvi	*	Stem	1 part
4	*Curcuma longa* L.	Zingiberaceae	Nisa	24235	Rhizome	1 part
5	*Glycyrrhiza glabra* L.	Fabaceae	Yastimadhu	24236	Root	1 part
6	*Hemidesmus indicus* (L.) R. Br. ex. Schult	Apocynaceae	Sariva (black)	24234	Root	1 part
7	*Jasminum officinale* Linn.	Oleaceae	Jati	24241	Leaf	1 part
8	*Picrorhiza kurroa* Royle ex. Benth	Plantaginaceae	Katuka	24240	Root/ rhizome	1 part
9	*Pongamia pinnata* (L.) Pierre	Fabaceae	Karanja	24232	Seed	1 part
10	*Rubia cordifolia* L.	Rubiaceae	Manjistha	24225	Root	1 part
11	*Trichosanthes dioica* Roxb.	Cucurbitaceae	Patola	24419	Leaf	1 part

*Identified as per standards mentioned in API [19].

2.4. Gas Chromatography-Mass Spectrometry (GC-MS) Analysis. Four millilitres of 0.5 N methanolic sodium hydroxide was added to the 150 mg of *JT*-Hex extracts and heated on a steam bath until the fat globules went into solution. After 5 min, 5 mL of BF3-methanol was added to the flask and the mixture was boiled for 2 min. A saturated sodium chloride solution was added to the flask to float the methyl esters. They were transferred with a syringe to a separatory funnel and 20 mL of petroleum ether (b.p. 30–60°C reagent grade redistilled) was added. The layers were separated by 1 min vigorous shaking. The petroleum ether layer was drained through filter paper and the solvent was then evaporated on a 60°C water bath. A 1 mL aliquot ester of the *JT*-Hex extracts was subjected to analysis by GC-MS.

GC-MS analysis was conducted on an Agilent 7890A GC coupled with a 5975 mass selective detector (Agilent Technologies, USA). Samples were separated on a DB-5MS capillary column (30 m length x 0.25 mm diameter x 0.25 μm film thickness). The oven temperature was held at 40°C for 5 min and raised to 280°C at a rate 5°C/min. Pure helium was used as a carrier gas at a constant flow rate of 1 mL/min. Diluted samples in methanol of 3 μL were injected in the split mode with a split ratio of 50 : 1. The chemical composition of the extracts was identified from the chromatograms and mass spectra using the database of NIST08 Library.

2.5. Bacterial Strains. The following reference and clinical bacterial strains were used in this study: *S. aureus* ATCC 25923, *S. aureus* (MRSA) ATCC 33592, *S. epidermidis* RP62 A, *Enterococcus faecalis* 29212, *Escherichia coli* ATCC 25922, *Pseudomonas aeruginosa* ATCC 27853, multidrug-

resistant (MDR) *P. aeruginosa* ATCC BAA-2108, *Proteus mirabilis* ATCC 29245, and *Klebsiella pneumoniae* ATCC 33495. All the reference strains were obtained from the microbiology laboratory at Riga East University Hospital (REUH). The microorganisms were revived for bioassay by subculturing in fresh nutrition Trypticase soy broth for 24 h before use. The clinical material was collected by a sterile cotton swab from diabetic foot ulcers from DFI patients admitted to REUH. Collection of clinical samples from diabetic foot wounds for bacterial isolates was approved by the ethics committee at the Institute of Cardiovascular and Regenerative Medicine, University of Latvia. Four *S. aureus* cultures were isolated and identified microbiologically up to a species level at the REUH microbiology laboratory using the BBL Crystal system (Becton, Dickinson, UK). Susceptibility to a panel of antimicrobials was tested according to Clinical and Laboratory Standard Institute guidelines [30] by the agar disk diffusion test and the E-test using Mueller–Hinton (MH) agar (Becton Dickinson, UK) against the following panel of antibacterials: penicillin, gentamicin, cefazolin, erythromycin, clindamycin, vancomycin, ciprofloxacin, and trimethoprim-sulfamethoxazole. Methicillin resistance was tested by a cefoxitin disk on an agar screen plate. Plates inoculated with clinical *S. aureus* cultures were incubated for 20–24 h. The antibiogram of four *S. aureus* strains showed susceptibility to methicillin (cefoxitin).

2.6. Broth Microdilution Method. The antibacterial efficacy of the *JT* extracts was tested by determining the minimum inhibitory concentration (MIC) by broth microdilution method as described by Balouiri [31] with modifications. Stock solutions of gentamicin (0.4 mg/mL) and streptomycin (1 mg/mL) were used as MIC controls in each experiment according to CLSI standards CLSI-2017-M02-A12 [30]. Unsupplemented MH broths with and without the bacterial inoculate were used as positive and negative controls, respectively, in each experiment. DMSO was used as vehicle control for the inhibitory effect on all bacterial strains. The twofold dilution series of diluent DMSO were made in each well (starting from 12.5% in the first well, 6.25% in the second well, and so forth). The concentration of DMSO at 6.25% in the second well was below the toxic level as tested separately and did not inhibit the growth of bacteria.

Twofold dilution series of each extract were prepared in MH broth (starting from a concentration of 250 mg/mL) and added to 96-well microtiter plate (100 μL/well). Overnight grown fresh bacterial cells were suspended in sterile saline and adjusted to a turbidity of McFarland standard No 0.5, bacterial cell suspension containing 1.5×10^8 colony-forming units (CFU/mL). The bacterial cell suspension was further diluted 1 : 100 in distilled water and aliquoted into a microplate 100 μL per well. To calculate MIC, after 20 h of incubation at 35°C, 10 μL aliquots of the appropriate dilution were withdrawn from the microtiter plate and inoculated on MH agar in a Petri dish and incubated for 24 h. Colony-forming units of each dilution were counted and compared to the control Petri dish inoculated 24 h earlier with 10 μL of the same strain suspension for MIC determination. The MIC value was calculated manually and assumed the same as minimum bactericidal concentration when 99.9% inhibition of bacterial growth after inoculation in a Petri dish was observed [31]. Each extract was tested in triplicate for statistical reliability.

2.7. Cell Culture and Differentiation Induction. The human THP-1 monocyte cell line was obtained from ATCC (American Type Culture Collection). THP-1 cells were maintained in RPMI-1640 medium containing 10% fetal bovine serum and antibiotics and incubated in 5% CO_2 at 37°C. THP-1 monocytes were stimulated to differentiate into macrophages with phorbol 12-myristate 13-acetate (PMA) (20 ng/mL) for 24 h. Medium was exchanged for PMA-free medium for 48 h before cells were used for experiments.

2.8. Cell Viability Testing. Cell viability was tested by Cell Counting Kit-8 (CCK-8) (Sigma-Aldrich, USA), according to the manufacturer's instructions. THP-1 cells (100 μL) were seeded into a 96-well tissue culture plate at the density of 10^4 cells per well and grown in the presence or absence of various concentrations (3–200 μg/mL) of *JT* plant extracts. Wells with dead THP-1 cells were used as the negative control wells. CCK-8 solution (10 μL) was added to the cells at 24 and 48 h and plates were incubated for 1 h at 37°C. The absorbance of each well was measured at 450 nm using a microplate reader Victor3^{TM} (Perkin Elmer, USA). Wells without cells but containing medium were used as a blank value that was subtracted from all values. Each assay was performed in triplicate.

2.9. RNA Extraction and Quantitative Real-Time Polymerase Chain Reaction (qRT-PCR). Total RNA was isolated from cultured cells using TRIzol reagent (Sigma, USA), according to the manufacturer's protocol. First-strand cDNA was synthesized from 2 μg RNA using oligo (dT) primers with Revert Aid H Minus kit (Thermo Fisher Scientific, USA). qRT-PCR was performed using Absolute Blue SYBR green Master Mix reagent (Thermo Fisher Scientific, USA) with a ViiA7 real-time PCR detection system (Applied Biosystems, USA). The primer pairs used for the gene amplifications are listed in Table 3 mRNA levels were quantified and normalized to levels of reference gene *RPS29* using the $2^{-\Delta\Delta Ct}$ method and presented as relative expression compared with values of untreated cells.

2.10. Quantification of Cytokines and Chemokines. Conditioned media were obtained from untreated and *JT* extract-treated THP-1 macrophages. The concentrations of the IL-6, IL-1β, MCP-1, and CXCL10 biomolecules were measured by Luminex Multiplex immunoassay (R&D Systems, USA) according to the manufacturer's instructions and analyzed on a Luminex 200 (Luminex Corporation, USA). At least three independent repetitions in duplicate were made per sample. Concentrations of the analytes were quantified with five parameters logistic (5-PL) curve fit and expressed in pg/mL.

Table 3: Sequences for qRT-PCR primers used in this study.

Primer name	Sequence (5′- 3′)	Product length, bp
IL-6 Fw	AGACAGCCACTCACCTCTTCAG	132
IL-6 Rv	TTCTGCCAGTGCCTCTTTGCTG	
IL-1β Fw	CCACAGACCTTCCAGGAGAATG	131
IL-1β Rv	GTGCAGTTCAGTGATCGTACAGG	
TNF-α Fw	CCCAGGGACCTCTCTCTAATCA	116
TNF-α Rv	AGCTGCCCCTCAGCTTGAG	
MCP-1 Fw	AGAATCACCAGCAGCAAGTGTCC	98
MCP-1 Rv	TCCTGAACCCACTTCTGCTTGG	
CXCL10 Fw	GGTGAGAAGAGATGTCTGAATCC	134
CXCL10 Rv	GTCCATCCTTGGAAGCACTGCA	
RPS29 Fw	CAAGATGGGTCACCAGCAG	106
RPS29 Rv	ATATTTCCGGATCAGACCGT	

2.11. Statistical Analysis. Statistical analysis of MIC data was done using chi-square test. The median value for each MIC was calculated. Gene expression results are expressed as mean ± standard deviation (SD) of the indicated number of experiments. Student's *t*-test was used to assess the statistical significance of differences. Significant differences were assumed for $p < 0.05$. The statistical analysis was performed using GraphPad Prism 5.0 software (GraphPad Software Inc, USA).

3. Results

3.1. Phytochemical Evaluation of JT Extracts. The quantitative phytochemical screening of obtained *JT* plant extracts revealed the presence of phenols, proteins, tannins, sterols,and terpenoids in JT_{YG}-EE, JT_{AFI}-EE, and JT_{AFI}-Hex extracts, as shown in Table 4. All *JT* extracts had flavonoids with the highest content in JT_{YG}-EE extract. Both JT_{YG}-EE and JT_{AFI}-EE were rich in proteins. Alkaloids were detected only in JT_{AFI}-EE and saponins only in JT_{YG}-EE extracts. Glycosides were found to be present only in hexane extracts of both *JT* formulations with the higher concentration in JT_{YG}-Hex. Anthocyanins were present only in JT_{YG} extracts. Overall, *JT*-EE extracts had a higher content in phenols, proteins, tannins, sterols, and flavonoids.

3.2. Chemical Composition of JT Extracts. The presence of chemical components in the *JT* hexane extracts was analyzed by GC-MS. The analysis of JT_{YG}-Hex extract has shown the presence of 36 peaks in the gas chromatogram and 21 components corresponding to the major peaks have been determined and are listed in Table 5. Major chemical compounds were 9,12-octadecadienoic acid or linoleic acid (24.86%), n-hexadecanoic acid or palmitic acid (17.17%), cis 13- octadecenoic acid (15.19%), cis-13,16-docosadienoic acid (5.29%), ar-turmerone (2.49%), alpha-turmerone (2.03%), beta-turmerone or curlone (1.84%), 9-octadecenoic acid (Z) methyl ester or oleic acid (1.46%), phytol (1.61%), and squalene (1.84%), while other compounds were present in minor quantities with peak areas ranging from 0.09 to 1.61%.

Table 4: Quantitative phytochemical evaluation of the *JT* extracts.

Phytochemical (%)	Extracts			
	JT_{YG}-Hex	JT_{YG}-EE	JT_{AFI}-Hex	JT_{AFI}-EE
Alkaloids	—[a]	—	—	6.17
Phenols	—	6.20	4.60	8.28
Proteins	1.40	11.56	4.32	12.96
Tannins	—	9.80	5.69	14.32
Sterols	—	11.30	9.80	4.02
Glycosides	16.70	—	2.82	—
Saponins	—	11.04	—	—
Terpenoids	—	17.16	18.51	9.93
Flavonoids	3.06	9.02	2.70	5.26
Anthocyanins	0.19	0.50	—	—

[a]Quantitative evaluation of phytochemicals was not done as preliminary qualitative tests showing absence of these phytochemicals.

Gas chromatogram analysis of JT_{AFI}-Hex extract revealed 33 distinct peaks and the 25 components corresponding to the major peaks have been determined and listed in Table 6. Major chemical compounds were 6-octadecenoic acid (27.36%), n-hexadecanoic acid (10.17%), 3-dibenzofuranamine (13.24%), octadecane (5.67%), fumaric acid, 2, 4-dimethyl pent-3-yl isohexyl ester (5.36%), fumaric,3,5-dichlorophenyl isohexyl ester (4.99%), 9,12-octadecadienoic acid (Z, Z) (3.12%), and phytol (2.23%), while other compounds were present in minor quantities with peak areas ranging from 0.321 to .97%.

3.3. Antibacterial Activity of JT Extracts on Reference Bacterial Strains. The antibacterial properties of *JT* extracts were elucidated on four Gram (+) (*S. aureus* ATCC 25923, MRSA ATCC 33592, *S. epidermidis* RP62 A, and *E. faecalis* 29212) and five Gram (−) (*E. coli* ATCC 25922, *P. aeruginosa* ATCC 27853, MDR *P. aeruginosa* ATCC BAA-2108, *P. mirabilis* ATCC 29245, and *K. pneumoniae* ATCC 33495) reference bacterial strains. The results of MIC as determined by broth microdilution method are shown in Table 7. In general, MIC values ranged from 1.95 to 62.5 mg/mL. The extracts at bactericidal concentrations higher than 125 mg/mL were considered as having no inhibition since the bacterial growth was influenced by the diluent 12.5% DMSO.

All *JT* extracts showed better inhibitory activity for Gram (+) bacteria compared to Gram (−) (Table 7). When the cases of inhibition (MIC determined) were compared to the cases without inhibition, 100% of Gram (+) and only 40% of Gram (−) bacterial strains had cases of inhibition by extracts studied. Both JT_{YG}-Hex and JT_{YG}-EE extracts showed lower MIC for Gram (+) bacterial reference strains (median 11.7) than MIC for Gram (−) strains (median ≥125.0). Similarly, both JT_{AFI}-EE and JT_{AFI}-Hex extracts were also more active against Gram (+) (median 31.25) compared to MIC for Gram (−) (median 93.75) reference strains. The overall efficacy of JT_{YG} formulation extracts (median 11.7) was higher than that of JT_{AFI} formulation extracts (median 31.25).

In order to investigate the best efficacy for Gram (+) bacteria, the MICs were further compared between the extracts. The lowest MIC was detected for biofilm-forming *S. epidermidis* RP62 A strain by JT_{YG}-EE and JT_{YG}-Hex

Table 5: Biologically active chemical compounds of JT_{YG}-Hex extract.

S. No.	Retention time, min	Active components	Peak area, %
1	42.529	Ar-Turmerone	2.49
2	42.767	Turmerone	2.03
3	44.349	Curlone (beta-turmerone)	1.84
4	45.518	Bicyclo (3.1.1) heptanes,6,6-dimethyl-2methylene-(1S)	0.09
5	46.128	Bicyclo (2.2.1) heptan-2-ol,1,7,7-trimethyl-acetate	0.18
6	45.827	Cyclohexane carboxylic acid, dimethyl phenyl ester	0.60
7	46.548	2,6,6-trimethylbicyclo (3.1.1) hepatane	0.57
8	46.606	2-Hexadecane,3,7,11,15-tetramethyl-(R-R*, R*-(E))	0.21
9	46.775	3-Tetradecyne	0.19
10	47.311	Hexadexanoic acid methyl ester	0.16
11	47.502	Cyclotetradecane	0.57
12	47.790	n-Hexadecanoic acid	17.17
13	48.411	Phytol	1.61
14	48.674	9,12-Octadecadienoic acid (Z, Z)	24.86
15	48.847	*cis*-13-Octadecadienoic acid	15.19
16	49.484	*cis*-13,16-Docasadienoic acid	5.29
17	50.042	1H- Indole	1.19
18	50.226	Imidazole,1-(9-borabicyclo (3.1.1) non-9-yl)	1.08
19	50.306	Hexadecanoic acid,2-hydroxy-1-(Hydroxymethyl) ethyl ester	1.51
20	52.295	Squalene	1.84
21	53.065	Tetracosane	0.57

Table 6: Biologically active chemical compounds of JT_{AFI}- Hex extract.

S. No.	Retention time, min	Active components	Peak area %
1	42.509	Ar-Turmerone	0.85
2	42.748	Turmerone	0.35
3	44.348	Curlone (beta-turmerone)	0.52
4	46.555	Bicyclo (3.1.1) heptanes,6,6-dimethyl-,(1.alpha.,2.beta.,5.alpha)	0.32
5	47.686	n-Hexadecanoic acid	10.17
6	47.985	Cyclopentene,1-pentyl	0.89
7	48.060	1,19-Eicosadiene	1.09
8	48.412	Phytol	2.23
9	48.669	6-Octadecanoic acid	27.36
10	49.086	3-Dibenzofuranamine	13.24
11	49.435	Fumaric acid, 2, 4-dimethyl pent-3-yl isohexyl ester	5.36
12	49.503	Fumaric,3,5-dichlorophenyl isohexyl ester	4.99
13	49.666	Hentriacontane	5.67
14	50.124	Cis-13 = octadecenoic acid, methyl ester	1.16
15	50.258	Bezzoic anhyide, 4,4′,6,6′- Tetramethoxy -2,2′-dimethyl	2.68
16	50.428	Benzaldehyde, 6-Hydroxy-4-methoxy-2,3-dimethyl	1.65
17	50.573	4H-Pyran-4-one-2,6-diethyl-3,5-diemthyl	1.46
18	50.877	1-H-Imidazole-5-carboxamde,4-bebzoyl-N-(2-Pyridyl)	1.08
19	51.032	Lycopodan-5-1,12 hydroxy-15-methyl,(15 R)-	2.64
20	51.177	2,6-Dihydroxynaphthalene	1.97
21	51.335	Cylcopropaneoctanal,2-octyl-	1.00
22	51.438	9,12-Octadecadienoic acid (Z, Z)	3.12
23	52.292	2,6,10,14,18,22-Tetracosahexane	2.34
24	52.778	Stigmasterol	1.21
25	53.072	Tetracosane	0.82

extracts (1.95 mg/mL) followed by JT_{AFI}-EE extract (15.6 mg/mL) and by JT_{AFI}-Hex (31.25 mg/mL), as shown in Table 7. Notably, the results indicated that all four extracts were active against MRSA ATCC 33592 strain, with the highest inhibitory activity shown by JT_{YG}-EE and JT_{AFI}-EE extracts (15.6 mg/mL) (Table 7).

Further, the overall inhibitory efficacy for Gram (+) and Gram (−) bacteria was compared between the extracts. Gram (-) bacteria were susceptible only to EE extracts, except for *P. aeruginosa* MDR ATCC BAA-2108. There was no significantly important difference ($p = 0.527$) in the frequency of inhibition between JT_{YG}-EE (median 31.25) and JT_{YG}-Hex (median 62.5). There was also no significantly important difference ($p = 0.836$) in the frequency of inhibition between JT_{AFI}-EE (median 62.52) and JT_{AFI}-Hex (median ≥125), between JT_{YG}-EE (median 31.25) and JT_{AFI}-EE

Table 7: MIC values of *JT* extracts against reference bacterial strains.

Reference bacterial strains	Gram (±)	MIC, mg/mL[a]					
		JT_{YG}-EE	JT_{YG}-Hex	JT_{AFI}-EE	JT_{AFI}-Hex	Gentamicin control	Streptomycin control
S. aureus ATCC 25923	+	7.81	7.81	15.60	31.25	≤0.0156	0.0019
MRSA ATCC 33592[b]	+	15.60	31.25	15.60	31.25	ND[c]	ND
S. epidermidis RP62 A	+	1.95	1.95	15.60	31.25	0.012	≤0.0780
E. faecalis ATCC 29212	+	31.25	62.50	62.50	NI[d]	0.0039	0.0048
E. coli ATCC 25 922	−	62.50	NI	31.25	NI	0.0015	0.0039
P. aeruginosa ATCC 27853	−	15.60	NI	62.50	NI	0.2500	0.0078
P. aeruginosa MDR ATCC BAA-2108[e]	−	NI	62.5	62.50	NI	ND	ND
P. mirabilis ATCC 29245	−	NI	NI	NI	NI	≤0.00003	0.0780
K. pneumoniae ATCC 33495	−	62.50	NI	62.50	NI	≤0.0007	0.0004

[a]MICs were determined by broth microdilution method and all experiments were done in triplicate; [b]MICs were determined as 0.125 μg/mL to ciprofloxacin and 1.5 μg/mL to vancomycin; [c]ND: not determined; [d]NI: no inhibition; [e]MICs were determined as > 32 μg/mL to imipenem and ciprofloxacin.

(median 31.25), and between JT_{YG}-Hex (median 62.5) and JT_{AFI}-Hex extract (median 62.5) (Table 7).

3.4. Antibacterial Activity of JT Extracts on Clinical S. aureus Strains. Additionally, four *S. aureus* clinical strains, namely, 704, 526, 250, and 588, isolated from DFIs, were examined for antibacterial activity by broth microdilution method. The results of MICs are shown in Table 8. The values of MIC varied from 1.95 to 62.5 mg/mL among clinical strains and among extracts, except for JT_{YG}-Hex extract (7.81 mg/mL). There was no difference in MIC between JT_{YG}-EE (median 15.6) and JT_{AFI}-EE (median 15.6) extracts and, similarly, between JT_{YG}-Hex (median 62.5) and JT_{AFI}-Hex extracts (median 62.5), with the EE extracts showing higher activity compared to that of Hex extracts. Our data showed that the frequency of inhibition was not significantly different between *S. aureus* clinical strains and the reference group ($p = 0.590$).

As a component of the original JT_{AFI} formulation, possessing antibacterial potential on the skin, the inhibitory effect of copper sulfate was additionally tested on *S. aureus* clinical strains by broth microdilution method. Copper sulfate stock solution was prepared at a concentration of 3.53 mg/mL, which is equal to that used in the original JT_{AFI} product (10.6 g/3 L of water). Our data indicate that MIC was achieved by copper sulfate already at concentration 0.88 μg/mL, which is much lower than the concentration in the original JT_{AFI} product (Table 8).

3.5. Effects of JT Plant Extracts on Cell Viability. The effects of *JT* extracts on the viability of THP-1 macrophages were examined to determine the concentrations of the extracts that are nontoxic for the cells. As can be seen from Figure 1, no cytotoxic effect was observed following a 24 and 48 h treatment of the cells with both the JT_{YG}-Hex and JT_{AFI}-Hex at concentrations less than 50 μg/mL and the JT_{YG}-EE and JT_{AFI}-EE at concentrations less than 12 μg/mL. Therefore, for subsequent experiments, concentrations of 50 μg/mL for JT_{YG}-Hex and JT_{AFI}-Hex and 10 μg/mL for JT_{YG}-EE and JT_{AFI}-EE were used to induce a maximal response without causing cell toxicity. Exposure to vehicle control DMSO ranging from 0.2 to 0.003% had no effect on cell viability (data not shown).

3.6. JT Extracts Suppresses Gene Expression of Inflammatory Cytokines and Chemokines in THP-1 Macrophages. We quantified the expression levels of the proinflammatory cytokines IL-6, IL-1β, TNF-α, and chemokines-MCP-1 and CXCL10, which are chemoattractant factors involved in monocyte/macrophage and T-cell recruitment. THP-1 macrophages were stimulated with LPS (1 μg/mL) with or without the addition of various concentrations of *JT*-Hex (50, 10, and 1 μg/mL) and *JT*-EE (10 and 1 μg/mL) plant extracts. Expression of each molecule at mRNA level was upregulated after 4 h stimulation with LPS in THP-1 macrophages (Figure 2). All extracts in a dose-dependent manner showed the most potent inhibition of IL-6, CXCL10 and MCP-1 gene expression. The addition of JT_{YG}-Hex at 50, 10, and 1 μg/ml resulted in significant reduction of LPS- stimulated IL-6 mRNA levels by 95%, 84% ($p < 0.0001$), 22% ($p = 0.0019$), CXCL10 mRNA levels by 95% ($p < 0.0001$), 61% ($p = 0.0006$), and 21% ($p = 0.005$) and MCP-1 levels by 81% ($p < 0.0001$), 60% ($p = 0.005$), and 11% ($p = 0.096$), respectively (Figures 2(a) and 2(d)). The addition of JT_{AFI}-Hex at 50, 10 and 1 μg/mL resulted in significant reduction of LPS-stimulated IL-6 mRNA levels by 92% ($p < 0.0001$), 66% ($p = 0.0003$), and 28% ($p = 0.009$), CXCL10 mRNA levels by 92% ($p < 0.0001$), 54% ($p = 0.001$), and 34% ($p = 0.002$) and MCP-1 levels by 74%, 44% ($p < 0.0001$), and 15% ($p = 0.062$), respectively (Figures 2(a) and 2(d)). The addition of JT_{YG}-EE at 10 and 1 μg/mL resulted in significant reduction of LPS-stimulated IL-6 mRNA levels by 95% and 51% ($p < 0.0001$), CXCL10 mRNA levels by 94 ($p < 0.0001$) and 30% ($p = 0.003$) and MCP-1 levels by 56% ($p = 0.0002$) and 22% ($p = 0.011$), respectively (Figures 2(a) and 2(d)). The addition of JT_{AFI}-EE at 10 and 1 μg/mL resulted in significant reduction of LPS-stimulated IL-6 mRNA levels by 80% ($p < 0.0001$) and 20% ($p = 0.004$), CXCL10 mRNA levels by 74% ($p < 0.0001$) and 10% ($p = 0.058$) and MCP-1 levels by 24% ($p = 0.001$) and 3% ($p = 0.069$), respectively (Figures 2(a) and 2(d)). A significant 65% ($p = 0.0004$) and 43% ($p = 0.005$) decrease in IL-1β mRNA and 72% ($p < 0.0001$) and 36% ($p = 0.008$) decrease in TNF-α mRNA was detectable at 50 μg/mL for JT_{YG}-Hex and

Table 8: MIC values of *JT* extracts against clinical isolates of *S. aureus*.

	MIC, mg/mL[a]						
Clinical isolates, *S. aureus*	JT_{YG}- EE	JT_{YG}- Hex	JT_{AFI}- EE	JT_{AFI}- Hex	Gentamicin control	Streptomycin control	Copper sulfate
704	1.95	7.81	7.81	62.50	≤0.0015	≤0.0004	0.00088
526	7.81	7.81	15.60	31.25	≤0.0015	≤0.0004	0.00088
250	15.60	7.81	15.60	62.50	≤0.0015	0.0078	0.00088
588	31.25	7.81	15.60	31.25	≤0.0015	0.0039	0.00088

[a]- MICs were determined by broth microdilution method and all experiments were done in triplicate.

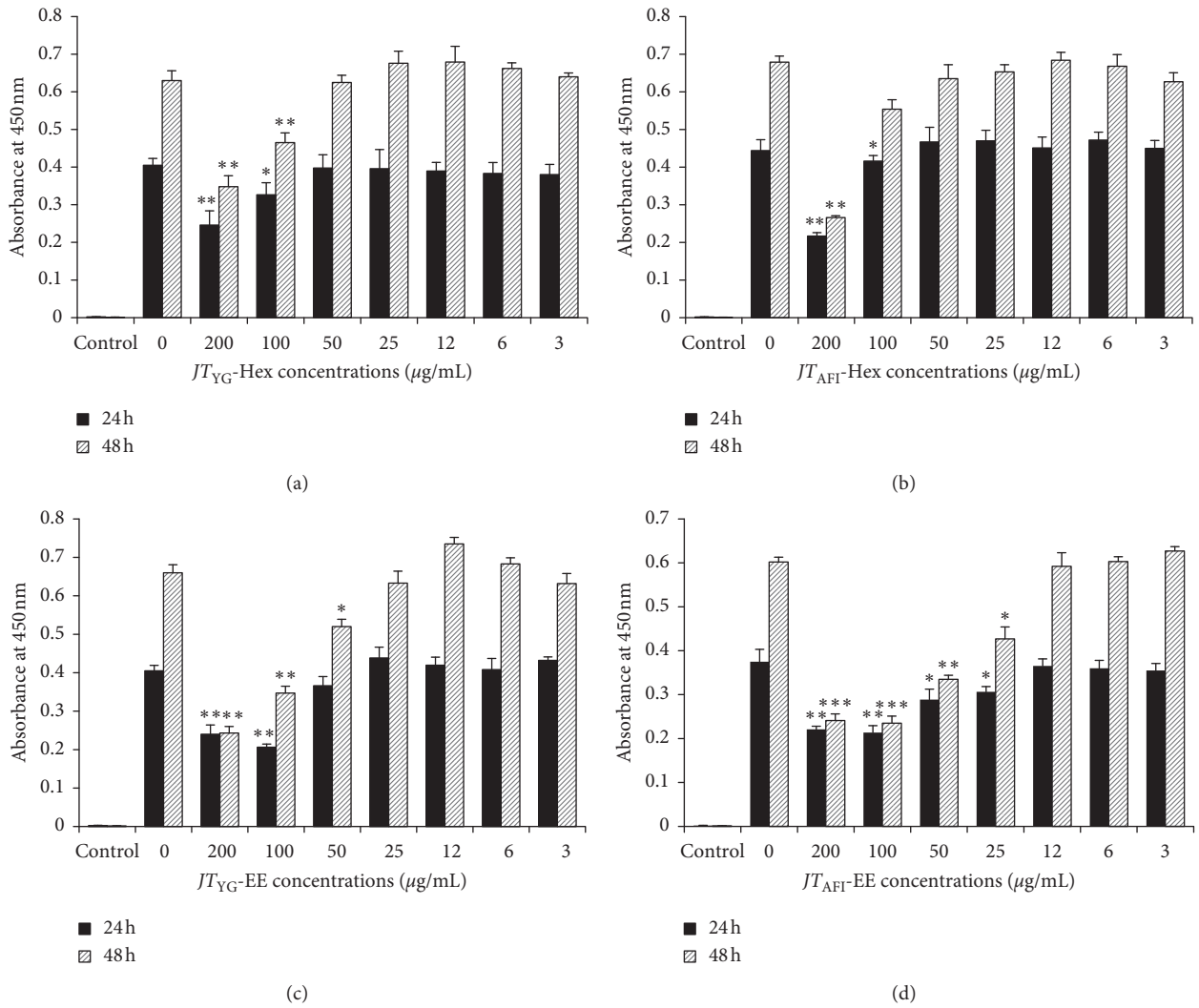

Figure 1: Effects of JT_{YG} and JT_{AFI} plant extracts on THP-1 cells viability. THP-1 macrophages were grown in the presence of indicated concentrations of JT_{YG}-Hex (a), JT_{AFI}-Hex (b), JT_{YG}-EE (c), and JT_{AFI}-EE (d) extracts for 24 and 48 h. Cell viability was measured using the CCK-8 solution. Data are a summary of three independent experiments performed in duplicate and expressed as mean ± SD. $^{*}p < 0.05$, $^{**}p < 0.01$, $^{***}p < 0.0001$ are significantly different from untreated cells.

JT_{AFI}-Hex extracts, respectively (Figures 2(b) and 2(c)). However, only JT_{YG}-EE at 10 μg/mL was able to significantly ($p = 0.001$) inhibit IL-1β gene expression (Figure 2(c)). Exposure to 10 μM dexamethasone used as positive control significantly decreased LPS-stimulated mRNA levels of all tested molecules (Figure 2). Exposure to vehicle control DMSO had no effect on cytokine expression in LPS- stimulated cells (data not shown).

3.7. Plant Extracts Suppresses Secretion of Inflammatory Cytokines and Chemokines in THP-1 Macrophages. As the next step, we measured cytokine levels secreted into the medium when THP-1 macrophages were exposed to LPS (1 μg/mL) in the presence or absence of *JT*- Hex (50 μg/mL) and *JT*- EE (10 μg/mL) extracts. After 24 h, the culture medium was collected, and cytokine concentrations were measured with Luminex kit. All cytokine secretion

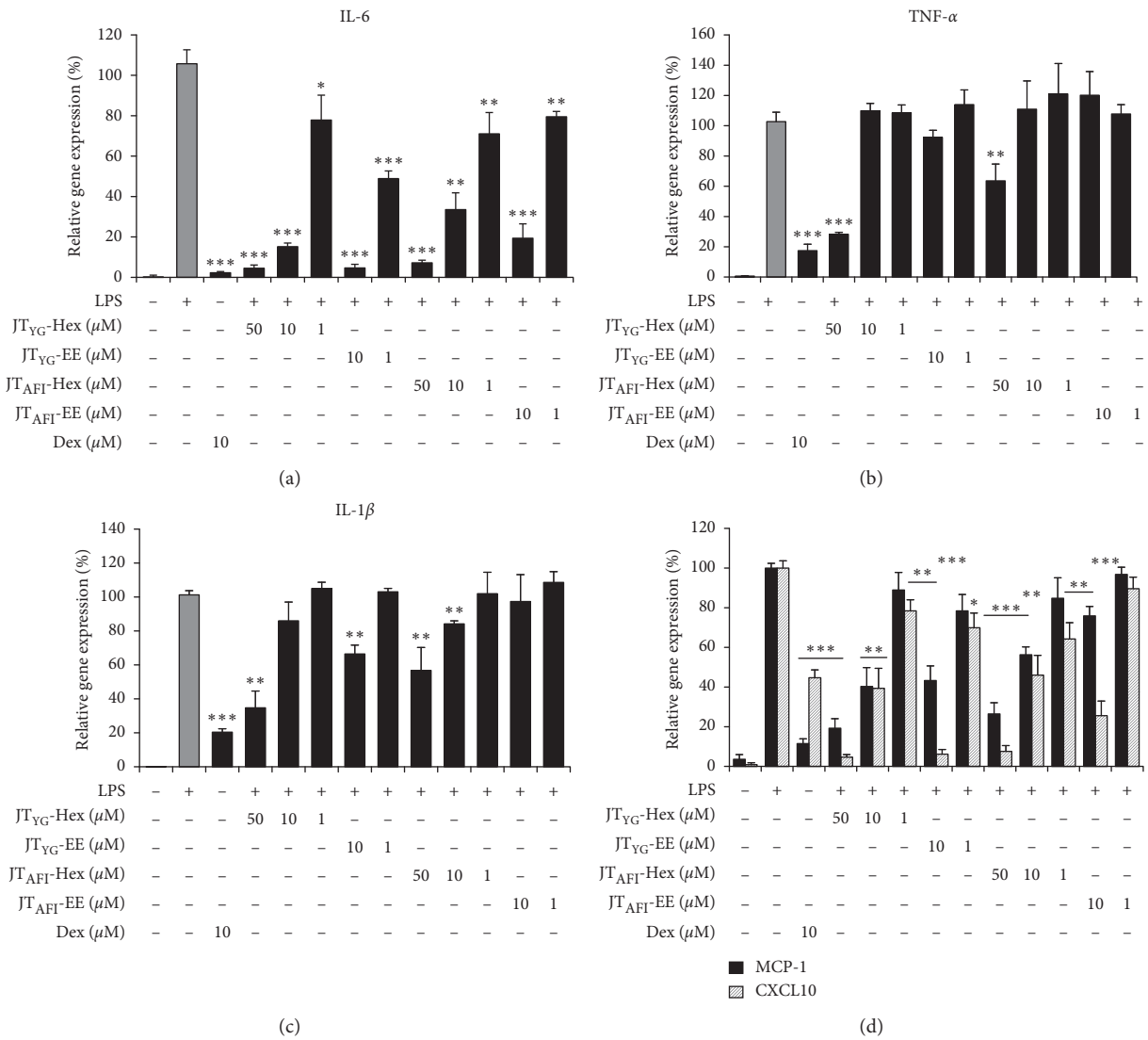

Figure 2: Suppression of proinflammatory cytokine and chemokine gene expression by *JT* extracts in THP-1 macrophages. Cells were treated 4 h with LPS (1 μg/mL) in the presence or absence of various concentrations of *JT*-EE and *JT*-Hex extracts. The levels of cytokine IL-6 (a), TNF-α (b), IL-1β (c), and chemokine MCP-1 and CXCL10 (d) mRNA were determined by real-time PCR. Data were normalized to *RpS29* and values were calculated using the comparative ($2^{-\Delta Ct}$) method. Results are mean ± SD from at least three independent experiments. $^{*}p < 0.05$, $^{**}p < 0.01$, $^{***}p < 0.0001$ are significantly different from LPS-stimulated cells.

significantly increased following macrophage treatment with LPS (Figure 3). JT_{AFI}-Hex and JT_{YG}-Hex extracts were able to significantly reduce the secretion of IL-6, IL-1β, MCP-1, and CXCL10 from macrophages (Figure 3). IL-6, MCP-1, and CXCL10 secretion was also significantly decreased by both *JT*-EE extracts (Figures 3(a), 3(c), and 3(d)). However, only JT_{YG}-EE extract at 10 μg/mL significantly decreased LPS-stimulated secretion of IL-1β ($p = 0.005$, Figure 3(b)).

4. Discussion

The reverse pharmacology approach can be applied to study formulations used in Ayurveda to understand their mode of actions. Few reports have offered clear underlying mechanisms of synergistic therapeutic actions of herbal ingredients [32]. This study attempts to understand the potentials of both traditional *JT* versions and the biological activities of hexane and ethanol extracts of herbal fractions of JT_{AFI} and JT_{YG} formulations *in vitro*.

So far, the wound healing mechanisms and efficacy of the *JT* formulation have been investigated using *in vivo* excision wound model and burn injury in rats [15, 33]. The authors reported faster wound healing process in rats treated with *JT* due to increased proliferation of fibroblasts, protein synthesis, enhanced collagen formation, reepithelization, and wound contracting ability. However, to the best of our knowledge, there are no studies on antimicrobial and anti-inflammatory potential of *JT*. Therefore, this study evaluated the antimicrobial and anti-inflammatory activities of ethanol and hexane extracts obtained from both JT_{YG} and JT_{AFI} formulations. JT_{AFI} formulation is composed of thirteen herbal ingredients along with copper sulfate fortified in oil.

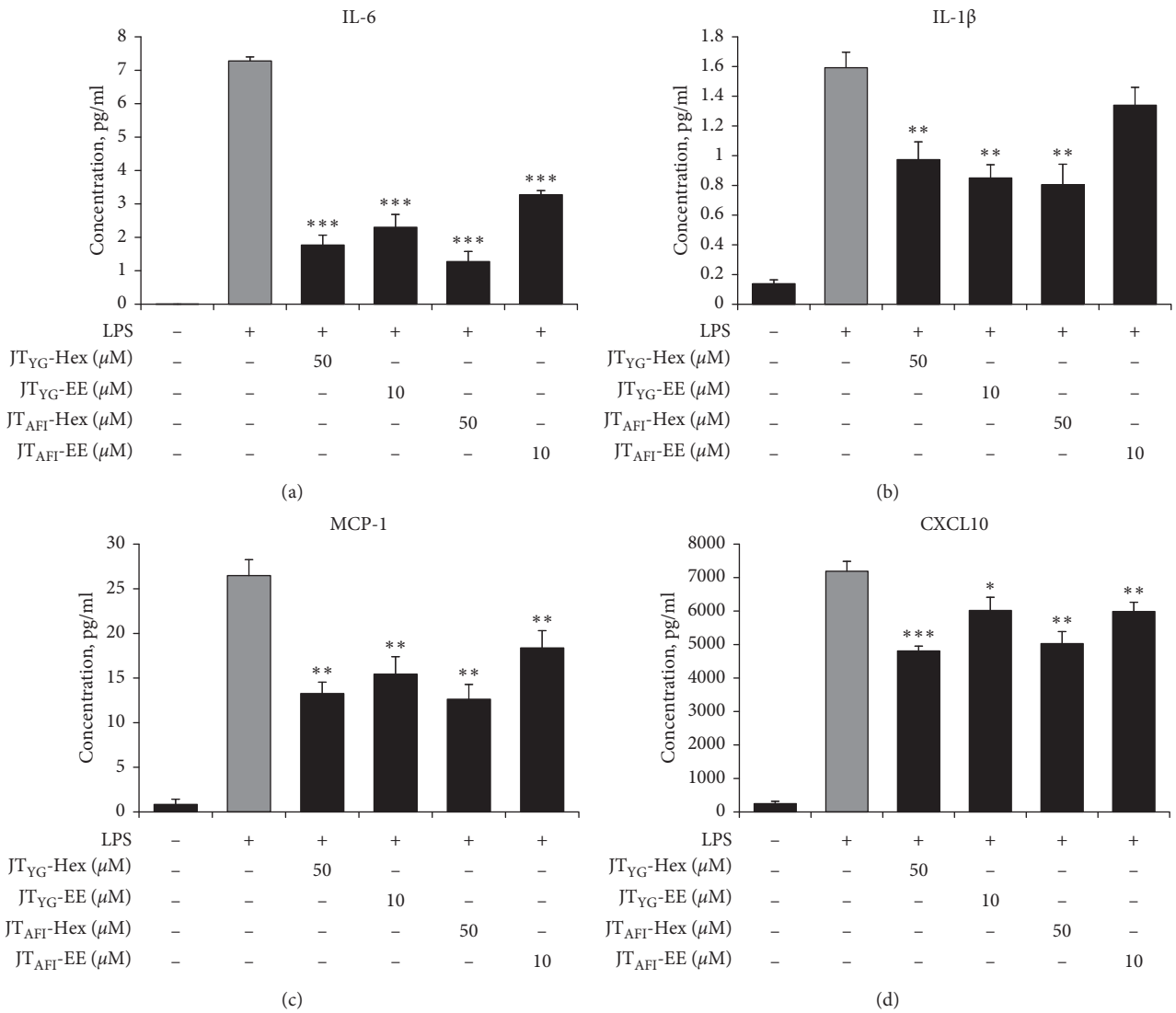

Figure 3: Suppression of proinflammatory cytokine and chemokine secretion by *JT* extracts in THP-1 macrophages. Supernatants from 4 h LPS and/or extracts-treated THP-1 macrophages were subjected to Luminex assay to detect proinflammatory cytokine IL-6 (a) and IL-1β (b) and chemokine MCP-1 (c) and CXCL10 (d) levels. Results are mean ± SD from three independent experiments. $^{*}p < 0.05$, $^{**}p < 0.01$, $^{*}p < 0.0001$ are significantly different from LPS-stimulated cells.

This study focuses only on the herbal fractions of both *JT* formulations. JT_{AFI} was evaluated without copper sulfate to understand the role of herbal combinatorics, as the efficacy of copper sulfate for its antimicrobial [34] and wound healing activity is well established [35].

Recent studies using molecular methods such as 16S rRNA sequencing on diabetic ulcers revealed much higher levels of microbial diversity, especially more anaerobes and Gram (−) species than those previously known through culture-based methods [36]. Other bacteria involved in DFI in Europe, as revealed by conventional culturing, include *P. mirabilis, P. aeruginosa, Klebsiella* spp., *E. coli*, and anaerobes [37]. Contrary to this, in warmer countries (particularly in Asia and Africa), aerobic Gram (−) bacilli, especially *P. aeruginosa,* are more often the cause of DFIs. The antibacterial activity of *JT* extracts was evaluated against both Gram (+) and Gram (−) reference bacterial strains and against four *S. aureus* strains isolated from clinically infected diabetic foot ulcers. We observed that all *JT* extracts showed better inhibitory activity for Gram (+) bacteria than Gram (−) strains. Notably, Gram (-) bacteria were susceptible only to EE extracts, except in the case of bacterial strain *P. aeruginosa* MDR ATCC BAA-2108. This can be explained by the higher presence of phenols, tannins, sterols, and flavonoids in EE extracts. A direct correlation between the summary content of phenols and flavonoids and antibacterial activity of different plant extracts has been reported [38].

Interestingly, the most potent antibacterial activity of *JT* extracts was observed against the reference bacterial strains, namely, *S. aureus* (MRSA, MSSA) and *S. epidermidis*. Moreover, the extracts were effective against all four clinical strains of *S. aureus*, with the highest MIC value of 7.81 mg/mL for JT_{YG}-Hex extract and varying in MICs from 1.95 to

62.5 mg/mL among clinical strains and JT_{YG}-EE, JT_{AFI}-EE, and JT_{AFI}-Hex extracts. It has been shown that *S. aureus* is the most common pathogen among the Gram (+) bacteria isolated from infected diabetic foot wounds [39, 40]. Moreover, both *S. aureus* and *S. epidermidis* strains are able to form biofilms in a number of chronic wound states, including DFIs, which appear to impair wound healing by delaying wound reepithelization, reducing the effects of antimicrobials and immune response, and further increasing the infection of the wound [41].

In the recent past, treating DFIs has become more challenging due to the increased prevalence of multidrug-resistant pathogens, particularly MRSA. Interestingly, the prevalence of MRSA in DFI varies among countries with an increase in less developed countries [8]. Therefore, we have elucidated the antibacterial activity of *JT*-EE and *JT*-Hex extracts against two predominant multiresistant bacteria found in diabetic wounds-MRSA and MDR *P. aeruginosa*. All four extracts had the greatest potential value against MRSA, with the highest inhibitory activity by ethanol extracts of both *JT* formulations with MIC 15.60 mg/mL and following hexane fractions with MIC 31.25 mg/mL. However, only JT_{YG}-Hex and JT_{AFI}-EE extracts were able to inhibit the growth of the Gram (-) MDR *P. aeruginosa,* albeit with a higher MIC value of 62.5 mg/mL. The antibacterial effect of *JT* extracts found in this study could be one of the mechanisms, which accelerates wound healing activity and thus supports its traditional use.

Such microbial infections and higher levels of biofilm in chronic wounds could influence the activity of the cells involved in wound healing and the composition of secreted cytokines and growth factors. Proinflammatory cytokines in the wound are required for initiating normal wound repair, but their increased expression levels are required only transiently. Moreover, both bacteria and their produced endotoxins can lead to the prolonged elevation of proinflammatory cytokines such as IL-1β, IL-6, and TNF-α and downregulation of the anti-inflammatory cytokines TGF-β and IL-10 in diabetic wounds, resulting in prolonged inflammation stage of wound healing [5]. The present study explored whether *JT* extracts were able to modulate inflammatory activity in LPS-challenged THP-1 macrophage cells. Our results showed that all *JT* plant extracts dose-dependently decreased IL-6, MCP-1 and CXCL10 gene expression and protein secretion in THP-1 macrophages in response to LPS; however, only JT_{YG}-EE was able to significantly reduce the protein secretion and gene expression of IL-1β cytokine. Hexane extracts of both *JT* formulations also showed the potency to modulate TNF-α gene expression. The *JT* extracts could be able to normalize overexpressed cytokines in chronic wounds and, therefore, could shorten the prolonged inflammation.

In the present study, the phytochemical analysis and GC-MS showed the presence of a considerable number of bioactive compounds and phytochemicals like flavonoids, terpenoids, sterols, glycosides, and fatty acids in the *JT* plant extracts, which can contribute to their antibacterial and anti-inflammatory activities. It has been shown that saponins, flavonoids, and phenols possess potent anti-inflammatory and antifungal activity. Terpenoids exhibit antibacterial activity and play an active role in wound healing, increase the concentration of antioxidants in wounds and restore inflamed tissues [42]. Furthermore, the *JT*- Hex extracts were rich in ar-turmerone, *a*-turmerone, and *ß*-turmerone, which are the major compounds in the essential oils of turmeric from *Curcuma longa*. Several studies have demonstrated that turmeric essential oils possessed potent antibacterial activity against a wide range of bacteria such as *S.aureus, E.coli*, *P.aeruginosa*, and *B.subtilis* [43–45]. Other phytoconstituents in *JT* extracts, such as squalene from *Cynodon dactylon,* phytol from *Erythrina variegate* and *Azadirachta indica*, and stigmasterol derived from *Pongamia pinata* may also contribute to the biological effects of the *JT* extracts. Studies have demonstrated that squalene promotes remodelling and tissue repair response signals by inhibiting the nuclear factor-kappa B, inducible nitric oxide synthase, the production of proinflammatory cytokines, such as IL-1β and TNF-α, and stimulation of anti-inflammatory cytokines IL-10 and IL-4 [46, 47]. The biological activities of phytol and phytosterols can be attributed to anti-inflammatory activities through reduction of leukocyte and neutrophil migration, IL-1β, IL-6, and TNF-α levels and oxidative stress, as well as antibacterial effects [48–50].

JT extracts showed a considerable number of free fatty acids such as palmitic, oleic, linoleic, stearic acids, and their esters. Free fatty acids have shown a vital effect in the prevention of antibacterial growth by targeting the structure and function of bacterial cell walls and membranes and inflammatory process via modulation of nitric oxide and cytokine production at the wound site [51, 52].

5. Conclusions

This study provides evidence that the ethanol and hexane extracts of both *JT* formulations possess potent antibacterial activity against Gram (+) and, to a lesser extent, Gram (−) bacteria and play an essential role in the anti-inflammatory response to LPS in macrophages. So, the study provides a rationale for the synergistic contribution of various herbs in the use of *JT* in the management of nonhealing wounds.

Data Availability

All data used during this study are available from the corresponding author.

Conflicts of Interest

The authors declare that they have no conflicts of interest.

Acknowledgments

The authors are grateful to Kaspars Jekabsons (University of Latvia, Faculty of Medicine, Department of Pharmacology) for his help with the statistical analysis. The research was funded by the Effective Collaboration Project from University of Latvia and AVP Research Foundation (Grant no. ZD2016/20226).

References

[1] B. A. Lipsky, A. R. Berendt, P. B. Cornia et al., "2012 infectious diseases society of America clinical practice guideline for the diagnosis and treatment of diabetic foot infections," *Clinical Infectious Diseases*, vol. 54, no. 12, pp. e132–e173, 2012.

[2] N. H. Cho, J. E. Shaw, S. Karuranga et al., "IDF Diabetes Atlas: global estimates of diabetes prevalence for 2017 and projections for 2045," *Diabetes Research and Clinical Practice*, vol. 138, pp. 271–281, 2018.

[3] M. P. Rodero and K. Khosrotehrani, "Skin wound healing modulation by macrophages," *International Journal of Clinical and Experimental Pathology*, vol. 3, no. 7, pp. 643–653, 2010.

[4] R. E. Mirza, M. M. Fang, E. M. Weinheimer-Haus, W. J. Ennis, and T. J. Koh, "Sustained inflammasome activity in macrophages impairs wound healing in type 2 diabetic humans and mice," *Diabetes*, vol. 63, no. 3, pp. 1103–1114, 2014.

[5] G. Zhao, M. L. Usui, R. A. Underwood et al., "Time course study of delayed wound healing in a biofilm-challenged diabetic mouse model," *Wound Repair and Regeneration*, vol. 20, no. 3, pp. 342–352, 2012.

[6] S. E. Dowd, R. D. Wolcott, Y. Sun, T. McKeehan, E. Smith, and D. Rhoads, "Polymicrobial nature of chronic diabetic foot ulcer biofilm infections determined using bacterial tag encoded FLX amplicon pyrosequencing (bTEFAP)," *PLoS One*, vol. 3, no. 10, Article ID e3326, 2008.

[7] M. Malone, K. Johani, S. O. Jensen et al., "Next generation DNA sequencing of tissues from infected diabetic foot ulcers," *EBioMedicine*, vol. 21, pp. 142–149, 2017.

[8] C. Dunyach-Remy, C. Ngba Essebe, A. Sotto, and J.-P. Lavigne, "*Staphylococcus aureus* toxins and diabetic foot ulcers: role in pathogenesis and interest in diagnosis," *Toxins*, vol. 8, no. 7, p. 209, 2016.

[9] P. Rao, *Bhaishajya Kalpana Vijnanam*, pp. 250–274, Chaukhamba Publications, Varanasi, India, 2013.

[10] Ayurvedic Formulary of India (AFI), *Part I*pp. 75–247, Government of India, Ministry of Health and Family Welfare, Department of Indian system of Medicines and Homeopathy, New Delhi, India, 2nd edition, 2003.

[11] B. Kumar, M. Vijayakumar, R. Govindarajan, and P. Pushpangadan, "Ethnopharmacological approaches to wound healing-exploring medicinal plants of India," *Journal of Ethnopharmacology*, vol. 114, no. 2, pp. 103–113, 2007.

[12] M. Kumar, "Jaatyadi Ghrita and its use in treating vrana (wound)," *International Research Journal of Pharmacy*, vol. 5, no. 3, pp. 128–130, 2014.

[13] Y. Kulkarni, S. Emmi, T. Dongargaon, and A. Wali, "Wound healing effect of Vimlāpanakarma with Jātyādi tailam in diabetic foot," *Ancient Science of Life*, vol. 34, no. 3, pp. 171–174, 2015.

[14] S. Singh and K. Rajoria, "Ayurvedic management of life-threatening skin emergency erythroderma: a case study," *AYU (An International Quarterly Journal of Research in Ayurveda)*, vol. 36, no. 1, pp. 69–72, 2015.

[15] S. Shailajan, S. Menon, S. Pednekar, and A. Singh, "Wound healing efficacy of Jatyadi Taila: in vivo evaluation in rat using excision wound model," *Journal of Ethnopharmacology*, vol. 138, no. 1, pp. 99–104, 2011.

[16] P. S. Jamadagni, S. Jamadagni, K. Mukherjee et al., "Experimental and histopathological observation scoring methods for evaluation of wound healing properties of Jatyadi Ghrita," *Ayu*, vol. 37, no. 3-4, pp. 222–229, 2016.

[17] S. R. Ayyar, P Vaidhyaratnam, and S. Warrier's, pp. 97-98, Arya Vaidhya Sala, Kottakal, India.

[18] B. Vijakumar, P. N. Rao, and K. P. Hemant, "A Case discussion on Dushta vrana (chronic wound)," *International Journal of Ayurvedic Medicine*, vol. 3, no. 1, pp. 53–57, 2012.

[19] Ayurvedic pharmacopoeia of India (API), *Part I*pp. 33-34, Government of India, Ministry of Health and Family Welfare, Department of AYUSH, New Delhi, India, 1st edition, 2008.

[20] W. C. Evance, *Trease and Evans' Pharmacognosy*pp. 96–98, Harcourt, Brace, San Diego, CA, USA, 14th. edition, 1997.

[21] S. Kamtekar, V. Keer, and V. Patil, "Estimation of phenolic content, flavonoid content, antioxidant and alpha amylase inhibitory activity of marketed polyherbal formulation," *Journal of Applied Pharmaceutical Science*, vol. 4, no. 9, pp. 061–065, 2014.

[22] H. P. S. Makkar, "Measurement of total phenolics and tannins using Folin-Ciocalteu method," in *Quantification of Tannins in Tree and Shrub Foliage*Springer, Berlin, Germany, 2003.

[23] J. Zhishen, T. Mengcheng, and W. Jianming, "The determination of flavonoid contents in mulberry and their scavenging effects on superoxide radicals," *Food Chemistry*, vol. 64, no. 4, pp. 555–559, 1999.

[24] C. Egbuna, J. C. Ifemeje, M. C. Maduako et al., "Phytochemical test methods: qualitative, quantitative and proximate analysis," *In Phytochemistry Fundamentals, Modern Techniques, and Applications*, Apple Academic Press, New York, NY, USA, 2018.

[25] P. Brenac and Y. Sauvaire, "Accumulation of sterols and steroidal sapogenins in developing fenugreek pods: possible biosynthesis in situ," *Phytochemistry*, vol. 41, no. 2, pp. 415–422, 1996.

[26] J. B. Harborne, *Phytochemical Methods: A Guide to Modern Techniques of Plant Analysis*, Chapman & Hall, London, 3rd edition, 1998.

[27] R. K. Upadhyay, M. B. Pandey, R. N. Jha, V. P. Singh, and V. B. Pandey, "Triterpene glycoside fromTerminalia arjuna," *Journal of Asian Natural Products Research*, vol. 3, no. 3, pp. 207–212, 2001.

[28] W. Yam, K. Ohtani, R. Hasai et al., "Steroidal saponins from fruits of Tribulus terrestris," *Phytochemistry*, vol. 42, no. 5, pp. 1417–1422, 1996.

[29] O. Lowry, N. Rosebrough, A. L. Farr, and R. Randall, "Protein measurement with the Folin phenol reagent," *Journal of Biological Chemistry*, vol. 193, no. 1, pp. 265–275, 1951.

[30] Clinical and Laboratory Standards Institute, *Performance Standards for Antimicrobial Susceptibility Testing. CLSI-M100-S27, CLSI M02-A12*, p. 282, 27th edition, Clinical and Laboratory Standards Institute, Pennsylvania, PA, USA, 2017.

[31] M. Balouiri, M. Sadiki, and S. K. Ibnsouda, "Methods for in vitro evaluating antimicrobial activity: a review," *Journal of Pharmaceutical Analysis*, vol. 6, no. 2, pp. 71–79, 2016.

[32] Y. Yang, Z. Zhang, S. Li, X. Ye, X. Li, and K. He, "Synergy effects of herb extracts: pharmacokinetics and pharmacodynamic basis," *Fitoterapia*, vol. 92, no. 2, pp. 133–147, 2014.

[33] P. P. Dhande, S. Raj, N. I. Kureshee et al., "Burn wound healing potential of Jatyadi formulations in rats," *Research Journal of Pharmaceutical, Biological and Chemical Sciences*, vol. 3, no. 4, pp. 747–754, 2012.

[34] F. M. Aarestrup and H. Hasman, "Susceptibility of different bacterial species isolated from food animals to copper sulfate, zinc chloride and antimicrobial substances used for disinfection," *Veterinary Microbiology*, vol. 100, no. 1-2, pp. 83–89, 2004.

[35] C. K. Sen, S. Khanna, M. Venojarvi et al., "Copper-induced vascular endothelial growth factor expression and wound healing," *American Journal of Physiology-Heart and Circulatory Physiology*, vol. 282, no. 5, p. H1821, 2002.

[36] K. Smith, A. Collier, E. M. Townsend et al., "One step closer to understanding the role of bacteria in diabetic foot ulcers: characterising the microbiome of ulcers," *BMC Microbiology*, vol. 16, no. 1, p. 54, 2016.

[37] W. Xavier, M. T. Sukumaran, A. K. Varma et al., "Emergence of multi drug resistant bacteria in diabetic patients with lower limb wounds," *Indian Journal of Medical Research*, vol. 140, no. 3, pp. 435–437, 2014.

[38] D. P. Basak, T. Adhikary, P. Das, and S. Biswas, "Phytochemical analysis and comparative study of antibacterial effect of turmeric extracts using different solvent," *IOP Conference Series: Materials Science and Engineering*, vol. 410, Article ID 012018, 2018.

[39] Y. Ge, D. MacDonald, H. Hait et al., "Microbiological profile of infected diabetic foot ulcers," *Diabetic Medicine*, vol. 19, no. 12, pp. 1032–1034, 2002.

[40] S. E. Gardner, S. L. Hillis, K. Heilmann, J. A. Segre, and E. A. Grice, "The neuropathic diabetic foot ulcer microbiome is associated with clinical factors," *Diabetes*, vol. 62, no. 3, pp. 923–930, 2013.

[41] C. F. Schierle, M. De la Garza, T. A. Mustoe, and R. D. Galiano, "Staphylococcal biofilms impair wound healing by delaying reepithelialization in a murine cutaneous wound model," *Wound Repair and Regeneration*, vol. 17, no. 3, pp. 354–359, 2009.

[42] J. R. S. Rex, N. M. S. A. Muthukumar, and P. M. Selvakumar, "Phytochemicals as a potential source for anti-microbial, antioxidant and wound healing - a review," *MOJ Bioorganic & Organic Chemistry*, vol. 2, no. 2, pp. 61–70, 2018.

[43] P. S. Negi, G. K. Jayaprakasha, and K. K. Sakariah, "Antibacterial activity of turmeric oil: a byproduct from curcumin manufacture," *Journal of Agricultural and Food Chemistry*, vol. 47, no. 10, pp. 4297–4300, 1999.

[44] R. Singh, R. Chandra, M. Bose et al., "Antibacterial activity of Curcuma longa rhizome extract on pathogenic bacteria," *Current Science*, vol. 83, no. 6, pp. 737–740, 2002.

[45] L. Czernicka, A. Grzegorczyk, Z. Marzec, B. Antosiewicz, A. Malm, and W. Kukula-Koch, "Antimicrobial potential of single metabolites of Curcuma longa assessed in the total extract by thin-layer chromatography-based bioautography and image analysis," *International Journal of Molecular Sciences*, vol. 20, no. 4, p. 898, 2019.

[46] C. Li, F. Xi, J. Mi et al., "Two new 3,4;9,10-secocycloartane type triterpenoids from Illicium difengpi and their anti-inflammatory activities," *Evidence Based Complementary and Alternative Medicine*, vol. 2013, Article ID 942541, 9 pages, 2013.

[47] C. Sanchez-Quesada, A. Lopez-Biedma, E. Toledo et al., "Squalene Stimulates a Key innate immune cell to Foster wound healing and Tissue repair," *Evidence Based Complementary and Alternative Medicine*, vol. 2018, Article ID 9473094, 2018.

[48] A. Navarro, B. De las Heras, and A. Villar, "Anti-inflammatory and immunomodulating properties of a sterol fraction from Sideritis foetens," *Biological and Pharmaceutical Bulletin*, vol. 24, no. 5, pp. 470–473, 2011.

[49] R. O. Silva, F. B. M. Sousa, S. R. B. Damasceno et al., "Phytol, a diterpene alcohol, inhibits the inflammatory response by reducing cytokine production and oxidative stress," *Fundamental & Clinical Pharmacology*, vol. 28, no. 4, pp. 455–464, 2014.

[50] M. T. Islam, S. A. Ayatollahi, S. M. N. K. Zihad et al., "Phytol anti-inflammatory activity: pre-clinical assessment and possible mechanism of action elucidation," *Cellular and Molecular Biology*, vol. 66, no. 4, pp. 264–269, 2020.

[51] B. Yoon, J. Jackman, E. Valle-González, and N.-J. Cho, "Antibacterial free fatty acids and monoglycerides: biological activities, experimental testing, and therapeutic applications," *International Journal of Molecular Sciences*, vol. 19, no. 4, p. 1114, 2018.

[52] C. Ribeiro Barros Cardoso, M. Aparecida Souza, E. Favoreto, and J. Deolina Oliveira Pena, "Influence of topical administration of n-3 and n-6 essential and n-9 nonessential fatty acids on the healing of cutaneous wounds," *Wound Repair and Regeneration*, vol. 12, no. 2, pp. 235–243, 2004.

Hindawi
Evidence-Based Complementary and Alternative Medicine
Volume 2021, Article ID 6671130, 11 pages
https://doi.org/10.1155/2021/6671130

Research Article

Ethanolic Extract of *Centella asiatica* Treatment in the Early Stage of Hyperglycemia Condition Inhibits Glomerular Injury and Vascular Remodeling in Diabetic Rat Model

Wiwit A. W. Setyaningsih,[1] **Nur Arfian**,[1] **Akbar S. Fitriawan**,[2] **Ratih Yuniartha**,[1] **and Dwi C. R. Sari**[1]

[1]*Department of Anatomy, Faculty of Medicine, Public Health, and Nursing, Universitas Gadjah Mada, Yogyakarta 55281, Indonesia*
[2]*Department of Nursing, Faculty of Health Sciences, Universitas Respati Yogyakarta, Yogyakarta 55282, Indonesia*

Correspondence should be addressed to Nur Arfian; nur_arfian@ugm.ac.id

Received 12 November 2020; Revised 31 March 2021; Accepted 8 June 2021; Published 6 July 2021

Academic Editor: Youhua Xu

Background. Diabetes mellitus (DM) is marked by oxidative stress, inflammation, and vascular dysfunction that caused diabetic nephropathy that resulted in end-stage renal disease (ESRD). Vascular dysfunction is characterized by an imbalance in vasoconstrictor and vasodilator agents which underlies the mechanism of vascular injury in DM. Additionally, diminished podocytes correlate with the severity of kidney injury. Podocyturia often precedes proteinuria in several kidney diseases, including diabetic kidney disease. *Centella asiatica* (CeA) is known as an anti-inflammatory and antioxidant and has neuroprotective effects. This research aimed to investigate the potential effect of CeA to inhibit glomerular injury and vascular remodeling in DM. *Methods*. The DM rat model was induced through intraperitoneal injection of streptozotocin 60 mg/kg body weight (BW), and then rats were divided into 1-month DM (DM1, $n = 5$), 2-month DM (DM2, $n = 5$), early DM concurrent with CeA treatment for 2 months (DMC2, $n = 5$), and 1-month DM treated with CeA for 1-month (DM1C1, $n = 5$). The CeA (400 mg/kg BW) was given daily via oral gavage. The control group (Control, $n = 5$) was maintained for 2 months. Finally, rats were euthanized and kidneys were harvested to assess vascular remodeling using Sirius Red staining and the mRNA expression of superoxide dismutase, podocytes marker, ACE2, eNOS, and ppET-1 using RT-PCR. *Results*. The DM groups demonstrated significant elevation of glucose level, glomerulosclerosis, and proteinuria. A significant reduction of SOD1 and SOD3 promotes the downregulation of nephrin and upregulation of TRPC6 mRNA expressions in rat glomerular kidney. Besides, this condition enhanced ppET-1 and inhibited eNOS and ACE2 mRNA expressions that lead to the development of vascular remodeling marked by an increase of wall thickness, and lumen wall area ratio (LWAR). Treatment of CeA, especially the DMC2 group, attenuated glomerular injury and showed the reversal of induced conditions. *Conclusions*. *Centella asiatica* treatment at the early stage of diabetes mellitus ameliorates glomerulosclerosis and vascular injury via increasing antioxidant enzymes.

1. Introduction

Diabetic nephropathy (DN) is one of the late complications of the diabetes mellitus (DM) and results in end-stage renal disease (ESRD) [1, 2]. It is widely known that uncontrolled chronic hyperglycemia disturbs the mitochondrial electron-transport chain producing superoxides. An excess of superoxides enhances the alteration of various pathways such as protein kinase-C (PKC) pathways, advanced glycation end (AGE) product, hexosamine, and polyol pathways [3]. The formation of superoxides leads to an increase of reactive oxygen species (ROS) which causes oxidative stress, inflammation, and vascular complications [4, 5]. It is widely reported that the plasma level of superoxide dismutase (SOD) and glutathione peroxidase (GSH-Px) were lower in the diabetic condition [6, 7] which increases the risk of

cardiovascular disease. Superoxide dismutase catalyzes superoxide anion (O_2^-) into hydrogen peroxide; however, the high glucose level inside the cells promotes production of ROS. There are three types of SOD: (1) SOD1 (Cu/Zn SOD) or intracellular SOD found in the cytoplasm and nuclei, (2) SOD2 (MnSOD) localized in the mitochondrial matrix, and (3) SOD3 (ZnSOD) or extracellular SOD found in the vascular extracellular space and highly expressed in the blood vessels and heart [8, 9].

Podocyte loss is the early injury in DN, then resulting in decreasing podocyte density and increasing albuminuria [10, 11]. Podocyte injury occurs since the early stage of DM and it dramatically worsens with the progressivity of diabetes. Podocyte loss also induces downregulation of podocyte protein, such as WT-1, that undergoes shifting localization of from the nucleus to cytoplasmic [12], and nephrin, an adhesion protein between the foot processes of the podocyte. At the early stage of glomerular injury, the urinary expression of nephrin can be detected before the proteinuria [13, 14]. Furthermore, in the glomeruli of patients with diabetes, the protein expression of nephrin reduces compared to the control subjects [15, 16]. Hyperglycemic itself may induce activation of the transient receptor potential canonical channel C6 (TRPC6), a receptor-operated cation channel, which is expressed in podocytes, mesangial cells, and endothelial cells; several conditions produce different results in TRPC6 expression. Downregulation of TRPC6 occurs in mesangial cells culture under high glucose treatment [17, 18]. On the other hand, several studies suggested that the treatment of high glucose increases TRPC6 in both the glomerulus and the heart which associated with ROS production and the renin-angiotensin system (RAS) activation [14, 19].

DM is often associated with microvascular and macrovascular diseases, as complication of the early to late hyperglycemia condition [20, 21]. Chronic hyperglycemia activates RAS that contributes to the glomerular hypertension exacerbating endothelial dysfunction. However, this mechanism is not fully understood [22]. Endothelin-1 (ET-1) has been known as a potent vasoconstrictor which promotes the imbalance between vasoconstrictor and vasodilator substances [23]. Diminished production of nitrite oxide (NO) contributes to the progressivity of cardiovascular and kidney damage mediated by impairment of vascular damage [24–26]. Plasma ET-1 and microangiopathy are positively correlated with the severity of type 2 DM that leads to vascular dysfunction [27]. Imbalance in vasoactive substances and local growth factors contribute to the pathophysiology of vascular injury [28]. Moreover, activation of vasoactive, such as RAS, induces oxidative stress which promotes vascular injury and remodeling that alter lumen and wall areas [28]. The essential landmark for the new concept of RAS is the characterization of angiotensin 1–7 (Ang-1-7) produced by ACE2 which has a vasodilatation effect [29]. On the other hand, ET-1 also contribute to vascular remodeling of intrarenal arteries in kidney ischemic/reperfusion injury [30].

Centella asiatica (CeA) is an herbaceous plant that is found in tropical climate countries. It has been widely used as a traditional herbal medicine due to its anti-inflammatory, antioxidant, and neuroprotective effects [31–34]. The main components of CeA are triterpenoids that consist of asiatic acid, madecassic acid, asiatocoside, and madecassicoside. Madecassic acid-contained CeA demonstrated antidiabetic effects through diminished ROS, increased catalase and glutathione, and reduced inflammatory processes [34, 35]. In addition, madecassic acid has an important role as the activator of peroxisome proliferator-activated receptor γ (PPARγ) through binding in the 5′ upstream element of peroxisome proliferator response element (PPRE). This process enhances the sensitivity of insulin even though this process remains unclear. PPARγ is widely found in the adipose tissue, intestines cells, macrophages, and endothelial cells. Once it is activated, agonist PPARγ promotes inhibition of tumor necrosis factor-alpha (TNF-α), nuclear factor kappa-beta (NFκB), and activator protein-1 (AP-1). Unless, madecassic per se induces the elevation of low-density lipoproteins (LDL) through upregulation of CD36 [34, 36, 37].

In this study, we aimed to elucidate role of CeA treatment either at the early or late hyperglycemia condition of DM. We focused on the glomerular injury and vascular remodeling that are mediated by its antioxidant properties.

2. Materials and Methods

2.1. Animal Experiment and Kidney Harvesting. The DM rat model was performed through intraperitoneally injection of streptozotocin (60 mg/kg body weight (BW)) single dose [38, 39]. Wistar male rats (3 months old, 160–200 grams) were then divided into DM for 1 month (DM1, $n = 5$), DM 2 months (DM2, $n = 5$), DM-treated CeA for 2 months started from the first diagnosis of DM (DMC2, $n = 5$), and DM-treated CeA after one month of DM (DM1C1, $n = 5$). The ethanolic extract of CeA (400 mg/kg BW) was given daily via oral gavage. At the end of study (after 2 months), rats were anesthetized with ketamine (50 mg/kg BW), xylazine (2 mg/kg BW), and acepromazine (0.5 mg/kg BW). Then, the abdomen and thorax were opened to access the heart and kidney. Next, the organs were perfused using NaCl 0.9% from left ventricle. Finally, the kidney was harvested, the left kidney was immersed in RNA Later (Ambion, AM7021), and the right kidney was kept in neutral buffer formalin (NBF).

This research was conducted according to the guidelines for animal care of the Universitas Gadjah Mada and had been approved by the Medical and Health Research Ethics Committee of the Faculty of Medicine, Public Health, and Nursing, Universitas Gadjah Mada, with ethical expediency number KE/FK/1211/EC/2019.

2.2. Centella asiatica Extraction. The CeA leaves were attained from Merapi Herbal Farma (the commercial herbal manufacturer) and the isolation method has been described according to the previous study [40]. *Centella asiatica* (400 mg/kg BW) [41] was administered via oral gavage for 1 month and 2 months after diabetes mellitus induction. This

process was performed in the Department of Pharmacology and Therapeutics, Faculty of Medicine, Public Health, and Nursing, Universitas Gadjah Mada.

2.3. RNA Extraction and cDNA Synthesis. Kidney was extracted using Genezol RNA Solution (GENEzol™, GZR100) according to the protocol from the manufacturer. The RNA concentration was quantified using a nanodrop (Maestrogen, MN-913A). The RNA was synthesized into cDNA using cDNA synthesis kit (SMOBio, RP1400) with PCR condition: 30°C for 10 min., 42°C for 60 min., and 85°C for 5 min.

2.4. Reverse Transcriptase-PCR (RT-PCR). Reverse Transcriptase-PCR was performed to amplify several specific target genes which consisted of antioxidant enzymes, nephrin, TRPC6, ACE2, eNOS, and ppET-1 using the following primers' sequences (Table 1):

2.5. Vascular Remodeling. The kidney-embedded paraffin was cut into 4 μm in thickness followed with deparaffinized using xylene and rehydrated using 100%, 90%, 80%, and 70% ethanol. Afterwards, slides were incubated using Sirius Red for an hour to assess wall thickness in intrarenal arteries (diameter 10–50 μm) [30]. Finally, the slides were captured using Optilab software in 400x magnification of 15 random areas.

2.6. Immunohistochemical (IHC) Staining of SOD-1 and WT-1. The slides were deparaffinized using xylene and rehydrated using 100%, 90%, 80%, and 70% ethanol which was then followed with antigen retrieval using citrate buffer pH 6 and blocking peroxidase using H_20_2 3% in PBS solution. Afterwards, slides were incubated with blocking serum (Finetest, IHC007), and rabbit 1st monoclonal antibody SOD1 (1 : 100, Bioss, bs-10216R) and WT-1 (1 : 50, Santa Cruz, sc-192) overnight. Finally, the slides were incubated with poly-HRP Goat-anti rabbit and diaminobenzidine tetrahydrochloride (DAB) (Finetest, IHC007). The results were assessed with light microscope (Olympus, CX22®), and captured with Optilab software with 400x magnification.

2.7. Western Blot. The kidney was extracted according to the protocol from Pro-Prep™ (Intron Biotechnology, 17081). Twenty milligrams of kidney was homogenized with 600 μL of Pro-Prep™ solution. Then, the homogenates were centrifugated in 15,000 rpm at 4 °C for 20 min. Afterwards, the supernatants were separated onto 10% SDS-PAGE and transferred to a polyvinylidene fluoride (PVDF) membrane. Next, it was incubated with the primary antibodies, β-actin (1 : 1000, Abcam, ab8227) and SOD1 (1 : 200, Bioss, bs-10216R) overnight and ended with visualization using ECL Prime Western Blotting Detection Reagents (GE Healthcare, RPN2232) under Geldoc machine (Geldoc Syngene Gbox Seri Chemi xrq).

2.8. Statistical Analysis. The SPSS 23 software (IBM Corp., Chicago) for Windows was used for analyses data. Data normality test was conducted using Shapiro–Wilk and one-way ANOVA for normal data distribution. The p-value less than 0.05 ($p < 0.05$) was considered statistically significant.

3. Results

3.1. Depletion of Glucose Level, Proteinuria, and Glomerulosclerosis in CeA-Treated Groups. We demonstrated that streptozotocin injection consistently elevated glucose level compared to the control group ($p \leq 0.001$), and it lowered when the CeA was administered. The CeA treatment at the early stage of DM (DMC2) significantly reduced glucose level compared to the DM2 ($p = 0.009$). Otherwise, the DM1C1 did not show any significant reduction of glucose level compared to DM groups. The proteinuria was obviously seen in the DM2 group compared to the control group ($p \leq 0.001$) and DM1 group ($p \leq 0.001$). The CeA treatment groups, either DMC2 or DM1C1, demonstrated a significant reduction of the proteinuria compared to the DM2 ($p \leq 0.001$).

The histological staining of glomerulosclerosis demonstrated normal morphological features in the control group; however, the DM groups showed sclerosis, synechiae, thickening of the basement membrane, and narrowing of the glomerular arteriolar. When the CeA was administered, these injuries significantly ameliorated compared to the control group.

3.2. Centella asiatica Elevated Superoxide Dismutase. The mRNA expression of SOD1 and SOD3 significantly lowered in the DM groups; however, there was no alteration of SOD2 mRNA expression. The mRNA expression of SOD-1 was sharply reduced in the DM1 ($p = 0.005$) and DM2 ($p \leq 0.001$) compared to the control. The DMC2 showed a significant elevation of the mRNA expression of SOD1 compared to the DM2 ($p = 0.006$) while the DM1C1 showed no difference with the DM groups. We also demonstrated that the SOD1 protein expression decreased in the DM groups compared to the control group. The DMC2 exhibited a significant elevation of the SOD1 protein expression. The SOD1 protein expression reduced sharply in the DM1 ($p = 0.000$), DM2 ($p = 0.006$), DMC2 ($p = 0.004$), and DM1C1 ($p = 0.000$) groups compared to the control group. Administration of the CeA at the DMC2 ($p = 0.015$) improved SOD1 protein expression compared to the DM1 group.

Hyperglycemia-caused DM enhanced a significant reduction of the SOD3 in both DM1 ($p = 0.004$) and DM2 ($p = 0.003$) groups compared to the control group. Besides, the DMC2 demonstrated a significant upregulation of the SOD3 mRNA expression compared to the DM1 ($p = 0.017$), DM2 ($p = 0.010$), and DM1C1 ($p = 0.038$).

3.3. CeA Treatment May Associate with High Nephrin and Low TRPC6 mRNA Expressions. Next, our findings suggested that the mRNA expression of TRPC6 was higher in DM1 ($p = 0.002$) and DM2 ($p = 0.001$) groups compared to the

control group. Meanwhile, only the DMC2 ($p = 0.005$) had lowered the mRNA expression of TRPC6 compared to the control group. The nephrin was significantly lowered in the DM2 group compared to the control ($p \leq 0.001$) and DM1 groups ($p = 0.001$). The CeA groups elicited higher nephrin mRNA expression compared to the control group ($p = 0.001$). Lower nephrin mRNA expression aligned with reduction WT-1 protein expression in the kidney and CeA treatment restored the WT-1 protein expression in the glomerulus.

3.4. CeA Reduced ppET-1 and Increased Both eNOS and ACE2 mRNA Expressions. Then, we assessed the imbalance of vasoconstrictor and vasodilator agents that promotes vascular remodeling induced by DM. Early stage of hyperglycemia (DM1 group) increased eNOS mRNA level ($p = 0.045$) compared to the control group. Then, the eNOS mRNA expression in DM2 group plummeted ($p = 0.014$) compared to the control group. The eNOS mRNA expression increased significantly in DM1C1 ($p = 0.007$), and DMC2 ($p = 0.017$) compared to the DM1 group as well as DMC2 ($p = 0.038$) compared to the DM2 group. The vasoconstrictor agent, ppET-1, was significantly higher in DM1 ($p \leq 0.001$) and DM2 ($p \leq 0.001$) groups compared to the control group. CeA treatment at the early stage of hyperglycemia-induced DM significantly reduced ppET-1 mRNA expression compared to the DM1 ($p = 0.019$) and DM2 ($p = 0.001$) groups. Besides, we assessed the mRNA expression of ACE2 as the counter-arm of angiotensin II. The DM stimulated downregulation of the ACE2 mRNA expression that was obviously seen in DM2 ($p \leq 0.001$) compared to the control group. However, neither DMC2 ($p = 0.028$) nor DM1C1 (p=0.009) promoted significantly higher ACE2 compared to the DM2 group.

3.5. Centella asiatica-Treated Diabetes Mellitus Ameliorated Vascular Remodelling. Finally, we demonstrated that CeA inhibited vascular remodeling in the kidney which delineated an increase of wall thickness and lumen wall area ratio (LWAR) in the diabetes mellitus groups. Thickening of the vascular wall was obviously seen in DM2 (p<0.01) compared to the control and DM1 groups. Treatment of CeA markedly reduced the wall thickness in DMC2 compared to the DM2 ($p = 0.0255$) group as well as in DM1C1 compared to the DM1 ($p = 0.0219$) group. The lumen wall area ratio increased significantly in DM1 ($p = 0.005$) and DM2 ($p = 0.039$) groups compared to the control group. Treatment of CeA in the early stage of hyperglycemia-induced diabetes mellitus (DMC2, $p = 0.040$) remarkably reduced the lumen wall area ratio compared to the DM1 group.

4. Discussion

This study reveals the protective effect of CeA extract in the early hyperglycemia condition, but not in late hyperglycemia condition in kidney injury as DM progression. CeA treatment in DMC2 group which represented the early CeA treatment, as early as hyperglycemia occurred, may attenuate the diabetic nephropathy (DN). DN initiates chronic kidney disease (CKD) and ESRD that exacerbates the mesangial cell expansion, thickening of the glomerular basement membrane (GBM), and glomerulosclerosis [40, 41]. Since the glomerular filtration barrier (GFB) consists of endothelial cells, GBM, and slit diaphragm (SD), the impairment of the layers contributes to the proteinuria [42]. In this study, diabetes kidney disease was induced through a single intraperitoneal injection (60 mg/kg BW) which resulted in an elevation of blood glucose level and kidney impairment showed by a high level of proteinuria and glomerulosclerosis (Figure 1). High glucose level resulted in damage to the endothelial and mesangial cells due to glucose flooding inside the cells [43]. Lower blood glucose level was associated with CeA treatment in the early-hyperglycemic condition, but not in late hyperglycemic state (Figure 1). This finding demonstrated that attenuation of injury might partially have association with blood glucose reduction.

The CeA treatment significantly reduced the proteinuria and glomerulosclerosis compared to the DM2 group (Figure 1). Oral administration of CeA, both 500 mg/kg BW and 1000 mg/kg BW, showed antihyperglycemic effect that is mediated by α-amylase and disaccharidase enzymes inhibition in the intestines [39]. Then, it attenuates blood glucose level and lipid profile serum followed by diminished polyphagia, polydipsia, and polyuria [38, 42]. A previous study mentioned that CeA has several potent active compounds such as asiatic acid, asiatocoside, madecassic acid, madecassoside, astragaloside, and triptolide [33, 44, 45] that cause a reduction in proteinuria and glomerulosclerosis. In addition, the administration of the asiatocoside and asiatic acid significantly reduced urinary protein excretion and blood glucose level in DM rat models [33, 45]. Elucidating active compound in this study might give better understanding for the reno-protective effect of CeA in the future.

Early treatment of CeA in DM might attenuate oxidative stress and podocyte injury with upregulation of SOD-1, SOD-3, and nephrin mRNA expression Figures 2 and 3. DM promotes activation of both enzymatic and nonenzymatic pathways that leads to ROS production. Activation of the AGE and its ligand and receptor, receptor advance glycated-end product (RAGE), in the endothelial surface leads to proinflammatory cytokines and free radicals productions [3, 46–48]. Control glucose loss inside the cell stimulates transport-chain electron dysfunction in the mitochondria that contributes to the biggest source of ROS [3, 5, 48, 49]. Antioxidant enzyme SOD has an essential role in catalyzing superoxide anion (o_2^-) into hydrogen peroxide and molecular oxygen, thus protecting cellular and histological damage from ROS [50, 51]. However, during the hyperglycemia, the SOD is unable to eliminate the excess ROS, which results in suppression of the antioxidant enzymes such as SOD1 [52,53], SOD3 [53], and catalase [52] but not SOD2. Reduction of the kidney SOD enzymes was demonstrated in KK/Ta-Akita mice after 5-week hyperglycemia mediated by TNF-α and interleukin-1β (IL-1β) [53]. Overexpression of SOD1 in the SOD1-Tg mice suppressed lipid peroxidation in the maternal hyperglycemia that leads to diminished susceptibility of diabetic embryopathy [53, 54]. Knockout of SOD3 resulted in reduced basal NO activity and increased

Table 1: Primer sequences.

Gene	Forward primer ($5' \longrightarrow 3'$)	Reverse primer ($5' \longrightarrow 3'$)	Annealing temperature
SOD1	GCGGTGAACCAGTTGTGGTG	AGCCACATTGCCCAGGTCTC	55
SOD2	ATGTTGTGTCGGGCGGCGTGCAGC	GCGCCTCGTGGTACTTCTCCTCGGTG	57
SOD3	AGGCAGCTCAGAGGCTCTTT	GAGGTTCCACACCTGACAAGC	63
Nephrin	ACTCAGGCTGACATCTGGGAT	AGAGCTGGAATGACAGTGATGG	55
TRPC6	AAGTGAACGAAGGGGAGCTG	ACAGTCTCTCCCCAAGCTTTC	60
ACE2	GCCCAAAAGATGAACGAGGC	GACGCTTGATGGTCGCATTC	60
eNOS	CCGGCGCTACGAAGAATG	AGTGCCACGGATGGAAATT	55
ppET-1	GTCGTCCCGTATGGACTAGG	ACTGGCATCTGTTCCCTTGG	57
β-Actin	GCAGATGTGGATCAGCAAGC	GGTGTAAAACGCAGCTCAGTAA	53

The cDNA was mixed with Taq Master Mix (Promega, GoTaq Green, M7122) and primers and then incubated in 94 °C denaturation for 10 s, annealing (according to the table) for 30 sec, and extension 72 °C for 1 min final extension phase ending with the conditions of 72 °C for 10 minutes for 35 cycles. The PCR products were separated using 2% agarose gel along with 100 bp DNA ladder (SMOBio, DM2400). The expression of the genes was quantified with a densitometry analysis using the ImageJ software, and the mRNA expression of β-actin was used as the housekeeping genes.

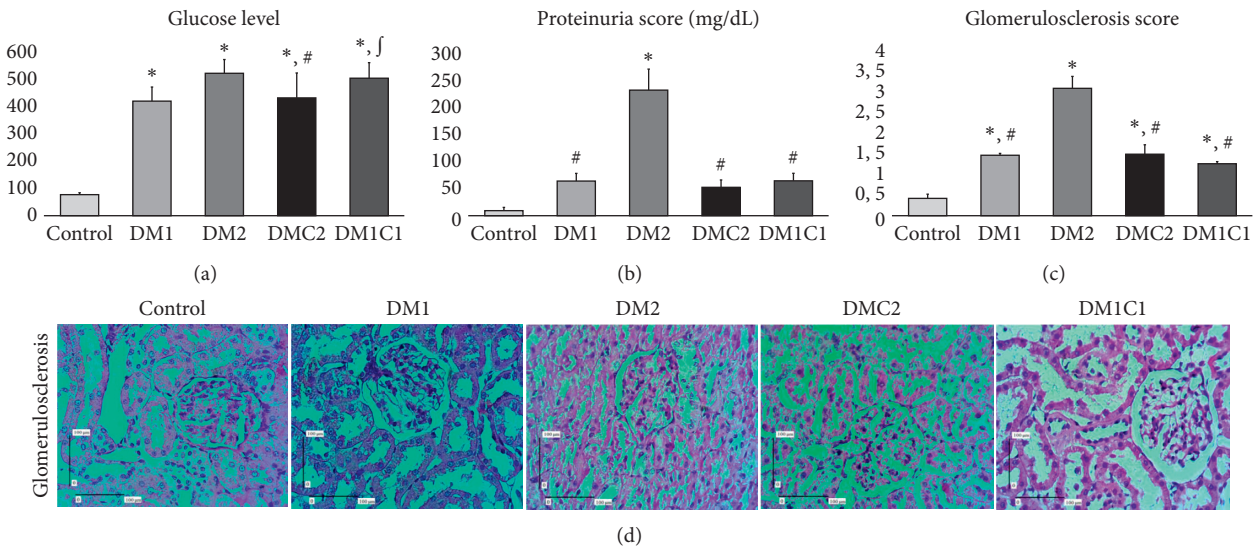

Figure 1: Ethanolic extract of *Centella asiatica* alleviated glucose level, proteinuria, and glomerulosclerosis under DM. (a–c) The results of glucose level, proteinuria, and glomerulosclerosis score. (d) The representative figure of glomerulosclerosis (magnification 400X; scale bar 100 μm). $^{*}p < 0.01$ vs. control, $\int p < 0.01$ vs. DM1, and $^{\#}p < 0.01$ vs. DM2.

superoxides in the endothelial and vascular that then led to impaired endothelial relaxation [55]. Oral treatment of CeA improves antioxidant enzymes by preventing lipid peroxidation [56], activates PPARγ that then promotes insulin sensitivity, and represses TNF-α and NFκB [37].

Hyperglycemic condition also induces podocyte injury. The detachment of the podocytes in the urinary sediment can be seen in patients with DM that precedes the proteinuria [56–58]. The diminished mRNA and protein level of nephrin in the DN-induced adriamycin alter the podocyte structure and integrity [33]. We showed STZ-induced DM markedly reduced the mRNA nephrin expression (Figure 2). The TRPC6 may play a key role in podocyte injury during DN. Knockout TRPC-6 in Akita mice attenuated glomerulosclerosis, tubular injury, and proteinuria while even promoting mesangial cell expansion [14, 59]. ROS induces glomerulosclerosis with the upregulation of the TRPC6 in podocytes [59, 60]. Podocyte culture transfected with scrambled siRNA targeted TRPC6 and Syndecan4 (Syn4), exposure to high d-glucose increased ROS, and TRPC6 via Syn4 [19]. Besides, the upregulation of the TRPC6 mRNA expression was observed in the monocytes of patients with type-2 DM that promotes atherosclerosis [61]. Based on our data, attenuation of podocyte injury may be associated with reducing hyperglycemia, upregulation of SOD-1/SOD-3 mRNA expression, and downregulation of the TRPC6 mRNA expression in the CeA treatment in early hyperglycemia condition (Figures 2 and 3). However, our study cannot correlate precisely the podocyte detachment with the reduction of podocyte marker expression in our study. The underlying mechanism of podocyte detachment may give a better understanding of the mechanism.

In this study, we observed that STZ-induced DM rat model promoted upregulation of ET-1 mRNA expression and downregulation of eNOS and ACE2 mRNA expressions (Figure 4). High production of ROS in DM plays an essential

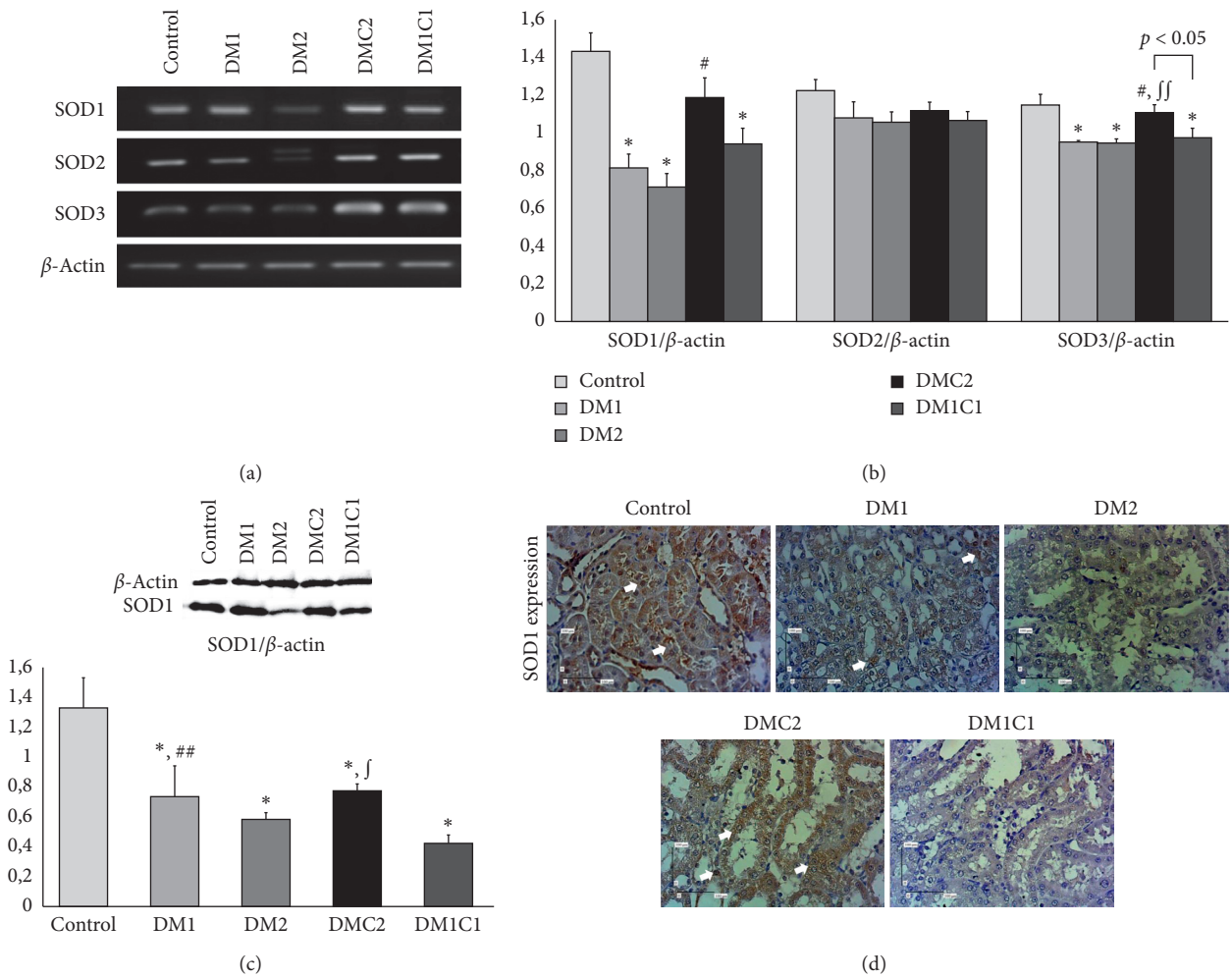

Figure 2: Ethanolic extract of *Centella asiatica* enhanced SOD1 and SOD3 mRNA expressions. (a, b) The representative figures of SOD1, SOD2, and SOD3 mRNA expressions according to the RT-PCR. (c) The representative images of SOD1 protein expression (magnification 400x; scale bar 100 μm). *: <0.01 vs. control, $^{\int}$: <0.01 vs. DM1 and <0.05 vs. DM1, and $^{\#}$: <0.01 vs. DM2.

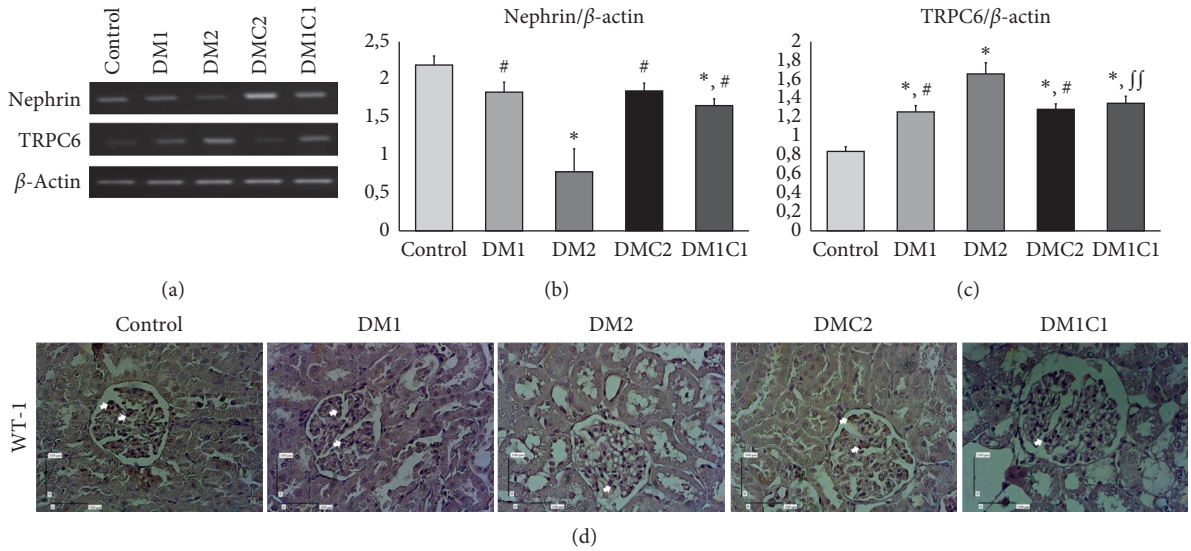

Figure 3: *Centella asiatica* upregulated nephrin and downregulated TRPC6 mRNA expressions with preservation of WT-1 protein staining. (a) The representative pictures of nephrin and TRPC6 mRNA expression based on RT-PCR. (b, c) The bar charts of semiquantitative analysis of nephrin and TRPC6 mRNA expression. (d) The representative figures of WT-1 protein expression (magnification 400X; scale bar 100 m). *<0.01 vs. control, $^{\int\int}$<0.05 vs. DM1, and $^{\#}$<0.01 vs. DM2.

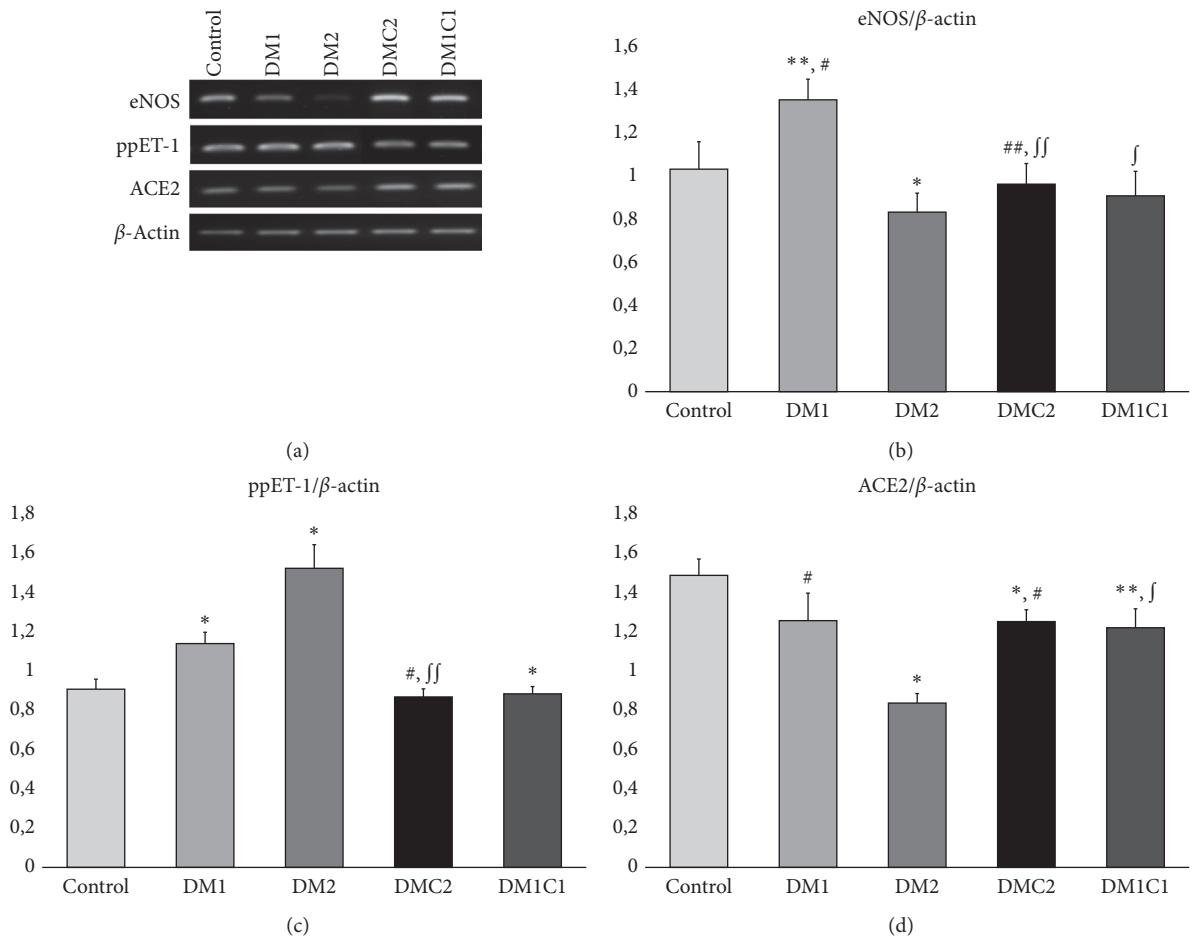

Figure 4: *Centella asiatica* preserved eNOS and down-regulated ACE2 and ppET-1 mRNA expression in DMC2 compared to DM2 groups. (a) The representative pictures of eNOS, ACE2, and ppET-1 based on RT-PCR quantification. (b -d) The bar charts of semiquantitative analysis of eNOS, ppET-1, and ACE2 mRNA expression. *<0.01 vs. control, **<0.05 vs. control, $^{\int}$<0.01 vs. DM1, $^{\int\int}$<0.05 vs. DM1, $^{\#}$<0.01 vs. DM2, and $^{\#\#}$<0.01 vs. DM2.

role in endothelial dysfunction through the inactivation of nitrite oxide (NO) and activation of renin-angiotensin-system (RAS). The eNOS has an essential role as an anti-atherogenic that has a significant relevancy with the development of vascular injury in diabetes. The eNOS knockout mice demonstrated severe diabetic nephropathy concomitant with high blood pressure [62] and vascular hypertrophy [63]. Furthermore, deletion of the ET-1 in endothelial cells reduced oxidative stress after kidney ischemic/reperfusion injury (IRI) [30] which may correlate with the downregulation of SOD3 mRNA expression (Figure 2). ET-1 shows different effects through the Endothelin-A receptor (EDNRA) and Endothelin-B receptor (EDNRB) that exert various impacts. Several studies showed that the correlation between an increase of plasma ET-1 and elevation of GFR, mesangial cell expansion, and proteinuria [27]. Enhanced ET-1 level promotes vascular dysfunction via inhibition of the NO production that then leads to insufficient eNOS bioavailability and production [64]. The role of ET-1 promotes glomerulosclerosis is mediated by EDNRB; the administration of BQ-788, EDNRB antagonist, showed downregulation of the ET-1-induced calcium transient pathway that leads to podocyte detachment [65].

It has been demonstrated that RAS can play a role through the ACE-angiotensin II axis and ACE2-Ang1-7 axis. Angiotensin II raises renal ET-1 formation from podocyte cells and drives glomerulosclerosis and podocyte detachment [64, 65]. On the other hand, angiotensin II cleaved by angiotensin-converting enzyme2 (ACE2) produces Ang1-7 that exhibits a vasodilatation effect [29]. This enzyme significantly decreases in the DM condition as shown by the DM2 group. The pharmacological administration of ACE2 inhibitor elicited albuminuria and associated with the severity of the glomerular lesions [29]. The antioxidant effect from CeA is associated with the diminishment of ET-1 mRNA expression followed by the enhancement of eNOS and ACE2 mRNA expression.

The early stage of DM showed hyperfiltration marked by vascular hypertrophy, and vascular injury [59]. An elevation of the GFR, one of the characteristics of early diabetes, correlates with an increase of vessel diameter and renal blood flow [66]. Our findings were consistent with the previous research that showed the dilatation of

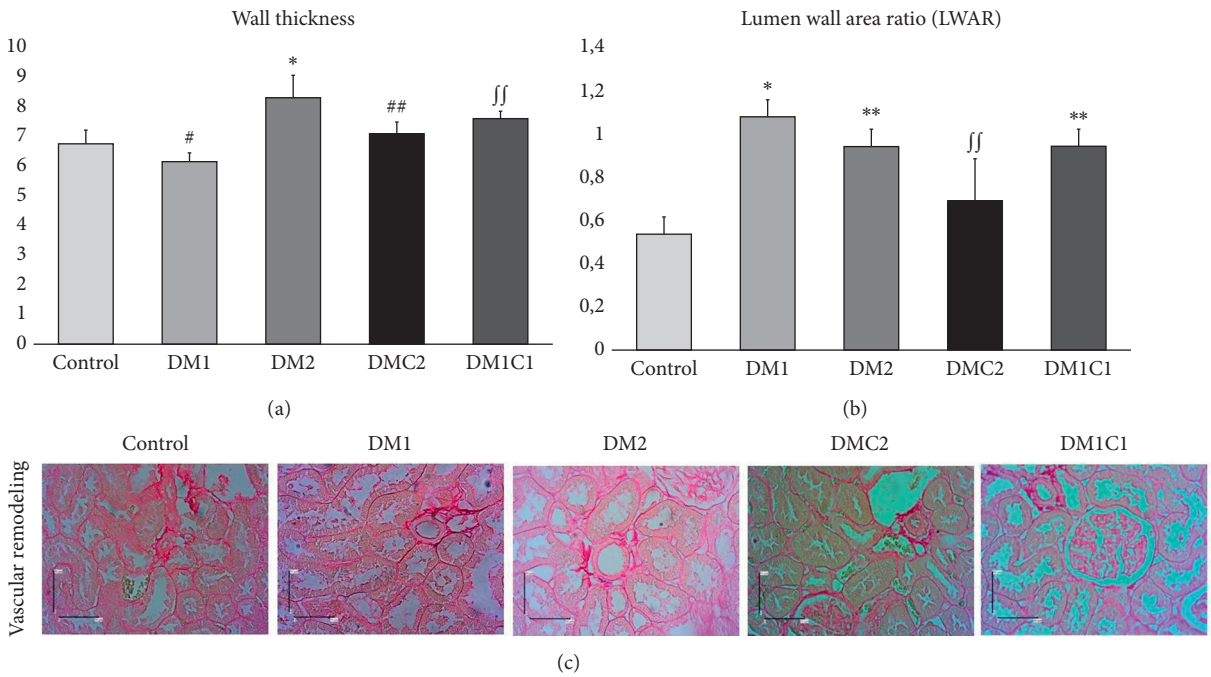

Figure 5: Ethanolic extract of *Centella asiatica* treatment in DMC2 group attenuated vascular remodeling with reducing wall thickness. (a, b) The quantification of wall area and wall/lumen area ratio which represented vascular remodeling measurement. (c) Representative pictures of intra-renal arteries for vascular remodeling assessment. *<0.01 vs. control, **<0.05 vs. control, $^{\int\int}$<0.05 vs. DM1, $^{\#}$<0.01 vs. DM2, and $^{\#\#}$<0.01 vs. DM2.

the lumen, basal membrane thickening, and increasing wall thickness (Figure 5). We demonstrated that the CeA treatment since the early hyperglycemia condition of the DM reduced the vascular lumen area and wall thickness area. However, the effect of CeA extract treatment during late hyperglycemia condition may not demonstrate kidney injury attenuation.

In this study, we want to focus on the protective effect of CeA in reducing the progression of DM in the early and late stage of diabetes mellitus. We explore several aspects, including oxidative stress, podocyte injury, glomerulosclerosis, and endothelial injury that become our main focus. Despite this, there are limitations in this study. One important limitation is that this study did not provide a positive control group which might not be compared with standardized therapeutics drugs, such as glibenclamide [67, 68], and metformin [69]. Even though our study reported that CeA treatment at the early stage of diabetes mellitus could improve random blood glucose level, glomerulosclerosis, antioxidant level, podocyte injury, and diabetic nephropathy, we cannot elucidate the effectiveness of CeA compared to the standardized therapeutic drugs. Besides, we did not provide the quality control of the extract. We are fully aware that the quality control process provides more information for the reader. Therefore, we cannot determine which active compound of CeA gives an essential role as a reno-protective agent in DM or the hazardous effect. In the future, these limitations need further investigation.

5. Conclusions

Centella asiatica (CeA) treatment at the early stage of DM ameliorates glomerulosclerosis and vascular injury via increasing antioxidant enzymes. However, treatment of CeA at the middle stage of DM less effectively ameliorates glomerular and vascular injury in diabetes mellitus .

Data Availability

Data are available on request through contacting the corresponding author and can be assessed through the supplementary files.

Conflicts of Interest

The authors declare that there are no conflicts of interest regarding the publication of this study.

Acknowledgments

The authors thank Mr. Mulyana for maintaining the animal and laboratory assistant and Klinik Bahasa Faculty of Medicine, Public Health, and Nursing for assisting in the language editing. This work was funded by Universitas Gadjah Mada, Indonesia, with the grant no. 2403/UN1.P.III/DIT-LIT/PT/2020.

Supplementary Materials

Supplementary Table 1: specific antibody information for immunohistochemistry. Supplementary Table 2: specific primer pair information for RT-PCR. (*Supplementary Materials*)

References

[1] K. G. M. M. Alberti and P. Z. Zimmet, "Definition, diagnosis and classification of diabetes mellitus and its complications. Part 1: diagnosis and classification of diabetes mellitus. Provisional report of a WHO Consultation," *Diabetic Medicine*, vol. 15, no. 7, pp. 539–553, 1998.

[2] W. T. Cade, "Diabetes-Related microvascular and macrovascular diseases in the physical therapy setting," *Physical Therapy*, vol. 88, no. 11, pp. 1322–1335, 2008.

[3] M. Brownlee, "The pathobiology of diabetic complications: a unifying mechanism," *Diabetes*, vol. 54, no. 6, pp. 1615–1625, 2005.

[4] T. Fukai and M. Ushio-fukai, "Superoxide dismutases: role in redox signaling, vascular function, and diseases," *Antioxidants & Redox Signaling*, vol. 15, no. 6, pp. 1583–1606, 2011.

[5] N. Arfian, W. A. W. Setyaningsih, M. M. Romi, and D. C. R. Sari, "Heparanase upregulation from adipocyte associates with inflammation and endothelial injury in diabetic condition," *BMC Proceedings*, vol. 13, no. Suppl 11, pp. 17-18, 2019.

[6] M. I. Yilmaz, M. Saglam, K. Caglar et al., "The determinants of endothelial dysfunction in CKD: oxidative stress and asymmetric dimethylarginine," *American Journal of Kidney Diseases*, vol. 47, no. 1, pp. 42–50, 2006.

[7] A. G. Miranda-díaz, L. Pazarín-villaseñor, F. G. Yanowsky-escatell, J. Andrade-sierra, and E. K. Changes, "Oxidative stress in diabetic nephropathy with early chronic kidney disease," *Journal of Diabetes Research*, vol. 2016, pp. 1–8, Article ID 7047238, 2016.

[8] J.-R. Peng, T.-T. Lu, H.-T. Chang, X. Ge, B. Huang, and W.-M. Li, "Elevated levels of plasma superoxide dismutases 1 and 2 in patients with coronary artery disease," *BioMed Research International*, vol. 2016, pp. 1–9, Article ID 3708905, 2016.

[9] P. Mondola, S. Damiano, A. Sasso, and M. Santillo, "The Cu, Zn superoxide dismutase: not only a dismutase enzyme," *Front. Physiol.*vol. 7, pp. 1–8, 2016.

[10] A. Minakawa, A. Fukuda, Y. Sato et al., "Podocyte hypertrophic stress and detachment precedes hyperglycemia or albuminuria in a rat model of obesity and type2 diabetes-associated nephropathy," *Scientific Reports*, vol. 9, no. 1, pp. 18485–18515, 2019.

[11] B. Liu, X. He, S. Li, B. Xu, L. Birnbaumer, and Y. Liao, "Deletion of diacylglycerol-responsive TRPC genes attenuates diabetic nephropathy by inhibiting activation of the TGFβ1 signaling pathway," *American Journal of Translational Research*, vol. 9, no. 12, pp. 5619–5630, 2017.

[12] J. Su, S.-J. Li, Z.-H. Chen et al., "Evaluation of podocyte lesion in patients with diabetic nephropathy: wilms' tumor-1 protein used as a podocyte marker," *Diabetes Research and Clinical Practice*, vol. 87, no. 2, pp. 167–175, 2010.

[13] Y. Kandasamy, R. Smith, E. R. Lumbers, and D. Rudd, "Nephrin - a biomarker of early glomerular injury," *Biomarker Research*, vol. 2, no. 21, pp. 1–8, 2014.

[14] A. Staruschenko, "TRPC6 in diabetic kidney disease: good guy or bad guy?" *Kidney International*, vol. 95, no. 2, pp. 256–258, 2019.

[15] S. Doublier, G. Salvidio, E. Lupia et al., "Nephrin expression is reduced in human diabetic nephropathy: evidence for a distinct role for glycated albumin and angiotensin II," *Diabetes*, vol. 52, no. 4, pp. 1023–1030, 2003.

[16] B. Jim, M. Ghanta, A. Qipo et al., "Dysregulated nephrin in diabetic nephropathy of type 2 diabetes: a cross sectional study," *PLoS One*, vol. 7, no. 5, p. e36041, 2012.

[17] S. Graham, M. Ding, S. Sours-Brothers, T. Yorio, J. X. Ma, and R. Ma, "Downregulation of TRPC6 protein expression by high glucose, a possible mechanism for the impaired Ca^{2+} signaling in glomerular mesangial cells in diabetes," *American Journal of Physiology: Renal Physiology*, vol. 293, no. 4, 2007.

[18] P. Menè, G. Pugliese, F. Pricci, U. Di Mario, G. A. Cinotti, and F. Pugliese, "High glucose inhibits cytosolic calcium signaling in cultured rat mesangial cells," *Kidney International*, vol. 43, no. 3, pp. 585–591, 1993.

[19] F. Thilo, M. Lee, S. Xia, A. Zakrzewicz, and M. Tepel, "High glucose modifies transient receptor potential canonical type 6 channels via increased oxidative stress and syndecan-4 in human podocytes," *Biochemical and Biophysical Research Communications*, vol. 450, no. 1, pp. 312–317, 2014.

[20] G. Spinetti, N. Kraenkel, C. Emanueli, and P. Madeddu, "Diabetes and vessel wall remodelling: from mechanistic insights to regenerative therapies," *Cardiovascular Research*, vol. 78, no. 2, pp. 265–273, 2010.

[21] G. K. Kolluru, S. C. Bir, and C. G. Kevil, "Endothelial dysfunction and diabetes: effects on angiogenesis, vascular remodeling, and wound healing," *International Journal of Vascular Medicine*, vol. 2012, pp. 1–30, Article ID 918267, 2012.

[22] A. Kuwabara, M. Satoh, N. Tomita, T. Sasaki, and N Kashihara, "Deterioration of glomerular endothelial surface layer induced by oxidative stress is implicated in altered permeability of macromolecules in Zucker fatty rats," *Diabetologia*, vol. 53, no. April, pp. 2056–2065, 2010.

[23] S. Fakhruddin, W. Alanazi, and K. E. Jackson, "Diabetes-induced reactive oxygen species: mechanism of their generation and role in renal injury," *Journal of Diabetes Research*, vol. 2017, pp. 1–30, Article ID 8379327, 2017.

[24] B. S. Dellamea, C. B. Leitão, R. Friedman, and L. H. Canani, "Nitric oxide system and diabetic nephropathy," *Diabetology & Metabolic Syndrome*, vol. 6, no. 17, pp. 17–26, 2014.

[25] Y. Qian, E. Feldman, S. Pennathur, M. Kretzler, and F. C. Brosius, "Mechanisms of glomerulosclerosis in diabetic nephropathy," *Diabetes*, vol. 57, no. 6, pp. 1439–1445, 2014.

[26] M. A. Creager, T. F. Lüscher, F. Cosentino, and J. A. Beckman, "Diabetes and vascular disease," *Circulation*, vol. 108, no. 12, pp. 1527–1532, 2003.

[27] M. Kalani, "The importance of endothelin-1 for microvascular dysfunction in diabetes," *Vascular Health and Risk Management*, vol. 4, no. 5, pp. 1061–1068, 2008.

[28] N. F. Renna, N. de las Heras, and R. M. Miatello, "Pathophysiology of vascular remodeling in hypertension," *International Journal of Hypertension*, vol. 2013, pp. 1–7, Article ID 808353, 2013.

[29] A. Ribeiro-Oliveira Jr, A. I. Nogueira, R. M. Pereira, W. W. V. Boas, R. A. S. dosSantos, and A. C. S. eSilva, "The renin – angiotensin system and diabetes: an update," *Vascular Health Risk Management*, vol. 4, no. 4, pp. 787–803, 2008.

[30] N. Arfian, N. Emoto, N. Vignon-Zellweger, K. Nakayama, K. Yagi, and K.-i. Hirata, "ET-1 deletion from endothelial cells

protects the kidney during the extension phase of ischemia/reperfusion injury," *Biochemical and Biophysical Research Communications*, vol. 425, no. 2, pp. 443–449, 2012.

[31] S. Shakir Jamil, Q. Nizami, and M. Salam, "*Centella asiatica* (Linn.) urban óa review," *Indian Journal of Natural Products and Resources*, vol. 6, no. 2, pp. 158–170, 2007.

[32] B. Tang, B. Zhu, Y. Liang et al., "Asiaticoside suppresses collagen expression and TGF-β/Smad signaling through inducing Smad7 and inhibiting TGF-βRI and TGF-βRII in keloid fibroblasts," *Archives of Dermatological Research*, vol. 303, no. 8, pp. 563–572, 2011.

[33] Z. Wang, J. Liu, and W. Sun, "Effects of asiaticoside on levels of podocyte cytoskeletal proteins and renal slit diaphragm proteins in adriamycin-induced rat nephropathy," *Life Sciences*, vol. 93, no. 8, pp. 352–358, 2013.

[34] D. C. R. Sari, S. Aswin, R. Susilowati et al., "Ethanol extracts of *Centella asiatica* leaf improves memory performance in rats after chronic stress via reducing nitric oxide and increasing Brain- Derived Neurotrophic Factor (BDNF) concentration," *International Journal of Psychology*, vol. 1, no. 1, pp. 61–67, 2014.

[35] X. Xu, Y. Wang, Z. Wei et al., "Madecassic acid, the contributor to the anti-colitis effect of madecassoside, enhances the shift of Th17 toward Treg cells via the PPAR γ/AMPK/ACC1 pathway," *Nature*, vol. e273, pp. 1–15, 2017.

[36] Y.-M. Hsu, Y.-c. Hung, L. Hu, Y.-j. Lee, and M.-c. Yin, "Antidiabetic effects of madecassic acid and rotundic acid," *Nutrients*, vol. 7, no. 12, pp. 10065–10075, 2015.

[37] J. C. Oates, C. M. Reilly, M. B. Crosby, and G. S. Gilkeson, "Peroxisome proliferator-activated receptor? agonists: potential use for treating chronic inflammatory diseases," *Arthritis & Rheumatism*, vol. 46, no. 3, pp. 598–605, 2002.

[38] N. Wang, L. Verna, N.-G. Chen et al., "Constitutive activation of peroxisome proliferator-activated receptor-γ suppresses pro-inflammatory adhesion molecules in human vascular endothelial cells," *Journal of Biological Chemistry*, vol. 277, no. 37, pp. 34176–34181, 2002.

[39] S. Kumar, V. Kumar, and O. Prakash, "Antidiabetic and hypolipidemic activities of Kigelia pinnata flowers extract in streptozotocin induced diabetic rats," *Asian Pacific Journal of Tropical Biomedicine*, vol. 2, no. 7, pp. 543–546, 2012.

[40] D. C. R. Sari, N. Arfian, U. Tranggono, W. A. W. Setyaningsih, M. M. Romi, and N. Emoto, "Hippocampal brain-derived neurotrophic factor (BDNF), tyrosine kinase B (TrkB) and extracellular signal-regulated protein kinase 1/2 (ERK1/2) signaling in chronic electrical stress model in rats," *Iran. Journal of Basic Medical Sciences*, vol. 22, no. 8, pp. 1218–1224, 2019.

[41] S. Sasikala, S. Lakshminarasaiah, and M. D. Naidu, "Antidiabetic activity of *Centella asiatica* on streptozotocin induced diabetic male albino rats," *World Journal Pharmarcy Science*, vol. 3, no. 8, pp. 2321–3086, 2015.

[42] H. Dai, Q. Liu, and B. Liu, "Research progress on mechanism of podocyte depletion in diabetic nephropathy," *Journal Diabetes Research*, vol. 2017, Article ID 2615286, 10 pages, 2017.

[43] F. P. Schena and L. Gesualdo, "Pathogenetic mechanisms of diabetic nephropathy," *Journal of the American Society of Nephrology*, vol. 16, no. 4, pp. 30–33, 2005.

[44] Q. Zhu, J. Zeng, J. Li et al., "Effects of compound *Centella* on oxidative stress and Keap1-Nrf2-ARE pathway expression in diabetic kidney disease rats," *Evidence-Based Complementary and Alternative Medicine*, vol. 2020, Article ID 9817932, 13 pages, 2020.

[45] Y. Zhao, P. Shu, Y. Zhang et al., "Effect of *Centella asiatica* on oxidative stress and lipid metabolism in hyperlipidemic animal models," *Oxidative Medicine and Cellular Longevity*, vol. 2014, Article ID 154295, 8 pages, 2014.

[46] A. C. Maritim, R. A. Sanders, and J. B. Watkins III, "Diabetes, oxidative stress, and antioxidants: a review," *Journal of Biochemical and Molecular Toxicology*, vol. 17, no. 1, pp. 24–38, 2003.

[47] S. Yamagishi, K. Fukami, and T. Matsui, "Crosstalk between advanced glycation end products (AGEs)-receptor RAGE axis and dipeptidyl peptidase-4-incretin system in diabetic vascular complications," *Cardiovascular Diabetology*, vol. 14, pp. 1–12, 2015.

[48] M. Brownlee, "Biochemistry and molecular cell biology of diabetic complications," *Nature*, vol. 414, no. 6865, pp. 813–820, December, 2001.

[49] J. Zhao, H. Jin, J. Gao et al., "Serum extracellular superoxide dismutase is associated with diabetic retinopathy stage in Chinese patients with type 2 diabetes mellitus," *Disease Markers*, vol. 2018, Article ID 8721379, 8 pages, 2018.

[50] B. K. Tiwari, K. B. Pandey, A. B. Abidi, and S. I. Rizvi, "Markers of oxidative stress during diabetes mellitus," *Journal Biomark*, vol. 2013, Article ID 378790, 8 pages, 2013.

[51] A. Ullah, "Diabetes mellitus and oxidative stress–A concise review," *Saudi Pharmaceutical Journal*, vol. 24, no. 5, pp. 547–553, 2016.

[52] G. Sadi and G. Sahin, "Modulation of renal insulin signaling pathway and antioxidant enzymes with streptozotocin-induced diabetes : effects of resveratrol," *Mediacal MDPI*, vol. 55, no. 3, pp. 1–12, 2019.

[53] H. Fujita, H. Fujishima, S. Chida et al., "Reduction of renal superoxide dismutase in progressive diabetic nephropathy," *Journal of the American Society of Nephrology*, vol. 20, no. 6, pp. 1303–1313, 2009.

[54] H. Weng, X. Li, E. A. Reece, and P. Yang, "SOD1 suppresses maternal hyperglycemia-increased iNOS expression and consequent nitrosative stress in diabetic embryopathy," *American Journal of Obstetrics and Gynecology*, vol. 206, pp. 448.e1–448.e7, 2012.

[55] O. Jung, S. L. Marklund, H. Geiger, T. Pedrazzini, R. Busse, and R. P. Brandes, "Extracellular superoxide dismutase is a major determinant of nitric oxide bioavailability," *Circulation Research*, vol. 93, no. 7, pp. 622–629, 2003.

[56] V. Ramachandran and R. Saravanan, "Asiatic acid prevents lipid peroxidation and improves antioxidant status in rats with streptozotocin-induced diabetes," *Journal of Functional Foods*, vol. 5, no. 3, pp. 1077–1087, 2013.

[57] Z. Kang, J. Zeng, T. Zhang et al., "Hyperglycemia induces NF-κB activation and MCP-1 expression via downregulating GLP-1R expression in rat mesangial cells: inhibition by metformin," *Cell Biology International*, vol. 43, no. 8, pp. 940–953, 2019.

[58] J. Reiser and M. M. Altintas, "Podocytes [version 1; referees: 2 approved]," *F1000 Research*, vol. 5, pp. 1–19, 2016.

[59] M. Pourghasem, H. Shafi, and Z. Babazadeh, "Histological changes of kidney in diabetic nephropathy," *Caspian Journal of internal Medicine*, vol. 6, no. 3, pp. 120–127, 2015.

[60] G. Hall, L. Wang, and R. F. Spurney, "TRPC channels in proteinuric kidney diseases," *Cells*, vol. 9, no. 1, pp. 1–24, 2019.

[61] T. Wuensch, F. Thilo, K. Krueger, A. Scholze, M. Ristow, and M. Tepel, "High glucose–induced oxidative stress increases transient receptor potential channel expression in human monocytes," *Diabetes*, vol. 59, no. April, pp. 3–8, 2010.

[62] T. Kosugi, M. Heinig, T. Nakayama, S. Matsuo, and T. Nakagawa, "eNOS knockout mice with advanced diabetic nephropathy have less benefit from renin-angiotensin blockade than from aldosterone receptor antagonists," *The American Journal of Pathology*, vol. 176, no. 2, pp. 619–629, 2010.

[63] S. Savard, P. Lavoie, C. Villeneuve, M. Agharazii, M. Lebel, and R. Lariviere, "eNOS gene delivery prevents hypertension and reduces renal failure and injury in rats with reduced renal mass," *Nephrology Dialysis Transplantation*, vol. 27, no. 6, pp. 2182–2190, 2012.

[64] B. Ozdemir and A. Yazici, "Could the decrease in the endothelial nitric oxide (NO) production and NO bioavailability be the crucial cause of COVID-19 related deaths?" *Med. Hypotheses*, vol. 144, no. January, pp. 19–22, 2020.

[65] O. Lenoir, M. Milon, A. Virsolvy et al., "Direct action of Endothelin-1 on podocytes promotes diabetic glomerulosclerosis," *Journal of the American Society of Nephrology*, vol. 25, no. 5, pp. 1050–1062, 2014.

[66] R. S. Awad Allah, M. A. Dkhil, and M. A. Danfour, "Structural alterations of the glomerular wall and vessels in early stages of diabetes mellitus (light and transmission electron microscopic study)," *Libyan Journal of Medicine*, vol. 2, no. 3, pp. 135–138, 2007.

[67] M. Candasamy, T. E. K. Murthy, K. Gubiyappa, D. Chellappan, and G. Gupta, "Alteration of glucose lowering effect of glibenclamide on single and multiple treatments with fenofibrate in experimental rats and rabbit models," *Journal of Basic and Clinical Pharmacy*, vol. 5, no. 3, p. 62, 2014.

[68] N. Bunyapraphatsara, S. Yongchaiyudha, V. Rungpitarangsi, and O. Chokechaijaroenporn, "Antidiabetic activity of Aloe vera L. juice II. Clinical trial in diabetes mellitus patients in combination with glibenclamide," *Phytomedicine*, vol. 3, no. 3, pp. 245–248, 1996.

[69] S. H. Yoon, E. J. Han, J. H. Sung, and S. H. Chung, "Antidiabetic effects of compound K versus metformin versus compound K-metformin combination therapy in diabetic db/db mice," *Biological and Pharmaceutical Bulletin*, vol. 30, no. 11, pp. 2196–2200, 2007.

Hindawi
Evidence-Based Complementary and Alternative Medicine
Volume 2021, Article ID 1282957, 12 pages
https://doi.org/10.1155/2021/1282957

Research Article

Study on the TCM Syndromes Evolution and Chinese Herbal Characteristics of Type 2 Diabetes Patients with Different Courses of Disease in TCM "Heat Stage": A Real-World Study

Ying Xing,[1] Min Pi,[2] Runshun Zhang,[3] and Tiancai Wen[1,4]

[1]*Institute of Basic Research in Clinical Medicine, China Academy of Chinese Medical Sciences, Beijing, China*
[2]*Shenzhen Traditional Chinese Medicine Hospital, Guangdong, China*
[3]*Guang'anmen Hospital, China Academy of Chinese Medical Sciences, Beijing, China*
[4]*Traditional Chinese Medicine Data Center, China Academy of Chinese Medical Sciences, Beijing, China*

Correspondence should be addressed to Tiancai Wen; wentiancai@ndctcm.cn

Received 10 April 2021; Revised 21 May 2021; Accepted 3 June 2021; Published 17 June 2021

Academic Editor: Youhua Xu

Objective. The purpose of this study is to analyze and summarize the syndrome distribution, syndrome evolution, and Chinese herb medicine characteristics of T2D in heat stage. *Method*. In this study, 228 heat-stage T2D patients were divided into three groups based on the course of disease. Group 1 (the course of disease ≤5 years) included 118 patients. Group 2 (5< the course of disease ≤10 years) had 73 patients. Group 3 (the course of disease >10 years) consisted of 37 patients. The main methods used in our study were complex network community partitioning algorithms and Sankey diagram visualization, based on the clinical electronic medical record data we collected. *Result*. In the three groups, the nodes with the highest node degree are all "heat syndrome." Edge weight between "heat" and "dampness," "qi stagnation," "phlegm," "liver," and "stomach" is the largest. During the whole course of treatment, 60.17%, 63.01%, and 62.16% of the patients' syndromes in groups 1, 2, and 3, respectively, were ascribed to the heat stage all the time. The patients' syndromes in groups 1 and 2 easily transformed to the syndrome of deficiency of both qi and yin of the spleen and stomach. In group 3, 27% of the patients' syndromes were easily transformed into kidney yin deficiency and qi deficiency and blood stasis syndrome. The largest Chinese herb communities of the patients whose syndromes did not change after treatment in the three groups were all heat-clearing drugs. The proportion of blood-activating drugs in patients with syndrome changes increased significantly after treatment. *Conclusion*. (1) The basic syndrome of T2D patients in the heat stage is liver-stomach heat syndrome. (2) T2D patients in the heat stage tend to deteriorate towards the direction of qi and yin deficiency syndrome. However, the longer the course of the disease is, the more likely it is to deteriorate to the direction of kidney yin deficiency syndrome and blood stasis syndrome. (3) Drugs that can help T2D patients in the heat stage to maintain their condition stably are heat-clearing drugs represented by *Coptis chinensis*, which usually need to be combined with warming interior drugs such as Zingiberis Rhizoma and Pinelliae Rhizoma.

1. Introduction

Type 2 diabetes (T2D), namely, "xiaoke" of TCM, is a chronic and complex disease with diverse etiologies, long course, and different stages. In TCM, we concluded that diabetes had four different pathological stages based on clinical symptoms and manifestations, namely, stagnation stage, heat stage, deficiency stage, and injuring stage [1]. The heat stage is equivalent to the heat stage-to-mid period of diabetes and indicates the attack of disease [2]. Therefore, the heat stage is an extremely critical stage in the development of T2D. The study in [3] had shown that T2D patients in the heat stage are mostly obese, and the main syndrome is excess heat syndrome, but the specific type and the evolution direction of heat syndrome had not been explained clearly at present.

The course of disease is an important factor affecting the adverse control of blood glucose and chronic complications

in T2D [4]. Related studies have revealed that patients with a course of more than 5 years have more than twice as much unsatisfactory blood glucose control as other patients [5], and the incidence of T2D retinopathy, nephropathy, and neuropathy will increase with the course of diabetes [6]. Considering the irreversibility of the increase in the course of the disease, at the key treatment point of the heat stage, if we can make clear the evolution direction of the syndrome of patients with different courses of disease and use effective Chinese herb medicine to treat them pertinently, then it will be of great help to prevent the aggravation of the disease or even to reverse the current poor state of the disease. But now we have not found related reports.

Clinical epidemiological investigation or clinical trial research had always been the golden standard for studying the evolution of syndrome. But, with the popularity of real-world study concepts, knowledge captured during routine clinical pathways in Electronic Medical Records (EMRs) has ushered a new way of syndromes evolution study that can provide evidence for medical decision-making beyond that from formal clinical studies. However, the current research [7–9] on syndrome evolution based on EMRs has an obvious shortcoming. Their method is usually to extract the distribution changes of syndrome frequency at different time points to describe the changes of syndrome, which will entirely isolate the syndrome at different time points and cannot completely describe the continuous evolution pattern of syndrome in the time dimension. In recent years, there are some new methods to study the evolution of syndrome, such as transition probability matrix [10], nonlinear mixed effect model [11], hidden structure model [12], and potential category analysis [13], but they are still rarely used in T2DM. Based on the above situation, this study mainly uses complex network community discovery algorithm and Sankey diagram to find out the syndrome evolution and Chinese herb medicine characteristics of T2D patients with different courses of disease in TCM heat stage, so as to provide reference for clinic.

2. Materials and Methods

2.1. Data Source and Data Screening Criteria. The real-world data used in this study are the EMRs of 590 T2D patients, which are obtained from the clinical data warehouse of the Traditional Chinese Medicine Data Center of the China Academy of Chinese Medical Sciences. We extracted the information we need from the EMRs, including the patient's unique code, treatment date, syndrome diagnosis, and Chinese herb medicine prescription and dosage. Since we need to include T2D patients in the heat stage, we refer to the definition of T2D heat stage in *international traditional Chinese medicine guideline for diagnostic and treatment principles of diabetes* [2], an international standard for T2D TCM treatment. When the patient's initial visit symptoms meet the criteria for the heat stage, then the patient is considered to be in the T2D heat stage. In addition, we have strict restrictions on the patient's total disease duration and the date interval between the adjacent prescriptions: the total number of visits ≥3 times. The total duration of treatment ≥ 30 days. The time span of adjacent prescriptions is between 7 and 30 ± 5 days. Our goal is to prevent certain special circumstances from affecting the accuracy of the results, such as too few visits (such as only one treatment) or too long interval between two treatments (such as a year from the last treatment).

2.2. Patient Grouping and Syndrome Division. We selected 228 patients who met the screening criteria from 590 patients. These patients were divided into three groups: Group 1 (the course of disease ≤5 years) included 118 patients. Group 2 (5< the course of disease ≤10 years) had 73 patients. Group 3 (the course of disease >10 years) consisted of 37 patients. In the real TCM clinical work scene, doctors' writing of TCM syndromes of patients is often not standard enough, such as the same syndrome but different ways of writing, which cause many restrictions to our research. Therefore, we disassembled all the syndromes into a combination of disease location syndrome elements and disease nature syndrome elements. The problem of syndrome heterogeneity is well solved by this method, which makes the clinical syndrome differentiation results more accurate and reliable. We refer to the *Syndrome Element Dialectics* [14] to split the syndrome.

2.3. Data Analysis. Our research mainly uses two kinds of data mining methods: complex network community partition algorithm and Sankey diagram. Here are several important concepts [15] that need our attention in complex networks: a node in a complex network is an entity. Edge is the relationship between nodes in a complex network, namely, the relationship between different entities in a complex system. Node degree is the number of edges connected to a node. Edge weight indicates the closeness of the relationship between the two nodes.

First of all, we first establish the undirected weighted complex network of T2DM syndrome and Chinese herb medicine. In this study, the node represents the syndrome element or Chinese herb medicine, and the edge signifies a pair of syndrome elements or the compatibility of Chinese herb medicine:

$$\deg(v_i) = w_i \sum_{i,j \in G} e(i,j). \tag{1}$$

In formula (1), G is a complex network, and v_i represents node I in G. $e(i,j)$ indicates whether there is an edge between nodes I and j; if it exists, the value is 1; otherwise it is 0. w_i represents the weight of node I, and the value of w_i in syndrome network is 1. In the traditional Chinese medicine network, w_i is expressed as the average dose of Chinese herb medicine.

Based on undirected weighted complex network, we use the FastUnfolding algorithm for community division. In complex networks, some nodes are closely connected and some are sparse. Then the tightly connected parts of the nodes can be regarded as a community, while the connections between communities are relatively sparse [16].

The FastUnfolding algorithm takes modularity as an index to divide closely connected nodes into a community [17]. In our study, the purpose of this algorithm is to find the clustering rule of syndrome and Chinese herb medicine in the heat-stage T2D population. Due to the large complex network caused by many kinds of Chinese herb medicine, we screened the nodes with a node degree ≥50 to find more core Chinese herb medicine. The establishment of complex networks and communities division all rely on Gephi 0.9.2.

Secondly, according to the statistical results of the outpatient visit distribution, we take the representative time point as the observation end point and draw the Sankey diagram of syndrome evolution. Sankey diagram, also known as heat balance diagram or energy flow chart, is composed of edges, flow rates, and nodes. Nodes represent different categories to divide different energy flow stages or zones. Edges connect nodes of different stages or zones, representing the flow of energy or data [18]. In this study, Sankey diagram was used to show the evolution of heat stage syndrome of T2DM. The node is the outpatient visit, the edge is the syndrome, and the width of the edge indicates the number of people who have syndrome transformation. Figure 1 clearly reflects the data analysis process.

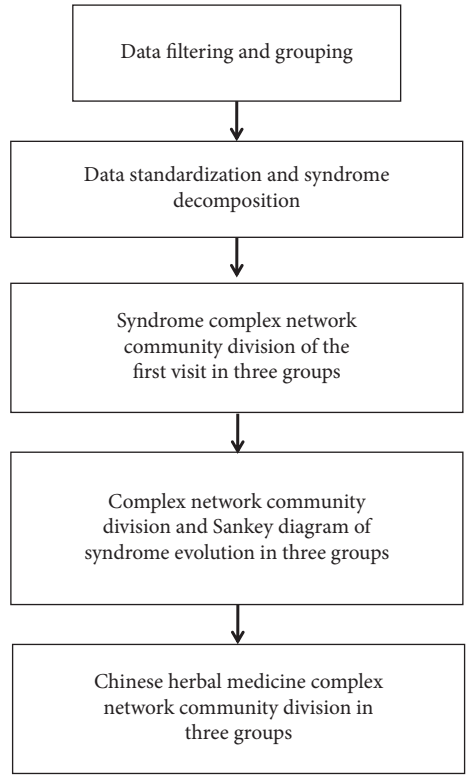

Figure 1: Data analysis flow chart.

3. Results

3.1. Characteristics of the Participants. 228 patients were enrolled in the study, with a total of 1435 outpatient visits. Most of patients in the three groups were male, and there was no statistical difference in gender composition among the three groups ($P = 0.864$). Most of the patients in group 1 were 18~40 years old and 40~60 years old ($n = 95$, 41.67%). Most of the patients in group 2 were 40~60 years old and over 60 years of age ($n = 67$, 29.39%). All the patients in group 3 were 40~60 years old and over 60 years of age ($n = 37$, 16.23%), and no one was 18~40 years old. The difference in age composition among the three groups was statistically significant ($P < 0.001$). The total number of overweight and obese patients in the three groups was 109 (71.24%). There was no statistically significant difference in BMI values among the three groups ($P = 0.383$) (Table 1).

The number of visits of most patients ranged from 3 to 5 ($n = 174$, 76.32%), and the average number of visits was 6.29 (Figure 2(a)). The number of days from the first visit of all patients remained stable before the 13th visit but then began to fluctuate sharply (Figure 2(b)).

3.2. Syndromes Distribution of T2D Patients in Heat Stage with Different Courses. By analyzing the results of syndrome elements complex network community division of patients with different disease courses at the first visit, we found that the core syndrome combinations of patients in the three groups were highly similar. In the three groups, the largest syndrome communities (syndrome communities aI, bI, and cI) accounted for 56.52%, 57.14%, and 69.57%, respectively (Figures 3(a)–3(c)). Among the syndrome communities aI, bI, and cI, the syndrome nodes with the highest node degree are all "heat" (Figures 3(a)–3(c)). In addition, edge weight between "heat" and "dampness," "qi stagnation," "phlegm," "liver," and "stomach" is the largest (Figures 3(a)–3(c)). Syndrome communities aII, bII, and cII were the second largest syndrome communities in the three groups, accounting for 21.74%, 33.33%, and 21.74%, respectively, with blood stasis syndrome and meridians as the core nodes (Figures 3(a)–3(c)).

3.3. Syndromes Evolution of T2D Patients in Heat Stage. The syndromes of T2D patients in the heat stage mainly evolved to two types of syndromes. The first is class A syndrome: the largest syndrome community A1 included 85.71% of syndrome element nodes, with heat, yin deficiency, qi deficiency syndrome and spleen, and stomach having the largest node degree and edge weight (Figure 4(a)). The second is class B syndrome: the largest syndrome community B1 accounted for 48.28%, and the node degree and edge weighting degree of qi deficiency, blood deficiency, blood stasis, yang deficiency, and meridians were the largest. The proportion of syndrome community B2 was 34.48%, and the node degree and edge weighting degree of heat, yin deficiency, essence deficiency, liver, and kidney were the highest (Figure 4(b)).

Since most of the T2D patients in this study were seen for follow-up visits within 6 times (Figure 2(a)), we intercepted the syndrome data of all patients from 1 to 6 visits to draw a Sankey diagram, and less than 6 times we regarded it as a loss of follow-up.

For patients in group 1, the syndrome conversion rate reached the highest rate of 20% at the fourth consultation point (average of 61 days). It is important to note that 60.17% of the patients' syndromes always belong to the heat stage

Table 1: Basic information of patients.

Basic information	Classification	Group 1	Group 2	Group 3	χ^2 value	P value
Gender	Male	76 (33.33%)	49 (21.49%)	23 (10.09%)	0.293	0.864
	Female	42 (18.42%)	24 (10.53%)	14 (6.14%)		
Age	(18~40)	38 (16.67%)	6 (2.63%)	0 (0%)	40.769	<0.001
	(40~60)	57 (25%)	42 (18.42%)	14 (6.14%)		
	≥60	23 (10.09%)	25 (10.96%)	23 (10.09%)		
BMI	18.5~23.9	26 (16.99%)	15 (9.8%)	3 (1.96%)	4.174	0.383
	24.0~27.9	36 (23.53%)	19 (12.42%)	13 (8.5%)		
	≥28	19 (12.42%)	15 (9.8%)	7 (4.58%)		

BMI: body mass index. The classification criteria come from *the Guidelines for the Prevention and Control of Overweight and Obesity in Chinese Adults* [19]: BMI = 24 is the limit of overweight for Chinese adults, and BMI ≥ 28 is the limit of obesity. BMI records of 75 patients were missing in this study.

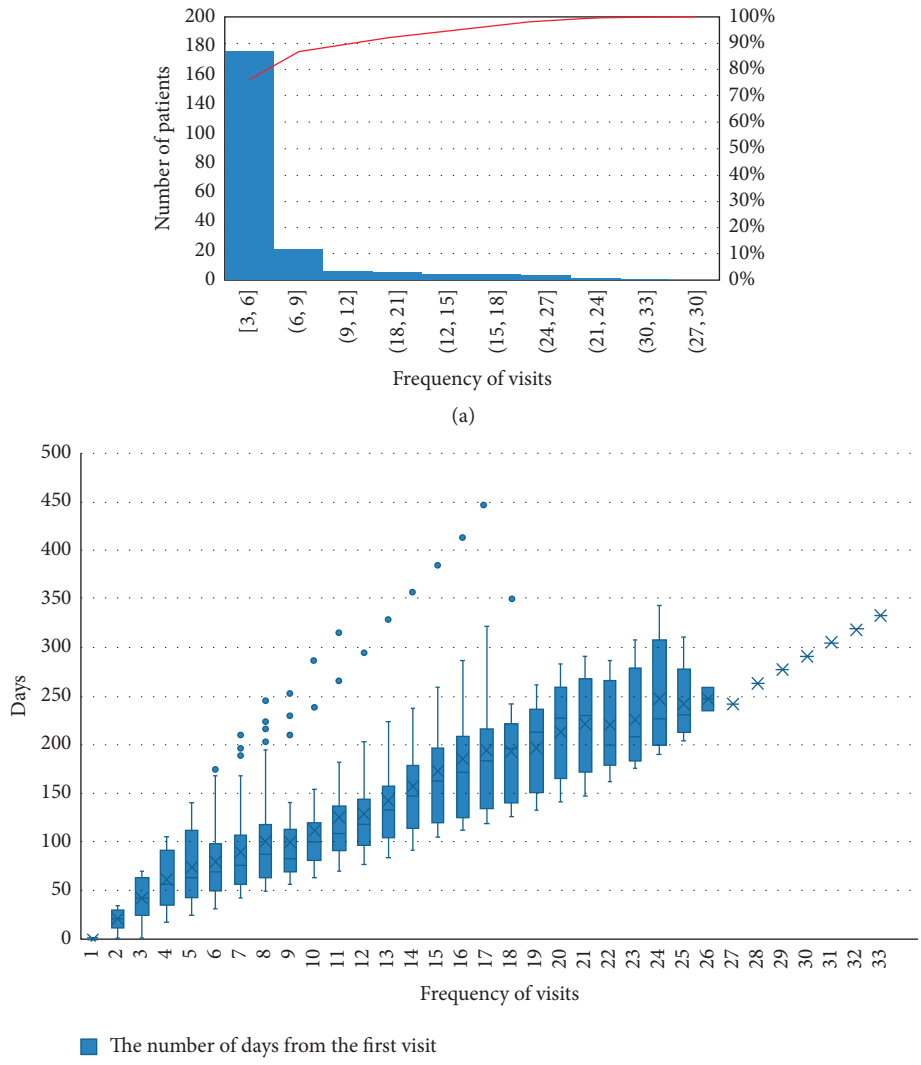

Figure 2: The distribution of visits and the time interval between hospital visits of T2D patients. (a) Cumulative distribution table of outpatient visits. (b) Boxplot of the number of days from the first visit.

during treatment. Similarly, the highest conversion rate to class A syndrome was 18.67% at the fourth consultation (average of 61 days). However, the highest conversion rate of patients to class B syndrome was only 5.5%, which occurred at the third consultation (an average of 42.4 days) (Figure 5(a)).

For patients in group 2, the syndrome conversion rate was the highest (19.18%) at the second time point (average of 21 days). More specifically, during the whole course of treatment, 63.01% of the patients' syndromes were always ascribed to the heat stage. The conversion rate of patients to

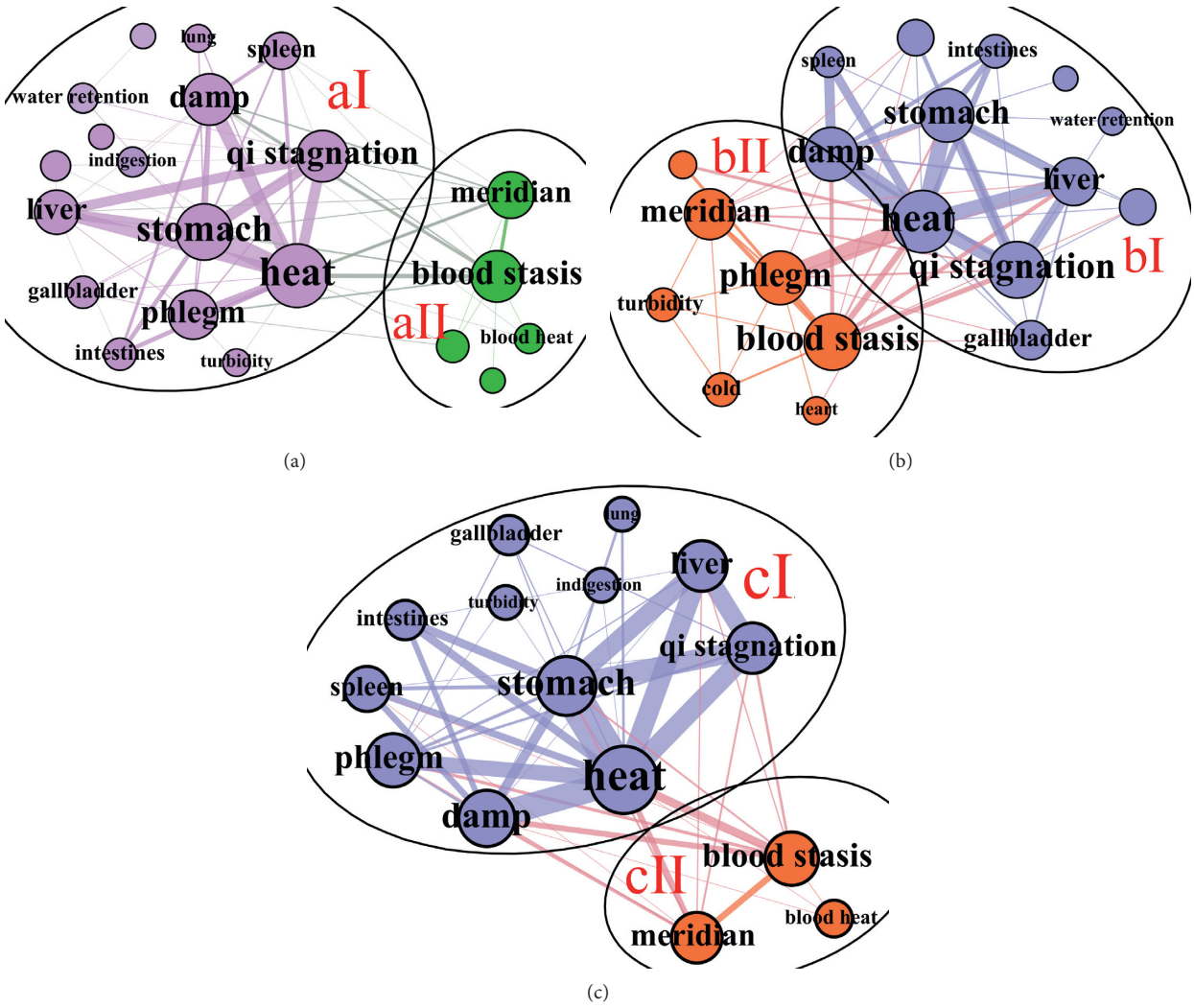

Figure 3: Syndrome complex network community division of T2D patients with different courses in the heat stage. (a) Syndrome complex network community division of group 1. (b) Syndrome complex network community division of group 2. (c) Syndrome complex network community division of group 3.

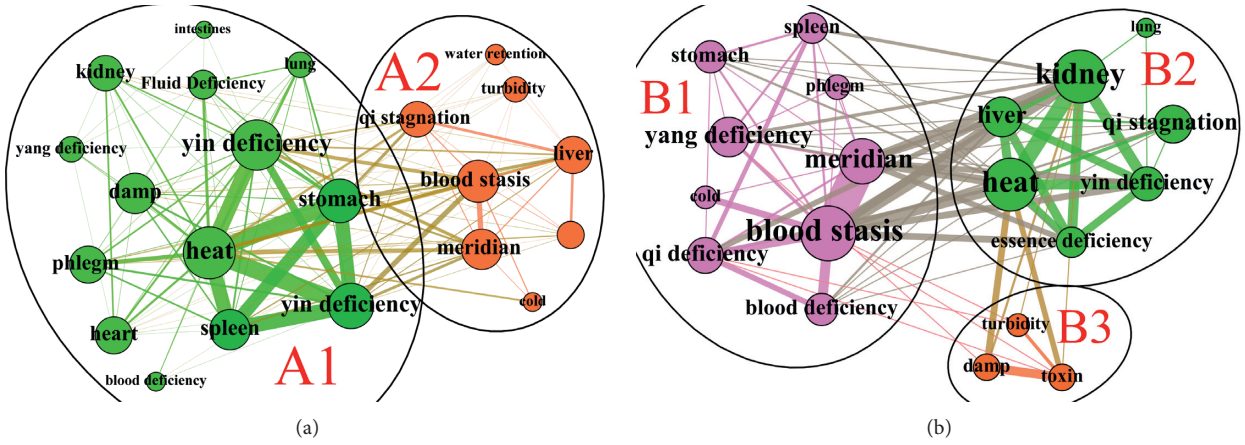

Figure 4: Complex network community division of syndrome evolution in heat stage. (a) Class A syndrome. (b) Class B syndrome.

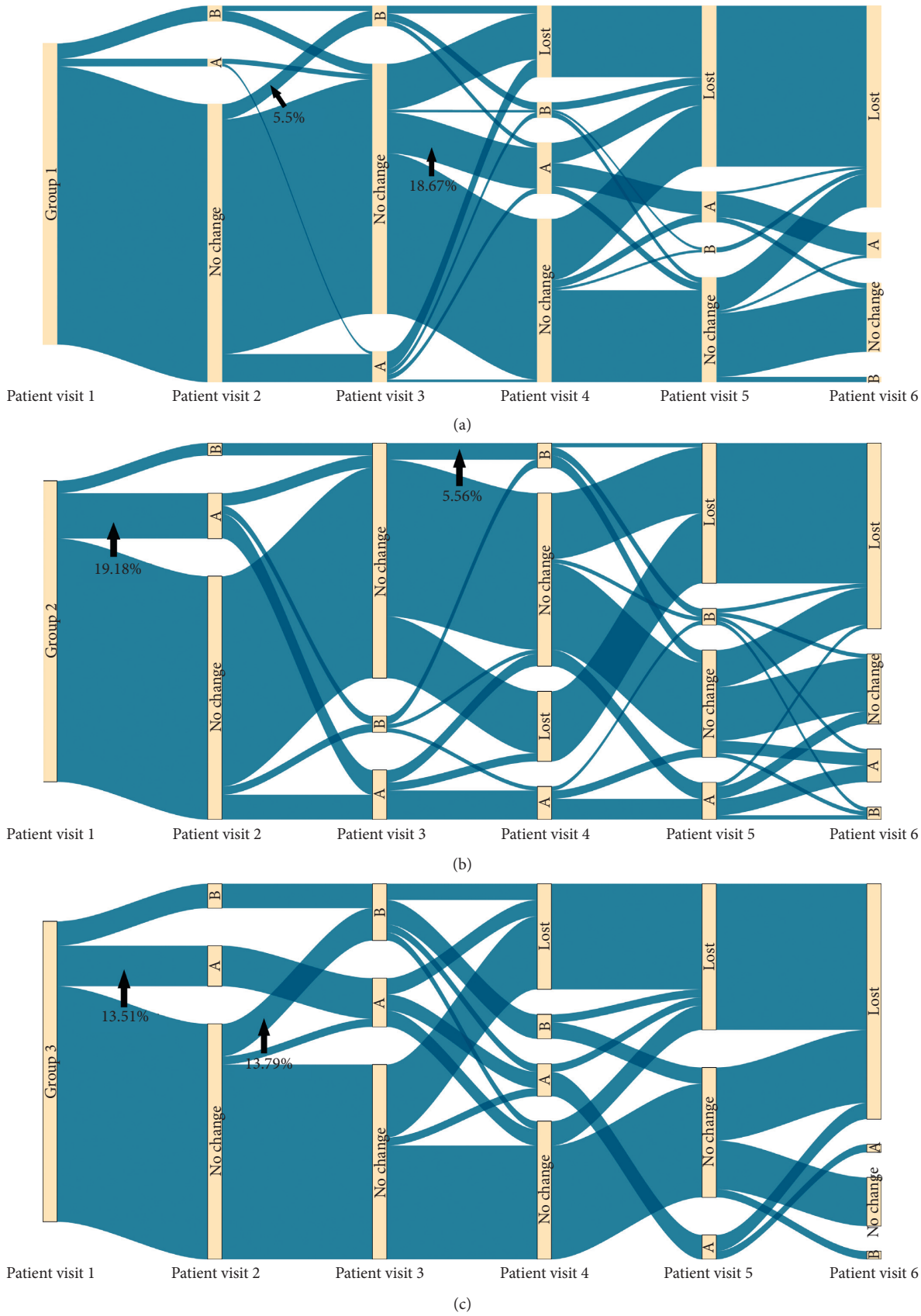

Figure 5: Sankey diagram of syndrome evolution of T2D patients in heat stage. (1) A: class A syndrome; (2) B: class A syndrome; (3) Lost: loss to follow-up patients; (4) No change: patients' syndrome had no change. (a) Syndrome evolution Sankey diagram of group 1. (b) Syndrome evolution Sankey diagram of group 2. (c) Syndrome evolution Sankey diagram of group 3.

class A syndrome was the highest (15.07%) at the second consultation time point (average 21 days) and the highest to class B syndrome at the fourth consultation time point (average of 61 days) (5.56%) (Figure 5(b)).

Patients with a course of more than 10 years had the highest syndrome conversion rate of 21.62% at the second consultation point (average of 21 days). At the second consultation (average of 21 days), the conversion rate to class A syndrome was the highest (13.51%). At the third consultation point (average of 42.4 days), the conversion rate to class B syndrome was the highest (13.79%). In particular, note that 62.16% of the patients' syndromes in group 3 always remained at the heat stage (Figure 5(c)).

3.4. Chinese Herb Medicine Characteristics of T2D Patients in Heat Stage. In the syndrome evolution Sanji diagram, our results show that more than 60% of the patients in the three groups have no change in syndrome, and other patients have syndrome transformation. In this case, we divided all patients' drugs of three groups into two categories: syndrome unchanged group (Figures 6(a), 6(c), and 6(e)) and syndrome change group (Figures 6(b), 6(d), and 6(f)).

The Chinese herb communities **a1**, **c1**, and **e1** are the largest communities, accounting for 42.42%, 37.93%, and 39.13%. All the drugs in communities **a1**, **c1**, and **e1** have the effect of clearing away heat and invigorating fluid, and Coptidis Rhizoma, Scutellariae Radix, Anemarrhenae Rhizoma, Trichosanthis Radix, and Puerariae Lobatae Radix have large node degree. Communities **a2** (27.27%), **c2** (31.03%), and **e2** (37.35%) all contain drugs with the effect of tonifying qi and nourishing yin. The difference is that community **e2** includes more drugs for nourishing kidney yin, such as Rehmanniae Radix, Corni Fructus, Polygonati Rhizoma, and Cistanches Herba. The drugs belonging to communities **a4** (12.12%), **c3** (31.03%), and **e3** (23.53%), such as Astragali Radix, Cinnamomi Ramulus, Spatholobi Caulis, and Chuanxiong Rhizoma, are all drugs with the effect of tonifying qi or promoting blood circulation. However, the proportion of community **a4** in patients with no syndromes change of group 1 was very small. Chinese herb community **a3** (18.18%) included *Trichosanthes*, Hawthorn, and *Monascus*, which mainly had the effect of resolving phlegm (Figures 6(a), 6(c), and 6(e)).

In group 1, the drugs included in Chinese herb communities **b2** (32.35%) and **a3** (18.18%) were phlegm-dissipating drugs, but the proportion of **b2** was higher than that of **a3** (Figures 6(a) and 6(b)). Blood-activating drugs are included in community **b3** (29.41%) and community **a4** (12.12%), but the proportion of **b3** is higher than that of **a4** (Figures 6(a) and 6(b)). In Figures 6(d) and 6(f), **d1** (41.67%) and **f1** (35.14%) are the largest Chinese herb communities, mainly including drugs for benefiting qi and activating blood, which are quite different from the results shown in Figures 6(c) and 6(e).

4. Discussion

In this study, 228 T2D patients were divided into three groups based on the course of disease: within 5 years, 5–10 years, and more than 10 years. Moreover, with the increase of the course of the disease, the age of the patients also increased, and the patients with a course of disease of more than 10 years were all over 40 years of age. According to the results in Section 3.2, regardless of the course of disease, the basic syndrome of T2D patients in the heat stage is liver-stomach heat syndrome. Moreover, heat often does not exist alone but is combined with phlegm, dampness, qi stagnation, and blood stasis. Therefore, according to the specific conditions of different patients, there will be different types of compound heat syndrome such as phlegm-heat, damp-heat, stagnant-heat, and stasis-heat syndrome. The studies in [20–23] have shown that there is obvious high expression of tumor necrosis factor-α (TNF-α), interleukin-6 (IL-6), C-reactive protein (CRP), and other inflammatory factor-related genes in TCM heat syndrome, and more and more studies [24–26] suggest that T2D may be an inflammatory response mediated by cytokines and is an immune disease. In particular, the proportion of overweight and obese patients included in this study is as high as 70%. Obesity can cause chronic low-grade inflammation in adipose tissue, liver, and pancreas, leading to insulin resistance and T2D [27, 28], and obese patients show symptoms of phlegm-dampness and heat in TCM [29]. Zhou et al.'s [30] prospective study on TCM syndromes of early T2D patients showed that obese patients were more common in early T2D, and phlegm-heat syndrome was the main syndrome type in early T2D. In addition, there were more male patients in this study. The studies in [31] have shown that the majority of male patients with T2D are dampness-heat constitutionally, so they are more prone to dampness-heat syndrome.

There was a significant relationship between the direction of syndrome evolution and the duration of the disease in patients with T2D in the heat stage. First of all, patients with a disease course of 5 years and 5–10 years are more likely to deteriorate to the syndrome of deficiency of spleen and stomach qi and Yin. Heat consumes qi and yin in TCM theory, which leads to the syndrome transformation from heat syndrome to qi deficiency and yin deficiency syndrome. This is clearly stated in a large number of ancient books of TCM and the views of modern Chinese medicine scholars [32–34]. Although the syndrome of patients with a course of disease of more than 10 years is also easy to transform to yin deficiency syndrome, its transformation direction is kidney yin deficiency syndrome. This is significantly different from those of the first two groups. TCM theory believes that the disease for a long time is easy to damage the kidney yin, the origin of the whole body yin fluid. For patients with a course of more than 10 years, the heat syndrome lasts so long that it damages the kidney yin, so the disease location of the yin deficiency syndrome has changed. In addition, the syndrome of patients greater than 10 years is also easily converted to the direction of qi deficiency. The occurrence of blood stasis is related to a variety of factors, such as heat injuring body fluid, phlegm-dampness blocking meridians, and impaired viscera function [35]. Moreover, with the gradual increase of the course of the disease, the meridian obstruction of the patients became serious incrementally, and finally blood

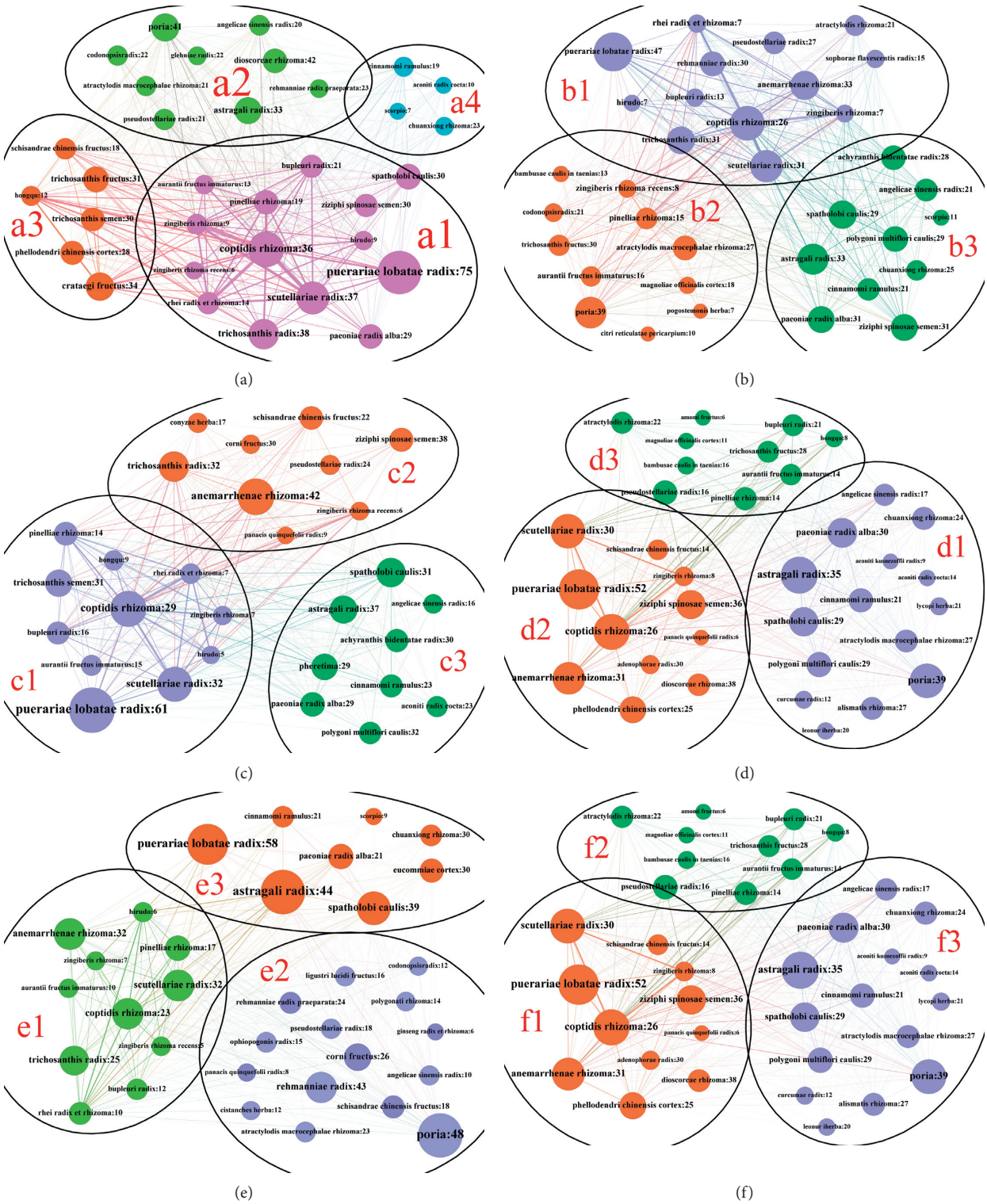

(a) (b) (c) (d) (e) (f)

Figure 6: Chinese herb medicine complex network community division of T2D patients with different courses in the heat stage. For example, "Coptidis Rhizoma: 28.8"—the number after the node name in Figure 6 represents the drug dose. (a) Chinese herb medicine community division of patients with unchanged syndromes in group 1. (b) Chinese herb medicine community division of patients with syndromes change in group 1. (c) Chinese herb medicine community division of patients with unchanged syndromes in group 2. (d) Chinese herb medicine community division of patients with syndromes change in group 2. (e) Chinese herb medicine community division of patients with unchanged syndromes in group 3. (f) Chinese herb medicine community division of patients with syndromes change in group 3.

stasis became the main factor leading to diabetic complications such as retina, nephropathy, coronary heart disease, and myocardial infarction [36]. The studies in [37] have shown that patients with blood stasis syndrome have more serious disorders of fat metabolism, amino acid metabolism, and energy metabolism than those without blood stasis syndrome, and blood stasis syndrome is common in T2D patients with a course of 10–15 years [38].

When discussing the medication characteristics of the patient, we discuss them separately according to whether the patient's syndrome has changed or not. In Section 3.2, more than 60% of the patients in all three groups had no change in syndrome after treatment, which means that the Chinese herb medicine used by these patients helps in keeping their condition stable. Here, we believe that patients whose syndromes do not deteriorate after taking Chinese herbs, to some extent, demonstrate the effectiveness of TCM or at least prove that TCM is beneficial in keeping their condition stable. For this chronic disease, portraying "cure of diabetes" as a goal for all persons with diabetes, however, is misleading and has the potential to do harm [39]. Even for insulin, it is not a cure for diabetes; it is just a treatment [40]. *Standards of Medical Care in Diabetes-2020* [41] mentioned the following: "The goals of treatment for diabetes are to prevent or delay complications and optimize quality of life." There is no doubt that keeping the patient's condition stable helps to delay complications. Therefore, in our results, we found that all those patients were treated with antipyretic drugs, such as Coptidis Rhizoma, Scutellariae Radix, Anemarrhenae Rhizoma, Trichosanthis Radix, and Puerariae Lobatae Radix. The studies in [42] have shown that heat-clearing herbs can generally reduce the abundance and species diversity of intestinal flora, maintain intestinal barrier function, reduce inflammatory reaction, and improve insulin resistance by regulating intestinal flora disorder. For example, regarding Coptidis Rhizoma, one of the representative heat-clearing drugs, its core component berberine in reducing blood lipids and improving insulin resistance has been fully proved in many randomized clinical trials [43]. In addition, studies have proved that the therapeutic effect of Coptidis Rhizoma is closely related to the dose, and the significant hypoglycemic effect can be observed when the dose is high [44]. In our results, the average high dose of *Coptis chinensis* in heat-stage T2D patients was 24–28 g. However, heat-clearing herbs are cold, especially for T2D patients with weak function of spleen and stomach, which should not be taken for a long time. Therefore, a commonly used compatibility is a combination of heat-clearing herbs and warm herbs such as Zingiberis Rhizoma and Pinelliae Rhizoma to neutralize the cold nature of heat-clearing herbs. The studies in [45] have shown that this compatibility can increase the expression of insulin receptor in the pancreas of T2D model mice and improve insulin resistance. Secondly, patients in the hot stage tend to evolve in the direction of qi and yin deficiency syndrome. Therefore, the three groups of patients also used Pseudostellariae Radix, Astragali Radix, Panacis Quinquefolii Radix, Glehniae Radix, and Ophiopogonis Radix, which have the effect of tonifying qi and nourishing yin. These Chinese herbs are compatible with heat-clearing drugs, the basic medication for T2D patients in the heat stage, which embodies the idea of "treating predisease" in TCM. However, for patients with a disease course of more than 10 years, additional traditional Chinese medicines with kidney yin nourishing effect should be added to cope with their possible deterioration to kidney yin deficiency syndrome at any time, such as Corni Fructus, Schisandrae Chinensis Fructus, Ligustri Lucidi Fructus, Polygonati Rhizoma, and Angelicae Sinensis Radix.

With the exception of 60% of the patients who are in a more stable condition, the rest of the patients inevitably have syndrome changes even after treatment, which means that the disease has taken a turn for the worse. We compared the drugs used in two parts of patients with different conditions and found that the proportion of blood-activating drugs used in patients with worsening conditions increased significantly. In group 2 and group 3, for example, the blood-activating drugs became the most commonly used drugs rather than the generally thought heat-clearing drugs. Therefore, it is valid to consider that blood stasis may be the main factor leading to the disease deterioration in patients with T2D in the heat stage. Consequently, in order to prevent the gradual accumulation of blood stasis leading to aggravation of the condition, many Chinese medical experts [46–48] believe that patients should use drugs to promote blood circulation and remove blood stasis as soon as possible. In our study, except for heat-clearing drugs as basic drugs, patients with more stable conditions used drugs for promoting blood circulation and removing blood stasis, and the longer the course of disease, the greater the proportion of use. The representative drugs are Astragali Radix, Cinnamomi Ramulus, Spatholobi Caulis, Chuanxiong Rhizoma, *Hirudo*, and *Pheretima*. The studies in [49] have shown that "Buqi Huoxue recipe" can improve glucose and lipid metabolism, reduce the level of oxidative stress in myocardial tissue to a certain extent, downregulate the expression of some inflammatory factors in blood, and improve the related symptoms of diabetic angiopathy in many aspects.

In addition, we also found an interesting result that high-dose Puerariae Lobatae Radix is often used to treat T2D, with an average of 41–60 g. Puerariae Lobatae Radix not only is nontoxic but also has the dual effects of clearing heat and nourishing yin. Puerarin, the core component of Puerariae Lobatae Radix, may directly benefit DM by decreasing blood glucose levels, improving insulin resistance, protecting islets, inhibiting inflammation, decreasing oxidative stress, and inhibiting Maillard reaction and advanced glycation end products (AGEs) formation [50]. But its efficacy is low, so it needs to be used in large doses or in combination with other herbs. For example, Gegen Qinlian Decoction, composed of Coptidis Rhizoma, Scutellariae Radix, Puerariae Lobatae Radix, and Glycyrrhizae Radix et Rhizome, is a classic traditional Chinese medicine prescription that is widely used to clinically treat diabetes mellitus, and it has been proved that it can significantly reduce blood glucose and increase serum insulin level in type 2 diabetic mice [51].

5. Conclusion

The basic syndrome of T2D patients in the heat stage is liver-stomach heat syndrome, and heat is often combined with phlegm, dampness, qi stagnation, and blood stasis. Therefore, patients generally have phlegm-heat, dampness-heat, stagnation-heat, and stasis-heat syndrome as well as other compound-heat syndromes. In the process of syndrome evolution, the patients mainly evolved to the syndrome of qi-yin deficiency. But, for patients with a course of more than 10 years, because of their longer course of disease, they tend to evolve in the direction of deficiency of qi and blood stasis or syndrome of liver-kidney yin deficiency. Drugs that can help T2D patients in the heat stage to maintain their condition stable are heat-clearing drugs represented by *Coptis chinensis*, which usually need to be combined with warming interior drugs such as Zingiberis Rhizoma and Pinelliae Rhizoma. At the same time, according to the different syndrome evolution trends of patients with different courses, patients with shorter course of disease should appropriately increase the proportion of herbs for tonifying qi and nourishing yin, while patients with longer course of disease can use more herbs for nourishing kidney yin. In addition, we also found that blood stasis was the main factor leading to the deterioration of the condition of T2D patients in the heat stage. Therefore, for patients in the heat stage, it is also necessary to use blood-activating drugs to prevent the deterioration of the disease, and representative drugs include Astragali Radix, Spatholobi Caulis, Cinnamomi Ramulus, Chuanxiong Rhizoma, and *Pheretima*.

The advantage of this study is that we introduce a new data mining method, Sangji diagram, to study the evolution of TCM syndromes. Moreover, we have made a complete study of the syndromes distribution, syndromes evolution, and the corresponding herb characteristics and doses in the heat stage of T2D, which is more helpful for doctors to use in clinical treatment according to the actual situation of patients. However, an obvious disadvantage of our research is that we have a small amount of data. This is mainly due to our strict data filtering conditions. Moreover, we did not control for some variables that might affect the results. For example, we think that the drugs of patients with unaltered symptoms will help them stabilize their condition, but in fact regular diet and exercise may also improve their condition.

Data Availability

The data used to support the findings of this study are included within the article.

Conflicts of Interest

The authors declare that there are no conflicts of interest.

Acknowledgments

This study was supported by the National Natural Science Foundation of China (no. 81774158) and the National Science and Technology Major Project of China (no. 2017ZX10106001-001).

References

[1] Diabetes Branch of Chinese Medical Association, "Chinese guidelines for prevention and treatment of type 2 diabetes (2020 edition)," *Chinese Journal of Endocrinology and Metabolism*, vol. 4, no. 37, pp. 311–398, 2021.

[2] F. Lian, Q. Ni, Y. Shen, S. Yang et al., "International traditional Chinese medicine guideline for diagnostic and treatment principles of diabetes," *Annals of Palliative Medicine*, vol. 4, no. 9, pp. 2237–2250, 2020.

[3] X. L. Tong, G. Z. Bi, Z. Zhen et al., "TCM syndrome differentiation of 2518 T2DM cases," *World Journal of Integrated Traditional Chinese and Western Medicine*, vol. 1, pp. 26–28, 2008.

[4] D. H. Yin, X. C. Liang, Y. L. Pu et al., "Analysis of Chinese medicine syndrome pattern in patients with type 2 diabetes mellitus and its relationship with diabetic chronic complications," *Chinese Journal of Integrated Traditional Chinese and Western Medicine*, vol. 29, no. 6, pp. 506–510, 2009.

[5] J. Zhou, F. H. Zhou, J. Shi et al., "Status and influencing factors of glycemic control in type 2 diabetes patients over 35 years old in Nanning City," *China Journal of Disease Control and Prevention*, vol. 18, no. 9, pp. 816–819, 2014.

[6] B. Zhang, H. D. Xiang, M. B. Mao et al., "Epidemiological survey of chronic vascular complications of type 2 diabetic Inpatients in Four municipalities," *Acta Academiae Medicinae Sinicae*, vol. 24, no. 5, pp. 452–456, 2002.

[7] W. He, M. Cheng, W.-B. Qiao et al., "Analysis on research methods of syndrome elements and their evolution," *Journal of Traditional Chinese Medicine*, vol. 11, no. 54, pp. 901–904, 2013.

[8] R.-Z. Yan, Y.-X. Wang, X.-N. Wang et al., "Study on distribution characteristics of traditional Chinese medicine heat syndrome in diabetic kidney disease patients," *China Journal of Traditional Chinese Medicine and Pharmacy*, vol. 8, no. 35, pp. 4153–4156, 2020.

[9] C. Zhao, G. Li, J.-H. Si et al., "Exploration on design forms and elements of studies on variation of traditional Chinese medicine syndrome based on the literatures survey," *China Journal of Traditional Chinese Medicine and Pharmacy*, vol. 5, no. 31, pp. 1914–1919, 2016.

[10] M.-X. Zhang, J. Li, H. Li et al., "Evolvement rule of Chinese medicine syndrome of coronary heart disease complicated with hypertension," *Journal of Traditional Chinese Medicine*, vol. 11, no. 57, pp. 953–956, 2016.

[11] M. Yuan, X.-S. Xu, Y. Yang et al., "A quick and accurate method for the estimation of covariate effects based on empirical bayes estimates in mixed-effects modeling: correction of bias due to shrinkage," *Statistical Methods in Medical Research*, vol. 12, no. 28, pp. 3568–3578, 2019.

[12] W.-Q. Zhang, R. Zhang, and Y.-L. Xu, "Application progress of implicit structure analysis in research of traditional Chinese medicine," *Traditional Chinese Medicine Research*, vol. 6, no. 33, pp. 68–71, 2020.

[13] H.-Y. Zhang, J.-Z. Ye, Y. Zhou et al., "The application of the latent structural equation in the analysis of TCM syndrome evolution," *Lishizhen Medicine and Materia Medica Research*, vol. 10, no. 29, pp. 2476-2477, 2018.

[14] W.-F. Zhu, *Syndrome Element Dialectics*, People's Health Publishing House, Beijing, China, 2008.

[15] M. Jacomy, T. Venturini, S. Heymann et al., "ForceAtlas2, a continuous graph layout algorithm for handy network visualization designed for the Gephi software," *PLoS One*, vol. 6, no. 9, Article ID 98679, 2014.

[16] B. Liu, X. Zhou, Y. Wang et al., "Data processing and analysis in real-world traditional Chinese medicine clinical data: challenges and approaches," *Statistics in Medicine*, vol. 7, no. 31, pp. 653–660, 2012.

[17] V. D. Blondel, J. L. Guillaume, R. Lambiotte et al., "Fast unfolding of communities in large networks," *Journal of Statistical Mechanics: Theory and Experiment*, vol. 10, p. 1000, 2008.

[18] M. Schmidt, "The sankey diagram in energy and material flow management: part I: history," *Journal of Industrial Ecology*, vol. 1, no. 12, pp. 82–94, 2008.

[19] Chinese Obesity Working Group, "Guidelines for the prevention and control of overweight and obesity in Chinese adults (excerpt)," *Journal of Nutrition*, vol. 1, pp. 1–4, 2004.

[20] X. Han, Y. Gao, B. Ma et al., "The clinical relevance of serum NDKA, NMDA, PARK7, and UFDP levels with phlegm-heat syndrome and treatment efficacy evaluation of traditional Chinese medicine in acute ischemic stroke," *Evidence-Based Complementary and Alternative Medicine*, vol. 2015, Article ID 270498, 7 pages, 2015.

[21] S. Guan, J. Chen, and Y. Ma, "Relation between the initial state fiery syndrome of acute cerebral infarction and immune cell factors," *Journal of Radioimmunoassay*, vol. 13, pp. 331-332, 2000.

[22] M.-Y. Li, X.-M. Huang, M.-M. Yin et al., "Treatment of type 2 diabetes based on heat syndrome," *Journal of Traditional Chinese Medicine*, vol. 6, no. 57, pp. 476–479, 2016.

[23] F.-M. Zhao, Y. Huang, M.-J. Wu et al., "Expressions of spectrum of inflammation-related and clotting-related genes in hemorrhagic stroke patients with stagnated heat syndrome," *Journal of Traditional Chinese Medicine*, vol. 20, no. 59, pp. 1753–1757, 2018.

[24] N. Esser, S. Legrand-Poels, J. Piette et al., "Inflammation as a link between obesity, metabolic syndrome and type 2 diabetes," *Diabetes Research and Clinical Practice*, vol. 2, no. 105, pp. 141–150, 2014.

[25] O. Chávez-Talavera, A. Tailleux, P. Lefebvre et al., "Bile acid control of metabolism and inflammation in obesity, type 2 diabetes, dyslipidemia, and nonalcoholic fatty liver disease," *Gastroenterology*, vol. 7, no. 152, pp. 1679–1694, 2017.

[26] X.-J. Li and Y.-H. Wu, "Is diabetes an inflammatory disease?" *Chinese Journal of Endocrinology and Metabolism*, vol. 4, pp. 5–7, 2003.

[27] N. Ouchi, J. L. Parker, J. J. Lugus et al., "Adipokines in inflammation and metabolic disease," *Nature Reviews Immunology*, vol. 2, no. 11, pp. 85–97, 2011.

[28] C. Kang, D. LeRoith, and E. J. Gallagher, "Diabetes, obesity, and breast cancer," *Endocrinology*, vol. 11, no. 159, pp. 3801–3812, 2018.

[29] C.-h. Zhang, J.-q. Sheng, W.-h. Xie et al., "Mechanism and basis of traditional Chinese medicine against obesity: prevention and treatment strategies," *Frontiers in Pharmacology*, vol. 12, Article ID 615895, 2021.

[30] L.-B. Zhou, J.-P. Wei, F. Liu et al., "Study on the TCM pathology and syndrome characteristics of first attack diabetes II," *Journal of Sichuan of Traditional Chinese Medicine*, vol. 11, pp. 34–36, 2008.

[31] X. Y. Xiang and Y. Z. Ran, "Study on TCM constitutional types and clinical syndromes of 270 patients with type II diabetes," *World Chinese Medicine*, vol. 9, no. 12, pp. 1599–1602, 2014.

[32] Y.-J. Ding, S.-D. Wang, Y.-H. Wang et al., "Discussion on the basic pathogenesis of diabetes mellitus "yin and qi consumption caused by internal heat injury"," *Journal of Traditional Chinese Medicine*, vol. 5, pp. 389–391, 2008.

[33] J.-N. Huang, "Theoretical discussion on treating diabetes from deficiency of both qi and yin," *Chinese Journal of Basic Medicine in Traditional Chinese Medicine*, vol. 9, pp. 1-2, 2000.

[34] Y.-H. Wang, J.-X. Zhao, S.-D. Wang et al., "TCM syndrome development research of diabetic nephropathy in different stage," *China Journal of Traditional Chinese Medicine and Pharmacy*, vol. 10, no. 27, pp. 2687–2690, 2012.

[35] W.-J. Wu, J.-X. Zhao, S.-D. Wang et al., "Retrospective analysis on characteristics of syndrome and pathogenesis of diabetic kidney disease," *Journal of Traditional Chinese Medicine*, vol. 3, no. 57, pp. 216–219, 2016.

[36] K.-C. Huang, C.-C. Chen, Y.-C. Su et al., "The relationship between stasis-stagnation constitution and peripheral arterial disease in patients with type 2 diabetes," *Evidence-Based Complementary and Alternative Medicine*, vol. 2014, Article ID 903798, 6 pages, 2014.

[37] S.-F. Chu, H.-L. Li, D.-L. Liu et al., "Characteristics of plasma metabonomics of patients of diabetes mellitus type 2 with blood stasis syndrome," *Journal of Traditional Chinese Medicine*, vol. 8, no. 58, pp. 664–668, 2017.

[38] Z.-Z. Xu, "Characteristics of syndromes in patients with different course of diabetes," *Journal of Traditional Chinese Medicine*, vol. 1, pp. 44-45, 2000.

[39] S. Kalra, A. Singal, and T. Lathia, "What's in a name? Redefining type 2 diabetes remission," *Diabetes Therapy*, vol. 12, no. 3, pp. 647–654, 2021.

[40] K. Verhoeff, S. J. Henschke, B. A. Marfil-Garza, N. Dadheech, and A. M. J. Shapiro, "Inducible pluripotent stem cells as a potential cure for diabetes," *Cells*, vol. 10, no. 2, p. 278, 2021.

[41] E. Johnson, H. Feldman, A. Butts et al., "Standards of medical Care in diabetes—2020 abridged for primary Care providers," *Clinical Diabetes*, vol. 43, pp. S1–S212, 2019.

[42] H. Wang and M. Wang, "Research progress on heat-clearing Chinese herbal compounds against diabetes based on regulating intestinal flora," *Chinese Journal of Experimental Traditional Medical Formulae*, vol. 3, no. 27, pp. 238–244, 2021.

[43] A. F. G. Cicero and A. Baggioni, "Berberine and its role in chronic disease," *Advances in Experimental Medicine and Biology*, vol. 928, pp. 27–45, 2016.

[44] X.-H. Zhang, Y.-H. Zhang, Z.-J. Hu et al., "Thoughts on effects of xinkai kujiang formula with different amounts of coptis on hypoglycemic action in KKAy mice with incipient type 2 diabetes mellitus," *China Journal of Traditional Chinese Medicine and Pharmacy*, vol. 5, no. 29, pp. 1547–1549, 2014.

[45] M. Jiang, X.-H. Zhang, Y.-H. Zhang et al., "Impacts of xinkai kujiang Formula on the expressions of InR and bax inKKAy mice of early T2DM," *World Journal of Integrated Traditional Chinese and Western Mdicine*, vol. 7, no. 10, pp. 991–994, 2015.

[46] Q. H. Yan and Y. Q. Zou, "The treatment of diabetic nephropathy by national Chinese medicine master Zou Yanqin from spleen and kidney," *Journal of Nanjing University of Traditional Chinese Medicine*, vol. 34, no. 2, pp. 109–111, 2018.

[47] T. X. Han and Q. Z. Yan, "Professor YAN de-xin's experience in treating diabetes," *Journal of Zhejiang Chinese Medical University*, vol. 36, no. 10, pp. 1067–1069, 2012.

[48] B. Che, F. Shao, S. D. Wang et al., "Study on medication experience of national TCM master lü renhe inheritance team in the treatment of diabetes mellitus," *Chinese Journal of Information on Traditional Chinese Medicine*, vol. 27, no. 11, pp. 111–115, 2020.

[49] Y.-H. Hu, J. Yang, C.-K. Xiu et al., "Research progress of Yi-qi Huoxue prescription in treatment of diabetic angiopathy," *Chinese Journal of Experimental Traditional Medical Formulae*, vol. 8, no. 26, pp. 1–12, 2020.

[50] X. Chen, J. Yu, and J. Shi, "Management of diabetes mellitus with puerarin, a natural isoflavone from pueraria lobata," *The American Journal of Chinese Medicine*, vol. 46, no. 8, pp. 1771–1789, 2018.

[51] X. Xu, L. Niu, Y. Liu et al., "Study on the mechanism of gegen qinlian decoction for treating type II diabetes mellitus by integrating network pharmacology and pharmacological evaluation," *Journal of Ethnopharmacology*, vol. 262, pp. 113–129, 2020.

Hindawi
Evidence-Based Complementary and Alternative Medicine
Volume 2021, Article ID 6655555, 11 pages
https://doi.org/10.1155/2021/6655555

Research Article

Mulberroside A from Cortex Mori Enhanced Gut Integrity in Diabetes

Yinyan Xu,[1] **Hengli Guo**,[2,3] **Tingting Zhao**,[2] **Jing Fu**,[1] **and Youhua Xu**[2]

[1]*Department of Pharmacy, Women's Hospital of Nanjing Medical University, Nanjing Maternity and Child Health Care Hospital, Nanjing 210004, Jiangsu, China*
[2]*Faculty of Chinese Medicine, State Key Laboratory of Quality Research in Chinese Medicine, Macau University of Science and Technology, Avenida Wai Long, Taipa, Macao SAR 999078, China*
[3]*Department of Traditional Chinese Medicine, Zhuhai Maternal and Child Health Hospital, Zhuhai 519000, Guangdong, China*

Correspondence should be addressed to Jing Fu; jingfu6_6@126.com and Youhua Xu; yhxu@must.edu.mo

Received 31 December 2020; Revised 7 April 2021; Accepted 29 April 2021; Published 20 May 2021

Academic Editor: Md. Akil Hossain

Background. Diabetic endotoxemia has been recognized as one of the hallmarks of type 2 diabetes mellitus (T2DM). Recent findings suggest that gut leak plays a pivotal role in diabetic endotoxemia. Cortex Mori (CM) has been widely applied in China to ameliorate development of T2DM, but its effect on endotoxemia is unknown. *Methods*. The study was constructed with two parts: (1) in vivo study of CM on diabetic endotoxemia in db/db mice. Eight C57BL/6 mice were set as normal control; (2) in vitro study of mulberroside A (MBA) from CM on diabetic endotoxemia. Potential mechanism of MBA on ameliorating diabetic endotoxemia was also explored. *Results*. The present study found that CM water extract decreased levels of blood glucose, ameliorated liver and renal damage in db/db mice, and ameliorated diabetic endotoxemia ($p < 0.01$). We also found that the water extract enhanced gut integrity and decreased gut inflammatory protein ICAM-1 expression in db/db mice as detected by H&E staining and immunohistochemistry methods. In the in vitro study, MBA decreased levels of MDA and ROS induced by LPS ($p < 0.01$) and enhanced the integrity of gut epithelial barrier ($p < 0.01$). *Conclusions*. We found that Cortex Mori and its active component mulberroside A could ameliorate diabetic endotoxemia by preserving gut integrity.

1. Introduction

Type 2 diabetes mellitus (T2DM) has now been regarded as an epidemic disease. Although a series of anti-T2DM agents are emerging within this decade, such as GLP-1 analogues [1], this epidemic tendency seems not to be shacked. More importantly, with the prevalent of Western food, this trend is becoming worsened. Because genetic factors should not have dramatic alteration within a few decades, environmental factors must play a role in it. Previously, Hotamisligil and colleagues [2] first demonstrated that neutralizing proinflammatory cytokines helps to ameliorate development of T2DM; since then on, the term "diabetic endotoxemia" is suggested, and "anti-inflammation" has been labeled as one of the indices that evaluate therapeutic efficacy in clinical settings. Within this decade, it is gradually recognized that gut dysbacteriosis might be the source of diabetic endotoxemia [3, 4], as dysbiosis of gut microbiota will contribute to the increase of gut permeability which finally leads to metabolic endotoxemia and higher plasma lipopolysaccharide (LPS) [5, 6]. In this sense, preserving gut integrity is believed to have a beneficial effect on reversing this endotoxemia.

Cortex Mori (CM) is the dried root bark of *Morus alba* L. For centuries, CM has been used in the treatment of diabetes in China. Previously, Qi and colleagues [7] found that CM extract can effectively ameliorate diabetic hyperlipidaemia. A previous study [8] indicated that CM extract concentration dependently suppressed the production of COX-2 and PGE_2 in vivo and in vitro and showed the anti-inflammatory effects. However, influence of CM on diabetic endotoxemia had not been well investigated.

The current study was constructed with two parts: (1) in vivo study of CM on diabetic endotoxemia in db/db mice and (2) in vitro study of the component from CM (mulberroside A) on diabetic endotoxemia and its potential mechanism.

2. Materials and Methods

2.1. Materials, Reagents, and Animals. Cortex Mori (CM) was bought from Bozhou Chinese Medicinal Herb Market (Anhui, China). Standard mulberroside A (MBA) was derived from National Institutes for Food and Drug Control of China (Beijing, China). Metformin was purchased from GBCBIO technology (Guangzhou, China). Lipopolysaccharide (LPS) was derived from Sigma (St. Louis, MO, USA). ELISA kits for advanced glycation end products (AGEs) and LPS were purchased from Cheng Lin Biotechnology Company (Beijing, China). Kits for alanine aminotransferase (ALT or GPT), glutamic oxaloacetic transaminase (AST or GOT), HbA1c, and creatinine (Cr) are from Jiancheng (Nanjing, Jiangsu, China). 3-(4,5)-Dimethylthiazo (-z-y1)-3,5-diphenytetrazoli-umromide (MTT), primary antibodies for zona occludens protein-1 (ZO-1), occludin, ICAM-1, p-p38 MAPK, and p38 MAPK were purchased from Santa Cruz (USA). Kit for mAlb was derived from Westang (Shanghai, China). Kits for IL-1β, IL-8, MCP-1, and TNF-α were purchased from Neobioscience (Shenzhen, China). MDA and ROS detection kits were from Beyotime Biotechnology (Beijing, China). Dulbecco's modified eagle medium (DMEM), fetal bovine serum (FBS), trypsin, MEM nonessential amino acids solution, and L-glutamine were obtained from Gibco (Big Cabin, OK, USA). DAPI, Cy3-, and FITC-conjugated secondary antibodies were supplied by Boster (Wuhan, China). 24-well transwell cell culture plates (hanging insert well diameter 6.5 mm, membrane area 0.3 cm^2) were obtained from Corning (Corning, NY, USA). The electrical resistance detection system (Millicell ESR-2) was bought from Millipore (Billerica, MA, USA). The other reagents and kits are from commercial sources.

Male C57BL/6 and db/db mice weighing 20–30 g were supplied by Cavens Lab Animal Co. Ltd. (Changzhou, China), and normal chow diet or high-fat diet was, respectively, administrated to the animals. All animal care and investigation conformed to the Guide for the Care and Use of Laboratory Animals published by the US National Institutes of Health (NIH Publication No. 85–23, revised 1996) and was approved by Macau University of Science and Technology. The animals were maintained on a 12/12 h light/dark cycle. Before drug intervention, all animals were kept in animal house for 3 days to make them adapt for the environment.

2.2. Preparation of Cortex Mori Water Extract (ECM). Dry powder of Cortex Mori (CM, 300 g) was immersed with double distilled water (3,000 ml) and continuously boiled on thermostat for 2 h. The water extraction mixture was filtrated and concentrated to 150 ml with the R2002 rotary evaporator, and stock solution for water extract of CM (ECM) was obtained with a concentration of 2 g/ml. The crude drug solution was filtered through a 0.45 μm membrane. Finally, the stock solution was diluted with water to 1.25 g/ml (high dose), 0.58 g/ml (medium dose), and 0.31 g/ml (low dose) and then stored at 4°C until use.

2.3. Animals Grouping and Drug Administration. Diabetic animals (db/db mice) were randomly divided into 5 groups as follows: (1) negative control group ($n = 6$); (2) positive control group in which animals were administrated with metformin (0.15 g/kg bodyweight, $n = 6$); (3) low dose Cortex Mori group (0.91 g/kg bodyweight, $n = 6$); (4) medium dose Cortex Mori group (1.82 g/kg bodyweight, $n = 6$); and (5) high dose Cortex Mori group (3.64 g/kg bodyweight, $n = 6$). Eight C57BL/6 mice were set as normal control. Each day, all animals were administrated with drugs as mentioned above or 0.45 ml normal saline (for normal and model group animals) by gavage for 5 continuous weeks. At the end of the experiment, blood samples were collected for biochemical examination, the animals were sacrificed, and colon samples were collected for histological evaluation.

2.4. Blood Assay. Blood cell count was measured by the clinical laboratory of Jihua Hospital affiliated to Jinan University (Guangzhou, China). Blood HbA1c, AGEs, AST, ALT, BUN, Cr, LPS, and MCP-1 were determined by kits according to the protocol provided by the manufacturers.

2.5. Hematoxylin and Eosin Staining and Immunohistological Evaluation of Colon. Colon was fixed in 4% paraformaldehyde for 24 h and then paraffinized. For observation, sections (0.4 μm) were stained with hematoxylin and eosin (H&E) solution for 5 min, and the histopathological images of colon were observed under a light microscope (Olympus, Tokyo, Japan). For immunohistological evaluation of the colon, sections were first incubated with primary antibody for ICAM-1 (1 : 200); then, biotin-conjugated secondary antibody and streptavidin-biotin enzyme complex were added to the sections to develop brown deposit (positive staining).

2.6. Cell Culture. Human epithelial colorectal adenocarcinoma (Caco-2) cell was purchased from the American Type Tissue Collection (Manassas, VA, USA). The cells were maintained in DMEM with 10% fetal bovine serum (FBS), 1% penicillin/streptomycin, 1% MEM nonessential amino acids, and L-glutamine in a cell culture incubator.

2.7. MTT Assay. To evaluate influence of LPS and mulberroside A (MBA) on cell viability, cells were treated with MTT (5 mg/ml) for 4 h followed by dimethyl sulphoxide (DMSO) incubation. The absorbance at 490 nm was determined by a spectrophotometer.

2.8. Cell Antioxidant Activity Experiment. Cell antioxidant activity was evaluated by determining levels of

malondialdehyde (MDA) and reactive oxygen species (ROS) after drugs intervention according to the manufacturer's instruction.

2.9. Immunofluorescence Assay. Caco-2 cells were seeded on the slide. After being treated with vehicle, LPS (100 μg/ml), or LPS + MBA (70 μM), cells were fixed with 4% paraformaldehyde. Then, primary antibodies including ZO-1 (1 : 100), occludin (1 : 100), p-p38 MAPK (1 : 100), or p38 MAPK (1 : 100) were added to the cultured cells. DAPI was used for nuclear staining, and FITC- or Cy3-conjugated secondary antibodies were applied to observe proteins' expression or activation under a fluorescence microscope (Olympus, Tokyo, Japan).

2.10. Inflammatory-Related Cytokines Assay. Levels of LPS and inflammatory cytokines including IL-1β, TNF-α, and IL-8 after drugs intervention were determined according to the manufacturer's instruction.

2.11. Gut Epithelial Barrier Evaluation. An in vitro gut epithelial barrier model was developed according to our previous report [9]. In general, Caco-2 cells at the density of 1×10^5 were seeded on the upper well membrane of the transwell system and further cultured for 21 days; then, a confluent monolayer was obtained for which transepithelial electrical resistance (TEER) would exceed 400 Ωcm^2. After drug administration for 24 h, the upper well was added with LPS; finally, level of LPS in the lower chamber of transwell was determined.

2.12. Statistical Analysis. The data were expressed as mean ± standard deviation (SD). SPSS 19.0 software with the one-way ANOVA method was applied for data analysis. The p value of 0.05 or less was considered to be statistical significant.

3. Results

3.1. Blood Glycated Proteins. High blood glucose is the most significant phenomenon in diabetic population. Long-term exposure of hemoglobin and other forms of proteins to plasma glucose will promote a nonenzymatic glycation pathway and generate glycated proteins, namely, HbA1c or advanced glycation end products (AGEs). Therefore, the level of glycated proteins can reflect average plasma glucose concentration over prolonged periods of time. To identify if oral CM administration could affect this glycation, levels of HbA1c and AGEs were detected by kits. As shown in Figures 1(a) and 1(b), drug administration with either metformin or CM could significantly decrease HbA1c and AGEs levels compared with the diabetic model group, and CM at medium dose had more effect on lowering the AGEs level compared with high or low dose (Figure 1(b)).

3.2. Liver and Renal Function. To evaluate influence of CM water extract on target organs of diabetes, liver and renal functions were determined. As depicted in Figures 2(a) and 2(b), CM administration at low dose and medium dose would not deteriorate liver function as levels of ALT and AST were not significantly higher than that of the DM group. For renal function, we determined urine BUN (Figure 2(c)), Cr (Figure 2(d)), and ratio of mAlb/Cr (Figure 2(e)). We found that renal function in DM mice was dramatically damaged; in that, all of the three indicators were significantly elevated, while administration with CM at low or medium doses could significantly decrease the renal function indicators.

3.3. CM Ameliorated Diabetic Endotoxemia in db/db Mice. T2DM has now been recognized as a low-grade inflammatory disease, and inflammatory cell infiltration is one of the characteristics [10]. In the present study, we found that the amount of white blood cell (WBC) was dramatically increased compared with normal mice (Figure 3(a)), and administration with either low or medium dose of CM could significantly decrease the level of WBC; more importantly, medium dose of CM possessed more significant effect compared with its low or high dose. We also observed that the number of abnormal lymphocytes (ALY) was significantly increased in diabetic animals, and this elevation could be decreased by any drug intervention in this experiment (Figure 3(b)). The present data suggested that CM at medium dose have a beneficial effect on ameliorating both diabetes and diabetic-inflammatory cell infiltration.

Inflammatory cell infiltration relies on inflammatory chemoattractant protein's expression. MCP-1 is well studied for its role in mediating inflammatory cell infiltration [11]. We observed in the present study that MCP-1 was significantly increased in the diabetic model group compared with normal mice, and administration with metformin or low/medium dose of CM could significantly decrease the level of MCP-1 (Figure 3(c), $p < 0.01$ vs. the diabetic group).

Lipopolysaccharides (LPS), also known as endotoxin, have been found to be elevated in diabetic population and share an important composition in diabetic endotoxemia [12]. In the present study, we found that the serum level of LPS in diabetic mice was increased by about 7 times compared with normal mice (Figure 3(d)); metformin and CM treatment significantly decreased the level of LPS ($p < 0.01$ vs. the diabetic group); more importantly, low or medium dose of CM administration had more significant effect compared with that of metformin on decreasing serum LPS ($p < 0.01$). It is well-known that LPS is an important component of the cell wall in Gram-negative bacteria. In this sense, gut-sourced Gram-negative bacteria (or the so-called bad-microbiota) overproliferation accompanied with gut barrier integrity damage may play a role in diabetic endotoxemia.

3.4. CM Preserved Gut Integrity and Decreased Proinflammatory Cytokine's Expression. To verify if CM intervention could preserve gut integrity and inhibit "gut-leak" mediated diabetic endotoxemia, we carried out hematoxylin and eosin (H&E) staining and immunohistological

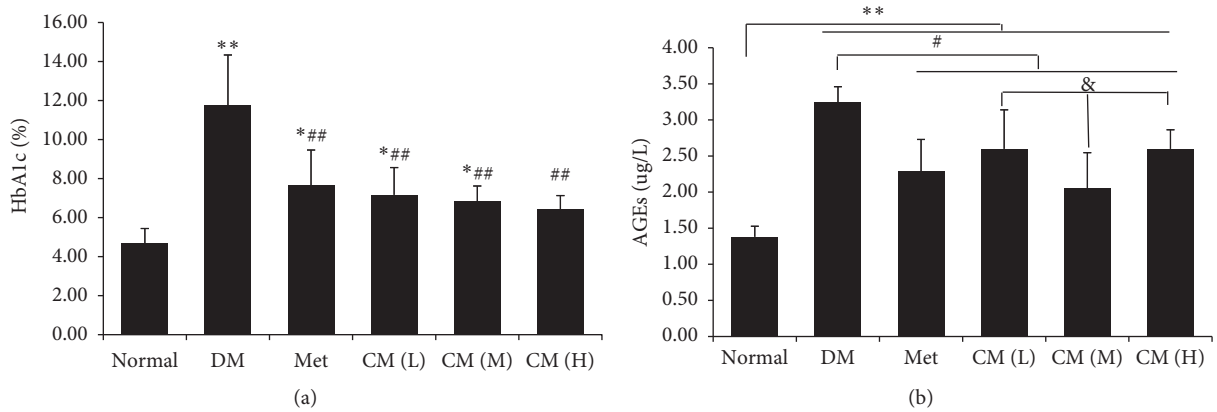

Figure 1: Cortex Mori water extract decreased levels of blood (a) HbA1c and (b) AGEs in db/db mice. DM, diabetic group; Met, metformin group; CM (L), CM (M), and CM (H) indicate diabetic mice administrated with low, medium, and high dose of Cortex Mori water extract. $^{*}p < 0.05$, $^{**}p < 0.01$ vs. normal mice; $^{\#}p < 0.05$, $^{\#\#}p < 0.01$ vs. DM; $^{\$\$}p < 0.01$ vs. Met; & $p < 0.05$ vs. CM (M).

evaluation on gut. As shown in Figure 4(a), the gut physical barrier was severely damaged as amounts of gut epithelial cells were detached from the basal lamina; once the animals were treated with metformin or CM, gut integrity was obviously recovered; more importantly, medium dose of CM had more significant effect on preserving gut integrity; in that, this dose administration could restore gut integrity to that of normal state in view of histological evaluation.

As inflammatory cell infiltration was significantly reduced by CM administration at medium dose, we would like to know if any inflammatory protein was involved in this process. ICAM-1 is well recognized to participate in development of diabetes and thereafter inflammatory cell infiltration [13]. To demonstrate our hypothesis, its expression was determined by the immunohistochemistry method. As shown in Figure 4(b), ICAM-1 expression accompanied with inflammatory cell infiltration was dramatically increased in diabetic mice, and medium dose of CM significantly reversed both expression of ICAM-1 and infiltration of WBC. Converging from above findings, we concluded that oral administration with CM had positive effects against diabetic endotoxemia, and the potential mechanism might attribute to its function on preserving gut barrier integrity.

3.5. Mulberroside A from CM Enhanced Antioxidative Activity of Caco-2 Cells. Mulberroside A is found to be an active component that has been demonstrated to possess multiple activities. Oxidative stress damage is believed to participate in the development of gut leak and diabetic endotoxemia. To investigate if MBA possess some effect on this aspect, Caco-2 cells were incubated with drugs for 24 h; then, the culture supernatant was collected for MDA detection, and the level of ROS in the cells was observed by the immunofluorescence method. As shown in Figures 5(a) and 5(b), LPS stimulation significantly elevated the level of both MDA and ROS in Caco-2 cells, and MBA intervention showed satisfactory effects on decreasing their levels to normal.

3.6. MBA Increased Gut Integrity. To evaluate influence of MBA on gut epithelial barrier, we constructed a Caco-2 cell monolayer by a transwell cell culture system. Transepithelial electrical resistance (TEER) across the monolayer was measured with a Millicell-ERS electric resistance system, and the amount of LPS from the upper chamber to the lower chamber across the monolayer was determined. As shown in Figures 6(a) and 6(b), LPS significantly decreased TEER which was accompanied by higher permeability of LPS across the monolayer to the lower chamber ($p < 0.01$), and treatment with MBA strengthened the monolayer integrity.

Two pivotal factors including cell viability and tight junction between cells contribute to the integrity of gut barrier [14]. In the current study, we did not find a significant effect of MBA on increasing Caco-2 cell viability (Figure 7(a)), and we would like to know about the tight junction condition after drug administration. In the present study, expression of two tight junction proteins including ZO-1 and occludin was studied. As can be seen in Figure 6(c), these junction proteins are highly expressed on normal Caco-2 cells, and LPS administration strikingly decreased their expression; expectedly, MBA intervention ameliorated this decrease.

To further investigate the potential mechanism, the intracellular signaling pathway activation status was observed. The p38MAPK signaling pathway has been well studied in its role on development of diabetic endotoxemia. As shown in Figure 6(d), the amount of total-p38MAPK in normal, LPS, and LPS + MBA groups were at the similar level. LPS incubation significantly activated p38MAPK, as its phosphor form (p-p38MAPK) was dramatically increased; when the cell was further administrated with MBA after LPS, activation of p38MAPK was significantly inhibited.

4. Discussion

Metabolic endotoxemia has now been recognized as a risk factor that is closely accompanied with both the onset and the progress of T2DM [15, 16]. Although there is still a

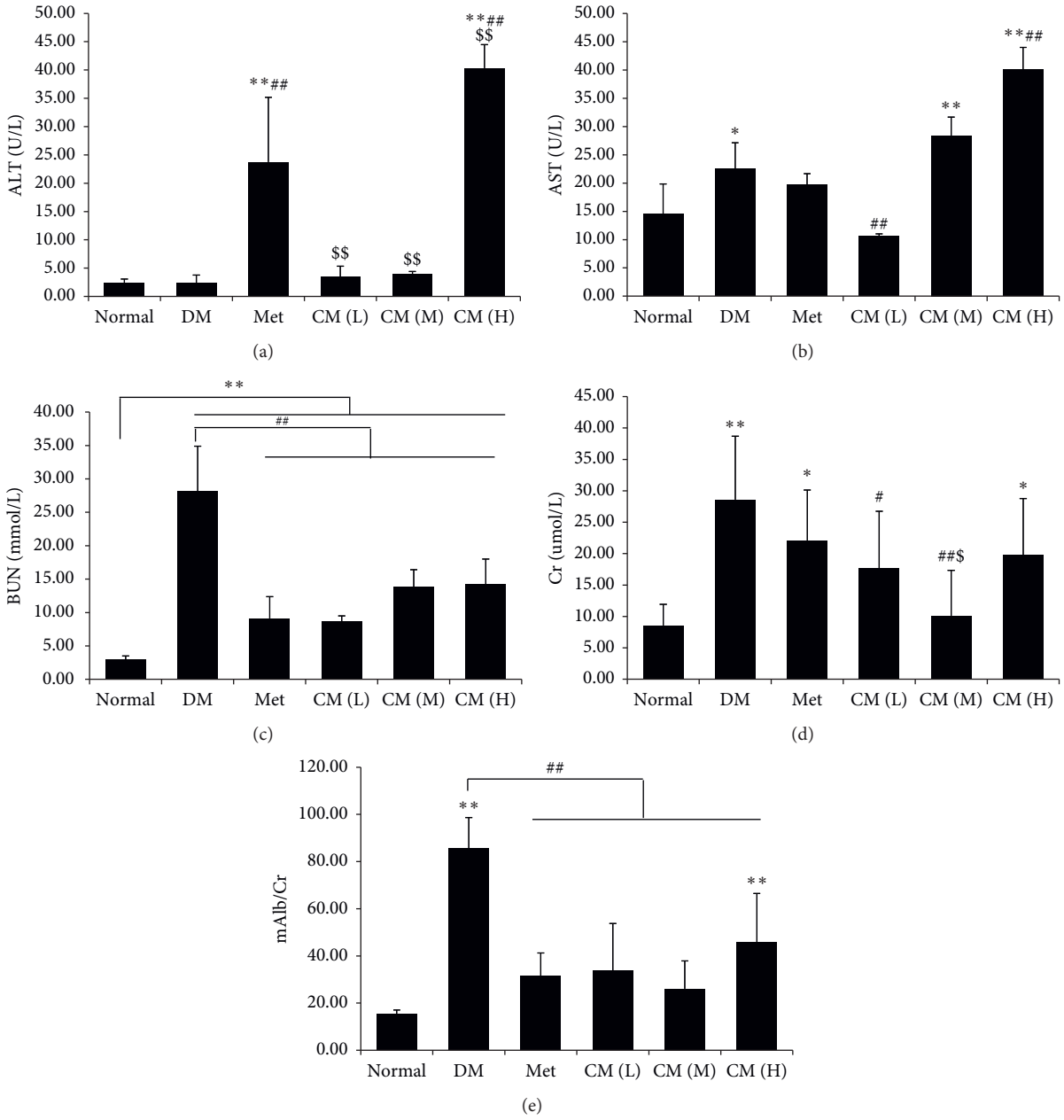

Figure 2: Cortex Mori water extract ameliorate liver and renal damage in db/db mice. Levels of (a) alanine aminotransferase (ALT), (b) aspartate aminotransferase (AST), (c) blood urea nitrogen (BUN), (d) creatinine (Cr), and (e) microalbuminuria (mAlb)/Cr were determined. DM, diabetic group; Met, metformin group; CM (L), CM (M), and CM (H) indicate diabetic mice administrated with low, medium, and high dose of Cortex Mori water extract. $^{*}p < 0.05$, $^{**}p < 0.01$ vs. normal mice; $^{\#}p < 0.05$, $^{\#\#}p < 0.01$ vs. DM; $^{\$}p < 0.05$, $^{\$\$}p < 0.01$ vs. Met.

conflict concerning the source of endotoxemia, scholars from both basic research and clinical physician have achieved a consensus that inhibit endotoxemia to help to attenuate the development of T2DM. Many herbal medicines have been used in China to treat diabetes for hundreds of years. However, most of their effecting mechanisms are unknown. In the present study, we investigated influence of Cortex Mori (CM) on diabetic endotoxemia in db/db mice; effects of an active component from it were also evaluated in the in vitro study.

Previously, Hotamisligil and colleagues [2] first demonstrated that neutralizing proinflammatory cytokines helped to ameliorate development of T2DM; since then on, the term "diabetic endotoxemia" is suggested, and "anti-inflammation" has been labeled as one of the indices that evaluate therapeutic efficacy in clinic. Recently, the pivotal role of gut in guarding the body in a healthy status has been more and more recognized. The dysfunction of the gut barrier will result in "gut-leak" and facilitate the entrance of gut-sourced pathogens or toxins into blood circulation; in

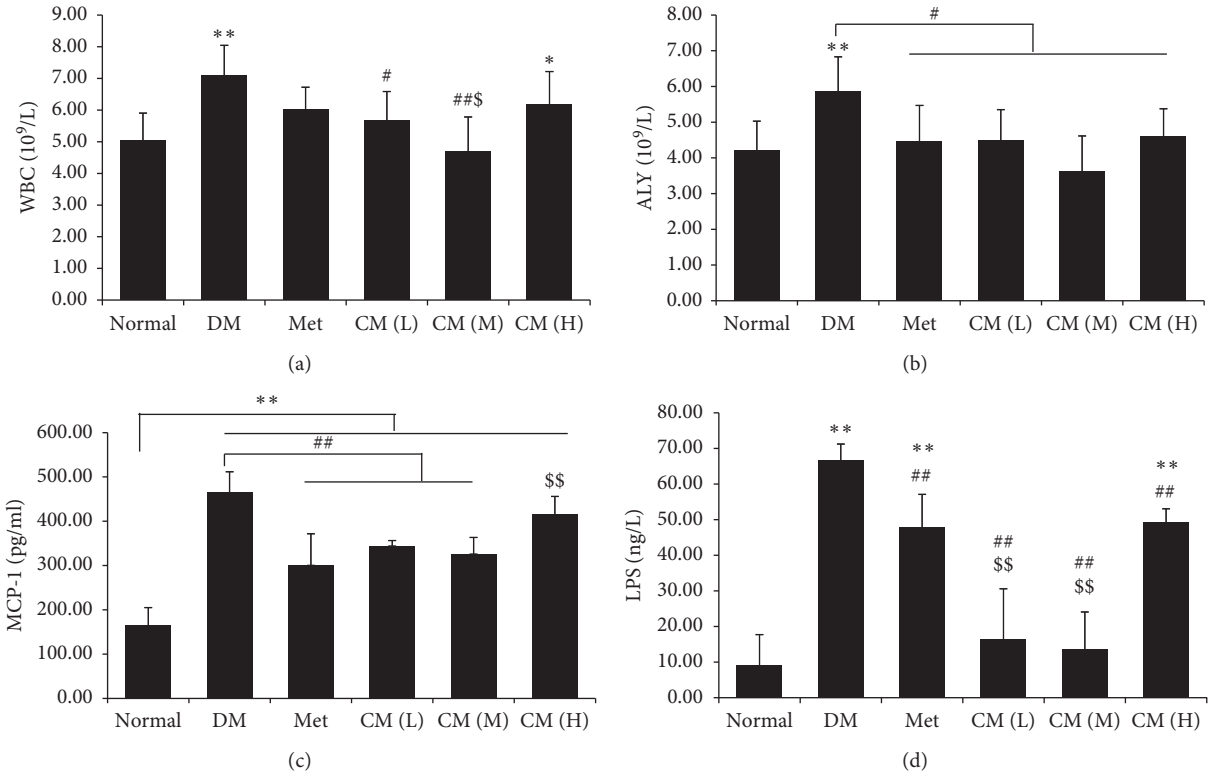

Figure 3: Cortex Mori water extract ameliorated diabetic endotoxemia. Levels of (a) white blood cells (WBC), (b) atypical lymphocytes (ALY), (c) inflammatory cytokine monocyte chemoattractant protein-1 (MCP-1), and (d) lipopolysaccharides (LPS) in blood of db/db mice were determined by kits. DM, diabetic group; Met, metformin group; CM (L), CM (M), and CM (H) indicate diabetic mice administrated with low, medium, and high dose of Cortex Mori water extract. $^{*}p < 0.05$, $^{**}p < 0.01$ vs. normal mice; $^{\#}p < 0.05$, $^{\#\#}p < 0.01$ vs. DM; $^{\$}p < 0.05$, $^{\$\$}p < 0.01$ vs. Met.

this sense, if this source is not intervened, it may persistently activate inflammatory cells and enlarge the production of internal-derived inflammatory cytokines, and finally, diabetic endotoxemia occurs. Unfortunately, there is no satisfactory strategy or drug that can solve this problem at present.

Cortex Mori (CM, Sang Bai Pi in Chinese) is the root of *Morus alba* L, which has been traditionally applied to treat diabetic inflammation [17, 18]. To first observe its effect on db/db mice, both hematological and histological experiments were carried out. We found that oral administration of CM water extract at medium dose possessed a significant effect on reducing glycated protein levels (HbA1c and AGEs), ameliorating diabetic nephropathy, and reducing diabetic inflammation in db/db mice. An important finding was that the level of blood LPS was significantly reduced on CM extract application. As LPS cannot be generated from the internal source, we postulated that CM may possess protective effects on inhibiting outsourced LPS entrance into the body. To this end, histological experiment was carried out. By H&E staining, we observed that the gut barrier was severely damaged in diabetic mice, and CM administration significantly preserved its integrity. Moreover, CM administration significantly decreased expression of ICAM-1 and inflammatory cell infiltration in gut wall. Our findings suggest that CM may ameliorate diabetic endotoxemia via enhancing gut integrity. To our knowledge, this is the first report that CM has this effect on gut.

In the present study, we found that low or medium dose of CM possessed protective effects in diabetic mice, while high-dose CM increased serum ALT, AST, creatinine, and LPS levels. We postulated that these adverse effects might be attributed to the over-high-dose CM application. On the one hand, high-dose CM exceeds metabolic ability of the mice and thus induced damage of related organs, e.g., the liver and kidney; on the other hand, oral administration with high-dose CM induced a hypertonic injury in the gut and therefore promoted gut leak and diabetic inflammation. However, exact reason is still waiting to be fully explained.

MBA is one of active components that have been reported to have various activities. To verify if MBA has effects on preserving gut integrity thereafter ameliorating diabetic endotoxemia, a series of in vitro studies were designed. Caco-2 cell is a colon epithelial cell line that has been widely applied to serve as a model to study gut barrier integrity [19]. Previously, we have successfully constructed a monocellular gut barrier model using Caco-2 cells [9]. In the present study, Caco-2 cell line was adopted, and LPS was applied to stimulate Caco-2 cell damage to mimic diabetic gut epithelial barrier damage. Our present in vitro disease model was supported by a previous report from Song and colleagues [20] that LPS administration will induce gut leak accompanied with the epithelial cell loss in mice.

As the epithelial cell loss and inflammation is the characteristic of diabetic endotoxemia, to verify in vitro

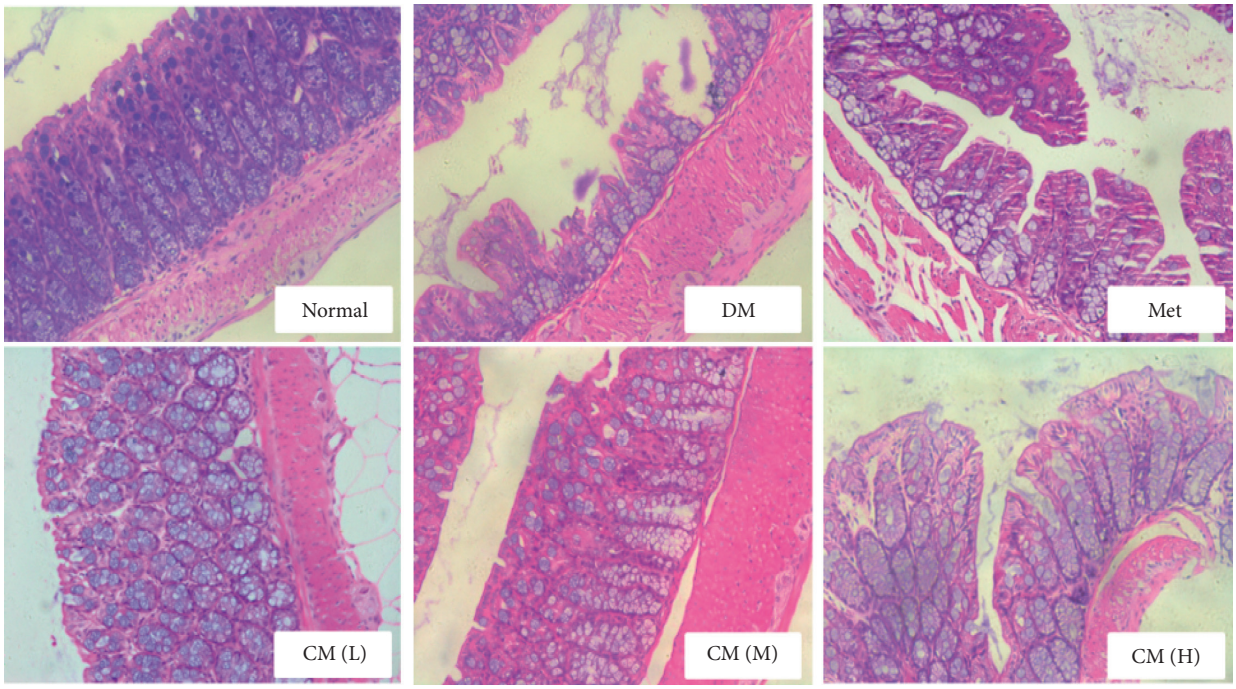

(a)

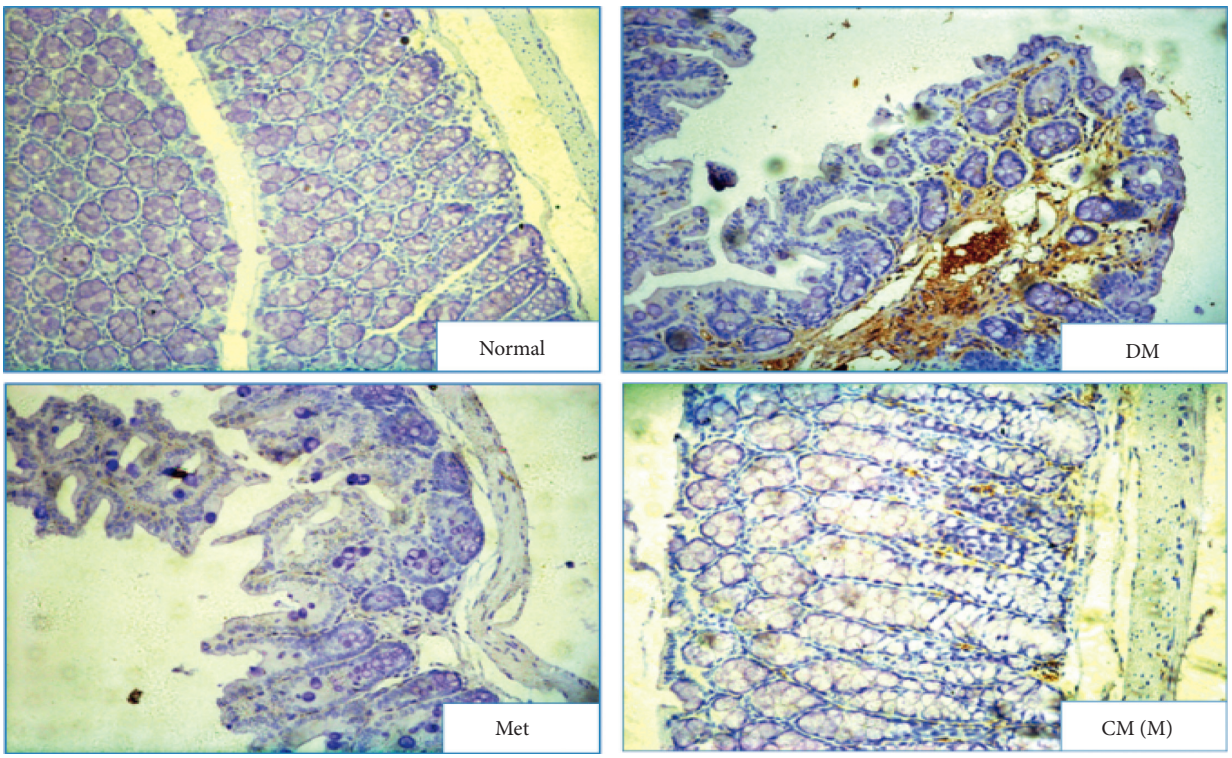

(b)

Figure 4: Cortex Mori water extract (a) enhanced gut integrity and (b) decreased gut inflammatory protein ICAM-1 expression in db/db mice as detected by H&E staining and immunohistochemistry methods. DM, diabetic group; Met, metformin group; CM (L), CM (M), and CM (H) indicate diabetic mice administrated with low, medium, and high dose of Cortex Mori water extract. Representative pictures are shown (magnification: 200).

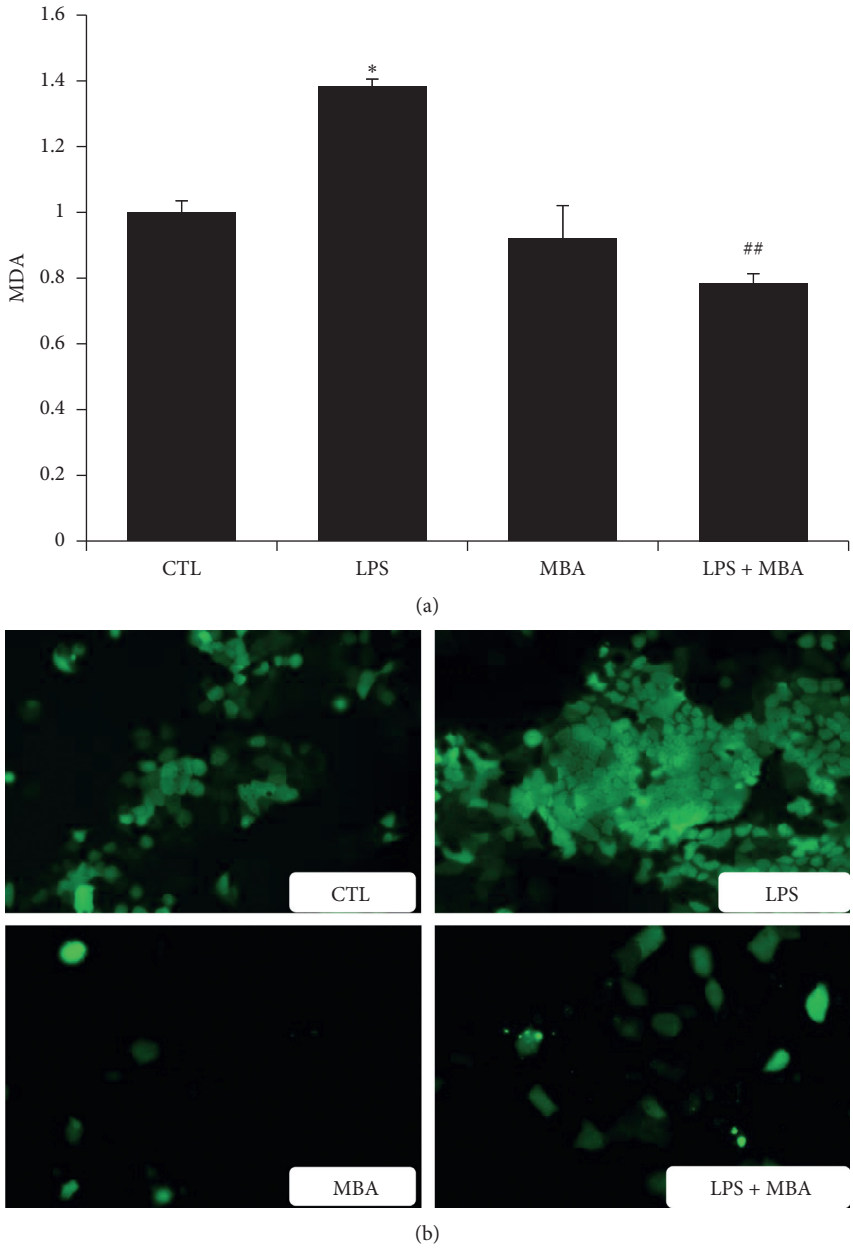

Figure 5: Mulberroside A (MBA) decreased levels of (a) MDA and (b) ROS induced by LPS. CTL, normal control; LPS, lipopolysaccharides group; ROS, reactive oxygen species. $^{*}p < 0.05$ vs. CTL; $^{\#\#}p < 0.01$ vs. LPS.

effects of MBA on LPS-induced Caco-2 cell damaged, the cell viability and inflammatory cytokines secretion were first studied. Report has demonstrated that cytokines including TNF-α and IL-1β promote the recruitment and infiltration of inflammatory cells and thereafter exaggerate inflammatory damage [21]. Unexpectedly, we did not observe a significant effect of MBA on enhancing cell viability and reversing LPS-induced inflammatory cytokines secretion in Caco-2 cells. So, we conclude from this finding that MBA may not have a direct effect on inhibiting inflammatory cytokines secretion. Oxidative stress is one of the characteristics of diabetes, and excessive oxidative stress may directly induce cell loss which will contribute to gut leak. We noticed that MBA has amounts of "-OH" structure, and we postulate it may possess some effect against oxidative stress. Fortunately, we found that MBA has definite effects against LPS-induced oxidative stress by reducing the level of MDA and ROS within cells.

As discussed above, gut leak will result in the paracellular invading of luminal antigens and toxins into blood circulation [22, 23]. Recent understanding depicts the importance of gastrointestinal tract leaky barrier in the development of DM [24]. The tight junction between intestinal epithelial cells is a natural barrier against invasion of intestinal toxins and bacteria into blood circulation [25, 26], and cell quantity and tight junction proteins among cells are two important

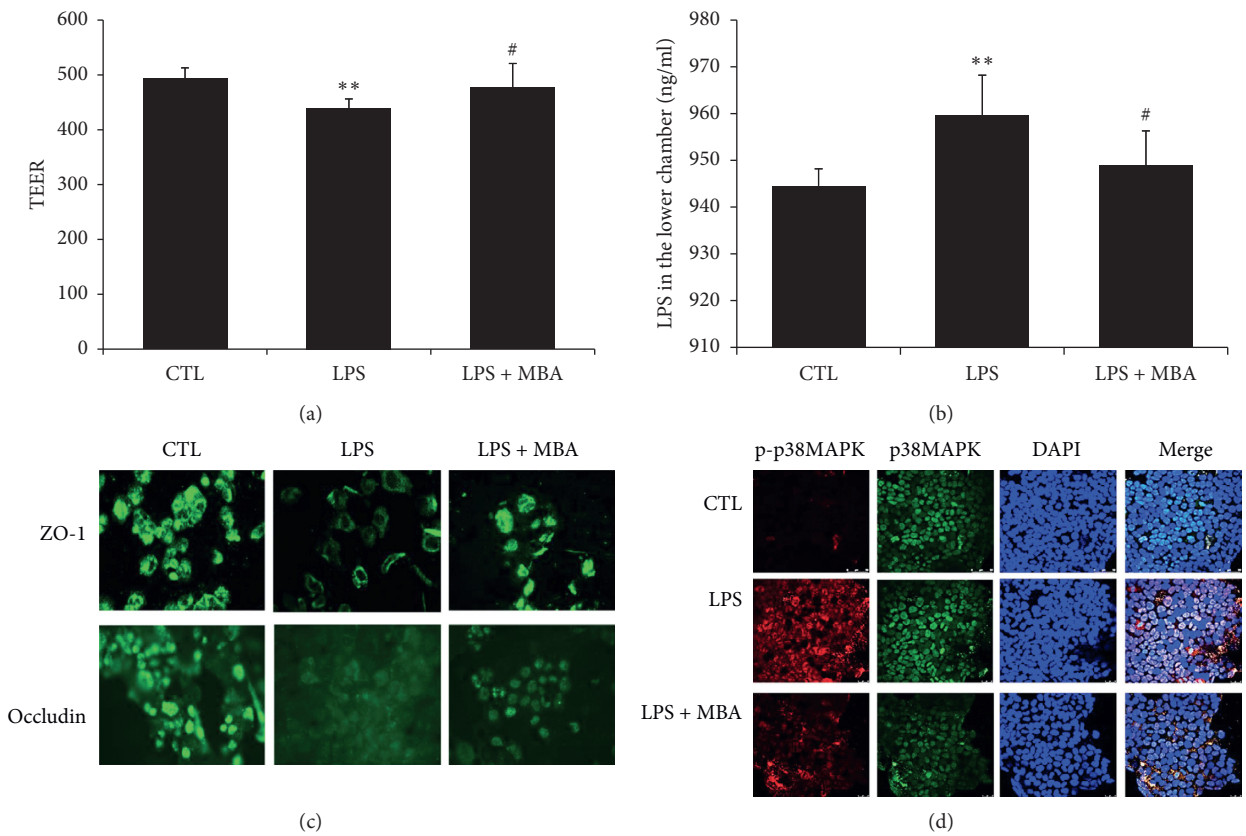

Figure 6: Mulberroside A (MBA) enhanced the integrity of gut epithelial barrier. (a) Transepithelial electrical resistance (TEER) across the monolayers was measured with a Millicell-ERS electric resistance system. (b) LPS was added into the upper chamber, and the permeability of LPS across the barrier to the lower chamber was assayed. (c) Expression of intercellular adhesion molecules proteins including ZO-1 and occludin damaged by LPS in Caco-2 cells was assayed by the immunofluorescence method. (d) Activation of the p38MAPK signaling pathway was studied. Phosphor-p38MAPK was stained by Cy3-conjugated secondary antibody (red), and total-p38MAPK was stained by FITC-conjugated secondary antibody (green); the cell nucleus was stained with DAPI. CTL, normal control; LPS, lipopolysaccharides group. $^{**}p < 0.01$ vs. CTL; $^{\#}p < 0.05$ vs. LPS.

factors that ensure gut barrier integrity [19, 27]. As we did not observe, MBA had a protective effect on gut epithelial cell viability, and we would like to know if it has some effects on expressions of tight junction proteins. We found that MBA administration significantly elevated expression of tight junction proteins expression, including ZO-1 and occludin. Our present finding is in accordance that LPS administration can decrease tight junction proteins' expression and increase the paracellular permeability [20]. Our finding was further verified; in that, the permeability of LPS across gut epithelial barrier was decreased, and TEER was enhanced on MBA administration.

As discussed above, endotoxemia has been found to be one of pivotal factors that promote development of diabetes, and gut leak might be a new target on preventing disease progression [15, 16]. In the present study, we found oral administration with the extract of Cortex Mori decreased the serum level of LPS and preserved integrity of gut barrier. Therefore, we detected the underlying mechanism in Caco-2 cells. Previously, Koistinen and colleague found the p38 MAPK signaling pathway contributed to insulin resistance in skeletal muscle cells [28]. Besides that, p38 MAPK has also been demonstrated to be the pivotal cell signaling pathway that mediates both inflammation and tight junction proteins expression. It is reported that activation of p38 MAPK will increase inflammatory cytokines expression and secretion, while it will decrease expression of tight junction proteins among epithelial cells [29, 30]. To further investigate its role in MBA-mediated function in gut barrier integrity, its activation was studied by the immunofluorescence method. We found that LPS significantly decreased TEER and activated p38 MAPK, while MBA administration significantly reduced the level of p-p38 MAPK and increased gut barrier integrity in Caco-2 cells.

In conclusion, we demonstrated in the present that oral administration with Cortex Mori water extract could ameliorate diabetic endotoxemia by enhancing gut integrity. By in vitro study, we demonstrated that MBA had a significant effect against LPS-induced gut epithelial barrier damage, anti-inflammation, antioxidative stress, and enhancing tight junction proteins expression involved in its protective effect, and p38MAPK participated in this process. Our present findings may supply novel idea on R&D of antidiabetic drugs from Chinese medicines.

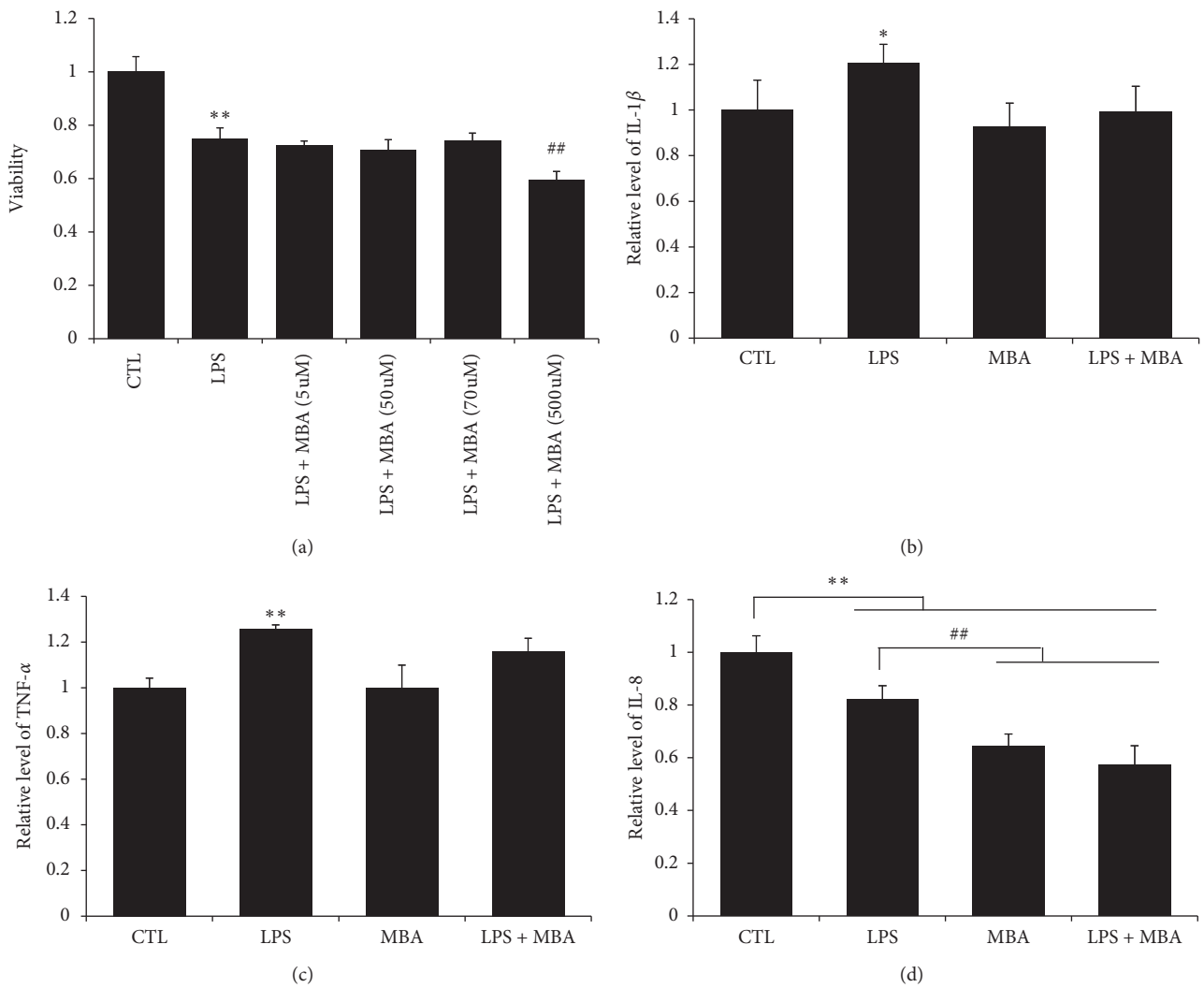

Figure 7: Mulberroside A (MBA) did not influence the viability and inflammation of Caco-2 cells induced by LPS. (a) Viability of cell was determined by the MTT method; levels of (b) IL-1β, (c) TNF-α, and (d) IL-8 were determined by kits. CTL, normal control; LPS, lipopolysaccharides group. $^{*}p < 0.05$ and $^{**}p < 0.01$ vs. CTL; $^{\#\#}p < 0.01$ vs. LPS + MBA (70 μM).

Data Availability

The datasets used to support the findings of this study are available from the corresponding author upon request.

Conflicts of Interest

The authors declare that they have no conflicts of interest.

Acknowledgments

This study was supported by the National Natural Science Foundation of China (81501271) and the Nanjing Medical Science and Technique Development Foundation, Nanjing, Jiangsu, China (QYK11142 and YKK15149).

References

[1] R. L. Smith, M. R. Soeters, R. C. I. Wüst, and R. H. Houtkooper, "Metabolic flexibility as an adaptation to energy resources and requirements in health and disease," *Endocrine Reviews*, vol. 39, no. 4, pp. 489–517, 2018.

[2] G. Hotamisligil, N. Shargill, and B. Spiegelman, "Adipose expression of tumor necrosis factor-alpha: direct role in obesity-linked insulin resistance," *Science*, vol. 259, no. 5091, pp. 87–91, 1993.

[3] P. D. Cani, J. Amar, M. A. Iglesias et al., "Metabolic endotoxemia initiates obesity and insulin resistance," *Diabetes*, vol. 56, no. 7, pp. 1761–1772, 2007.

[4] J. Qin, Y. Li, Z. Cai et al., "A metagenome-wide association study of gut microbiota in type 2 diabetes," *Nature*, vol. 490, no. 7418, pp. 55–60, 2012.

[5] M.-C. Denis, Y. Desjardins, A. Furtos et al., "Prevention of oxidative stress, inflammation and mitochondrial dysfunction in the intestine by different cranberry phenolic fractions," *Clinical Science*, vol. 128, no. 3, pp. 197–212, 2015.

[6] A. Camargo, R. Jimenez-Lucena, J. F. Alcala-Diaz et al., "Postprandial endotoxemia may influence the development of type 2 diabetes mellitus: from the CORDIOPREV study," *Clinical Nutrition*, vol. 38, no. 2, pp. 529–538, 2019.

[7] S.-Z. Qi, N. Li, Z.-D. Tuo et al., "Effects of Morus root bark extract and active constituents on blood lipids in

hyperlipidemia rats," *Journal of Ethnopharmacology*, vol. 180, pp. 54–59, 2016.

[8] K. O. Chung, B. Y. Kim, M. H. Lee et al., "In-vitro and in-vivo anti-inflammatory effect of oxyresveratrol from Morus alba L," *The Journal of Pharmacy and Pharmacology*, vol. 55, no. 12, pp. 1695–1700, 2003.

[9] H. Guo, Y. Xu, W. Huang et al., "Kuwanon G preserves LPS-induced disruption of gut epithelial barrier in vitro," *Molecules*, vol. 21, no. 11, Article ID E1597, 2016.

[10] Q. Ma, Y. Li, M. Wang et al., "Progress in metabonomics of type 2 diabetes mellitus," *Molecules*, vol. 23, no. 7, p. 1834, 2018.

[11] M. Ibi, S. Horie, S. Kyakumoto et al., "Cell-cell interactions between monocytes/macrophages and synoviocyte-like cells promote inflammatory cell infiltration mediated by augmentation of MCP-1 production in temporomandibular joint," *Bioscience Reports*, vol. 38, no. 2, 2018.

[12] J. Wang, S. S. Ghosh, and S. Ghosh, "Curcumin improves intestinal barrier function: modulation of intracellular signaling, and organization of tight junctions," *American Journal of Physiology-Cell Physiology*, vol. 312, no. 4, pp. C438–C445, 2017.

[13] E. Burlet and S. K. Jain, "Manganese supplementation increases adiponectin and lowers ICAM-1 and creatinine blood levels in Zucker type 2 diabetic rats, and downregulates ICAM-1 by upregulating adiponectin multimerization protein (DsbA-L) in endothelial cells," *Molecular and Cellular Biochemistry*, vol. 429, no. 1-2, pp. 1–10, 2017.

[14] N. J. Ronaghan, J. Shang, V. Iablokov et al., "The serine protease-mediated increase in intestinal epithelial barrier function is dependent on occludin and requires an intact tight junction," *American Journal of Physiology-Gastrointestinal and Liver Physiology*, vol. 311, no. 3, pp. G466–G479, 2016.

[15] J. M. G. Gomes, J. D. A. Costa, and R. D. C. G. Alfenas, "Metabolic endotoxemia and diabetes mellitus: a systematic review," *Metabolism*, vol. 68, pp. 133–144, 2017.

[16] P. D. Cani, "Human gut microbiome: hopes, threats and promises," *Gut*, vol. 67, no. 9, pp. 1716–1725, 2018.

[17] C. Guo, R. Li, N. Zheng, L. Xu, T. Liang, and Q. He, "Anti-diabetic effect of ramulus mori polysaccharides, isolated from Morus alba L., on STZ-diabetic mice through blocking inflammatory response and attenuating oxidative stress," *International Immunopharmacology*, vol. 16, no. 1, pp. 93–99, 2013.

[18] W. Yu, H. Chen, Z. Xiang, and N. He, "Preparation of polysaccharides from ramulus mori, and their antioxidant, anti-inflammatory and antibacterial activities," *Molecules*, vol. 24, no. 5, p. 856, 2019.

[19] R. Singh, S. Chandrashekharappa, S. R. Bodduluri et al., "Enhancement of the gut barrier integrity by a microbial metabolite through the Nrf2 pathway," *Nature Communications*, vol. 10, no. 1, p. 89, 2019.

[20] D. Song, X. Zong, H. Zhang et al., "Antimicrobial peptide Cathelicidin-BF prevents intestinal barrier dysfunction in a mouse model of endotoxemia," *International Immunopharmacology*, vol. 25, no. 1, pp. 141–147, 2015.

[21] F. Sanchez-Muñoz, A. Dominguez-Lopez, and J. K. Yamamoto-Furusho, "Role of cytokines in inflammatory bowel disease," *World Journal of Gastroenterology*, vol. 14, no. 27, pp. 4280–4288, 2008.

[22] S. Ménard, N. Cerf-Bensussan, and M. Heyman, "Multiple facets of intestinal permeability and epithelial handling of dietary antigens," *Mucosal Immunology*, vol. 3, no. 3, pp. 247–259, 2010.

[23] K. R. Groschwitz and S. P. Hogan, "Intestinal barrier function: molecular regulation and disease pathogenesis," *Journal of Allergy and Clinical Immunology*, vol. 124, no. 1, pp. 3–20, 2009.

[24] J. G. Daft and R. G. Lorenz, "Role of the gastrointestinal ecosystem in the development of type 1 diabetes," *Pediatric Diabetes*, vol. 16, no. 6, pp. 407–418, 2015.

[25] J. R. Turner, "Intestinal mucosal barrier function in health and disease," *Nature Reviews Immunology*, vol. 9, no. 11, pp. 799–809, 2009.

[26] M. González-González, C. Díaz-Zepeda, J. Eyzaguirre-Velásquez, C. González-Arancibia, J. A. Bravo, and M. Julio-Pieper, "Investigating gut permeability in animal models of disease," *Front Physiol*, vol. 9, p. 1962, 2018.

[27] K. Shi, F. Wang, H. Jiang et al., "Gut bacterial translocation may aggravate microinflammation in hemodialysis patients," *Digestive Diseases and Sciences*, vol. 59, no. 9, pp. 2109–2117, 2014.

[28] H. A. Koistinen, A. V. Chibalin, and J. R. Zierath, "Aberrant p38 mitogen-activated protein kinase signalling in skeletal muscle from Type 2 diabetic patients," *Diabetologia*, vol. 46, no. 10, pp. 1324–1328, 2003.

[29] T.-M. Ma, N. Xu, X. D. Ma, Z. H. Bai, X. Tao, and H. C. Yan, "Moxibustion regulates inflammatory mediators and colonic mucosal barrier in ulcerative colitis rats," *World Journal of Gastroenterology*, vol. 22, no. 8, pp. 2566–2575, 2016.

[30] Y. Ni, T. Teng, R. Li, A. Simonyi, G. Y. Sun, and J. C. Lee, "TNFα alters occludin and cerebral endothelial permeability: role of p38MAPK," *PLoS One*, vol. 12, no. 2, Article ID e0170346, 2017.

Hindawi
Evidence-Based Complementary and Alternative Medicine
Volume 2021, Article ID 6675567, 9 pages
https://doi.org/10.1155/2021/6675567

Research Article

Total flavonoids of *Astragalus* Ameliorated Bile Acid Metabolism Dysfunction in Diabetes Mellitus

Zhe Wang,[1] Xu-Ling Li,[1] Kin-Fong Hong,[1] Ting-Ting Zhao,[1] Rui-Xue Dong,[2] Wei-Ming Wang,[1] Yun-Tong Li,[1] Gui-Lin Zhang,[1] Jing Lin,[3] Ding-Kun Gui,[4] and You-Hua Xu[1,2,5]

[1]*Faculty of Chinese Medicine, State Key Laboratory of Quality Research in Chinese Medicine, Macau University of Science and Technology, Taipa, Macao, China*
[2]*School of Pharmacy, State Key Laboratory of Quality Research in Chinese Medicine, Macau University of Science and Technology, Taipa, Macao, China*
[3]*Guangdong Provincial Hospital of Chinese Medicine-Zhuhai Hospital, Zhuhai, Guangdong, China*
[4]*Department of Nephrology, Shanghai Jiao Tong University Affiliated to Sixth People's Hospital, Shanghai 200233, China*
[5]*Department of Endocrinology, Zhuhai Hospital of Integrated Traditional Chinese and Western Medicine, Zhuhai, China*

Correspondence should be addressed to Ding-Kun Gui; dick7837@163.com and You-Hua Xu; yhxu@must.edu.mo

Received 29 December 2020; Revised 27 March 2021; Accepted 2 April 2021; Published 13 April 2021

Academic Editor: Daniel Dias Rufino Arcanjo

Astragalus Radix is one of the common traditional Chinese medicines used to treat diabetes. However, the underlying mechanism is not fully understood. Flavones are a class of active components that have been reported to exert various activities. Existing evidence suggests that flavones from *Astragalus Radix* may be pivotal in modulating progression of diabetes. In this study, total flavones from *Astragalus Radix* (TFA) were studied to observe its effects on metabolism of bile acids both *in vivo* and *in vitro*. C57BL/6J mice were treated with STZ and high-fat feeding to construct diabetic model, and HepG2 cell line was applied to investigate the influence of TFA on liver cells. We found a serious disturbance of bile acids and lipid metabolism in diabetic mice, and oral administration or cell incubation with TFA significantly reduced the production of total cholesterol (TCHO), total triglyceride, glutamic oxalacetic transaminase (AST), glutamic-pyruvic transaminase (ALT), and low-density lipoprotein (LDL-C), while it increased the level of high-density lipoprotein (HDL-C). The expression of glucose transporter 2 (GLUT2) and cholesterol 7α-hydroxylase (CYP7A1) was significantly upregulated on TFA treatment, and FXR and TGR5 play pivotal role in modulating bile acid and lipid metabolism. This study supplied a novel understanding towards the mechanism of *Astragalus Radix* on controlling diabetes.

1. Introduction

Although a giant leap has been made in the prevention and treatment of diabetes mellitus (DM), the number of patients continues to rise. The International Diabetes Federation estimates that the DM patients will increase to 700 million by 2045 [1].

Studies have proved that bile acids are closely related to DM and glycolipid metabolism [2]. Liver is the main organ that secretes bile acids, and hepatoenteral circulation of bile acids plays an important role in maintaining the homeostasis of glycolipids in the body [3, 4]. It has been well demonstrated that metabolic changes of bile acid may induce glycolipidemia via FXR and TGR5 pathways [5, 6]. Alternatively, long-lasting hyperglycemia will influence liver function and secretion of bile acids [7]. Therefore, modulating metabolism of bile acids is believed to be a potential target on preventing DM.

Studies concerning effects of *Astragalus Radix* (*Huang Qi* in Chinese) on DM are abundant. The active components of *Astragalus Radix* mainly include polysaccharide, astragalosides, and flavones [8, 9]. Previously, we

have reported that flavones calycosin and calycosin-7-O-β-D-glucopyranoside could ameliorate vascular endothelial cell dysfunction under diabetic settings [10–12]; moreover, calycosin also possessed protective effects on hepatocyte function [13]. Besides that, other research groups have also reported that total flavonoids of *Astragalus Radix* (TFA) has anti-inflammatory effects [14, 15]. Recently, it was reported that *Astragalus Radix* decoction has a regulatory effect on bile acid [16]. However, the role and mechanism of TFA in the metabolism of bile acids still need to be elucidated. For this aim, we designed this study.

2. Materials and Methods

2.1. Materials. The TFA was provided by Chengdu Pusi Biotechnology, Co., Ltd. (Chengdu, Sichuan, China). Metformin was purchased from GBCBIO technology (Guangzhou, Guangdong, China). Insulin was provided by Yuanye Bio-Technology Co., Ltd. (Shanghai, China). Lipopolysaccharide (LPS) was purchased from Sigma (St. Louis, MO, USA). ELISA kits for measuring total bile acid (TBA), total cholesterol (TCHO), total triglyceride (TG), glutamic oxalacetic transaminase (AST), glutamic-pyruvic transaminase (ALT), high-density lipoprotein (HDL-C), and low-density lipoprotein (HDL-C) were purchased from Jiancheng (Nanjing, Jiangsu, China). Primary antibodies for apical sodium-dependent bile acid transporter (ASBT) were purchased from PL Laboratories (Richmond, Canada). CYP7A1 and FXR were purchased from Santa Cruz (Dallas, TX, USA). TGR5 was provided by Abcam (Cambridge, MA, USA). GLUT2 was derived from Bioss (Beijing, China). Other reagents are from commercial sources.

2.2. Animals. The NIH (U.S. National Institutes of Health publication no. 85–23, revised 1996) Guide for the Care and Use of Laboratory Animals was followed, and the study was approved by Macau University of Science and Technology. C57BL/6J mice were provided from Guangdong Medical Laboratory Animal Center. All mice were housed in an animal house with a 12 h daylight cycle at 25°C. Before drug intervention, all mice were fed adaptively for 7 days. The animals were fed a high-fat diet (15% protein, 43% carbohydrate, 42% fat; obtained from Guangdong Medical Experimental Animal Center) for 8 weeks and then treated with streptozotocin (50 mg/kg per day) for 4 days to make the model. The animals were randomly divided into groups as follows: (1) normal control group ($n = 6$, animals were fed normal chow); (2) DM model group ($n = 6$), where animals were given streptozotocin; (3) intervention group where DM animal models were orally treated with low TFA (L-TFA, 5 mg/kg per day, $n = 6$), medium TFA (M-TFA, 25 mg/kg per day, $n = 6$), and high TFA (H-TFA, 50 mg/kg per day, $n = 6$); (4) positive control group where animals were orally administrated metformin (Met, 0.15 g/kg per day, $n = 6$). At the end of the experiment, liver was collected for histological or biochemical study.

2.3. Cell Lines and Cell Culture. HepG2 cells were derived from American Type Culture Collection (Manassas, VA, USA). All cells were cultured using MEM medium (Gibco) supplemented with 10% fetal bovine serum, 100 U/mL penicillin, and 100 mg/mL streptomycin at 37°C in 5% CO_2 incubator.

2.4. MTT Assay for Cell Viability. The HepG2 cells were inoculated into a 96-well cell culture plate with 1×10^5 cells per well. Different concentrations of TFA (0–40 μg/mL) were added to the cells. After 24 h, MTT (3-(4,5-dimethylthiazol-2-yl)-2,5-diphenyltetrazolium bromide)) (0.5 mg/ml) was added to the culture system and cultured in dark for 4 h. Thyroid crystal was dissolved with 10% SDS (sodium dodecyl sulfate). Cell activity was analyzed at 595 nm using a plate reader (Molecular Devices, USA).

2.5. Histological Analysis. Liver slices were observed for hematoxylin-eosin (H&E) and periodic acid-schiff (PAS) staining. The liver slices were fixed within 4% paraformaldehyde over 24 h; after being paraffinized, sections (0.4 μm) were stained with H&E or PAS staining solution according to the standard procedure. Finally, the slices were covered with coverslip and imaged using the Leica DM2500 Fluorescence Microscope Imaging System (Leica, Germany).

2.6. Western Blot Analysis. Liver tissue was lysed in 1 × RIPA buffer with a protease inhibitor cocktail and phosphatase inhibitor. Total protein was quantified by using the Bio-Rad Protein Assay (USA). Samples were separated by 10% SDS-polyacrylamide gels and then transferred to polyvinylidene difluoride (PVDF) membranes (EMD Millipore, MA, USA). After blocking with 5% BSA in TBST buffer, the PVDF membrane was incubated with primary antibodies including anti-GAPDH antibody (1 : 1000), anti-CYP7A1 antibody (1 : 800), anti-FXR antibody (1 : 800), anti-TGR5 antibody (1 : 1000), or anti-GLUT2 antibody (1 : 1000) overnight at 4°C. After that, the membranes were washed with TBST buffer for three times and then further incubated with secondary antibody (Invitrogen, USA) for 1 h at room temperature. Protein detection was carried out by the Odyssey CLx Imaging System (Li-COR Biosciences, Belfast, ME, USA).

2.7. Immunofluorescence Assay. Immunofluorescence assay was performed as previously described [17]. HepG2 cells in the exponential phase were seeded on glass slides, normal MEM was used in normal group, Ins + LPS (insulin, 10^{-7} mol/L; LPS: 1 μg/ml) was added in DM group, Ins + LPS + TFA was added in TFA group, and metformin (Met, 0.5 mM) was added in positive control group [18, 19]. Twenty-four hours later, cells were treated with 4% paraformaldehyde for 30 min. After being blocked with 5% BSA, cells were incubated with antibodies including anti-GLUT2 (1 : 200), anti-FXR (1 : 200), anti-CYP7A1 (1 : 200), anti-TGR5 (1 : 200), or anti-ASBT (1 : 200) at 4°C overnight and then were further incubated with FITC- or CY3 -conjugated secondary antibody. The nucleus was stained with DAPI.

Finally, the cells were observed under a confocal laser scanning microscopy (Leica TCS SP8, Germany), and the fluorescent density was determined by Image-J software.

2.8. Statistical Analysis. Figure preparation and statistical analysis were carried out using GraphPad Prism 7.00 software (GraphPad Software Inc., CA, USA). Fluorescent images were processed with open-source software Image-J. All data were obtained from more than three independent repeated experiments. All data that fit into the normal distribution were expressed as mean ± standard deviation (SD), and the difference among groups was analyzed by one-way ANOVA method. Significance was accepted at $p < 0.05$ or less.

3. Results

3.1. TFA Ameliorated Liver Injury and Regulated Blood Glucose in Diabetic Mice. The level of fasting blood glucose (FBG) is a sensitive parameter that reflects control of diabetes. As shown in Figure 1(e), TFA administration significantly decreased FBG in diabetic mice, suggesting definite effect of TFA on ameliorating progression of diabetes.

The liver plays a pivotal role in modulating the level of blood glucose. The H&E staining and PAS staining images (Figures 1(a)–1(d)) show that, compared with the normal group, steatosis was obviously observed in T2DM mice; moreover, the content of glycogen in hepatocytes was significantly decreased as observed by PAS staining (Figures 1(c) and 1(d)). Alternatively, TFA preserves lobular structure, maintains cellular morphology, and improves intracellular glycogen levels. The liver index was also reduced in mice treated with TFA (Figure 1(f)). These results suggest that TFA administration in T2DM mice preserved the liver function.

3.2. Effect of TFA on Serum Lipid Profile. To investigate the influence of TFA on liver function, serum lipid profile is measured. As shown in Figures 2(a)–2(c) and Figures 2(e)–2(g), serum levels of TBA, TG, TC, LDL-C, ALT, and AST in diabetic mice were significantly increased compared with normal control, while level of HDL-C was decreased in diabetic mice, but no statistical significance was found compared with normal control (Figure 2(d)). Expectedly, administration with TFA significantly ameliorated lipid metabolism damage and restored liver function compared with diabetic mice. The most significant effect was observed in medium TFA (M-TFA) group. These results indicated that TFA can not only reduce the cholesterol level in diabetic mice but also reverse the elevated serum bile acid level in diabetic mice.

3.3. TFA Improved Glucose and Lipid Metabolism in the Liver of Diabetic Mice. Existing studies have found that proteins that regulate lipid and glucose metabolism are significantly inhibited under diabetic settings, such as glucose transporter 2 (GLUT2), cholesterol 7 alpha-hydroxylase (CYP7A1), G-protein-coupled bile receptor (TGR5), and Farnesyl X receptor (FXR) [20, 21]. To study the mechanism of TFA on bile acid metabolism, their protein expression was determined by western blot. As shown in Figure 3, TFA significantly increased the expressions of GLUT2 (Figure 3(b)), CYP7A1 (Figure 3(c)), and TGR5 (Figure 3(e)) compared with those in the diabetic model group; FXR was also increased by administration of TFA, but no statistical significance was observed (Figure 3(d)).

3.4. TFA Improves Lipid Metabolism in HepG2 Cells. To verify the aforementioned findings, effects of TFA on HepG2 cells were further studied. MTT method was used to preliminarily detect the influence of TFA on cell viability. As shown in Figure 4(a), low concentration of TFA slightly increased the viability of HepG2 cells, but cell viability toxicity was observed once the concentration exceeds 10 μg/ml; therefore, we applied "10 μg/ml" in the following study.

Lipid metabolism of HepG2 cell was determined by kits. In line with findings in animals, TG, TCHO, AST, ALT, and LDL-C were significantly increased and HDL-C was decreased in diabetic mice, while TFA incubation significantly increased HDL-C and decreased other parameters (Figures 4(b)–4(g)).

3.5. TFA Modulated Expression of GLUT2 and Proteins Regulating Cholic Acid Metabolism in HepG2 Cells. Glucose transporters play pivotal roles in mediating hepatocyte glucose uptake. By immunofluorescence assay, we found the expression of GLUT2 was significantly decreased in DM model while TFA inhibited this decrement (Figures 5(a) and 5(g)).

CYP7A1 is an enzyme that plays an important role in mediating cholesterol metabolism. In the present study, we observed that CYP7A1 was also located on HepG2 cell membranes (Figure 5(b)); moreover, DM significantly inhibited its expression ($p < 0.01$ vs. normal), and this reduction was reversed by TFA administration ($p < 0.01$ vs. DM) (Figure 5(f)).

The apical sodium-dependent bile acid transporter (ASBT) in small intestinal epithelial cells is reabsorbed into ileum cells [22], and FXR and TGR5 play key roles in cholesterol balance, fat absorption, and bile acid synthesis. In this study, we found that the reduced expression of ASBT, FXR, and TGR5 in diabetic model was significantly reversed by addition of TFA (Figures 5(c)–5(e) and 5(h)–5(j)).

4. Discussion

Bile acids are synthesized by hepatocytes and play a pivotal role in the digestion and absorption of lipids [23]. Recent findings have indicated its role in modulating glucose metabolism and controlling progression of diabetes. *Astragalus Radix* is a common Chinese medicine used to treat diabetes [26], and a report has demonstrated that *Astragalus Radix* can regulate blood lipid and blood glucose levels in HFD-fed mice [27]. Previously, we found active

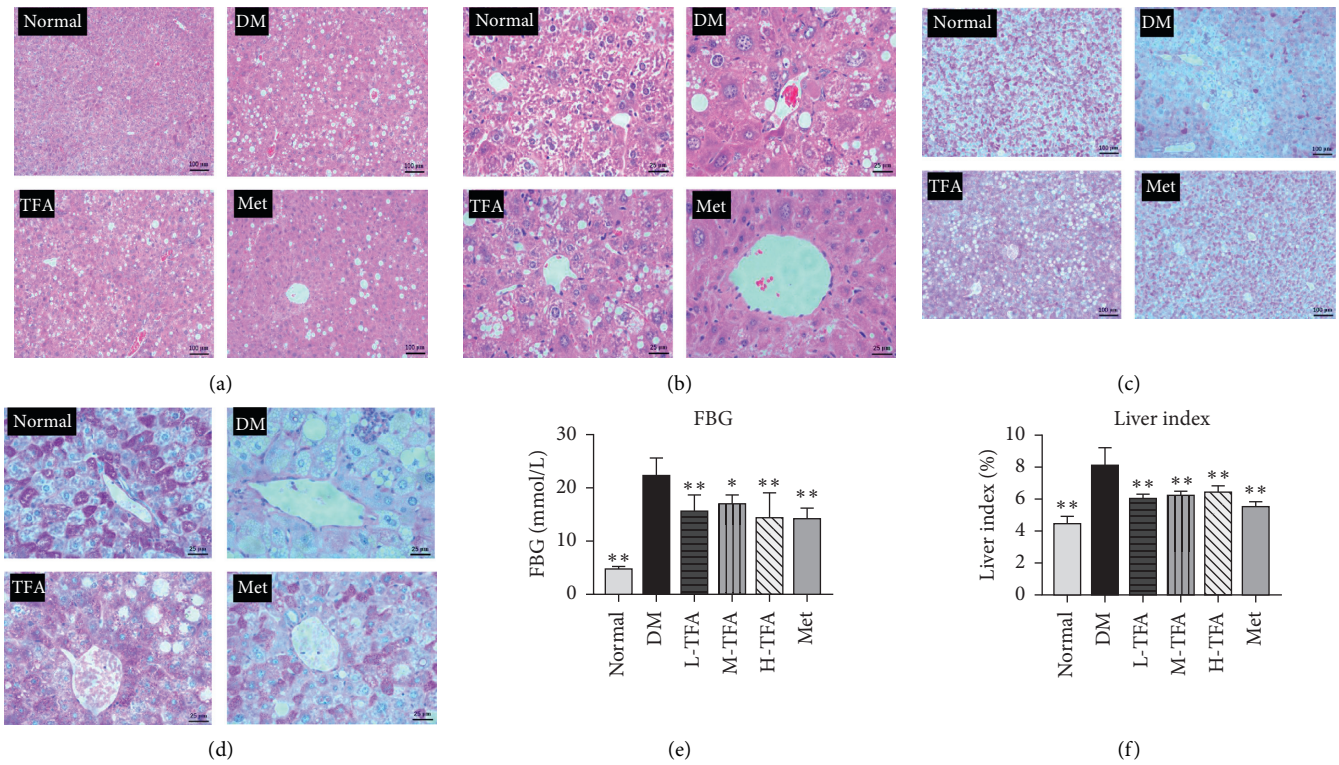

Figure 1: Effects of total *Astragalus* flavones (TFA) on blood glucose and liver histology in diabetic mice. H&E staining of liver (magnification: (a) 100x and (b) 400x). PAS staining of liver (magnification: (c) 100x and (d) 400x). (e) Fasting blood glucose (FBG) test. (f) Liver index; liver index = (liver weight/body weight) %. ($n = 6$). Met: metformin. $^{*}p < 0.05$; $^{**}p < 0.01$ vs. DM group.

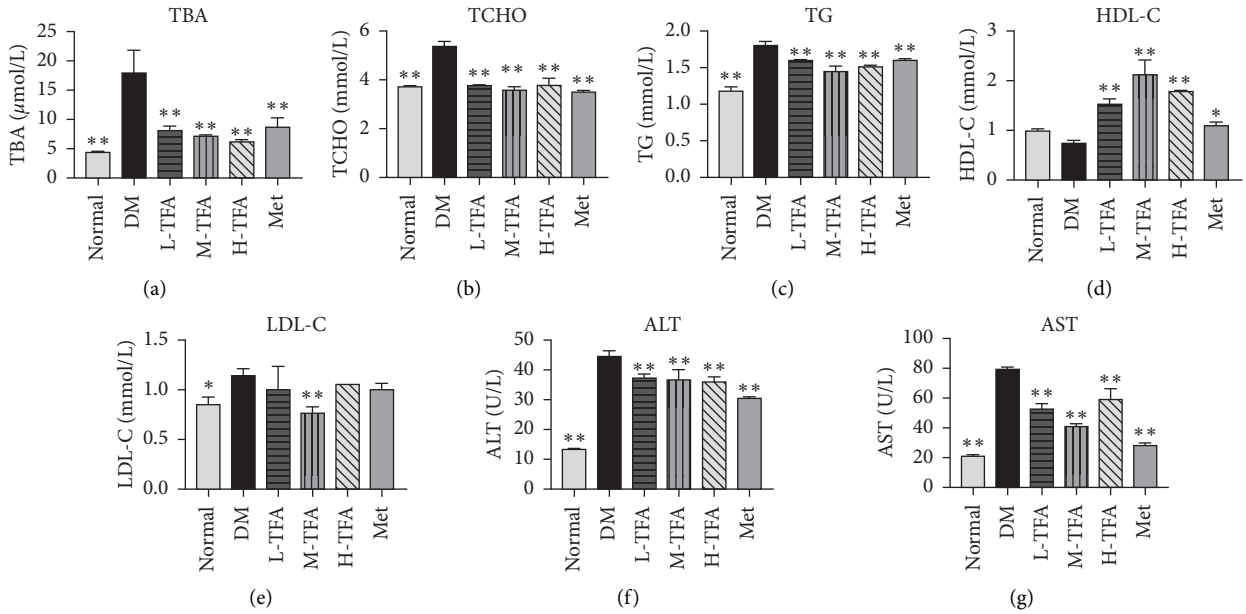

Figure 2: Total *Astragalus* flavones (TFA) improved lipid metabolism in mice. Serum levels of (a) total bile acid (TBA), (b) total cholesterol (TCHO), (c) total triglyceride (TG), (d) high-density lipoprotein (HDL-C), (e) low-density lipoprotein (LDL-C), (f) glutamic-pyruvic transaminase (ALT), and (g) glutamic oxalacetic transaminase (AST) were determined by kits ($n = 6$). Met: metformin. $^{*}p < 0.05$; $^{**}p < 0.01$ vs. DM group.

flavonoid components of *Astragalus Radix* have protective effects against diabetic damage *in vitro* [10–13], but its influence on bile acid metabolism was not studied. In the present study, we found that TFA could modulate metabolism of bile acid both *in vivo* and *in vitro*, and the potential mechanism was also studied.

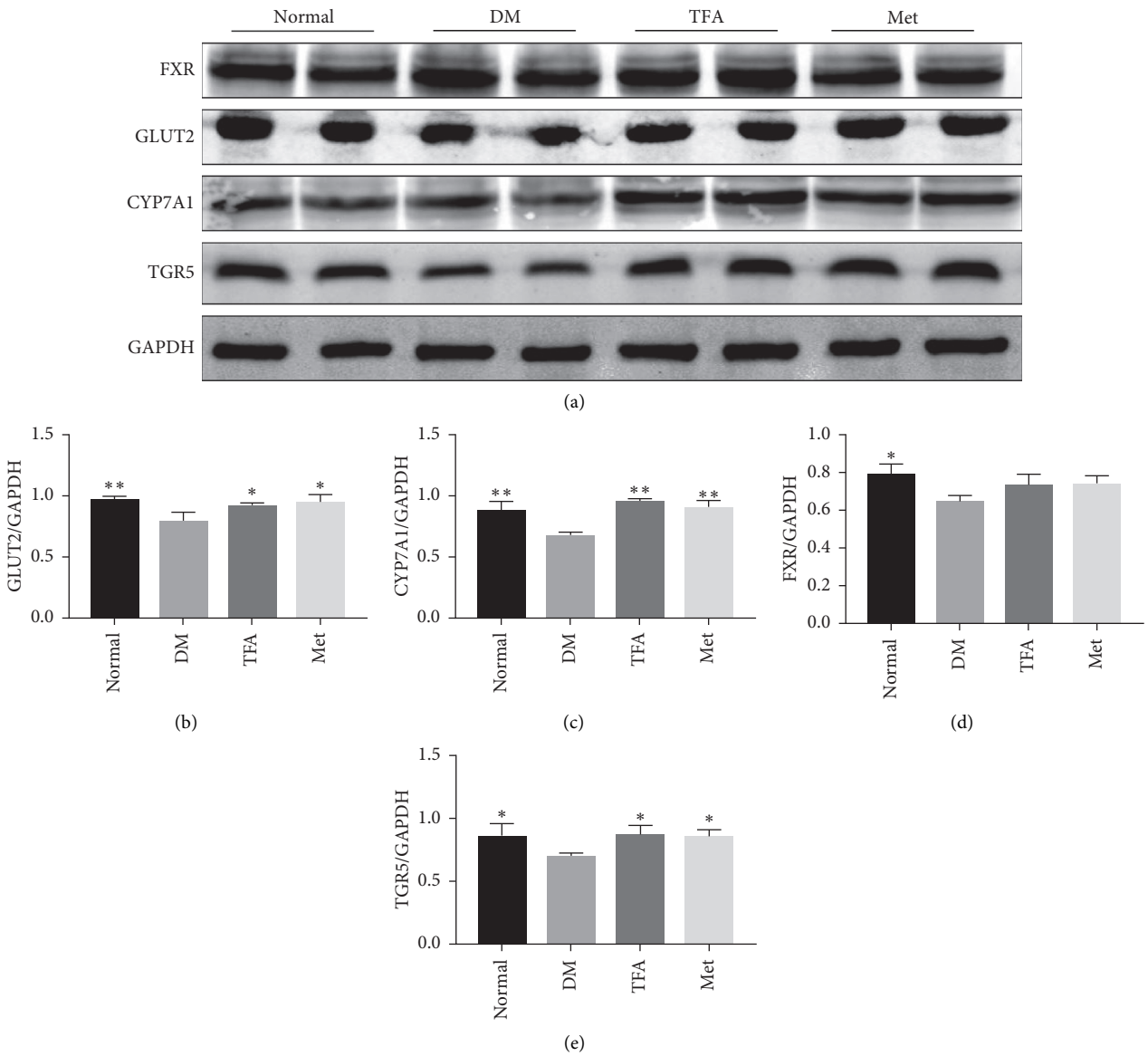

Figure 3: TFA increased the expression of proteins related to glucose and lipid metabolism under diabetic settings. (a) WB detection for proteins expression. Quantitative analysis of (b) GLUT2, (c) CYP7A1, (d) FXR, and (e) TGR5. Glyceraldehyde-3-phosphate dehydrogenase (GAPDH) was used as an internal control ($n = 3$). $^{*}p < 0.05$; $^{**}p < 0.01$ vs. DM group.

The liver plays a pivotal role in modulating metabolism. With the increasing understanding of the mechanism of T2DM, the role of bile acid in disease progression has attracted scholars' interest. Within the organism, bile acids are recollected in the intestine by ASBT and transported back to the liver in a process known as the hepatointestinal circulation of bile acids. Several types of bile acid receptors have been found, one of which is the nuclear receptor, the representative of which is FXR [24]; the other group is g-protein-coupled membrane receptors, of which the representative is TGR5 [25]. Therefore, expression and activation of FXR and TGR5 will significantly influence metabolism of bile acids.

The role of bile acids in progression of diabetes has been increasingly recognized. It is found that activation of TGR5 can promote the secretion of insulin GLP-1, improve the function of pancreatic tissues, promote insulin sensitivity [28], and inhibit inflammation [29]. A rise in cholic acid within the body can activate TGR5, and binding between bile acid and TGR5 will further activate adenylate cyclase pathway and increase AMP content [30]. FXR receptor was the first bile acid receptor discovered. It was reported that cholesterol within the liver is digested by CYP7A1 to become bile acid, and the latter will be reabsorbed by ASBT in the ileum. Binding and activation of FXR-FGF19 will further inhibit the activity of CYP7A1 by activating the MAP kinase pathway, thereby inhibiting bile acid synthesis [31, 32]. Therefore, TGR5 and FXR are pivotal in modulating both genesis and metabolism of bile acid. In the present study, we found that the expressions of CYP7A1, ASBT, TGR5, and

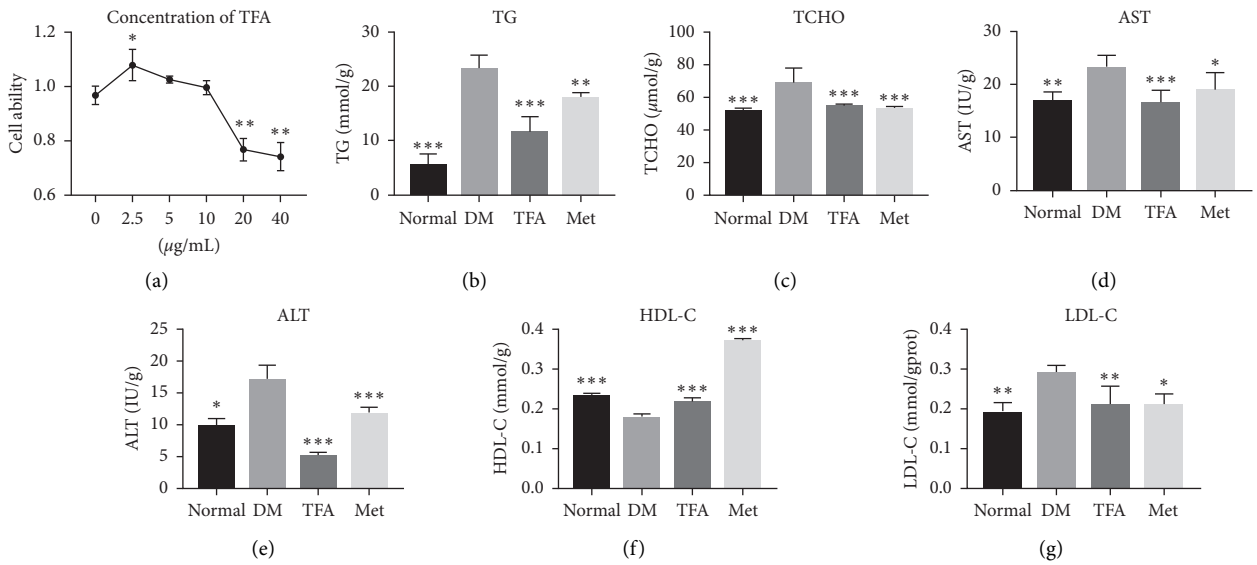

FIGURE 4: Total *Astragalus* flavones (TFA) regulated lipid metabolism in HepG2 cells. (a) MTT assay was used to evaluate the influence of TFA on cell viability. The effects of TFA on the biochemical indexes including (b) total triglyceride (TG), (c) total cholesterol (TCHO), (d) glutamic oxalacetic transaminase (AST), (e) glutamic-pyruvic transaminase (ALT), (f) high-density lipoprotein (HDL-C), and (g) low-density lipoprotein (LDL-C) were detected by the kits according to the manufacturers' protocol ($n = 6$). Met: metformin. $*p < 0.05$; $**p < 0.01$; $***p < 0.001$ vs. DM group.

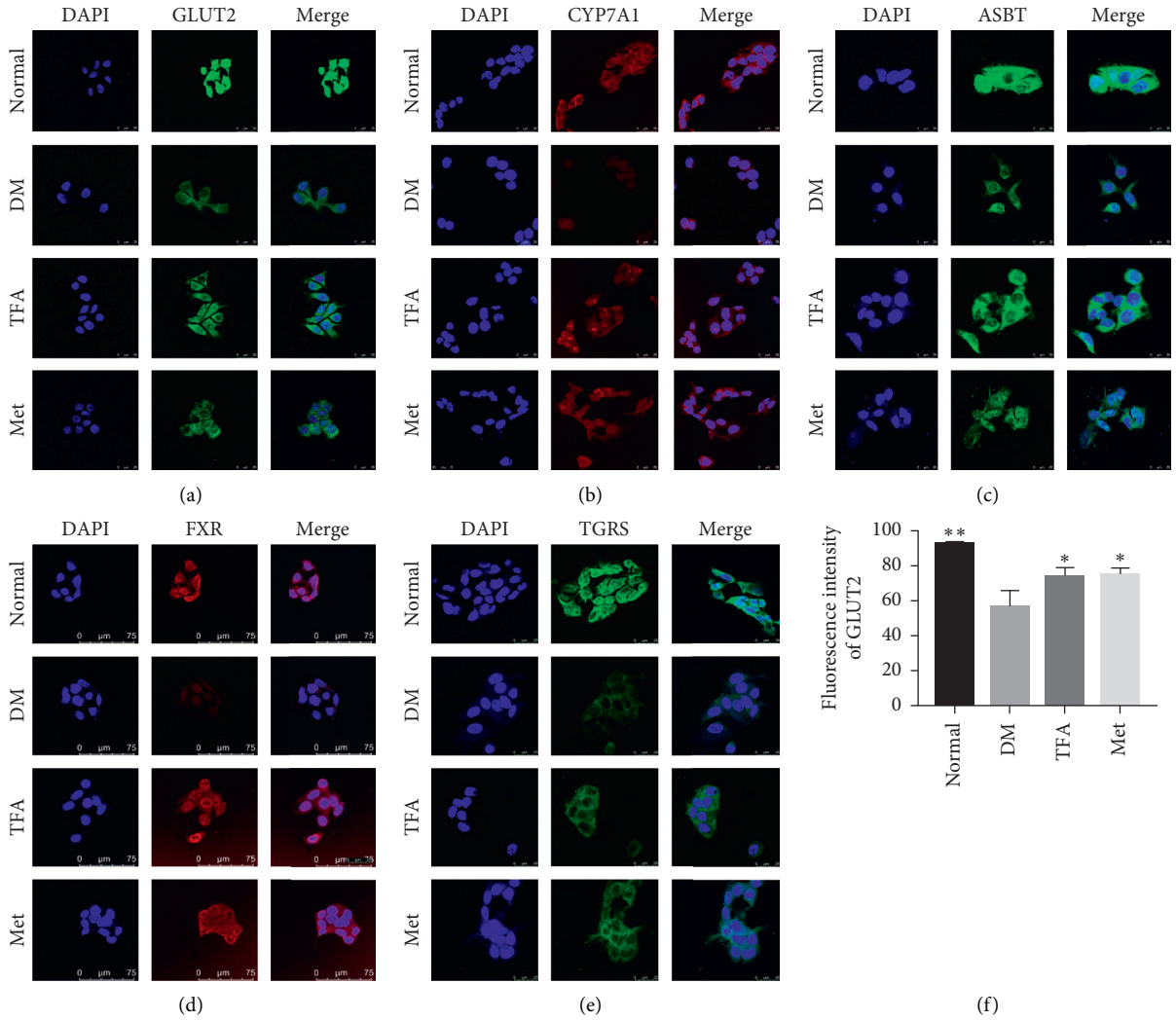

FIGURE 5: Continued.

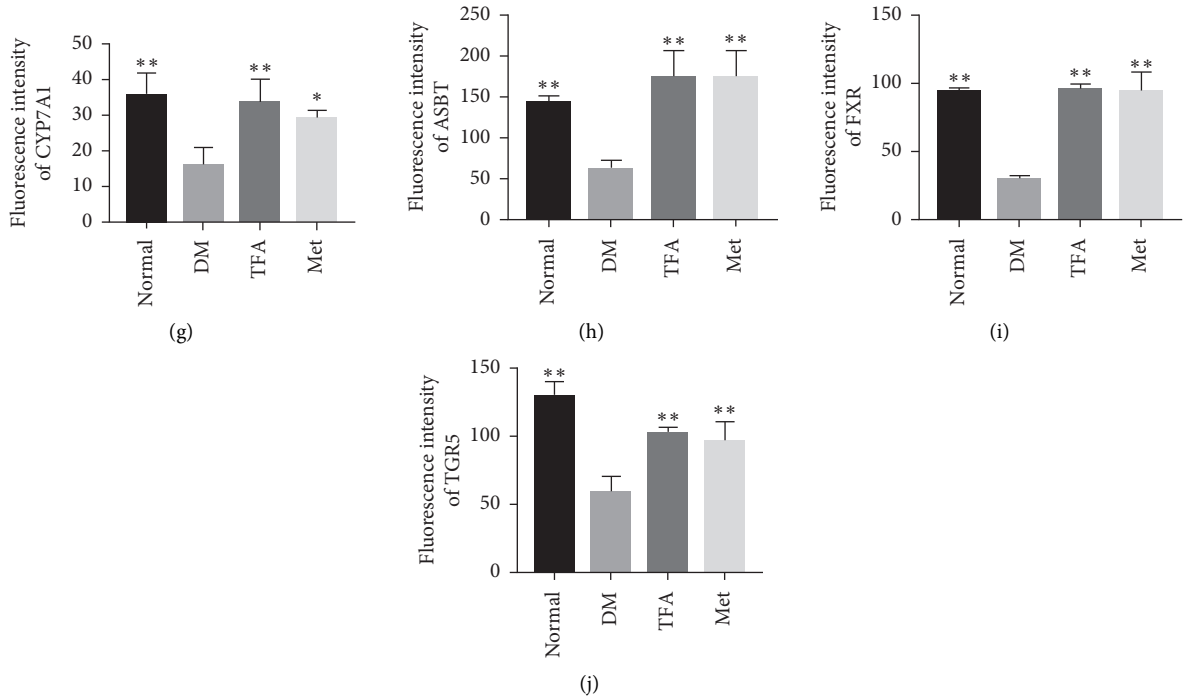

Figure 5: Effects of total *Astragalus* flavones (TFA) on lipid metabolism related proteins in HepG2 cells. Expressions of (a) GLUT2, (b) CYP7A1, (c) ASBT, (d) FXR, and (e) TGR5 were determined by immunofluorescence assay under laser scanning confocal microscope (magnification: 800x), and relative fluorescence intensities of (f) GLUT2, (g) CYP7A1, (h) ASBT, (i) FXR, and (j) TGR5 were determined by Image-J software. DAPI (4′,6-diamidino-2-phenylindole) was used to stain the nucleus ($n = 3$). Met: metformin. $*p < 0.05$; $**p < 0.01$ vs. DM group.

FXR were significantly reduced under diabetic settings, suggesting bile acid was inhibited in the whole process of its metabolism, and administration with TFA significantly improves its generation and metabolism.

The negative feedback of bile acid hepatointestinal circulation is mediated by small molecule heterodimer partner (SHP), which is the downstream target of FXR [34]. It was found that the activation of FXR will induce SHP-inhibited expression of CYP7A1 and ASBT in liver cells [35, 36]. Binding between SHP and transcription factor LRH-1 will regulate the expression of CYP7A1 in that LRH-1 inhibition will result in the decreased expression of CYP7A1 [37]. Studies have demonstrated that activation of FXR can promote lipoprotein metabolism [38] and reduce plasma triglyceride and cholesterol levels [39]. Moreover, the agonist of FXR was also shown to inhibit hepatic gluconeogenic genes such as glucose-6-phosphatase and increase liver glycogen synthesis [40]. Our present findings are in line with previous reports that state that a serious disturbance of lipid and bile acid metabolism was observed in diabetic mice, and administration with TFA significantly increased FXR expression and restored lipid metabolism. It has been well recognized that elevated TCHO, TG, AST, ALT, and LDL-C levels and decreased HDL-C levels are manifestations of hepatocyte injury [41, 42]. Our present findings obviously suggest that TFA have protective effects against progression of diabetes.

In conclusion, we found in the present study that TFA ameliorated lipid and bile acid metabolism under diabetic settings, and regulation of FXR and TGR5 should contribute to its effects. Our present findings provide a new understanding on mechanism of *Astragalus Radix* against progression of diabetes.

Data Availability

The data used to support the results of this study are included within the manuscript and may be obtained from the corresponding author upon reasonable request.

Conflicts of Interest

All the authors declare that they have no conflicts of interest.

Acknowledgments

This work was supported by the Science and Technology Development Fund of Macau, Macau SAR, China (0006/2019/A).

References

[1] P. Saeedi, I. Petersohn, P. Salpea et al., "Global and regional diabetes prevalence estimates for 2019 and projections for 2030 and 2045: results from the international diabetes federation diabetes atlas, 9th edition," *Diabetes Research and Clinical Practice*, vol. 157, Article ID 107843, 2019.

[2] A. Nguyen and B. Bouscarel, "Bile acids and signal transduction: role in glucose homeostasis," *Cellular Signalling*, vol. 20, no. 12, pp. 2180–2197, 2008.

[3] A. L. Ticho, P. Malhotra, P. K. Dudeja, R. K. Gill, and W. A. Alrefai, "Intestinal absorption of bile acids in health and disease," *Comprehensive Physiology*, vol. 10, pp. 21–56, 2019.

[4] J. Y. L. Chiang, "Bile acid metabolism and signaling," *Comprehensive Physiology*, vol. 3, pp. 1191–1212, 2013.

[5] B. Kong, M. Zhang, M. Huang et al., "FXR deficiency alters bile acid pool composition and exacerbates chronic alcohol induced liver injury," *Digestive and Liver Disease*, vol. 51, no. 4, pp. 570–576, 2019.

[6] Y. J. Y. Wan and L. Sheng, "Regulation of bile acid receptor activity," *Liver Research*, vol. 2, no. 4, pp. 180–185, 2018.

[7] Y. Wu, A. Zhou, L. Tang, Y. Lei, B. Tang, and L. Zhang, "Bile acids: key regulators and novel treatment targets for type 2 diabetes," *Journal of Diabetes Research*, vol. 2020, Article ID 6138438, 11 pages, 2020.

[8] X. Wu, X. Li, W. Wang et al., "Integrated metabolomics and transcriptomics study of traditional herb Astragalus membranaceus Bge. var. mongolicus (Bge.) Hsiao reveals global metabolic profile and novel phytochemical ingredients," *BMC Genomics*, vol. 21, no. S10, p. 697, 2020.

[9] X. Li, L. Qu, Y. Dong et al., "A review of recent research progress on the astragalus genus," *Molecules*, vol. 19, no. 11, pp. 18850–18880, 2014.

[10] Y. Xu, L. Feng, S. Wang et al., "Phytoestrogen calycosin-7-O-β-D-glucopyranoside ameliorates advanced glycation end products-induced HUVEC damage," *Journal of Cellular Biochemistry*, vol. 112, no. 10, pp. 2953–2965, 2011.

[11] Y. Xu, L. Feng, S. Wang et al., "Calycosin protects HUVECs from advanced glycation end products-induced macrophage infiltration," *Journal of Ethnopharmacology*, vol. 137, no. 1, pp. 359–370, 2011.

[12] Y. H. Xu, J. Xiong, S. S. Wang, D. Tang, R. S. Wang, and Q. Zhu, "Calycosin entered HUVECs and ameliorated AGEs-promoted cell apoptosis via the Bcl-2 pathway," *Journal of Natural Medicines*, vol. 68, no. 1, pp. 163–172, 2014.

[13] Y. Xu, J. Xiong, Y. Zhao et al., "Calycosin rebalances advanced glycation end products-induced glucose uptake dysfunction of hepatocyte in vitro," *The American Journal of Chinese Medicine*, vol. 43, no. 6, pp. 1191–1210, 2015.

[14] V. M. Bratkov, A. M. Shkondrov, P. K. Zdraveva, and I. N. Krasteva, "Flavonoids from the genus Astragalus: phytochemistry and biological activity," *Pharmacognosy Reviews*, vol. 10, pp. 11–32, 2016.

[15] Z. Guo, H. Y. Xu, L. Xu, S. S. Wang, and X. M. Zhang, "In vivo and in vitro immunomodulatory and anti-inflammatory effects of total flavonoids of Astragalus," *Africa Journal of Traditional Complementary and Alternative Medicine*, vol. 13, no. 4, pp. 60–73, 2016.

[16] J. S. Wu, Y. F. Li, Y. Y. Li et al., "Huangqi decoction alleviates alpha-naphthylisothiocyanate induced intrahepatic cholestasis by reversing disordered bile acid and glutathione homeostasis in mice," *Frontiers in Pharmacology*, vol. 8, p. 938, 2017.

[17] J. Gu, W. Huang, W. Zhang et al., "Sodium butyrate alleviates high-glucose-induced renal glomerular endothelial cells damage via inhibiting pyroptosis," *International Immunopharmacology*, vol. 75, Article ID 105832, 2019.

[18] Y. H. Xu, C. L. Gao, H. L. Guo et al., "Sodium butyrate supplementation ameliorates diabetic inflammation in db/db mice," *Journal of Endocrinology*, vol. 238, no. 3, pp. 231–244, 2018.

[19] W. Q. Zhang, T. T. Zhao, D. K. Gui et al., "Sodium butyrate improves liver glycogen metabolism in type 2 diabetes mellitus," *Journal of Agricultural and Food Chemistry*, vol. 67, no. 27, pp. 7694–7705, 2019.

[20] T. Zhao, J. Gu, H. Zhang et al., "Sodium butyrate-modulated mitochondrial function in high-insulin induced HepG2 cell dysfunction," *Oxidative Medicine and Cellular Longevity*, vol. 2020, Article ID 1904609, 16 pages, 2020.

[21] Y. Hamada, M. Goto, G. Nishimura et al., "The alpha-glucosidase inhibitor miglitol increases hepatic CYP7A1 activity in association with altered short-chain fatty acid production in the gut of obese diabetic mice," *Metabolism Open*, vol. 5, Article ID 100024, 2020.

[22] L. Xiao and G. Pan, "An important intestinal transporter that regulates the enterohepatic circulation of bile acids and cholesterol homeostasis: the apical sodium-dependent bile acid transporter (SLC10A2/ASBT)," *Clinics and Research in Hepatology and Gastroenterology*, vol. 41, no. 5, pp. 509–515, 2017.

[23] S. H. Lee, J. M. Choi, S. Y. Jung et al., "The bile acid induced hepatokine orosomucoid suppresses adipocyte differentiation," *Biochemical and Biophysical Research Communications*, vol. 534, p. 864, 2021.

[24] M. Song, Q. Yang, F. Zhang et al., "Hyodeoxycholic acid (HDCA) suppresses intestinal epithelial cell proliferation through FXR-PI3K/AKT pathway, accompanied by alteration of bile acids metabolism profiles induced by gut bacteria," *The FASEB Journal*, vol. 34, no. 5, pp. 7103–7117, 2020.

[25] I. R. Tough, T. W. Schwartz, and H. M. Cox, "Synthetic G protein-coupled bile acid receptor agonists and bile acids act via basolateral receptors in ileal and colonic mucosa," *Neurogastroenterology & Motility*, vol. 32, no. 12, Article ID e13943, 2020.

[26] J. Zhao, Y. Li, L. Xin et al., "Clinical features and rules of Chinese herbal medicine in diabetic peripheral neuropathy patients," *Evidence-Based Complementary and Alternative Medicine*, vol. 2020, Article ID 5795264, 8 pages, 2020.

[27] D. J. Choi, S. C. Kim, G. E. Park et al., "Protective effect of a mixture of Astragalus membranaceus and lithospermum erythrorhizon extract against hepatic steatosis in high fat diet-induced nonalcoholic fatty liver disease mice," *Evidence-Based Complementary and Alternative Medicine*, vol. 2020, Article ID 8370698, 11 pages, 2020.

[28] S. Hui, L. Huang, X. Wang et al., "Capsaicin improves glucose homeostasis by enhancing glucagon-like peptide-1 secretion through the regulation of bile acid metabolism via the remodeling of the gut microbiota in male mice," *The FASEB Journal*, vol. 34, no. 6, pp. 8558–8573, 2020.

[29] J. Rao, C. Yang, S. Yang et al., "Deficiency of TGR5 exacerbates immune-mediated cholestatic hepatic injury by stabilizing the β-catenin destruction complex," *International Immunology*, vol. 32, no. 5, pp. 321–334, 2020.

[30] J. M. Kowal, K. A. Haanes, N. M. Christensen, and I. Novak, "Bile acid effects are mediated by ATP release and purinergic signalling in exocrine pancreatic cells," *Cell Communication and Signaling*, vol. 13, no. 1, p. 28, 2015.

[31] M. Li, Q. Wang, Y. Li et al., "Apical sodium-dependent bile acid transporter, drug target for bile acid related diseases and delivery target for prodrugs: current and future challenges," *Pharmacology & Therapeutics*, vol. 212, Article ID 107539, 2020.

[32] F. J. Gonzalez, "Nuclear receptor control of enterohepatic circulation," *Comprehensive Physiology*, vol. 2, pp. 2811–2828, 2012.

[33] M. J. D. Robin, M. D. Appelman, H. R. Vos et al., "Calnexin depletion by endoplasmic reticulum stress during cholestasis

inhibits the Na^+-taurocholate cotransporting polypeptide," *Hepatology Communications*, vol. 2, no. 12, pp. 1550–1566, 2018.

[34] J. Wei, J. Chen, L. Fu et al., "Polygonum multiflorum Thunb suppress bile acid synthesis by activating Fxr-Fgf15 signaling in the intestine," *Journal of Ethnopharmacology*, vol. 235, pp. 472–480, 2019.

[35] L. Wang, Y.-K. Lee, D. Bundman et al., "Redundant pathways for negative feedback regulation of bile acid production," *Developmental Cell*, vol. 2, no. 6, pp. 721–731, 2002.

[36] Y. C. Kim, H. Jung, S. Seok et al., "MicroRNA-210 promotes bile acid-induced cholestatic liver injury by targeting mixed-lineage leukemia-4 methyltransferase in mice," *Hepatology*, vol. 71, no. 6, pp. 2118–2134, 2020.

[37] C. Gardès, E. Chaput, A. Staempfli, D. Blum, H. Richter, and G. M. Benson, "Differential regulation of bile acid and cholesterol metabolism by the farnesoid X receptor in $Ldlr^{-/-}$ mice versus hamsters," *Journal of Lipid Research*, vol. 54, no. 5, pp. 1283–1299, 2013.

[38] C.-J. Ling, J.-Y. Xu, Y.-H. Li et al., "Lactoferrin promotes bile acid metabolism and reduces hepatic cholesterol deposition by inhibiting the farnesoid X receptor (FXR)-mediated enterohepatic axis," *Food & Function*, vol. 10, no. 11, pp. 7299–7307, 2019.

[39] M. Ghosh Laskar, M. Eriksson, M. Rudling, and B. Angelin, "Treatment with the natural FXR agonist chenodeoxycholic acid reduces clearance of plasma LDL whilst decreasing circulating PCSK9, lipoprotein(a) and apolipoprotein C-III," *Journal of Internal Medicine*, vol. 281, no. 6, pp. 575–585, 2017.

[40] D. Duran-Sandoval, B. Cariou, F. Percevault et al., "The farnesoid X receptor modulates hepatic carbohydrate metabolism during the fasting-refeeding transition," *Journal of Biological Chemistry*, vol. 280, no. 33, pp. 29971–29979, 2005.

[41] D. Sheng, S. Zhao, L. Gao et al., "BabaoDan attenuates high-fat diet-induced non-alcoholic fatty liver disease via activation of AMPK signaling," *Cell & Bioscience*, vol. 9, no. 1, p. 77, 2019.

[42] M. Davaatseren, H. J. Hur, H. J. Yang et al., "Taraxacum official (dandelion) leaf extract alleviates high-fat diet-induced nonalcoholic fatty liver," *Food and Chemical Toxicology*, vol. 58, pp. 30–36, 2013.

Hindawi
Evidence-Based Complementary and Alternative Medicine
Volume 2021, Article ID 5563660, 15 pages
https://doi.org/10.1155/2021/5563660

Research Article

Curcumin Ameliorates Palmitic Acid-Induced Saos-2 Cell Apoptosis Via Inhibiting Oxidative Stress and Autophagy

Baicheng Ma,[1,2] Gaopeng Guan,[1,3] Qizhuang Lv,[4] and Lei Yang[1]

[1]*Jiangxi Provincial Key Lab of System Biomedicine, Jiujiang University, Jiujiang 332000, Jiangxi, China*
[2]*School of Medicine, Jiujiang University, Jiujiang 332000, Jiangxi, China*
[3]*Affiliated Hospital of Jiujiang University, Jiujiang University, Jiujiang 332000, Jiangxi, China*
[4]*College of Biology & Pharmacy, Yulin Normal University, Yulin 537000, Guangxi, China*

Correspondence should be addressed to Qizhuang Lv; lvqizhuang062@163.com and Lei Yang; yangleigeili@163.com

Received 16 January 2021; Revised 6 March 2021; Accepted 10 March 2021; Published 26 March 2021

Academic Editor: Youhua Xu

Objectives. We aimed to determine the effects of curcumin on palmitic acid- (PA-) induced human osteoblast-like Saos-2 cell apoptosis and to explore the potential molecular mechanisms in vitro level. *Methods*. Saos-2 cell were cultured with PA with or without curcumin, N-acetylcysteine (NAC, anti-oxidant), 3-methyladenine (3-MA, autophagy inhibitor) AY-22989 (autophagy agonist) or H_2O_2. Then, the effects of PA alone or combined with curcumin on viability, apoptosis, oxidative stress, and autophagy in were detected by CCK-8, flow cytometry assay and western blot. *Results*. We found that autophagy was induced, oxidative stress was activated, and apoptosis was promoted in PA-induced Saos-2 cells. Curcumin inhibited PA-induced oxidative stress, autophagy, and apoptosis in Saos-2 cells. NAC successfully attenuated oxidative stress and apoptosis, and 3-MA attenuated oxidative stress and apoptosis in palmitate-induced Saos-2 cells. Interestingly, NAC inhibited PA-induced autophagy, but 3-MA had no obvious effects on oxidative stress in PA-treated Saos-2 cells. In addition, curcumin inhibited H_2O_2 (oxidative stress agonist)-induced oxidative stress, autophagy, and apoptosis, but curcumin had no obvious effect on AY-22989 (autophagy agonist)-induced autophagy and apoptosis. *Conclusion*. The present study demonstrated that oxidative stress is an inducer of autophagy and that curcumin can attenuate excess autophagy and cell apoptosis by inhibiting oxidative stress in PA-induced Saos-2 cells.

1. Introduction

Diabetes mellitus is a pandemic metabolic disease and has a worldwide distribution. Patients with diabetes mellitus have various skeletal disorders, including osteopenia or osteoporosis [1]. Diets rich in high-fat foods, especially saturated fats, are usually the cause of the clinical symptoms of metabolic syndrome, such as obesity, insulin resistance, and type 2 diabetes, which eventually increase the likelihood of osteoporosis [2]. Moreover, obesity and type 2 diabetes trigger a prolonged elevation of circulating free fatty acid levels (FFAs) especially the saturated FFAs such as palmitate (PA), which causes lipotoxicity in many cell types, including human osteoblast-like Saos-2 cell [3]. Additionally, PA-induced lipotoxicity plays a vital role in the development and progression of osteoporosis [4, 5]. Numerous studies have focused on factors involved in the mechanism of PA-induced lipotoxicity, such as oxidative stress and autophagy [5].

Oxidative stress is essentially an imbalance between the generation of reactive oxygen species (ROS) and the ability of the body to counteract or detoxify their harmful effects through neutralization by antioxidants [6]. ROS are produced in all cellular compartments as a result of exposure to toxic agents and natural by-products of mitochondrial respiration and can disrupt the normal mechanisms of cellular signaling and function, resulting in DNA damage and apoptosis [7]. Previous studies have reported that oxidative stress plays an important role in the pathophysiology of many diseases, including osteoporosis [6].

Autophagy is a complex catabolic process in eukaryotes that enables cells to recycle cytoplasmic components through degradation in the lysosomes. Under stressful conditions, such as nutrient deprivation and oxidative stress, autophagy is activated as a pathway to promote cell survival by maintaining energy and reducing toxic substances [8]. In addition, there is increasing evidence that excessive or uncontrolled levels of autophagy may be essential for cell apoptosis in certain settings [9]. Moreover, some studies have reported that autophagy is related to diabetic osteoporosis, [8] and oxidative stress has been reported to be a novel autophagy inducer [10].

Curcumin, a non-flavonoid polyphenol found in the plant Curcuma longa, has been extensively investigated because of its anti-inflammatory, anti-oxidative, and cytoprotective properties [11]. Previous studies have reported that curcumin is a promising drug for the prevention and treatment of diabetes and diabetes-related diseases, including osteoporosis [12]. Moreover, both oxidative stress and autophagy are related to diabetic osteoporosis [13]. In addition, previous study has reported that curcumin can regulate oxidative stress and autophagy in vivo and in vitro [14].

In this study, we aimed to determine the effects of curcumin on PA-induced human osteoblast-like Saos-2 cell apoptosis and to explore the potential molecular mechanisms in vitro level. Herein, we investigated the participation and relationship of oxidative stress and autophagy and evaluated the effects and molecular mechanisms of curcumin in PA-induced Saos-2 cell apoptosis.

2. Materials and Methods

2.1. Cell Culture and Treatment. Saos-2 cells were cultured in DMEM supplemented with 10% FBS, 50 μg/mL penicillin, and 50 μg/mL gentamicin in a humidified incubator at 37°C with 5% CO_2. When the cells reached 70%–80% confluence, they were treated with different concentrations (1.25–20 μM) of curcumin and 200 μM PA to determine their effects on cell activity. At the same time, the cells were exposed to 200 μM PA in the presence or absence of 10 μM curcumin, 5 mM 3-MA, 10 μM AY-22989, 100 μM H_2O_2, or 2 mM NAC for 24 h.

2.2. Measurement of Cell Viability. After the treatment, 10 μl of CCK-8 was added to each well, and the cells were incubated for 2 h at 37°C. The number of viable cells was measured at 450 nm with a microplate reader (Bio-Rad 680). The results are presented as a percentage of the values measured for untreated control cells.

2.3. Cell Apoptosis Measurement. After the treatment, cell apoptosis was quantified with an Annexin V-FITC/PI Apoptosis Analysis Kit according to the manufacturer's instructions. The cells were analyzed using a flow cytometer (Becton, Dickinson and Company, USA) within 1 h. Early apoptotic cells were determined by counting the percentage of Annexin V-FITC+/PI− cells, progressed apoptotic cells were obtained by counting the percentage of Annexin V-FITC+/PI+ cells, and necrotic cells were detected by counting the percentage of Annexin V-FITC−/PI+ cells and Annexin V-FITC−/PI− cells.

2.4. Western Blot. After the treatment, cells were collected and washed with ice-cold PBS and lysed with RIPA buffer, and the total protein concentration was measured using the BCA assay. Fifty micrograms of total protein from each sample were loaded into each well of a 13% SDS-PAGE gel, and then, proteins were separated by electrophoresis. Proteins were then transferred to PVDF membranes. After blocking in TBST with 10% nonfat milk for 2 h, the samples were incubated with primary antibody against B-cell lymphoma-2 (Bcl-2, 1 : 1,000), Bcl-2 associated X protein (BAX, 1 : 500), glyceraldehyde-phosphate dehydrogenase (GAPDH, 1 : 2,000), Autophagy protein 5 (ATG5, 1 : 1,000), polyubiquitin-binding protein (P62, 1 : 1,000), and microtubule-associated protein light chain 3 (LC3, 1 : 1,000) overnight at 4°C. After washing, the membranes were incubated with secondary antibody (1 : 4,000) conjugated to horseradish peroxidase at 37°C for 30 min. The immunoreactive bands were visualized using a Super Signal West Pico kit according to the manufacturer's instructions, and the densities of the protein bands were measured by densitometric analysis using ImageJ software 1.48 (National Institutes of Health, Bethesda, Maryland, USA).

2.5. mCherry-GFP-LC3 Adenovirus Transfection and Autophagy Assay. Cells cultured in 24-well plates (1 × 105 cells/well) were transfected with mCherry-GFP-LC3 adenovirus at 40 MOI for 24 h. After transfection, the cells were incubated with fresh culture medium again for 24 h. The numbers of GFP and mCherry dots per cell were counted in three randomly selected fields under a fluorescence microscope (Olympus Corporation, Tokyo, Japan). GFP degrades in an acidic environment, while mCherry does not. Thus, yellow spots (formed from the overlap of red and green) indicate autophagosomes, while red spots indicate autophagic lysosomes. If autophagy is activated, the red signal will dominate over yellow. If autophagy is suppressed, there will be more yellow signal than red signal.

2.6. ROS Measurements. After the treatment, the cells were incubated with DCFH-DA (10 μM) at 37°C for 20 min. Then, the cells were subsequently washed three times with PBS, and the ROS-sensitive dye in cells was assessed under an inverted fluorescence microscope (Olympus Corporation, Tokyo, Japan) with an excitation wavelength of 488 nm and an emission wavelength of 525 nm. Fluorescent intensity was acquired using ImageJ 1.48 image analysis software.

2.7. Superoxide Dismutase (SOD) Detection. After the treatment, the cells were harvested and sonicated in PBS containing 1.0 mM PMSF to obtain cell homogenates. The homogenates were then centrifuged at 15,000 × g and 4°C for 15 min, and the protein content was determined using the

BCA Protein Assay Kit. Then, the supernatants were used for measuring cellular SOD. The SOD activity was determined at 450 nm using a microplate reader (Bio-Rad 680).

2.8. Caspase-3 Activity Measurement. After the treatment, the cells were harvested by centrifugation and incubated in lysis buffer on ice for 15 min. The lysates were then centrifuged at 15,000 × g and 4°C for 15 min, and the protein content was determined using the BCA Protein Assay Kit according to the manufacturer's instructions. Then, each sample was incubated with the Caspase-3 substrate at 37°C in a microplate for 4 h. The samples were measured at 405 nm using a microplate reader.

2.9. Statistical Analyses. All experiments were repeated at least three times for each group, and the data are expressed as the mean ± standard error of the mean (SEM). The data were analyzed by one-way analysis of variance (ANOVA) followed by Fisher's least significant difference test and independent samples Student's t-test with SPSS software, version 13.0 (SPSS, Chicago, IL, USA). Differences were considered statistically significant when $P < 0.05$.

3. Results

3.1. Curcumin Attenuated the PA-Induced Cell Viability Decrease and Cell Apoptosis in Saos-2 Cells. We first assessed the cytotoxicity of curcumin (1.25, 2.5, 5, 10, 20 μM) on Saos-2 cells. The CCK-8 results showed that 1.25–10 μM curcumin had no significant cytotoxicity, but 20 μM curcumin decreased cell viability after 24 h of culture (Figure 1(a)). Moreover, 200 μM PA and 1.25–20 μM curcumin were added to the culture medium for 24 h to determine the effects of curcumin on PA-induced Saos-2 cell viability. The results showed that 200 μM PA reduced cell viability by about 50%, and 1.25–10 μM curcumin prevented this reduction in cell viability in a dose-dependent manner. However, 20 μM curcumin had no obvious effects on cell viability compared with the control treatment (Figure 1(b)). Flow cytometry analysis revealed that curcumin prevented cell apoptosis caused by PA in a dose-dependent manner. However, 20 μM curcumin had no obvious effects on PA-induced cell apoptosis (Figure 1(c)). The colorimetric assay and western blot results showed that curcumin attenuated the expression of BAX and Caspase-3 but increased the expression of Bcl-2 in PA-treated Saos-2 cells (Figures 1(d) and 1(e)).

3.2. Curcumin Reduced PA-Induced Oxidative Stress and Autophagy in Saos-2 Cells. To determine the effects of curcumin on oxidative stress and autophagy in PA-treated Saos-2 cells, the cells were treated with 200 μM PA with or without 1.25–10 μM curcumin for 24 h, and oxidative stress-related parameters were analyzed. DCFH-DA assay revealed that PA increased intracellular ROS production, but curcumin treatment decreased the PA-induced ROS generation in a dose-depend manner (Figure 2(a)). Moreover, PA reduced the activity of the anti-oxidant enzyme SOD, which was rescued by 1.25–10 μM curcumin in a dose-dependent manner (Figure 2(b)). These results showed that curcumin attenuates PA-induced cell apoptosis in Saos-2 cells. The western blot results indicated that the 200 μM PA treatment increased the protein expression of ATG5 and LC3II and the degradation of p62. Meanwhile, we found that the protein expression levels of ATG5 and LC3II in PA-treated cells significantly decreased but that of p62 increased following the addition of different doses of curcumin (Figures 2(c)–2(f)).

3.3. Roles of Oxidative Stress and Autophagy in the Protective Effect of Curcumin on PA-Induced Saos-2 Cell Apoptosis. Because both oxidative stress and autophagy can be induced during Saos-2 cell apoptosis, we designed the following experiment to determine whether oxidative stress and autophagy are involved in PA-induced Saos-2 cell apoptosis. The oxidative stress inhibitor NAC and autophagy inhibitor 3-MA were added to the culture medium during the PA treatment. The CCK-8 assay results showed that NAC and 3-MA clearly increased cell viability in PA-induced Saos-2 cells (Figure 3(a)). The flow cytometry results indicated that NAC and 3-MA reduced cell apoptosis caused by PA (Figures 3(b) and 3(c)). The western blot and colorimetric assay results demonstrated that the decreases in BAX and Caspase-3 expression and the increase in Bcl-2 expression were also rescued by NAC and 3-MA in PA-induced Saos-2 cells (Figures 3(d) and 3(e)). Moreover, NAC and 3-MA had the same protective effect as curcumin on PA-induced Saos-2 cell apoptosis. Therefore, these results indicate that PA induces Saos-2 cell apoptosis by stimulating oxidative stress and activating autophagy and that curcumin may attenuate cell apoptosis by inhibiting oxidative stress and autophagy.

3.4. Relation of Oxidative Stress and Autophagy to the Protective Effect of Curcumin on PA-Induced Saos-2 Cell. To determine whether there is an association between oxidative stress and autophagy in PA-induced Saos-2 cells, we assessed the oxidative stress parameters and autophagy makers in PA-induced Saos-2 cells with or without NAC and 3-MA. The oxidative stress parameter results indicated that NAC, but not 3-MA, inhibited the ROS generation and SOD downregulation (Figures 4(a)–4(c)), suggesting that NAC, but not 3-MA, abrogated PA-induced oxidative stress. In addition, NAC and 3-MA clearly reduced the protein levels of ATG5 and LC3II and the degradation of P62 (Figures 4(d)–4(g)). Moreover, the NAC and 3-MA treatments inhibited the PA-induced increases in autophagosomes and autolysosomes (Figures 4(h) and 4(i)), suggesting that NAC and 3-MA alleviated PA-activated autophagy. Therefore, NAC, but not 3-MA, had the same effect as curcumin on PA-induced oxidative stress and autophagy in Saos-2 cells. These results indicated that oxidative stress is an inducer of autophagy in PA-induced Saos-2 cells and that curcumin may reduce oxidative stress and oxidative stress-induced autophagy in PA-induced Saos-2 cells.

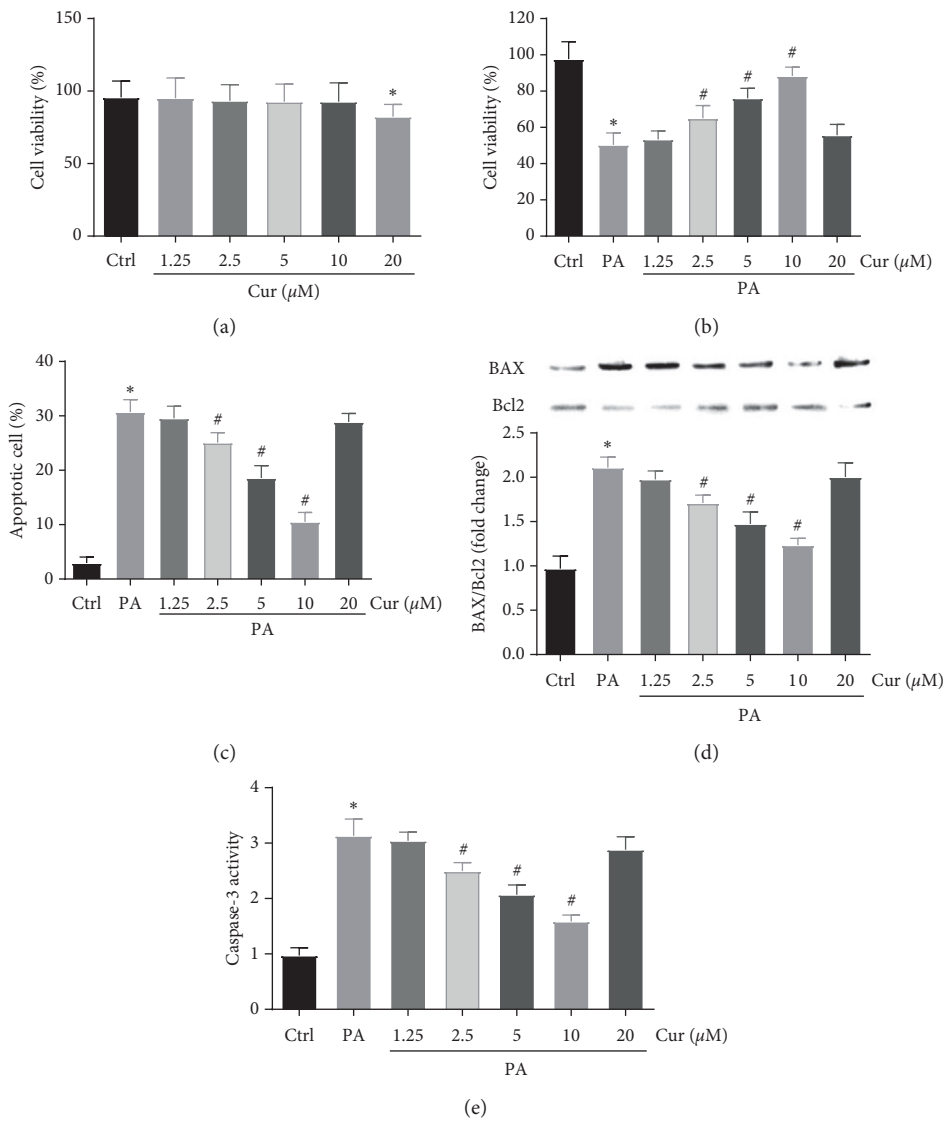

Figure 1: Effects of curcumin on PA-induced cell viability and apoptosis in Saos-2 cells. Saos-2 cells were treated with different concentrations of curcumin for 24 h. Cell viability was measured using CCK-8 assay (a). Cells were incubated with 200 μM PA for 24 h with or without curcumin at different concentrations. Cell viability was measured using CCK-8 assay (b). Apoptosis analysis was performed via flow cytometry (c). The protein expression levels of Bcl-2 and BAX were detected by western blot analysis. The analysis of band intensities is presented as the relative ratio of BAX to Bcl-2 (d). The Caspase-3 activity was detected using a microplate reader (e). Ctrl, control; Cur, different concentrations of curcumin; PA, 200 mM palmitic acid. Statistical analysis is shown on the bar graphs. Data are presented as the mean ± SEM of the three independent experiments. $^{*}P < 0.05$ versus control; $^{\#}P < 0.05$ versus PA.

3.5. Effects of Curcumin on Oxidative Stress- or Autophagy-Induced Saos-2 Cell Apoptosis. To further explored the roles of oxidative stress and autophagy in the mechanism of the protective effect of curcumin on PA-induced Saos-2 cell apoptosis, we added the oxidative stress inducer H_2O_2 or the autophagy agonist AY-22989 to the culture medium with or without curcumin. The results showed that H_2O_2 and AY-22989 clearly decreased cell viability and induced cell apoptosis in Saos-2 cells (Figures 5(a)–5(c)). Curcumin improved cell viability, prevented cell apoptosis, and altered the expression of apoptotic regulatory genes (Caspase-3, BAX, and Bcl-2) in H_2O_2-treated Saos-2 cells (Figures 5(d) and 5(e)). However, curcumin did not have a protective effect on AY-22989-induced Saos-2 cell apoptosis and cell viability decrease. These results indicated that curcumin inhibited oxidative stress-induced apoptosis not autophagy-induced apoptosis in Saos-2 cells.

3.6. Effects of Curcumin on Oxidative Stress or Autophagy in Saos-2 Cells. Moreover, we assessed oxidative stress and autophagy after adding H_2O_2 or AY-22989 to the culture medium with or without curcumin. The results showed that H_2O_2 increased the levels of ROS and inhibited the activity of SOD in Saos-2 cells (Figures 6(a)–6(c)). Curcumin reduced the levels of ROS and increased the activity of SOD in H_2O_2-treated Saos-2 cells. AY-22989 did not change the levels of ROS or the activity of SOD in Saos-2 cells. The western blot analysis showed that the expression of ATG5

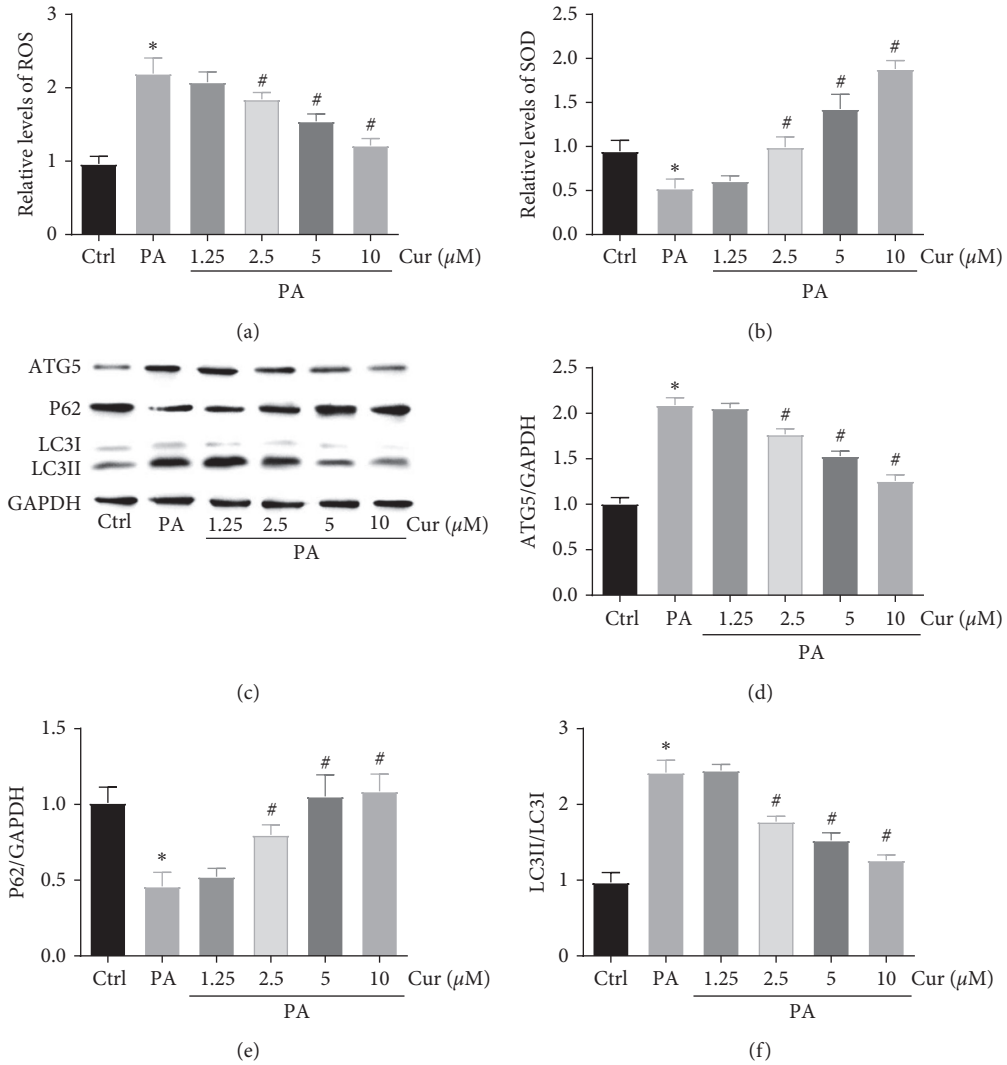

Figure 2: Effects of curcumin on PA-induced oxidative stress and autophagy in Saos-2 cells. Saos-2 cells were incubated with 200 μM PA for 24 h with or without curcumin at different concentrations. The generation of ROS was measured by using the DCFH-DA. Saos-2 cells were stained with DCFH-DA and analyzed by fluorescent microscopy. Statistical analysis of fluorescence intensity in Saos-2 cells by image J software (a). The relative levels of SOD were detected by a microplate reader (b). Western blot detected ATG5, P62, and LC3 (c). Ratio of ATG5 and P62 to GAPDH, and ratio of LC3- II to LC3- I (d, e, and f). Ctrl, control; Cur, different concentrations of curcumin; PA, 200 mM palmitic acid. Statistical analysis is shown on the bar graphs. Data are presented as the mean ± SEM of the three independent experiments. $^{*}P < 0.05$ versus control; $^{\#}P < 0.05$ versus PA.

and LC3II and the degradation of P62 increased in H_2O_2- and AY-22989-treated Saos-2 cells (Figures 6(d)–6(g)). We also found that the formation of autophagosomes and autolysosomes increased, suggesting that H_2O_2 and AY-22989 activated autophagy in Saos-2 cells (Figures 6(h) and 6(i)). Curcumin reduced the expression of ATG5 and LC3II, degradation of P62, and formation of autophagosomes and autolysosomes in H_2O_2-treated but not AY-22989-treated Saos-2 cells. These results indicated that curcumin inhibited oxidative stress and oxidative stress-induced autophagy but did not have a direct effect on autophagy in Saos-2 cells.

4. Discussion

In the past few decades, with the dramatic increase in the type 2 diabetes epidemic, our understanding of the role of dyslipidemia and lipotoxicity in many diseases has grown considerably. The association between hyperlipidemia and osteoporosis has been established clinically and in experimental models [15]. Palmitate is the main saturated FFA in plasma that stimulates ROS production and autophagy activity in cultured cardiomyocytes and endothelial cells [16]. In our previous study, we reported that PA triggers Saos-2 cell apoptosis via excessive autophagy [3], and several studies have reported that curcumin protects cells against oxidative stress-mediated apoptosis [14, 17]. However, the cryoprotective effect of curcumin on PA-treated cells and the underlying mechanisms have not been reported. Here, we demonstrated for the first time that curcumin can attenuate PA-induced Saos-2 cell apoptosis via inhibiting oxidative stress and autophagy (Figure 7).

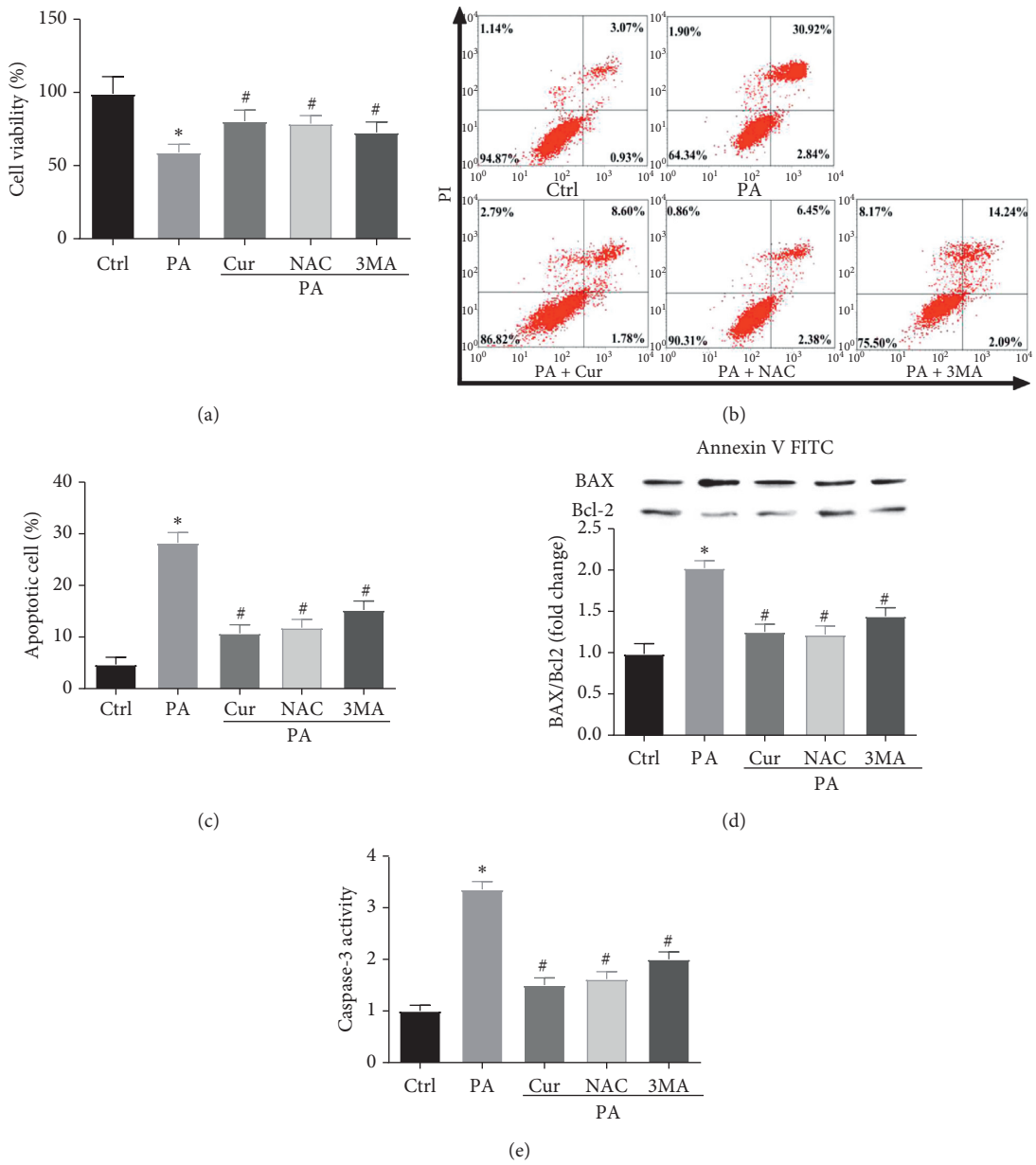

Figure 3: Oxidative stress and autophagy is involved in curcumin against PA-induced Saos-2 cell apoptosis (a). Saos-2 cells were incubated with 200 μM PA for 24 h with or without curcumin, NAC, or 3-MA. Cell viability was measured using CCK-8 assay (b). Apoptosis analysis was performed via flow cytometry (c). The protein expression levels of Bcl-2 and BAX were detected by western blot analysis. The analysis of band intensities is presented as the relative ratio of BAX to Bcl-2 (d). The Caspase-3 activity was detected using a microplate reader (e). Ctrl, control; Cur, 10 μM curcumin; PA, 200 mM palmitic acid; NAC, 2 mM N-acetylcysteine; 3-MA/3-MA, 5 mM 3-methyladenine. Statistical analysis is shown on the bar graphs. Data are presented as the mean ± SEM of the three independent experiments. $^{*}P < 0.05$ versus control; $^{\#}P < 0.05$ versus PA.

Curcumin has a range of pharmacological effects, including anticancer, anti-inflammatory, antioxidative as well as antioxidant, and cryoprotective activities [18, 19]. In our research, curcumin rescued the PA-induced cell viability decrease and cell apoptosis. Our results are different from those of previous studies that reported that curcumin triggers apoptosis in many tumor cells, including HT29 cells [20] and upper aerodigestive tract cancer cells [21], suggesting that curcumin is a potential anticancer drug. Meanwhile, our results further supported the conclusion that curcumin protects cells against various injuries such as ischemic injury [18, 22] and diabetes [23, 24] in vivo and in vitro. Therefore, curcumin seems to have a bidirectional effect on cell proliferation and apoptosis. On the one hand, it can promote cell apoptosis, especially in cancer cells; on the other hand, it can prevent cell apoptosis. The reasons for the different results (cell die or live) caused by curcumin may be due to differences in cell types, drug doses, and experimental methods.

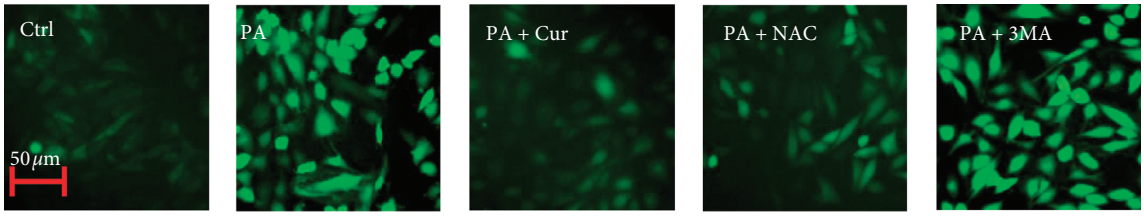

(a)

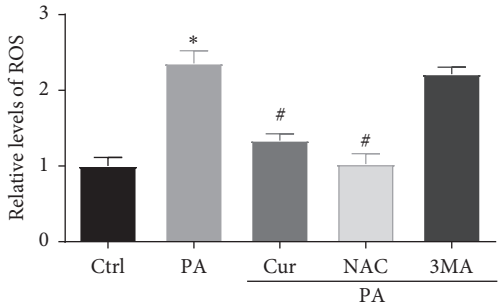

(b)

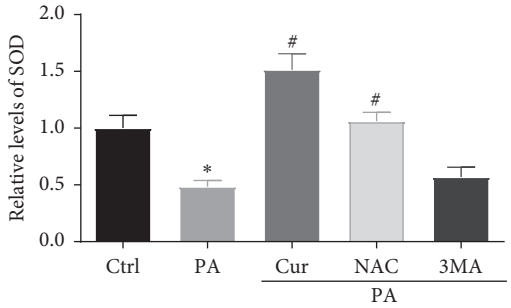

(c)

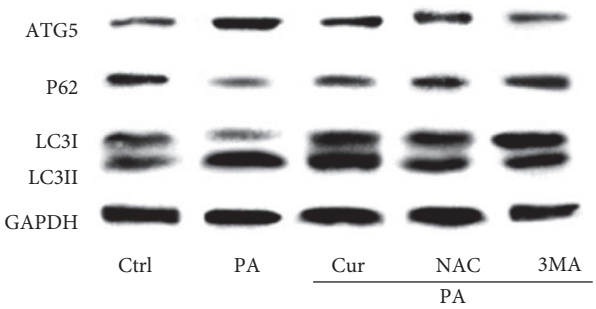

(d)

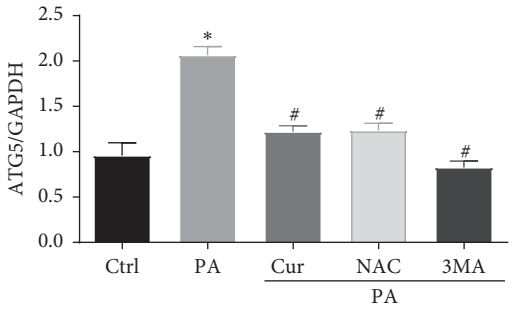

(e)

Figure 4: Continued.

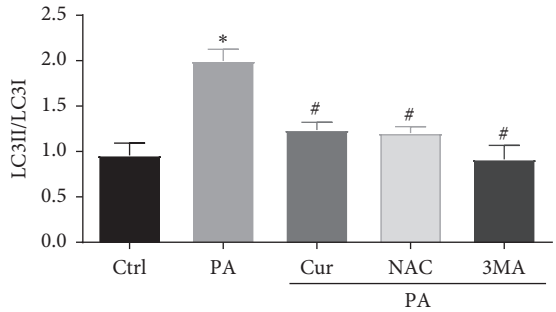

(f)

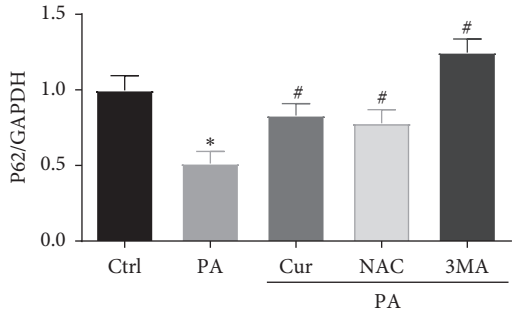

(g)

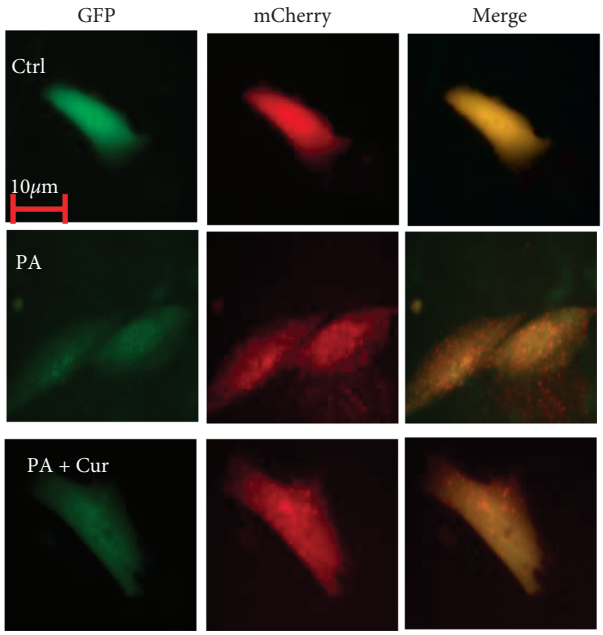

(h)

Figure 4: Continued.

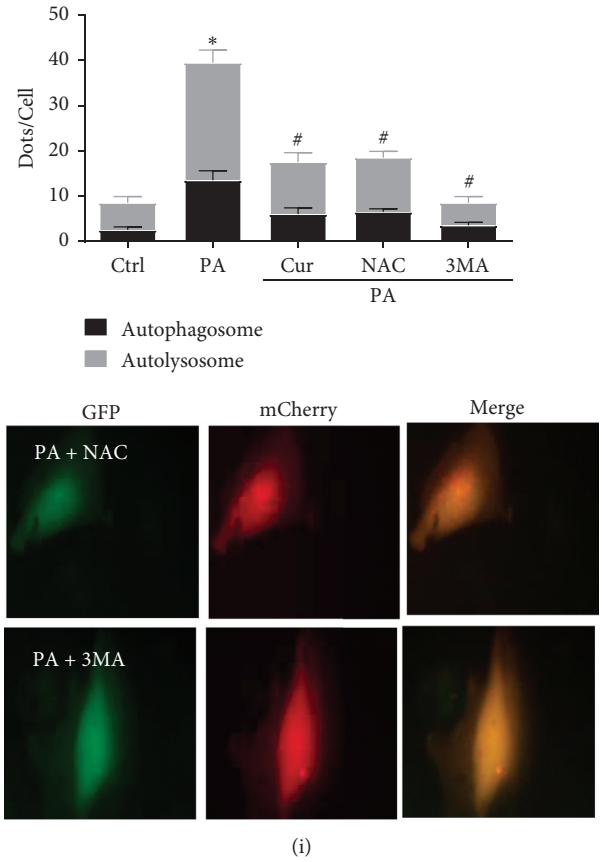

Figure 4: Curcumin reduces oxidative stress and oxidative stress-induced autophagy in PA-induced Saos-2 cell. Saos-2 cells were incubated with 200 μM PA for 24 h with or without curcumin, NAC, or 3-MA. The generation of ROS was measured by using the DCFH-DA. Saos-2 cells were stained with DCFH-DA and analyzed by fluorescent microscopy (a). Statistical analysis of fluorescence intensity in Saos-2 cells by image J software (b). The relative levels of SOD were detected by a microplate reader (c). Western blot detected ATG5, P62, LC3I, and LC3II (d). Ratio of ATG5 and P62 to GAPDH, and ratio of LC3- II to LC3- I (e, f, and g). Fluorescent microscopy analysis of Saos-2 cells transfected with mCherry-GFP-LC3B adenovirus (h). Statistical analysis of fluorescent dots in Saos-2 cells (i). Yellow spots indicate autophagosomes, and red spots indicate autolysosomes after the pictures were merged. Ctrl, control; Cur, 10 μM curcumin; PA, 200 mM palmitic acid; NAC, 2 mM N-acetylcysteine; 3-MA/3-MA, 5 mM 3-methyladenine. Statistical analysis is shown on the bar graphs. Data are presented as the mean ± SEM of the three independent experiments. $^{*}P < 0.05$ versus control; $^{\#}P < 0.05$ versus PA.

We further examined apoptotic regulatory genes, including Caspase-3, BAX, and Bcl-2. The results showed that curcumin decreased the expression of the pro-apoptotic molecule BAX and increased the expression of the anti-apoptotic molecule Bcl-2. Our results were consistent with the findings of previous studies that reported that curcumin ameliorated cell apoptosis by regulating Bcl-2 family proteins, which can downregulate BAX and upregulate Bcl-2 expression [25]. Caspase-3 acts as an executioner in Caspase-mediated apoptosis, and the expression of Caspase-3 positively correlates with the rate of apoptosis in cells [11]. In our study, we found that curcumin can inhibit Caspase-3 activity, suggesting that curcumin can maintain cell survival by restraining Caspase-3. Therefore, we propose that curcumin affects cell proliferation and apoptosis in PA-treated cells by regulating Bcl-2 family proteins and mitigating Caspase-3 activity.

In previous studies, oxidative stress was found to be involved in the process of PA-mediated apoptosis [7, 26]. In addition, ROS production is a particularly destructive aspect of oxidative stress. Apoptosis is induced by excess free radicals when ROS production exceeds the capacity of antioxidant defenses [7]. In our study, we found that PA enhanced ROS generation. SOD is an antioxidant that protect cells against oxidative damage. However, the downregulation of SOD further promotes oxidative stress and damages cells. Previous studies have demonstrated that curcumin can prevent cell damage via suppressing oxidative stress [27]. Our data indicated that curcumin alleviates oxidative stress in a dose-dependent manner, indicating the protective ability of curcumin to prevent PA-induced oxidative stress in Saos-2 cells.

Autophagy is an important intracellular bulk degradation process involving the lysosome-dependent turnover of damaged cytosolic proteins and organelles, and it is critical for the maintenance of the normal cell phenotype and its functions. However, excess autophagy triggers cell apoptosis by destroying large proportions of the cytosol and organelles [28]. In our previous study we found that PA activated autophagy in a dose- and time-dependent manner in Saos-2

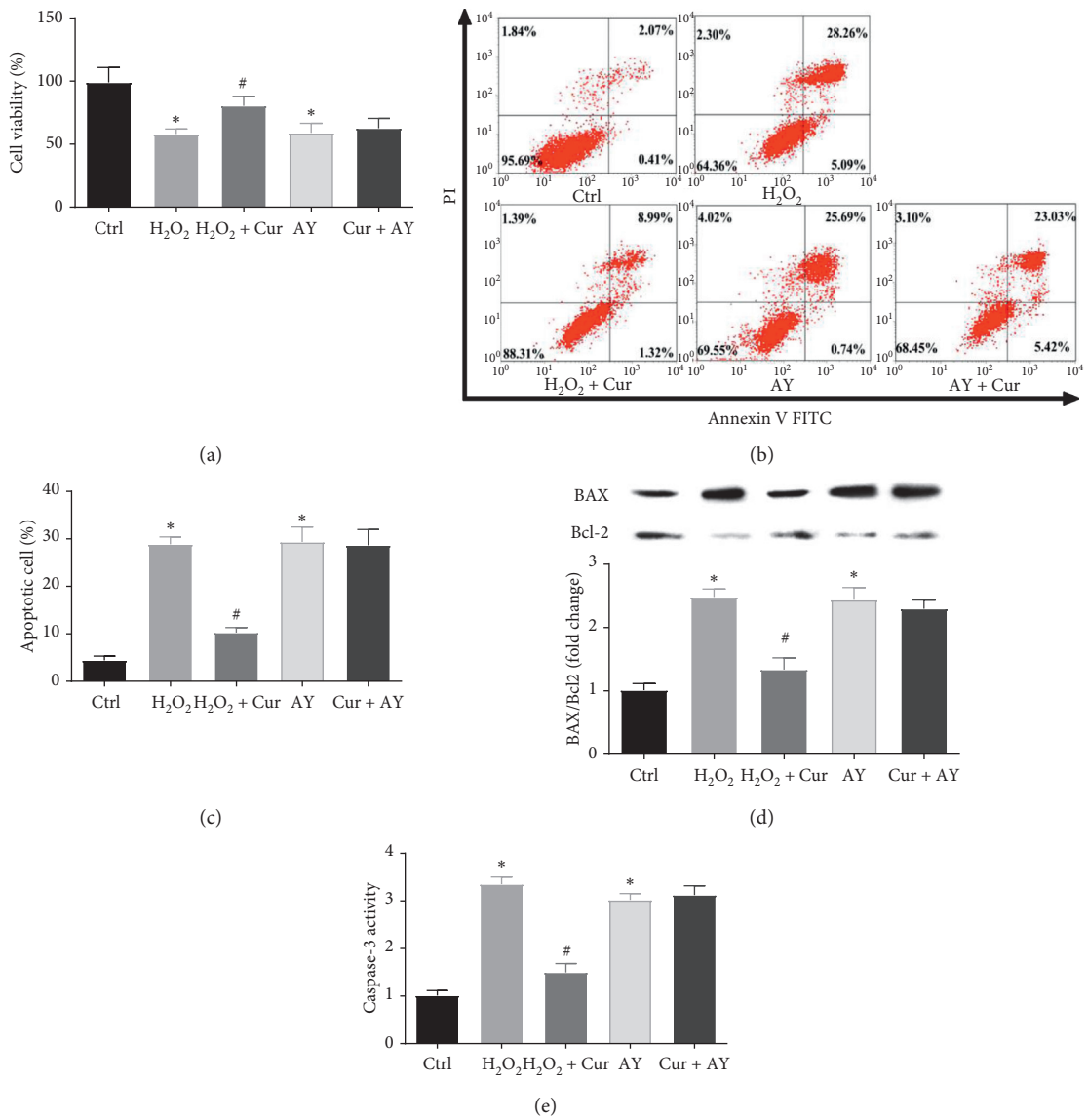

Figure 5: Curcumin attenuated oxidative stress-induced Saos-2 cell apoptosis. Saos-2 cells were incubated with H_2O_2 or AY-22989 for 24 h with or without curcumin. Cell viability was measured using CCK-8 assay (a). Apoptosis analysis was performed via flow cytometry using Annexin V-FITC/PI double staining (b, c). The protein expression levels of Bcl-2 and BAX were detected by western blot analysis. The analysis of band intensities is presented as the relative ratio of BAX to Bcl-2 (d). The Caspase-3 activity was detected using a microplate reader (e). Ctrl: control; Cur: 10 μM curcumin; H_2O_2: 100 μM H_2O_2; AY: 10 μM AY-22989. Statistical analysis is shown on the bar graphs. Data are presented as the mean ± SEM of the three independent experiments. $^{*}P < 0.05$ versus control, $^{\#}P < 0.05$ versus PA.

cells. Moreover, the PA-induced excessive autophagy caused cell apoptosis in Saos-2 cells. Furthermore, we analyzed the effects of curcumin on PA-induced autophagy. The results showed that PA successfully induced the expression of autophagy-related genes and that curcumin inhibited autophagy in a dose-dependent manner, suggesting that curcumin blocked.

To clarify whether oxidative stress and autophagy triggered PA-induced Saos-2 cell apoptosis, we used the oxidative stress inhibitor NAC and the autophagy inhibitor 3-MA to treat Saos-2 cells during the PA treatment. Apoptosis was inhibited by NAC and 3-MA. These results further indicated that PA-induced oxidative stress and autophagy cause Saos-2 cell apoptosis. Together, the results that curcumin inhibits autophagy, oxidative stress, and apoptosis indicate that curcumin may attenuate cell apoptosis by inhibiting oxidative stress and autophagy in PA-induced Saos-2 cells.

Previous studies have shown that oxidative stress can induce autophagy under starvation conditions [29]. Consistent with this previous study, we found that H_2O_2 activated autophagy in Saos-2 cells. Moreover, the PA-induced autophagy activity was inhibited by NAC in Saos-2 cells. In addition, AY-22989 and 3-MA did not have an effect on Saos-2 cells with or without PA treatment. These results indicated that oxidative stress is an inducer of autophagy in

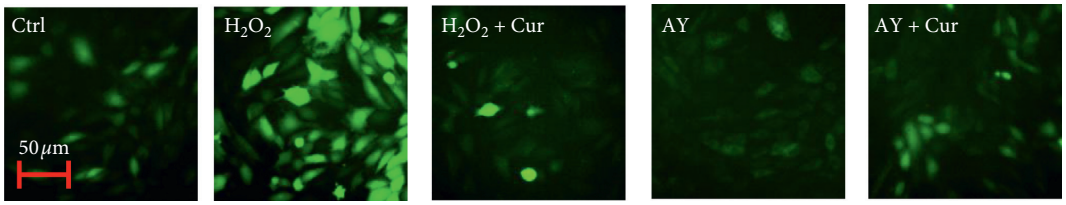

(a)

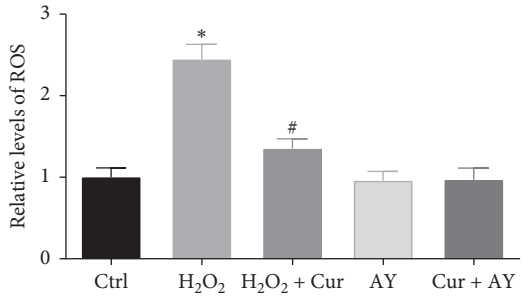

(b)

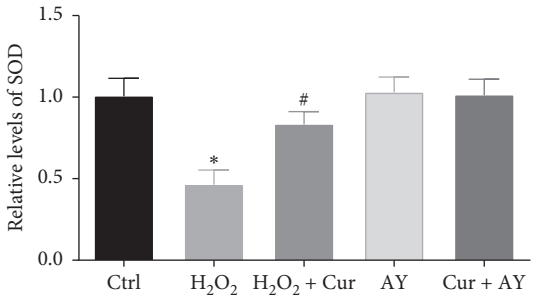

(c)

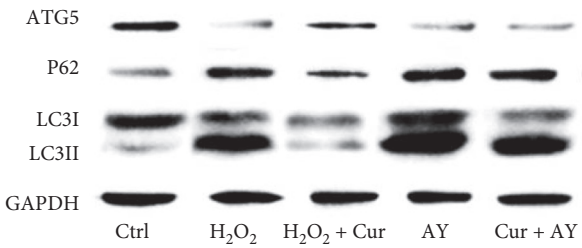

(d)

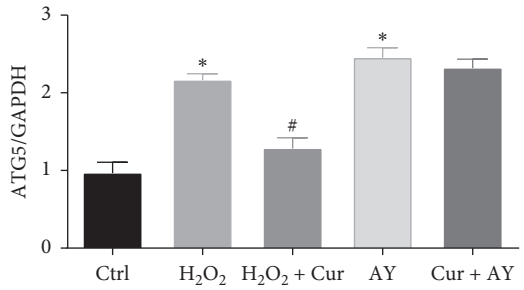

(e)

Figure 6: Continued.

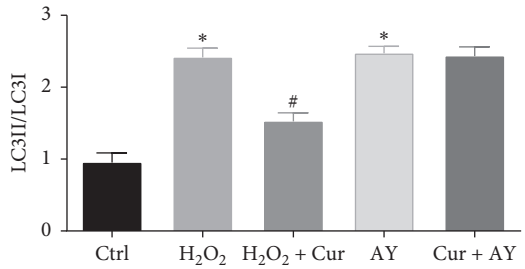

(f)

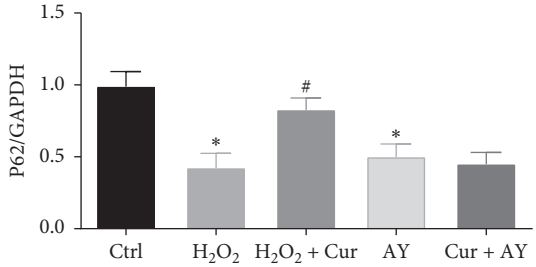

(g)

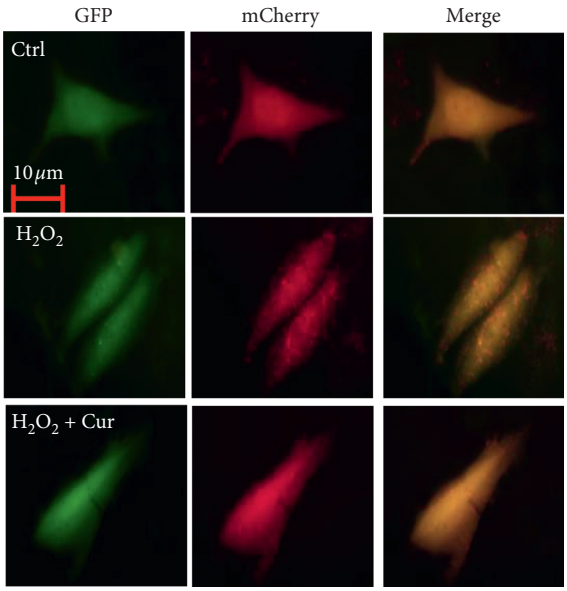

(h)

Figure 6: Continued.

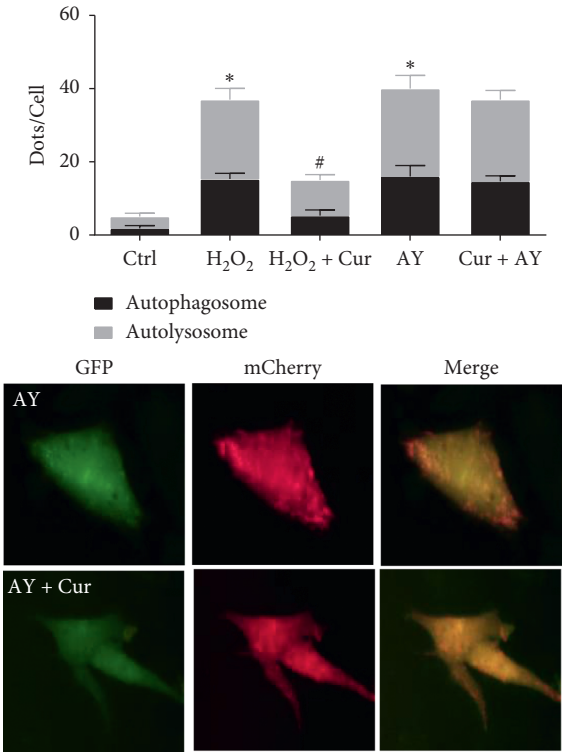

(i)

Figure 6: Curcumin inhibited oxidative stress and autophagy in H_2O_2- induced Saos-2 cells apoptosis. Saos-2 cells were incubated with H_2O_2 or AY-22989 for 24 h with or without curcumin. The generation of ROS was measured by using the DCFH-DA. Saos-2 cells were stained with DCFH-DA and analyzed by Fluorescent microscopy (a). Statistical analysis of fluorescence intensity in Saos-2 cells by image J software (b). The relative levels of SOD were detected by a microplate reader (c). Western blot detected ATG5, P62, LC3I and LCII (d). Ratio of ATG5 and P62 to GAPDH, and ratio of LC3- II to LC3- I (e) (f), and (g). Fluorescent microscopy analysis of Saos-2 cells transfected with mCherry-GFP-LC3B adenovirus (h). Statistical analysis of fluorescent dots in Saos-2 cells (i). Yellow spots indicate autophagosomes, and red spots indicate autolysosomes after the pictures were merged. Ctrl: control; Cur: 10 μM curcumin; H_2O_2: 100 μM H_2O_2; AY: 10 μM AY-22989. Statistical analysis is shown on the bar graphs. Data are presented as the mean ± SEM of the three independent experiments. $^{*}P < 0.05$ versus control, $^{\#}P < 0.05$ versus PA.

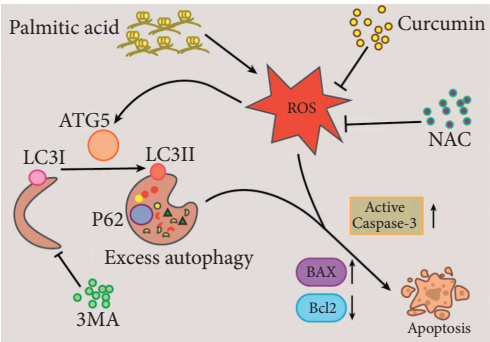

Figure 7: The mechanism by which curcumin ameliorates palmitic acid-induced Saos-2 cell apoptosis.

PA-induced Saos-2 cells. However, it is still unclear whether curcumin directly affects autophagy in PA-induced Saos-2 cells. Moreover, some studies have also reported that curcumin induces autophagy activation, such as in osteosarcoma MG63 cells [30] and oral cancer cells [31].

To further determine the effects of curcumin on autophagy in Saos-2 cells, we used AY-22989 to activate autophagy during the treatment. The results showed that curcumin had no obvious effects on autophagy and autophagy-induced apoptosis, indicating that curcumin has no effect on autophagy in Saos-2 cells. In addition, we found that the apoptosis, oxidative stress, and autophagy induced by H_2O_2 were rescued by curcumin, suggesting that curcumin can inhibit oxidative stress-induced autophagy and apoptosis in Saos-2 cells.

In summary, we found that curcumin can inhibit PA-induced oxidative stress, autophagy, and apoptosis. Moreover, previous studies have reported that oxidative stress can activate these processes in many cells and tissues [7, 32]. Our results showed that NAC can inhibit PA-induced autophagy but that 3-MA had no obvious effects on oxidative stress in Saos-2 cells with PA treatment. Thus, we assume that curcumin indirectly inhibits the PA-induced autophagy via suppressing oxidative stress. To further clarify this hypothesis, we found that curcumin inhibited H_2O_2-induced oxidative stress, autophagy, and apoptosis, but curcumin had no obvious effects on AY-22989-induced autophagy. Therefore, curcumin ameliorates PA-induced human Saos-2 cell apoptosis by inhibiting oxidative stress-mediated

autophagy. However, there were still a notable limitation in our study. The effects of curcumin on the lipotoxicity of Saos-2 cell in our present study might not represent the actual condition of human diabetic osteoporosis. Therefore, this study is the first step toward assessing the use of curcumin as a bioagent for the treatment of diabetic osteoporosis. To this end, we intend to establish an animal model to further confirm our results with the same way.

5. Conclusions

This is the first study to report that curcumin protects against PA-induced human Saos-2 cell apoptosis via inhibiting oxidative stress and autophagy (Figure 7). Our result may offer new insights into the molecular mechanisms and treatment of lipotoxicity in diabetic osteoporosis.

Data Availability

The data used to support the findings of this study are available from the corresponding author upon request.

Conflicts of Interest

The authors declare that they have no conflicts of interest.

Authors' Contributions

LY and QL designed the work; LY conceived and supervised the work; BM and GG performed experiments, performed the statistical analysis, and interpreted the results; LY and GG and drafted the study. BM and GG contributed equally to this work.

Acknowledgments

This study was supported by the Natural Science Foundation of Jiangxi Province (no. 20192BAB215011), the Project of Health Commission of Jiangxi Province (nos. 20193010 and 20195629), and the Project of Science and Technology of Jiangxi Provincial Education Department (GJJ180901).

References

[1] I. Kanazawa, A. Takeno, K.-I. Tanaka, Y. Yamane, and T. Sugimoto, "Osteoporosis and vertebral fracture are associated with deterioration of activities of daily living and quality of life in patients with type 2 diabetes mellitus," *Journal of Bone and Mineral Metabolism*, vol. 37, no. 3, pp. 503–511, 2019.

[2] P. Vestergaard, "Discrepancies in bone mineral density and fracture risk in patients with type 1 and type 2 diabetes-a meta-analysis," *Osteoporosis International*, vol. 18, no. 4, pp. 427–444, 2007.

[3] L. Yang, G. Guan, L. Lei et al., "Palmitic acid induces human osteoblast-like Saos-2 cell apoptosis via endoplasmic reticulum stress and autophagy," *Cell Stress and Chaperones*, vol. 23, no. 6, pp. 1283–1294, 2018.

[4] K. Gunaratnam, C. Vidal, R. Boadle, C. Thekkedam, and G. Duque, "Mechanisms of palmitate-induced cell death in human osteoblasts," *Biology Open*, vol. 2, no. 12, pp. 1382–1389, 2013.

[5] Y. Liu, R. Palanivel, E. Rai et al., "Adiponectin stimulates autophagy and reduces oxidative stress to enhance insulin sensitivity during high-fat diet feeding in mice," *Diabetes*, vol. 64, no. 1, pp. 36–48, 2015.

[6] S. Wehinger, R. Ortiz, M. I. Díaz et al., "Phosphorylation of caveolin-1 on tyrosine-14 induced by ROS enhances palmitate-induced death of beta-pancreatic cells," *Biochimica et Biophysica Acta (BBA)—Molecular Basis of Disease*, vol. 1852, no. 5, pp. 693–708, 2015.

[7] L. Yang, G. P. Guan, L. J. Lei, J. Y. Liu, L. L. Cao, and X. G. Wang, "Oxidative and endoplasmic reticulum stresses are involved in palmitic acid-induced H9c2 cell apoptosis," *Bioscience Reports*, vol. 39, no. 5, 2019.

[8] X. Xia, R. Kar, J. Gluhak-Heinrich et al., "Glucocorticoid-induced autophagy in osteocytes," *Journal of Bone and Mineral Research*, vol. 25, no. 11, pp. 2479–2488, 2010.

[9] Y. Liu and B. Levine, "Autosis and autophagic cell death: the dark side of autophagy," *Cell Death & Differentiation*, vol. 22, no. 3, pp. 367–376, 2015.

[10] W. L. Zheng, B. J. Wang, L. Wang et al., "ROS-mediated cell cycle arrest and apoptosis induced by zearalenone in mouse sertoli cells via er stress and the ATP/AMPK pathway," *Toxins*, vol. 10, no. 1, p. 24, 2018.

[11] G. Guan, L. Lei, Q. Lv, Y. Gong, and L. Yang, "Curcumin attenuates palmitic acid-induced cell apoptosis by inhibiting endoplasmic reticulum stress in H_9C_2 cardiomyocytes," *Human & Experimental Toxicology*, vol. 38, no. 6, pp. 655–664, 2019.

[12] Z. Chen, J. Xue, T. Shen, G. Ba, D. Yu, and Q. Fu, "Curcumin alleviates glucocorticoid-induced osteoporosis by protecting osteoblasts from apoptosisin vivoandin vitro," *Clinical and Experimental Pharmacology and Physiology*, vol. 43, no. 2, pp. 268–276, 2016.

[13] Y. Yang, X. Zheng, B. Li, S. Jiang, and L. Jiang, "Increased activity of osteocyte autophagy in ovariectomized rats and its correlation with oxidative stress status and bone loss," *Biochemical and Biophysical Research Communications*, vol. 451, no. 1, pp. 86–92, 2014.

[14] T. Jaroonwitchawan, N. Chaicharoenaudomrung, J. Namkaew, and P. Noisa, "Curcumin attenuates paraquat-induced cell death in human neuroblastoma cells through modulating oxidative stress and autophagy," *Neuroscience Letters*, vol. 636, pp. 40–47, 2017.

[15] F. Parhami, "Possible role of oxidized lipids in osteoporosis: could hyperlipidemia be a risk factor?" *Prostaglandins, Leukotrienes and Essential Fatty Acids*, vol. 68, no. 6, pp. 373–378, 2003.

[16] J. Li, Y. Zhou, W. Zhang, C. Bao, and Z. Xie, "Relief of oxidative stress and cardiomyocyte apoptosis by using curcumin nanoparticles," *Colloids and Surfaces B: Biointerfaces*, vol. 153, pp. 174–182, 2017.

[17] Y. Gao, Z. Zhuang, S. Gao et al., "Tetrahydrocurcumin reduces oxidative stress-induced apoptosis via the mitochondrial apoptotic pathway by modulating autophagy in rats after traumatic brain injury," *American Journal of Translational Research*, vol. 9, no. 3, pp. 887–899, 2017.

[18] C. J. Xie, A. P. Gu, J. Cai, Y. Wu, and R. C. Chen, "Curcumin protects neural cells against ischemic injury in N2a cells and mouse brain with ischemic stroke," *Brain and Behavior*, vol. 8, Article ID e00921, 2018.

[19] Z. Chen, D. Wen, F. Wang, C. B. Wang, and L. Yang, "Curcumin protects against palmitic acid-induced apoptosis via the inhibition of endoplasmic reticulum stress in testicular

leydig cells," *Reproductive Biology and Endocrinology*, vol. 17, no. 1, 2019.

[20] A. Agarwal, A. Kasinathan, R. Ganesan et al., "Curcumin induces apoptosis and cell cycle arrest via the activation of reactive oxygen species-independent mitochondrial apoptotic pathway in Smad4 and p53 mutated colon adenocarcinoma HT29 cells," *Nutrition Research*, vol. 51, pp. 67–81, 2018.

[21] A. R. M. R. Amin, A. Haque, M. A. Rahman, Z. G. Chen, F. R. Khuri, and D. M. Shin, "Curcumin induces apoptosis of upper aerodigestive tract cancer cells by targeting multiple pathways," *PLoS One*, vol. 10, no. 4, Article ID e0124218, 2015.

[22] H. Liu, C. Wang, Z. Qiao, and Y. Xu, "Protective effect of curcumin against myocardium injury in ischemia reperfusion rats," *Pharmaceutical Biology*, vol. 55, no. 1, pp. 1144–1148, 2017.

[23] S. Chuengsamarn, S. Rattanamongkolgul, R. Luechapudiporn, C. Phisalaphong, and S. Jirawatnotai, "Curcumin extract for prevention of type 2 diabetes," *Diabetes Care*, vol. 35, no. 11, pp. 2121–2127, 2012.

[24] N. Poolsup, N. Suksomboon, P. D. M. Kurnianta, and K. Deawjaroen, "Effects of curcumin on glycemic control and lipid profile in prediabetes and type 2 diabetes mellitus: a systematic review and meta-analysis," *PLoS One*, vol. 14, no. 4, Article ID e0215840, 2019.

[25] L. Zhao, Q. Gu, L. Xiang et al., "Curcumin inhibits apoptosis by modulating Bax/Bcl-2 expression and alleviates oxidative stress in testes of streptozotocin-induced diabetic rats," *Therapeutics Clinical Risk Management*, vol. 13, pp. 1099–1105, 2017.

[26] X. Shen, L. Yang, S. Yan et al., "The effect of FFAR1 on pioglitazone-mediated attenuation of palmitic acid-induced oxidative stress and apoptosis in βTC6 cells," *Metabolism*, vol. 63, no. 3, pp. 335–351, 2014.

[27] H. He, Y. Luo, Y. Qiao et al., "Curcumin attenuates doxorubicin-induced cardiotoxicity via suppressing oxidative stress and preventing mitochondrial dysfunction mediated by 14-3-3γ," *Food & Function*, vol. 9, no. 8, pp. 4404–4418, 2018.

[28] M. C. Maiuri, E. Zalckvar, A. Kimchi, and G. Kroemer, "Self-eating and self-killing: crosstalk between autophagy and apoptosis," *Nature Reviews Molecular Cell Biology*, vol. 8, no. 9, pp. 741–752, 2007.

[29] R. Scherz-Shouval, E. Shvets, E. Fass, H. Shorer, L. Gil, and Z. Elazar, "Reactive oxygen species are essential for autophagy and specifically regulate the activity of Atg4," *The EMBO Journal*, vol. 26, no. 7, pp. 1749–1760, 2007.

[30] Y. Zhang, P. Chen, H. Hong, L. Wang, Y. Zhou, and Y. Lang, "JNK pathway mediates curcumin-induced apoptosis and autophagy in osteosarcoma MG63 cells," *Experimental and Therapeutic Medicine*, vol. 14, no. 1, pp. 593–599, 2017.

[31] J. Y. Kim, T. J. Cho, B. H. Woo et al., "Curcumin-induced autophagy contributes to the decreased survival of oral cancer cells," *Archives of Oral Biology*, vol. 57, no. 8, pp. 1018–1025, 2012.

[32] H. H. Liu, X. F. Zhang, S. S. Zhang et al., "Oxidative stress mediates microcystin-LR-induced endoplasmic reticulum stress and autophagy in KK-1 cells and C_{57}BL/6 mice ovaries," *Frontiers Physiology*, vol. 9, 2018.

Hindawi
Evidence-Based Complementary and Alternative Medicine
Volume 2021, Article ID 6649331, 9 pages
https://doi.org/10.1155/2021/6649331

Research Article

An Apriori Algorithm-Based Association Rule Analysis to Identify Acupoint Combinations for Treating Diabetic Gastroparesis

Ping-Hsun Lu,[1,2] **Jui-Lin Keng**,[3] **Fu-Ming Tsai**,[4] **Po-Hsuan Lu**,[5,6] **and Chan-Yen Kuo**[4]

[1]*Department of Chinese Medicine, Taipei Tzu Chi Hospital, Buddhist Tzu Chi Medical Foundation, New Taipei City, Taiwan*
[2]*School of Post-Baccalaureate Chinese Medicine, Tzu Chi University, Hualien, Taiwan*
[3]*Department of Applied Mathematics, University of Washington, Seattle, WA, USA*
[4]*Department of Research, Taipei Tzu Chi Hospital, Buddhist Tzu Chi Medical Foundation, New Taipei City, Taiwan*
[5]*Department of Medicine, Mackay Medical College, New Taipei City, Taiwan*
[6]*Department of Dermatology, Mackay Memorial Hospital, Taipei, Taiwan*

Correspondence should be addressed to Po-Hsuan Lu; pohsuan@gmail.com and Chan-Yen Kuo; cykuo863135@gmail.com

Received 4 December 2020; Revised 25 February 2021; Accepted 28 February 2021; Published 26 March 2021

Academic Editor: Youhua Xu

We explored the potential association rules within acupoints in treating diabetic gastroparesis (DGP) using Apriori algorithm complemented with another partition-based algorithm, a frequent pattern growth algorithm. Apriori algorithm is a data mining-based analysis that is widely applied in various fields, such as business and medicine, to mine frequent patterns in datasets. To search for effective acupoint combinations in the treatment of DGP, we implemented Apriori algorithm to investigate the association rules of acupoints among 17 randomized controlled trials (RCTs). The acupoints were extracted from the 17 included RCTs. In total, 29 distinct acupoints were observed in the RCTs. The top 10 frequently selected acupoints were CV12, ST36, PC6, ST25, BL21, BL20, BL23, SP6, BL18, and ST21. The frequency pattern of acupoints achieved by using a frequent pattern growth algorithm also confirms the result. The results showed that the most associated rules were {BL23, BL18} ≥ {SP6}, {BL20, BL18} ≥ {PC6}, {PC6, BL18} ≥ {BL20}, and {SP6, BL18} ≥ {BL23} in the database. Acupoints, including BL23, BL18, SP6, BL20, and PC6, can be deemed as core elements of acupoint combinations for treating DGP.

1. Introduction

With the changes in lifestyle and the prevalence of obesity, International Diabetes Federation has reported a total of 451 million people with diabetes in the world, and the number of diabetes mellitus (DM) patients may rise to 693 million in 2045. DM is a non-negligible problem in developing countries [1]. Diabetic gastroparesis (DGP) is a common complication of autonomic neuropathy that occurs in patients with hyperglycemia or DM. Furthermore, DGP affects around 4.8% of patients with type I DM and 1% of those with type II DM [2]. Nausea, vomiting, early satiety, postprandial fullness, abdominal distension, and abdominal pain are often observed in patients with DGP. Wide glycemic fluctuations and impact on quality of life are also noticed in DGP patients [3, 4]. The possible pathogenesis of DGP includes multiple factors, such as vagus neuropathy, abnormal myenteric neurotransmission, damage of inhibitory neuronal function, and the impaired function of smooth muscle cells and interstitial Cajal cells (ICCs) [5–7]. The suggested treatment for DGP depends on the severity. For mild-to-moderate patients, recommendations consist of controlling blood sugar, adjusting diet, and using prokinetic agents. For severe patients, gastric electrical stimulation or placement of a feeding jejunostomy to provide nutrition is suggested. Gastrectomy is the last resort for DGP refractory to treatment [5]. Metoclopramide, erythromycin, domperidone, and cisapride are prokinetic agents that are commonly used to treat DGP, but they present short-term efficacy and may have adverse

effects, including insomnia, extrapyramidal symptoms, and cardiac arrhythmias [5, 8]. To date, sufficient evidence that supports surgical treatment as beneficial for DGP is still lacking [8, 9]. Therefore, other alternative treatment options for DGP must be developed.

Acupuncture, an ancient therapy that has been used in China for over 2500 years, has become popular for its adjunctive role to ameliorate certain disease symptoms and to treat gastrointestinal tract disorders with limited side effects [10]. Acupuncture can improve gastric motility in animal models and humans [11, 12]. The possible mechanisms to improve the dyspeptic symptoms in DGP by acupuncture include restoration of the enteric nervous system (ENS), restoration of the ultrastructure and pacing function of ICCs, calibration of gastrointestinal hormone disorders, and improvement of gastrointestinal motility [13, 14]. The choice and combination of acupoints have been broadly accepted as important for successful acupuncture treatment. Yellow Emperor's Internal Classic and the ancient Meridian theory serve as guidelines for the selection of acupoints and their combination [15, 16]. Nevertheless, no consensus has been reached regarding the standard acupoint combinations for DGP treatment.

Data mining methods have been broadly applied in acupuncture. Data mining methods have been applied to evaluate the option and combination of acupuncture to treat reflux esophagitis [17], chronic atrophic gastritis [18], diarrhea [19], and diabetic peripheral neuropathy [20]. Given that acupuncture therapy focuses on numerous acupoints simultaneously in clinical practice, Apriori algorithm-based association rule analysis can be an essential and useful approach to explore the basic rules. Nevertheless, the acupoint combination for DGP treatment based on randomized controlled trials (RCTs) with a high level of evidence remains lacking. Data mining algorithms are frequently used in Chinese medicine and acupuncture combination analyses in the attempt to treat different types of syndromes [21]. Apriori, one of the association rule mining algorithms, proceeds by identifying the frequency of item sets in large databases and then determining their corresponding association rules [22]. Thus, Apriori algorithm provides comprehensive association rule analysis and offers insights into databases. Certain metrics, support, confidence, and lift are specified in Apriori to help us understand the strength of association rules [22]. Frequent pattern growth algorithm, on the other hand, mines the most frequent pattern and presents a dataset in the form of a tree with its structure constructed by the associations between items in the dataset. Similar to Apriori algorithm, it uses basic metrics, support, confidence, lift, and expected confidence to evaluate the frequent patterns [23].

In this paper, we primarily use Apriori algorithm to achieve the results, which are then further compared with the results obtained from the frequent pattern algorithm. We focused on the exploration of the promising core combination of acupoint combination to treat DGP by applying the Apriori association rule learning analysis based on RCTs [24].

2. Materials and Methods

2.1. Literature Search. Articles published up to January 2020 were searched for in PubMed, EMBASE, CENTRAL, and clinicaltrials.gov. The following MeSH and Emtree search headings were used: (diabet* AND gastroparesis) AND (acupuncture OR electroacupuncture OR acup*). For different databases, we have adjusted the search terms accordingly. Unpublished studies were sought out from the ClinicalTrials.gov registry (http://clinicaltrials.gov/). Only human studies were included. We extracted data on the acupoints used for DGP treatment from these 17 RCTs, fourteen of which were included in a meta-analysis article (Table 1) [24–27].

2.2. Study Selection. We selected RCTs to assess the efficacy of acupuncture in the treatment of DGP patients. The following inclusion criteria were applied: randomized controlled trials with DGP diagnosis without gastric outlet ulceration or obstruction by radiographic examination, treatment including acupuncture, electroacupuncture (EA), abdomen acupuncture, eye acupuncture, ear acupuncture, scalp acupuncture, acupuncture combined with acupuncture-related auxiliary techniques and with the sham acupuncture, or gastroprokinetic agents as the control groups, and quantified data available for DGP symptoms. The exclusion criteria were the use of moxibustion, transcutaneous electroacupuncture, acupoint injection, acupuncture therapy combined with Chinese materia medica, incomplete data, and quantified data available for dyspeptic symptoms.

2.3. Risk of Bias (RoB) Assessment. Two authors independently assessed the methodological quality of the included studies using the Cochrane Collaboration's RoB tool [18]. Any disagreement between the investigators was resolved by the third author. Several domains were assessed, namely, allocation generation; allocation concealment; blinding of participants, personnel, and outcome assessors; completeness of outcome data; freedom from selective reporting; and freedom from other forms of bias.

2.4. Data Analysis. In this study, software RStudio (version 1.2.5033, Integrated Development for R, RStudio, PBC, Boston, MA) was used to conduct Apriori association rule learning analysis and plot charts [28]. The dataset contains 14 columns, where each column represents individual formulas. The dataset was then fitted by using the R package "arules." Data visualization of the charts was performed by fitting the dataset into the R package, "arulesViz." In contrast, we utilized Python programming language's open-source package (Python Software Foundation, Python Language Reference, version 3.7), "pyfpgrowth," to conduct a frequent pattern growth algorithm [29].

Association rule learning algorithm is one of the widely used techniques to detect and analyze relations and useful information from transaction data. Numerous studies implemented association rule learning algorithms to identify

Table 1: Summary of 17 RCTs of acupuncture treatment for DGP.

Study (year)	Study design	Inclusion criteria	Acupoints	Overall bias
Wang et al. (2008)	RCT	DGP	ST36, LI4	High
Ge et al. (2010)	RCT	DGP	CV12, ST36, PC6	High
Shen et al. (2010)	RCT	DGP	PC6, CV12, CV6, ST36, SP6	High
Wang et al. (2010)	RCT	DGP	BL20, BL21, BL18, BL23, PC6, ST36, SP6, CV12	High
Zeng and Chai (2008)	RCT	DGP	BL21, CV12, BL20, LR13, BL23, BL18, LR14, GB25, ST25, ST36	High
Zhang et al. (2007)	RCT	DGP	CV12, ST36, PC6	High
Zheng and Ge (2010)	RCT	DGP	CV12, ST36, PC6	High
Han et al. (2001)	RCT	DGP	ST36, ST25, PC6, ST39, CV12	High
Li (2006)	RCT	DGP	ST36, CV12, ST25, BL21, BL20, LR3, BL23, PC6	High
Wang (2007)	RCT	DGP	BL21, CV12, BL20, LR13, BL23, BL18, LR14, GB25, ST25, ST36	High
Wang et al. (2009)	RCT	DGP	CV17, CV13, CV12, CV4, CV10, CV8, CV6	High
Chen (2008)	RCT	DGP	CV12, ST36, ST25, ST21, ST37	High
Zhao (2011)	RCT	DGP	ST36, CV12, ST25, ST21, ST37	High
Chen (2005)	RCT	DGP	CV12, ST21, ST25, BL21, ST36	High
Zhang et al. (2013)	RCT	DGP	CV12, ST36, PC6	High
Li et al. (2015)	RCT	DGP	CV12, ST36, PC6	Low
Song et al. (2020)	RCT	DGP	CV12, ST36, PC6, SP9, SP10, SP6, SP8, LI11, LI4, ST40, LR3, SP4	High

RCT: randomized controlled trial; DGP: diabetic gastroparesis.

medicine compatibility and to find interdependence within medical record data [22]. The association rule learning algorithm contains an antecedent and consequent set, both of which are a set of items.

Support and confidence factors are essential parameters in association rule learning. Support estimates the frequency of an acupoint appearing in the 14 formulas. On the other hand, confidence measures the frequency of acupoint A appearing in the formula, given that acupoint B appears simultaneously. Expected confidence is the number of formulas that include the consequent set of acupoints divided by the total number of formulas. Lift is the likelihood of an increase in the consequent given a particular antecedent. Namely, lift is the probability of the acupoint B appearing when acupoint A is present in a DGP formula given an expected confidence. It equals the confidence divided by expected confidence. During the exploration of the association rules, users need to test multiple combinations of minimum values for support and confidence factors to discover the significant association rules. However, the selection of thresholds showed slight ambiguity and varied from case to case. If the parameter thresholds were set at extremely high values, then certain meaningful information would be discarded.

In this study, the minimum thresholds for support and confidence factors were 20% and 60%, respectively. The highest value of the support factor was 0.6, and by increasing the minimum value of support from 0.1 to 0.2, we can filter out 82 rules down to 19 rules given that the confidence's minimum value was set to 0.6. The association rules were sorted by support factor in descending order.

3. Results

3.1. Study Characteristics. The acupuncture treatment for DGP used an average of five acupoints, and the average duration of treatment was 22 days. In the meta-analysis, compared with the control group, acupuncture therapy showed a higher response rate (RR, 1.20 (95% confidence interval (CI), 1.12 to 1.29), $P < 0.00001$) and significantly improved dyspeptic symptoms like stomach fullness, loss of appetite, and nausea and vomiting in the treatment group, but there is no real difference between the two groups of gastric emptying [24]. Li et al. reported that in patients with diabetic gastroparesis, acupuncture reduces gastric retention, improves gastroparesis symptoms [25], and is effective for epigastric fullness [27]. Song et al. showed acupuncture treatment improved the DGP symptom score and reduced serum content of transmembrane protein 16A (a selective marker of ICC) [26].

3.2. RoB Assessment. Table 1 summarizes the methodological quality of the included studies, whereas Supplementary Figure 1 provides the detailed RoB assessment. The 17 RCTs exhibited variable overall quality. This finding can be possibly explained by one of the following reasons. The random sequences of 11 studies out of 17 trials were correct and had apparent descriptions [24–27]. None of the retrieved studies gave a detailed description of allocation concealment, only two trials used patient blinding with sham electro-acupuncture [24, 25], seven studies reported incomplete data, and seven studies did not give the baseline comparison of the severity of DGP symptoms [24].

3.3. Acupoint Distribution. We identified 29 acupoints from the 17 RCTs on acupuncture treatment for DGP. Figure 1 shows the frequency distribution of acupoints. The 10 most frequently selected acupoints for treating DGP were CV12, ST36, PC6, ST25, BL21, BL20, BL23, SP6, BL18, and ST21.

3.4. Apriori Algorithm-Based Association Rule Analysis for Item Sets of Herb Combinations. We investigated 11 association rules in accordance with the 17 acupoint formulas for

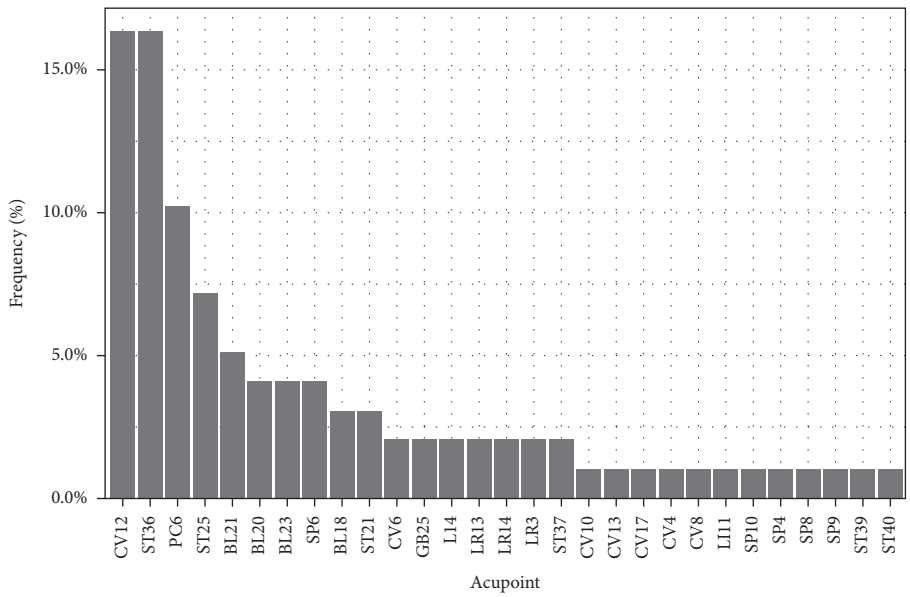

Figure 1: Frequency distribution of acupoints used in the 17 RCTs of acupuncture treatment for DGP.

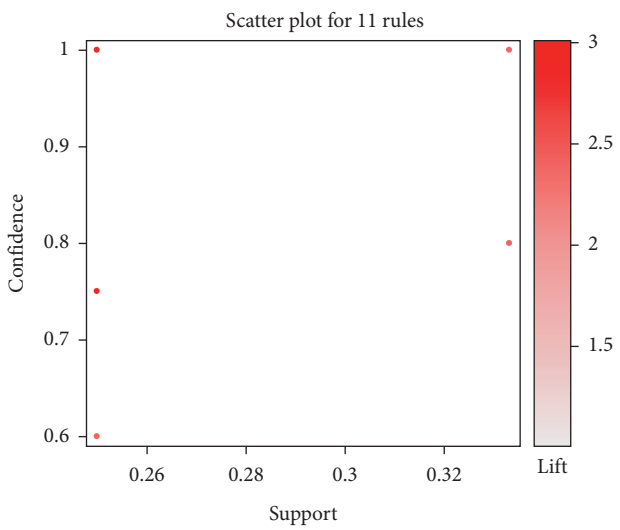

Figure 2: Scatter plot for the 11 association rules obtained in the 17 RCTs of acupuncture treatment for DGP via an Apriori algorithm-based association rule analysis.

treating DGP. The association rules were shown based on the scatter plot with support on the x-axis and confidence on the y-axis. The color of each association rule was decided by the metric's corresponding value and lift (Figure 2). The results demonstrated that the lift values of 11 association rules were larger than 1. Thus, the likelihood of the antecedent and consequent acupoints being selected in the same formula was statistically significantly larger than that of consequent acupoint being selected alone. The metric values for the confidence of all 11 association rules were at least larger than 0.6. Therefore, for each rule, the likelihood of the consequent acupoint being selected when antecedent acupoints are selected is relatively high. By contrast, the metric values for support ranged from 0.2 to 0.6, indicating the frequency of each individual antecedent acupoint appearing in the formula. This finding suggests the presence of a core list of acupoints to select from for the treatment of DGP. All 11 association rules were ordered by the metric and support (Table 2).

A grouped matrix diagram was used to cluster similar rules into groups (circles) and display the general distribution of association rules (Figure 3). Six clusters were on the horizontal ordinate, and the vertical ordinate represented the acupoints generated by these six clusters (rules). The darker the color of a circle was, the higher was the degree of lift of a group. The size of a circle represents the degree of support. Thus, the larger the circle was, the higher was the degree of support. Figure 4 shows the network graph visualization. The figure shows the 11 association rules found among the 17 acupoint formulas. Acupoints ST36 and CV12 were most likely to be used in association with other acupoints.

3.5. Apriori Algorithm-Based Association Rule Analysis for Item Sets of Herb Combinations Complemented with Frequent Pattern Growth Algorithm. Table 3 shows the frequent patterns of acupoint used in the 17 RCTs based on frequent pattern growth algorithm, and its results are coherent with the result in Figure 4. However, the values of lift to the association rules containing ST36 and CV12 were low, and thus they were not selected in the following result. Acupoints {BL23, BL18} ≥ {SP6}, {BL20, BL18} ≥ {PC6}, {PC6, BL18} ≥ {BL20}, and {SP6, BL18} ≥ {BL23} were selected, revealing item sets of antecedent and consequent acupoints. The results of selected association rules matched the association rule #8 {BL23} ≥ {SP6}, #3 {BL20} ≥ {PC6}, #4 {PC6} ≥ {BL20}, and #9 {SP6} ≥ {BL23} in Table 2. Likewise, the results of selected association rules are consistent with #17 ("PC6," "SP6") ≥ ("CV12," "ST36"), #19 (CV12, SP6) ≥ (PC6, ST36), # 6 (BL18, CV12) ≥ (BL20, BL21, BL23), #9 (BL23, CV12) ≥ (BL20, BL21), #4 (BL20, BL21) ≥ (BL23,

Table 2: Apriori algorithm-based association rules for acupoints used in the 17 RCTs on acupuncture treatment for DGP.

No.	Association rules	Support	Confidence	Expected confidence	Lift
1	{PC6} ≥ {CV12}	0.3333333	1.0000000	0.4166667	2.400000
2	{CV12} ≥ {PC6}	0.3333333	0.8000000	0.4166667	2.400000
3	{BL20} ≥ {PC6}	0.2500000	1.0000000	0.3333333	3.000000
4	{PC6} ≥ {BL20}	0.2500000	0.7500000	0.3333333	3.000000
5	{BL20} ≥ {CV12}	0.2500000	1.0000000	0.4166667	2.400000
6	{CV12} ≥ {BL20}	0.2500000	0.6000000	0.4166667	2.400000
7	{BL21} ≥ {ST36}	0.2500000	1.0000000	0.5000000	2.000000
8	{BL23} ≥ {SP6}	0.2500000	1.0000000	0.3333333	3.000000
9	{SP6} ≥ {BL23}	0.2500000	0.7500000	0.3333333	3.000000
10	{SP6} ≥ {ST36}	0.2500000	0.7500000	0.6666667	1.500000
11	{CV12} ≥ {ST36}	0.2500000	0.6000000	0.8333333	1.200000

DGP: diabetic gastroparesis.

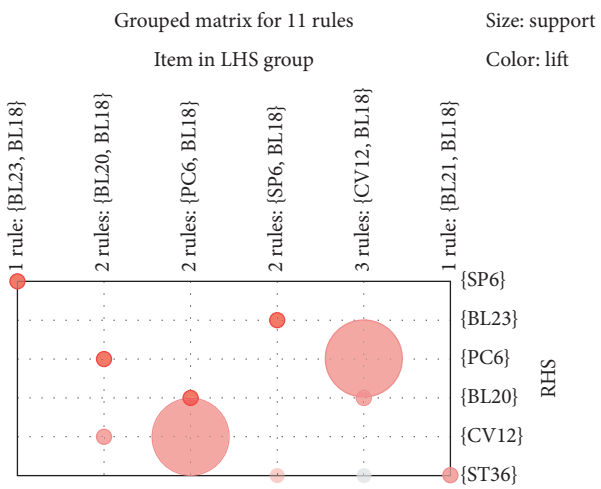

Figure 3: Grouping matrix for the 11 association rules obtained in the 17 RCTs of acupuncture treatment for DGP via an Apriori algorithm-based association rule analysis.

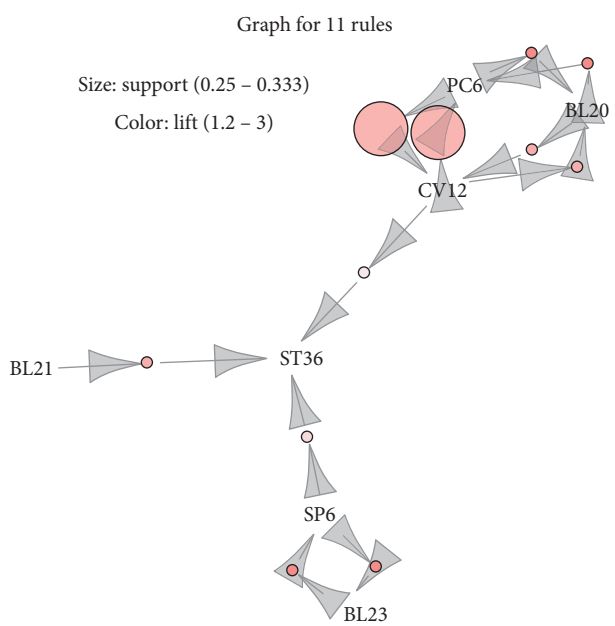

Figure 4: Combination matrix of association rules obtained in the 17 RCTs of acupuncture treatment for DGP via an Apriori algorithm-based association rule analysis.

Table 3: Frequent patterns of acupoints used in the 17 RCTs on acupuncture treatment for DGP.

No.	Frequent pattern	Support
1	("CV12," "ST36")	1.071429
2	("CV12," "PC6")	0.714286
3	("PC6," "ST36")	0.714286
4	("CV12," "ST25")	0.500000
5	("ST25," "ST36")	0.500000
6	("BL21," "ST36")	0.357143
7	("BL21," "CV12")	0.357143
8	("BL23," "ST36")	0.285714
9	("BL23," "CV12")	0.285714
10	("BL21," "BL23")	0.285714
11	("BL20," 'BL23")	0.285714
12	("BL20," "ST36")	0.285714
13	("BL20," "CV12")	0.285714
14	("BL20," "BL21")	0.285714
15	("CV12," "SP6")	0.285714
16	("SP6," "ST36")	0.285714
17	("PC6," "SP6")	0.285714
18	("CV12," "ST21")	0.214286
19	("ST21," "ST36")	0.214286
20	("ST21," "ST25")	0.214286
21	("BL18," "ST36")	0.214286
22	("BL18," "CV12")	0.214286
23	("BL18," "BL21")	0.214286
24	("BL18," "BL20")	0.214286
25	("BL18," "BL23")	0.214286

DGP: diabetic gastroparesis.

ST36), #5 (BL21, BL23) ≥ (BL20, ST36), #17 (PC6, SP6) ≥ (CV12, ST36), and #7 (BL21, CV12) ≥ (ST36) in Table 4.

4. Discussion

This study indicated BL23, BL18, and SP6 and BL20, BL18, and PC6 as the major acupoint combinations in treating DGP, as confirmed by Apriori association-mining analysis (Figure 5). RCTs of acupuncture for DGP revealed that the acupoint combination played a role in relieving dyspeptic symptoms in patients with DGP.

The evidence-based strategies help to ascertain the efficacy of selecting acupoints for further treatment. To the

Table 4: 24 frequent pattern growth algorithm-based association rules obtained in the 17 RCTs on acupuncture treatment for DGP.

No.	LHS	RHS	Confidence
1	(BL18, BL20)	(BL21, BL23, ST36)	1.00
2	(BL18, BL23)	(BL20, BL21, ST36)	1.00
3	(BL20, BL23)	(BL21, ST36)	1.00
4	(BL18, BL21)	(BL20, BL23, ST36)	1.00
5	(BL20, BL21)	(BL23, ST36)	1.00
6	(BL21, BL23)	(BL20, ST36)	1.00
7	(BL18, CV12)	(BL20, BL21, BL23)	1.00
8	(BL21, CV12)	(ST36)	0.60
9	(BL20, CV12)	(BL21, BL23)	1.00
10	(BL23, CV12)	(BL20, BL21)	1.00
11	(BL18, ST36)	(BL20, BL21, BL23)	1.00
12	(BL21, ST36)	(CV12)	0.60
13	(BL20, ST36)	(BL21, BL23)	1.00
14	(BL23, ST36)	(BL20, BL21)	1.00
15	(ST21, ST25)	(CV12)	1.00
16	(ST21, ST36)	(ST25)	1.00
17	(CV12, ST21)	(ST25)	1.00
18	(PC6, SP6)	(CV12, ST36)	0.75
19	(SP6, ST36)	(CV12, PC6)	0.75
20	(CV12, SP6)	(PC6, ST36)	0.75
21	(CV12, ST25)	(ST36)	1.00
22	(ST25, ST36)	(CV12)	1.00
23	(CV12, PC6)	(ST36)	1.00
24	(CV12, ST36)	(PC6)	0.66

DGP: diabetic gastroparesis.

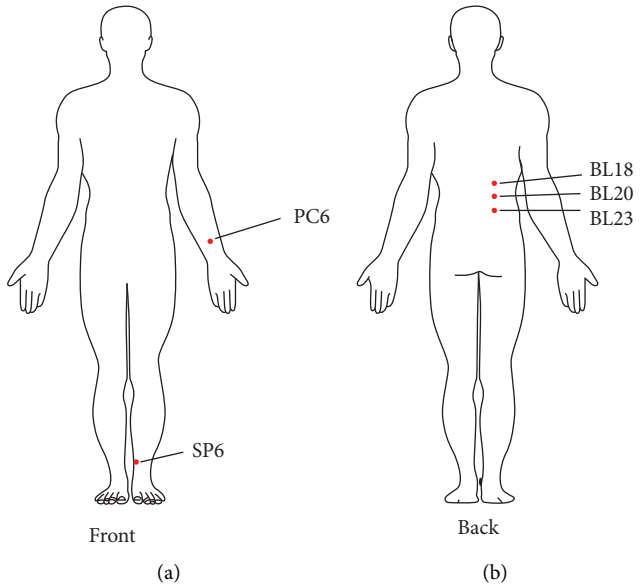

Figure 5: Location of core acupoints derived from association rules obtained in the 17 RCTs of acupuncture treatment for DGP.

best of our knowledge, this study is the first report on potential core acupoint combinations to treat patients with DGP based on RCTs and data mining analysis. The core acupoint combinations are helpful for patients with DGP; the possible fundamental mechanisms include restoration of ICC [13, 30], mediation of hormones, restoration of the ENS, and enhancement of gastrointestinal motility [14, 31]. Stimulating ST36 and CV12 points of the DGP rat with EA can reduce ICC apoptosis and restore ICC structure and pacing function, possibly through the mouse stem cell factor (SCF)/KIT-ETV1 signaling pathway to upregulate the mRNA of SCF and neuronal nitric oxide synthase [32–34]. Hou et al. reported an RCT that included 40 postoperative patients with gastrointestinal tumors; this RCT showed that electrical stimulation on acupoints ST36 and ST37 can elevate the serum levels of gastrin and motilin and

Table 5: Potential efficacy of the core acupoints for DGP treatment.

Point	Chinese name	English name	Primary meridians	Efficacy
BL18 [49]	Ganshu	Liver locus	Bladder	Activation of CRH-like neurons; modulation of the expressions of CRH and GR in the PVN
BL20 [54]	Pishu	Spleen locus	Bladder	Suppresses acid secretion and increases β-EP and SS
BL23 [49]	Shenshu	Kidney locus	Bladder	Activation of CRH-like neurons; modulation of the expressions of CRH and GR in the PVN
SP6 [50–52]	Sanyinjiao	Crossroad at three Yin	Spleen	Protection of ICCs, amelioration of vascular endothelial dysfunction, and modulation of ghrelin
PC6 [54–56]	Neiguan	Inner pass	Pericardium	Suppresses acid secretion, increases β-EP and SS, modulates vagovagal neurocircuits, and decreases the number of double-labeled OT neurons and c-fos neurons

DGP: diabetic gastroparesis; CRH: corticotropin-releasing hormone; GR: glucocorticoid receptor; PVN: paraventricular nucleus of the hypothalamus; β-EP; beta-endorphin; SS: somatostatin; GD: gastric distention; ICCs: interstitial Cajal cells; OT: oxytocin.

electrogastrogram frequency. Additionally, the recovery of gastrointestinal function and reduction of complications, such as flatulence, abdominal pain, and diarrhea, were noted [35]. Jang et al. reported that stimulation with acupoint ST36 in mice can promote the motility of the small intestine via the decrease in serum levels of vasoactive intestinal peptide and an increase in serum levels of motilin, ghrelin, and gastrin [36]. Liang et al. demonstrated that electrical stimulation on acupoints ST36 and ST25 of a constipation mouse model can improve gastrointestinal motility by regulating excitatory and inhibitory neurons in ENS [37]. High-frequency electrical stimulation of ST36 in diabetic rats can promote the regeneration of lost enteric neurons through glial cell-derived neurotrophic factor and phosphatidylinositol-3 kinase/Akt signaling pathways [38].

The combination of acupoints was reported to exhibit greater therapeutic efficacy than a single acupoint [39, 40]. Wang et al. reported that the combination of multiple acupoints resulted in improved the score of the Pittsburgh sleep quality index and Athens Insomnia Scale via regulation of the activity of the brain area related to sleep experience [39]. The RCT which enrolled 30 patients with hypertension showed that the combined acupuncture points LR3 and KI3 can activate a wider area of the brain than a single point acupuncture based on the resting-state functional magnetic resonance imaging scan [41]. Gao et al. demonstrated that stimulating acupoint combination in slow transit constipation mice showed higher defecation grain number and intestinal propulsion rate compared with a single acupoint [42]. In DGP model rats, stimulation of the combined acupoints ST36 and CV12 can produce more ICCs than the single point ST36 [43]. Hence, an acupoint combination displays better pharmacological efficacy than a single acupoint. Even though there are also articles discussing the compatibility laws of acupuncture in the treatment of DGP, it uses fewer databases, not selects a higher level of evidence article, such as RCT, and does not elaborate on the association analysis [44, 45]. We implemented systemic review and Apriori algorithm to investigate the association rules of acupoints among 17 RCTs to demonstrate the effectiveness of acupuncture on patients with DGP. Moreover, research studies indicate that the core acupoint combinations we discovered can improve DGP through the protection of ICCs, amelioration of vascular endothelial dysfunction, hormone modulation, and stimulation of neurons [46–53] (Table 5).

4.1. Limitation. Despite our results on potential core acupoint combinations for the treatment of DGP, our study has several limitations. First, most RCTs included in this meta-analysis revealed a high RoB, and only two studies used the blinding method. Thus, a high RoB should be considered to explain these results. Second, most RCTs lacked a careful follow-up. The treatment duration was 22 days on average in this meta-analysis. Therefore, further research should be carried out regarding the long-term efficacy and safety of these core acupoint combinations for DGP. Third, as the mechanisms of action of acupoint combinations are unclear, more basic and clinical studies are required for a comprehensive assessment.

5. Conclusions

Based on RCTs and data mining analysis, the acupoint combinations of BL23, BL18, and SP6 and BL20, BL18, and PC6 are potential acupuncture treatments for DGP. The acupoint combinations also significantly improved stomach fullness, nausea and vomiting, and loss of appetite. However, further trials with larger sample sizes and appropriate controls are recommended.

Data Availability

The data utilized to support the findings of this study are included within the article.

Conflicts of Interest

The authors declare that there are no conflicts of interest regarding the publication of this article.

Acknowledgments

The authors thank Taipei Tzu Chi Hospital and the participants for their contribution to the study. This study was supported by Taipei Tzu Chi Hospital, Buddhist Tzu Chi Medical Foundation, New Taipei City, Taiwan (TCRD-TPE-109-12, TCRD-TPE-109-06(1/2), and TCRD-TPE-110-49).

Supplementary Materials

Supplementary Figure 1: RoB assessment of the retrieved RCTs. (*Supplementary Materials*)

References

[1] N. H. Cho, J. E. Shaw, S. Karuranga et al., "IDF diabetes atlas: global estimates of diabetes prevalence for 2017 and projections for 2045," *Diabetes Research and Clinical Practice*, vol. 138, pp. 271–281, 2018.

[2] B. Moshiree, M. Potter, and N. J. Talley, "Epidemiology and pathophysiology of gastroparesis," *Gastrointestinal Endoscopy Clinics of North America*, vol. 29, no. 1, pp. 1–14, 2019.

[3] S. Krishnasamy and T. L. Abell, "Diabetic gastroparesis: principles and current trends in management," *Diabetes Therapy*, vol. 9, no. 1, pp. 1–42, 2018.

[4] W. A. Hoogerwerf, P. J. Pasricha, A. N. Kalloo, and M. M. Schuster, "Pain: the overlooked symptom in gastroparesis," *American Journal of Gastroenterology*, vol. 94, no. 4, pp. 1029–1033, 1999.

[5] G. S. Aswath, L. A. Foris, A. K. Ashwath, and K. Patel, *Diabetic Gastroparesis*, StatPearls Publishing LLC., Treasure Island, FL, USA, 2020.

[6] S. S. Yarandi and S. Srinivasan, "Diabetic gastrointestinal motility disorders and the role of enteric nervous system: current status and future directions," *Neurogastroenterology & Motility*, vol. 26, no. 5, pp. 611–624, 2014.

[7] K. Kishi, N. Kaji, T. Kurosawa, S. Aikiyo, and M. Hori, "Hyperglycemia in the early stages of type 1 diabetes accelerates gastric emptying through increased networks of interstitial cells of Cajal," *PLoS One*, vol. 14, no. 10, p. e0222961, 2019.

[8] H. P. Parkman, W. L. Hasler, and R. S. Fisher, "American gastroenterological association technical review on the diagnosis and treatment of gastroparesis," *Gastroenterology*, vol. 127, no. 5, pp. 1592–1622, 2004.

[9] M. P. Jones and K. Maganti, "A systematic review of surgical therapy for gastroparesis," *American Journal of Gastroenterology*, vol. 98, no. 10, pp. 2122–2129, 2003.

[10] "Acupuncture NCDPo. Acupuncture," *JAMA*, vol. 280, no. 17, pp. 1518–1524, 1998.

[11] J. Chen, G.-Q. Song, J. Yin, T. Koothan, and J. D. Z. Chen, "Electroacupuncture improves impaired gastric motility and slow waves induced by rectal distension in dogs," *American Journal of Physiology-Gastrointestinal and Liver Physiology*, vol. 295, no. 3, pp. G614–G620, 2008.

[12] J. Yin and J. D. Chen, "Gastrointestinal motility disorders and acupuncture," *Autonomic Neuroscience*, vol. 157, no. 1-2, pp. 31–37, 2010.

[13] Y. Gao, G. Lu, Y. Y. Wang, L. Chen, R. Chen, and F. X. Liang, "[Prospects and progress on the mechanisms of acupuncture underlying improvement in diabetic gastroparesis]," *Zhen Ci Yan Jiu*, vol. 42, no. 4, pp. 367–371, 2017.

[14] Y. Feng, Y. Fang, Y. Wang, and Y. Hao, "Acupoint therapy on diabetes mellitus and its common chronic complications: a review of its mechanisms," *BioMed Research International*, vol. 2018, Article ID 3128378, 9 pages, 2018.

[15] W. Zhou and P. Benharash, "Effects and mechanisms of acupuncture based on the principle of meridians," *Journal of Acupuncture and Meridian Studies*, vol. 7, no. 4, pp. 190–193, 2014.

[16] W. B. Zhang, Y. P. Wang, and H. Y. Li, "[Analysis on correlation between meridians and viscera in book the yellow emperor's internal classic]," *Zhen Ci Yan Jiu*, vol. 43, no. 7, pp. 424–429, 2018.

[17] Y. Yi, L. X. Pei, H. Chen et al., "[Analysis on acupoint selection rules for reflux esophagitis]," *Zhongguo Zhen Jiu*, vol. 40, no. 5, pp. 557–564, 2020.

[18] Y. Liu, H. Gong, J. Liu, and H. Zhang, "[Acupoint selection pattern of chronic atrophic gastritis based on data mining methods of latent structure model and frequency item set]," *Zhongguo Zhen Jiu*, vol. 38, no. 6, pp. 667–671, 2018.

[19] Z. W. Su, Y. L. Ren, S. Y. Zhou et al., "[Analysis on characteristics of meridians and acupoints of acupuncture and moxibustion for diarrhea in ancient based on data mining]," *Zhongguo Zhen Jiu*, vol. 33, no. 10, pp. 905–909, 2013.

[20] H. Pan, H. Wang, Y. Wang, and H. Huang, "[Rules of acupoint selection for diabetic peripheral neuropathy based on data mining technology]," *Zhongguo Zhen Jiu*, vol. 36, no. 10, pp. 1111–1114, 2016.

[21] P.-H. Lu, J.-L. Keng, K.-L. Kuo, Y.-F. Wang, Y.-C. Tai, and C.-Y. Kuo, "An Apriori algorithm-based association rule analysis to identify herb combinations for treating uremic pruritus using Chinese herbal bath therapy," *Evidence-Based Complementary and Alternative Medicine*, vol. 2020, Article ID 8854772, 9 pages, 2020.

[22] R. J. Bayardo Jr. and R. Agrawal, "Mining the most interesting rules," in *Proceedings of the Fifth ACM SIGKDD International Conference on Knowledge Discovery and Data Mining*, San Diego, CA, USA, August 1999.

[23] J. Han and J. Pei, "Mining frequent patterns by pattern-growth: methodology and implications," *ACM SIGKDD Explorations Newsletter*, vol. 2, no. 2, pp. 14–20, 2000.

[24] M. Yang, X. Li, S. Liu et al., "Meta-analysis of acupuncture for relieving non-organic dyspeptic symptoms suggestive of diabetic gastroparesis," *BMC Complementary Medicine and Therapies*, vol. 13, p. 311, 2013.

[25] G. Li, C. Huang, X. Zhang et al., "The short-term effects of acupuncture on patients with diabetic gastroparesis: a randomised crossover study," *Acupuncture in Medicine*, vol. 33, no. 3, pp. 204–209, 2015.

[26] Y. J. Song, X. Wang, X. J. Li, and Z. L. Zhang, "[Effect of Tiaoli Piwei needling technique on diabetic gastroparesis and transmembrane protein 16A]," *Zhongguo Zhen Jiu*, vol. 40, no. 8, pp. 811–815, 2020.

[27] B. M. Zhang, Z. H. Hu, Y. Shou, Y. Wang, S. W. Xu, and Y. Yang, "Treatment of diabetic gastroparesis by acupuncture therapy: a multi-center randomized controlled trial," *Shanghai Journal of Traditional Chinese Medicine*, vol. 47, no. 3, pp. 31–34, 2013.

[28] J. Verzani, *Getting Started with RStudio:*, O'Reilly Media, Inc., Newton, MA, USA, 2011.

[29] R. Gv and F. L. Drake, *The Python Language Reference Manual*, Network Theory Ltd., London, UK, 2011.

[30] X. Wei, Y. Lin, D. Zhao et al., "Electroacupuncture relieves suppression of autophagy in interstitial cells of cajal of diabetic

gastroparesis rats," *Canadian Journal of Gastroenterology and Hepatology*, vol. 2020, Article ID 7920715, 10 pages, 2020.

[31] X. F. Wu, X. L. Chen, X. N. Zheng et al., "[Effect of different stimulating strength of electroacupuncture on gastrointestinal motility and RhoA/ROCK signaling in gastric antral smooth muscle in diabetic gastroparesis rats]," *Zhen Ci Yan Jiu*, vol. 43, no. 3, pp. 169–174, 2018.

[32] C.-C. Zhang, Y.-P. Lin, Y. Peng et al., "Study on the mechanisms of electroacupuncture for promoting gastrointestinal motility in rats with diabetic gastroparesis," *Journal of Acupuncture and Tuina Science*, vol. 15, no. 3, pp. 158–164, 2017.

[33] L. Tian, B. Zhu, and S. Liu, "Electroacupuncture at ST36 protects ICC networks via mSCF/kit-ETV1 signaling in the stomach of diabetic mice," *Evidence-based Complementary and Alternative Medicine*, vol. 2017, Article ID 3980870, 13 pages, 2017.

[34] C. C. Zhang, Y. P. Lin, Y. Peng et al., "[Effects of electroacupuncture on ultrastructure of interstitial cells of cajal and stem cell factor-kit signal pathway of gastric antrum in diabetic gastroparesis rats]," *Zhen Ci Yan Jiu*, vol. 42, no. 6, pp. 482–488, 2017.

[35] L. Hou, L. Xu, Y. Shi, and F. Gu, "Effect of electric acupoint stimulation on gastrointestinal hormones and motility among geriatric postoperative patients with gastrointestinal tumors," *Journal of Traditional Chinese Medicine*, vol. 36, no. 4, pp. 450–455, 2016.

[36] J.-H. Jang, D.-J. Lee, C.-H. Bae et al., "Changes in small intestinal motility and related hormones by acupuncture stimulation at Zusanli (ST 36) in mice," *Chinese Journal of Integrative Medicine*, vol. 23, no. 3, pp. 215–220, 2017.

[37] C. Liang, K. Y. Wang, M. R. Gong, Q. Li, Z. Yu, and B. Xu, "Electro-acupuncture at ST37 and ST25 induce different effects on colonic motility via the enteric nervous system by affecting excitatory and inhibitory neurons," *Neurogastroenterologu and Motility*, vol. 30, no. 7, p. e13318, 2018.

[38] F. Du and S. Liu, "Electroacupuncture with high frequency at acupoint ST-36 induces regeneration of lost enteric neurons in diabetic rats via GDNF and PI3K/AKT signal pathway," *American Journal of Physiology-Regulatory, Integrative and Comparative Physiology*, vol. 309, no. 2, pp. R109–R118, 2015.

[39] Y. K. Wang, T. Li, L. J. Ha et al., "Effectiveness and cerebral responses of multi-points acupuncture for primary insomnia: a preliminary randomized clinical trial and fMRI study," *BMC Complementary Medicine and Therapies*, vol. 20, no. 1, p. 254, 2020.

[40] P. C. Hsieh, C. F. Cheng, C. W. Wu et al., "Combination of acupoints in treating patients with chronic obstructive pulmonary disease: an apriori algorithm-based association rule analysis," *Evidence-Based Complementary and Alternative Medicine*, vol. 2020, Article ID 8165296, 7 pages, 2020.

[41] J. Zhang, X. Cai, Y. Wang et al., "Different brain activation after acupuncture at combined acupoints and single acupoint in hypertension patients: an rs-fMRI study based on ReHo analysis," *Evidence-Based Complementary and Alternative Medicine*, vol. 2019, Article ID 5262896, 10 pages, 2019.

[42] F. Gao, H. M. Sheng, T. N. Zhang, S. B. Wu, J. Cao, and M. Q. Zhou, "[Effect of manual acupuncture stimulation of single acupoint or acupoints combination on intestinal movement in slow transit constipation mice]," *Zhen Ci Yan Jiu*, vol. 42, no. 1, pp. 62–66, 2017.

[43] Y. Q. Li, B. Yu, T. Li, Z. J. Zhao, M. J. Yang, and F. C. Wang, "Effect of acupuncture at single acupoint and combined acupoints on antral interstitial cells of cajal in diabetic gastroparesis model rats," *World Chinese Medicine*, vol. 11, no. 2, pp. 214–218, 2016.

[44] F. Cao, T. Li, L. J. Ha, C. X. Shan, M. J. Zhi, and F. C. Wang, "[Analysis of compatibility laws for acupoint selection of acupuncture in treating diabetic gastroparasis]," *Zhongguo Zhong Xi Yi Jie He Za Zhi*, vol. 36, no. 5, pp. 549–552, 2016.

[45] P. Li, Y. Z. Hui, Q. Q. Wen, and Y. Wang, "Analysis of acupoint selection rules to treat diabetic gastroparesis with acupuncture based on the clinical controlled trials," *Journal of Clinical Acupuncture and Moxibustion*, vol. 31, no. 6, pp. 37–39, 2015.

[46] E. Siegel, *The Acupuncture Point Functions Charts and Workbook*, Jessica Kingsley Publishers, London, UK, 2019.

[47] C. Liang, Y. Wang, B. Xu, and Z. Yu, "[Effect of acupuncture at different acupoints on electric activities of rat cerebellar fastigial nuclear]," *Zhongguo Zhong Xi Yi Jie He Za Zhi*, vol. 35, no. 4, pp. 476–480, 2015.

[48] H. Wang, W. J. Liu, G. M. Shen, M. T. Zhang, S. Huang, and Y. He, "Neural mechanism of gastric motility regulation by electroacupuncture at RN12 and BL21: a paraventricular hypothalamic nucleus-dorsal vagal complex-vagus nerve-gastric channel pathway," *World Journal of Gastroenterology*, vol. 21, no. 48, pp. 13480–13489, 2015.

[49] S. J. Wang, J. J. Zhang, H. Y. Yang, F. Wang, and S. T. Li, "Acupoint specificity on acupuncture regulation of hypothalamic- pituitary-adrenal cortex axis function," *BMC Complementary and Alternative Medicine*, vol. 15, p. 87, 2015.

[50] L. Liu, X. F. Wu, X. N. Zheng et al., "[Effect of point-moxibustion and electroacupuncture on the expression of endothelial nitric oxide synthase mRNA and angiotensin 2 mRNA in gastric antrum in diabetic gastroparesis rats]," *Zhen Ci Yan Jiu*, vol. 42, no. 3, pp. 240–245, 2017.

[51] Y. Peng, Y.-P. Lin, F.-E. He, and S.-X. Yi, "Effect of electroacupuncture on gastric motility, expressions of ghrelin and GHSR mRNA in gastric antrum tissue of diabetic gastroparesis rats," *Journal of Acupuncture and Tuina Science*, vol. 15, no. 2, pp. 88–93, 2017.

[52] J. W. Yang, Y. Peng, H. J. Chen et al., "[Effect of electroacupuncture intervention on gastrointestinal motility and expression of insulin-like growth factor 1 and its receptor proteins in gastric antrum in diabetic gastroparesis rats]," *Zhen Ci Yan Jiu*, vol. 42, no. 4, pp. 315–320, 2017.

[53] L. Chao, W. Yuan, X. Bin, and Y. Zhi, "Effect of acupuncture at three different acupoints on electrical activity of gastric distention-affected neurons in rat medial vestibular nucleus," *Journal of Traditional Chinese Medicine*, vol. 38, no. 1, pp. 125–131, 2018.

[54] H. Li, T. He, Q. Xu et al., "Acupuncture and regulation of gastrointestinal function," *World Journal of Gastroenterology*, vol. 21, no. 27, p. 8304, 2015.

[55] M. Lu, C. Chen, W. Li, Z. Yu, and B. Xu, "EA at PC6 promotes gastric motility: role of brainstem vagovagal neurocircuits," *Evidence-Based Complementary and Alternative Medicine*, vol. 2019, Article ID 7457485, 10 pages, 2019.

[56] C.-Y. Yong, S. Chen, H. Chen et al., "Effects of needling acupoints at different nerve segments on oxytocin neurons in rat's hypothalamic paraventricular nucleus and intragastric pressure," *Journal of Acupuncture and Tuina Science*, vol. 17, no. 5, pp. 297–304, 2019.

Hindawi
Evidence-Based Complementary and Alternative Medicine
Volume 2021, Article ID 6699935, 13 pages
https://doi.org/10.1155/2021/6699935

Review Article

A Meta-Analysis of the Effects of Tai Chi on Glucose and Lipid Metabolism in Middle-Aged and Elderly Diabetic Patients: Evidence from Randomized Controlled Trials

Ya-nv Liu,[1] Lin Wang,[1,2] Xin Fan,[2] Shijie Liu,[3] Qi Wu,[1] and You-Ling Qian[4,5]

[1]*Department of Physical Education, Wuhan University of Technology, Wuhan 430070, China*
[2]*School of Physical Education, Hubei Normal University, Huangshi 435002, China*
[3]*School of Physical Education, Jianghan University, Wuhan 430056, China*
[4]*School of Physical Education, Hubei Minzu University, Enshi 445000, China*
[5]*Graduate School, Adamson University, Manila 1000, Philippines*

Correspondence should be addressed to Lin Wang; wanglin123@126.com

Received 31 December 2020; Revised 2 March 2021; Accepted 6 March 2021; Published 22 March 2021

Academic Editor: Youhua Xu

This research review aimed to evaluate the effect of practicing Tai Chi on glucose and lipid metabolism in middle-aged and elderly diabetic patients. Furthermore, it aimed to provide a theoretical basis for the practice of Tai Chi as a way to improve glucose and lipid metabolism in middle-aged and elderly diabetic patients. Therefore, we searched for randomized controlled trials on the practice of Tai Chi in middle-aged and elderly diabetic patients in Chinese- and English-language electronic databases, such as Web of Science, PubMed, the Cochrane Library, EMBASE, Google Scholar, CNKI, Wanfang Database, and Weipu. We collected articles published no later than August 1, 2020. The methodological quality of the included studies was evaluated according to the standards of the Cochrane Collaboration System Evaluation Manual (version 5.1.0). Finally, 14 articles were included, showing an average Physiotherapy Evidence Database scale score of 6.57. The articles were meta-analyzed using Stata 14.0 software, showing that practicing Tai Chi improved middle-aged and elderly diabetic patients' fasting blood glucose (WMD = −0.60, 95% CI [−1.08, −0.12], $p = 0.015$), glycosylated hemoglobin (WMD = −0.87, 95% CI [−1.60, −0.14], $p = 0.019$), total cholesterol (WMD = −0.48, 95% CI [−0.83, −0.14], $p = 0.006$), triglycerides (WMD = −0.21, 95% CI [−0.37, −0.04], $p = 0.014$), and low-density lipoprotein cholesterol level significantly (WMD = −0.32, 95% CI [−0.63,−0.00], $p = 0.050$). Conversely, patients' high-density lipoprotein cholesterol levels (WMD = 0.09, 95% CI [−0.01, 0.17], $p = 0.136$) showed no obvious improvement. In conclusion, practicing Tai Chi in sessions lasting longer than 50 minutes (at least three times per week, for at least 12 weeks) can effectively improve glucose and lipid metabolism in middle-aged and elderly diabetic patients. However, several other factors affect glucose and lipid metabolism; therefore, further high-quality research is needed. Protocol registration number: INPLASY2020120107.

1. Introduction

In 2007, the American Academy of Sports Medicine and the American Medical Association jointly launched the *Exercise is Medicine* initiative in the United States. Taken as an academic philosophy and health-promotion initiative, the concept of exercise as medicine was received enthusiastically in many countries. The main goals of this initiative were the following: To provide professional training programs and continuing education programs for primary-care doctors and nurses (to ensure that they fully understand the importance of sports for health self-management), and to improve the overall national health level and happiness index through exercise prescriptions formulated by professional health-care personnel [1].

The concept of exercise as medicine is based on the findings of several previous studies showing that exercise ameliorates chronic disease. For example, Igarashi et al. found that water sports improved blood pressure in patients with hypertension [2]. Furthermore, Nalbant et al.

implemented a six-month aerobic intervention for elderly patients with chronic obstructive pulmonary disease and found that their lung function and lower limb strength were significantly improved [3]. Additionally, Wang et al. found that practicing yoga promoted the recovery of stroke patients' neurological functions and improved their overall health [4].

Diabetes is a metabolic disease that impairs the body's insulin production, leading to unstable blood sugar levels. Chronic hyperglycemia (low blood sugar) accelerates the aging of diabetic patients' organs and, in severe cases, causes organ dysfunction or failure [5]. According to the World Health Organization, diabetes has become the third most serious threat to human health [6]. The Global Diabetes Map (released by the International Diabetes Federation) shows that the number of diabetic patients aged 20–79 in 2019 was about 463 million, marking a three-fold increase since the year 2000. The World Health Organization estimates that the number of diabetic patients aged 20–79 will reach 700 million by 2045 and has shown that the global annual expenditure on diabetes health is approximately 760 billion US dollars.

The high cost of diabetes treatment not only has a significant impact on patients and their families but also represents a heavy burden to society. In view of the serious harm of diabetes to the world, research on this disease has increased in recent years. While seeking new drugs to treat diabetes, researchers are actively exploring non-pharmaceutical treatment options. Exercise has proven to be an effective means of prevention and treatment of chronic diseases. Additionally, encouraging results have also been observed in exercise-based interventions for patients with diabetes. Researchers have used aerobic and resistance exercises in interventions with diabetic patients; their studies have shown that aerobic and resistance exercises effectively improved patients' level of glucose and lipid metabolism [7, 8].

Tai Chi is a physical and mental exercise that integrates martial arts with mental and breathing exercises. Practicing Ta Chi can effectively improve flexibility, balance, and coordination, while it has also proven effective against heart disease [9], coronary heart disease [10], hypertension [11], and cancer [12]. However, researchers hold different views regarding the effects of Tai Chi on diabetic patients' glucose and lipid metabolism. For example, Xia et al. found that Tai Chi reduced moderately the fasting blood glucose and glycosylated hemoglobin levels of patients with type 2 diabetes (T2D) [13]. Furthermore, Zhou et al. found that Tai Chi had a significant effect on reducing fasting blood glucose, glycosylated hemoglobin, and total cholesterol level of patients with T2D [14]. Additionally, Tang Qing et al. found that Tai Chi reduced fasting blood glucose level and glycosylation in patients with T2D and that hemoglobin, triglycerides, and body weight also exhibited improvements; however, the adjustment of total cholesterol was not statistically significant [15]. Conversely, other studies have noted that Tai Chi had no significant effects on glycosylated hemoglobin in patients with T2D [16, 17].

Therefore, results regarding the effectiveness of Tai Chi in the prevention and treatment of glucose and lipid metabolism in diabetes are inconclusive. Additionally, there is a lack of systematic reviews focused on glucose and lipid metabolism in middle-aged and elderly diabetic patients. Furthermore, prior studies have seldom taken into account multiple variables, such as single-session duration, exercise frequency, and overall duration. Therefore, through this research review, we aimed to explore the influence of Tai Chi on the metabolism of glucose and lipids in middle-aged and elderly diabetic patients and to assess whether there is a scientific basis to support the implementation of Tai Chi interventions for middle-aged and elderly diabetic patients.

2. Methods

2.1. Data Sources. To identify studies on the effects of Tai Chi on diabetes, we conducted a search of Chinese and English electronic databases, such as Web of Science, PubMed, the Cochrane Library, EMBASE, Google Scholar, CNKI, Weipu, and Wanfang. Chinese search keywords were the following: "Tai Chi," "diabetes," "type 1 diabetes," and "type 2 diabetes." English search keywords were the following: "Tai Chi," "Tai Ji," "Tai Chi Exercise," "Tai Ji Chuan," "Tai Ji Quan," "Tai Chi Chuan," "Tai Chi Quan," "Taichi," "Taichiquan," and "diabetes," "diabetes mellitus," "type 2 diabetes mellitus," and "type 1 diabetes mellitus." The upper limit for the publication date of articles was August 1, 2020. Taking the Web of Science as an example, the detailed search strategy is presented in Table 1.

2.2. Inclusion Criteria and Exclusion Criteria

2.2.1. Eligibility Criteria. Among our inclusion criteria, we included the following: (1) The randomized controlled trial (RCT) also explored the relationship between Tai Chi and diabetes; (2) the study included at least one outcome measurement of diabetes-related indicators; (3) the study population comprised middle-aged and elderly patients with a diabetes diagnosis; and (4) the article was published no later than August 1, 2020.

Among our exclusion criteria, we included the following: (1) duplicate studies; (2) literature reviews, theories, abstracts, and nonrandomized controlled experiments; (3) the study included patients with severe complications; (4) the article did not provide sufficient result data, while the original data could not be obtained after contacting the author; and (5) studies with poor quality assessment.

2.2.2. Trial Inclusion. Study selection was carried out by two researchers independently. By carefully reading studies' title, abstract, and full text, studies that were not related to the main subject of this review were discarded. If there was any disagreement during the literature review process, the three researchers discussed it and sought a consensus regarding the inclusion of the reviewed study. Finally, the researchers determined which studies were qualified for inclusion in this review.

Table 1: Web of Science search strategy.

Order	Search terms
#1	Tai Chi
#2	Tai Ji
#3	Tai Chi exercise
#4	Tai Ji Chuan
#5	Tai Ji Quan
#6	Tai Chi Chuan
#7	Tai Chi Quan
#8	Taichi
#9	Taichiquan
#10	#1 OR #2 OR #3 OR #4 OR #5 OR #6 OR #7 OR #8 OR #9
#11	Diabetes
#12	Diabetes mellitus
#13	Type 2 diabetes mellitus
#14	Type 1 diabetes mellitus
#15	#11 OR #12 OR #13 OR #14
#16	#10 AND #15

2.2.3. Trial Quality Assessment. The quality of the studies was assessed according to the Physiotherapy Evidence Database (PEDro) scale [18]. The PEDro scale comprises 11 dimensions: eligibility criteria evaluation, randomization, allocation hiding, similar baseline, participant blinding, instructor blinding, evaluator blinding, a retention rate of over 85%, treatment intention analysis, comparison between groups, and point measurement and variability measurement [9]. Satisfying one of the indicators was counted as a 1-point addition to the score. Since the first item of the PEDro scale is not included in the total score, the total score of the scale is 10 points. A total score of ≥7 indicates high quality, 5-6 points indicate medium quality, and anything lower indicates poor quality [19, 20].

2.2.4. Data Extraction. The coding of the included literature was independently completed by two researchers. The basic information extracted included the name of the first author, the year of publication, the characteristics of the test, the intervention methods, the intervention period, the intervention frequency, and the type of outcome indicators. If two researchers encountered differences in the process of extracting basic information, the three researchers discussed and resolved them together.

2.3. Statistical Analysis. To conduct this meta-analysis, we used Stata 14.0 software. Analysis modules included the combined effect size, publication bias analysis, heterogeneity analysis, sensitivity analysis, and subgroup analysis. Since the outcome indicators of studies included in this review were continuous variables, the measurement data are shown as the Weighted Mean Difference (WMD). The included studies were tested for heterogeneity before merging their effect sizes. The heterogeneity test between the studies was performed using the χ^2 test. When the included studies had statistical homogeneity ($I^2 < 50\%$), a fixed meta-analysis was performed on the effect model. When the statistical heterogeneity between the included studies was large ($I^2 \geq 50\%$), a random-effects model was used for meta-analysis. When I^2 was greater than 75%, it was considered highly heterogeneous. The source and control of heterogeneity adopted the method of subgroup analysis, and publication bias adopted the funnel chart.

3. Results

3.1. Study Selection. Our database search yielded 1,068 studies. After discarding duplicate documents and reading studies' titles and abstracts to assess their relevance for this review, 56 articles remained. These studies were rescreened after reading the full text. We excluded 15 nonrandomized controlled trial studies, 20 studies with inconsistent research designs, and 7 studies with missing or unavailable data. Thus, 14 articles were finally included (Figure 1), including 10 articles in Chinese and 4 articles in English.

3.2. Study Characteristics. All 14 studies (Table 2) were randomized controlled trials. About 64.3% of the articles were published in 2010. The sample sizes ranged from 16 to 108. Twelve studies specified the gender distribution of their samples, which, in total, comprised 285 women and 232 men. The average duration of Tai Chi interventions varied. The shortest duration registered was 8 weeks, and the longest was 24 weeks. The number of exercise sessions per week ranged from 1 to 7, while a single-session duration ranged from 30 to 60 min.

4. Methodological Quality

The PEDro scale showed that the methodological quality of the 14 studies ranged from 6 to 8 with an average score of 6.57 (Table 3), indicating that the overall methodological quality of the included studies was good. All 14 studies were randomized controlled trials. We reviewed inclusion conditions, statistical results between groups, point measurement values, and variation measurement values. Two of the studies blinded the assessors of the test, subjects of 8 studies received experimental interventions according to the allocation plan, and 14 studies obtained measurement results.

4.1. Influence of Tai Chi on Middle-Aged and Elderly Diabetic Patients

4.1.1. Fasting Blood Glucose. Twelve studies evaluated the effect of Tai Chi on fasting blood glucose in middle-aged and elderly diabetic patients. We used funnel plots to detect publication bias. Three outliers were excluded, namely, the work of Wu et al. (2010), Li Qi et al. (2013), and Zhu et al. (2017). The final funnel diagram is shown in Figure 2. The heterogeneity test of these 12 studies showed heterogeneity ($p \leq 0.01$, $I^2 = 70.6\%$). Therefore, a random-effects model was used for meta-analysis (Figure 3). The results showed that the improvement effect of Tai Chi on fasting blood glucose levels among elderly diabetic patients was statistically significant (WMD = −0.60, 95% CI [−1.08, −0.12], $p = 0.015$).

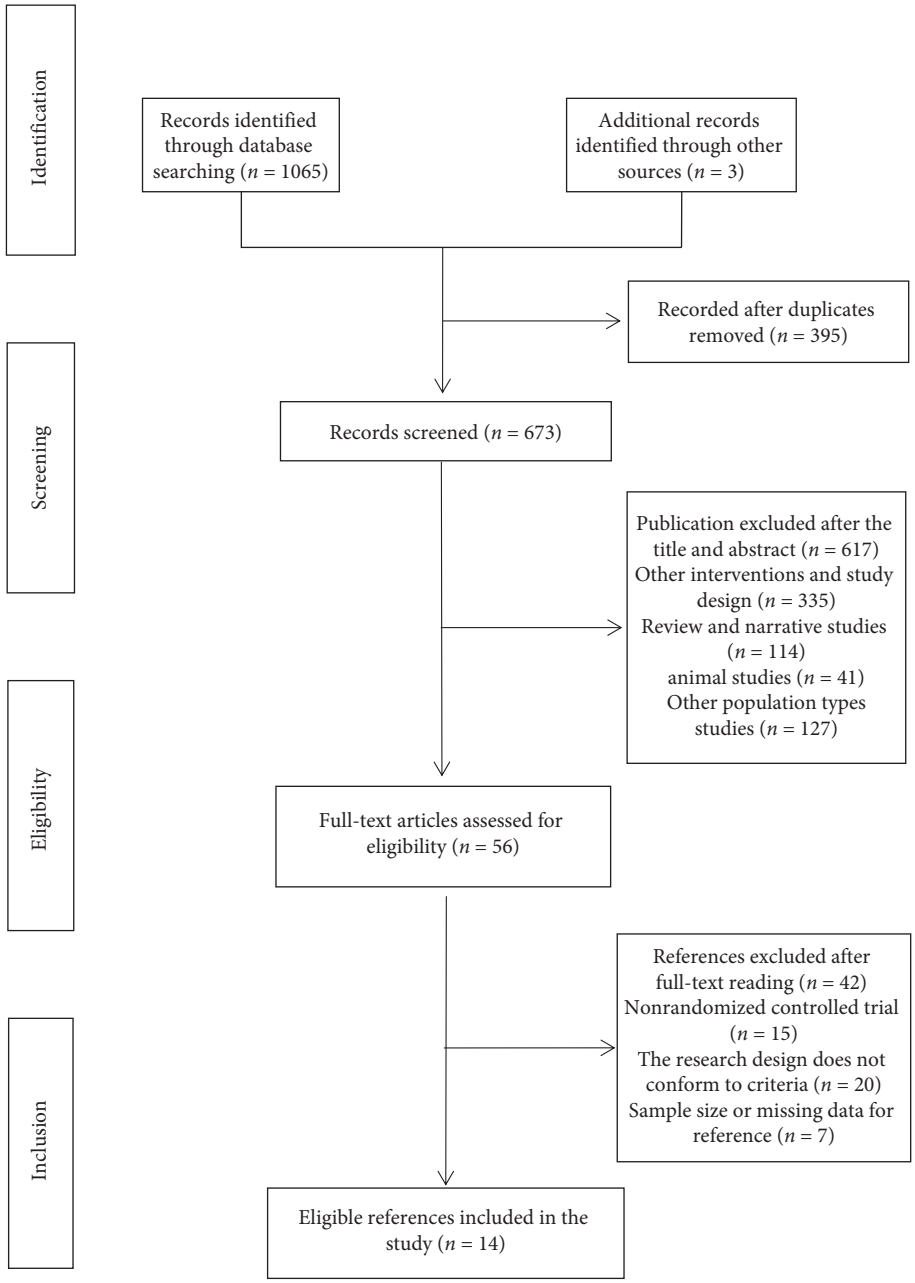

Figure 1: Flow of study selection.

In order to explore whether the heterogeneity among the included studies was caused by a single study, a sensitivity analysis of heterogeneity was carried out to assess the stability of the overall effect size. After excluding the articles by Wu et al. (2010), Zhu et al. (2017), and Li Qi et al. (2013), a meta-analysis of the remaining nine studies showed that the studies showed heterogeneity in sexual decline ($I^2 = 40.3\%$, $p = 0.099$) and combined effect size (WMD = −0.20, 95% CI [−0.57, 0.17], $p = 0.294$).

Subgroup analysis was performed on the outcome index of fasting blood glucose levels. We also performed a subgroup analysis of exercise cycle, exercise frequency, and single-session exercise time, according to the research intervention characteristics that could cause heterogeneous differences (Table 4). Among them, the combined effect size of Tai Chi exercises with an exercise period of more than 12 weeks was WMD = −0.78, 95% CI (−1.47, −0.08), $p = 0.029$, indicating that practicing Tai Chi over a 12-week period can significantly improve the fasting blood glucose levels of middle-aged and elderly diabetic patients. In the subgroup of single-session exercise time, the combined effect size of Tai Chi sessions lasting longer than 50 minutes was WMD = −1.04, 95% CI (−1.70, −0.37), $p = 0.002$, indicating that Tai Chi sessions longer than 50 minutes can significantly improve the fasting blood sugar levels of middle-aged and elderly diabetic patients.

Table 2: Characteristics of the studies included in the meta-analysis.

References	F/M	Sample size (attrition rate)	Population	Course of disease	Duration (week)	Time (min)	Frequency (weekly)	Motion intensity	Intervention program	Outcome measured
Wu et al. [21], China, 2010	25/15	40 (0%)	M	EG: 1.35 (0.62) CG: 1.36 (0.7)	24	60	3	Moderate	EG : TC (Yang style) + DT CG : DT	FBG and HbA1c
Li et al. [22], China, 2015	NR	100 (0%)	E	EG: 7.83 (2.16) CG: 8.14 (3.19)	24	40–50	7	NR	EG : TC (Chen style) CG : AE	FBG, HbA1c, TC, TG, HDL-C, and LDL-C
Li Qi et al. [23], China, 2013	NR	108 (19.4%)	M + E	EG: 6.95 (3.63) CG: 7.22 (4.14)	12	30	7	NR	EG : TC (Yang style) + DT CG : DT	FBG, HbA1c, TC, and HDL-C
Wang et al. [24], China, 2009	24/30	54 (0%)	M	EG: 1.35 (0.62) CG: 1.36 (0.7)	24	30–50	5	Moderate	EG : TC (Yang style) CG : AE	FBG, HbA1c, TC, TG, HDL-C, and LDL-C
Xiao et al. [25], China, 2010	10/14	24 (0%)	M	NR	24	60	6	Moderate	EG : TC (Yang style) + DT CG : DT	FBG
Zhao et al. [26], China, 2017	0/16	16 (11%)	M	NR	16	60	7	Moderate	EG : TC (Chen style) + DT CG : DT	FBG, TC, TG, HDL-C, and LDL-C
Zhang et al. [27], China, 2008	20/0	20 (5%)	M + E	NR	14	60	5	Low	EG : TC (Yang style) + DT CG : CE + DT	FBG, TC, TG, HDL-C, and LDL-C
Lam et al. [28], Australia, 2008	29/24	53 (17%)	M + E	NR	24	60	1	NR	EG : TC (other types) CG : CE	HbA1c, TC, and TG
Tracey et al. [29], Australia, 2008	30/8	38 (2.6%)	E	NR	16	60	2	Low	EG : TC (other types) CG : MM	HbA1c
Chen et al. [30], China, 2010	59/45	104 (9%)	M + E	EG: 7.8 (3.1) CG: 8.5 (3.5)	12	60	3	NR	EG : TC (Chen style) + DT CG : AE + DT	FBG, HbA1c, TC, TG, HDL-C, and LDL-C
Li et al. [31], China, 2013	24/36	60 (0%)	M + E	NR	8	45	7	Moderate	EG : TC (other types) + UC CG : UC	FBG
Zhang et al. [32], China, 2014	31/9	40 (0%)	M + E	NR	14	60	3	Moderate	EG : TC (Yang style) CG : AE	FBG and HbA1c
Kan et al. [33], China, 2004	23/25	48 (0%)	M	NR	12	60	7	NR	EG : TC (Yang style) CG : AE	FBG, TC, TG, HDL-C, and LDL-C
Zhu et al. [34], China, 2017	10/10	20 (0%)	M + E	EG: 5.15 (2.53) CG: 5.30 (2.65)	12	60	5	Moderate	EG : TC (Chen style) CG : UC	FBG, HbA1c, TC, TG, HDL-C, and LDL-C

Note. EG = exercise group; CG = control group; NR = not reported; outcome measured (FBG = fasting blood glucose; HbA1c = glycosylated hemoglobin; TC = total cholesterol; TG = triglyceride; HDL-C = high-density lipoprotein cholesterol; and LDL-C = low-density lipoprotein cholesterol); intervention program (TC = Tai Chi; DT = drug therapy; UC = usual care; AE = aerobic exercise; MM = mixed movement; and CE = conventional exercise); and population type (M = middle-aged; *E* = elderly).

4.1.2. Glycated Hemoglobin. Nine studies evaluated the effect of Tai Chi on glycated hemoglobin levels in middle-aged and elderly diabetic patients. Heterogeneity analysis showed that there was heterogeneity among the included studies ($p \leq 0.01$, $I^2 = 94.0\%$); therefore, a randomized meta-analysis of the effect model (Figure 4) showed that Tai Chi improved the glycosylated hemoglobin of middle-aged and elderly diabetic patients, and the difference was statistically significant (WMD = −0.87, 95% CI [−1.60, −0.14], $p = 0.019$).

Table 3: Study-quality assessment of eligible randomized controlled trials.

Reference	Item 1	Item 2	Item 3	Item 4	Item 5	Item 6	Item 7	Item 8	Item 9	Item 10	Item 11	Score
Wu et al. (2010) [21]	1	1	0	1	0	0	0	1	1	1	1	7
Li et al. (2015) [22]	1	1	0	1	0	0	0	1	1	1	1	7
Li Qi et al. (2013) [23]	1	1	0	1	0	0	0	1	0	1	1	6
Wang et al. (2009) [24]	1	1	0	1	0	0	0	1	1	1	1	7
Xiao et al. (2010) [25]	1	1	0	1	0	0	0	0	1	1	1	6
Zhao et al. (2017) [26]	1	1	0	1	0	0	0	1	0	1	1	6
Zhang et al. (2008) [27]	1	1	0	1	0	0	0	1	0	1	1	6
Lam et al. (2008) [28]	1	1	0	1	0	0	1	1	0	1	1	7
Tracey et al. (2008) [29]	1	1	0	1	1	0	1	1	0	1	1	8
Chen et al. (2010) [30]	1	1	0	1	0	0	0	1	0	1	1	6
Li et al. (2013) [31]	1	1	0	1	0	0	0	1	1	1	1	7
Zhang et al. (2014) [32]	1	1	0	1	0	0	0	1	1	1	1	7
Kan et al. (2004) [33]	1	1	0	0	0	0	0	1	1	1	1	6
Zhu et al. (2017) [34]	1	1	0	0	0	0	0	1	1	1	1	6

Note. Item 1 = eligibility criteria; item 2 = random sequence; item 3 = allocation concealment; item 4 = similar at baseline; item 5 = subjects blinded; item 6 = therapists blinded; item 7 = assessors blinded; item 8 = <15% dropouts; item 9 = intention-to-treat analysis; item 10 = between-group comparison; item 11 = point measures and variability data; 1 = meets the criteria; 0 = did not meet the criteria.

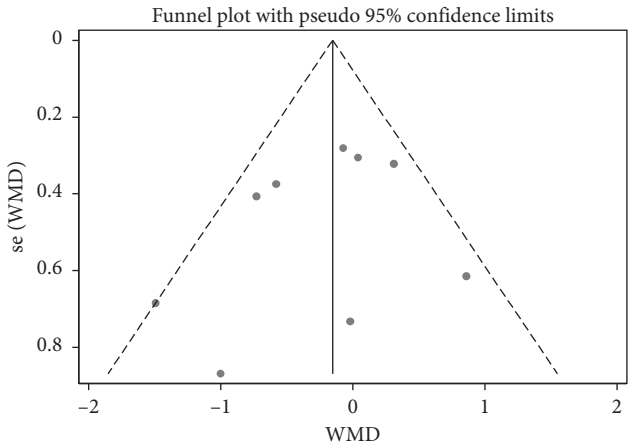

Figure 2: Funnel plot of Tai Chi's effect on fasting blood glucose levels in middle-aged and elderly diabetic patients.

In order to explore whether the heterogeneity among the included studies was caused by a single study, a sensitivity analysis of heterogeneity was carried out to assess the stability of the overall effect size. We found that the articles by Wu et al. (2010), Li et al. (2015), Tracey et al. (2008), and Wang et al. (2009) were quite heterogeneous. After excluding these four articles, five studies remained. The meta-analysis showed that the heterogeneity decreased after excluding the aforementioned four studies: $I^2 = 17.5\%$, $p = 0.303$, WMD = −0.75, 95% CI (−1.10, −0.39), $p \leq 0.01$.

A subgroup analysis was performed on the outcome indices of glycosylated hemoglobin, exercise period, exercise frequency, and single-session exercise time, according to the research intervention characteristics that could cause heterogeneous differences (Table 4). In the subgroup of exercise frequency, the combined effect size of practicing Tai Chi more than 3 times per week was WMD = −0.91, 95% CI (−1.56, −0.25), $p = 0.007$, indicating that practicing Tai Chi more than three times per week can significantly improve the glycosylated hemoglobin levels of middle-aged and elderly diabetic patients.

4.1.3. Total Cholesterol. Nine studies evaluated the effect of Tai Chi on total cholesterol levels among middle-aged and elderly diabetic patients. Heterogeneity analysis showed that there was heterogeneity among the included studies ($p \leq 0.01$, $I^2 = 78.1\%$). Subsequently, a randomized meta-analysis of the effect model (Figure 5) showed that Tai Chi improved the total cholesterol levels of middle-aged and elderly diabetic patients and that the difference was statistically significant (WMD = −0.48, 95% CI [−0.83, −0.14], $p = 0.006$).

In order to explore whether the heterogeneity among the included studies was caused by a single study, a sensitivity analysis of heterogeneity was carried out to assess the stability of the overall effect size and found significant heterogeneity in the articles by Li Qi et al. (2013), Wang et al. (2009), and Chen et al. (2010). After excluding these three articles, a meta-analysis of the remaining six studies showed decreased heterogeneity ($I^2 = 34.2\%$, $p = 0.180$), WMD = −0.62, 95% CI (−0.90, −0.33), $p \leq 0.01$.

A subgroup analysis was performed on the outcome indices of total cholesterol, exercise period, exercise frequency, and single-session exercise time. Each subgroup was analyzed according to the research intervention characteristics that could cause heterogeneous differences (Table 4). In the exercise cycle subgroup, the combined effect size of Tai Chi practice lasting no longer than 12 weeks was WMD = −0.61, 95% CI (−1.11, −0.11), and $p = 0.016$. This indicates that Tai Chi practice lasting no longer than 12 weeks significantly improved the total cholesterol level of middle-aged and elderly diabetic patients, which is inconsistent with the results of previous studies. This could be because of human exercise stress and adaptability. Practicing Tai Chi for no longer than 12 weeks promoted the uptake of fatty acids by muscle tissue and accelerated the transport and degradation of total cholesterol. Additionally, practicing Tai Chi for more than 12 weeks may prompt the human body to adapt to the physical demands of exercise, leading to a plateau in stress level and a decrease in the efficiency of adipose tissue mobilization. In the exercise frequency

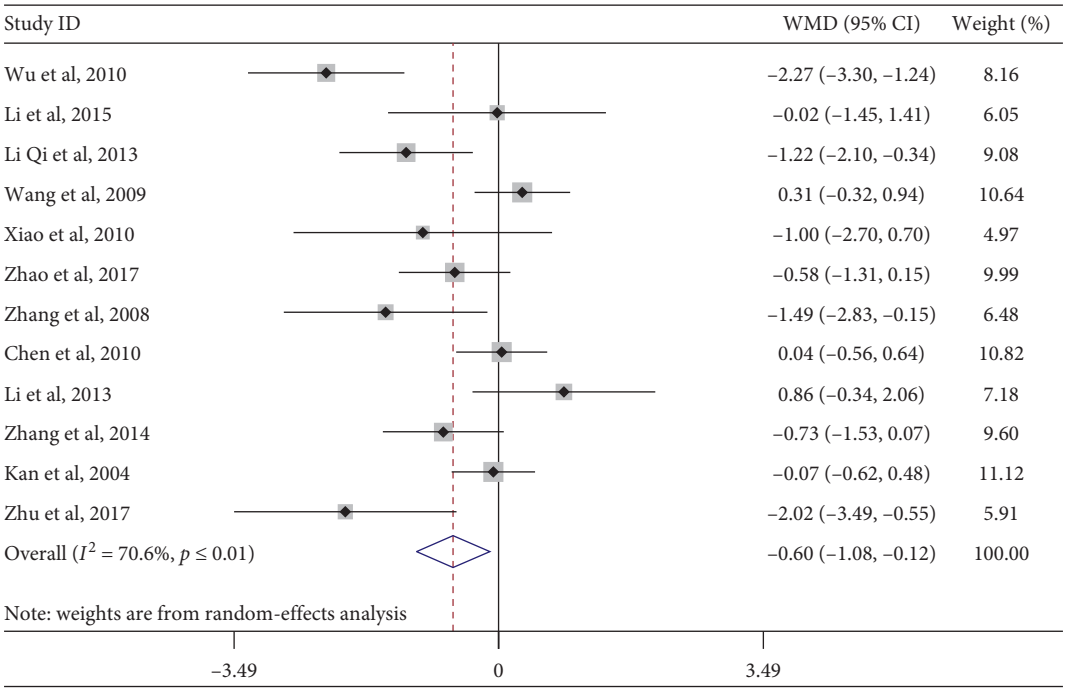

Figure 3: Forest plot of the effects of Tai Chi on fasting blood glucose levels in middle-aged and elderly diabetic patients.

subgroup, the combined effect size of practicing Tai Chi more than three times per week was WMD = −0.58, 95% CI (−0.94, −0.22), $p = 0.002$, indicating that practicing Tai Chi more than three times per week significantly improves the total cholesterol levels of middle-aged and elderly diabetic patients. Regarding single-session exercise time, the combined effect amount of Tai Chi sessions lasting longer than 50 minutes was WMD = −0.40, 95% CI (−0.77, −0.03), $p = 0.036$, indicating that Tai Chi sessions lasting longer than 50 minutes can significantly improve the total cholesterol of middle-aged and elderly diabetic patients.

4.1.4. Triglycerides. Eight studies evaluated the effect of Tai Chi on triglyceride levels in middle-aged and elderly patients with diabetes. Heterogeneity analysis showed that there was heterogeneity among the included studies ($p = 0.027$, $I^2 = 55.8\%$). A meta-analysis of the random-effects model (Figure 6) showed that Tai Chi improved triglyceride levels of middle-aged and elderly diabetic patients and that the difference was statistically significant (WMD = −0.21, 95% CI [−0.37, −0.04], $p = 0.014$).

In order to explore whether the heterogeneity among the included studies was caused by a single study, a sensitivity analysis of heterogeneity was carried out to assess the stability of its overall effect size. Wang et al.'s (2009) study was relatively heterogeneous. After excluding this article, a meta-analysis of the remaining seven studies showed that the heterogeneity decreased ($I^2 = 0.0\%$, $p = 0.814$), WMD = −0.27, 95% CI (−0.37, −0.18), $p \leq 0.01$.

A subgroup analysis was performed on the outcome indices of total cholesterol, exercise period, exercise frequency, and single-session exercise time according to the research intervention characteristics that could cause heterogeneous differences (Table 4). The results showed that the three different subgroups found no significant improvement in triglyceride levels in middle-aged and elderly diabetic patients.

4.1.5. High-Density Lipoprotein Cholesterol. Eight studies evaluated the effect of Tai Chi on high-density lipoprotein (HDL) cholesterol in middle-aged and elderly diabetic patients. Heterogeneity analysis showed that these studies exhibited heterogeneity ($p = 0.051$, $I^2 = 50.0\%$). Therefore, a random-effects model was used for meta-analysis (Figure 7), which showed that Tai Chi did not significantly improve HDL cholesterol levels in middle-aged and elderly diabetic patients (WMD = 0.09, 95% CI [−0.01, 0.17], $p = 0.136$).

To explore whether the heterogeneity among the included studies was caused by a single study, a sensitivity analysis of heterogeneity was carried out to assess the stability of the overall effect size. Zhu et al.'s (2017) article exhibited relatively large heterogeneity. After excluding this article, a meta-analysis of the remaining seven articles showed that the heterogeneity decreased ($I^2 = 35.1\%$, $p = 0.160$), WMD = 0.07, 95% CI (0.00, 0.14), $p = 0.045$.

Although practicing Tai Chi did not significantly improve HDL cholesterol in middle-aged and elderly diabetic patients, this review further explored the influence of different factors on HDL cholesterol, hoping to provide a scientific basis for future clinical exercise interventions for diabetes. According to the research intervention characteristics that could cause heterogeneous differences, we analyzed exercise period, exercise frequency, and single-session exercise time by subgroup analysis (Table 4). Tai Chi's improvement of protein cholesterol levels was not evident.

Table 4: Subgroup analysis of Tai Chi on glucose and lipid metabolism in diabetic patients.

Outcomes	Group	Subgroup	N	WMD	95%CI	p	I^2 (%)	(WMD) p value
FBG	Duration	≤12 weeks	5	−0.39	−1.12, 0.34	0.005	73.00	0.293
		>12 weeks	7	−0.78	−1.47, −0.08	0.002	71.10	0.029
	Frequency	≤3 times/week	4	−0.67	−1.51, 0.17	0.001	82.10	0.12
		>3 times/week	8	−0.57	−1.22, 0.08	0.004	66.10	0.084
	Time	≤50 min	5	−0.06	−0.67, 0.55	0.036	61.00	0.84
		>50 min	7	−1.04	−1.70, −0.37	0.004	69.00	0.002
HbA1c	Duration	≤12 weeks	4	−0.82	−1.24, −0.39	0.243	28.20	≤0.01
		>12 weeks	5	−0.88	−2.07, 0.30	≤0.01	96.90	0.144
	Frequency	≤3 times/week	4	−0.77	−2.44, 0.89	≤0.01	97.10	0.363
		>3 times/week	5	−0.91	−1.56, −0.25	≤0.01	84.90	0.007
	Time	≤50 min	3	−0.88	−2.02, 0.27	≤0.01	90.70	0.132
		>50 min	6	−0.87	−1.91, 0.18	≤0.01	95.30	0.103
TC	Duration	≤12 weeks	4	−0.61	−1.11, −0.11	≤0.01	85.80	0.016
		>12 weeks	5	−0.34	−0.81, 0.13	0.027	63.50	0.159
	Frequency	≤3 times/week	2	0.02	−0.34, 0.38	0.441	0.00	0.902
		>3 times/week	7	−0.58	−0.94, −0.22	≤0.01	76.80	0.002
	Time	≤50 min	3	−0.61	−1.31, 0.10	≤0.01	89.80	0.091
		>50 min	6	−0.4	−0.77, −0.03	0.021	62.40	0.036
TG	Duration	≤12 weeks	3	−0.28	−0.40, −0.16	0.369	0.00	≤0.01
		>12 weeks	5	−0.09	−0.45, 0.27	0.018	66.50	0.625
	Frequency	≤3 times/week	2	−0.2	−0.38, −0.04	0.854	0.00	0.016
		>3 times/week	6	−0.19	−0.42, 0.04	0.008	68.10	0.098
	Time	≤50 min	2	0.09	−0.62, 0.79	0.001	90.70	0.808
		>50 min	6	−0.28	−0.40, −0.17	0.719	0.00	≤0.01
HDL-C	Duration	≤12 weeks	4	0.17	0.05, 0.28	0.072	57.20	0.004
		>12 weeks	4	0.00	−0.08, 0.08	0.67	0.00	0.967
	Time	≤50 min	3	0.09	−0.07, 0.25	0.024	73.30	0.268
		>50 min	3	0.11	0.01, 0.20	0.208	32.00	0.038
LDL-C	Duration	≤12 weeks	2	−0.62	−0.82, −0.43	0.349	0.00	≤0.01
		>12 weeks	4	−0.17	−0.57, 0.23	0.011	73.20	0.407
	Time	≤50 min	2	−0.05	−0.67, 0.56	0.005	87.30	0.868
		>50 min	4	−0.47	−0.83, −0.12	0.047	62.30	0.008

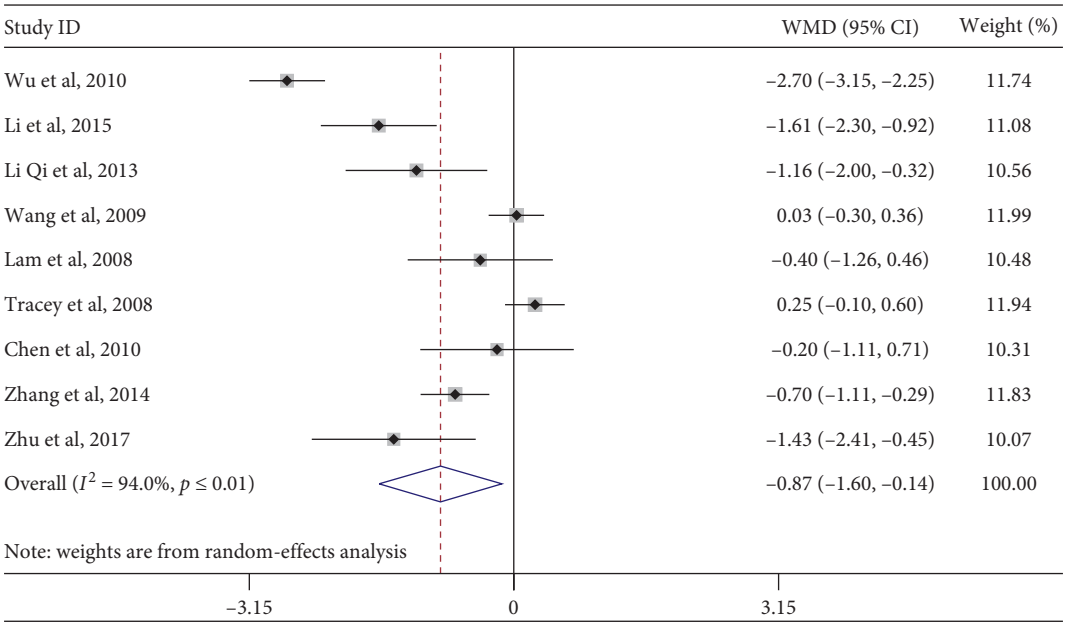

Figure 4: Forest plot of the influence of Tai Chi on glycosylated hemoglobin levels in middle-aged and elderly diabetic patients.

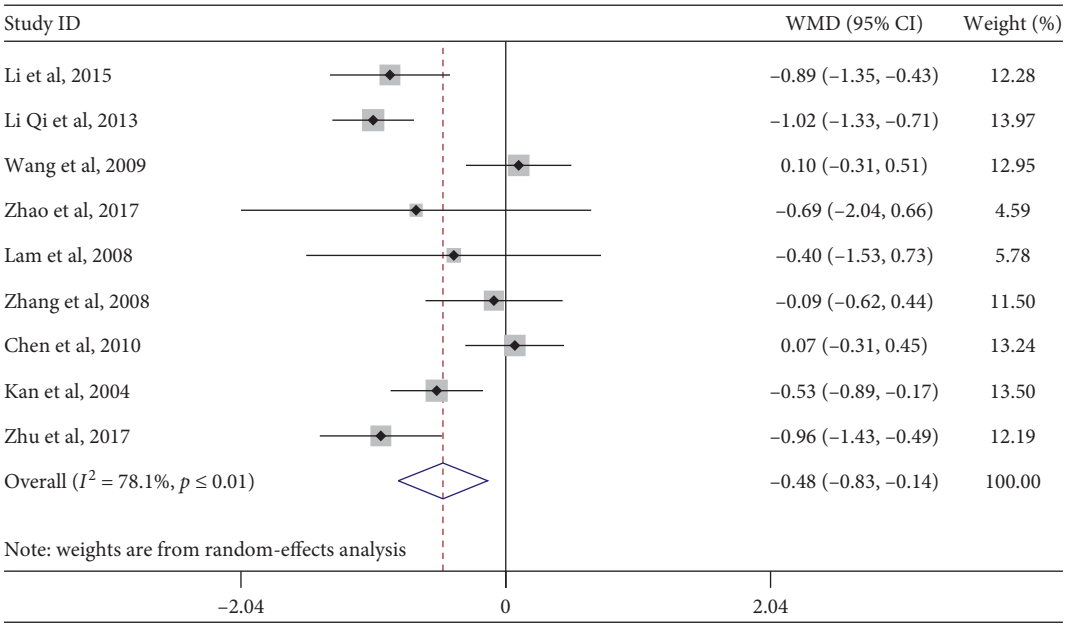

Figure 5: Forest plot of the effect of Tai Chi on total cholesterol levels among middle-aged and elderly diabetic patients.

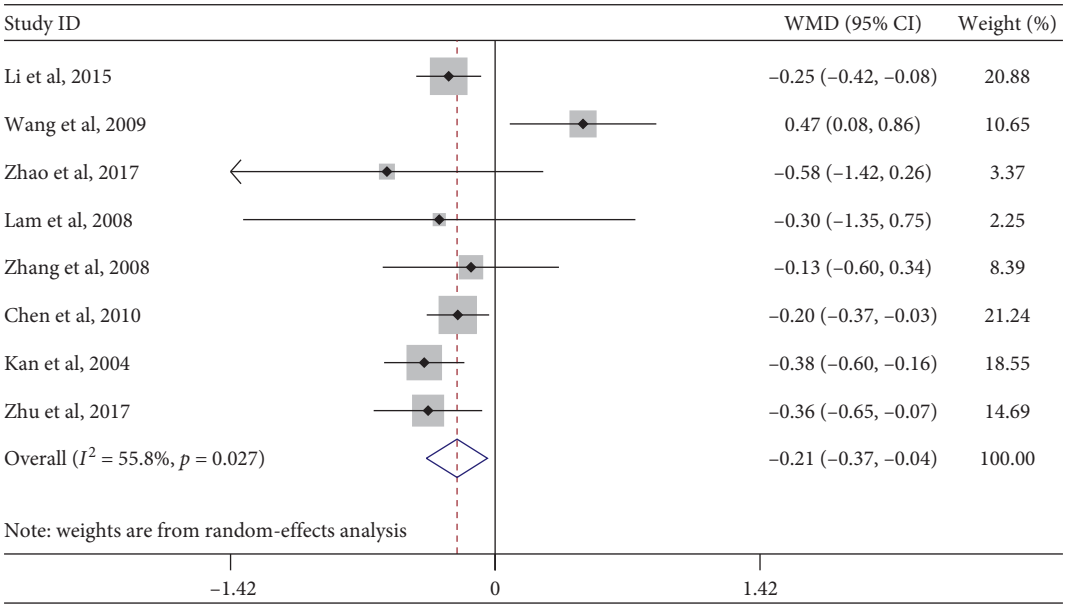

Figure 6: Forest plot of Tai Chi influence on triglyceride in middle-aged and elderly diabetic patients.

4.1.6. Low-Density Lipoprotein Cholesterol. Six studies evaluated the effect of Tai Chi on low-density lipoprotein cholesterol levels in middle-aged and elderly people. Heterogeneity analysis showed that there was heterogeneity among the included studies ($p \leq 0.01$, $I^2 = 78.4\%$). Therefore, a random-effects model was used for meta-analysis (Figure 8), showing that Tai Chi improved the low-density lipoprotein cholesterol levels of middle-aged and elderly diabetic patients, and the difference was statistically significant (WMD = −0.32, 95% CI [−0.63,− 0.00], $p = 0.050$).

In order to explore whether the heterogeneity among the included studies was caused by a single study, a sensitivity analysis of heterogeneity was carried out to assess the stability of the overall effect size. We found that the articles by Zhao et al. (2017) and Wang et al. (2009) were relatively heterogeneous. After excluding these two articles, the meta-analysis of the remaining four studies showed that the heterogeneity decreased ($I^2 = 24.6\%$, $p = 0.264$), WMD = −0.33, 95% CI (−0.57, −0.10), $p = 0.006$.

A subgroup analysis was performed for the outcome indicator of low-density lipoprotein cholesterol. According to the research intervention characteristics that could cause heterogeneous differences, subgroup analysis was performed on the exercise cycle and single-session exercise time

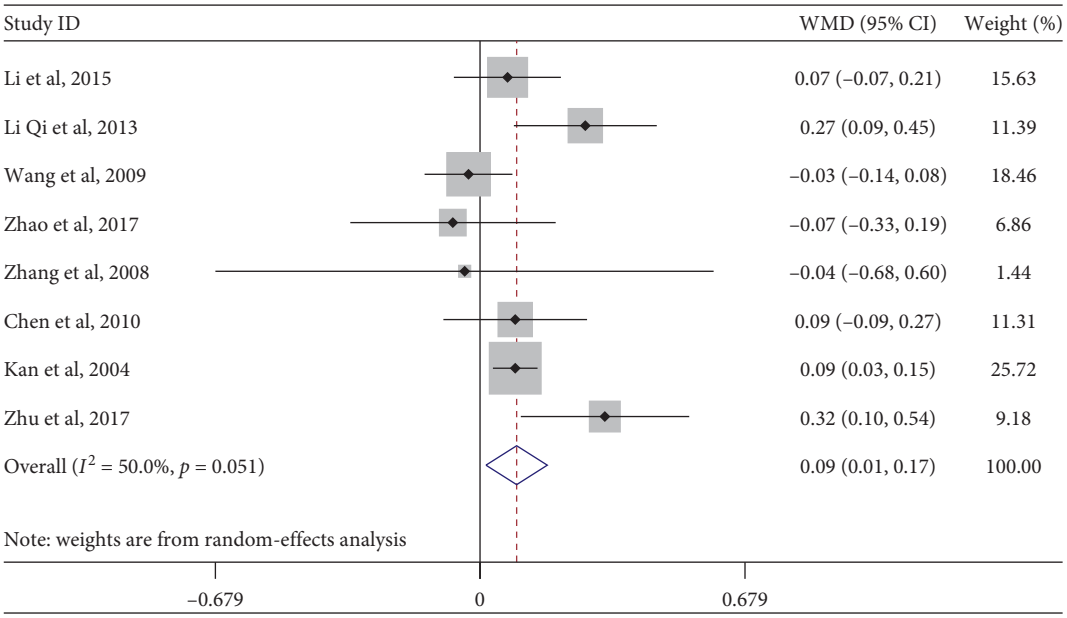

Figure 7: Forest plot of Tai Chi influence on high-density lipid-cholesterol in middle-aged and elderly diabetic patients.

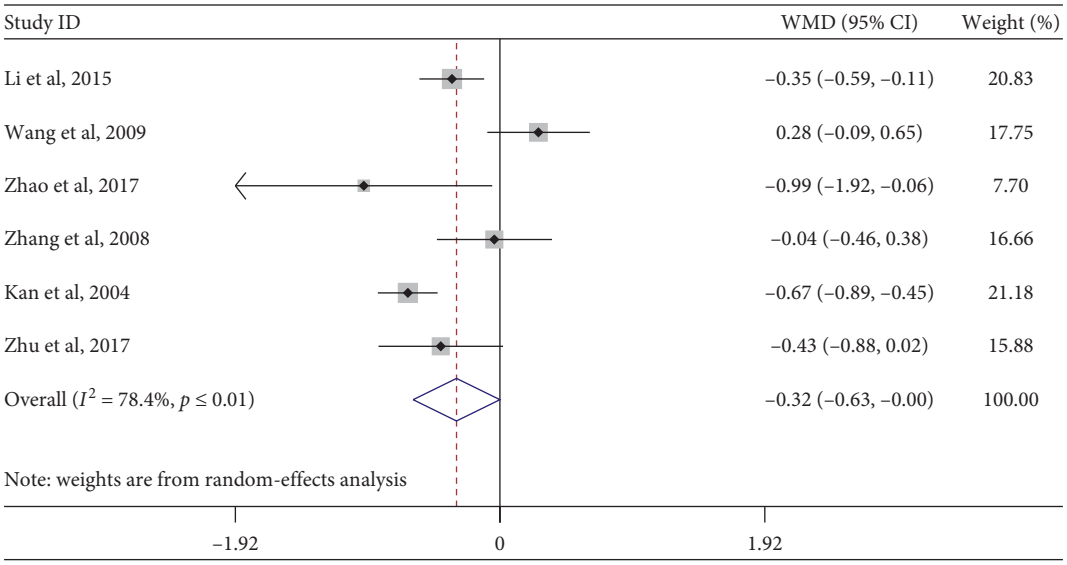

Figure 8: Forest plot of Tai Chi influence on low-density lipid-cholesterol in middle-aged and elderly diabetic patients.

variables (Table 4). In the subgroup, the combined effect size of Tai Chi sessions lasting longer than 50 min was WMD = −0.47, 95% CI [−0.83, −0.12], p = 0.008, indicating that practicing Tai Chi in +50-minute sessions can significantly improve low-density lipoprotein cholesterol in middle-aged and elderly diabetic patients.

5. Discussion

The International Diabetes Federation has stated that a healthy diet and regular physical exercise play a large role in preventing type 2 diabetes and controlling blood sugar [35]. Studies have found that engaging in aerobic and resistance exercise for 30 minutes every day can reduce the risk of diabetes by 43% [36]. Furthermore, Peng et al. found that the longer the diabetic patients persisted in performing exercise (specifically, Baduanjin qigong), the greater the decrease in glycosylated hemoglobin they exhibited [7]. Moreover, the research by Zhang et al. pointed out that a 14-week Tai Chi exercise can significantly improve blood glucose, glycosylated serum protein, triglyceride, and other related indicators in elderly women with type 2 diabetes [27].

Some scholars have conducted a review on Taijiquan's improvement of glucose and lipid metabolism in diabetic patients, but some reviews [14, 37, 38] only explored the effect of Taijiquan on the blood sugar of diabetic patients without involving the effect of Taijiquan on diabetic patients' blood lipids. Studies have confirmed that, in addition to

abnormal blood glucose, the factors which cause cardiovascular complications in diabetic patients are important, so attention should also be paid to their blood lipids. The second part of the review [16, 38] included studies that used nonrandomized controlled trials, which would increase the degree of bias in the research and affecting its results [13–17, 37, 39, 40]. The intervention methods included in the study were Qigong, Dayuan Hypoglycemic (Tai Chi) Exercise, and Tai Chi Soft Ball. Like Dayuan Hypoglycemic (Tai Chi) Exercise, Tai Chi Soft ball is created through Tai Chi thinking, but it is still different from Tai Chi exercise. It is difficult to sink the dantian and guide the qi with the mind, and it is even more difficult to coordinate the heart, mind, and qi. This is bound to have a certain impact on the final intervention effect, which then affects the system review's objectivity. Only one study [37] explored the dose effect of Tai Chi on the blood sugar of patients with type 2 diabetes according to different types of exercise and total exercise volume (single exercise time * exercise days per week * exercise weeks); instead, the total exercise volume was used. The dose effect on glucose and lipid metabolism in diabetic patients is insufficient as the same total exercise amount has different effects. This study did not explore the effect of Tai Chi exercises when different times and frequencies were used or the effect of a single exercise period on diabetic patients' blood sugar. The influence of Tai Chi on diabetic patients' blood lipids has not been explored.

The innovations of this article are as follows: (1) Conduct a subgroup analysis considering the dimensions of "exercise cycle," "exercise frequency," and "single exercise time" and deeply explore the dose effect of Tai Chi on the glucose and lipid metabolism of diabetic patients. (2) All research methods in the study are randomized controlled trials, and the experimental group uses Tai Chi as an intervention technique. (3) The research on diabetic patients in this article includes not only blood sugar (fasting blood glucose and glycosylated hemoglobin) but also blood lipids (total cholesterol, triglycerides, low-density lipoprotein cholesterol, and high-density lipoprotein cholesterol) and systematically studied Tai Chi effects on glucose and lipid metabolism in diabetic patients.

This research review shows that Tai Chi can significantly improve fasting blood glucose and glycosylated hemoglobin in middle-aged and elderly diabetic patients, which is consistent with the results of previous studies [13–15, 37, 39]. Additionally, we found that Tai Chi significantly improved triglycerides, total cholesterol, and low-density lipoprotein levels in middle-aged and elderly diabetic patients, but it had no significant effect on high-density lipoprotein cholesterol. Similarly, Xia et al. found that Tai Chi significantly improved triglyceride levels in diabetic patients [13]. Additionally, the research by Liu Yongjin et al. found that Tai Chi significantly improved triglycerides, total cholesterol, and low-density lipoprotein levels in diabetic patients [39].

Among the outcome indicators of glucose metabolism, Tai Chi improved fasting blood glucose and glycosylated hemoglobin levels in middle-aged and elderly diabetic patients. The reasons for this may be that (1) Tai Chi can promote skeletal muscle's uptake and use of glucose in the blood and increase the activity of insulin in the body to convert blood sugar. The activity of the glucose transporter on the skeletal muscle cell membrane is to further improve the blood glucose concentration in the body [22]; (2) Tai Chi has both the advantages and characteristics of oxygen and resistance exercise. Middle-aged and elderly diabetic patients maintain a standing posture for a long time during the practice of Tai Chi. Therefore, leg muscle strength is increased and the cross section of muscle fibers is enlarged, which causes the leg muscles to grow. (3) Absorption and utilization of blood sugar: Practicing Tai Chi engages the whole body in the exercise, especially small muscle groups and peripheral tissues, and promotes the absorption of glucose [41].

Additionally, Tai Chi can improve total cholesterol and triglyceride levels in middle-aged and elderly diabetic patients. The reason for this may be that exercise increases the activity of lipoprotein lipase in the body, which promotes the hydrolysis of triglycerides in the body. Lipoprotein lipase promotes lipolysis in the body after an increase in activity, reducing total cholesterol levels and triglycerides in plasma, accelerating the conversion and degradation of triglycerides, and increasing the body's ability to remove cholesterol in the blood [42]. Second, exercise increases the permeability of skeletal muscle capillaries, increases the surface area of the capillary endothelium, increases lipoprotein lipase activity in skin cells, and promotes the decomposition of total cholesterol and triglycerides in plasma. A decrease in low-density lipoprotein cholesterol is related to activity in low-density lipoprotein (LDL) receptors and ApoB levels. When LDL receptor activity increases or ApoB levels decrease, serum low-density lipoprotein cholesterol levels decrease [43].

The possible reasons why the effect of Tai Chi on HDL cholesterol in middle-aged and elderly diabetic patients was not statistically significant (compared with the control group) are exercise intensity and gender. Studies have found that moderate-intensity (50% VO_2max) and greater-intensity (70% VO_2max) exercise are more suitable for elderly diabetic patients [44]. Five of the studies we reviewed did not specify exercise intensity, while two studies specified having implemented low-intensity exercise. An unsuitable exercise intensity cannot guarantee that fat is the main component. As the functional substance of HDL, cholesterol did not change significantly. Furthermore, Xiao et al. implemented an aerobic exercise intervention for 12 weeks and found that the level of high-density lipoprotein cholesterol in men's plasma increased significantly, while the level of HDL cholesterol in women's plasma had not changed significantly [45].

This review has some limitations. First, the subjects included in the study have a large difference in their illness duration. Existing studies have shown that the risk of complications from diabetes, including strokes, will increase as the duration of disease increases. Increasing duration also increases the difficulty of controlling diabetes, which may be one of the causes of heterogeneity. Second, the control group included in the study received different intervention methods, mainly divided into three types: drug therapy,

exercise intervention, and drug therapy combined with exercise intervention. Different intervention methods have different effects in terms of controlling the subjects' condition, which will affect the research results. Third, the postures and familiarity of the participants in the included study of Taijiquan are not explained. Taijiquan training in different postures will affect the cardiovascular function and athletic ability of the participants. The inconsistency in proficiency of Taijiquan will interfere with the subjects as their mind and breath of the participants during the practice have a certain impact on the effect of the intervention. Fourth, among the elements of Tai Chi intervention, differences in exercise intensity, exercise time, exercise frequency, and exercise items also have different effects on the glucose and lipid metabolism of the subjects, thereby affecting the authenticity of the research results.

6. Conclusions

Tai Chi can significantly improve fasting blood glucose, glycosylated hemoglobin, total cholesterol, triglycerides, and low-density lipoprotein cholesterol metabolism in middle-aged and elderly diabetic patients, but it has no significant effect on high-density lipoprotein cholesterol metabolism; practicing Tai Chi in sessions lasting longer than 50 minutes (at least three times per week, for at least 12 weeks) can effectively improve glucose and lipid metabolism in middle-aged and elderly diabetic patients. However, several other factors affect glucose and lipid metabolism; therefore, further high-quality research is needed.

Data Availability

The (continuous) data supporting this meta-analysis are from previously reported studies and datasets, which have been cited. The processed data are available in the supplementary files.

Conflicts of Interest

No conflicts of interest exist in this study.

Authors' Contributions

Ya-nv Liu, Lin Wang, and Xin Fan conceptualized the study. Shijie Liu, Qi Wu, and You-Ling Qian curated data. Ya-nv Liu, Lin Wan, and Xin Fan conducted formal analysis. Lin Wang acquired funding. Ya-nv Liu, Lin Wang, Xin Fan, and Shijie Liu conducted investigation. Ya-nv Liu, Lin Wang, and Xin Fan formulated the methodology. Ya-nv Liu, Lin Wang, and Xin Fan were responsible for the software. Lin Wang, Xin Fan, and Shijie Liu supervised the work. Ya-nv Liu, Lin Wang, and Xin Fan wrote the original draft. Ya-nv Liu, Lin Wang, Xin Fan, Shijie Liu, Qi Wu, and You-Ling Qian reviewed and edited the manuscript.

Acknowledgments

This work was supported by the National Social Science Foundation (20BTY104) and the Fundamental Research Funds for the Central Universities (WUT: 2020VI001).

Supplementary Materials

The data of this study are derived from 14 published documents. (*Supplementary Materials*)

References

[1] J. S. Coombes, J. Law, B. Lancashire et al., ""Exercise is Medicine": curbing the burden of chronic disease and physical inactivity," *Asia-Pacific Journal of Public Health*, vol. 27, no. 2, pp. 600–605, 2015.

[2] Y. Igarashi and Y. Nogami, "The effect of regular aquatic exercise on blood pressure: a meta-analysis of randomized controlled trials," *European Journal of Preventive Cardiology*, vol. 25, no. 2, pp. 190–199, 2018.

[3] O. Nalbant, H. Nur, C. Öğüş et al., "Effects of long-term aerobic exercise program in chronic obstructive pulmonary disease," *FTR-Turkiye Fiziksel Tip ve Rehabilitasyon Dergisi*, vol. 57, no. 1, pp. 8–13, 2011.

[4] F. Wang, "Research on the effect of yoga on the recovery of motor and neurological functions of stroke patients," *NeuroQuantology*, vol. 16, no. 3, 2018.

[5] Expert Committee on the Diagnosis and Classification of Diabetes Mellitus, "Report of the expert committee on the diagnosis and classification of diabetes mellitus," *Diabetes Care*, vol. 26, pp. S4–S19, 2000.

[6] WHO, *The World Health Report*, World Health Organization, Geneva, Switzerland, 1998.

[7] P. Niu, "Effect of Ba Duan Jin exercise on the blood glucose control in type 2 diabetic patients," *Chinese Journal of Nursing*, vol. 47, no. 8, pp. 701–703, 2012.

[8] Z. T. Liu, "Effect of different modes of exercise training on glycemic indices in patients with type 2 diabetes," *Journal of Shandong Sport University*, vol. 26, no. 7, pp. 46–51, 2010.

[9] A. H. Zhao, A. R. Han, and Z. H. Tao, "The effect of yoga exercise on blood glucose and quality of life in female patients with type 2 diabetes," *Chinese Nursing Research*, vol. 32, no. 16, pp. 2608–2610, 2018.

[10] M. R. Irwin, R. Olmstead, and S. J. Motivala, "Improving sleep quality in older adults with moderate sleep complaints: a randomized controlled trial of Tai Chi Chih," *Sleep*, vol. 31, no. 7, pp. 1001–1008, 2008.

[11] J.-C. Tsai, W.-H. Wang, P. Chan et al., "The beneficial effects of Tai Chi Chuan on blood pressure and lipid profile and anxiety status in a randomized controlled trial," *The Journal of Alternative and Complementary Medicine*, vol. 9, no. 5, pp. 747–754, 2003.

[12] K. M. Mustian, J. A. Katula, D. L. Gill, J. A. Roscoe, D. Lang, and K. Murphy, "Tai Chi Chuan, health-related quality of life and self-esteem: a randomized trial with breast cancer survivors," *Supportive Care in Cancer*, vol. 12, no. 12, pp. 871–876, 2004.

[13] T. W. Xia, Y. Yang, W. H. Li et al., "Different training durations and styles of tai chi for glucose control in patients with type 2 diabetes: a systematic review and meta-analysis of controlled trials," *BMC Complementary and Alternative Medicine*, vol. 19, no. 1, p. 63, 2019.

[14] Z. Zhou, R. Zhou, K. Li et al., "Effects of tai chi on physiology, balance and quality of life in patients with type 2 diabetes: a systematic review and meta-analysis," *Journal Of Rehabilitation Medicine*, vol. 51, no. 6, pp. 405–417, 2019.

[15] Q. Tang, C. J. Guo, P. Li et al., "Meta-analysis of the effect of Tai Chi in patients with type 2 diabetes mellitus," *Modern Preventive Medicine*, vol. 44, no. 14, pp. 2516–2521, 2017.

[16] J.-H. Yan, W.-J. Gu, and L. Pan, "Lack of evidence on Tai Chi-related effects in patients with type 2 diabetes mellitus: a meta-analysis," *Experimental and Clinical Endocrinology & Diabetes*, vol. 121, no. 5, pp. 266–271, 2013.

[17] M. S. Lee, J. H. Jun, H.-J. Lim, and H.-S. Lim, "A systematic review and meta-analysis of tai chi for treating type 2 diabetes," *Maturitas*, vol. 80, no. 1, pp. 14–23, 2015.

[18] L. G. Macedo, M. R. Elkins, C. G. Maher, A. M. Moseley, R. D. Herbert, and C. Sherrington, "There was evidence of convergent and construct validity of physiotherapy evidence database quality scale for physiotherapy trials," *Journal of Clinical Epidemiology*, vol. 63, no. 8, pp. 920–925, 2010.

[19] L. Harvey, R. Herbert, and J. Crosbie, "Does stretching induce lasting increases in joint ROM? A systematic review," *Physiotherapy Research International*, vol. 7, no. 1, pp. 1–13, 2002.

[20] N. A. Lannin and R. D. Herbert, "Is hand splinting effective for adults following stroke? A systematic review and methodological critique of published research," *Clinical Rehabilitation*, vol. 17, no. 8, pp. 807–816, 2003.

[21] F. Wu, E. F. Song, Y. Bao et al., "Effect of simplified 24 movement forme of tai chi on the level of inflammatory cytokines and the quality of life of type2 diabetes patients," *Chinese Journal Physical Medicine Rehabilitation*, vol. 32, no. 3, pp. 205–207, 2010.

[22] H. C. Li, Y. Qiu, and Y. Tie, "Effects of Chen style Taijiquan on blood biochemical parameters and cardiopulmonary function in elderly patients with type 2 diabetes," *Chinese Journal of Gerontology*, vol. 35, no. 5, pp. 1293-1294, 2015.

[23] Z. B. Li, L. L. Qi, L. Zhao et al., "Study on advantages of treating type 2 diabetes mellitus with Baduanjin for aerobic exercise," *Liaoning Journal of Traditional Chinese Medicine*, vol. 40, no. 9, pp. 1858–1860, 2013.

[24] P. Wang, Q. Y. Han, G. T. Li et al., "Evaluation of varying aerobics interferential effects on type 2 diabetes patients in the community," *China Medical Herald*, vol. 6, no. 9, pp. 34-35, 2009.

[25] L. Xiao, Y. Zhou, and J. Li, "Effects of fasting blood sugar nitrogen monoxide content and nitric oxide synthase activity in blood serum content in patients with diabetes after the intervention of Taijiquan exercise and Puerarin," *Journal of Shaanxi Normal University(Natural Science Edition)*, vol. 39, no. 2, pp. 104–108, 2011.

[26] G. Zhao, M. S. Chen, L. Zhuang et al., "Intervention effects of taijiquan exercise on body shape, blood lipid and insulin resistance in patients with type II diabetes," *Journal of Nanjing Sports Institute*, vol. 16, no. 1, pp. 1–7, 2017.

[27] Y. Zhang and F. H. Fu, "Effects of 14-week Tai Ji Quan exercise on metabolic control in women with type 2 diabetes," *The American Journal of Chinese Medicine*, vol. 36, no. 4, pp. 647–654, 2008.

[28] P. Lam, S. M. Dennis, T. H. Diamond, and N. Zwar, "Improving glycaemic and BP control in type 2 diabetes. The effectiveness of Tai Chi," *Australian Family Physician*, vol. 37, no. 10, pp. 884–887, 2008.

[29] T. Tsang, R. Orr, P. Lam, E. Comino, and M. F. Singh, "Effects of Tai Chi on glucose homeostasis and insulin sensitivity in older adults with type 2 diabetes: a randomised double-blind sham-exercise-controlled trial," *Age and Ageing*, vol. 37, no. 1, pp. 64–71, 2008.

[30] S.-C. Chen, K.-C. Ueng, S.-H. Lee, K.-T. Sun, and M.-C. Lee, "Effect of T'ai chi exercise on biochemical profiles and oxidative stress indicators in obese patients with type 2 diabetes," *The Journal of Alternative and Complementary Medicine*, vol. 16, no. 11, pp. 1153–1159, 2010.

[31] X. B. Li, "Effects of tai chi exercise on oxidative stress and inflammation in elderly patients with type 2 diabetes mellitus," *Chinese Journal of Gerontology*, vol. 33, no. 21, pp. 5465-5466, 2013.

[32] E. M. Zhang, *Research on the Effects of 24-Style Taijiquan on Depression of Middle-Aed and Elderlv Patients with Diabetes*, Beijing Sport University, Beijing, China, 2014.

[33] Y. Kan and H. Shao, "Effects of taijiquan exercise on insulin sensitivity in obese patients with type 2 diabetes," *Journal of Traditional Chinese Medicine*, vol. 10, p. 11, 2014.

[34] N. Zhu, *Study the Effects of Yang and Chen Taijiquan Style on T2DM Patients*, Liaoning Normal University, Dalian, China, 2017.

[35] International Diabetes Foundation, *Type 2 Diabetes*, International Diabetes Foundation, Brussels, Belgium, 2020, https://www.idf.org/aboutdiabetes/type-2-diabetes.html.

[36] J. Lindström, P. Ilanne-Parikka, M. Peltonen et al., "Sustained reduction in the incidence of type 2 diabetes by lifestyle intervention: follow-up of the Finnish Diabetes Prevention Study," *The Lancet*, vol. 368, no. 9548, pp. 1673–1679, 2006.

[37] M. Chao, C. Wang, X. Dong et al., "The effects of Tai Chi on type 2 diabetes mellitus: a meta-analysis," *Journal of Diabetes Research*, vol. 2018, Article ID 7350567, 9 pages, 2018.

[38] M. S. Lee, T.-Y. Choi, H.-J. Lim, and E. Ernst, "Tai chi for management of type 2 diabetes mellitus: a systematic review," *Chinese Journal of Integrative Medicine*, vol. 17, no. 10, pp. 789–793, 2011.

[39] Y. Liu, B. Du, B. Huang, L. Yang, and S. Huang, "Systematic review on effect of tai chi regarding to glucolipid metabolism and life quality of type 2 diabetes mellitus," *Rehabilitation Medicine*, vol. 27, no. 4, pp. 55–59+64, 2017.

[40] Q. Wang, *The Systematic Review and Meta-Analysis of Randomized Controlled Trials for Tai Chi in the Treatment of Type 2 Diabetes*, Beijing Sport University, Beijing, China, 2017.

[41] W. H. Li, Z. F. Wu, C. X. Jing et al., "Effects of Chen-style Taijiquan on cardiorespiratory endurance of pre-diabetic patients," *China Journal of Traditional Chinese Medicine and Pharmacy*, vol. 34, no. 6, pp. 2807–2809, 2019.

[42] J. S. Wooten, K. D. Biggerstaff, and C. Anderson, "Response of lipid, lipoprotein-cholesterol, and electrophoretic characteristics of lipoproteins following a single bout of aerobic exercise in women," *European Journal of Applied Physiology*, vol. 104, no. 1, pp. 19–27, 2008.

[43] Joint Committee on the Development of Guidelines for Prevention and Treatment of Adult Dyslipidemia in China, "Chinese guidelines for the prevention and treatment of dyslipidemia in adults," *Chinese Journal of Cardiology*, vol. 35, no. 5, pp. 390–419, 2007.

[44] X. Y. Shen, D. L. Zhang, H. Fu et al., "Research progress on the effect of exercise prescription on elderly patients with type 2 diabetes," *Chinese Journal of Gerontology*, vol. 388, no. 5, pp. 251–253, 2018.

[45] X. R. Xi, I. A. Qureshi, X. D. Wu, I. H. Khan, Y. B. Huang, and E. Shiarkar, "The effect of exercise training on physical fitness and plasma lipids in young Chinese men and women," *Zhonghua yi xue za zhi = Chinese Medical Journal; Free China Ed*, vol. 59, no. 6, pp. 341–347, 1997.

Hindawi
Evidence-Based Complementary and Alternative Medicine
Volume 2021, Article ID 6656362, 14 pages
https://doi.org/10.1155/2021/6656362

Research Article

Effect of Bushen Huoxue Prescription on Cognitive Dysfunction of KK-Ay Type 2 Diabetic Mice

Shao-Yang Zhao,[1,2] Huan-Huan Zhao,[3] Ting-Ting Hao,[1] Wei-Wei Li,[2] and Hao- Guo[1]

[1]*Institute of Basic Medical Sciences, Xiyuan Hospital, China Academy of Chinese Medical Sciences, Beijing 100091, China*
[2]*Research Studio of Integration of Traditional and Western Medicine, First Hospital, Peking University, Beijing 100034, China*
[3]*Nutrition Department, LinYi People's Hospital, Linyi 276000, China*

Correspondence should be addressed to Wei-Wei Li; weiwei_ivy@163.com and Hao- Guo; g0502g@163.com

Received 10 November 2020; Revised 24 January 2021; Accepted 18 February 2021; Published 13 March 2021

Academic Editor: Youhua Xu

Diabetic cognitive impairment is one of the common complications of type 2 diabetes, which can cause neurological and microvascular damage in the brain. Bushen Huoxue prescription (BSHX), a compound Chinese medicine, has been used clinically to treat diabetes-induced cognitive impairment. However, its underlying mechanisms remain unclear. In this study, KK-Ay diabetic model mouse was administered BSHX daily for 12 weeks. Bodyweight, random blood glucose (RBG), and fasting blood glucose (FBG) were measured every 4 weeks. Triglycerides (TG), cholesterol (TC), high-density lipoprotein cholesterol (HDL-C), low-density lipoprotein cholesterol (LDL-C), fasting serum insulin (FINS), and Morris water maze were tested after 12 weeks of administration. On the day of sacrifice, the hippocampus was collected for pathological staining and advanced glycation end products (AGEs) analysis to evaluate the neuroprotective effect of BSHX. Our results showed that BSHX treatment significantly ameliorated the T2DM related insults, including the increased bodyweight, blood glucose, TG, insulin levels, AGEs, the reduced HDL-C, the impaired spatial memory, and the neurological impairment. Moreover, Western blot analysis showed that increased expression of receptors of AGEs (RAGEs), inducible nitric oxide synthase (iNOS), cyclooxygenase-2 (COX-2), and activation of nuclear factor-κB (NF-κB) in the hippocampus were significantly inhibited by BSHX treatment. These results indicate that BSHX can significantly ameliorate glucose and lipid metabolism dysfunction, reduce the morphological changes in hippocampus tissues, and improve the cognitive function of KK-Ay mice. These protective effects of BSHX may involve regulation of the AGEs/RAGE/NF-κB signaling pathway.

1. Introduction

Type 2 diabetes mellitus (T2DM) is a metabolic disease mainly characterized by long-term hyperglycemia, which is affected by multiple factors [1]. According to a survey, 693 million people worldwide will suffer from T2DM by 2045 [2]. During the occurrence and development of this disease, the metabolism of carbohydrates, lipids, and proteins is abnormal, resulting in long-term damage to various tissues such as the eye, kidney, nerve, cardiocerebral vessel, and eventually functional impairment and failure. Diabetic cognitive dysfunction is one of the main chronic complications. A foreign epidemiological survey shows that T2DM can increase the risk of cognitive dysfunction by 40% [3, 4]. Diabetes has become an independent risk factor for cognitive dysfunction [5]. Diabetes combined with cognitive dysfunction can eventually result in memory disorder, cognitive dysfunction, aphasia, and apraxia and bring heavy burden to society [6–11]. Therefore, the prevention and treatment of diabetic cognitive dysfunction is of great significance to improve the prognosis and quality of life of T2DM patients.

According to traditional Chinese medicine, the core pathogenesis of diabetic cognitive dysfunction is kidney deficiency and blood stasis. Bushen Huoxue prescription (BSHX), a newly formulated compound Chinese medicine, is to add leech on the basis of modified Wuzi Yanzong prescription (Table 1) to increase the function of promoting

Table 1: Composition of BSHX.

Herbal composition	Part used	Percentage of total weight
Cuscuta chinensis Lam. (菟丝子)	Fruit	25
Lycium barbarum L (枸杞子)	Fruit	25
Rubus chingii Hu. (覆盆子)	Fruit	12
Schisandra chinensis (Turcz.) Baill.(五味子)	Fruit	3
Plantago asiatica L. (车前子)	Seed	6
Epimedium brevicornu Maxim. (淫羊藿)	Stem and leaf	25
Hirudo nipponica Whitman (水蛭)	The whole body	4

blood circulation and dredging collaterals on the basis of tonifying kidney. Its clinical application has proven that BSHX can significantly alleviate memory decline in the patients in addition to its hypoglycemic effect [12–15]. Previous studies have reported that some traditional Chinese medicines or monomers in this prescription have good glucose-controlling and neuroprotective effects, in which Chinese wolfberry can not only reduce blood glucose but also improve cognitive impairment in T2DM mice [16–19]. Icariside can improve cerebral ischemia-reperfusion-induced microcirculatory disturbance, improve blood flow, and reduce neuron loss and apoptosis in the CA1 area of the hippocampus in *Gerbillinae* [15], while hyperoside and schisandrin *B* can inhibit the neurotoxicity of amyloid β-protein (Aβ) by inhibiting the activation of the mitochondrial apoptosis pathway [19, 20]. However, the improvement effect of BSHX on diabetic cognitive dysfunction still lacks systematic pharmacodynamic evaluation. The aim of the present study was to investigate the effect of BSHX on diabetic cognitive impairment in a spontaneous T2DM animal model: KK-Ay mice.

2. Materials and Methods

2.1. Materials. BSHX was purchased from Beijing Kangrentang Pharmaceutical Co., Ltd. (Beijing, China). The medicinal components of BSHX are listed in Table 1. Protamine zinc recombinant human insulin was from Eli Lilly and Company (Indiana, USA). Metformin was purchased from Shanghai Squibb Pharmaceutical Co., Ltd. (Shanghai, China). High-fat diet for mice was obtained from Beijing HFK Bioscience Co., Ltd. (Beijing, China). Normal diet for mice was obtained from Beijing Keao Xieli Feed Co., Ltd. (Beijing, China). Stroke-physiological saline solution was from Beijing Double-Crane Pharmaceutical Co., Ltd. (Beijing, China). Mouse ultrasensitive insulin ELISA kit was from ALPCO (USA). TUNEL kit was purchased from Roche Group (Basel, Switzerland). Triglyceride assay kit (GPO-PAP) and total cholesterol assay kit (COD-PAP) were obtained from BioSino Biotechnology and Science Inc. (Beijing, China). High-density lipoprotein cholesterol (HDL-C) and low-density lipoprotein cholesterol (LDL-C) assay kits were purchased from Nanjing Jiancheng Co., Ltd. (Nanjing, China). AGEs ELISA kit was purchased from Andy Gene Biotechnology Co., Ltd. (Beijing, China). Nuclear extraction kit was obtained from KeyGEN Biotech Inc. (Nanjing, China). Primary antibodies for RAGE, iNOS, COX-2, p-NF-κB, NF-κB, and rabbit IgG were obtained from Cell Signaling Technology (Boston, MA, USA).

2.2. HPLC Analysis. Referring to the study of our research group [21], BSHX extracts were analyzed using a Shimadzu prominence liquid chromatography platform (Kyoto, Japan) equipped with two LC-20AT pumps, a CTO-20A column oven, a DGU-20A5R degasser, an SIL-20A autosampler, and an SPD20AD detector. Chromatographic separation was conducted on a AichromBond-AQ C18 column (250 mm × 4.6 mm, 5 μm; Abel Industries Ltd., Canada), protected by a Phenomenex® C18 guard cartridge (3 × 4 mm, 5 μm; Torrance, CA, USA). The mobile phase consisted of ACN (A) and 0.1% aqueous formic acid (B) and was delivered at 1.0 mL/min with the following gradient program: 0–35 min, 0–3% B; 35–100 min, 3–22% B; 100–115 min, 22–35% B; 115–130 min, 35–35% B; 130–140 min, 35–100% B; 140–145 min, 40–100% B; and 145–155 min, 100–100% B. The column was maintained at 40°C. At the end of each run, the delivery of 100% A was performed for another 14 min for system reequilibration. The monitor wavelength was set at 235 nm, 254 nm, and 280 nm, respectively.

2.3. Animal Grouping and Drug Administration. All animal experiments complied with the European Union Guidelines (2010/63/EU) and were performed as per the Guidelines of the Animal Research Committee of Peking University after being approved by the Institutional Animal Care and Use Committee of Peking University First Hospital.

Twelve-week-old male KK-Ay mice ($N = 50$), weighing 30–35 g, were purchased from Beijing HFK Bioscience Co., Ltd. (license no. SCXK (Jing) 2016–0005). Twelve-week-old male C57BL/6J mice ($N = 10$), weighing 23–25 g, were purchased from Beijing Vital River Laboratory Animal Technology Co., Ltd. (License No. SCXK (Jing) 2016–0001). KK-Ay mice were fed with high-fat diet, and C57BL/6J mice were fed with general diet. All animals were kept in the animal room of Xiyuan Hospital, China Academy of Chinese Medical Sciences. The mice could drink water freely and were reared for 10 days under the conditions of 22 ± 1°C, 40% ± 5% humidity, and a 12 h light cycle. Blood glucose was measured by the glucose oxidase method. Only KK-Ay mice satisfying the requirement of random blood glucose (RBG) ≥11.1 mmol/L or fasting blood glucose (FBG) ≥7.0 mmol/L were taken as DM samples.

The mice were randomly divided into six groups as follows: (1) control (untreated C57BL/6J mice); (2) model

(untreated KK-Ay mice); (3) low BSHX (KK-Ay mice treated with 0.5 g/kg BSHX); (4) medium BSHX (KK-Ay mice treated with 1 g/kg BSHX); (5) high BSHX (KK-Ay mice treated with 2 g/kg BSHX); and (6) metformin (KK-Ay mice treated with 250 mg/kg metformin). All drugs were given orally, 0.1 mL/10g each day for 12 weeks. The control group and model group were given the equivalent volume of distilled water in the same manner for contrast.

2.4. Oral Glucose Tolerance Test (OGTT). Blood was taken from caudal veins of mice fasted for 8 hours for FBG measuring. After giving mice 2 g/kg glucose solution orally, the blood glucose levels at the timepoints of 30 min (BG30), 60 min (BG60), and 120 min (BG120) were measured, and the curve was drawn. The area under the curve (AUC) was then calculated according to the formula $AUCg = (FBG + BG30) \times 0.5 \div 2 + (BG30 + BG60) \times 0.5 \div 2 + (BG60 + BG120) \times 1 \div 2$.

2.5. Insulin Tolerance Test (ITT). Blood was taken from caudal veins of mice fasted for 8 hours for FBG detection. The blood glucose levels of mice were detected at 30 min (BG30), 60 min (BG60), and 120 min (BG120) after 0.26 IU/kg insulin was injected intraperitoneally, and the curve was drawn. The AUC was computed by $AUCg = (FBG + BG30) \times 0.5 \div 2 + (BG30 + BG60) \times 0.5 \div 2 + (BG60 + BG120) \times 1 \div 2$.

2.6. Fasting Serum Insulin (FINS) and the Blood Lipid Test. Concentrations of FINS in blood taken from caudal veins of mice fasted for 8 hours were tested using commercial ELISA kits following the manufacturer's protocol. Concentrations of total triglycerides (TG) and total cholesterol (TC) in serum were measured using triglyceride assay kits (GPO-PAP) and total cholesterol assay kits (COD-PAP), respectively. High-density lipoprotein cholesterol (HDL-C) and low-density lipoprotein cholesterol (LDL-C) in serum were detected with corresponding assay kits according to manufacturer's protocol.

2.7. Morris Water Maze (MWM) Test. After 12 weeks of treatment, spatial and related forms of learning and memory were assessed by the MWM test [22]. Briefly, mice were individually trained in a circular pool (120 cm in diameter and 50 cm in height), which was filled with 30 cm deep water at a constant temperature of 25 ± 1°C. There was a platform (9 cm in diameter) at the center of each of four quadrants of the pool. On each side of the walls of the four quadrants, distinctly colored papers were disposed as a visual positional hint. On the first 2 days, each mouse was subjected to visible platform training, in which the platform was submerged 1 cm beneath the water surface and was indicated by a flag. On days 3–5, hidden platform training was carried out with the flags removed for cultivating the spatial learning and memory retention ability of mice to find the platform.

The escape latency of mice in finding the platform was then tested for 5 days. Briefly, four trials were performed on each mouse per day with about 1 h interval in between. During each trial, mice were released into the water facing the pool wall from one of the 4 starting positions and allowed to locate the submerged platform for a maximum of 120 s. Mice failing to find the platform within 120 s were gently guided to the platform and allowed to stay on it for 15 s. On day 6, the platform was removed, and a probe trial was performed to record the time spent in the target quadrant where the escape platform was placed and the number of crossings over the original position of the platform.

2.8. Hematoxylin and Eosin (H&E) Staining. Normal saline was infused into mice under anesthesia via the left ventricle, followed by injection of 4% paraformaldehyde for fixation. After being harvested, brains were kept in 10% modified formaldehyde fixative, embedded in paraffin, and cut into 4 μm thick slices successively for H&E staining and optical observation of pathological changes.

2.9. Nissl Staining. The paraffin sections were dewaxed, debenzoled by gradient alcohol, and washed with distilled water. After being dyed at 37°C for 10 minutes and washed with distilled water for 3 times, the samples were differentiated and decolorized by 95% and 75% ethanol until the background under the microscope was clear. The samples were dehydrated routinely and sealed with transparent and neutral gum prior to observation under an optical microscope.

2.10. TUNEL Staining. The paraffin sections were fixed with 4% paraformaldehyde and washed with distilled water before being incubated at 37°C for 20 min with protein digestive enzyme. The TUNEL apoptosis kit was then used for staining as directed.

2.11. Measurement of Advanced Glycation End Products (AGEs). The hippocampal tissues of mice were collected after 12 weeks of treatment. The concentrations of AGEs in hippocampus were detected by ELISA kit (Andy Gene Biotechnology Co., Ltd., Beijing, China) according to the manufacturer's instructions.

2.12. Western Blot Analysis. After the anesthetized mice were transcardially perfused with saline through the left ventricle, brains were collected and lysed with RIPA buffer (50 mM Tris-HCl, 300 mM NaCl, 0.5% TritonX-100, 5 mM EDTA, and protease inhibitor cocktail) for 30 min on ice. The cell lysates were centrifuged at 13,000 rpm and 4°C for 15 min before determination of protein concentrations by Bradford assay. Nuclear and cytoplasmic proteins were extracted with the Nuclear Extraction Kit (KeyGEN Biotech Inc., Nanjing, China) according to manufacturer's instructions. Equal amounts of protein were separated with SDS-PAGE and subsequently transferred to polyvinylidene fluoride membranes. The blots were blocked with 5% nonfat milk in PBST and then incubated with primary antibodies at 4°C overnight. Afterward, the blots were washed adequately in PBST and incubated with horseradish peroxidase-labeled goat

anti-rabbit secondary antibody at room temperature for 1 h. The washed blots were then developed with the enhanced chemiluminescent substrate and visualized with the Tanon 5200 Imaging Analysis System (Tanon Science & Technology Co. Ltd., Shanghai, China).

2.13. Statistical Methods. All data were expressed as mean ± standard deviation (SD). One-way analysis of variance (ANOVA) and Bonferroni's post hoc test were adopted for statistical analysis. $P < 0.05$ was considered statistically significant, and $P < 0.01$ was considered statistically highly significant.

3. Results

3.1. Identification of the Components of BSHX Extract. Combining application of high-performance liquid chromatography (HPLC) and mass spectrometry (HPLC-MS) to analyze the main components of BSHX extract, a total of 114 compounds were identified, including 43 flavonoids (F1–F43), 28 small molecular phenolic acids (P1–P28), 17 cinnamoyl polyamines (A1–A17), 11 glycolipids (G1–G11), 8 fatty acids (FA1–FA8), 4 lignins (L1–L4), 2 semiterpene glycosides (T1-T2), and 1 saponin compound (S1). LC/ESI-IT-TOF-MS^n analysis results showed that the flavonoids in BSHX were mainly derived from *Epimedium*, cinnamoyl polyamines and glycolipids were mainly derived from wolfberry, and small molecular phenolic acids were the main sources in *Plantago* seed, *Cuscuta* seed, and raspberry (Figure 1 and Supplementary Data).

3.2. BSHX Helps Prevent KK-Ay Mice from Gaining Bodyweight. As shown in Table 2, untreated KK-Ay mice gained significantly more bodyweight than C57BL/6J mice from the beginning ($P < 0.01$ vs. the C57BL/6J group), and they developed obesity at the 12th week. The weight growth of KK-Ay mice fed by BSHX was slower than that of untreated KK-Ay mice (Figure 2). There were statistical differences regarding the bodyweight between the KK-Ay mice fed by 2 g/kg BSHX and the untreated KK-Ay mice after 8 weeks of treatment ($P < 0.05$ vs. the KK-Ay group). Twelve weeks later, the bodyweight of mice treated by different doses of BSHX was statistically different from that of untreated KK-Ay mice ($P < 0.05$ or $P < 0.01$ vs. the KK-Ay group). The bodyweight showed no significant increase and maintained at a stable level in the high BSHX (2 g/kg) group.

Bodyweight of mice in each group was examined every 4 weeks. Data were expressed as mean ± SD ($n = 10$). $^{**}P < 0.01$ vs. the C57BL/6J group. $^{\#}P < 0.05$, $^{\#\#}P < 0.01$ vs. the KK-Ay group.

3.3. BSHX Inhibits the Increase of Random Blood Glucose (RBG). According to Table 3, the RBG of mice in the model group rose continuously and was significantly different from that in the control group ($P < 0.01$ vs. the C57BL/6J group). Four weeks after gavaging, blood glucose increased significantly in the model group and all treatment groups, but no difference was found between each treatment group and the model group. Eight weeks after treatment, the blood glucose level of mice in the high BSHX (2 g/kg) group was significantly lower than that in the model group ($P < 0.01$ vs. the KK-Ay group). BSHX (2 g/kg) showed the similar effect to metformin in reducing blood glucose. After continuous administration for 12 weeks, blood glucose was notably improved in both medium BSHX (1 g/kg) and high BSHX (2 g/kg) groups ($P < 0.01$ vs. the KK-Ay group), and a high dose of BSHX (2 g/kg) showed a better effect (Figure 3).

Blood samples were collected from mice caudal veins in each group to detect random blood glucose every 4 weeks. Data were expressed as mean ± SD ($n = 10$). $^{**}P < 0.01$ vs. the C57BL/6J group. $^{\#\#}P < 0.01$ vs. the KK-Ay group.

3.4. BSHX Reduces the Fasting Blood Glucose (FBG) Level. After gavage for 8 weeks, the FBG levels of mice were improved in the metformin group and all BSHX groups, especially in the medium BSHX (1 g/kg) group. After gavage for 12 weeks, the FBG levels of mice in the medium BSHX (1 g/kg) and high BSHX (2 g/kg) groups were significantly improved ($P < 0.01$ vs. KK-Ay group), and a high dose of BSHX (2 g/kg) had a similar effect to metformin in reducing the FBG level (Table 4 and Figure 4).

Blood samples were collected from mice caudal veins in each group to detect fasting blood glucose every 4 weeks. Data are expressed as mean ± SD ($n = 10$). $^{**}P < 0.01$ vs. the C57BL/6J group. $^{\#\#}P < 0.01$ vs. the KK-Ay group.

3.5. BSHX Ameliorates Glucose Tolerance and Insulin Resistance. The oral glucose tolerance of mice in each group was measured after continuous gavage for 12 weeks (Figure 5(a)). Specifically, high glucose solution was given to mice in each group. Within the first 30 min, the blood glucose level of all mice increased, especially the KK-Ay mice in the model group. For the next 30 min, the blood glucose level in all BSHX groups began to decrease, while that of the model group peaked. After 120 min, the blood glucose level tended to stabilize in all groups. The statistical analysis results suggested that the AUC of OGTT in the medium BSHX (1 g/kg) group and the metformin group was significantly lower than that in the model group ($P < 0.05$ or $P < 0.01$ vs. the KK-Ay group). However, compared with the model group, the AUC of low (0.5 g/kg) and high BSHX (2 g/kg) groups decreased but showed no statistical difference.

As indicated in Figure 5(b), the blood glucose level in the KK-Ay model mice presented an increasing trend due to stress hyperglycemia within the first 30 min after insulin injection. In contrast, the blood glucose levels of mice in all BSHX groups and the metformin group decreased in varying degrees within the first 30 min. After insulin injection for 60–120 min, the blood glucose level of mice in all groups gradually decreased and finally maintained unchanged. Moreover, compared with the model group, all BSHX groups, especially the medium BSHX (1 g/kg) group, had a significantly smaller AUC of ITT ($P < 0.01$ vs. the KK-Ay group). The above results demonstrated that the 12-week

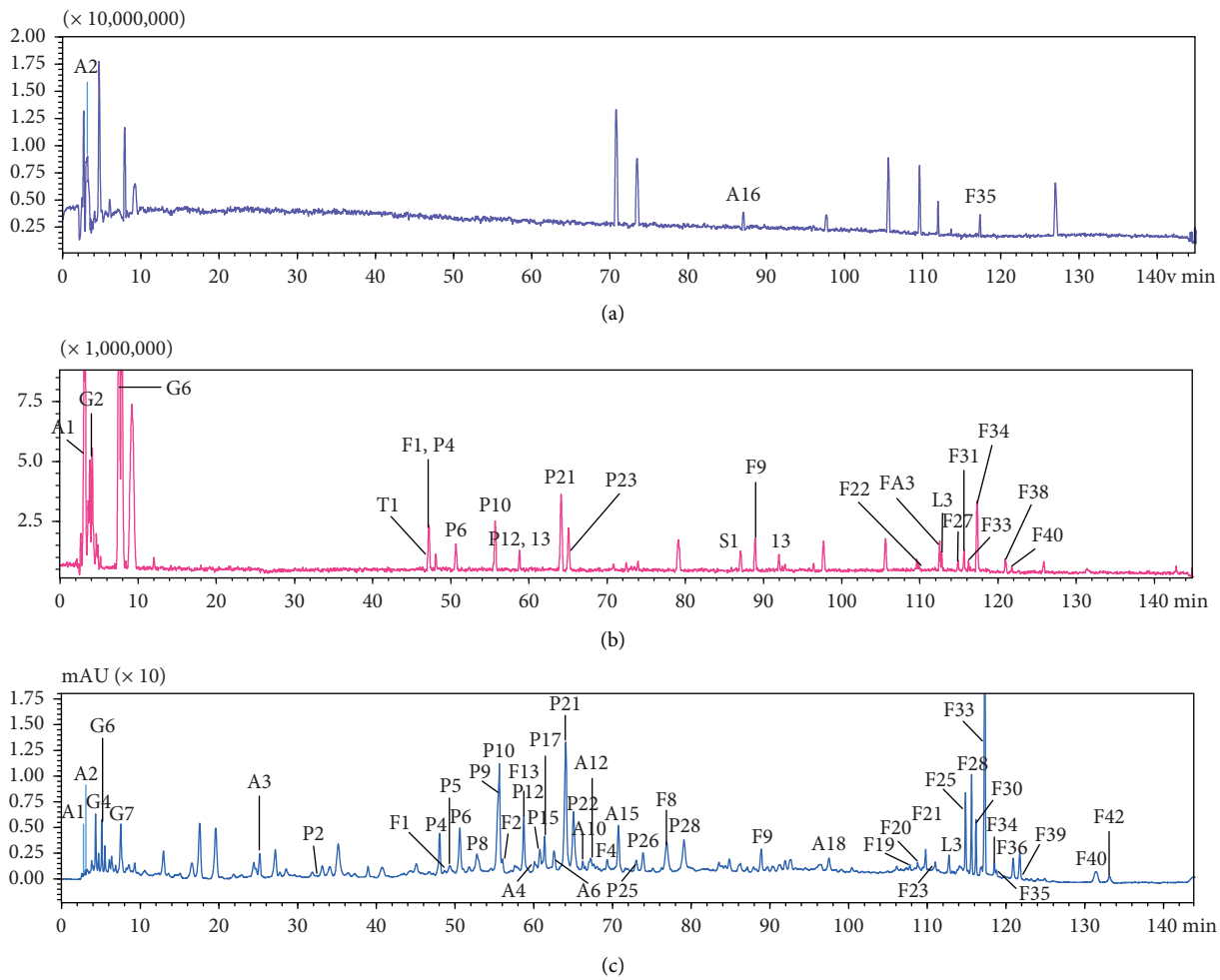

Figure 1: Representative chromatograms analysis of BSHX. (a) Detection in the positive polarity. (b) Detection in the negative polarity. (c) HPLC fingerprint of BSHX with a monitoring wavelength of 280 nm.

Table 2: Bodyweight in each group after 12 weeks of administration (g, $\overline{\chi} \pm s$, $n = 10$).

	Week 0	Week 4	Week 8	Week 12
C58BL/6J	23.58 ± 0.74	27.16 ± 0.46	28.71 ± 1.7	30.10 ± 1.6
KK-Ay	35.33 ± 1.39**	44.74 ± 1.39**	49.13±±1.34**	52.28 ± 1.11**
KK-Ay + BSHX 0.5 g/kg	36.41 ± 1.44	45.10 ± 1.14	49.39 ± 1.75	50.38 ± 1.29#
KK-Ay + BSHX 1 g/kg	35.88 ± 1.63	45.07 ± 1.2	47.58 ± 1.5	48.39 ± 1.26#
KK-Ay + BSHX 2 g/kg	37.07 ± 1.58	43.8 ± 1.7	46.35 ± 1.23#	46.28 ± 1.37##
KK-Ay + Met 250 mg/kg	35.86 ± 1.92	44.34 ± 2.5	46.41 ± 2.3#	47.39 ± 1.35##

Data are expressed as mean ± SD ($n = 10$). **$P < 0.01$ vs. the C57BL/6J group. #$P < 0.05$, ##$P < 0.01$ vs. the KK-Ay group.

administration of BSHX (especially with a dose of 1 g/kg) could tremendously ameliorate insulin resistance of mice.

3.6. BSHX Downregulates the FINS Level and Promotes Blood Lipid Metabolism. FINS, TC, TG, LDL-C, and HDL-C levels were detected in mice after 12 weeks of gavage. Table 5 shows that FINS, TC, TG, and LDL-C levels of the KK-Ay mice in the model group were significantly higher than those in the control group, while the HDL-C level was on the contrary ($P < 0.01$ or $P < 0.001$ vs. the C57BL/6J group). Compared with that of the model group, the FINS level was significantly reduced in the metformin group ($P < 0.01$ vs. the KK-Ay group) and decreased in all BSHX groups. For TC, TG, LDL-C, and HDL-C, a high dose of BSHX (2 g/kg) significantly reduced TG and increased HDL-C ($P < 0.05$ vs. the KK-Ay group).

3.7. BSHX Improves the Cognitive Function of KK-Ay Mice. The MWM test was carried out to examine the spatial and related forms of learning and memory of mice. The escape latency gradually decreased in all groups over 5 days of training (Figure 6(a) and Table 6), and the decrease rate was

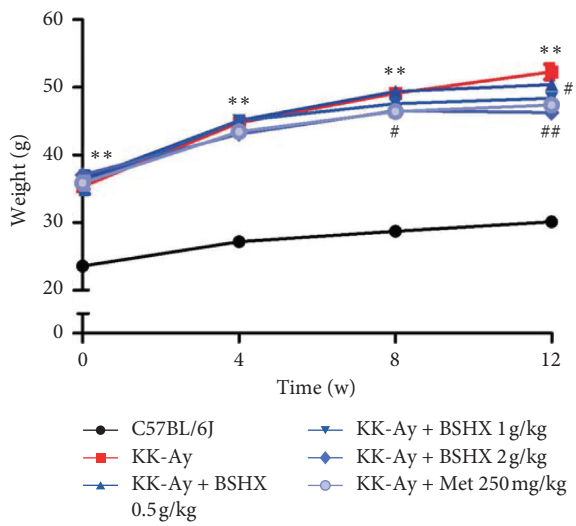

Figure 2: Weight changes of mice in each group after 12 weeks of administration.

Table 3: Random blood glucose changes of mice in each group (mmol/L, $\overline{\chi} \pm s$, $n = 10$).

	Week 0	Week 4	Week 8	Week 12
C57BL/6J	5.5 ± 0.36	6.39 ± 0.86	5.19 ± 0.31	6.43 ± 0.51
KK-Ay	13.53 ± 0.99**	19.93 ± 1.19**	25.87±±0.44**	26.80 ± 0.47**
KK-Ay + BSHX 0.5 g/kg	13.27 ± 1.54	21.3 ± 0.64	26.63.39 ± 0.75	26.37 ± 0.76
KK-Ay + BSHX 1 g/kg	13.88 ± 1.63	19.89 ± 1.1	23.97.58 ± 0.9	21.79 ± 1.06##
KK-Ay + BSHX 2 g/kg	11.75 ± 1.58	19.17 ± 0.67	21.46 ± 0.51##	18.95 ± 0.57##
KK-Ay + Met 250 mg/kg	12.36 ± 1.92	21.6 ± 1.24	21.83 ± 1.64##	19.93 ± 0.75##

Data are expressed as mean ± SD ($n = 10$). **$P < 0.01$ vs. the C57BL/6J group. ##$P < 0.01$ vs. the KK-Ay group.

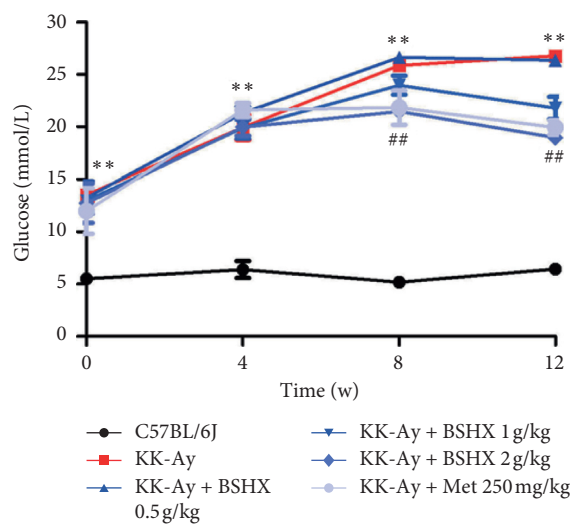

Figure 3: Random blood glucose changes of KK-Ay in each group after 12 weeks of administration.

Table 4: Fasting blood glucose changes of KK-Ay in each group (mmol/L, $\overline{\chi} \pm s$, $n = 10$).

	Week 0	Week 4	Week 8	Week 12
C57BL/6J	6.23 ± 0.37	4.93 ± 0.6	5.3 ± 0.41	6 ± 0.36
KK-Ay	12.77 ± 0.78**	18.87 ± 0.85**	23.40 ±± 0.5**	23.67 ± 0.86**
KK-Ay + BSHX 0.5 g/kg	13.33 ± 1.26	21.23 ± 0.78	19.53.39 ± 0.46##	23.11 ± 0.91
KK-Ay + BSHX 1 g/kg	12.15 ± 0.76	18.27 ± 0.85	18.87 ± 0.33##	19.93 ± 0.74##
KK-Ay + BSHX 2 g/kg	13.43 ± 1.69	19.49 ± 1.43	19.1 ± 0.72##	16.84 ± 0.56##
KK-Ay + Met 250 mg/kg	11.36 ± 1.52	20.43 ± 0.81	18.2 ± 0.72##	17.10 ± 0.81##

Data are expressed as mean ± SD ($n = 10$). **$P < 0.01$ vs. the C57BL/6J group. ##$P < 0.01$ vs. the KK-Ay group.

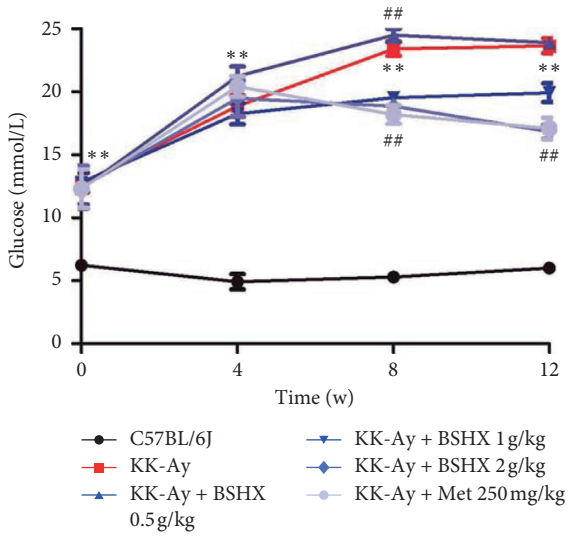

Figure 4: Fasting blood glucose changes of KK-Ay in each group after 12 weeks of administration.

significantly lower in the model group than that in the control group from the third day ($P < 0.01$ vs. the C57BL/6J group). However, compared with the model group, the decline of the escape latency was accelerated in the medium BSHX (1 g/kg) group on day 5 ($P < 0.01$ vs. the KK-Ay group). The escape latency on day 6 further confirmed that BSHX (1 g/kg) significantly improved memory impairment, as displayed in Figure 6(b) and Table 6 ($P < 0.01$ vs. the KK-Ay group). Besides, the escape latency in other BSHX groups also deceased, but the difference between them and the model group was not significantly different.

In the probe trial (Figures 6(c) and 6(d)), a putative measurement of spatial learning and memory retention, there were significantly less platform crossings and a smaller percentage of time spent in the target quadrant in the model group than in the control group ($P < 0.05$ or $P < 0.01$ vs. the C57BL/6J group). The time that mice in the medium BSHX (1 g/kg) group spent in the target quadrant was significantly more than that in the model group ($P < 0.05$ vs. the KK-Ay group). The forementioned two indexes were improved in the other two BSHX groups (Figures 6(c) and 6(d)), but no significant difference was observed.

3.8. BSHX Reduces the Morphological Changes in Hippocampus Tissues. Neuronal damage, especially in the hippocampus, is the pathological basis of cognitive dysfunction in DM [23–27]. The staining patterns of CA1 pyramidal cells in the hippocampus of mice in the control, model, and medium BSHX (1 g/kg) groups were measured after the MWM test (Figure 7). The H&E staining results of brain tissues revealed that the hippocampal neurons of the C57BL/6J mice were well-stained and closely arranged with intact structure, while the nuclei of the hippocampal neurons of the KK-Ay model mice were fixed and contracted with enlarged extracellular spaces and disordered arrangement. In the medium BSHX (1 g/kg) group, the neurons in the hippocampus were arranged neatly and stained homogeneously, and neuronal damage was partially recovered (as shown by the yellow arrow). Nissl staining showed that Nissl bodies in the control group were dark blue, and the cells were closely arranged. In the model group, edema appeared around the neurons and the number of cell layers decreased. Besides, Nissl bodies were lightly stained and indistinctly demarcated. In the medium BSHX (1 g/kg) group, no significant edema of neurons was observed, the cells were closely arranged, and Nissl bodies were stained more homogeneously than those in the model group (as shown by the white arrows). In addition, according to the results of TUNEL staining (which could stain apoptotic cells into dark brown), the dark brown color of neurons in the CA1 region of the hippocampus in the model group suggested that many neurons were apoptotic. The neurons in the medium BSHX (1 g/kg) group were more lightly stained than those in the model group, indicating that cell apoptosis was improved (as shown by the black arrows).

3.9. BSHX Inhibits the Expression of the AGEs/RAGE/NF-κB Signaling Pathway. AGEs play an important role in the pathological development of diabetic cognitive impairment. First, the content of AGEs in the hippocampus of mice was detected by ELISA. According to Figure 8(a), compared with the control group, the model group had significantly increased AGEs content ($P < 0.001$ vs. the C57BL/6J group), and the medium BSHX (1.0 g/kg) group had significantly decreased AGEs content ($P < 0.01$ vs. the KK-Ay group). As for the receptor of AGEs (RAGE), it also dramatically increased in the model group ($P < 0.01$ vs. the C57BL/6J group), but BSHX (0.5 g/kg and 1.0 g/kg) significantly inhibited its expression ($P < 0.05$ or $P < 0.001$ vs. the KK-Ay group) (Figure 8(b)). When AGEs bind to RAGE, they can activate the NF-κB signaling pathway and produce inflammatory factors to destroy the neuron. Therefore, Western blot was adopted to detect whether the NF-κB signaling pathway was activated. As shown in Figure 8(c),

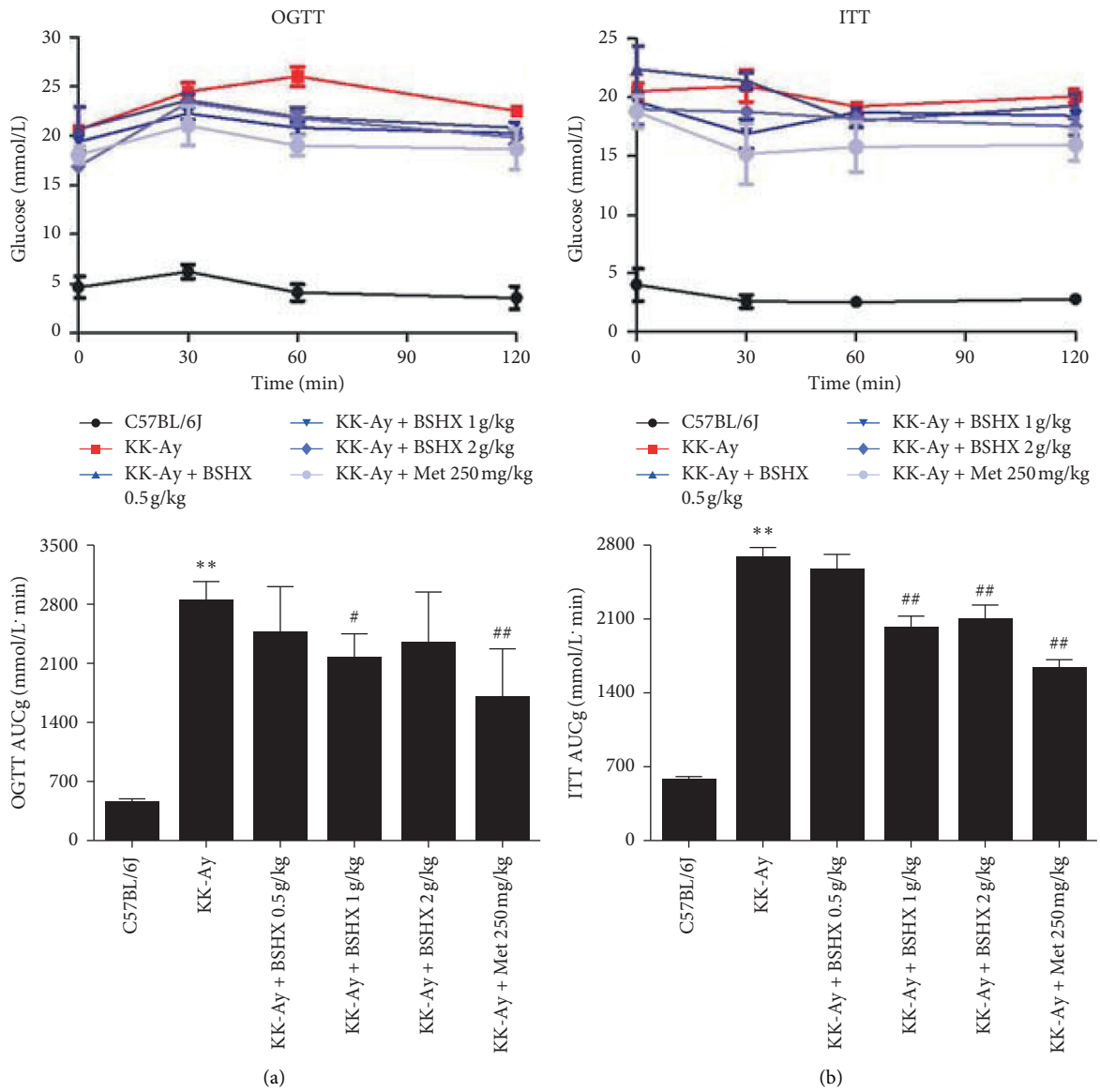

Figure 5: The effect of BSHX on OGTT and ITT. (a) After 12 weeks of administration, glucose solution was given 2 g/kg orally to mice in each group, and the blood glucose curve was drawn at the timepoints of 30 min, 60 min, and 120 min, respectively. (b) After injecting insulin intraperitoneally with a dosage of 0.26 IU/kg to mice in each group, the blood glucose curve was drawn at the timepoints of 30 min, 60 min, and 120 min, respectively. Data are expressed as mean ± SD ($n = 10$). $^{**}P < 0.01$ vs. the C57BL/6J group. $^{\#}P < 0.05$, $^{\#\#}P < 0.01$ vs. the KK-Ay group.

Table 5: Determination of FINS, TC, and TG in each group at week 12 ($\overline{\chi} \pm s$, $n = 10$).

	FINS (ng/mL)	TC (mmol/L)	TG (mmol/L)	LDL-C (mmol/L)	HDL-C (mmol/L)
C57BL/6J	1.32 ± 0.67	1.39 ± 0.12	0.57 ± 0.12	0.31 ± 0.06	1.68 ± 0.30
KK-Ay	10.4 ± 2.31**	3.55 ± 0.63**	2.16±±0.44**	0.50 ± 0.08**	0.75 ± 0.13***
KK-Ay + BSHX 0.5 g/kg	9.25 ± 2.21	2.80 ± 0.88	1.62.39 ± 0.97	0.47 ± 0.09	0.78 ± 0.39
KK-Ay + BSHX 1 g/kg	7.54 ± 1.43	3.07 ± 0.48	1.54 ± 0.41	0.44 ± 0.08	0.73 ± 0.22
KK-Ay + BSHX 2 g/kg	8.58 ± 1.3	2.88 ± 0.85	1.36 ± 0.62#	0.45 ± 0.04	1.30 ± 0.16#
KK-Ay + Met 250 mg/kg	6.52 ± 1.17##	2.74 ± 0.90	1.6 ± 0.36	0.42 ± 0.05	0.80 ± 0.15

Data are expressed as mean ± SD ($n = 10$). $^{**}P < 0.01$, $^{***}P < 0.001$ vs. the C57BL/6J group. $^{\#}P < 0.05$, $^{\#\#}P < 0.01$ vs. the KK-Ay group.

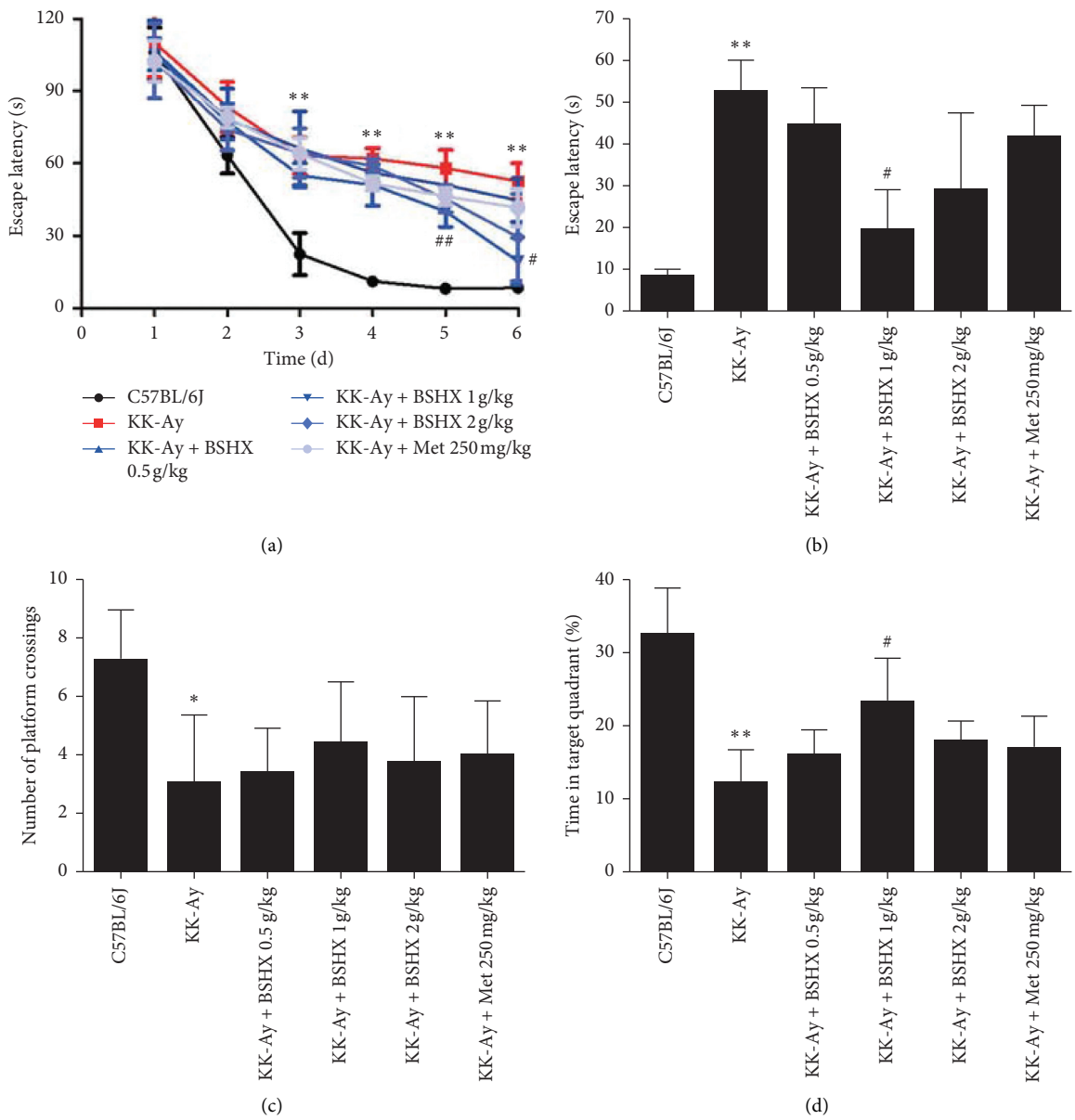

Figure 6: The effect of BSHX on spatial memory of KK-Ay. (a) The mean escape latency time during the training period of mice in each group. Time, seconds. (b) Analysis of escape latency of each group of mice in the formal navigation test. Time, seconds. (c) The number of platform crossings during the spatial probe test. (d) The percent of total time spent in the target of quadrant during the spatial probe test. Data are expressed as mean ± SD ($n = 10$). $^{*}P < 0.05$, $^{**}P < 0.011$ vs. the C57BL/6J group. $^{\#}P < 0.05$, $^{\#\#}P < 0.01$ vs. the KK-Ay group.

Table 6: The escape latency of mice in the navigation test ($\overline{\chi} \pm s$, $n = 10$).

	Day 1 (s)	Day 2 (s)	Day 3 (s)	Day 4 (s)	Day 5 (s)	Day 6 (s)
C57BL/6J	106 ± 10.5	63.33 ± 7.50	22.33 ± 8.74	11.10 ± 2.6	8.04 ± 1.12	8.33 ± 1.53
KK-Ay	110 ± 14.11	83.35 ± 10.41	63.33±±7.64**	62.3 ± 4.7**	58.47 ± 7.55**	52.67 ± 7.5**
KK-Ay + BSHX 0.5 g/kg	106.7 ± 12.58	78.16 ± 12.74	66.57 ± 15.18	56.86 ± 3.60	51.23 ± 2.71	44.67 ± 8.96
KK-Ay + BSHX 1 g/kg	105.3 ± 6.66	77.33 ± 7.37	55.01 ± 5.21	51. 9 ± 3.36	40.09 ± 6.26$^{\#\#}$	19.33 ± 9.71$^{\#}$
KK-Ay + BSHX 2 g/kg	105.8 ± 15.53	74 ± 8.54	64.93 ± 10.21	59.87 ± 5.37	45.33 ± 5.67	29.54 ± 18.15
KK-Ay + Met 250 mg/kg	102.3 ± 8.62	79.4 ± 4.12	64 ± 6.57	51.74 ± 4.89	46.33 ± 3.51	41.67 ± 7.64

Data are expressed as mean ± SD ($n = 10$). Time, seconds. $^{**}P < 0.01$ vs. the C57BL/6J group. $^{\#}P < 0.05$, $^{\#\#}P < 0.01$ vs. the KK-Ay group.

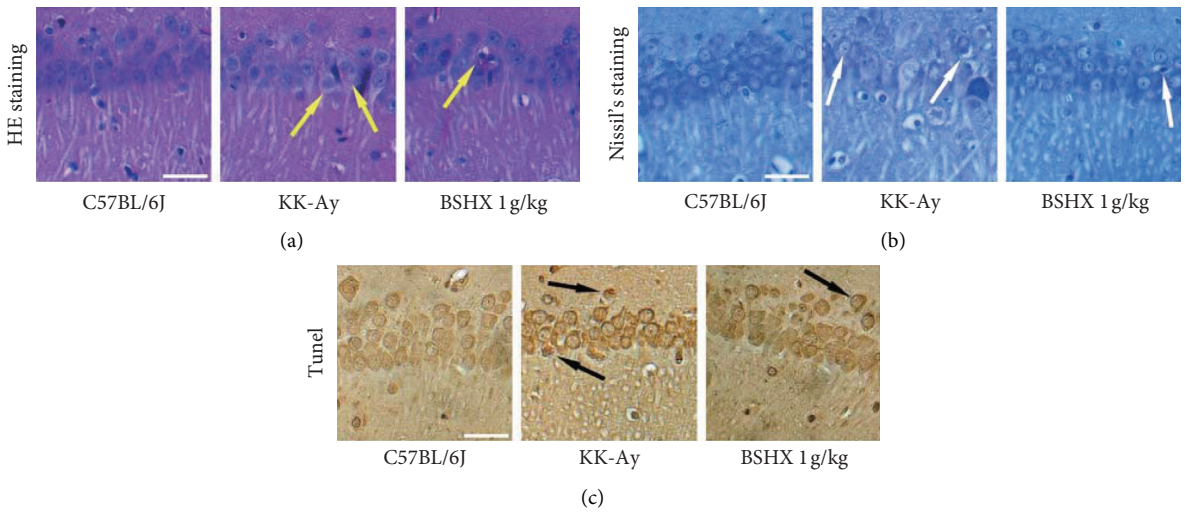

Figure 7: Staining analysis of the effect of BSHX on hippocampal tissue of KK-Ay mice. (a) The results of H&E stain of neurons in hippocampal CA1 region of mice in the C57BL/6J group, KK-Ay group, and KK-Ay + BSHX 1 g/kg group. (b) The results of Nissl stain of neurons in hippocampal CA1 region of mice in each group. (c) The results of TUNEL stain of neurons in hippocampal CA1 region of mice in each group. Scale bar = 50 μm.

iNOS and COX-2, two important inflammatory proteins in the NF-κB signaling pathway, were significantly increased in the brain of the KK-Ay model mice ($P < 0.001$ vs. the C57BL/6J group), while BSHX could notably downregulate the expression of these two proteins ($P < 0.01$ or $P < 0.001$ vs. the KK-Ay group). Meanwhile, a remarkable increase in the phosphorylated NF-κB level was observed in the model group ($P < 0.05$ vs. C57BL/6J group). After 12 weeks of BSHX treatment, the phosphorylated NF-κB level significantly declined ($P < 0.05$ vs. the KK-Ay group) (Figure 8(d)). In addition, the Western blot analysis showed that the model group provoked the translocation of NF-κB p65 from the cytoplasm to the nucleus, and this process was significantly blocked by BSHX (1 g/kg and 2 g/kg) treatment ($P < 0.01$ or $P < 0.001$ vs. the KK-Ay group, Figure 8(e)).

4. Discussion

In this study, the spontaneously mutated KK-Ay model mice with T2DM were intervened with drugs, and the effects of BSHX of different doses on the bodyweight, blood glucose and lipid, insulin level, behavioral cognition, and brain morphology of T2DM mice were analyzed. Besides, the pharmacodynamics of BSHX was assessed. The results showed that the bodyweight, blood glucose, TG, TC, LDL-C, and insulin level of T2DM KK-Ay mice in the model group increased significantly, while the HDL-C level was on the contrary. These results suggested that mice in the model group showed hyperglycemia, hyperlipidemia, and insulin resistance. The MWM test also revealed obvious learning and memory disorders in mice aged 25 weeks in the model group. After intragastric administration for 12 weeks, the above symptoms of KK-Ay mice treated with different doses of BSHX or with metformin were alleviated and improved in varying degrees. These results were consistent with the previous related study by our group [28].

However, different doses of BSHX had different effects. BSHX improved bodyweight and blood glucose in a dose-dependent manner. In the high BSHX (2 g/kg) group, the blood glucose level was significantly reduced by the 8th week after gavage. What is more, 2 g/kg of BSHX achieved the same hypoglycemic effect as metformin by the 12th week after gavage. The results of OGTT and ITT were different. After 12 weeks of administration, 1 g/kg of BSHX showed a better performance than 2 g/kg of BSHX in improving the OGTT and ITT of mice. Besides, the FINS level in the medium BSHX (1 g/kg) group was also lower than that in the low (0.5 g/kg) and high BSHX (2 g/kg) groups. However, the metformin was superior to 1 g/kg of BSHX in improving OGTT and ITT, and only the metformin could significantly reduce the insulin level. It suggested that metformin should be preferred in the treatment of T2DM patients in case of no contraindications.

In the aspect of blood lipid and cholesterol, only a high dose of BSHX (2 g/kg) could significantly reduce TG and increase the HDL-C level after 12 weeks of intragastric administration. No significant reduction was found in blood lipid or cholesterol in the low (0.5 g/kg) and medium BSHX (1 g/kg) groups and the metformin group. The reason might be that taking metformin alone was not enough to reduce blood lipid in T2DM mice with a severe condition in the later stage. Moreover, KK-Ay mice were always fed with high-fat feed without diet control, resulting in the sustained high blood lipid level. The high dose of BSHX, however, could lower the lipid level since its concentration of lipid-decreasing components was higher than that in low-dose and medium-dose BSHX. The specific lipid-lowering components required further screening and separation. In terms of learning and memory, the MWM test in the 25th week demonstrated that only the escape latency and stay time in the target quadrant of mice in the medium BSHX (1 g/kg) group were significantly improved, compared with those in

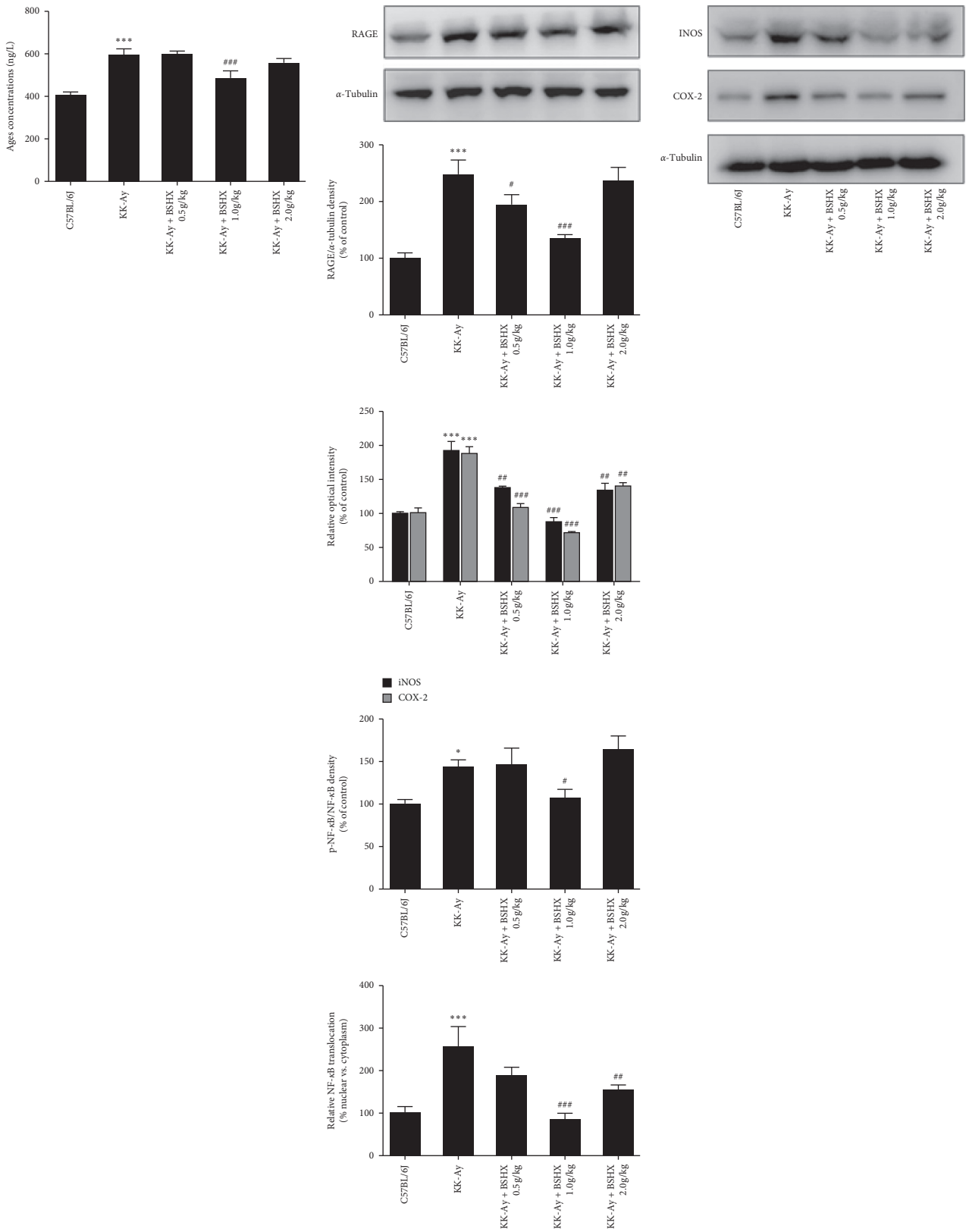

(a) (b) (c)

Figure 8: Continued.

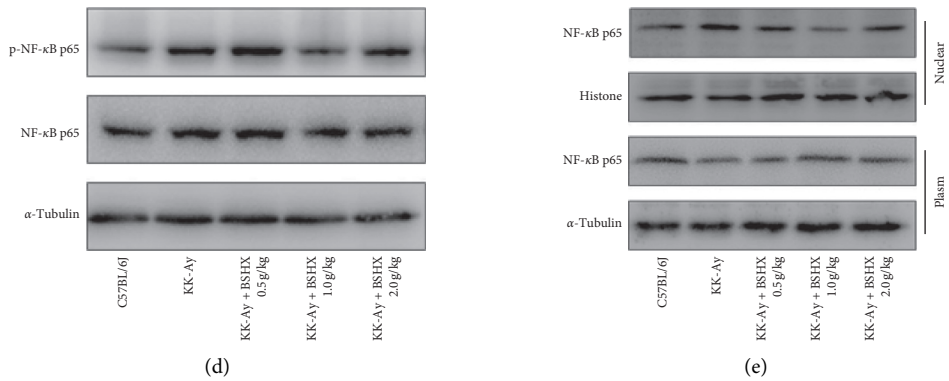

Figure 8: The effect of BSHX on the expression of AGEs, RAGE, iNOS, COX-2, and p-NF-κB. (a) Level of AGEs. (b) Representative Western blots and quantitative analysis of RAGE in each group. (c) Representative Western blots and quantitative analysis of iNOS and COX-2 in each group. (d) Representative Western blots and quantitative analysis of NF-κB and p-NF-κB in each group. (e) Representative Western blot analysis of NF-κB p65 nuclear translocation. Data were expressed as mean ± SD ($n = 10$). $^{*}P < 0.05$, $^{***}P < 0.001$ vs. the C57BL/6J group. $^{\#}P < 0.05$, $^{\#}P < 0.01$, $^{\#\#\#}P < 0.001$ vs. the KK-Ay group.

the model group. The reason might be that a dose of 2 g/kg was higher than the clinical dosage. The components that originally showed significant efficacy had such a high concentration in the high BSHX group that they produced a negative effect. The specific causes needed to be further analyzed and investigated. The MWM test results reminded us that metformin should be used in combination with other drugs to improve cognitive impairment in T2DM patients. The pathomorphology of the mouse brain was observed through H&E staining, Nissl staining, and TUNEL staining. The results revealed that BSHX could improve the damage of hippocampal neurons in mice.

Neuroinflammatory mechanisms play a crucial role in the development of cognitive dysfunction in T2DM. The anti-inflammatory treatment stems from the "inflammatory theory" of T2DM, in which advanced glycation end products (AGEs) play an important role in the inflammatory response [29–31]. Kalninova et al. detected the levels of inflammatory markers and AGEs in blood of T2DM patients with cognitive impairment and normal people by high-performance liquid chromatography (HPLC) and fluorescence spectrophotometry [32]. The results showed that the levels of AGEs, IL-6, IL-8, TNF-α, and monocyte chemotactic protein-1 (MCP-1) in plasma of T2DM patients were significantly higher than those of the normal control group, indicating that there may be a relationship between AGEs and neuroinflammatory factors in T2DM. Advanced glycosylation end products (AGEs), the nonenzymatic glycosylation of proteins or lipids, are found in plasma, microglia, astrocytes, the hippocampus, and the brains of diabetic patients [33]. Therefore, some researchers suspect that AGEs may be involved in neuroinflammation in the brain of type 2 diabetics, leading to diabetic cognitive dysfunction. It has been found that AGEs and AGEs receptor (RAGE) in macrophages can cause oxidative stress and activate NF-κB through the mitogen-activated protein kinase (MAPK) signaling pathway [34, 35]. In addition, AGEs could bind to RAGE and activate the downstream NF-κB signaling pathway, leading to phosphorylation of IκB-α. The phosphorylated IκB-α is degraded by ubiquitination, and then, the released NF-κB is free in the cytoplasm and quickly transferred to the nucleus, where it specifically binds to the corresponding gene transcription site and induces the expression of inflammation factors, such as cytokines such as interleukin-6 (IL-6) and tumor necrosis factor-α (TNF-α) [36]. These cytokines could induce the recruitment of adaptive immune system cells into the central nervous system [35]. Wang et al. studied the effect of danshensu on the loss of learning and memory function of T2DM mice mediated by AGEs. The results showed that danshensu could partially block the expression of phosphorylated p38 mitogen-activated protease (p-p38), cyclooxygenase-2 (COX-2), NF-κB, and RAGE and inhibit the increase of TNF-α, IL-6, and prostaglandin E2 (PGE2), which indicated that AGEs could mediate the cognitive dysfunction of T2DM mice caused by neuroinflammation. Consistent with the above reports, in this study, we found that BSHX could not only significantly downregulate the expression of AGEs and RAGE but also reduce the levels of phosphorylated NF-κB, nitric oxide synthase (iNOS), and COX-2 in a dose-dependent manner. These results suggested that BSHX could resist neuroinflammation by inhibiting the activation of the AGEs/RAGE/NF-κB signaling pathway. Nevertheless, the specific mechanism required further research given the fact that traditional Chinese medicine compounds often exert their effects though multiple pathways and multiple targets.

5. Conclusion

BSHX can significantly ameliorate glucose and lipid metabolism dysfunction, reduce the morphological changes in hippocampus tissues, and improve the cognitive function of KK-Ay mice. The mechanism underlying the above effects of BSHX may be related to the inhibition of activation of the AGEs/RAGE/NF-κB signaling pathway. The results of this study provide a pharmacological basis for the application of BSHX in the treatment of diabetic cognitive dysfunction.

Abbreviations

AGEs: Advanced glycation end products
BSHX: Bushen Huoxue prescription
COX-2: Cyclooxygenase-2
FBG: Fasting blood glucose
FINS: Fasting serum insulin
HDL-C: High-density lipoprotein cholesterol
HPLC: High-performance liquid chromatography
IL-6: Interleukin-6
iNOS: Inducible nitric oxide synthase
ITT: Insulin tolerance test
LDL-C: Low-density lipoprotein cholesterol
MAPK: Mitogen-activated protein kinase
MWM: Morris water maze
NF-κB: Nuclear factor-κB
OGTT: Oral glucose tolerance test
PGE2: Prostaglandin E2
P-p38: Phosphorylated p38 mitogen-activated protease
RAGE: Receptors of AGEs
RBG: Random blood glucose
T2DM: Type 2 diabetes mellitus
TC: Total cholesterol
TG: Total triglycerides
TNF-α: Tumor necrosis factor-α.

Data Availability

The datasets used and analyzed during the current study are available from the corresponding author upon request.

Ethical Approval

All animal experiments complied with the European Union Guidelines (2010/63/EU) and were performed as per the Guidelines of the Animal Research Committee of Peking University after being approved by the Institutional Animal Care and Use Committee of Peking University First Hospital.

Disclosure

Shao-Yang Zhao and Huan-Huan Zhao are considered as the co-first authors

Conflicts of Interest

The authors declare that they have no conflicts of interest.

Authors' Contributions

Hao-Guo and Wei-Wei Li conceived and designed the experiments. Shao-Yang Zhao and Huan-Huan Zhao carried out the experiments, analyzed the data, and wrote the manuscript. Ting-Ting Hao, Hao-Guo, and Wei-Wei Li contributed to regents/materials/analysis tools. Shao-Yang Zhao and Huan-Huan Zhao contributed equally to this work. All authors have read and approved the manuscript.

Acknowledgments

This work was supported by the National Natural Science Foundation of China (Grant no. 81530099).

Supplementary Materials

Supplementary data file includes the main components and sources of BSHX Prescription. (*Supplementary Materials*)

References

[1] S. Y. Tan, J. L. M. Wong, Y. J. Sim et al., "Type 1 and 2 diabetes mellitus: a review on current treatment approach and gene therapy as potential intervention," *Diabetology & Metabolic Syndrome*, vol. 13, no. 1, pp. 364–372, 2018.

[2] N. H. Cho, J. E. Shaw, S. Karuranga et al., "IDF Diabetes Atlas: global estimates of diabetes prevalence for 2017 and projections for 2045," *Diabetes Research and Clinical Practice*, vol. 138, no. 1, pp. 271–281, 2018.

[3] B. van Harten, F.-E. de Leeuw, H. C. Weinstein, P. Scheltens, and G. J. Biessels, "Brain imaging in patients with diabetes: a systematic review," *Diabetes Care*, vol. 29, no. 11, pp. 2539–2548, 2006.

[4] A. Ott, R. P. Stolk, F. van Harskamp, H. A. P. Pols, A. Hofman, and M. M. B. Breteler, "Diabetes mellitus and the risk of dementia: the Rotterdam study," *Neurology*, vol. 53, no. 9, p. 1937, 1999.

[5] M. G. Dik, C. Jonker, H. C. Comijs et al., "Contribution of metabolic syndrome components to cognition in older individuals," *Diabetes Care*, vol. 30, no. 10, pp. 2655–2660, 2007.

[6] M. W. J. Strachan, "R D Lawrence Lecture 2010. The brain as a target organ in Type 2 diabetes: exploring the links with cognitive impairment and dementia," *Diabetic Medicine*, vol. 28, no. 2, pp. 141–147, 2011.

[7] K. Talbot, H.-Y. Wang, H. Kazi et al., "Demonstrated brain insulin resistance in Alzheimer's disease patients is associated with IGF-1 resistance, IRS-1 dysregulation, and cognitive decline," *Journal of Clinical Investigation*, vol. 122, no. 4, pp. 1316–1338, 2012.

[8] S. Prasad, R. K. Sajja, P. Naik, and L. Cucullo, "Diabetes mellitus and blood-brain barrier dysfunction: an overview," *Journal of Pharmacovigilance*, vol. 2, no. 2, pp. 125–143, 2014.

[9] H. Ascher-Svanum, Y.-F. Chen, A. Hake et al., "Cognitive and functional decline in patients with mild alzheimer dementia with or without comorbid diabetes," *Clinical Therapeutics*, vol. 37, no. 6, pp. 1195–1205, 2015.

[10] P. J. Fried, L. Schilberg, A. K. Brem et al., "Humans with Type-2 diabetes show abnormal long-term potentiation-like cortical plasticity associated with verbal learning defificits," *Journal of Alzheimer's Disease*, vol. 55, no. 1, pp. 89–100, 2017.

[11] T. B. Chen, S. Y. Yiao, Y. Sun et al., "Comorbidity and dementia: a nationwide survey in Taiwan," *PLoS One*, vol. 12, no. 4, pp. 1–12, 2017.

[12] S. P. Zhou, X. L. Tong, and L. Pan, "Influence of leech on the morphologic changes of retinal microvessel in diabetic rats," *Journal of Traditional Chinese Ophthalmology*, vol. 12, no. 2, pp. 79–82, 2002.

[13] F. Hong, X. M. Wang, and G. X. Liu, "The effect of Jiawei Wuzi Yanzong particle on memory ability and level of serum beta-amyloid protein of mild cognitive impairment patients," *Chinese Journal of Gerontology*, vol. 27, no. 8, pp. 715–717, 2007.

[14] K.-W. Zeng, H. Ko, H. O. Yang, and X.-M. Wang, "Icariin attenuates β-amyloid-induced neurotoxicity by inhibition of tau protein hyperphosphorylation in PC12 cells," *Neuropharmacology*, vol. 59, no. 6, pp. 542–550, 2010.

[15] B.-Y. Yan, C.-S. Pan, X.-W. Mao et al., "Icariside II improves cerebral microcirculatory disturbance and alleviates hippocampal injury in gerbils after ischemia-reperfusion," *Brain Research*, vol. 1573, pp. 63–73, 2014.

[16] O. J. Olatunji, H. Chen, and Y. Zhou, "Lycium chinensis Mill attenuates glutamate induced oxidative toxicity in PC12 cells by increasing antioxidant defense enzymes and down regulating ROS and Ca2+ generation," *Neuroscience Letters*, vol. 616, pp. 111–118, 2016.

[17] V. Cavallucci, M. D'Amelio, and F. Cecconi, "Aβ toxicity in alzheimer's disease," *Molecular Neurobiology*, vol. 45, no. 2, pp. 366–378, 2012.

[18] W. Chen, X. Cheng, J. Chen et al., "Lycium barbarum polysaccharides prevent memory and neurogenesis impairments in scopolamine-treated rats," *PLoS One*, vol. 9, no. 2, pp. 1–13, 2014.

[19] K. W. Zeng, X. M. Wang, H. Ko, H. C. Kwon, J. W. Cha, and H. O. Yang, "Hyperoside protects primary rat cortical neurons from neurotoxicity induced by amyloid beta-protein via the PI3K/Akt/Bad/Bcl(XL)-regulated mitochondrial apoptotic pathway," *European Journal of Pharmacology*, vol. 672, no. 1-3, pp. 45–55, 2011.

[20] B. Wang and X. M. Wang, "Schisandrin B protects rat cortical neurons against Abeta1-42-induced neurotoxicity," *Die Pharmazie*, vol. 64, no. 7, pp. 450–454, 2009.

[21] Q. Yu, F.-J. Song, J.-F. Chen et al., "Antineuroinflammatory effects of modified Wu-Zi-Yan-Zong prescription in β-amyloid-stimulated BV2 microglia via the NF-κB and ERK/p38 MAPK signaling pathways," *Evidence-based Complementary and Alternative Medicine*, vol. 2017, Article ID 8470381, 10 pages, 2017.

[22] X. Song, W. Wang, Y. Kang et al., "Tangzhining exhibits a protective effect against cognitive dysfunction in diabetic rats," *International Journal of Clinical and Experimental Medicine*, vol. 8, no. 6, pp. 9013–9021, 2015.

[23] J. Liu, T. Liu, W. Wang et al., "Reduced gray matter volume in patients with type 2 diabetes mellitus," *Frontiers in Aging Neuroscience*, vol. 9, no. 22, pp. 1–10, 2017.

[24] A. M. Wessels, S. Simsek, P. L. Remijnse et al., "Voxel-based morphometry demonstrates reduced grey matter density on brain MRI in patients with diabetic retinopathy," *Diabetologia*, vol. 49, no. 10, pp. 2474–2480, 2006.

[25] G. Wu, L. Lin, Q. Zhang, and J. Wu, "Brain gray matter changes in type 2 diabetes mellitus: a Meta-analysis of whole-brain voxel-based morphometry study," *Journal of Diabetes and Its Complications*, vol. 31, no. 12, pp. 1698–1703, 2017.

[26] J. Zhang, Y. Wang, J. Wang et al., "White matter integrity disruptions associated with cognitive impairments in type 2 diabetic patients," *Diabetes*, vol. 63, no. 11, pp. 3596–3605, 2014.

[27] R. Hempel, R. Onopa, and A. Convit, "Type 2 diabetes affects hippocampus volume differentially in men and women," *Diabetes/Metabolism Research and Reviews*, vol. 28, no. 1, pp. 76–83, 2012.

[28] Y. Li, Q. Li, C. S. Pan et al., "Bushen Huoxue attenuates diabetes-induced cognitive impairment by improvement of cerebral microcirculation: involvement of RhoA/ROCK/moesin and src signaling pathways," *Frontiers in Physiology*, vol. 9, pp. 527–541, 2018.

[29] N. C. Chilelli, S. Burlina, and A. Lapolla, "AGEs, rather than hyperglycemia, are responsible for microvascular complications in diabetes: a "glycoxidation-centric" point of view," *Nutrition, Metabolism and Cardiovascular Diseases*, vol. 23, no. 10, pp. 913–919, 2013.

[30] I. K. Hwang, J. H. Choi, S. M. Nam et al., "Activation of microglia and induction of pro-inflammatory cytokines in the hippocampus of type 2 diabetic rats," *Neurological Research*, vol. 36, no. 9, pp. 824–832, 2014.

[31] E. Cudaback, N. L. Jorstad, Y. Yang, T. J. Montine, and C. D. Keene, "Therapeutic implications of the prostaglandin pathway in Alzheimer's disease," *Biochemical Pharmacology*, vol. 88, no. 4, pp. 565–572, 2014.

[32] J. Kalninova, V. Jakus, M. Glejtkova, L. Kuracka, and E. Sandorova, "Impact of glycemic control on advanced glycation and inflammation in overweight and obese patients with type 2 diabetes mellitus," *Bratislava Medical Journal*, vol. 115, no. 8, pp. 457–468, 2014.

[33] A. Wong, H.-J. Lüth, W. Deuther-Conrad et al., "Advanced glycation endproducts co-localize with inducible nitric oxide synthase in Alzheimer's disease," *Brain Research*, vol. 920, no. 1-2, pp. 32–40, 2001.

[34] C. E. Finch and D. M. Cohen, "Aging, metabolism, and alzheimer disease: review and hypotheses," *Experimental Neurology*, vol. 143, no. 1, pp. 82–102, 1997.

[35] S. Amor, F. Puentes, D. Baker, and P. van der Valk, "Inflammation in neurodegenerative diseases," *Immunology*, vol. 129, no. 2, pp. 154–169, 2010.

[36] B. B. Di, H. W. Li, W. Li et al., "Liraglutide inhibited AGEs induced coronary smooth muscle cell phenotypic transition through inhibiting the NF-κB signal pathway," *Peptides*, vol. 112, no. 1, pp. 125–132, 2018.

Hindawi
Evidence-Based Complementary and Alternative Medicine
Volume 2020, Article ID 8848676, 17 pages
https://doi.org/10.1155/2020/8848676

Review Article

Ethnopharmacological Use and Biological Activities of *Tragia involucrata* L.

Mumtaz S. Pallie,[1,2] Pathirage K. Perera,[2] Nishantha Kumarasinghe,[1] Menuka Arawwawala,[3] and Charitha L. Goonasekara[1]

[1]*Faculty of Medicine, General Sir John Kotelawala Defence University, Ratmalana, Sri Lanka*
[2]*Institute for Indigenous Medicine, University of Colombo, Colombo, Sri Lanka*
[3]*Industrial Technology Institute, Colombo, Sri Lanka*

Correspondence should be addressed to Charitha L. Goonasekara; charithalg@kdu.ac.lk

Received 16 September 2020; Revised 16 November 2020; Accepted 23 November 2020; Published 15 December 2020

Academic Editor: Youhua Xu

Plants have been utilized as medicines to treat various ailments since ancient times. Formulations made by plant materials have been used in traditional, complementary, and alternative medicine and remain widespread in both developing and developed countries. In developing countries, traditional medicines are widely practiced due to its accessibility and affordability, while in developed countries, complementary and alternative medicine are widely popular due to the adverse effects of chemical drugs. *Tragia involucrata* Linn. (family: Euphorbiaceae) is a highly used medicinal plant used in both Sri Lankan and Indian traditional medical systems. Since this plant is a weed, it is being extensively destroyed due to the lack of knowledge regarding the medicinal value of this plant. Hence, the objective of this study was to collect data on the medicinal value of this plant by correlating its scientifically validated biological activities with its ethnopharmacological uses. An attempt was made to gather as much information available regarding the ethnopharmacological uses and scientifically validated biological activities of *Tragia involucrata* through authentic traditional texts, scientific journals, and other authentic texts regarding medicinal plants. Thus, the review provides an insight to the capability of *Tragia involucrata* to be used as a monoherbal formulation for diseases pertaining to multiple systems of the body. With all the scientifically validated biological activities and the ethnopharmacological uses, *Tragia involucrata* may qualify as a potent candidate to be developed into a phytomedicine to be utilized as both a preventive and as a therapeutic agent.

1. Introduction

Plants have been in use as medicines in different formulations to treat various ailments since ancient times. Even at present, medicinal plants play a key role in world health. Use of traditional, complementary, and alternative medicine, which mainly uses plant material for their formulations, remains widespread in both developing and developed countries. According to the World Health Organization (WHO), about 65–80% of the world's population which lives in developing countries depends essentially on medicinal plants for their primary healthcare [1]. Due to this wide use of medicinal plants, the WHO has recommended the initiation of studies to identify and characterize new herbal preparations from traditionally known plants and the development of new effective therapeutic agents, especially in the areas where there is a lack of modern drugs, such as for chronic diseases [2].

Tragia involucrata Linn. (family: Euphorbiaceae) is a medicinal plant, which has been used for centuries in Sri Lankan Traditional Medicine as well as in the Ayurveda medical system [3, 4]. This plant is mainly found and used by South Asian countries such as Sri Lanka, India, and Bangladesh. The ethnopharmacological uses of TI illustrates that it has been used in the treatment of disorders in different systems of the body. TI has a great market potential due to its

abundant medicinal values and thus has been scientifically investigated for a variety of biological activities.

TI is a weed and therefore propagates easily and survives in harsh weather conditions. Although this plant has been in use for thousands of years, at present, the public is not aware of the medicinal value of this plant, and since it causes a severe stinging effect when touched, the plant is being extensively destroyed especially in Sri Lanka. Due to the destruction of the plant, it is restricted to certain districts of the country. Therefore, the aim of this study was to collect data on the medicinal value of this plant by correlating its biological activities with its ethnopharmacological uses in order to interpret the importance of the plant so that it may be conserved. This review also provides an insight to the capability of *Tragia involucrata* to be used as a monoherbal formulation for noncommunicable diseases due to its many scientifically validated biological activities and its many ethnopharmacological uses which date backs to thousands of years.

2. Botanical Evaluation of *Tragia involucrata* Linn.

Tragia involucrata L. belonging to family Euphorbiaceae is commonly known as Wel Kahambiliya, Helkahambiliya [5], Kahambiliya, or Kasambiliya [6] in Sinhala and Indian stinging nettle or climbing nettle in English. It is called as Indian stinging nettle or climbing nettle in English. In Tamil, the plant is called Ambu or Cherukanjuru [5], and in Sanskrit, it is called Duralabha, Dusparcha, Grahini, and Kachchura [5]. It is a well-known fact that this perennial herb with hispid stem and leaves causes injurious itching and stinging which limit the tangibility. The Sinhala name Kahambiliya is derived from the vesicant effect of TI which causes stinging and itchiness on the skin.

In the book "A revised handbook to the Flora of Ceylon [7]," four types of plants are mentioned under the genus Tragia. They are *Tragia hispida* Willd., *Tragia involucrata* L., *Tragia plukenetii* Radcliffe-Smith, and *Tragia muelleriana* Pax and Hoffm. The vernacular name given for *Tragia hispida* Willd., *Tragia involucrata* L., and *Tragia plukenetti* Radcliffe-Smith are Wel kahambiliya. A vernacular name had not been given to *Tragia muelleriana* Pax and Hoffm. in Dassanayake and Clayton [7].

2.1. Morphology. TI [5, 7] is a perennial, densely hispid-pubescent herb, with scattered, stinging hairs throughout (Figure 1). The stem is elongate, slender, and twining. Leaves are simple, alternate, serrate, stipulate, 2.5–12.5 cm long, 2–4.5 cm broad, densely hispid-pubescent. Regular, unisexual, and apetalous flowers are borne in terminal axillary. The flowering period is February, March, and June. Fruit is a capsule of 8 mm diameter, 3-lobed, more or less hispid. Seeds are subglobose, grayish brown, and smooth, with slight mottling. TI is geographically distributed in India, Sri Lanka, Burma, and China. In Sri Lanka, it is common in Jaffna, Anuradhapura, Minneriya, Galle, and Matara, as a weed of cultivation and waste grounds.

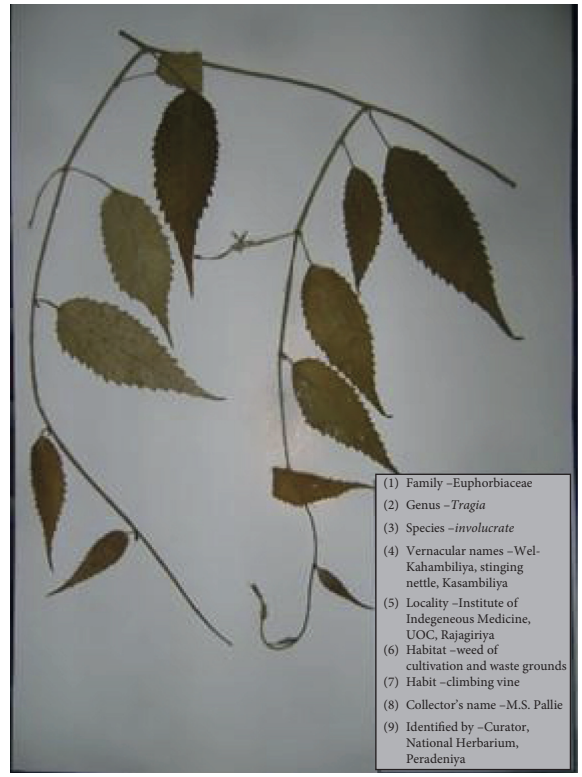

Figure 1: Voucher specimen of *Tragia involucrata*.

Moreover, there are two morphologically different plants which are known by the vernacular name "Wel Kahambiliya" in Sri Lanka (unpublished data). One plant being a vine (Figure 2) and the other being a shrub (Figure 3). Both plants have been identified by the National Herbarium, Department of National Botanic Gardens, Peradeniya, Sri Lanka, as *Tragia involucrata* L. According to Dassanayake and Clayton [7], the morphological characters which have been used for the "key to the species" in Tragia species under family Euphorbiaceae are the shape of the leaf (whether palmately lobed or simple), base of the leaf (whether cuneate or cordate), and fruiting calyx (whether lobes are linear, variously toothed and stellately spreading, and exposing fruit or broadly ovate, enclosing fruit). The nature of the stem is not considered as a key. Therefore, both the abovementioned two morphological forms fall into the same species. In Dassanayake and Clayton [7], the common stem type for Tragia species has been mentioned as climbing or twining. Hence, it would be worth conducting further investigations into the genetic composition of these two morphologically distinct forms, in order to understand their taxonomical stand in comparison to each other.

2.2. Wel Kahambiliya (TI) as a Substitute. As mentioned in Ayurveda Pharmacopoeia, Wel Kahambiliya is used as a substitute for Dhanwayasa, Duralabha, and Yawasa in Sri Lanka [8]. According to most Ayurvedic texts, however, Dhanwayasa and Duralabha are considered one plant, having the botanical name as *Fagonia cretica* Linn. belonging to family Zygophyllaceae [9], and the texts mention

Figure 2: The vine type of *Tragia involucrata*.

Figure 3: The shrub type of *Tragia involucrata*.

that they are synonyms for each other. In Ayurveda authentic text Bhavaprakasha [10], it is mentioned that Duralabha and Yawasa are two different plants. The botanical name of Yawasa is *Alhagi camelorum* Fisch and belongs to family Fabaceae. According to the book, "Medicinal Plants (Indigenous and Exotic) Used in Ceylon [5]" by D.M.A. Jayaweera, the vernacular name of *Alhagi camelorum* is mentioned as Wel Kahambiliya, which further notes that *Alhagi camelorum* is not found in Sri Lanka. Dhanwayasa or Duralabha and Yawasa could be having the same ethnopharmacological properties as *Tragia involucrata*, and thus, the latter is used as a substitute in Sri Lanka due to its availability in the region. The same reason could have led to the use of the vernacular name "Wel Kahambiliya" for those other plants as well.

3. Study Design

Data for the study were collected using relevant authentic texts as well as scientific journal articles. Authentic texts that were used for the study were prominent texts used in Ayurveda medicine and Sri Lankan indigenous medicine. The main treatise in Ayurveda which were used in the study included Charaka Samhita [4], Sushruta Samhita [11], Ashtangahrida Samhita [10], and Bhavaprakasha Nighantu [10]. The Sri Lankan texts which were used related to Ayurveda and indigenous medicine were Sarartha Samgraha [3] by King Buddhadasa (340–368 AC) and Ayurveda pharmacopoeia volume II and Ayurveda pharmacopoeia volume III.

Published studies reporting details regarding the biological activities, phytochemistry, and ethnomedicinal uses of *Tragia involucrata* was undertaken according to Figure 4 (illustrates a flow diagram of the study selection process). A comprehensive search of the literature was conducted in the following databases: PubMed (U.S. National Library of Medicine, USA), ScienceDirect (RELX group, Netherlands), and Semantic Scholar (Allen Institute for Artificial Intelligence, USA) for studies published between 1st January 1984 and 31st December 2018. The following medical headings and keywords were used for the search: "*Tragia involucrata*," "Biological activities of *Tragia involucrata*," "Phytochemistry of *Tragia involucrata*," and "Ethnomedicinal use of *Tragia involucrata*." From a total of 168 results, 24 were excluded because of duplication, 46 being irrelevant judged on the abstract or full paper. Finally, 98 articles were included in this review.

4. Ethnomedicinal Uses of *Tragia involucrata* L.

The earliest documentation of the ethnopharmacological use of *Tragia involucrata* dates back to 1st century AD. The three main treatises of Ayurveda, Charaka Samhita, Sushruta Samhita, and Vagbhata Samhita, have mentioned TI by the vernacular name of Vrishchakali. In Charaka Samhita [4] documented in 1st century AD, TI is mentioned under Apasmara Chikitsa (treatment for epilepsy). In Sushruta Samhita [11] documented in 4th century AD, TI is mentioned under Jwara Chikitsa (treatment for fever), and in Vagbhata/Ashtangahrida Samhita [10] documented in 5th century AD, TI is mentioned under Chikitsa Sthana as an ingredient of Vidaryadi Gritha, a preparation made from cow's ghee, internally used for disorders of the respiratory tract symptoms.

In Sri Lanka, the earliest documentation of TI goes back to the reign of King Buddhadasa (341–370). The physician king of Sri Lanka compiled "Sarartha Samgraha," a comprehensive medical treatise, in Sanskrit. In Sarartha Samgraha [3], TI comes under a group of drugs called "welpasmul" (roots of five climbers), comprising of *Ipomoea mauritiana*, *Hemides musindicus, Tragia involucrata*, *Tinospora cordifolia,* and *Pergularia daemia*. The decoction is made from the root of these five climbers mainly for urinary tract disorders.

However, it appears that the use of TI in ethnomedicine has not been for the treatment of a single specific ailment but for a range of unrelated disorders. Various ethnomedicinal uses of TI, as gathered as mentioned in numerous articles and books related to Sri Lankan Traditional Medicine and Ayurveda medicine, are shown in Table 1. The ethnomedicinal use of TI spreads across disorders associated with a range of bodily systems. Therefore, Table 1 demonstrates these ethnomedical uses being categorized according to the body systems, ailments, and the parts of the plant used.

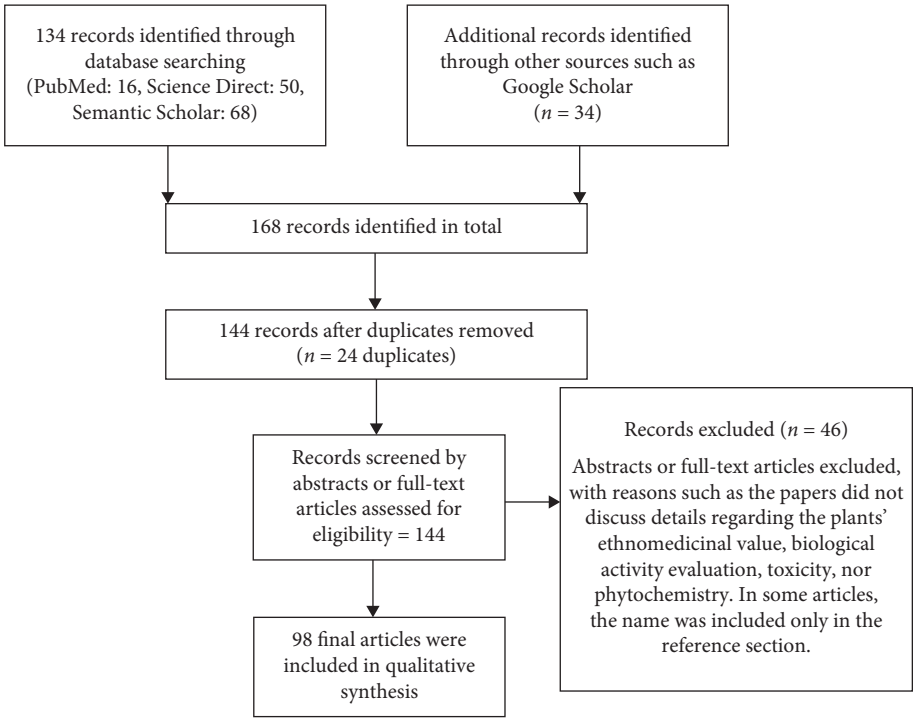

Figure 4: Flow diagram of the study selection process.

5. Biological Activities and Phytochemicals Found in *Tragia involucrata*

A number of controlled researches both in vitro and in vivo have been carried out to scientifically validate the ethnopharmacological properties of TI. Owing to the broader use of TI as an ethnomedicine in traditional medical practice, a larger number of investigations have devoted to scientifically evaluate its biological activities. Many of these studies have supported the value of TI in treating diseases pertaining to the major systems of the body and have further shown to possess a range of biological activities such as antibacterial/microbial activity, antidiabetic/hyperglycaemic activity, antioxidant activity, and anti-inflammatory activity. Since phytochemicals are responsible for these biological activities, simultaneous research carried out on phytochemical analysis of the whole part or parts of TI show that it is rich with phytochemicals, which agrees with its broader biological activities. The major phytochemical groups found to be present in different extracts of *Tragia involucrata*, the whole plant or its parts, as at present, are summarized in Table 2. These phytochemicals are distributed in different parts of the plant and are extractable with different solvent systems. Accordingly, the ethnomedicinal uses of *Tragia involucrata* also varies depending on the part of the plant involved. Further details into the biological activities of *Tragia involucrata*, shown by different parts of the plant under different extraction methods, and the chemical compounds identified as the potential biologically active ingredient are discussed and summarized in Table 3.

5.1. Antimicrobial Activity of Tragia involucrata. Many studies have been carried out to investigate the antimicrobial activity of *Tragia involucrata* (TI) against a number of microorganisms because of its ethnomedicinal use in wound healing and infections [71, 72]. These antibacterial studies are summarized in Table 4.

The most widely studied part of the plant is the leaf. Few studies have also been investigated for the antimicrobial activity in the stem and the root. The antibacterial activity appears to have depended on the solvent which was used to extract TI rather than the plant part. With respect to the solvents used for the extraction of TI for above antimicrobial studies, it appears that extracts of more polar solvents such as ethyl acetate, acetone, and methanol produced potent antimicrobial activity while that of less polar solvents such as petroleum ether was less active. Aqueous extracts of TI, on the other hand, showed very low antibacterial activity.

Most of the antibacterial investigations had been carried out against Gram-negative bacteria, mostly on *Escherichia coli*, while the choice of Gram-positive bacteria being *Staphylococcus aureus*. All the different extracts of TI leaf, which were tested, have shown potent anti-*S. aureus* activity [78].

Also the wound healing activity, which can be explained by antimicrobial activity, was investigated using the methanolic root extract [69] and Shellsol [79] isolated from fresh TI leaves. The test was carried out on *S. aureus*-induced excision wounds, and the extracts were topically applied. Both the extract and compound were active and showed

Table 1: Ethnomedicinal uses of *Tragia involucrata*.

System of the body/main action	Plant part used	Ailment	Reference
(1) Endocrinology system	Whole plant	(i) Madumeha (diabetes mellitus)	[12–18]
	Root	(ii) A major constituent of anti-diabetic formulations	[19]
(2) Digestive system	Whole plant	(i) Appetizer	Ayurveda pharmacopoeia [20]
		(ii) Gastropathy and antiemetic	[17, 21]
		(iii) Used as a mouth wash to cleanse oral cavity	[22]
	Root	(i) Diarrhoea, vomiting, and dysentery	[4]
		(ii) Constipation	[23]
		(iii) Haemorrhoids and gastropathy	[24]
		(iv) Anthelmintic–to get rid of Guinea worms	[11]
	Leaves and roots	(i) Bloody dysentery and stomachache	[4]
		(ii) Constipation, haemorrhoids, and vomiting	[25]
(3) Respiratory system	Whole plant	(i) Asthma	[19, 26]
		(ii) Cough and asthma	Ayurveda pharmacopoeia [20]
		(iii) Bronchitis, pneumonia, and laryngitis	[5]
	Root	(i) Bronchitis	Ayurveda pharmacopoeia [20, 27, 28]
		(ii) Dry cough	[5]
		(iii) Infants acute breathing complications	[29]
(4) Integumentary system	Whole plant	(i) Chronic inflammatory skin diseases (psoriasis, eczema, and seborrheic dermatitis)	[30, 31]
		(ii) Pruritic eruptions	[11]
		(iii) Elephant's skin diseases	[22]
	Root	(i) Pruritic skin eruptions	[24]
		(ii) Skin diseases including leprosy	Ayurveda pharmacopoeia [20, 32]
		(iii) Wounds	Ayurveda pharmacopoeia [20, 32]
		(iv) Abscess	[34]
	Leaves	(i) Skin infection, swellings, children scabies, and eczema in children	[19, 35]
	Fruit	(i) Bloody eruptions	Ayurveda pharmacopoeia [20]
		(ii) Indraluptha (hair loss causing patches of balding/alopecia areata)	Ayurveda pharmacopoeia [4, 20]
	Stem	(i) Dermatitis	[36]
	Leaves and root	(i) Skin diseases	[32]
	Stem and leaves	(i) Skin diseases	[4]
(5) Urinary system	Whole plant	(i) Diuretic	Ayurveda pharmacopoeia [20]
	Root	(i) Diuretic	Ayurveda pharmacopoeia [20]
		(ii) For all urinary problems	[37]
		(iii) Dysuria	[3, 38]
	Stem and leaves	(i) For renal stones	[39]
(6) Cardiovascular system	Whole plant	(i) Cardiotonic	[22]
	Root	(ii) As a blood purifier	[24]
(7) Nervous system	Whole plant	(i) Headache	[40]
	Root	(i) Epilepsy	[4, 41, 42]
		(ii) Headache	Ayurveda pharmacopoeia [20]
		(iii) Migraine	[19]
		(iv) Pain in the limbs	[4]
		(v) Pain in the waist	[34]
		(vi) Melalgia and brachialgia	[24]
	Leaves and roots	(i) Headache, vertigo, and giddiness	[25]
	Fruit	(i) For headaches	[16, 43]

Table 1: Continued.

System of the body/main action	Plant part used	Ailment	Reference
(8) Immune system			
Inflammation	Root	(i) Antiperiodic and depurative	[24]
		(ii) Tumor and elephantiasis	[19, 44]
		(iii) Arthritis and rheumatoid arthritis	[35, 45]
	Leaves	(i) Local swelling of hands and feet	[46]
Fever	Whole plant	(i) For pain and cold extremities due to high fever	Ayurveda pharmacopoeia [20]
		(ii) All types of fever	[37]
		(iii) For typhoid fever	[5]
		(iv) Malarial fever	[47]
	Root	(i) Diaphoretic	[24]
		(ii) Febrifuge	Ayurveda pharmacopoeia [20, 48]
Venereal diseases	Whole plant	(i) Chronic syphilis	Ayurveda pharmacopoeia [20]
	Root	(i) Venereal diseases	[24]
Allergies	Root	(i) Itches due to allergies	[23]
(9) Reproductive system	Whole plant	(i) As an aphrodisiac	[49]
	Stem and leaves	(i) A contraceptive drug called "shanti bori" is made from aerial parts of TI	[50, 51]
(10) Snake and scorpion bites	Whole plant	(i) Scorpion stings and snake bites	[48, 49]
	Roots	(i) Snake bites	[52–55]
	Leaves	(i) For scorpion stings, insect bites, and snake bites	[19, 32]
(11) Miscellaneous	Whole plant	(i) As anticancer agent	[56, 57]
		(ii) As a nutritional source	[49]
		(iii) Mosquito repellent	[58]
		(iv) Ophthalmic diseases	[47]
		(v) Eliminates toxins from the body, energy booster	[22]
	Root	(i) Protection of a new born baby	[34]
		(ii) To warm the body	[36]
		(iii) Ankle sprains and fractures	[59]
	Leaves	(i) Insect repellents	[22]

complete healing of the wound. Furthermore, antibacterial studies with fractionated TI leaf extracts have identified vinyl hexyl ether, Shellsol, and 2-methylnonane as the active compounds possessing antibacterial properties [80, 81]. Moreover, Shellsol isolated from TI leaves seems to be very potent against *S. aureus* Gram-positive bacteria [69, 73]. Another mechanism of action for the antibacterial activity of TI could be through quorum quenching. Bacteria depend on quorum sensing, which is a communication process of bacteria, to regulate gene expression for important cellular processes that are essential for surveillance, survival, and adaptation to their changing environments [82]. Quorum quenching is the inhibition of this quorum sensing. A study has shown that the aqueous leaf extract of TI possess quorum quenching activity [83].

The TI plant showed antifungal activity as well. A study carried out by Panda et al. [70] investigated the ethyl acetate extract of TI root against *Malassezia furfur* fungus. This study showed that the zone of inhibition of EAE of TI root was comparable to that of ketoconazole, which was used as the control. In another study, the ethanol and methanol extract of TI stem was used against *Aspergillus niger* and *Rhizopus arrhizus*, which also gave positive results. In the same study performed by Panda et al. [70], 10, 13-dimethoxy-17-(6-methylheptan-2-yl)-2, 3, 4, 7, 8, 9, 10, 11, 12, 13, 14, 15, 16, 17-tetradecahydro-1H-cyclopenta[a]phenanthrene and 3-(2,4-dimethoxyphenyl)-6,7-dimethoxy-2,3- dihydrochro-men-4-one identified from TI root have shown both antibacterial and antifungal effects. A latest study performed by Gupta et al. [84] showed that the leaf extract of TI possessed antifungal activity against *Chaetomium globosum* and few other pathogenic fungi.

In summary, it is evident that TI possesses antibacterial activity as well as antifungal activity; hence, TI is a potential candidate which qualifies into developing a phytomedicine as an antimicrobial agent.

5.2. Anti-Inflammatory Activity of Tragia involucrata. Extracts from roots, leaves, and whole plant of TI have been tested to investigate the anti-inflammatory effect. In vivo tests had been carried out on healthy Wistar rats using carrageenan-induced paw oedema and cotton pellet granuloma methods. Different solvent extracts had been used such as aqueous, methanolic, petroleum ether, and chloroform. All the extracts at the tested doses showed positive results both orally as well as intraperitoneal [73, 80, 81, 85–87]. The active component Shellsol has shown positive results for anti-inflammatory activity [73], further indicating that TI potentially mediates its antibacterial as well as anti-inflammatory activity via Shellsol.

Table 2: Major phytochemicals found in various extracts of different parts of *Tragia involucrata*.

Plant part	Extract	Phytochemical constituent											Reference
		Alkaloids	Coumarins	Catechins	Flavonoids	Glycosides	Phenols	Saponins	Sterols	Steroids	Tannins	Terpenoids	
Leaf	Fresh	+	NT	NT	+	NT	+	+	NT	+	+	+	[60]
	MeOH	+*	NT	NT	+**	+**	NT	NT	+**	NT	+**	NT	*[61], **[62]
	EtOH	+	NT	−	+	+	−	−	+	+	−	+	[63]
	Hexane	+	NT	−	+	+	−	−	NT	+	−	+	[64]
Root	H_2O	+*	NT	NT	+**	−**	NT	+*	−**	−**	+**	−**	*[65], **[66]
	MeOH	−**	NT	NT	+**	−**	NT	+**	−**	−**	+**	−**	**[66]
	PE	−**	NT	NT	+*	−**	NT	−**	+**	−**	+*	−**	*[65], **[66]
	EA	+**	NT	NT	−**	−**	NT	−**	−**	−**	−**	−**	**[66]
	CHL	+*	NT	NT	−**	−**	NT	−**	+**	−**	−**	−**	*[65], **[66]
Whole plant	Hot water	−	+	NT	+	+	NT	+	+	−	+	+	[67]
	Aq/EtOH	+	NT	NT	+	NT	+	+	+	NT	+	+	[12]
	Aq/MeOH	NT	NT	NT	+	NT	NT	NT	NT	NT	NT	NT	[68]

NT, not tested; +, present; −, negative; MeOH, methanol; EtOH, ethanol; H_2O/Aq, water; PE, petroleum ether; EA, ethyl acetate; CHL, chloroform. *,**Relevant references.

Table 3: Biologically active phytochemicals isolated from *Tragia involucrata*.

	Phytochemical	Structure	Biological activity	Reference
1	Ar-turmerone (identified by GC-MS)	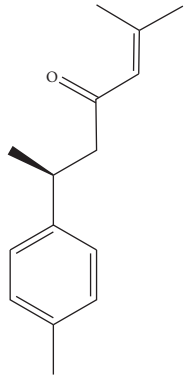	Antimicrobial Wound healing	[17]
2	Friedelan-3-one (identified by GC-MS)	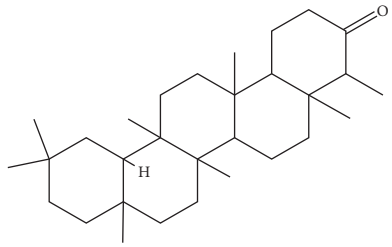	Antimicrobial Anti-inflammatory	[17]
3	Vinyl hexyl ether (identified by GC-MS)	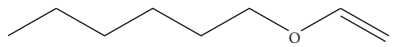	Antimicrobial Anti-inflammatory	[69]
4	Shellsol (identified by GC-MS)	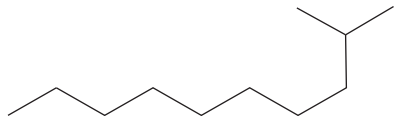	Antimicrobial Anti-inflammatory Wound healing	[69]
5	2,4-Dimethylhexane (identified by GC-MS)	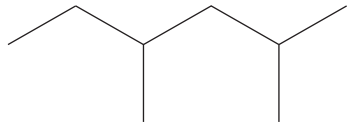	Antimicrobial Anti-inflammatory	[69]
6	2-Methylnonane (identified by GC-MS)	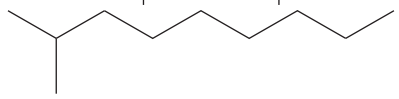	Antimicrobial Anti-inflammatory	[69]
7	2,6-Dimethylheptane (identified by GC-MS)	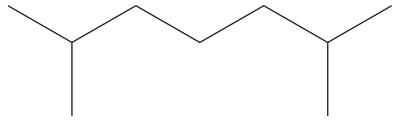	Antimicrobial Anti-inflammatory	[69]

Table 3: Continued.

	Phytochemical	Structure	Biological activity	Reference
8	Iridine (identified by LC/MS)	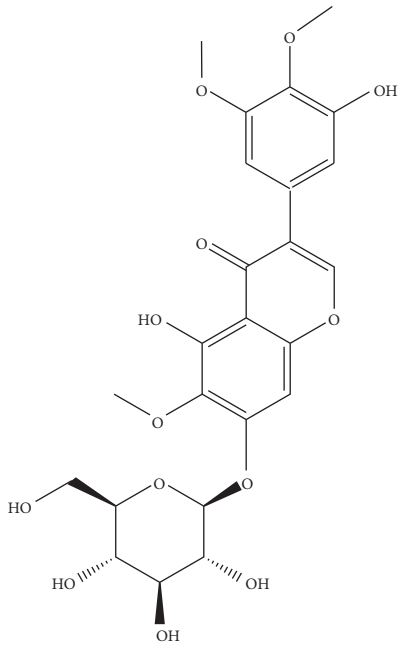	Antioxidant	[68]
9	Orientin (identified by LC/MS)	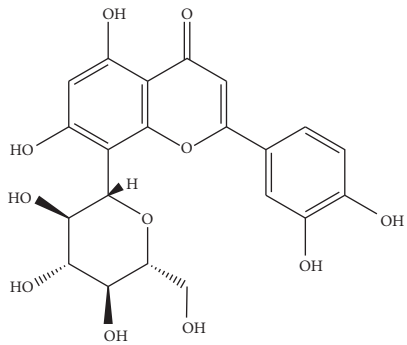	Antioxidant	[68]
10	10,13-Dimethoxy-17-(6-methylheptan-2-yl)-2,3,4,7,8,9,10,11,12,13,14,15,16,17-tetradecahydro-1H-cyclopenta-phenanthrene (identified by IR and H-NMR spectroscopy)	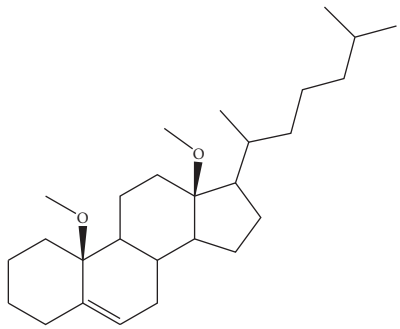	Antimicrobial Anti-inflammatory	[70]
11	Stigmasterol (identified by IR and H-NMR spectroscopy)	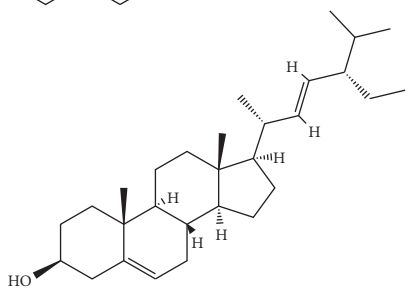	Antimicrobial Anti-inflammatory	[70]

Table 3: Continued.

	Phytochemical	Structure	Biological activity	Reference
12	Quercetin (identified by IR and H-NMR spectroscopy)	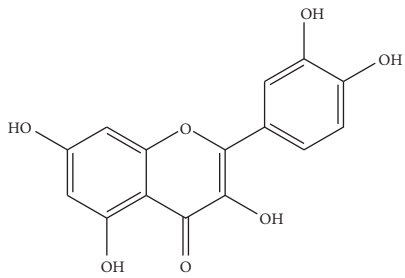	Antimicrobial Anti-inflammatory	[70]
13	Rutin (identified by IR and H-NMR spectroscopy)	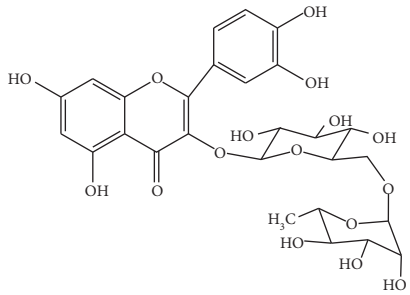	Antimicrobial Anti-inflammatory	[70]
14	3-(2,4-Dimethoxyphenyl)-6,7-dimethoxy-2,3-dihydrochromen-4-one (identified by IR and H-NMR spectroscopy)	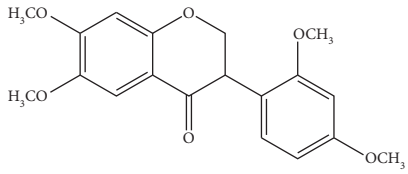	Antimicrobial Anti-inflammatory	[70]

5.3. Antidiabetic Activity of Tragia involucrata. *Tragia involucrata* (TI) has been used for diabetes mellitus in traditional medicine practiced in South Asian countries for centuries. In Sri Lankan traditional medical system, the decoction made out of TI whole plant is used for diabetes mellitus [88]. Using a single plant to prepare decoction is rare in traditional medicine; hence, it depicts the efficacy of TI towards treating diabetes mellitus. Many studies have been performed to investigate the antidiabetic activity of TI, both in vitro and in vivo, and discussed.

In vivo studies have been carried out using diabetes-induced rats. The rats had been induced with alloxan [19, 89] which mimic type I diabetes mellitus and streptozotocin-nicotinamide [12], and high-fat diet and low doses of streptozotocin [90] were also used to mimic type II diabetes mellitus. TI extracts showed potent antidiabetic activity in both types. The hypolipidaemic activity was also investigated during the same antidiabetic study because of the effect of insulin on triglyceride metabolism secondarily causing hyperlipidaemia. TI extracts normalized the values of the lipid profile, which showed that TI possesses insulin mimicking action.

An in vitro antidiabetic study [91] was carried out with the leaf extract of TI using α-amylase inhibition assay. The study showed that the extract restrained effective α-amylase enzyme inhibitory activity. α-Amylase is a protein enzyme which hydrolyses alpha bonds of large, alpha-linked polysaccharides, such as starch and glycogen, yielding glucose and maltose. By inhibiting α-amylase enzyme, the breakdown of polysaccharides is hindered, and thereby, the digestion of starch and glycogen is obstructed, and the release of glucose into the blood is inhibited [92]. This is a popular strategy for the treatment of disorders in carbohydrate uptake such as diabetes mellitus and obesity.

To add onto the benefits of TI in diabetes because of its antibacterial activities as discussed previously, TI has also shown potent activity against pathogens which cause diabetic foot ulcers and urinary tract infections [93], which are common complications of diabetes mellitus.

5.4. Antioxidant Activity of Tragia involucrata. A few antioxidant tests have been carried out using the whole plant and the aerial parts of TI. Alcoholic and ethyl acetate extracts were used for the tests. Most of the studies were in vitro studies using methods such as the free radical scavenging activity (IC 50), ABTS and DPPH radical scavenging methods, Griess reagent method, Phosphomolybdenum method, superoxide dismutase by nitroblue tetrazolium method, and superoxide radical scavenging method. Alcoholic and ethyl acetate extracts of TI showed potent antioxidant activities [51, 89, 94, 95].

5.5. Antinociceptive Activity of Tragia involucrata. Analgesic activity of TI has been investigated in vivo using acetic acid-induced writing and radian heat analgesiometer methods. Different solvent extracts of the root and the whole

Table 4: Summarized findings of antibacterial studies carried out on *Tragia involucrata*.

Type of extract	Bacterial type										Reference
	Gram (+)			Gram (−)							
	S.A.	V.C.	P.M.	P.A.	V.D.	K.P.	B.P.	E.C.	P.V.	S.M.	
Isolated compounds from TI leaves	+	NT	NT	NT	NT	NT	NT	+	+	NT	[69]
Ethyl acetate extract of root	+	NT	NT	NT	NT	NT	NT	+	NT	NT	[70]
Methanolic leaf extract	+	NT	NT	−	+	+*	+	NT	NT	NT	[73],*[74]
Acetone leaf extract	NT	NT	NT	NT	NT	NT	NT	+	NT	NT	[60]
Acetone root extract	−	NT	NT	+	NT	+	NT	+	NT	+	[75]
Acetone and methanol leaf extract	+	NT	−	−	NT	−	NT	+	NT	+	[76]
Ethanol leaf extract	+	NT	+	−	NT	−	NT	+	NT	+	[76]
Chloroform stem and ethanol leaf extract	NT	NT	+	+	NT	NT	NT	NT	NT	NT	[63]
Silver nanoparticles synthesized from TI stem	+	NT	NT	NT	NT	NT	NT	+	NT	NT	[77]

S.A., *Staphylococcus aureus*; V.C., *Vibrio cholera*; P.M., *Proteus mirabilis*; P.A., *Pseudomonas aeruginosa*; V.D., *Vibrio damsel*; K.P., *Klebsiella pneumonia*; B.P., *Burkholderia pseudomallei*; E.C., *Escherichia coli*; P.V., *Proteus vulgaris*; S.M., *Serratia marcescens*. NT, not tested. (+), activity present. (−), activity absent. *,** Relevant references.

plant have been used both orally and intraperitoneally to investigate the activity which proved positive for the tested doses [65, 85, 96].

5.6. Antiparasitic Activity of Tragia involucrata. Different types of parasites have been used to investigate the antiparasitic activity of TI. Anthelmintic activity was investigated using earthworms and aquarium worms, and the extracts caused paralysis and death of the worms at the tested dose [62, 87]. Larvicidal activity of root and leaf extracts of TI checked using mosquito larvae showed positive results [64, 97]. Also, phagodeterrence, oviposition deterrence, and mosquito repellant activities were also checked in adult female and gravid female mosquitos which showed positive results [58, 97].

5.7. Diuretic Activity of Tragia involucrata. In Ayurveda and traditional Sri Lankan medicine, TI is used in dysuria and other conditions related to the urinary tract. Hence, diuretic action has been evaluated using different extracts from the root and decoction made from the whole plant. The tests were carried out using healthy Wistar rats. The results showed that the activity of the aqueous root extract and the decoction of the whole plant was most potent as a diuretic, and other extracts such as petroleum ether and chloroform extracts had mild activities [67, 87].

5.8. Antitumor Activity of Tragia involucrata. Hexane and ethyl acetate extracts of the aerial parts of TI were used on Ehrlich's ascites carcinoma (EAC) bearing mice to investigate the antitumor effect. The extract proved to have antitumor activity at the tested doses [98]. Cytotoxic activity of aerial parts of TI was explored using MTT assay in an in vitro test which also showed potent antitumor activity [99]. Furthermore, the in vitro study performed on Ehrlich's ascites carcinoma-induced albino mice showed anticancer activity in the TI ethyl acetate extract [99].

5.9. Other Biological Activities of Tragia involucrata. An in vitro study on the antiarthritic activity of the TI leaf extract which has been investigated [100] showed the extracts having potent activity. Yadav et al. [61] shows antihistamine activity of 5-hydroxy-1-methylpiperidin-2-one (5-HMP) isolated from the TI leaf extract, which further found to be mediated through the formation of protein-ligand complex by binding to human serum albumin [61]. Also, a few in vivo studies have been performed to check antifertility activity [51], antiepileptic activity [101, 102], antihistamine activity [60], hepatoprotective activity [103], and nephroprotective activity [104] using different extracts of different parts of TI plant. All these activities showed positive results for the used extract and for the given dose.

6. Toxicities Associated with *Tragia involucrata*

TI consists of stinging hair/trichomes with sharp siliceous points which can be found on the whole plant. When the trichome is touched, the tip breaks triggering a basal pump mechanism which acts as a hypodermic syringe and release calcium oxalate and toxic peptides such as Shellsol [105]. These toxins on physical contact cause severe itching, burning pain, and inflammation that may persist for few hours to few days. These proteins like any other proteins are denatured once dried, and therefore, the inflammatory symptoms are present mildly in the dried plant. Furthermore, the water solubility of calcium oxalate is 0.67 mg/L (20°C). Therefore, the plant decoctions which is the medicinal preparation used in traditional medicine does not contain the toxins which cause the inflammatory action.

A number of in vivo investigations have been performed to assess possible toxic effects of various decoctions/extractions prepared of TI, which generally indicated that there is no toxicity associated with TI. These studies had been carried out with the whole plant, aerial parts, and leaf, extracted with various solvents such as water, methanol, petroleum ether, chloroform, and ethyl acetate. Most of the toxicity studies had been assessed up to the 14th day of daily administration of the TI extract using different doses.

Acute toxicity performed using the aqueous extract of whole plant of TI for fourteen days showed negative results

at a dose of 5000 mg/kg on healthy male Wistar rats [105]. The methanolic extract of whole plant and leaf did not show 14 days oral acute toxicity at a dose of 2000 mg/kg/day on healthy Wistar rats and Swiss albino mice [12, 101]. The ethyl acetate extract of the aerial part of TI was given to healthy Swiss albino mice through intraperitoneal administration [51] using different doses. Doses of 60, 75, and 90 mg/kg for 14 days IP did not show any toxicity or mortality.

Velu and Malipeddi [100] carried out an in vitro haemolytic activity for the TI leaf extract using human erythrocytes from healthy volunteers. The leaf extract of different solvents such as petroleum ether, chloroform, ethyl acetate, and aqueous extracts showed no haemolytic activity suggesting the nontoxic nature of TI towards erythrocytes.

7. Correlation between the Biological Activities and the Ethnomedicinal Uses of *Tragia involucrata*

Ethnomedicinal use of a medicinal plant correlates with the underlining biological activity possessed by the plant. As discussed earlier, *Tragia involucrata* possesses an abundance of ethnomedicinal uses pertaining to different systems of the body, and many of these uses can be correlated to a range of biological activities of the plant that have been scientifically validated by using systematically controlled in vitro and in vivo experiments. In certain instances, the proven biological activity does not correlate directly to the mentioned disease itself but relates to the underlying pathological condition which causes the disease. Furthermore, the medicinal outcome may be due not to the presence of one biological activity but due to a combination of activities.

One such example is TI's ability to act as a febrifuge. This therapeutic indication is found in most of the Ayurveda authentic texts and in Sri Lankan traditional medical texts. According to the traditional medical text Thalapathepiliyam, the whole plant of TI along with 4 other herbs, each comprising 12 g, are added to 1920 ml water to make the decoction of 240 ml, which is consumed daily. Fever can be a symptom of an infection. Therefore, the febrifuge action by TI could be mediated through its anti-inflammatory and antimicrobial activities. Furthermore, one of the psychopharmacological studies performed by Choudhuri Nag et al. [107] using TI methanol fraction of the root extract showed significant central nervous system depressant action, which also includes the decrease of body temperature. As shown by Samy et al. [69], the aqueous leaf extract of TI showed positive results for acute and subacute anti-inflammatory effects at doses of 50, 100, 200, 300, and 400 mg/kg on albino rats. Moreover, in a study carried out by Panda et al. [70], the ethyl acetate extract of TI root at a dose of 250 mg/kg showed a potent antimicrobial effect against many strains of Gram-positive and Gram-negative bacteria and 3 types of fungi. However, the information on the extractable amounts of ingredients in those traditional decoctions are not indicated. Therefore, in terms of the dose administered, the ethnopharmacological data cannot be compared with the effective doses of various biological activities. Moreover, since the method of extractions between these preparations is also different, the compositions and doses of active ingredients can be varied.

Furthermore, the diseases pertaining to the gastrointestinal tract which comes under ethnomedicinal uses such as dysentery [5] and haemorrhoids [24] are due to inflammation and microbial infection. Therefore, the anti-inflammatory [69, 85] and antimicrobial action [70] of TI as mentioned above can be correlated to the fact why it has been used to cure the aforesaid diseases mentioned in the ethnomedicinal uses. The traditional medical text Thalapathepiliyam [108] mentions that 15 g of the root of TI is made into a decoction with three other plants for bloody dysentery. It also mentions that 30 g of TI root, together with the root of another medicinal plant, is made into a decoction at 240 ml for haemorrhoids, in which this decoction is taken orally at a dose of 120 ml each morning and evening.

Ethnomedicinal uses of TI for diseases concerning the respiratory system [19, 20] such as asthma, cough, and bronchitis and integumentary system [19, 30] such as skin diseases are caused by allergies or microbial activity which in turn stimulate inflammation and histamine release. Hence, anti-inflammatory [85], antihistamine [61], and antimicrobial [70] actions can eliminate these diseases. To evaluate the antihistamine effect of TI, Yadav et al. [61] isolated the potent bioactive molecule, 5-hydroxy-1-methylpiperidin-2-one, from the methanol extract of TI leaves. At a dose of 12.5 mg/kg, this compound showed muscle relaxant, bronchodilating, and antiallergic effects, as tested on histamine-induced muscle contraction in the ileum, bronchoconstriction in the bronchioles, and triple response in the skin of guinea pig. To relieve the asthmatic condition, ethnomedically, the root of TI and two other plants, taken in equal portions, is boiled with rice-washed water [108] and used orally.

Some of the ethnomedicinal uses, such as for diabetes, can be directly correlated to scientifically proven biological activities. The antidiabetic activity [17, 18] of TI has been scientifically validated through in vitro and in vivo studies [12, 19, 65, 89, 91]. According to the study performed by Farook and Atlee [12], the oral administration of the aqueous ethanolic extract of TI whole plant showed potent antidiabetic activity on streptozotocin-nicotinamide-induced type 2 diabetes mellitus in rats, at doses 250 and 500 mg/kg. Similarly, in the ethnomedicinal use, 60 g of the dried and pulverized TI whole plant was prepared into a decoction of 240 ml [88] and used at 120 ml each twice a day. The therapeutic human dose of TI in this decoction, calculated by measuring its extractable matter, was 110 mg/kg [67].

Other therapeutic indications, such as the wound healing action, have been carried out by Samy et al. [80], which showed that 50 μg/kg of Shellsol, isolated from TI, exhibited complete healing after 24 days on *Staphylococcus aureus*-induced excision wound in albino rats. In ethnomedicinal use, the aerial parts of TI and two other plants are ground together into a paste and applied on wounds for wound healing [108]. Furthermore, TI is included in a group of drugs called "welpasmul," meaning the roots of five climbers, which is used for all types of kidney diseases. These

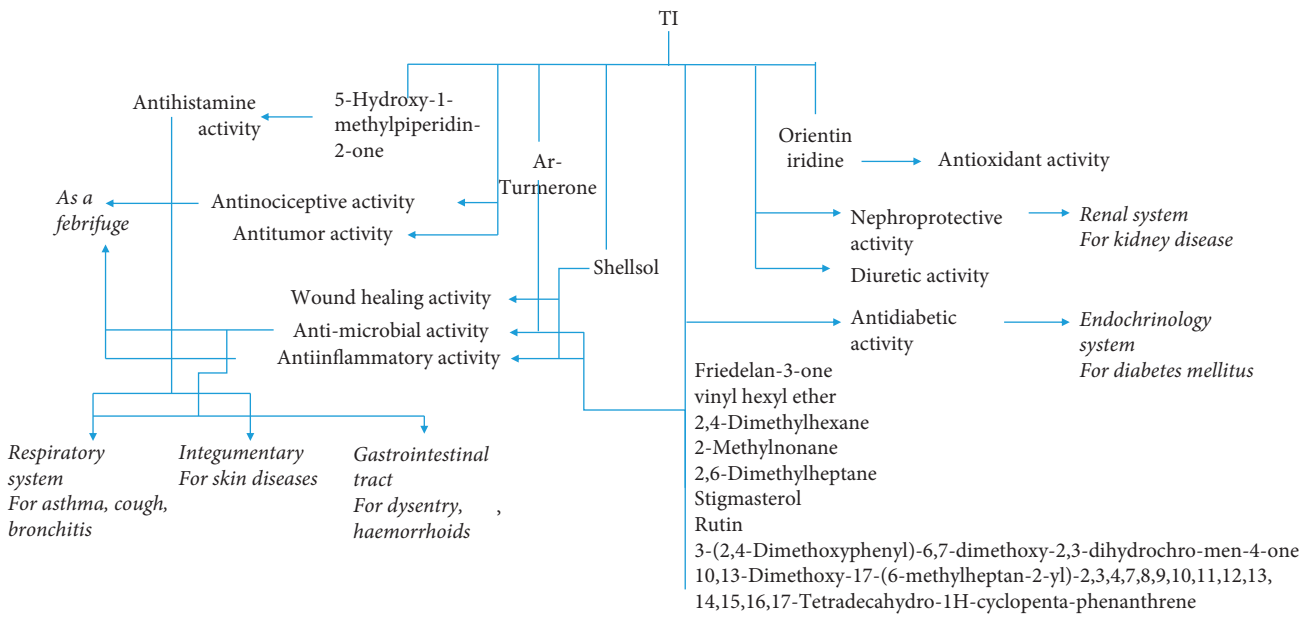

Figure 5: A schematic for the mechanism of action of major ethnopharmacological activities of TI. The validated biological activities of TI have been related to the ethnomedicinal use and the suggested active chemical ingredient.

herbs are used at a weight of 12 g each, and decoction is made at 240 ml for daily consumption [3]. In agreement, the ethanol leaf extract of TI at dose 250 and 500 mg/kg showed potent nephroprotective activity against acetaminophen-induced toxicity in male albino rats on a study performed by Palani et al. [104]. Its diuretic action was also studied by Pallie et al. [67], which showed dose-dependent diuretic activity of the TI decoction on healthy rats at 550, 1100, 1650, and 2200 mg/kg. The therapeutic rat dose of this TI decoction was 550 mg/kg.

The mechanism of action/s of ethnopharmacological activities of TI, based on the information currently available and described in the current manuscript, are summarized in Figure 5.

8. Discussion

In this study, an attempt was made to analyze available information with on phytochemistry, ethnomedicinal uses, and biological activities of the medicinal herb, *Tragia involucrata*, and to explore the correlation between its ethnomedicinal uses with the related biological activities. This study was therefore aimed to scientifically analyze the potential of *Tragia involucrata* having many therapeutic indications, which appears to be applicable in curing diseases pertaining to most of the body systems. In agreement with the broader nature of the ethnomedicinal use of TI, treating a number of diseases rather than a specific disease, TI has shown to possess a range of different biological activities. Moreover, the fact that TI possesses a variety of biological activities which can interplay to relieve symptoms in a particular ailment makes TI as a remedy with a broader therapeutic value. For example, having activities of antibacterial and analgesic for treating an infection and having activities of antidiabetic, antioxidant, and antibacterial for treating diabetes can be shown. It is currently not clear whether all these activities could be mediated by TI by triggering the activation or inhibition of a biochemical pathway that would be common to all the body systems. It would be interesting, therefore, to investigate the mechanism of action of TI in depth to clearly understand its broader therapeutic indications. Although most of the biological activities have been scientifically proven, except for the antioxidant activity, the mechanism of action of other biological activities have not been scientifically explained in literature. Further research needs to be carried out to investigate the mechanisms of action of these biological activities to get a more clear understanding about the pharmacodynamics of TI.

Regarding the available literature on the phytochemistry of TI, it is clear that only a number of chemical compounds have been isolated so far from TI. Also, most of these chemicals have been studied for their antimicrobial or anti-inflammatory actions alone. These chemicals have not been investigated for multiple biological activities so far. Therefore, studies should also be focused in isolating biologically active chemicals from TI and carry out investigations to understand its mechanism of action responsible for multiple activities.

Furthermore, no studies were found which evaluated the activities of TI in human since all of the studies were either in vitro studies in animals or in vivo studies. Therefore, it should be cautioned when generalizing the conclusions of those studies to the human population, despite the fact that TI has been in use for centuries in traditional medical systems. The way to bridge this gap is through extending those studies to the clinical level to scientifically evaluate the effectiveness of the plant on humans as well as to gain knowledge on its common side effects and drug interactions. Randomized clinical trials are required to be performed as future studies in order to scientifically prove the safety and efficacy of TI to be

used as a phytomedicine. It will strengthen the validation of the therapeutic efficacy of this medicinal plant.

9. Conclusion

In conclusion, this review was presented in the hope to discover a medicinal herb which has the potential to function in multiple systems of the body and which possess a range of different biological activities. It is of great importance to understand whether *Tragia involucrata* stimulates or inhibits a common biochemical pathway in all the body systems, to trigger those activities. Hence, it would be interesting to investigate the mechanism of action of TI in depth to clearly understand its broader therapeutic indications. Since most of the activities are preclinical trials, it would be necessary to carry out randomized controlled human trials to determine whether TI can be developed into a phytomedicine to be used as both as a preventive and a therapeutic agent.

Conflicts of Interest

The authors declare that there are no conflicts of interest.

Acknowledgments

The authors would like to extend their sincere appreciation to the University Grant Commission (UGC/DRIC/PG/2014MAY/IIM/01) of Sri Lanka for funding this research.

References

[1] B. H. Haroon, M. Kulandhaivel, S. Anbalagan, M. Sankareswaran, and K. Abirami, "Green synthesis of silver nanoparticles using 002 *Hybanthusenneaspermus* plant extract against nosocomial pathogens with nanofinished antimicrobial cotton fabric," *Global Journal of Nanomedicine*, vol. 1, no. 1, Article ID 555554, 2016.

[2] The Promotion and Development of Traditional Medicine, *WHO Technical Report Series No. 622:8*, World Health Organization, Geneva, Switzerland, 1978, http://apps.who.int/iris/bitstream/handle/10665/40995/WHO_TRS_622.pdf.

[3] A. Kumarasinghe, *King Buddhadasa'sSararthaSamgraha*, Department of National Museums, Colombo, Sri Lanka, 1910.

[4] R. K. Sharma, *Caraka Samhita (Based on CakrapaniDatta's Ayurveda Deepika) (Translation Reprinted)*, Chaukhambha Sasnskrit Series Office, Varnasi, India, 2017.

[5] D. M. A. Jayaweera, *Medicinal Plants (Indigenous and Exotic) Used in Ceylon. Part II*, The National Science Foundation, Colombo, Sri Lanka, 2006.

[6] Compendium of Medicinal plants, *A Sri Lankan Study*, Vol. 1, Department of Ayurveda, Colombo, Sri Lanka, 2004.

[7] M. D. Dassanayake and W. D. Clayton, *A Revised Handbook to the Flora of Ceylon*, Vol. XI, Oxford & IBH Publishing Co. Pvt. Ltd., New Delhi, India, 1997.

[8] Ayurveda Pharmacopoeia, *Ayurveda Pharmacopoeia*, Vol. I, Department of Ayurveda, Colombo, Sri Lanka, 2nd edition, 1979.

[9] S. K. R. Murthy, *Bhavaprakasa of Bhavamisra*, Vol. I, ChowkhambhaKrishnadas Academy, Varanasi, India, 2004.

[10] S. Murthy, *Vagbhata'sAstangahrdayam (Translation and Reprint)*, Chaukhambha Krishnadas Academy, Varnasi, India, 2004.

[11] S. Murthy, *Sushruta Samhita (Translation and Reprint)*, Chaukhambha Orientalia, Varnasi, India, 2017.

[12] S. M. Farook and W. C. Atlee, "Antidiabetic and hypolipidemic potential of *Tragia involucrata*linn. in streptozotocin-nicotinamide induced type II diabetic rats," *International Journal of Pharmacy and Pharmaceutical Sciences*, vol. 3, no. 4, pp. 103–109, 2011.

[13] E. Jarald, S. B. Joshi, and D. C. Jain, "Diabetes and herbal medicines," *Iranian Journal of Pharmacology & Therapeutics*, vol. 7, pp. 97–106, 2008.

[14] A. Kar, B. K. Choudhary, and N. G. Bandyopadhyay, "Preliminary studies on the inorganic constituents of some indigenous hypoglycaemic herbs on oral glucose tolerance test," *Journal of Ethnopharmacology*, vol. 64, no. 2, pp. 179–184, 1999.

[15] R. J. Marles and N. R. Farnsworth, "Antidiabetic plants and their active constituents," *Phytomedicine*, vol. 2, no. 2, pp. 137–189, 1995.

[16] I. Mohanram and J. S. Meshram, *Chapter 10: Treasures of Indigenous Indian Herbal Antidiabetics: An Overview. Discovery and Development of Antidiabetic Agents from Natural Products*, Elsevier, Amsterdam, Netherlands, 2017.

[17] M. M. Sundaram, R. Deepthi, D. Sudarsanam, R. Sivasubramanian, and P. Brindha, "Chemotaxonomic studies on *Tragia involucrata* Linn," *International Journal of Biological and Chemical Sciences*, vol. 3, no. 5, pp. 927–933, 2009.

[18] S. Surya, A. D. Salam, D. V. Tomy, B. Carla, R. A. Kumar, and C. Sunil, "Diabetes mellitus and medicinal plants-a review," *Asian Pacific Journal of Tropical Disease*, vol. 4, no. 5, pp. 337–347, 2014.

[19] A. Kar, B. K. Choudhary, and N. G. Bandyopadhyay, "Comparative evaluation of hypoglycaemic activity of some Indian medicinal plants in alloxan diabetic rats," *Journal of Ethnopharmacology*, vol. 84, no. 1, pp. 105–108, 2003.

[20] Ayurveda Pharmacopoiea, *Ayurveda Pharmacopoiea*, Vol. I, Department of Ayurveda, Colombo, Sri Lanka, 2nd edition, 1985.

[21] A. Dey and J. N. De, "Ethnobotanical survey of Purulia district, West Bengal, India for medicinal plants used against gastrointestinal disorders," *Journal of Ethnopharmacology*, vol. 143, no. 1, pp. 68–80, 2012.

[22] C. RamanKutty, P. K. Warrier, and V. P. Nambiar, *Indian Medicinal Plants: A compendium of 500 species*, Vol. 5, Orient Longman Publishers, Bengaluru, India, 1992.

[23] M. Rahmatullah, Z. Khatun, A. Hasan et al., "Survey and scientific evaluation of medicinal plants used by the pahan and teli tribal communities of natore district, Bangladesh," *African Journal of Traditional Complementary and Alternative Medicines*, vol. 9, no. 3, pp. 366–373, 2012.

[24] G. K. Dash, T. Subburaju, T. K. Khuntia, J. Khuntia, S. Moharana, and P. Suresh, "Some pharmacognostical characteristics of Tragia involucrata Linn. roots," *Ancient Science of Life*, vol. 20, no. 1-2, pp. 1–5, 2000.

[25] D. Rekha and A. Paneerselvam, "Studies on medicinal plants of Koradacheri village, Kodavasal Taluk, Thiruvarur district, Tamil nadu, India," *International Research Journal of Pharmacy*, vol. 4, no. 10, pp. 99–107, 2014.

[26] N. Savithramma, C. Sulochana, and K. N. Rao, "Ethnobotanical survey of plants used to treat asthma in Andhra

Pradesh, India," *Journal of Ethnopharmacology*, vol. 113, no. 1, pp. 54–61, 2007.

[27] Y. Jahan, T. Mahmood, P. Bagga, A. Kumar, K. Singh, and M. Mujahid, "Future prospects of cough treatment; herbal medicines V/S modern drugs," *International Journal of Pharmaceutical Research and Sciences*, vol. 6, no. 9, pp. 3689–3697, 2015.

[28] S. Shanmugam, K. Rajendran, and K. Suresh, "Traditional uses of medicinal plants among the rural people in Sivagangai district of Tamil Nadu, Southern India," *Asian Pacific Journal of Tropical Biomedicine*, vol. 2, no. 1, pp. s429–s434, 2012.

[29] A. Dey and J. Nath De, "Ethnobotanicals of the family Euphorbiaceae used by the ethnic groups of Purulia district, West Bengal, India," *Life Sciences Leaflets*, vol. 18, pp. 690–694, 2011.

[30] R. Solanki, "Treatment of skin diseases through medicinal plants in different regions of the world," *International Journal of Biomedical Research*, vol. 2, no. 1, pp. 73–80, 2011.

[31] S. Sundarrajan and M. Arumugam, "Documentation of traditional siddha medicines for skin diseases from Katpadi taluk, Vellore district, Tamil nadu, India," *European Journal of Integrative Medicine*, vol. 9, pp. 52–62, 2017.

[32] M. Ayyanar and S. Ignacimuthu, "Medicinal plants used by the Tribals of Tirunelveli hills, Tamila Nadu, to treat poisonous bites and skin diseases," *Indian Journal of Traditional Knowledge*, vol. 4, no. 3, pp. 229–236, 2005.

[33] B. Kumar, M. Vijayakumar, R. Govindarajan, and P. Pushpangadan, "Ethnopharmacological approaches to wound healing-exploring medicinal plants of India," *Journal of Ethnopharmacology*, vol. 114, no. 2, pp. 103–113, 2007.

[34] A. Khatun, A. A. Khan, A. Rahman et al., "Ethnomedicinal usage of plants and animals by folk medicinal practitioners of three villages in Chuadanga and Jhenaidah districts, Bangladesh," *American-eurasian Journal of Sustainable Agriculture*, vol. 7, no. 5, pp. 319–339, 2013.

[35] B. K. Mallik, T. Panda, and R. N. Padhy, "Traditional herbal practices by the ethnic people of kalahandi district of Odisha, India," *Asian Pacific Journal of Tropical Biomedicine*, vol. 2, no. 2, pp. s988–s994, 2012.

[36] F. Mawla, S. Khatoon, F. Rehana et al., "Ethnomedicinal plants of folk medicinal practitioners in four villages of Natore and Rajshahi districts, Bangladesh," *American-eurasian Journal of Sustainable Agriculture*, vol. 6, no. 4, pp. 406–416, 2012.

[37] S. B. Padal, P. P. Murty, D. S. Rao, and M. Venkaiah, "Ethnomedicinal plants from paderu division of Visakhapatnam district, A.P, India," *Journal of Phytology*, vol. 2, no. 8, pp. 70–91, 2010.

[38] M. F. Kadir, M. S. Bin Sayeed, N. I. Setu, A. Mostafa, and M. M. K. Mia, "Ethnopharmacological survey of medicinal plants used by traditional health practitioners in Thanchi, Bandarban Hill Tracts, Bangladesh," *Journal of Ethnopharmacology*, vol. 155, no. 1, pp. 495–508, 2014.

[39] V. Velu, M. Das, A. N. Raj N, K. Dua, and H. Malipeddi, "Evaluation of in vitro and in vivo anti-urolithiatic activity of silver nanoparticles containing aqueous leaf extract of Tragia involucrata," *Drug Delivery and Translational Research*, vol. 7, no. 3, pp. 439–449, 2017.

[40] A. Dey, P. Gorai, A. Mukherjee, R. Dhan, and B. K. Modak, "Ethnobiological treatments of neurological conditions in the Chota Nagpur plateau, India," *Journal of Ethnopharmacology*, vol. 198, pp. 33–44, 2017.

[41] J. Sharma, S. Gairola, R. D. Gaur, R. M. Painuli, and T. O. Siddiqi, "Ethnomedicinal plants used for treating epilepsy by indigenous communities of sub-Himalayan region of Uttarakhand, India," *Journal of Ethnopharmacology*, vol. 150, no. 1, pp. 353–370, 2013.

[42] Z.-J. Zhang, "Therapeutic effects of herbal extracts and constituents in animal models of psychiatric disorders," *Life Sciences*, vol. 75, no. 14, pp. 1659–1699, 2004.

[43] S. Ravi, R. Arumugam, and S. Ariyan, "Floristic diversity and ethnobotanical uses of Vedhagiri hills in Bhavani, Erode district, Tamil nadu," *Open Access Library Journal*, vol. 3, p. e2259, 2016.

[44] I. Lampronti, M. T. H. Khan, N. Bianchi et al., "Plants with antitumor properties: from biologically active molecules to drugs," *Lead Molecules from Natural Products-Discovery and New Trends*, vol. 2, pp. 45–63, 2006.

[45] A. Subramoniam, V. Madhavachandran, and A. Gangaprasad, "Medicinal plants in the treatment of arthritis," *Annals of Phytomedicine*, vol. 2, no. 1, pp. 3–36, 2013.

[46] Y. Uprety, R. C. Poudel, J. Gurung, N. Chettri, and R. P. Chaudhary, "Traditional use and management of NTFPs in Kangchenjunga landscape: implications for conservation and livelihoods," *Journal of Ethnobiology and Ethnomedicine*, vol. 12, no. 19, pp. 1–59, 2016.

[47] S. B. Padal, H. Ramakrishna, and R. Devender, "Ethnomedicinal studies for endemic diseases by the tribes of MunchingiputtuMandal, Visakhapatnam District, Andhra Pradesh, India," *International Journal of Aromatic Plants*, vol. 2, no. 3, pp. 453–459, 2012.

[48] R. A. Vasant, M. C. Khajuria, and A. Narasimhacharya, "Antioxidant and ACE enhancing potential of Pankajakasthuri in fluoride toxicity: anin vitrostudy on mammalian lungs," *Toxicology and Industrial Health*, vol. 27, no. 9, pp. 793–801, 2011.

[49] N. Savithramma, P. Yugandhar, K. Prasad, S. Ankanna, and K. Chetty, "Ethnomedicinal studies on plants used by Yanadi tribe of Chandragiri reserve forest area, Chittoor District, Andhra Pradesh, India," *Journal of Intercultural Ethnopharmacology*, vol. 5, no. 1, pp. 49–56, 2016.

[50] A. A. K. Chowdhury, R. A. Khaleque, and S. K. Chakder, "Antifertility activity of a traditional contraceptive pill comprising of Acacia catechu, A. Arabica, and Tragia involucrata," *Indian Journal of Medical Research*, vol. 80, pp. 372–374, 1984.

[51] G. C. Joshi and M. Gopal, "Antifertility activity of Hexane and ethyl acetate extracts of aerial parts of *Tragia involucrata* Linn," *Journal of Pharmacology and Toxicology*, pp. 2–6, 2011.

[52] G. Y. Dama, H. L. Tare, M. S. Gore, S. R. Deore, and J. S. Bidkar, "Herbal allies for snakebite envenomation," *Pharma Science Monitor an International Journal of Pharmaceutical Sciences*, vol. 3, no. 2, pp. 79–84, 2012.

[53] J. Félix-Silva, A. A. Silva-Junior, S. M. Zucolotto, and M. d. F. Fernandes-Pedrosa, "Medicinal plants for the treatment of local tissue damage induced by snake venoms: an overview from traditional use to pharmacological evidence," *Evidence-Based Complementary and Alternative Medicine*, vol. 2017, Article ID 5748256, 52 pages, 2017.

[54] R. P. Samy, M. M. Thwin, P. Gopalakrishnakone, and S. Ignacimuthu, "Ethnobotanical survey of folk plants for the treatment of snakebites in Southern part of Tamilnadu, India," *Journal of Ethnopharmacology*, vol. 115, no. 2, pp. 302–312, 2008.

[55] R. P. Samy, P. Gopalakrishakone, and V. T. K. Chow, "Therapeutic application of natural inhibitors against snake venom phospholipase A2," *Bioinformation*, vol. 8, no. 1, 2012.

[56] J. G. Graham, M. L. Quinn, D. S. Fabricant, and N. R. Farnsworth, "Plants used against cancer-an extension of the work of Jonathan Hartwell," *Journal of Ethnopharmacology*, vol. 73, no. 3, pp. 347–377, 2000.

[57] M. M. Rahman and M. A. Khan, "Anti-cancer potential of south Asian plants," *Natural Products and Bioprospecting*, vol. 3, no. 3, pp. 74–88, 2013.

[58] M. Nagendra and S. Mohanraghupathy, "Effect of natural mosquito repellent activity of Sticks of *Tragia involucrata* leaves," *World Journal of Pharmacy and Pharmaceutical Sciences*, vol. 5, no. 7, pp. 1106–1114, 2016.

[59] M. Saha, D. Sarker, P. Kar, P. Gupta, and A. Sen, "Indigenous knowledge of plants in local healthcare management practices by tribal people of Malda district, India," *Journal of Intercultural Ethnopharmacology*, vol. 3, no. 4, pp. 179–185, 2014.

[60] R. Gobalakrishnan, M. Kulandaivelu, R. Bhuvaneswari, D. Kandavel, and L. Kannan, "Screening of wild plant species for antibacterial activity and phytochemical analysis of *Tragia involucrata* L," *Journal of Pharmaceutical Analysis*, vol. 3, no. 6, pp. 460–465, 2013.

[61] S. A. Yadav, S. Ramalingam, A. J. Raj, and R. Subban, "Antihistamine from *Tragia involucrata* L. leaves," *Journal of Complementary and Integrative Medicine*, vol. 12, no. 3, pp. 217–226, 2015.

[62] B. S. Patil, I. D. Raut, M. A. Bhutkar, and S. K. Mohite, "Evaluation of anthelmintic activity of leaves of *Tragia involucrata* Linn," *Journal of Pharmacognosy and Phytochemistry*, vol. 4, no. 1, pp. 155–159, 2015.

[63] S. S. Sahaya, P. Vijayakanth, R. Palani, T. Thamizharasi, and A. Vimala, "Antimicrobial and phytochemical screening of Tragia involucrata L. using UV-VIS and FTIR," *International Journal of Research in Engineering and Bioscience*, vol. 1, no. 1, pp. 82–90, 2013.

[64] R. Ganasekar, J. Alagarmalai, and J. Alagarmalai, "Phytochemical constituents and larvicidal activity of Tragia involucrata Linn. (Euphorbiacea) leaf extracts against chikungunya vector, *Aedes aegypti* (Linn.) (Diptera: Culicidae)," *Journal of Coastal Life Medicine*, vol. 4, no. 1, pp. 53–55, 2016.

[65] N. Venkatrao, K. Benoyl, K. Hemamalini, S. M. S. Kumar, and S. Satyanarayana, "Pharmacological evaluation of root extracts of *Tragia involucrata*," *Pharmacologyonline*, vol. 2, pp. 236–244, 2007.

[66] B. S. Reddy, N. R. Rao, K. Vijeepallam, and V. Pandy, "Phytochemical, pharmacological and biological profiles of Tragia species (family: Euphorbiaceae)," *African Journal of Traditional, Complementary and Alternative Medicines*, vol. 14, no. 3, pp. 105–112, 2017.

[67] M. S. Pallie, P. K. Perera, C. L. Goonasekera, K. M. N. Kumarasinghe, and L. D. A. M. Arawwawala, "Evaluation of the diuretic effect of the hot water extract of standardized *Tragia involucrata* Linn. in rats," *International Journal of Pharmacology*, vol. 13, pp. 83–90, 2017.

[68] C. T. Sulaiman and I. Balachandran, "LC/MS characterization of antioxidant flavonoids from Tragia involucrata L," *Beni-Suef University Journal of Basic and Applied Sciences*, vol. 5, no. 3, pp. 231–235, 2016.

[69] R. P. Samy, P. Gopalakrishnakone, P. Houghton, and S. Ignacimuthu, "Purification of antibacterial agents from Tragia involucrata-a popular tribal medicine for wound healing," *Journal of Ethnopharmacology*, vol. 107, no. 1, pp. 99–106, 2006.

[70] D. Panda, S. K. Dash, and G. K. Dash, "Phytochemical examination and antimicrobial activity of various solvent extracts and the selected isolated compounds from roots of *Tragia involucrata* Linn," *International Journal of Pharmaceutical Sciences and Drug Research*, vol. 4, no. 1, pp. 44–48, 2012.

[71] R. P. Samy, S. Ignacimuthu, and A. Sen, "Screening of 34 Indian medicinal plants for antibacterial properties," *Journal of Ethnopharmacology*, vol. 62, no. 2, pp. 173–181, 1998.

[72] R. P. Samy and P. Gopalakrishnakone, "Therapeutic potential of plants as anti-microbials for drug discovery," *ECAM*, vol. 7, no. 3, pp. 283–294, 2010.

[73] R. P. Samy, J. Manikandan, and M. Al Qahtani, "Evaluation of aromatic plants and compounds used to fight multidrug resistant infections," *Evidence-Based Complementary and Alternative Medicine*, vol. 1, pp. 1–17, 2013.

[74] S. á Barros and M. T. Ralph, "Phytochemistry and preliminary assessment of the antibacterial activity of chloroform extract of amburanacearensis (allemão) A.C. Sm. against Klebsiellapneumoniae Carbapenemase-producing strains," *Evidence-Based Complementary and Alternative Medicine*, vol. 2014, Article ID 786586, 7 pages, 2014.

[75] T. Thomas, "Antibacterial behaviour of root extracts of *Tragia involucrata* L. in gradient extraction," *International Journal of Pharma Sciences and Research*, vol. 7, no. 11, pp. 419–422, 2016.

[76] T. F. Xavier, A. S. Auxilia, and M. Kannan, "An antibacterial potential of *Tragia involucrata* L. against opportunistic bacterial pathogens of HIV/AIDS positive patients of Karur District," *World Journal of Pharmacy and Pharmaceutical Sciences*, vol. 5, no. 3, pp. 871–877, 2016.

[77] N. Saraswathy and V. Thirumurugan, "Green synthesis of silver nanoparticles using Tragia involucrata stem extract and analysis of their antimicrobial property," *International Journal of Chemical and Pharmaceutical Analysis*, vol. 4, no. 2, 2017.

[78] R. A. A. Mothana, S. A. A. Abdo, S. Hasson, F. M. N. Althawab, S. A. Z. Alaghbari, and U. Lindequist, "Antimicrobial, antioxidant and cytotoxic activities and phytochemical screening of some Yemeni medicinal plants," *Evidence-based Complementary and Alternative Medicine*, vol. 7, no. 3, pp. 323–330, 2010.

[79] R. P. Samy, P. Gopalkrishakone, M. Sarumathi, and S. Ignacimuthu, "Wound healing potential of *Tragia involucrata* extract in rats," *Fitoterapia*, vol. 77, pp. 300–302, 2006.

[80] R. P. Samy, P. Gopalakrishnakone, P. Houghton, M. M. Thwin, and S. Ignacimuthu, "Effect of aqueous extract ofTragia involucrata Linn. on acute and subacute inflammation," *Phytotherapy Research*, vol. 20, no. 4, pp. 310–312, 2006.

[81] R. Samy, G. Sethi, V. Chow, and B. Stiles, "Plant-based hydrocarbon esters from Tragia involucrata possess antimicrobial and anti-inflammatory activities," *Infectious Disorders-Drug Targets*, vol. 13, no. 2, pp. 141–153, 2013.

[82] L. A. Hawver, S. A. Jung, and W. Ng, "Specificity and complexity in bacterial quorum-sensing systems," *FEMS Microbiology Reviews*, vol. 14, no. 40, pp. 738–752, 2016.

[83] K. Anitha and T. Mahalakshmi, "Screening of south Indian herbs for quorum quenching property," *International Journal of Pharma and Bio Sciences*, vol. 3, no. 4, pp. 974–979, 2012.

[84] S. M. Gupta, K. Kumar, S. K. Dwivedi, and M. Bala, "Bioactive potential of Indian stinging plants leaf extract against pathogenic fungi," *Journal of Complementary & Integrative Medicine*, vol. 16, no. 1, 2018.

[85] A. K. Dhara, V. Suba, T. Sen, S. Pal, and A. K. N. Chaudhuri, "Preliminary studies on the anti-inflammatory and analgesic activity of the methanolic fraction of the root extract of *Tragia involucrata* Linn," *Journal of Ethnopharmacology*, vol. 72, no. 1-2, pp. 265–268, 2000.

[86] P. Gopalakrishnakone, R. P. Samy, P. Houghton, M. Sarumathi, and S. Ignacimuthu, "Effect of aqueous extract of *Tragia involucrata* Linn. On acute and sub-acute inflammation," *Phytotherapy Research*, vol. 20, pp. 310–312, 2006.

[87] V. N. Rao, K. Benoy, K. Hemamalini, S. M. Shanta Kumar, and S. Satyanarayana, "Anti-diabetic activity of root extracts of Tragia involucrata," *Pharmacologyonline*, vol. 2, pp. 203–217, 2007.

[88] E. R. H. S. S. Ediriweera and W. D. Ratnasooriya, "A review on herbs used in treatment of diabetes mellitus by Sri Lankan ayurvedic and traditional physicians," *AYU*, vol. 30, no. 4, pp. 373–391, 2009.

[89] D. Prakash, P. Kumar, and N. Kumar, "Antioxidant and hypoglycaemic activity of some Indian medicinal plants," *Pharmacologyonline*, vol. 3, pp. 513–521, 2009.

[90] M. S. Pallie, P. K. Perera, C. L. Goonasekera, K. M. N. Kumarasinghe, and L. D. A. M. Arawwawala, "Tragia involucrata L.: safe and promising drug for type-2 diabetes mellitus," in *Proceedings of the Third International Conference on Natural Product Genomics and Drug Discovery (Held by Society of Natural Product Genomics and Drug Discovery on 2017)*, Colombo, Sri Lanka, 2017.

[91] V. Vinodhini, M. Himaja, V. SaiSaraswathi, and D. Poppy, "Invitroantidiabetic activity of Tragia involucrata Linn. leaf extracts," *International Journal of Research in Ayurveda and Pharmacy*, vol. 6, no. 1, 2015.

[92] B. M. Brena, C. Pazos, L. Franco-Fraguas, and F. Batista-Viera, "Chromatographic methods for amylases," *Journal of Chromatography B: Biomedical Sciences and Applications*, vol. 684, no. 1-2, p. 217, 1996.

[93] S. S. Lakshmi, G. Chelladurai, and B. Suresh, "In vitro studies on medicinal plants used against bacterial diabetic foot ulcer (BDFU) and urinary tract infected (UTI) causing pathogens," *Journal of Parasitic Diseases*, vol. 40, no. 3, pp. 667–673, 2016.

[94] S. M. Farook and W. C. Atlee, "Antioxidant potential of *Tragia involucrata* Linn. on streptozotocin induced oxidative stress in rats," *International Journal of Pharmaceutical Sciences and Research*, vol. 2, no. 6, pp. 1530–1536, 2011.

[95] M. G. Savithri, B. A. S. Chandanadevi, A. V. Krishnaraju, C. V. Rao, and G. Trimurtulu, "Antioxidant activity and brine ShrimpLethality of Tragia involucrata L," *Asian Journal of Chemistry*, vol. 22, no. 3, pp. 1684–1688, 2010.

[96] M. Alimuzzaman and M. Ahmed, "Analgesic activity of Tragia involucrata," *Dhaka University Journal of Pharmaceutical Sciences*, vol. 4, no. 1, 2005.

[97] K. Bhattacharya and G. Chandra, "Phagodeterrence, larvicidal and oviposition deterrence activity of Tragia involucrata L. (Euphorbiaceae) root extractives against vector of lymphatic filariasis *Culex quinquefasciatus* (Diptera: Culicidae)," *Asian Pacific Journal of Tropical Disease*, vol. 4, pp. S226–S232, 2014.

[98] C. G. Joshi, M. Gopal, and N. S. Kumari, "Antitumor activity of hexane and ethyl acetate extracts of Tragia involucrata," *International Journal of Cancer Research*, vol. 7, no. 4, pp. 267–277, 2011.

[99] C. G. Joshi, M. Gopal, and S. M. Byregowda, "Cytotoxic activity of *Tragia involucrata* Linn. extracts," *American Eurasian Journal of Toxicological Sciences*, vol. 3, no. 2, pp. 67–69, 2011.

[100] V. Velu and H. Malipeddi, "In vitro anti-arthritic and hemolytic activity of leaf extracts of Tragia involucrata," *International Journal of PharmTech Research*, vol. 8, no. 7, pp. 46–50, 2015.

[101] G. G. Varma, B. K. Mathai, K. Das, G. Gowda, S. Rammohan, and J. W. Einstein, "Evaluation of antiepileptic activity of methanolic leaves extract of *Tragia involucrata* Linn. in mice," *International Letters of Natural Sciences*, vol. 17, no. 2, pp. 167–179, 2014.

[102] A. K. Dhara, S. Pal, and A. K. Nag Chaudhuri, "Psychopharmacological studies on Tragia involucrata root extract," *Phytotherapy Research*, vol. 16, no. 4, pp. 326–330, 2002.

[103] A. S. ALAnazi, J. Anwar, and A. Ahmad, "Hepatoprotective and antioxidant activity of *Tragia involucrata* root extracts against CCl4 induced hepatotoxicity in rats," *Der Pharmacia Lettre*, vol. 7, no. 5, pp. 146–152, 2015.

[104] S. Palani, S. N. Kumar, R. Gokulan, D. Rajalingam, and B. S. Kumar, "Evaluation of Nephroprotective and antioxidant potential of *Tragia involucrata*," *Drug Invention Today*, vol. 1, no. 1, pp. 55–60, 2009.

[105] S. M. Gupta and K. Kumar, "Stinging plants: as future bioweapon," *Journal of Complementary and Integrative Medicine*, vol. 13, no. 3, pp. 217–219, 2016.

[106] M. S. Pallie, P. K. Perera, C. L. Goonasekera, K. M. N. Kumarasinghe, and L. D. A. M. Arawwawala, "Acute toxicity study on hot water extract of *Tragia involucrata* Linn. in rats," in *Proceedings of the Second International Conference on Natural Product Genomics and Drug Discovery*, Colombo, Sri Lanka, 2016.

[107] A. K. Chaudhuri Nag, A. K. Dhara, and S. Pal, "Psychopharmacological studies on *Tragia involucrata* root extract," *Phytotherapy Research*, vol. 16, pp. 326–330, 2002.

[108] Thalpathepiliyam, *Book 19, Borella*, Department of Ayurveda, Colombo, Sri Lanka, 1993.

Hindawi
Evidence-Based Complementary and Alternative Medicine
Volume 2020, Article ID 8836904, 13 pages
https://doi.org/10.1155/2020/8836904

Research Article

The Role of Oxymatrine in Amelioration of Acute Lung Injury Subjected to Myocardial I/R by Inhibiting Endoplasmic Reticulum Stress in Diabetic Rats

Yongpan Huang,[1,2] **Xian Long**,[1] **Xinliang Li**,[2] **Saihua Li**,[3] **and Jianbin He**[4]

[1]*Medicine School, Changsha Social Work College, Changsha, Hunan, China*
[2]*Institute of Chinese Meteria Medica, Hunan Academy of Chinese Medicine, Changsha, China*
[3]*Nursing Department, Guilin People's Hospital, Guilin, China*
[4]*Department of Respiratory and Critical Care Medicine, The First People's Hospital of Huaihua, affiliated to University of South China, Huaihua, Hunan, China*

Correspondence should be addressed to Saihua Li; lisaihuagl@163.com and Jianbin He; hjb0919hh@163.com

Received 15 September 2020; Revised 27 October 2020; Accepted 15 November 2020; Published 26 November 2020

Academic Editor: Xu-Jie Zhou

Background. Oxymatrine (OMT) is the primary pharmacological component of *Sophora flavescens* Aiton., which has been shown to possess potent antifibrotic, antioxidant, and anti-inflammatory activities. The aim of the present study was to clarify the protective mechanism of OMT on acute lung injury (ALI) subjected to myocardial ischemia/reperfusion (I/R). *Methods*. A myocardial I/R-induced ALI model was achieved in diabetic rats by occluding the left anterior descending coronary artery for 1 h, followed by reperfusion for 1 h. The levels of inflammatory factors (tumor necrosis factor-α, interleukin- (IL-) 6, and IL-17) in bronchoalveolar lavage fluid were assessed using commercially available kits. The index of myocardial injury, including the detection of cardiac troponin I (cTnI), cardiac troponin T (cTnT), lactate dehydrogenase (LDH), and creatine kinase-MB (CK-MB), was also determined using commercially available kits. Hematoxylin and eosin staining and terminal deoxynucleotidyl transferase-mediated dUTP nick end labeling were used to identify histological changes. The expression levels of endoplasmic reticulum chaperone BiP (GRP78), DNA damage-inducible transcript 3 protein (CHOP), eukaryotic translation initiation factor 2-alpha kinase 3 (PERK), inositol dependent enzyme 1α (IRE1α), ATF6, caspase-3, -9, and-12, Bcl-2, and Bax were determined by Western blotting. The mRNA expression levels of GRP78 and CHOP were detected by reverse transcription-quantitative PCR. *Results*. Myocardial I/R increased the levels of cTnI, cTnT, LDH, and CK-MB in diabetic rats. Damaged and irregularly arranged myocardial cells were also observed, as well as more serious ALI with higher lung injury scores and WET/DRY ratios and lower PaO_2. Moreover, the expression of key proteins of endoplasmic reticulum stress (ERS) was increased by I/R injury, including phosphorylated- (p-) PERK, p-IRE1α, and ATF6, as well as decreased levels of apoptosis. These effects were all significantly reversed by OMT treatment. *Conclusions*. OMT protects against ALI subjected to myocardial I/R by inhibiting ERS in diabetic rats.

1. Introduction

Diabetes is a metabolic disease with a high rate of mortality, which is characterized by hyperglycemia. Persistent hyperglycemia can lead to chronic tissue damage, including cardiomyopathy, nephropathy, diabetic foot, and diabetic neuropathy [1, 2]. Acute myocardial infarction is associated with higher mortality rates in patients with diabetes [3]. Diabetes also increases susceptibility myocardial ischemia/reperfusion (I/R) injury, which can induce endoplasmic reticulum stress (ERS) [4, 5]. ERS refers to ischemia, hypoxia, oxidative stress, and glucose/nutrition abnormalities where material deficiencies promote abnormal glycosylation reactions and calcium ion homeostasis, significantly increasing the number of unfolded proteins in the ER. As such, the processing capacity of the ER is exceeded causing

abnormal cellular reactions, and the intracellular conditions are altered in an attempt to restore the ER environment. Moderate ERS restores homeostasis and maintains cell survival, but persistently severe ERS results in apoptosis and even necrosis, accelerating I/R injury. Therefore, suppressing ERS may become an important therapeutic option for ameliorating I/R injury [6–8].

Oxymatrine (OMT) is a major active ingredient isolated from *Sophora flavescens* Aiton., which possesses diverse biological properties beneficial to human health, including anti-inflammatory, antiallergic, antiviral, and antifibrotic activities. Owing to its antioxidant activity, OMT has been reported to exert protective effects against cardiovascular diseases [9], diabetes [10], inflammation [11, 12], and cancer [13, 14]. Several lines of evidence have demonstrated that OMT exerts its protective effects by scavenging lipid free radicals, thereby decreasing cytotoxicity in vitro and in vivo [15, 16]. Studies have also revealed that OMT ameliorates diabetes-associated aortic endothelial dysfunction in streptozotocin- (STZ-) induced diabetic mice [10, 17, 18]. Based on the role of apoptosis during ERS and the effect of OMT in myocardial I/R-induced ALI in diabetic rats, the current study aimed to further investigate the protective effects of OMT in this setting and to confirm the contribution of ERS-associated signaling pathways against ALI-induced apoptosis in diabetic rats. The results suggest that the efficacy of OMT in ALI is associated with the attenuation of ERS-induced apoptosis, which provides novel insights for the treatment of myocardial I/R-induced ALI.

2. Materials and Methods

2.1. Induction and Assessment of Diabetes. Sprague–Dawley rats weighing 180–200 g (8–10 weeks old) were provided by the Department of Experimental Animal Science, Xiangya School of Medicine, Central South University. All animal experiments were approved by the Hunan Academy of Chinese Medicine Animal Care and Use Committee (approval no. Xiang 2019-0013) and conducted in accordance with the United States National Institutes of Health Guide for the Care and Use of Laboratory Animals (NIH Publication No. 85–23, revised 1996) and Ethics Committees in Science: European Perspectives (19). The rats were fed a normal diet of standard feed for 1 week and then randomly divided into the control ($n = 10$) and model ($n = 60$) groups. The control group continued to receive the normal diet, and the model group received a high-sugar, high-fat diet (67.5% standard feed, 10% lard, 20% sucrose 20%, 2% cholesterol, and 0.5% pig bile salt). After 4 weeks, the model group (with diabetes mellitus (DM)) received a single intraperitoneal injection of STZ (Sigma-Aldrich: 572201) (35 mg/kg) and the high-sugar, high-fat diet was continued; for the control group (control), an equal volume of sodium citrate buffer was administered (in place if STZ), and the normal diet was continued. At the 8th week, blood was taken from the tail vein, and the glucose concentration was determined; fasting blood glucose ≥7.0 mmol/l or random blood glucose ≥11.0 mmol/l was considered to indicate diabetes. The rats were then intragastrically administered with saline or OMT (Aladdin: A111285) for 7 weeks and then intraperitoneally injected with normal saline.

2.2. Establishment of Myocardial I/R Injury. The coronary artery ligation method was used to establish the I/R injury model. After anesthetization with an intraperitoneal injection of sodium pentobarbital (30 mg/kg), the rats received endotracheal intubation and artificial ventilation with oxygen-enriched room air using a rodent respirator (Chengdu Techman Software Co., Ltd) with 60 breaths per minute, and the tidal volume was set to 8 ml. The heart was exposed, and thread was passed through the left coronary artery. Another 2 threads were drawn from the knot to loosen the ligature. The left coronary artery was ligated to produce ischemia, after which the local myocardium appeared cyanotic. After 1 h ischemia, the ligature was loosened to restore blood flow and initiate reperfusion, which was sustained for an additional hour.

The rats were randomly divided into the seven following ($n = 8$ per group) groups: (i) control group; (ii) Sham group, surgery with no ischemia; (iii) I/R group, myocardial I/R; (iv) I/R + OMT group, myocardial I/R + OMT 30 mg/kg; (v) diabetes mellitus (DM) group; (vi) DM + I/R group, DM + myocardial I/R; and (vii) DM + I/R + OMT group, DM + myocardial I/R + OMT 30 mg/kg. OMT (30 mg/kg) was chosen from our preliminary pilot experiment and dissolved in isotonic saline and administered by gavage 10 min prior to occlusion of the left coronary artery. During the experiment, about two animals per group died. The rate of mortality reached to 20%, which is acceptable based on the ethical approval granted to our study. At the end of the study, rats were anesthetized by an intraperitoneal injection of pentobarbital sodium (30 mg/kg). Blood samples were collected from abdominal aorta for subsequent analysis. All the animals were sacrificed following anesthesia by exsanguination, and their heart tissues were collected for the following experiments (Figure 1).

2.3. Detection of Serum Myocardial Enzyme Levels. At the end of the 8th week, the rats were fasted for 12 h, sacrificed, and blood samples were collected. The serum was separated by centrifugation at 3000 × g for 10 min (4°C), and the levels of cardiac troponin I (cTnI) (Sigma-Aldrich: MABX7161), cardiac troponin T (cTnT) (Sigma-Aldrich: SAB1402377), lactate dehydrogenase (LDH) (Sigma-Aldrich: L7016), and creatine kinase-MB (CK-MB) (Sigma-Aldrich: MAK116) were quantified using commercial ELISA kits. The remaining serum was stored at −80°C for further studies.

2.4. Blood Gas Analysis and WET/DRY Ratio. Immediately after 1 h of reperfusion, the chest of each rat was opened, and arterial blood was taken from the left ventricle. Blood gas analysis was performed using the i-STAT blood gas analyzer (Abbott). Fresh lung tissues were weighed (wet weight) and dehydrated in an oven at 65°C for 48 h. The tissues were then weighed again until the weight

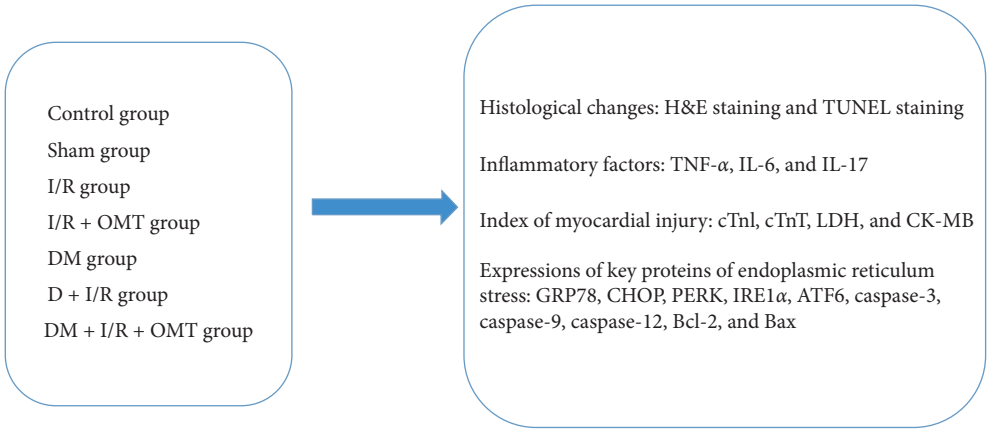

Figure 1: Experimental protocols.

did not fluctuate for ≥3 measurements. The ratio of wet weight to dry weight (the WET/DRY ratio) was then calculated.

2.5. Collection of Bronchoalveolar Lavage (BAL) Fluid. After sacrifice, the lungs were removed from each rat. The tissues were carefully separated, the left bronchial hilar was ligated, and scissors were used to cut a *V*-shaped incision under the tracheal annular cartilage. A blunt needle was inserted into the trachea along the incision, and the needle was ligated and fixed with a thin wire. Lung tissues were lavaged 3 times with PBS to collect BAL fluid. The collected samples were immediately centrifuged at 3000 × g for 10 min (4°C), and the supernatant was stored at −80°C until subsequent experimental testing.

2.6. Detection of Leukocytes, Tumor Necrosis Factor-α (TNF-α), Interleukin- (IL-) 6, and IL-17 in BAL Fluid. The obtained BAL fluid was centrifuged at 300 × g for 5 min (4°C), and the resulting supernatant was collected for protein concentration analysis; the cell pellet was stored for further use. Briefly, 6–10 times the amount of red blood cell lysis buffer (Roche Diagnostics: 11814389001) was added to the cell pellet, and the cells were incubated on ice for 5 min. Ice-cold PBS was added to the cell lysate, which was then centrifuged at 500 × g for 5 min (4°C). The supernatant was discarded, and the cells were centrifuged in 1 ml PBS (500 × g for 5 min, 4°C) to remove any remaining red blood cell debris. The supernatant was discarded, and the cells were resuspended in 0.5 ml PBS and counted using a hemocytometer. The levels of inflammatory factors were determined using commercial ELISA kits (Sigma-Aldrich: T5944, RAB0311, SRP6511), and all experiments were performed according to the manufacturer's instructions.

2.7. Hematoxylin and Eosin (H&E) Staining. Tissues of the left lung and myocardial tissues of the left ventricle were collected, fixed in 4% paraformaldehyde for 24 h, and then dehydrated until transparent. The tissues were embedded in paraffin and sectioned (4 μm), and H&E staining was conducted. The tissues were observed in 3 random areas under a light microscope (200x). Inflammatory cell infiltration, hemorrhage, and the interstitial and alveolar septum thickness of 5 random fields were observed, and scores for the corresponding indicators of lung injury were determined. For inflammatory cell infiltration (i) 0, without damage; (ii) 1, mild injury; (iii) 2, moderate injury; (iv) 3, severe damage; and (v) 4, very severe tissue damage. Other lung injury index scores were also calculated, and the average scores for each treatment group were determined.

2.8. Detection of Apoptosis. Tissue apoptosis was determined by terminal deoxynucleotidyl transferase-mediated dUTP nick end labeling (TUNEL). Briefly, at the end of reperfusion, the lungs were excised and fixed in 4% paraformaldehyde in PBS at room temperature for 24 h. Fixed tissues were embedded in paraffin and stained using an in situ cell death detection kit (Roche Diagnostics: 11684795910) as per the manufacturers' protocol. The apoptotic index (percentage of TUNEL-positive nuclei/total number of nuclei) was then determined.

2.9. Detection of Caspase-3 Activity. Tissues were collected and rinsed with PBS, homogenized and lysed as aforementioned, and then centrifuged at 12,000 × g for 10 min (4°C). Caspase-3 activity was detected using a caspase 3 assay kit (Roche Diagnostics: CASP3C) and normalized to the total protein content for quantification.

2.10. Western Blot Analysis. Total protein was extracted from the lung tissues and transferred to PVDF membranes by electrophoresis (SDS-PAGE). The membranes were incubated with primary antibodies for 2 h at room temperature, rinsed, and subsequently incubated with a horseradish peroxidase-conjugated secondary antibody. The chemiluminescence signals were detected using the EasySee Western Blot Kit (Beijing TransGen Biotech Co., Ltd.), and densitometric analysis was conducted with ImageJ Software 1.43 (National Institutes of Health). Primary antibodies against the following targets were used: endoplasmic

reticulum chaperone BiP (GRP78) (1 : 1000, G8918 : Sigma-Aldrich; Merck KGaA), DNA damage-inducible transcript 3 protein (CHOP) (1 : 1000, SAB4500631 : Sigma-Aldrich; Merck KGaA), inositol dependent enzyme 1 (IRE1)α (1 : 1000, P4334 : Sigma-Aldrich; Merck KGaA), p-IRE1α (1 : 1000, 5.32758: Sigma-Aldrich; Merck KGaA), eukaryotic translation initiation factor 2-alpha kinase 3 (PERK) (1 : 1000, P0073 : Sigma-Aldrich; Merck KGaA), p-PERK (1 : 1000, SAB4301310 : Sigma-Aldrich; Merck KGaA), ATF6 (1 : 1000, PRS3681 : Sigma-Aldrich; Merck KGaA), caspase-9 (1 : 1000, SAB4300683 : Sigma-Aldrich; Merck KGaA), caspase-3 (1 : 1000, C9598 : Sigma-Aldrich; Merck KGaA), caspase-12 (1 : 1000, C7611 : Sigma-Aldrich; Merck KGaA), Bax (1 : 1000, B8429 : Sigma-Aldrich; Merck KGaA), Bcl-2 (1 : 1000, B3170 : Sigma-Aldrich; Merck KGaA), and GADPH (1 : 1000, AF0006; Beyotime Biotechnology, China).

2.11. Real-Time PCR. Gene expression levels (mRNA) in lung tissue were determined by real-time PCR (Applied Biosystems). First, extracted total RNA were purified with 75% ethanol, and its concentration was determined by spectrophotometry. Then, the purified total RNA (200 ng each sample) was added into a transcription kit (DRR037A; TaKaRa, Dalian, China) and mixed to get the first strand template (reverse transcription reaction). GAPDH was used as the loading control. The primers were provided by GeneCopoeia Inc., as follows: CHOP forward, 5′-CAT ACA CCA CCA CAC CTG AAA G-3′; reverse, 5′-CAT ACA CCA CCA CAC CTG AAA G-3′; GRP78 forward, 5′-TCT CCA CGG CTT CCG ATA AT-3′; and reverse, 5′-GTA CCT TTG TCT TCA GCT GTC ACT C-3′. All oligonucleotide primers were designed by Sangon Biotech Co., Ltd (Shanghai, China). The Ct value of the target is normalized by subtracting the GAPDH Ct value to provide a ΔCt value. The relative expression level between treatments was then calculated using the following equation: relative gene expression = 2 − (ΔCt sample −ΔCt control).

2.12. Statistical Analysis. SPSS 21.0 (IBM Corp.) was used for statistical analysis, and all data are presented as the mean ± standard deviation (SD). For gene expressions, one-way ANOVA with the post hoc Tukey test was used to test for differences among groups. Lung injury scores were analyzed with the Kruskal–Wallis test followed by Dunn's multiple comparison test. The statistical significance of differences was assessed at $P < 0.05$.

3. Results

3.1. Myocardial I/R Accelerates ALI in Diabetic Rats. After the 8th week, blood was taken from the tail vein, and the glucose concentration was determined; fasting blood glucose ≥7.0 mmol/l or random blood glucose ≥11.0 mmol/l was considered to indicate diabetes (Supplementary Figure (available here)). To investigate the protective effect of OMT against I/R-induced myocardial damage in diabetic rats, alterations in the concentrations of serum myocardial injury markers (cTnI, cTnT, LDH, and CK-MB) were observed. The levels of serum cTnI, cTnT, LDH, and CK-MB were significantly increased in diabetic rats with I/R, compared with those in the Sham group. However, OMT treatment markedly suppressed the increases in these serum constituents (Figure 2). In addition, OMT ameliorated the damage and irregular arrangement of myocardial cells induced by I/R injury (Figure 2). These findings suggest that OMT attenuates myocardial I/R injury in diabetic rats.

ALI secondary to myocardial I/R is reportedly aggravated by diabetes [19, 20]. Following myocardial I/R, the BAL fluid was collected and analyzed. As indicated in Figure 3, the levels of TNF-α, IL-6, and IL-17A in the BAL fluid were significantly increased in diabetic rats, indicating the occurrence of a severe inflammatory reaction following myocardial I/R insult. Furthermore, OMT treatment suppressed these increases in TNF-α, IL-6, and IL-17A. The severity of lung injury was assessed by H&E staining and graded using an injury scoring system. As shown in Figure 3, H&E staining of the lung tissue revealed ALI with alveolar and interstitial edema, hemorrhage, and inflammatory cell infiltration. These pathological changes were more severe in diabetic rats. Compared with the Sham group, the degree of lung injury in the myocardial I/R group was also increased. These results confirmed that myocardial I/R could deteriorate ALI in the diabetic rats. However, OMT ameliorated myocardial I/R-induced ALI, suggesting a protective affect against ALI secondary to myocardial I/R in diabetic rats.

3.2. OMT Inhibits ALI-Induced ERS in Diabetic Rats. An increasing number of studies have suggested that excessive ERS accelerates the severity of I/R injury [21, 22]. To determine whether OMT treatment exerts a protective effect against myocardial I/R-associated ALI by inhibiting ERS, the expression levels of ERS markers GRP78 and CHOP were detected in diabetic rats. As shown in Figure 4, the expression of GRP78 and CHOP was markedly increased in the diabetic rats compared with the Sham group. Consistent with protein expression, the levels of GRP78 and CHOP mRNA were assessed by reverse transcription-quantitative PCR. We found that GRP78 and CHOP mRNA expressions are consistent with the protein expressions. Further findings showed no obvious differences between the I/R group and the DM + I/R group in the current experimental background, which does not mean that no differences in injury occurred between the two groups. Treatment with OMT downregulated GRP78 and CHOP mRNA expressions in myocardial I/R-associated ALI. These results suggest that OMT treatment alleviates ERS resulting from myocardial I/R-associated ALI in diabetic rats.

3.3. OMT Inhibits ERS-Induced Apoptosis in Diabetic Rats. To confirm whether ALI-induced ERS is involved in apoptosis, Western blotting was used to determine the expressions of apoptosis-related proteins, including caspase-9, caspase-3, caspase-12, Bcl-2, and Bax, in the lung tissues of diabetic rats. ALI caused significant increases in caspase-9, caspase-3, caspase-12, and Bax and a decrease in Bcl-2 expression (Figure 5), and OMT treatment reversed these

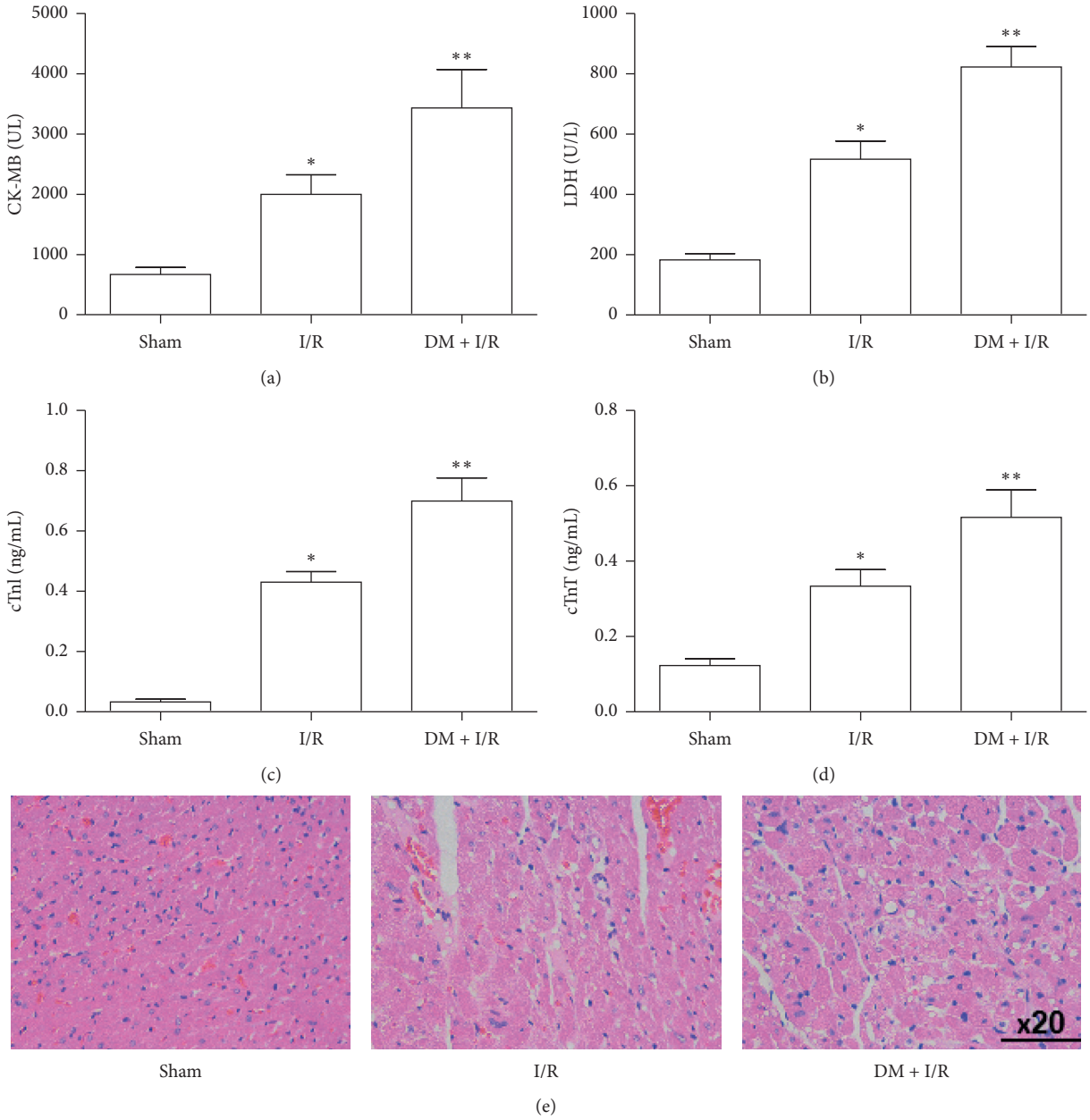

Figure 2: Myocardial I/R-accelerated acute lung injury in diabetic rats. (a), (b), (c), and (d) Serum levels of CK-MB, LDH, cTnI, and cTnT. (e) Hematoxylin and eosin staining of cardiac tissues (original magnification, 400x). Bars represent the mean ± SD of three independent experiments. $^{*}P < 0.05$ vs. the Sham group; $^{**}P < 0.01$ vs. the I/R group. I/R, ischemia/reperfusion; CK-MB, creatine kinase-MB; LDH, lactate dehydrogenase; cTnI, cardiac troponin I; cTnT, cardiac troponin T.

expression patterns. These results demonstrate that OMT inhibits ERS-induced apoptosis in rats including diabetes and nondiabetes. However, the present study does not provide any evidence for diabetes-specific effects.

3.4. OMT Exhibits Protective Effects against ALI-Induced ERS-Associated Signaling Pathway Activation in Diabetic Rats. Based on the aforementioned results, the mechanisms of OMT against myocardial I/R-induced ALI, which were associated with ERS-associated signaling proteins such as IRE1α, PERK, and ATF6, were investigated. As shown in Figure 6, ALI significantly upregulated the expressions of p-IRE1α and p-PERK, compared with the Sham group. Furthermore, these changes were reversed by OMT. These observations indicate that OMT inhibits IRE1α and/or PERK pathways, thereby attenuating ERS-mediated apoptosis and eliciting protection in ALI secondary to myocardial I/R.

4. Discussion

Myocardial I/R injury is regarded as a major public health threat with high rates of morbidity and mortality.

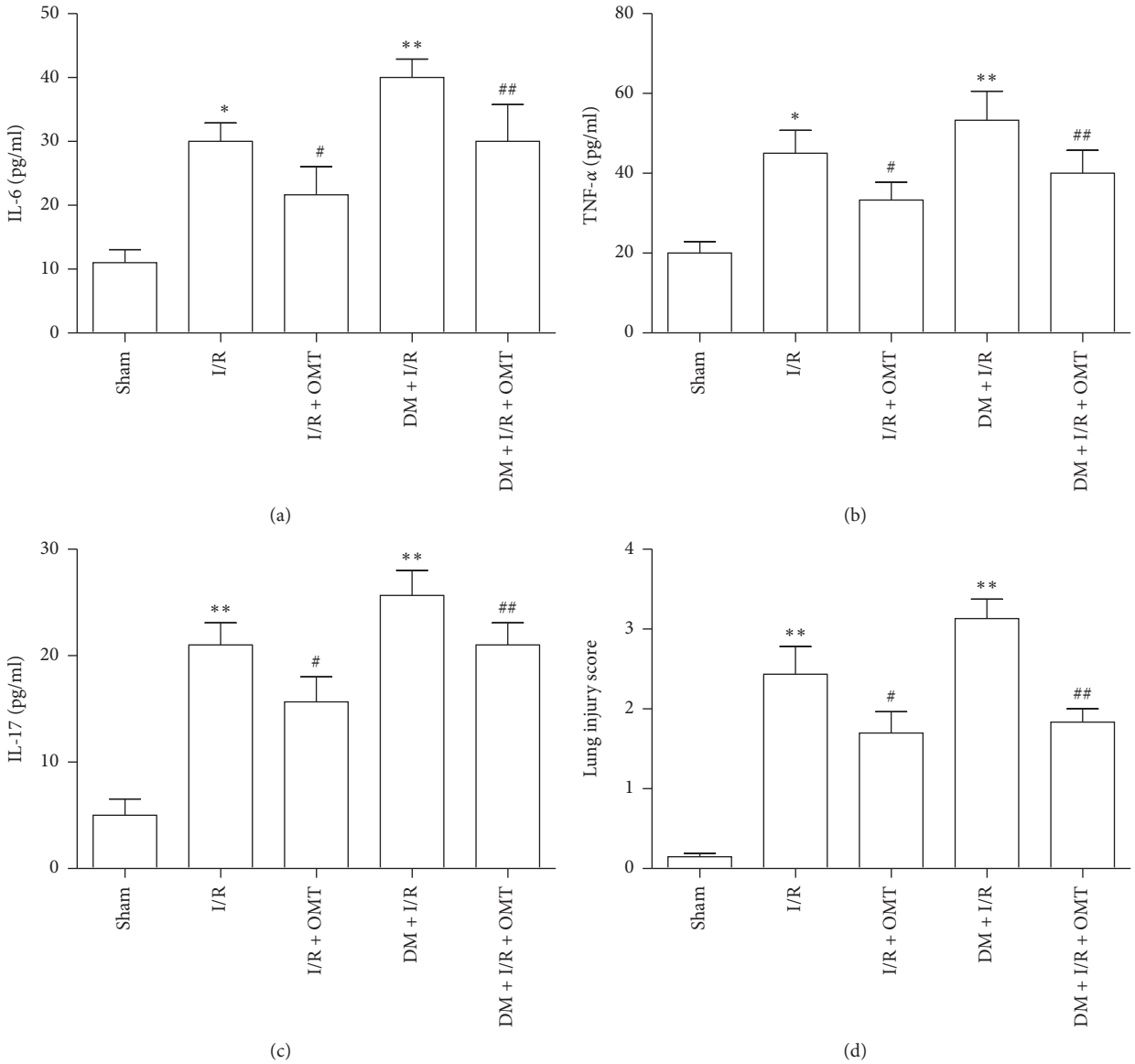

Figure 3: Continued.

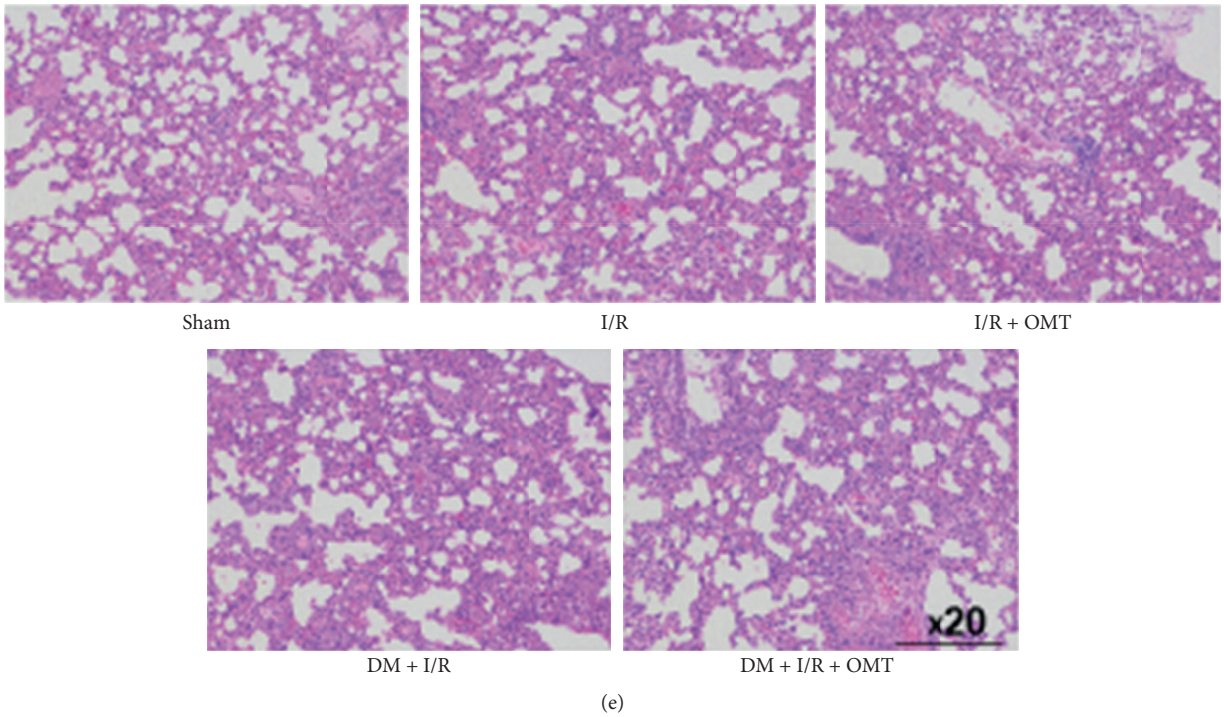

Figure 3: OMT ameliorates myocardial I/R-induced acute lung injury in diabetic rats. (a), (b), and (c) Expression levels of inflammatory factors IL-6, TNF-α, and IL-17. (d) Severity of lung injury expressed as the injury score. (e) Histopathological changes in rat lung tissues from control and diabetic rats subjected to sham or myocardial I/R surgery (original magnification, x200). All values are expressed as the mean ± SD, $n = 8$. $^{*}P < 0.05$ vs. the Sham group; $^{\#}P < 0.05$ vs. the I/R group; $^{\#\#}P < 0.01$ vs. the DM + I/R group. OMT, oxymatrine; I/R, ischemia/reperfusion; IL, interleukin; TNF-α, tumor necrosis factor-α; DM, diabetes mellitus.

Extensive studies have demonstrated that myocardial I/R may result in distant organ damage and that the lung may be one of the most vulnerable organs. The primary novelty of the present study was presenting evidence that myocardial I/R-induced ALI induces excessive lung ERS in diabetic rats and that OMT administration inhibits ERS-induced apoptosis. The myocardial protective effects of OMT suggest that it may be an effective agent for the treatment of I/R injury. However, recent studies showed that ER stress-induced apoptosis plays an important role in myocardial I/R-induced ALI. However, the more accurate functions have not been fully yet elucidated. In present study, the absence of DM without the I/R injury group might hinder understanding of myocardial I/R-induced ALI-associated ERS and the protective of OMT.

OMT is a major active ingredient isolated from *Sophora flavescens* Aiton. Several lines of evidence have demonstrated that OMT possesses diverse pharmacological characteristics, such as anti-inflammatory, antiallergic, antiviral, and antifibrotic properties [10, 11, 15–18]. OMT has been widely applied for the prevention and treatment of liver pathologies, cardiovascular diseases, vascular injury, and diabetes-associated dysfunction and inflammation [10, 15, 17]. In spite of these findings, the protective effects of OMT, as well as its potential mechanism, are yet to be elucidated. As such, the present study aimed to investigate the protective effects of OMT on myocardial I/R-associated ALI in diabetic rats.

Diabetes is the most common of all endocrine diseases. Diabetes is characterized by persistent hyperglycemia, which may lead to diverse representative complications including cardiomyopathy, nephropathy, diabetic foot, and diabetic neuropathy, which significantly contribute to the associated rates of morbidity and mortality [2]. Additionally, diabetes may accelerate the deterioration of respiratory function with characteristic anatomical and biological changes to the diabetic lung [5, 23, 24]. These abnormalities affect lung volume, pulmonary diffusing capacity, ventilation control, bronchomotor tone, and neuroadrenergic bronchial innervation. Although the practical implications of these functional alterations are frequently disregarded, the presence of an associated acute or chronic pulmonary and/or cardiac attack could influence severe respiratory derangement in diabetes [25]. During myocardial ischemia and/or reperfusion, the membranes of the myocardial tissues are attacked, resulting in the release of myocardial enzymes, including cTnI, cTnT, LDH, and CK-MB (which are often regarded as the markers of myocardial injury), into the peripheral blood. Therefore, detecting the peripheral blood levels of these enzymes (which reflect the degree of myocardial injury) has proven considerably valuable in the diagnosis of myocardial infarction. According to the results of the present study, OMT notably decreases the serum concentrations of these enzymes. Additionally, pathomorphological studies indicated a reduction in I/R-induced myocardial damage in diabetic rats treated with OMT.

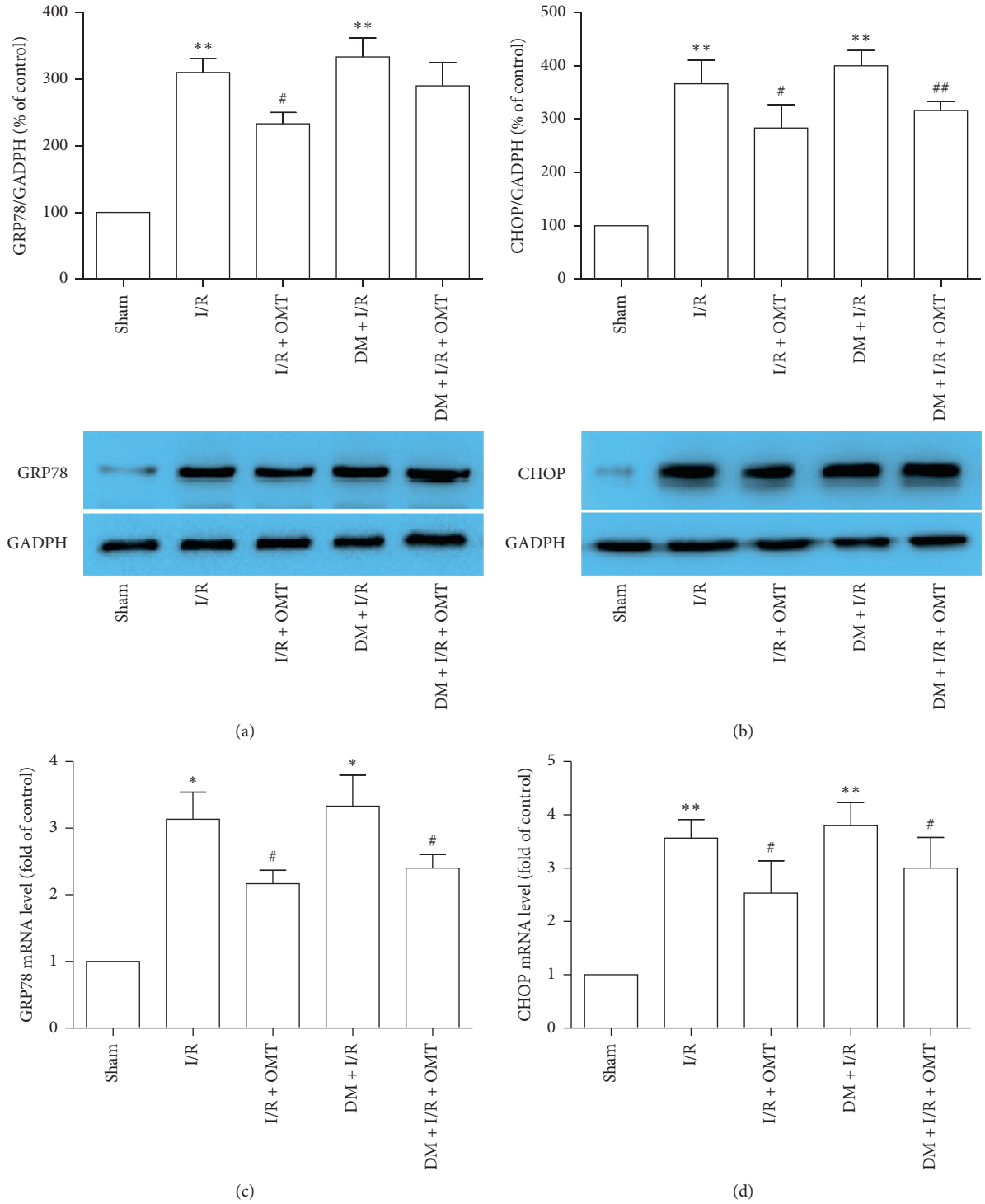

Figure 4: Effects of OMT on endoplasmic reticulum stress during myocardial I/R-induced acute lung injury in diabetic rats. mRNA expression levels of (a) GRP78 and (b) CHOP were detected using Western blot analysis. Protein expression levels of (c) GRP78 and (d) CHOP were determined using reverse transcription-quantitative PCR. Values are expressed as the mean ± SD from three independent experiments, $n = 3$. $^{*}P < 0.05$ and $^{**}P < 0.01$ vs. the Sham group; $^{\#\#}P < 0.01$ vs. the I/R group; $^{\#\#}P < 0.01$, vs. the DM + I/R group. OMT, oxymatrine; I/R, ischemia/reperfusion; GRP78, endoplasmic reticulum chaperone BiP; CHOP, DNA damage-inducible transcript 3 protein; DM, diabetes mellitus.

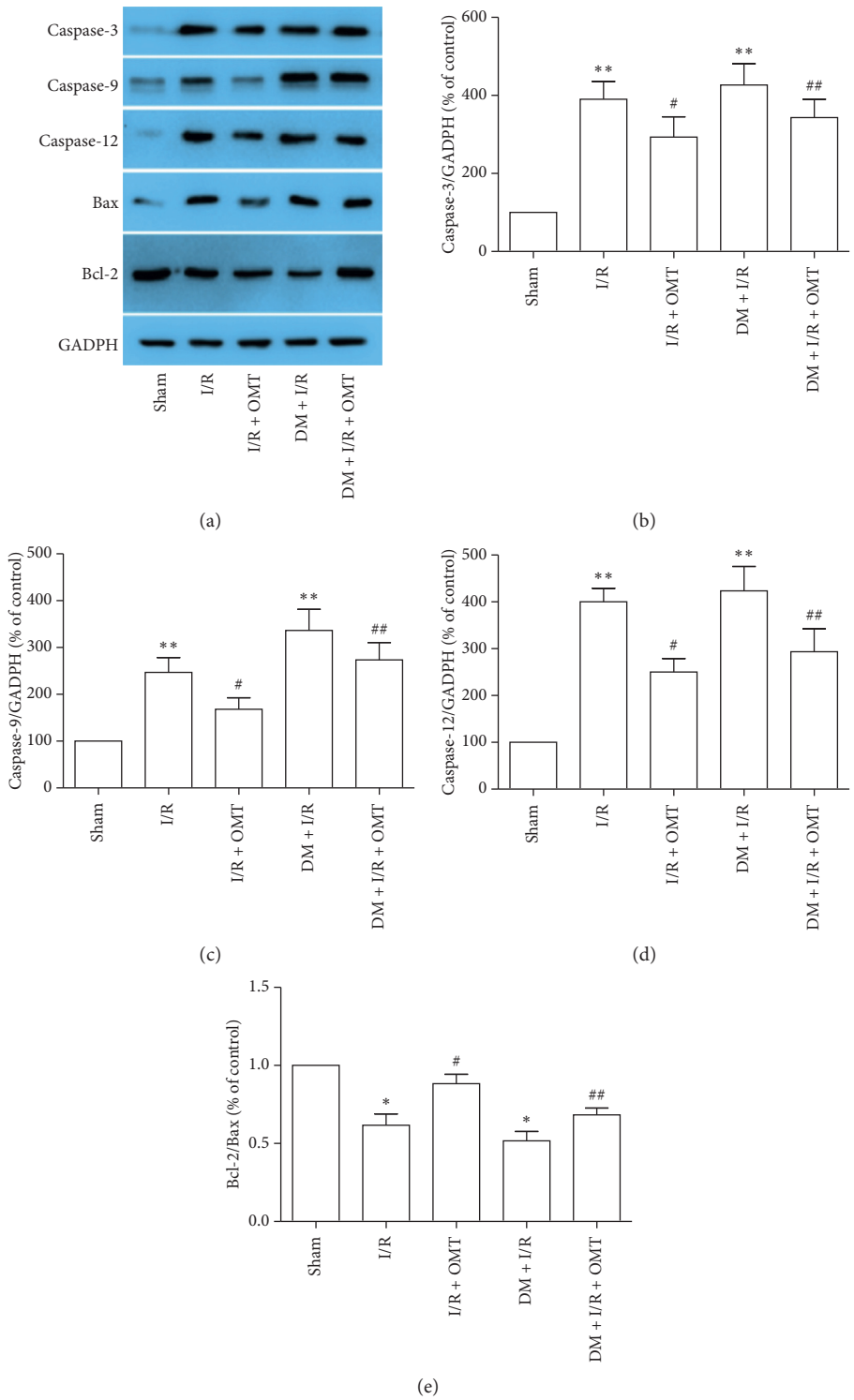

Figure 5: Continued.

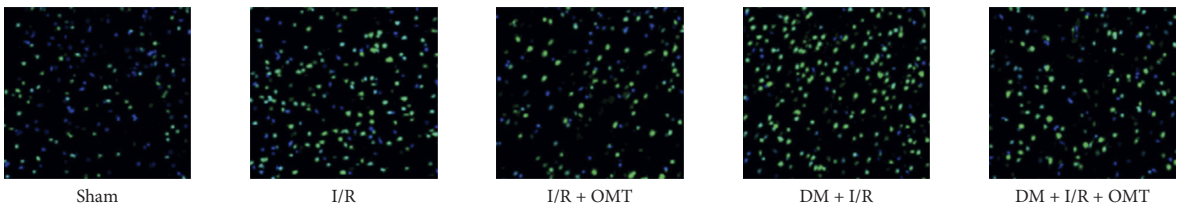

(f)

Figure 5: OMT inhibits ERS-induced apoptosis in diabetic rats. (a) Expression of caspase-3, caspase-9, caspase-12, Bax, and Bcl-2 was determined using Western blot analysis. (b), (c), (d), and (e) Quantification of Western blot results. (f) TUNNEL staining in lung tissues. Values are expressed as the mean ± SD from three independent experiments, $n = 3$. $^{*}P < 0.05$ and $^{**}P < 0.01$ vs. the Sham group; $^{\#\#}P < 0.01$ vs. the I/R group; $^{\#\#}P < 0.01$, vs. the DM + I/R group. OMT, oxymatrine; ERS, endoplasmic reticulum stress; I/R, ischemia/reperfusion; DM, diabetes mellitus.

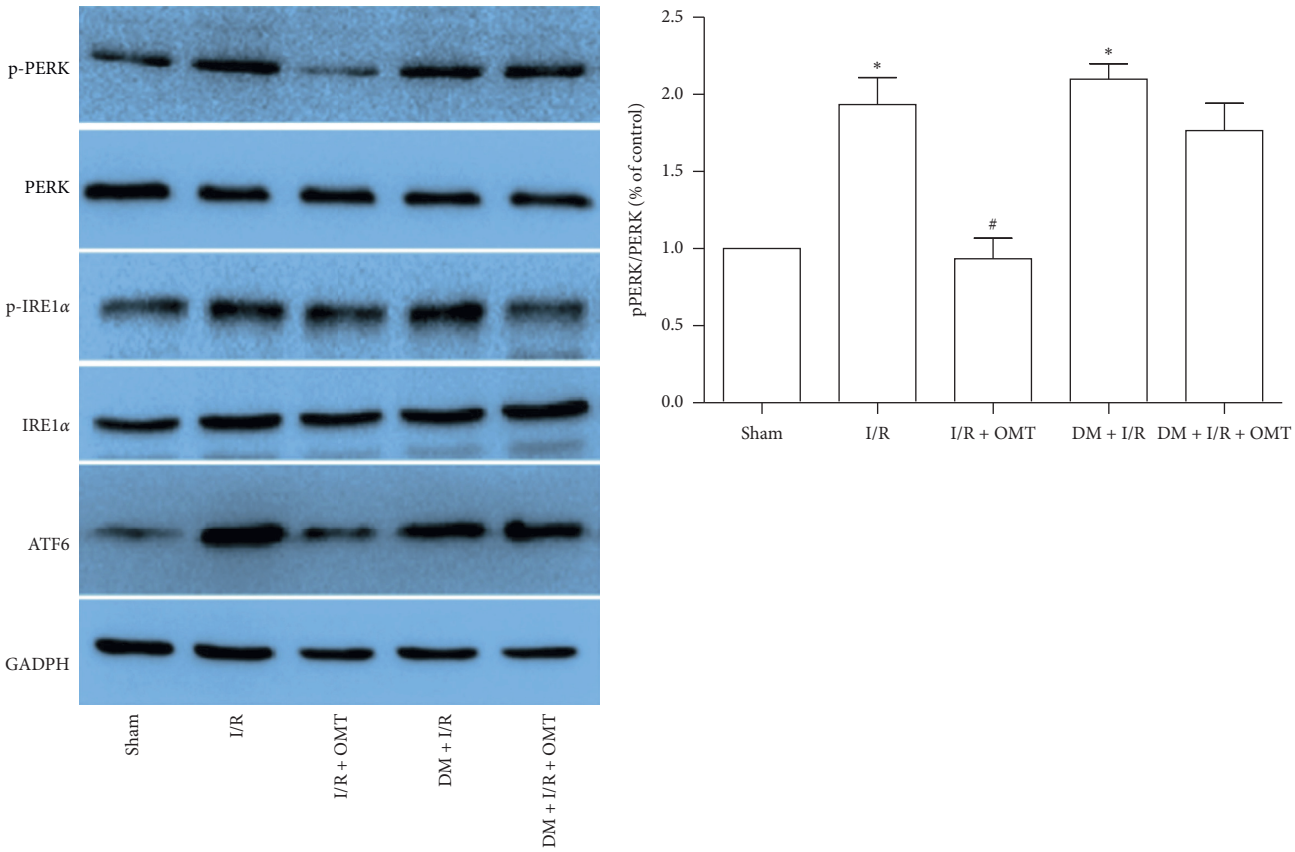

(a) (b)

Figure 6: Continued.

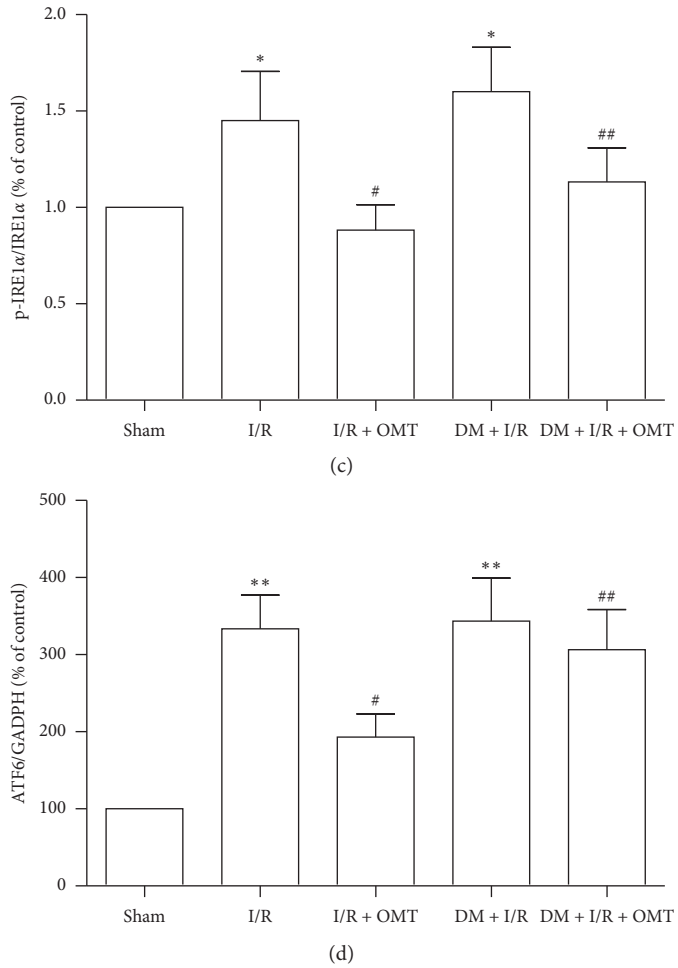

Figure 6: OMT inhibits acute lung injury-induced endoplasmic reticulum stress-associated signaling pathway activation in diabetic rats. (a) Protein expression levels of p-PERK, PERK, p-IRE1α, and IRE1α were determined using Western blot analysis. (b), (c), and (d) Quantification of Western blot results. Values are expressed as the mean ± SD from three independent experiments, $n = 3$. $^{*}P < 0.05$ and $^{**}P < 0.01$ vs. the Sham group; $^{\#}P < 0.05$ vs. the I/R group; $^{\#\#}P < 0.01$, vs. the DM + I/R group. OMT, oxymatrine; PERK, translation initiation factor 2-alpha kinase 3; IRE1, inositol dependent enzyme 1; p-, phosphorylated; I/R, ischemia/reperfusion; DM, diabetes mellitus.

Consistent with previously reports [19], the present study revealed that the lungs of diabetic rats are susceptible to myocardial I/R injury, indicated by increased levels of ALI-induced inflammatory factors (including IL-6, TNF-α, and IL-17) with higher lung injury scores and WET/DRY ratios, as well as a lower PaO_2. Moreover, the DM + I/R group showed more severe damages in levels of ALI-induced inflammatory factors (including IL-6, TNF-α, and IL-17) and lung injury scores but showed no obvious differences between the I/R + OMT group and the DM + I/R + OMT group. OMT could decrease the levels of inflammatory factors and lung injury scores and WET/DRY ratios in the I/R + OMT group or the DM + I/R + OMT group. But these results demonstrated that the effects of I/R + OMT is more obviously than DM + I/R + OMT. Overall, OMT exerts a beneficial effect on ALI secondary to I/R injury in diabetic rats.

The ER is a membrane-bound and structurally intricate organelle present in all eukaryotic cells. It is the specific site for monitoring intracellular protein and lipid synthesis, as well as intracytoplasmic calcium storage [26, 27]. Diabetes is known to be a chronic disorder characterized by low-grade chronic inflammation and a hypoxic microenvironment, which can result in the accumulation of misfolded and unfolded proteins in the ER lumen [4, 28]. ER homeostasis is disturbed in a condition referred to as ERS. Excessive ERS triggers an adaptive mechanism termed the unfolded protein response (UPR), which is implemented in the maintenance of cellular homeostasis. The UPR is primarily mediated by three ER transducers PERK, IRE1, and ATF6, which could detect unusual conditions and transmit signals to the cytosol. Once activated, these signals induced downstream responses. During ERS conditions, PERK, IRE1α, and ATF6 contributed to reactive oxygen species (ROS) generation and apoptosis. Sustained ERS ultimately leads to ERS-mediated apoptosis [9, 29, 30]. Caspase-12 is present in various tissues and is regarded as one of the major apoptotic signaling molecules of ERS. The imbalance of calcium ions in the ER or the accumulation of ER proteins can ultimately lead to

caspase-12 expression. Excessive ERS can trigger the activation of other caspases, such as caspase-9 and -3, causing cascade reactions that ultimately result in cell death [27, 31]. CHOP is an important proapoptotic signaling molecule and ERS-specific transcription factor. Under physiological conditions, CHOP is expressed at low levels; once activated by ERS, its expression level significantly increases, and this is considered to be an important marker of ERS [31]. Intracellular apoptotic signaling usually activates the mitochondrial pathway, facilitating the release of mitochondrial proapoptotic proteins and apoptosis-inducing factors and ultimately activating the caspase cascade and promoting apoptosis [32]. The present study revealed that the expression of ERS marker proteins GRP78 and CHOP in the I/R group and the DM + I/R group were markedly upregulated, demonstrating that ERS is involved in the occurrence of myocardial I/R-induced ALI, but showed no obvious differences between these groups in the current experimental background, and there seems to be no significant difference between these groups, which does not mean that no differences in injury occurred between the two groups. Furthermore, the present study demonstrated that the protein expression levels of PERK, p-PERK, p-IRE1α, ATF6, and CHOP in the lung tissues were upregulated. These results suggested that the lung tissue damage in the DM + I/R group was more severe than that in the I/R group. Further study confirmed that OMT treatment inhibited the upregulation in p-PERK, p-IRE1α, and ATF6 and also reduced the apoptosis index, suggesting that OMT exerts protective effects against myocardial I/R-induced ALI by suppressing ERS-associated apoptosis. Collectively, these findings demonstrate that OMT inhibits ERS-associated signaling pathways, which may further decrease ERS-induced apoptosis. This was subsequently investigated by detecting the expressions of apoptosis-associated proteins. Notably, OMT downregulated the high expression levels of caspase-3, caspase-9, caspase-12, and Bax associated with myocardial I/R-induced ALI and upregulated Bcl-2 expression in diabetic rats.

5. Conclusions

In summary, the present study revealed the significant protective effects of OMT against myocardial I/R-induced ALI in diabetic rats and illustrated that these effects are mediated by the inhibition of ERS-associated apoptosis. However, the overall mechanisms underlying the protective effects of OMT and its association with ERS required further investigation.

Abbreviations

ALI: Acute lung injury
cTnI: Cardiac troponin I
cTnT: Cardiac troponin T
CK-MB: Creatine kinase-MB
CHOP: DNA damage-inducible transcript 3 protein
ERS: Endoplasmic reticulum stress
GRP78: Endoplasmic reticulum chaperone BiP
I/R: Ischemia/Reperfusion
IL-6: Interleukin- (IL-) 6
IRE1-α: Inositol dependent enzyme 1α (IRE1α)
LDH: Lactate dehydrogenase
OMT: Oxymatrine
p-PERK: Phosphorylated- (p-) PERK
PERK: Eukaryotic translation initiation factor 2-alpha kinase 3
STZ: Streptozocin
TUNEL: Terminal deoxynucleotidyl transferase-mediated dUTP nick end labeling.

Data Availability

The data used to support the findings of this study are included within the manuscript and are available from the corresponding author upon request.

Conflicts of Interest

The authors declare that they have no conflicts of interest.

Authors' Contributions

YP. H. and XL. L. designed and undertook some parts of the experiment and analyzed, interpreted, and presented results for group discussion. SH. L. provided methods, description of results, and figures for the manuscript. SH. L. and JB. H. provided rationale, background, framework, and feedback.

Acknowledgments

The authors would like to thank all the colleagues who contributed to this study. This work was funded by Hunan Natural Science Foundation (2020JJ7090 to Yongpan Huang).

Supplementary Materials

Supplementary Figure1: effect of OMT on the serum glucose level. Bars represent the mean ± SD of three independent experiments. $^{*}P < 0.05$ vs. the control group. (*Supplementary Materials*)

References

[1] X. Mundet, A. Pou, N. Piquer et al., "Prevalence and incidence of chronic complications and mortality in a cohort of type 2 diabetic patients in Spain," *Primary Care Diabetes*, vol. 2, no. 3, pp. 135–140, 2008.

[2] S. Pichu, B. M. Patel, S. Apparsundaram, and R. K. Goyal, "Role of biomarkers in predicting diabetes complications with special reference to diabetic foot ulcers," *Biomarkers in Medicine*, vol. 11, no. 4, pp. 377–388, 2017.

[3] X. Zhou, S. S. Shrestha, E. Luman, G. Wang, and P. Zhang, "Medical expenditures associated with diabetes in myocardial infarction and ischemic stroke patients," *American Journal of Preventive Medicine*, vol. 53, no. 6S2, pp. S190–S196, 2017.

[4] T. W. Jung, H. C. Kim, H. U. Kim et al., "Asprosin attenuates insulin signaling pathway through PKCδ-activated ER stress

and inflammation in skeletal muscle," *Journal of Cellular Physiology*, vol. 234, no. 11, pp. 20888–20899, 2019.

[5] Y. Lee, S. H. Shin, K. A. Cho et al., "Administration of tonsil-derived mesenchymal stem cells improves glucose tolerance in high fat diet-induced diabetic mice via insulin-like growth factor-binding protein 5-mediated endoplasmic reticulum stress modulation," *Cells*, vol. 8, no. 4, p. 368, 2019.

[6] L. Cominacini, C. Mozzini, U. Garbin et al., "Endoplasmic reticulum stress and Nrf2 signaling in cardiovascular diseases," *Free Radical Biology and Medicine*, vol. 88, no. Pt B, pp. 233–242, 2015.

[7] W. Guo, T. Jiang, C. Lian, H. Wang, Q. Zheng, and H. Ma, "QKI deficiency promotes FoxO1 mediated nitrosative stress and endoplasmic reticulum stress contributing to increased vulnerability to ischemic injury in diabetic heart," *Journal of Molecular and Cellular Cardiology*, vol. 75, pp. 131–140, 2014.

[8] M. Liu, Y. Wang, Q. Zhu et al., "Protective effects of circulating microvesicles derived from ischemic preconditioning on myocardial ischemia/reperfusion injury in rats by inhibiting endoplasmic reticulum stress," *Apoptosis*, vol. 23, no. 7-8, pp. 436–448, 2018.

[9] R. Iijima, M. Nakamura, Y. Matsuyama et al., "Effect of optimal medical therapy before procedures on outcomes in coronary patients treated with drug-eluting stents," *The American Journal of Cardiology*, vol. 118, no. 6, pp. 790–796, 2016.

[10] L. Wang, X. Li, Y. Zhang, Y. Huang, and Q. Ma, "Oxymatrine ameliorates diabetes-induced aortic endothelial dysfunction via the regulation of eNOS and NOX4," *Journal of Cellular Biochemistry*, vol. 120, no. 5, pp. 7323–7332, 2019.

[11] Y. Jiang, W. Sang, C. Wang et al., "Oxymatrine exerts protective effects on osteoarthritis via modulating chondrocyte homoeostasis and suppressing osteoclastogenesis," *Journal of Cellular and Molecular Medicine*, vol. 22, no. 8, pp. 3941–3954, 2018.

[12] C. D. Resor, A. Nathan, D. J. Kereiakes et al., "Impact of optimal medical therapy in the dual antiplatelet therapy study," *Circulation*, vol. 134, no. 14, pp. 989–998, 2016.

[13] Y. Liu, Y. Xu, W. Ji et al., "Anti-tumor activities of matrine and oxymatrine: literature review," *Tumour Biology*, vol. 35, no. 6, pp. 5111–5119, 2014.

[14] C. Y. Shen, J. G. Jiang, L. Yang, D. W. Wang, and W. Zhu, "Anti-ageing active ingredients from herbs and nutraceuticals used in traditional Chinese medicine: pharmacological mechanisms and implications for drug discovery," *British Journal of Pharmacology*, vol. 174, no. 11, pp. 1395–1425, 2017.

[15] Y. Y. Zhang, M. Yi, and Y. P. Huang, "Oxymatrine ameliorates doxorubicin-induced cardiotoxicity in rats," *Cellular Physiology and Biochemistry*, vol. 43, no. 2, pp. 626–635, 2017.

[16] G. Jiang, X. Liu, M. Wang, H. Chen, Z. Chen, and T. Qiu, "Oxymatrine ameliorates renal ischemia-reperfusion injury from oxidative stress through Nrf2/HO-1 pathway," *Acta Cirurgica Brasileira*, vol. 30, no. 6, pp. 422–429, 2015.

[17] S. B. Wang and J. P. Jia, "Oxymatrine attenuates diabetes-associated cognitive deficits in rats," *Acta Pharmacologica Sinica*, vol. 35, no. 3, pp. 331–338, 2014.

[18] M. L. Zuo, A. P. Wang, Y. Tian, L. Mao, G. L. Song, and Z. B. Yang, "Oxymatrine ameliorates insulin resistance in rats with type 2 diabetes by regulating the expression of KSRP, PETN, and AKT in the liver," *Journal of Cellular Biochemistry*, vol. 120, no. 9, pp. 16185–16194, 2019.

[19] L. M. Wang, N. Z. Zhong, S. J. Liu, X. Y. Zhu, and Y. J. Liu, "Hypoxia-induced acute lung injury is aggravated in streptozotocin diabetic mice," *Experimental Lung Research*, vol. 41, no. 3, pp. 146–154, 2015.

[20] M. Fîlfan, R. E. Sandu, A. D. Zăvăleanu et al., "Autophagy in aging and disease," *Romanian Journal of Morphology and Embryology*, vol. 58, no. 1, pp. 27–31, 2017.

[21] F. Xu, R. Ma, G. Zhang et al., "Estrogen and propofol combination therapy inhibits endoplasmic reticulum stress and remarkably attenuates cerebral ischemia-reperfusion injury and OGD injury in hippocampus," *Biomedicine and Pharmacotherapy*, vol. 108, pp. 1596–1606, 2018.

[22] G. G. Zhang, H. Q. Cai, Y. H. Li et al., "Ghrelin protects heart against ERS-induced injury and apoptosis by activating AMP-activated protein kinase," *Peptides*, vol. 48, pp. 156–165, 2013.

[23] N. S. Kalman, G. D. Hugo, R. N. Mahon, X. Deng, N. D. Mukhopadhyay, and E. Weiss, "Diabetes mellitus and radiation induced lung injury after thoracic stereotactic body radiotherapy," *Radiotherapy and Oncology*, vol. 129, no. 2, pp. 270–276, 2018.

[24] H. Zheng, J. Wu, Z. Jin, and L. J. Yan, "Potential biochemical mechanisms of lung injury in diabetes," *Aging and Disease*, vol. 8, no. 1, pp. 7–16, 2017.

[25] B. Q. Xiang, H. Gao, M. L. Hao, Y. Y. Dai, and W. T. Wang, "Effects of excessive endoplasmic reticulum stress on lung ischemia/reperfusion induced myocardial injury in mice," *Zhongguo Ying Yong Sheng Li Xue Za Zhi*, vol. 34, no. 1, pp. 8–13, 2018.

[26] S. Song, J. Tan, Y. Miao, and Q. Zhang, "Crosstalk of ER stress-mediated autophagy and ER-phagy: involvement of UPR and the core autophagy machinery," *Journal of Cell Physiology*, vol. 233, no. 5, pp. 3867–3874, 2018.

[27] S. Song, J. Tan, Y. Miao, M. Li, and Q. Zhang, "Crosstalk of autophagy and apoptosis: involvement of the dual role of autophagy under ER stress," *Journal of Cell Physiology*, vol. 232, no. 11, pp. 2977–2984, 2017.

[28] W. Yang, F. Sheng, B. Sun, S. Fischbach, and X. Xiao, "The role of ORMDL3/ATF6 in compensated beta cell proliferation during early diabetes," *Aging (Albany NY)*, vol. 11, no. 9, pp. 2787–2796, 2019.

[29] J. Groenendyk, X. Fan, Z. Peng, L. Kurgan, and M. Michalak, "Endoplasmic reticulum and the microRNA environment in the cardiovascular system (1)," *Canadian Journal of Physiology and Pharmacology*, vol. 97, no. 6, pp. 515–527, 2019.

[30] S. Shirjang, B. Mansoori, S. Asghari et al., "MicroRNAs in cancer cell death pathways: apoptosis and necroptosis," *Free Radical Biology and Medicine*, vol. 139, pp. 1–15, 2019.

[31] Y. Li, Y. Guo, J. Tang, J. Jiang, and Z. Chen, "New insights into the roles of CHOP-induced apoptosis in ER stress," *Acta Biochimica et Biophysica Sinica (Shanghai)*, vol. 46, no. 8, pp. 629–640, 2014.

[32] G. Guan, J. Zhang, S. Liu, W. Huang, Y. Gong, and X. Gu, "Glucagon-like peptide-1 attenuates endoplasmic reticulum stress-induced apoptosis in H9c2 cardiomyocytes during hypoxia/reoxygenation through the GLP-1R/PI3K/Akt pathways," *Naunyn-Schmiedeberg's Archives of Pharmacology*, vol. 392, no. 6, pp. 715–722, 2019.